

Mohd Nazip Suratman *Editor*

Concepts and Applications of Remote Sensing in Forestry

 Springer

Concepts and Applications of Remote Sensing in Forestry

Mohd Nazip Suratman
Editor

Concepts and Applications of Remote Sensing in Forestry

 Springer

Editor

Mohd Nazip Suratman
Universiti Teknologi MARA
Shah Alam, Malaysia

ISBN 978-981-19-4199-3 ISBN 978-981-19-4200-6 (eBook)
<https://doi.org/10.1007/978-981-19-4200-6>

© Springer Nature Singapore Pte Ltd. 2022

This work is subject to copyright. All rights are solely and exclusively licensed by the Publisher, whether the whole or part of the material is concerned, specifically the rights of translation, reprinting, reuse of illustrations, recitation, broadcasting, reproduction on microfilms or in any other physical way, and transmission or information storage and retrieval, electronic adaptation, computer software, or by similar or dissimilar methodology now known or hereafter developed.

The use of general descriptive names, registered names, trademarks, service marks, etc. in this publication does not imply, even in the absence of a specific statement, that such names are exempt from the relevant protective laws and regulations and therefore free for general use.

The publisher, the authors, and the editors are safe to assume that the advice and information in this book are believed to be true and accurate at the date of publication. Neither the publisher nor the authors or the editors give a warranty, expressed or implied, with respect to the material contained herein or for any errors or omissions that may have been made. The publisher remains neutral with regard to jurisdictional claims in published maps and institutional affiliations.

This Springer imprint is published by the registered company Springer Nature Singapore Pte Ltd.
The registered company address is: 152 Beach Road, #21-01/04 Gateway East, Singapore 189721, Singapore

Preface

Remote sensing has been used for forestry applications for many decades. For example, aerial photographs were used as working tools in preparing forest inventory, size, type and condition maps of forest stands. Today, remote sensing is heavily utilised in forest management, which is acquired from airborne and spaceborne platforms using satellite data. In comparison with traditional aerial photography, satellite imagery has many advantages such as the frequency of data collection, global availability of satellite data, data suitability for digital analysis and classification, and data gathering at relatively low cost.

The new generations of satellite sensors are introduced not only to provide important information on forest ecosystems but also to improve the techniques and accuracies obtained by the traditional approaches. In recent years, there have been rapid advances in the new types of sensors. They have the potential to improve the accuracy in classification of forest types and species discrimination. In addition, the systems were reported to contribute to improving the estimations of forest variables such as forest biomass, stand volume, stand age and carbon stocks by linking the spectral reflectance and ground information via predictive models.

Researchers have become increasingly aware of the potential of remote sensing to address important forestry issues and challenges. The number of forestry publications using remote sensing has grown very rapidly, and this is noticeable with many recent technologies and applications. Therefore, this book chapter highlights the concepts and applications in remote sensing for forestry with a particular emphasis on the techniques, data, sensors and their applications. Novel applications of recent techniques in remote sensing are discussed. In addition, several constraints and future opportunities in the use of remote sensing for forestry applications are addressed.

Shah Alam, Malaysia

Mohd Nazip Suratman

Contents

Part I Introduction

Remote Sensing for Forest Inventory and Resource Assessment	3
Mohd Nazip Suratman, Zulkiflee Abd. Latiff, Tengku Mohd Zarawie Tengku Hashim, Ahmad Farid Mohsin, Nazlin Asari, and Nurul Ain Mohd Zaki	

Part II Overview of Remote Sensing

Multiple Sensors and Platforms for Biophysical and Biochemical Characterisations of Various Ecosystem Types of Tropical Forests in Malaysia: Advance, Limitation, and Opportunity	27
Hamdan Omar	

A Review on the Use of LiDAR Remote Sensing for Forest Landscape Restoration	49
Siti Munirah Mazlan, Wan Shafrina Wan Mohd Jaafar, Aisyah Marliza Muhmad Kamarulzaman, Siti Nor Maizah Saad, Norzalyta Mohd Ghazali, Esmaeel Adrah, Khairul Nizam Abdul Maulud, Hamdan Omar, Yit Arn Teh, Dzaeman Dzulkifli, and Mohd Rizaludin Mahmud	

Assessment and Modelling of Forest Biomass and Carbon Stock and Sequestration Using Various Remote Sensing Sensor Systems	75
Yousif Ali Hussin	

Part III Modelling and Monitoring

Spatial Modeling of Transport and Resources Accessibility for Protecting Forest Ecosystems Against Forest Fires	99
Abdullah Emin Akay, Ekaterina S. Podolskaia, and Burak Aricak	

Assessment of Forest Aboveground Biomass Estimation from SuperView-1 Satellite Image Using Machine Learning Approaches	115
Nurul Ain Mohd Zaki, Azinuddin Mohd Asri, Nur Ilyani Mohd Zulkiflee, Zulkiflee Abd Latif, Tajul Rosli Razak, and Mohd Nazip Suratman	

Potential Tree Species Distribution Modelling Using MaxEnt Model for Resource Partitioning in Azad Jammu and Kashmir (AJK), Pakistan . . .	135
Adeel Ahmad, Sajid Rashid Ahmad, and Hammad Gilani	
Application of Remote Sensing Vegetation Indices for Forest Cover Assessments	153
Weeraphart Khunrattanasiri	
Rainforest Assessment in Brunei Darussalam Through Application of Remote Sensing	167
Shafi Noor Islam and Surayah Banu Syed Hussain Haroon Rasheed	
Part IV Remote Sensing of Agricultural Tree Crops	
Rubber Trees and Biomass Estimation Using Remote Sensing Technology	185
Mohd Hasmadi Ismail, Iqbal Putut Ash Shidiq, Mohammad Firuz Ramli, Norizah Kamarudin, Pakhriazad Hassan Zaki, and Rokhmatuloh	
The Use of Landsat TM Imagery for the Application of Rubber Tree Area and Stand Volume Predictive Models in Rubber Plantations in Selangor, Malaysia	215
Mohd Nazip Suratman, Gary Bull, Valerie LeMay, Peter Marshall, and Donald G. Leckie	
Using Historical Disturbance Identified with LandTrendr in Google Earth Engine for Land Cover Mapping of Oil Palm Landscapes	237
Daniel Platt, Reza Azmi, Ahimsa Campos-Arceiz, Michelle Li Ern Ang, Darrel Tiang, Badrul Azhar, Hoong Chen Teo, Simon Jones, and Alex M. Lechner	
Part V Remote Sensing of Mangrove Ecosystems	
Geospatial Technology: Unlocking the Management and Monitoring in Malaysian Mangrove Forests	277
Norizah Kamarudin, Rhyma Purnamasayangsukasih Parman, Zulfa Abdul Wahab, Jamhuri Jamaluddin, and Mohd Hasmadi Ismail	
Effect of Tidal Regime, Relative Sea Level and Wind Intensity on Changes of Mangrove Area Using Remote Sensing Approach	289
Noorita Sahrman, Arnis Asmat, Fazlina Ahmat Ruslan, Ismail Maarof, and Abd Manan Samad	

Spatiotemporal Distribution of Mangrove at Kuala Sepetang Forest Reserve, Malaysia, Using Remotely Sensed Data	305
Zulkiflee Abd Latif, Nuraisah Anuar, Nurul Ain Mohd Zaki, Hamdan Omar, Mohd Nazip Suratman, and Biswajeet Pradhan	
 Part VI Remote Sensing of Urban Forestry	
Determination of the Effect of Urban Forests and Other Green Areas on Surface Temperature in Antalya	319
Mehmet Cetin, Fatih Adiguzel, and ilknur Zeren Cetin	
Conceptualising the Citizen-Driven Urban Forest Framework to Improve Local Climate Condition: Geospatial Data Fusion and Numerical Simulation	337
Siti Aekbal Salleh, Zulkiflee Abd. Latif, Faezah Pardi, Emad Mushtaha, and Yarina Ahmad	
 Part VII Remote Sensing of Forest Engineering and Restoration	
State of the Art on Airborne LiDAR Applications in the Field of Forest Engineering	357
Burak Aricak, Michael G. Wing, and Abdullah E. Akay	
Restoration of Damaged Forest and Roles of Remote Sensing	371
Kyungil Lee, Jieun Ryu, and Seung Hee Kim	
Recent Advances in UAV-Based Structure-from-Motion Photogrammetry for Aboveground Biomass and Carbon Storage Estimations in Forestry	395
Sercan Gülci, Abdullah Emin Akay, Burak Aricak, and Temel Sariyildiz	
 Part VIII Hyperspectral and Multi Source Remote Sensing	
Hyperspectral Identification of Selected Dipterocarp Montane at the Species Level	413
Nisfariza Mohd Noor	
Tree Biophysical Parameter Retrieval from Multi-source Remote Sensing Data Fusion	435
Nafisah Khalid, Noraain Mohamed Saraf, Juazer Rizal Abdul Hamid, and Zulkiflee Abd. Latif	
 Index	 453

Editor and Contributors

About the Editor



Mohd Nazip Suratman is a Professor of Forestry at the Faculty of Applied Sciences and a Principal Fellow at the Institute for Biodiversity and Sustainable Development, Universiti Teknologi MARA (UiTM), Malaysia. He earned a B.Sc. in Forestry from Universiti Putra Malaysia (UPM) and an M.S. from the University of Nebraska-Lincoln (UNL), USA. He was then honoured with a prestigious fellowship from the Canadian Commonwealth to pursue a Ph.D. degree at the University of British Columbia (UBC), Canada, where he worked on the application of remote sensing for sustainable forest management. He has been involved in numerous collaborative international research projects that led to publications in reputable journals. Altogether, he has published a total of 15 books and more than 200 research publications. His research interests cover several aspects across forestry, mainly on forest modelling, forest ecology and biodiversity. He received the UiTM's Best Researcher and Top Talent Awards in 2015 and 2021, respectively. He served as the Deputy Vice-Chancellor (Research and Innovation) from 2018 to 2021.

Contributors

Zulkiflee Abd. Latif Institute for Biodiversity and Sustainable Development, Universiti Teknologi MARA, Shah Alam, Malaysia
Centre of Studies for Surveying Science and Geomatics, Faculty of Architecture Planning and Surveying, Universiti Teknologi MARA, Shah Alam, Malaysia

Juazer Rizal Abdul Hamid Centre of Studies for Surveying Science and Geomatics, Faculty of Architecture Planning and Surveying, Universiti Teknologi MARA, Shah Alam, Malaysia

Khairul Nizam Abdul Maulud Earth Observation Centre, Institute of Climate Change, Universiti Kebangsaan Malaysia, Bangi, Selangor, Malaysia
Department of Civil Engineering, Faculty of Engineering and Built Environment, Universiti Kebangsaan Malaysia, Bangi, Selangor, Malaysia

Zulfa Abdul Wahab Department of Forestry Science and Biodiversity, Faculty of Forestry and Environment, Universiti Putra Malaysia, Serdang, Selangor, Malaysia

Fatih Adiguzel Faculty of Arts and Sciences, Department of Geography, Nevsehir Haci Bektas Veli University, Nevsehir, Turkey

Esmael Adrah Earth Observation Centre, Institute of Climate Change, Universiti Kebangsaan Malaysia, Bangi, Selangor, Malaysia

Adeel Ahmad College of Earth and Environmental Sciences, University of the Punjab, Lahore, Pakistan
Department of Geography, University of the Punjab, Lahore, Pakistan

Sajid Rashid Ahmad College of Earth and Environmental Sciences, University of the Punjab, Lahore, Pakistan

Yarina Ahmad Institute for Biodiversity and Sustainable Development, Universiti Teknologi MARA, Shah Alam, Malaysia
Faculty of Administrative Science and Policy Studies, Universiti Teknologi MARA, Shah Alam, Malaysia

Fazlina Ahmat Ruslan Centre of Studies for Surveying Science and Geomatics, Faculty of Architecture, Planning and Surveying, Universiti Teknologi MARA, Shah Alam, Selangor, Malaysia
School of Electrical Engineering, College of Engineering Studies, Universiti Teknologi MARA, Shah Alam, Selangor Darul Ehsan, Malaysia

Abdullah Emin Akay Faculty of Forestry, Forest Engineering Department, Bursa Technical University, Bursa, Turkey

Michelle Li Ern Ang School of Environmental and Geographical Sciences, University of Nottingham Malaysia, Semenyih, Malaysia

Nuraisah Anuar Centre of Studies for Surveying Science and Geomatics, Faculty of Architecture, Planning and Surveying, Universiti Teknologi MARA, Shah Alam, Selangor Darul Ehsan, Malaysia

Burak Aricak Faculty of Forestry, Forest Engineering Department, Bursa Technical University, Bursa, Turkey

Nazlin Asari Faculty of Applied Sciences, Universiti Teknologi MARA, Shah Alam, Malaysia

Iqbal Putut Ash Shidiq Department of Geography, Faculty of Mathematics and Natural Sciences, University of Indonesia, Depok City, West Java, Indonesia

Arnis Asmat Faculty of Applied Sciences, Universiti Teknologi MARA, Shah Alama, Malaysia

Badrul Azhar Department of Forestry Science and Biodiversity, Faculty of Forestry and Environment, Universiti Putra Malaysia, Serdang, Selangor Malaysia and Institute of Tropical Forestry and Forest Products, Universiti Putra Malaysia, Serdang, Selangor, Malaysia

Reza Azmi Wild Asia, Kuala Lumpur, Malaysia

Gary Bull Department of Forest Resources Management, Faculty of Forestry, University of British Columbia, Vancouver, BC, Canada

Ahimsa Campos-Arceiz Southeast Asia Biodiversity Research Institute, Chinese Academy of Sciences and Center for Integrative Conservation, Xishuangbanna Tropical Botanical Garden, Chinese Academy of Sciences, Mengla, Yunnan, China

Mehmet Cetin Faculty of Architecture, Department of City and Regional Planning, Ondokuz Mayıs University, Samsun, Turkey
Faculty of Engineering and Architecture, Department of Landscape Architecture, Kastamonu University, Kastamonu, Turkey

Dzaeman Dzulkiffi Tropical Rainforest Conservation and Research Centre, Kuala Lumpur, Malaysia

Hammad Gilani Department of Space Science, Institute of Space Technology, Islamabad, Pakistan

Sercan Gülcü Faculty of Forestry, Forest Engineering Department, Kahramanmaraş Sütçü İmam University, Kahramanmaraş, Turkey
Faculty of Forestry, Forest Engineering Department, Bursa Technical University, Bursa, Turkey

Yousif Ali Hussin Department of Natural Resources, Faculty of Geo-information Science and Earth Observation, University of Twente, Enschede, The Netherlands

Shafi Noor Islam Department of Geographical and Environmental Studies, Faculty of Arts and Social Sciences (FASS), Universiti Brunei Darussalam, Jalan Tungku Link, Bandar Seri Begawan, Brunei Darussalam

Mohd Hasmadi Ismail Department of Forestry Science and Biodiversity, Faculty of Forestry and Environment, Universiti Putra Malaysia, Serdang, Selangor, Malaysia

Jamhuri Jamaluddin Department of Forestry Science and Biodiversity, Faculty of Forestry and Environment, Universiti Putra Malaysia, Serdang, Selangor, Malaysia

Simon Jones School of Mathematical and Geospatial Sciences, RMIT University, Melbourne, VIC, Australia

Norizah Kamarudin Department of Forestry Science and Biodiversity, Faculty of Forestry and Environment, Universiti Putra Malaysia, Serdang, Selangor, Malaysia
Institute of Tropical Forestry and Forest Products, Universiti Putra Malaysia, Serdang, Selangor, Malaysia

Nafisah Khalid Centre of Studies for Surveying Science and Geomatics, Faculty of Architecture Planning and Surveying, Universiti Teknologi MARA, Shah Alam, Malaysia

Seung Hee Kim Schmid College of Science and Technology, Chapman University, Orange, CA, USA

Weeraphart Khunrattanasiri Department of Forest Management, Faculty of Forestry, Kasetsart University, Bangkok, Thailand

Alex M. Lechner School of Environmental and Geographical Sciences, University of Nottingham Malaysia, Semenyih, Malaysia
Monash University Indonesia, Tangerang, Banten, Indonesia

Donald G. Leckie Pacific Forestry Centre, Canadian Forest Service, Victoria, BC, Canada

Kyungil Lee AI Semiconductor Research Center, Seoul National University of Science and Technology, Nowon-gu, Seoul, Republic of Korea

Valerie LeMay Department of Forest Resources Management, Faculty of Forestry, University of British Columbia, Vancouver, BC, Canada

Ismail Maarof Centre of Studies for Surveying Science and Geomatics, Faculty of Architecture, Planning and Surveying, Universiti Teknologi MARA, Shah Alam, Selangor, Malaysia

Mohd Rizaludin Mahmud Geoscience & Digital Earth Centre, Faculty of Built Environment & Surveying, Universiti Teknologi Malaysia, Skudai, Johor, Malaysia

Peter Marshall Department of Forest Resources Management, Faculty of Forestry, University of British Columbia, Vancouver, BC, Canada

Siti Munirah Mazlan Earth Observation Centre, Institute of Climate Change, Universiti Kebangsaan Malaysia, Bangi, Selangor, Malaysia

Noraain Mohamed Saraf Centre of Studies for Surveying Science and Geomatics, Faculty of Architecture Planning and Surveying, Universiti Teknologi MARA, Shah Alam, Malaysia

Azinuddin Mohd Asri Centre of Studies for Surveying Science and Geomatics, Faculty of Architecture, Planning and Surveying, Universiti Teknologi MARA, Cawangan Perlis, Arau, Perlis, Malaysia

Norzalyta Mohd Ghazali Faculty of Science and Technology, Universiti Kebangsaan Malaysia, Bangi, Selangor, Malaysia

Nisfariza Mohd Noor Department of Geography, Faculty of Arts and Social Sciences, University Malaya, Kuala Lumpur, Malaysia

Nurul Ain Mohd Zaki Centre of Studies for Surveying Science and Geomatics, Faculty of Architecture, Planning and Surveying, Universiti Teknologi MARA, Perlis Branch, Arau, Perlis, Malaysia

Institute for Biodiversity and Sustainable Development (IBSD), Universiti Teknologi MARA, Shah Alam, Selangor, Malaysia

Nur Ilyani Mohd Zulkiflee Centre of Studies for Surveying Science and Geomatics, Faculty of Architecture, Planning and Surveying, Universiti Teknologi MARA, Cawangan Perlis, Arau, Perlis, Malaysia

Ahmad Farid Mohsin Faculty of Applied Sciences, Universiti Teknologi MARA, Shah Alam, Malaysia

Aisyah Marliza Muhammad Kamarulzaman Earth Observation Centre, Institute of Climate Change, Universiti Kebangsaan Malaysia, Bangi, Selangor, Malaysia

Emad Mushtaha Department of Architectural Engineering, University of Sharjah, Sharjah, United Arab Emirates

Hamdan Omar Geoinformation Programme, Division of Forestry and Environment, Forest Research Institute Malaysia (FRIM), Kepong, Selangor, Malaysia

Faezah Pardi Institute for Biodiversity and Sustainable Development, Universiti Teknologi MARA, Shah Alam, Malaysia
Faculty of Applied Science, Universiti Teknologi MARA, Shah Alam, Malaysia

Rhyma Purnamasayangasukasih Parman Department of Forestry Science and Biodiversity, Faculty of Forestry and Environment, Universiti Putra Malaysia, Serdang, Selangor, Malaysia

Daniel Platt School of Environmental and Geographical Sciences, University of Nottingham Malaysia, Semenyih, Malaysia

Ekaterina S. Podolskaia Laboratory of Forest Ecosystems Monitoring, Centre for Forest Ecology and Productivity of the Russian Academy of Sciences, Moscow, Russian Federation

Biswajeet Pradhan School of Civil and Environmental Engineering, University of Technology Sydney, Ultimo, NSW, Australia

Mohammad Firuz Ramli Department of Environment, Faculty of Forestry and Environment, Universiti Putra Malaysia, Serdang, Selangor, Malaysia

Tajul Rosli Razak Faculty of Computer and Mathematical Science, Universiti Teknologi MARA, Cawangan Perlis, Arau, Perlis, Malaysia

Rokhmatuloh Department of Geography, Faculty of Mathematics and Natural Sciences, University of Indonesia, Depok City, West Java, Indonesia

Jieun Ryu Inchoen Climate and Environment Research Center, Yeonsu-gu, Incheon, Republic of Korea

Siti Nor Maizah Saad Earth Observation Centre, Institute of Climate Change, Universiti Kebangsaan Malaysia, Bangi, Selangor
Malaysia and Universiti Teknologi MARA, Cawangan Perlis, Arau, Perlis, Malaysia

Noorita Sahrman Centre of Studies for Surveying Science and Geomatics, Faculty of Architecture, Planning and Surveying, Universiti Teknologi MARA, Shah Alam, Selangor, Malaysia

Siti Aekbal Salleh Institute for Biodiversity and Sustainable Development, Universiti Teknologi MARA, Shah Alam, Malaysia
Faculty of Architecture Planning and Surveying, Universiti Teknologi MARA, Shah Alam, Malaysia

Abd Manan Samad Centre of Studies for Surveying Science and Geomatics, Faculty of Architecture, Planning and Surveying, Universiti Teknologi MARA, Shah Alam, Selangor, Malaysia

Temel Sariyildiz Faculty of Forestry, Forest Engineering Department, Bursa Technical University, Bursa, Turkey

Mohd Nazip Suratman Faculty of Applied Sciences and Institute for Biodiversity and Sustainable Development, Universiti Teknologi MARA (UiTM), Shah Alam, Malaysia

Surayah Banu Syed Hussain Haroon Rasheed Department of Geographical and Environmental Studies, Faculty of Arts and Social Sciences (FASS), Universiti Brunei Darussalam, Jalan Tungku Link, Bandar Seri Begawan, Brunei Darussalam

Yit Arn Teh The School of Natural and Environmental Sciences of Newcastle University, Newcastle upon Tyne, UK

Tengku Mohd Zarawie Tengku Hashim Faculty of Applied Sciences, Universiti Teknologi MARA, Shah Alam, Malaysia

Hoong Chen Teo Department of Biological Sciences, National University of Singapore, Singapore, Singapore

Darrel Tiang School of Environmental and Geographical Sciences, University of Nottingham Malaysia, Semenyih, Malaysia

Wan Shafrina Wan Mohd Jaafar Earth Observation Centre, Institute of Climate Change, Universiti Kebangsaan Malaysia, Bangi, Selangor, Malaysia

Michael G. Wing Forest Engineering, Resources and Management Department, College of Forestry, Oregon State University, Corvallis, OR, USA

Pakhriazad Hassan Zaki Department of Forestry Science and Biodiversity, Faculty of Forestry and Environment, Universiti Putra Malaysia, Serdang, Selangor, Malaysia

ilknur Zeren Cetin Department of Park and Garden Plants, Program of Landscape and Ornamental Plants Cultivation, Samsun Vocational School, Ondokuz Mayıs University, Samsun, Turkey
Department of Forest Engineering, YOK 100/2000 Scholarship, Program of Sustainable Forestry, Institute of Graduate School, Bartin University, Bartin, Turkey

Part I

Introduction



Remote Sensing for Forest Inventory and Resource Assessment

Mohd Nazip Suratman, Zulkiflee Abd. Latiff,
Tengku Mohd Zarawie Tengku Hashim, Ahmad Farid Mohsin,
Nazlin Asari, and Nurul Ain Mohd Zaki

Abstract

There are multiple purposes of conducting forest inventories and forest resource assessment. One of them is to serve as information on the development of forest planning and management strategy which requires gathering of data about forest resources at the national level for the development of strategic policy. In order to characterise accurately both quantity and quality of the forest resources, enhanced information is required. Remote sensing technology offers potential gains in inventory efficiency based on its ability to quantitatively characterise stand canopies through spectral reflectance. Also, the frequency with which remote sensing data are acquired, and the availability of data for extensive areas,

M. N. Suratman (✉)

Faculty of Applied Sciences and Institute for Biodiversity and Sustainable Development, Universiti Teknologi MARA (UiTM), Shah Alam, Malaysia
e-mail: nazip@uitm.edu.my

Z. Abd. Latiff

Institute for Biodiversity and Sustainable Development (IBSD), Universiti Teknologi MARA (UiTM), Shah Alam, Selangor, Malaysia

Faculty of Architecture, Planning and Surveying, Universiti Teknologi MARA (UiTM), Shah Alam, Selangor, Malaysia

T. M. Z. Tengku Hashim · A. F. Mohsin · N. Asari

Faculty of Applied Sciences, Universiti Teknologi MARA (UiTM), Shah Alam, Selangor, Malaysia

N. A. Mohd Zaki

Institute for Biodiversity and Sustainable Development (IBSD), Universiti Teknologi MARA (UiTM), Shah Alam, Selangor, Malaysia

Centre of Studies for Surveying Science and Geomatics, Faculty of Architecture, Planning and Surveying, Universiti Teknologi MARA, Perlis Branch, Arau, Perlis, Malaysia

increases the attractiveness of these data for inventory purposes. For example, visible, near-, and mid-infrared radiance measurements, which are routinely available from the optical remotely sensed imagery, could be related to forest parameters and stand attributes such as biomass, basal area, diameter, stand age, and wood volume. The need for effective inventories for forest resources is the impetus for this chapter into reviewing traditional methods of ground-based surveys with information from satellite remote sensing. In addition, this chapter discusses the development of remote sensing sensors, which include their characteristics, applications, current practices, and future development of the remote sensor.

Keywords

Remote sensing · Forest inventory · Sampling design

1 Introduction

Forest inventory refers to the estimation by sampling of an area of a forest in its entirety or split up into forest types (Hildebrant 1989). In the planning phase of a forest inventory, it is necessary to define assessment units. For example, for a national forest inventory, the state or region could be the unit of assessment, while for a local inventory, the unit of assessment could be the stand or forest estate. A map or any form of remotely sensed imagery (e.g. aerial photographs, satellite, or radar imageries) can be utilised to delineate these units and obtain preliminary information. By means of these tools, the area can be stratified into several forest types and the variables of interest can be estimated precisely.

In many countries throughout the world, the issue of information requirements for forest resource management, conservation, and development at national and state levels has received much attention. Over the last decade, demand for more and better forestry information has continued to grow. There are many shortcomings regarding the method and efficiency of data collections required for planning the development of strategies within the forest sector at national and state levels. Remote sensing technology offers potential gains in inventory efficiency based on its ability to quantitatively characterise stand canopies through spectral reflectance (Ahern et al. 1991; Lillesand and Kiefer 2000). In addition, the frequency with which remote sensing data are acquired, and the availability of data for extensive areas, increases the attractiveness of these data for inventory purposes. Therefore, the need for effective inventories for forest resources was the impetus for this introductory chapter into reviewing the applications of remote sensing as a tool in providing information by linking ground information with satellite data.

2 Inventory and Sampling Design

Sampling design is of great importance for forest inventory and monitoring to ensure efficient data collection as measured by cost and reliability (IUFRO 1994). In applying any sampling method, it is essential to clearly define the population of interest. Freese (1962) and Cochran (1977) considered the population as the aggregate of units from which the sample is chosen. For example, if the sample is taken with plots, the population should be defined in terms of the plots.

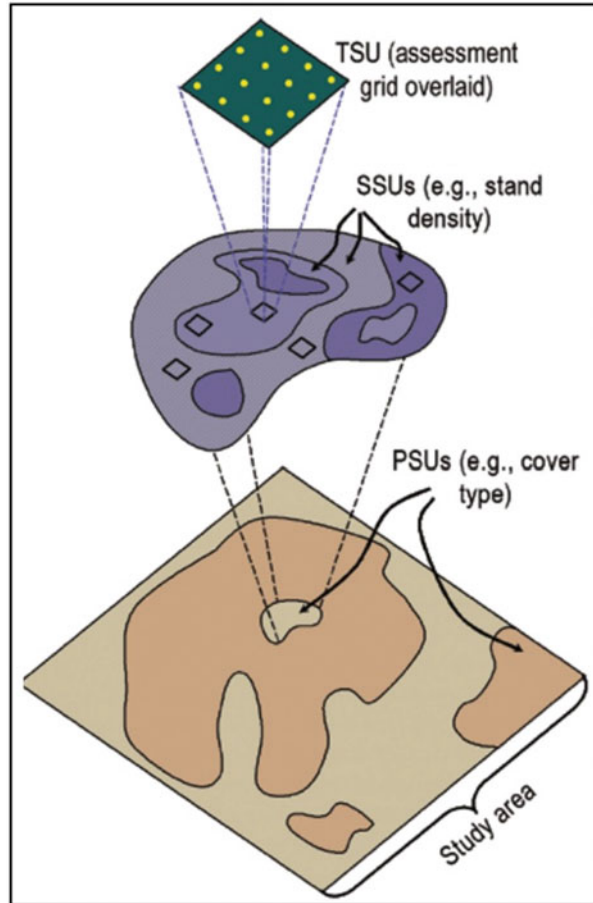
There are several sampling methods that can be applied to forest inventories. However, before considering the design, major information needs should be clarified. According to IUFRO (1994), the selection of the most appropriate sampling methods depends on (1) the objectives of the inventory, (2) the cost involved, (3) the extent of the area, (4) the forest types (whether only one or several), and (5) the availability of remotely sensed imagery.

In each sampling method, the sampling unit may be randomly or systematically selected. For example, in simple random sampling (SRS), the selection of sampling units from the population is such that every combination of n units has an equal chance of being selected (Freese 1962; Cochran 1977). In systematic sampling, sampling units are selected according to regular system. SRS yields unbiased estimates of the parameter of interest and allows estimation of the sampling error, which is a measure of precision of the estimate. The selection of the sampling units can be done with or without replacement (LeMay and Marshall 1990). In the former sampling process, a unit may appear in the sample more than once and in the latter a unit may appear in the sample only once. Sampling without replacement is used most frequently, since it is more precise than sampling with replacement (LeMay and Marshall 1990).

If sampling involves a subdivision of a forest area into smaller areas with more homogeneous characteristics, the method involves some form of stratified sampling. If the sampling units are selected randomly within each stratum, the method is called stratified random sampling (STRS). According to LeMay and Marshall (1990), STRS can be used effectively if (1) the separated strata are more homogeneous than the population, (2) the sizes of strata are known prior to sampling, (3) a sampling frame is available, and (4) one is interested in estimating parameters for the various strata. The greater the difference among stratum means, the greater the advantage to using STRS rather than SRS (Bickford 1961).

In some cases, it may be costly or impractical to select sample size using these methods. For example, if the distance between sample units is large, and time and cost are limiting factors, the sampling units can be aggregated into a number of mutually exclusive groups or clusters. This method of sampling is called cluster sampling (Frayer 1981) and is used if there is interest in getting proper interval estimates for the average element value within a cluster. However, if the units of assessment are large, clusters may be subdivided into units of hierarchical order, which constitutes multilevel sampling designs. As the name implies, this design uses more than one source of information in the estimation of population parameters (Frayer 1981). These sources generally, but not necessarily, involve one or more

Fig. 1 Sampling unit in multistage sampling; PSUs represents primary sampling units, SSUs is the secondary sampling units, and TSUs is the tertiary sampling units (Hamilton et al. 2010)



types of remotely sensed imagery and ground measurements (Kohl and Kushwaha 1994).

Multilevel sampling may be classified into multistage sampling and multiphase sampling (Kohl and Kushwaha 1994). Multistage sampling designs are based on dividing the population into subunits (Fig. 1). The first subset can be called primary sampling units (PSUs). Next, a subset of PSUs is selected and subdivided into secondary sampling units (SSUs) (Hamilton et al. 2010). Similarly, according to IUFRO (1994), in multistage sampling, the first stage can be divided into a secondary one, and the secondary stage can be divided into a tertiary one, and so forth. At each stage, different selection methods can be applied. On the other hand, multiphase sampling analyses information from every level. The variables of interest are derived from data from the lowest level. In multistage sampling the units are partitioned into smaller units at each succeeding stage. For multiphase sampling, the unit size remains the same, independent of the number of phases of information used. A first phase unit is the same as a second phase unit, and so on. According to Kohl and

Kushwaha (1994) the design must be such that the auxiliary variables are less expensive to derive than the variables of interest, and remote sensing is the ideal method for such purposes.

There are two types of multiphase sampling designs. They are known as multiphase sampling with regression estimators and multiphase sampling for stratification. In the first type, the relationship between the auxiliary variables and the variable of interest is described by means of regression. According to Kohl and Sutter (1991) this approach has repeatedly proved its worth in temperate latitudes. Bowden et al. (1979) and LaBau and Schreuder (1983) gave an overview of this method for large-scale inventories employing satellite data. In the second type, the auxiliary variable is not determined through the measurements; instead, it is an indicator variable showing the stratum to which the variable of interest is to be allocated (Kohl and Kushwaha 1994). In this method, volumes determined through a field survey in the last phase are weighted according to estimated strata sizes.

Double sampling is a commonly applied form of multiphase sampling, limited to two phases. Several authors reported this sampling method to be very efficient in terms of cost and precision of the estimate when applied in either temperate or tropical forests (Bickford et al. 1963; Hutchinson 1978; Temu 1981; Temu and Phillip 1981). More complex designs such as three and four stage methods have also been applied (Kohl and Kushwaha 1994).

There are two broad categories of sample plots, namely, permanent and temporary sample plots. The selection of type of sample plots to be adopted in forest inventory depending on the objectives of the inventory and the type of vegetation. Permanent sample plots are used when it involves measuring changes over a number of years, for example, measurement of changes in tree diameter growth, biomass, and carbon stocks in natural forests, in forest plantations, and in agroforestry settings. In temporary sample plots, measurements are made and the field data required for a given year. Suratman et al. (2004) and Asari et al. (2017) used temporary sample plots by establishing circular fixed plots based on the systematic sampling system with a random start (Fig. 2) to study the stand volume of rubber plantations and carbon stocks of oil palm plantations in Selangor, Malaysia, respectively. The values of radius of the circular plot and the distances between plots depend on the area and densities of the vegetation. Circular plots were established in each stand and the mean for stand variables was computed and used to represent the entire stand.

As seen from the review presented in this section, many sampling techniques have been applied in the inventory of natural resources. It is also possible to combine those techniques, creating more complex sampling designs. However, if a simpler technique will achieve the inventory objectives, it should be used in place of a more complex design. Multilevel sampling techniques have many applications and may become more efficient with the introduction of higher-resolution satellite and airborne imagery.

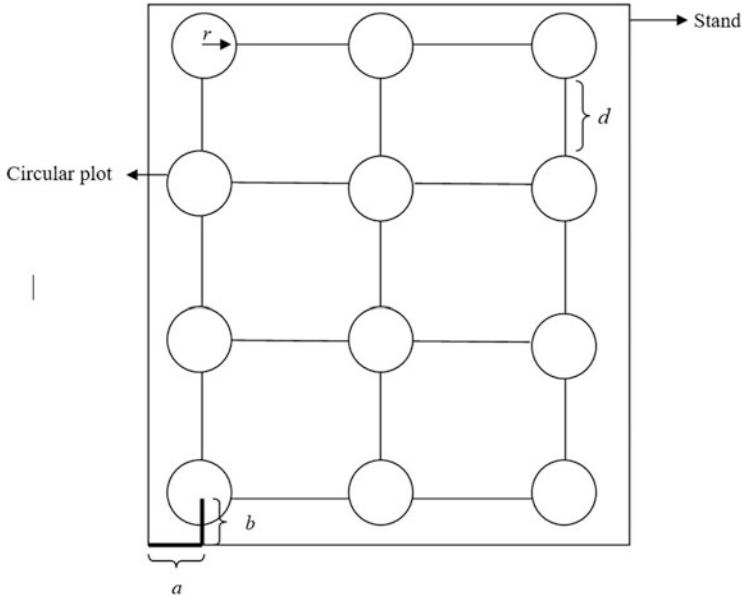


Fig. 2 Circular fixed plots in systematic sampling design; r represents the radius of the circular plot, d is the distance between circular plots and a and b are the random starting points (Asari 2017)

3 Tree Crop Inventory and Assessments

Considering its essential role in good forest management, tree crop assessment rarely receives the priority it deserves. For example, in the forest resource assessment (FRA) programme of the FAO, data on tree crops are not systematically recorded despite the fact that they have been identified as an essential element of sustainable forest management (FAO 1995). Reviews of inventory work in Kenya and India described below provide some insights on the assessment of specific tree crops in tropical areas.

In an agroforestry woody biomass survey in Kenya, Holmgren et al. (1994) used a two-phase sampling method. The first phase consisted of aerial photographs and the second was field measurements in a subsample of the photos. The survey, which covered 10 million ha where 80% of the country's population lives, revealed a rapid increase in planted woody biomass between 1986 and 1992. The average standing volume on farms was estimated to be $16.4 \text{ m}^3/\text{ha}$, of which 25% was planted and the remainder was natural woodland, including riverside areas. When calculated by district, the average standing volume of woody material outside of forests was estimated to be $4.7\text{--}36.2 \text{ m}^3/\text{ha}$. This study challenged some of the pessimistic opinions on land-use development and a fuel wood gap. Holmgren et al. also found that land degradation was not directly related to rapid population growth

and that Kenyan farmers seem to be applying wise and sustainable management practices on their holdings.

In India, two-stage stratified sampling was adopted for the inventory of trees outside of forests in 1992. The sampling unit in the first stage was a district, and the second stage was the village. The study was conducted by the Forest Survey of India with the purpose of assessing the extent of different tree crop components established by different agencies. Planted trees were classified into eight categories: farm forestry, village woodlot, block plantation, road, pond, rail, and canal side plantations and others. Standing trees in selected villages were enumerated and compilation and data processing was done at the district level. The inventory was completed for the State of Haryana in 1997. The total non-forest area and standing volume was estimated to be 4.4 million ha and 10.3 million m³, respectively. The study revealed that farm forestry contributes about 41% of the estimated total standing volume of wood in non-forest areas, followed by village woodlot (23%), roadside plantations (13%), and block plantations (11%) (FSI 1997).

4 Developments in Remote Sensing Technologies

Remote sensing has been used for many decades. An early practical application was aerial reconnaissance during the First World War. For example, aerial photography allowed the positions of the opposing armies to be monitored over wide areas more safely than a ground-based survey (USGS 2000). Aerial photographs also allowed for rapid and relatively accurate updates of military maps and strategic positions. Today, remote sensing is heavily utilised in environmental management. In comparison with traditional aerial photography, medium-resolution satellite imagery has the following advantages: (1) the frequency of data collection, (2) global availability of remote sensing data, (3) data being suitable for digital analysis and classification, and (4) data being gathered at relatively low cost (Wilkie and Finn 1996).

Remote sensing also has many advantages over ground-based surveys in that large land areas can be surveyed at one time, and areas of land or sea can be included that are otherwise inaccessible (Keiner and Yah 1998; Guidon and Edmonds 2002). The advent of satellite technology and multispectral sensors has further enhanced this capability, with the ability to capture images of very large areas of land in one pass, and by collecting environmental data that normally would not be visible to the human eye (Kushwaha 1987). Remote sensing can reduce cost and improve efficiency of forest inventories if remotely sensed data are well correlated with important field measurements, are available when needed in the sampling design (Czaplewski 1999), and cover large areas (Lindgren 1985).

On the other hand, remote sensing has limitations that prevent it from totally replacing ground-based survey methods. These are partly related to spatial, spectral, and temporal resolutions of the various sensors. Also, there are problems with the all-weather capabilities (see Table 1), data analysis, and data interpretations. Also, not all important information is related to the electromagnetic spectrum. In this respect, remotely sensed data should be considered as a complementary source of

Table 1 Characteristics of selected remote sensing sensor systems

Sensor	Spatial resolution	Image swath	Temporal resolution	Status as of August 2014	Potential uses
Landsat TM	30 m	185 × 185 km	16 days	End of operation	Mapping Stratification
Landsat ETM+ ^a	30 m	185 × 185 km	16 days	Operational	Mapping Stratification
SPOT 1–5 ^b	2.5–20 m	60 × 60 km	3–5 days	1, 3—end of operation 2, 4, 5—operational	Mapping Stratification
MODIS ^c	250–1000 m	2330 × 10 km	1–2 days	Operational	Mapping Stratification
AVHRR ^d	1000 m	2400 × 6400 km	1 day	Operational	Mapping Stratification
IKONOS ^e	1–4 m	11 × 11 km	3–5 days	Operational	Sampling Mapping Stratification
QuickBird	0.6–2.4 m	16.5 × 16.5 km	1–3.5 days	Operational	Sampling Mapping Stratification
ASTER ^f	15–90 m	60 × 60 km	16 days	Operational	Mapping Stratification
Hyperion	30 m	7.5 × 100 km	16 days	Operational	Mapping Stratification
ALOS PALSAR 1, 2 ^g	10 m	70 km	2 days	1—end of operation 2—operational	Mapping Stratification

Notes

^aLandsat Enhanced Thematic Mapper Plus^bSatellite Pour l'Observation de la Terre or Earth-Observing Satellites^cModerate-Resolution Imaging Spectroradiometer^dAdvanced Very High Resolution Radiometer^eIkon Observing Satellite^fAdvanced Spaceborne Thermal Emission and Reflection Radiometer^gAdvanced Land Observing Satellite-Phased Array L-band Synthetic Aperture Radar

Source: Lillesand and Kiefer (2000)

information, rather than a substitute for ground-based data gathering. However, the insight that it provides into the environmental status and processes is valuable.

Aerial photographs have been used routinely in forestry since the 1950s and have played a key role in forest mapping and inventory systems up to the present (Aldrich 1979; Leckie and Gillis 1995). Today, other remote sensing technologies have improved capability and resolution and are conducted using satellites or aircraft platforms and a variety of sensors.

The pixel sizes of selected operational sensor systems are compared in Fig. 3. The first earth resource technology satellite (ERTS-1 or Landsat 1), with an MSS, was

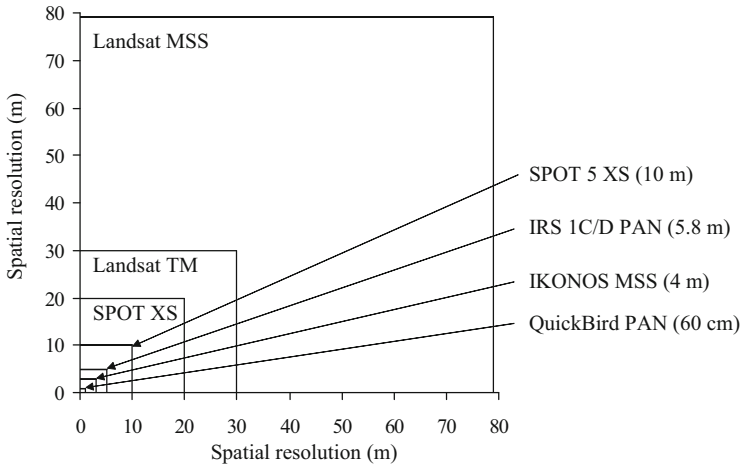


Fig. 3 Illustration of various sensor systems with respect to their spatial resolution (redrawn and from Kätsch and Vogt 1999 (revised))

launched in 1972 and had a resolution of 79×79 m with four spectral bands. Ten years later, it was improved with the addition of Landsat TM imagery. Landsat TM on Landsat 4 improved the resolution to 30 m and covered a wide range of the electromagnetic spectrum with seven bands, including thermal band and two mid-infrared bands. Together, Landsat series permit a retrospective image interpretation possible back to 1972 (IUFRO 1994).

The SPOT satellite was launched in 1986 and has a 20 m spatial resolution for multispectral and 10 m for panchromatic modes. SPOT with panchromatic, visible, and near-infrared bands is useful for vegetation studies including health assessments. By 1995, images with 5.8 m resolution were available from the IRS satellite (Lillesand and Kiefer 2000).

Canada's RADARSAT, which was launched in 1995, represents an operational spaceborne active sensor technology (Table 2). In this system, the target area on the ground is scanned by microwave radiation. The reflected and back-scattered radiation then provides information about the surface, sub-surface, physical, and dielectric properties (Leckie 1998). Microwave sensors have the highly advantageous properties of operating independently of sun illumination and are usually insensitive to weather conditions or cloud cover. These characteristics are particularly suitable to monitoring phenomena in the tropic regions (Thompson et al. 1993; Toan 1995; Salas et al. 2002), although the full capability of radar has yet to be exploited (Leckie 1998).

The first commercial imaging satellite (IKONOS) was launched in September 1999 from the Vandenberg Air Force Base, California. This satellite provides 1-m resolution panchromatic images and 4-m multispectral images (Lidov 1999). Test images from IKONOS prove the superior quality of the new system (Baltasvias et al. 2001). Many of the newly launched sensor systems feature high spatial geometric

Table 2 A selection of various previous and currently operational sensor platforms

Sensor	Country	Year of launch	Type of sensor	Spatial resolution (m)	Stereo capability
RADARSAT	Canada	1995	SAR ^a	28 × 25 10 × 9	
SUNSAT ^b	South Africa	1999	MSS	15	Yes
QuickBird	USA	2001	PAN ^c / MSS	0.6/2.44	
IKONOS 2	USA	1999	PAN/MSS	1.0/4.0	Yes
SPOT 4	France	1998	PAN/MSS	10/20	Yes
SPOT 5	France	2002	PAN/MSS	2.5/5/10	Yes
Landsat TM 7	USA	1999	PAN/MSS	15/30–60	

Notes

^aSynthetic aperture radar

^bThe sensor has not been active since 2001 due to technical problems

^cPanchromatic

Source: Kättsch and Vogt (1999) (revised)

resolutions in combination with stereo capabilities such as SUNSAT, IKONOS, SPOT 4, and SPOT 5 (Table 2). These characteristics will make images suitable for the application of traditional photogrammetric techniques to extract altimetric information, such as a digital elevation model (DEM). Evaluations using IKONOS images are still on-going for studying different topographic terrain and applications; however, recent results in mountainous areas are promising for small area mapping (Toutin and Cheng 2000).

Besides providing with necessary data and information on forest, the latest series of satellite platform also improvise to enhance the accuracies and techniques obtained as compared to the traditional approach. Recently, the new generation of platform shows more advanced sensors. The advancement includes enhancing the prediction of forest biomass, canopy height, and leaf area (Faridah-Hanum et al. 2014). Hyperion, Geoscience Laser Altimeter System (GLAS), GeoEye, and Panchromatic Remote Sensing Instrument for Stereo Mapping (PRISM) are examples of the recent very high-resolution (VHR) remote sensing.

Characterising ground parameters under the cloud cover obstacles is the application advantage of radar-imagery option. The synthetic aperture radar (SAR) systems include Phased Array type L-band Synthetic Aperture Radar (PALSAR), Advanced Synthetic Aperture Radar (ASAR), RADARSAT-1, RADARSAT-2, Japanese Earth Resources Satellite (JERS-1), European Remote Sensing Satellite (ERS-1), and Spaceborne Imaging Radar (SIR-C) (Marco and Kuenzer 2020). The ability of satellite imagery by remotely sensed data to appoint significant issues in forestry has generated strong interests from researchers for a long time. Previous studies also address unique aspects in the advancement of remote sensing of forestry function and traits, which can be grouped into two themes: (1) remote sensing-based estimation and monitoring of plant traits and (2) linking of forest to function and integration into models.

QuickBird is now the highest-resolution commercial remote sensing satellite offering imagery with 60 cm resolution. QuickBird was launched in October 2001 and collects multispectral and panchromatic imagery simultaneously with 16.5×16.5 km swath width at nadir (Euroimage 2002). SPOT 5 was launched from the Guiana Space Centre in Kourou, French Guiana, in May 2002. It offers enhanced capabilities compared to SPOT 4 in terms of improved resolution (up to 2.5 m) and will also be used to create coverage of five continents with digital terrain models. SPOT 6 and 7 were launched on 6 September 12 and 30 June 2014, respectively. Both sensors provide continuity of high-resolution, wide-swath data up to 2024 and carry New Astrosat Optical Modular Instrument (NAOMI) (European Space Agency 2022).

WorldView-1 was the first high-resolution commercial satellite from the WorldView series launched in 2007 with 50 cm resolution. Next in 2009 and 2014, WorldView-2 and WorldView-3 were launched respectively, equipped with 8-band multispectral bands. Most recently, WorldView-4 was launched in 2016 that consists of 31 cm which provided 31 cm panchromatic imagery and 1.23 m multispectral imagery. In Sabah, Malaysia, Mohsin et al. (2021) have used WorldView-2 data to develop predictive model for estimating stand volume of Eucalyptus plantation species and recorded a multiple coefficient of determination (R^2) value of 0.86.

5 Forestry Applications of Remote Sensing in Developing Countries

In developing countries, the use of satellite imagery data as a component in resource inventories and information systems has been reported by many authors (e.g. Lachowski and Dietrich 1978; Wacharakitti and Morain 1978; Aldrich 1979; Lal et al. 1990; Bong 1991; Rao et al. 1991). General conclusions were that remote sensor imagery has proven to be a more authoritative source of data than was formerly possible. For example, the Philippines government believed that its ever-green rainforest cover still accounted for 57% of the land base during the early 1970s, but a remote sensing survey carried out by Lachowski and Dietrich (1978) in 1976 revealed that the actual amount was only 38%. In this survey, the authors used Landsat imagery with support from ground data and considered that the methodology was sufficiently comprehensive for the results to be characterised as accurate within 95% accuracy. A similar example occurred in the early 1970s in Thailand, where the government believed that 48% of the country was under forest cover, largely monsoon deciduous forest. A 1978 Landsat survey revealed that the actual cover amounted to only 25% (Wacharakitti and Morain 1978). In India, the Department of Forestry estimated 23% of land area as forested, but a Landsat survey estimated the amount as less than 10% (Lal et al. 1990).

Inspired by the revealing results reported for the Philippines and Thailand, and motivated by growing evidence of forest depletion in their countries, a good number of other tropical countries have undertaken remote sensing surveys of their tropical

forest cover. In many different countries remote sensing revealed that forest cover was in fact less—often a good deal less—than was previously thought (Malingreau 1986).

Today, many developing countries are involved in the systematic monitoring of renewable resources. Given constraints of time, money, and skilled manpower, countries must evaluate effective methods to obtain reliable and timely resource data. Traditional ground methods are time-consuming and expensive for regional or national resource inventory programmes. Remote sensing from aircraft and satellites has gained worldwide recognition as an efficient method to provide resource information that is often technically and economically feasible compared to ground methods (FAO 1996).

In Malaysia, aerial photography has been used effectively for several decades. The first complete coverage was obtained in 1967 at a 1:25,000 scale with black-and-white panchromatic film (Kamaruzaman and Mohd Rasol 1995). Landsat MSS and TM data have been used for land-use surveys and the results have shown that it is possible to map various natural land-cover types and man-made features, including terrain change, forest areas, soil types, dams, and urban areas (Salleh 1976; Mahmood et al. 1983). However, the resolution of the MSS was found to be unsuitable for mapping Malaysian agricultural land utilisation due to small farm sizes and irregular cropping patterns (Darus 1989). Another study conducted by the ASEAN Institute of Forest Management (AIFM) in 1989 showed that Landsat TM imagery could be used to detect and classify forest disturbances and provide data to update forest resource maps through the integration of remote sensing and a geographic information system (GIS) (Zahriah et al. 1989). Landsat TM has been used to detect deforestation and to identify suitable areas for tourism-related development in Langkawi Island, Malaysia (Kamaruzaman and Mohd Rasol 1995; Kamaruzaman and Hasssan 1996). Another study was conducted by Kamaruzaman and D'Souza (1996) to determine the applicability of SPOT-HRV in the State of Pahang, Malaysia, for detecting logging activities. It was shown that physical features and forest disturbances could be detected by this image.

In Malaysia, the Forestry Department Peninsular Malaysia (FDPM) has begun the application of remote sensing and GIS for forest monitoring since 1986, however mostly focusing on the case studies at specific area. According to Hwai (2006), satellite imagery was used to help stratify the forest in the third National Forest Inventory (NFI) (1990–1992) with close help from the Malaysian Centre of Remote Sensing (MACRES). In the fourth NFI (2000–2002), satellite imagery was further used to map the forested areas. In 1998 onwards, the application of remote sensing imagery was continuously used to determine forest change, forest encroachment and illegal loggings, but at a less real time. With the more advanced technologies developed, the more real time imagery was used from 2006 onwards at which the forest boundaries were corrected using hyperspatial resolution. Meanwhile, the hyperspectral imageries were used at experimental stage to identify tree species and estimate time volume (Hwai 2006).

In 2004, Suratman et al. conducted a study to investigate the relationships between Landsat TM and rubber stand parameters and to develop and evaluate

models for estimating stand volume of rubber plantations. They found statistically significant models for estimating volume of rubber stands with the R^2 values being all higher than 0.70 and standard error of the estimate (SEE) values being lower than 54 m³/ha. In oil palm above-ground biomass (AGB) modelling study conducted by Asari et al. (2017) in Malaysia, they found a non-linear negative trend between AGB and all individual TM bands. Moderate relationships were recorded for AGB and bands 1, 4 and 5 with r values ranging from -0.33 to -0.42 . Meanwhile in Kedah, Malaysia, Tengku Hashim et al. (2020) used Landsat 8 (OLI) data to estimate the carbon stocks in mangroves. They found a positive correlation between field-measured carbon stocks with Landsat 8 individual bands (bands 2–7). The total carbon stocks were estimated to range from 16.88 Mg/ha to 138.20 Mg/ha with an overall mean of 67.29 Mg/ha.

In India, the use of remote sensing goes back over 30 years. The first aerial photographs for forestry purposes were acquired in 1963. Applications of satellite imagery in forestry date back to 1975. The first attempt to assess forest cover in India by satellite imagery interpretation was made in 1984–1985 by the National Remote Sensing Agency (NRSA 1983). This exercise was done visually and resulted in an estimate of the forest cover for the country of 0.64 million km², or 19.5% of the geographical area, in contrast to the previously recorded figure of 22.8% (Rao et al. 1991). The years between 1980 and 1990 were dominated by satellite remote sensing for forest resource assessment, monitoring, wildlife habitat evaluation, and fire damage assessment (Kushwaha 1987). Subsequently, vegetation cover and forest type mapping were done by the Forest Survey of India that involved preparing forest cover maps of 1:250,000 for the entire country, to be repeated every 2 years for monitoring (Kohl and Kushwaha 1994). This project revealed that non-forest areas could generally be mapped with an accuracy of 80–95% in flat undulating areas if the trees were in full foliage. Currently, approximately 70% of India has been covered on a thematic map (FAO 1998).

A FAO/UNDP project helped Myanmar assess forest resources with the use of satellite data from a 1970 Landsat image. This project, which was conducted from 1981 to 1991, provided reliable information on forest resources for about 90% of the area. Since 1991, the country has been conducting field forest inventories every year, covering 2 million ha using remote sensing and GIS technologies (FAO 1998).

In Sri Lanka, forest cover assessment maps using Landsat imagery were produced in 1991–1992. Indicative inventories of non-forest land and detailed periodic inventories of plantations were carried out for assessing resources. A forest resource assessment was done using 1:20,000 aerial photographs for natural forests and 1:10,000 and 1:20,000 for plantations (FAO 1998).

From 1995 to 1997, the Forest Department of Bangladesh completed an inventory programme in hill and coastal forest areas, with the assistance from an international development agency. This was a unique inventory in the sense that a socio-economic survey was also conducted along with the forest inventory to understand the behavioural pattern of the users. Forest statistics were generated with continuous resource change assessments. SPOT-HRV data were used to generate signatures of different types of forest vegetation (FAO 1998).

In some parts of the world, the conversion of mangrove forest into other types of land use (e.g. residential areas, airports, agricultural lands, fishponds, etc.) takes place continuously (Hartono 1994). Satellite imagery data have been used for various mangrove forest analyses and monitoring in many parts of the tropical world. For example, in Bangladesh, computer-processed Landsat data, with additional data from 1:30,000 aerial photographs, permitted two mangrove species to be distinguished with 71% classification accuracy (Heller and Ulliman 1983). SPOT-HRV satellite data have been used for more than 10 years in a mangrove forest analysis. For mapping purposes, SPOT-HRV images have been used in Vietnam (Bong 1991) and in Guinea (Moreau and Vercesi 1989). Monitoring of mangroves has been performed with SPOT-HRV and aerial photographs in East Java (Hartono and Muljosukojo 1990). More recently, SPOT-HRV satellite data were used for mangrove inventory in Cimanuk Delta, West Java, by Hartono (1994). Based on a combination of image analyses, five classes of mangrove vegetation were identified: (1) *Lumnitzera* spp. (2) *Avicennia* spp. (3) *Rhizophora* spp. (4) mixed floristries, and (5) degraded mangrove. In this study, a confusion matrix analysis was performed and an overall 94% classification accuracy was achieved. In other parts of the image, rice fields, villages, home state gardens, rivers, creeks, and irrigation channels were identified.

In Thailand, Landsat MSS images were used in the form of 1:1,000,000 diazo-chrome additive-colour composites and 1:500,000 black-and-white images of bands 4, 5, and 7 and of bands 5 and 7. Together with additional information from the field and from aerial photographs, maps made from the Landsat images were used to determine the total forest cover. Comparing this information with forest cover data either from aerial photographs or Landsat imageries with earlier dates permitted a rough calculation of the reduction of the forest cover over large areas, at a relatively low cost (Morain and Klankamsoon 1978). Miller et al. (1978) utilised Landsat imagery covering the years 1972 through 1977 for determining the expansion of shifting cultivation in northeastern Thailand. Additional information from 1:20,000 to 1:60,000 aerial photographs on shifting cultivation, irrigated rice, hill evergreen forest, and other forest types grouped together was also incorporated. Mapping of the different values of MSS band 7, displayed by assigning grey levels to various levels of difference in tone (scene brightness), permitted detection of shifting cultivation at 1-year intervals. The difference in maps of MSS band 5 was in showing where permanent agriculture was encroaching on the forest.

In Tanzania, remote sensing technology has been applied in the production of forest cover maps and inventories of plantations and natural forests. For example, Sylvander et al. (1988) successfully utilised satellite imagery for delineation of vegetation types in Eastern Tanzania using Landsat MSS false composites at a scale of 1:250,000. Double sampling with aerial photographs for estimating the volume of Miombo woodlands was done by Temu (1981). He found that the method was effective, especially for the areas where access was poor.

This review shows that forest inventories and monitoring work in developing countries makes extensive use of remote sensing data. Area information on forest

types from satellite data mapping has generally been successful, but identification of species has been difficult.

6 Relationship Between Forest Parameters and Remote Sensing Data

Information about forest conditions is essential for forest management planning. Forest management activities require reliable forecasts of the development of all constituent stands in the area being managed. Strategic decisions concerning forest policies to achieve management objectives require accurate information, including stand growth forecasts. In the last decade, many studies have shown that spectral radiance recorded by satellite remote sensing can be related to several forest parameters. Forest inventory studies have found that many tree and stand variables, such as wood volume, biomass, basal area, diameter, and stand age, show strong inverse relationships with red, near-, and mid-infrared bands from Landsat TM and red and near-infrared bands from SPOT (e.g. Horler and Ahern 1986; Danson 1987; Poso et al. 1987; Ripple et al. 1991; Ardö 1992; Brockhaus and Khorram 1992; Nilsson 1997; Suratman et al. 2002, 2004; Asari et al. 2017; Tengku Hashim et al. 2020; Mohsin et al. 2021). Ripple et al. (1991) argued that this was because the understory has a highly reflective shrub and herb layer. Young stands with lower wood volumes have higher radiance in all TM and HRV bands than older stands which have more shadows, thus causing the strong inverse relationships. Table 3 summarises the correlation coefficients (r) between some forest variables and Landsat TM and SPOT-HRV spectral data from various sources.

Studies using the near-infrared band of SPOT and the near- and mid-infrared bands of Landsat TM in Douglas-fir (*Pseudotsuga menziesii*) forests in Oregon have found reflectance and wood volume-related parameters to be well-correlated when using data averaged at the forest-stand scale with correlation values as high as -0.89 (Ripple et al. 1991). Studies that have not involved spatial averaging of data beyond the pixel scale produce relationships between reflectance and wood volume that have much lower r values, especially at higher wood volumes (Franklin 1986; Danson 1987). For example, Franklin (1986) presented a study, which included basal areas exceeding $100 \text{ m}^2/\text{ha}$, that showed a relationship between Landsat reflectance and wood volume with correlation values between -0.38 and -0.54 .

Image classification commonly uses statistical techniques to group pixels into various predefined classes, such as land-cover types, land-use classes, and vegetation types (e.g. Bolstad and Lillesand 1992; Brockhaus and Khorram 1992; Kamaruzaman and Mohd Rasol 1995; Suratman and Ahmad 2012). According to Leckie (1990), a discriminant analysis based on Bayesian maximum likelihood is the most common algorithm used for classification analysis. In addition, he stated that ancillary data describing soil type, slope, and previous management operations, for example, are important for improving the classification accuracy.

The ability of remotely sensed data to provide information on forest variables such as wood volume, tree height, tree diameter, and tree species composition has

Table 3 Correlation coefficients between forest variables and Landsat TM and SPOT-HRV spectral data

Spectral bands	Band	Spectral range (μm)	Volume (m^3/ha) ^a	Basal area (m^2/ha) ^b	Age (years)	Height (m)
TM band 1	Blue	0.45–0.52	–0.61	–0.27	–0.35 ^b	–0.44 ^c
TM band 2	Green	0.52–0.60	–0.72	–0.42	–0.54 ^b	–0.56 ^c
TM band 3	Red	0.63–0.69	–0.69	–0.47	–0.53 ^b	–0.48 ^c
TM band 4	Near-infrared	0.76–0.90	–0.76	–0.47	–0.45 ^b	–0.54 ^c
TM band 5	Mid-infrared	1.55–1.75	–0.63	–0.43	–0.62 ^b	–0.62 ^c
TM band 7	Mid-infrared	2.08–2.35	–0.55	–0.48	–0.59 ^b	–0.53 ^c
HRV band 1	Green	0.50–0.59	–0.77	–0.18	–0.67 ^d	–0.18 ^d
HRV band 2	Red	0.61–0.68	–0.63	–0.35	–0.40 ^d	–0.35 ^d
HRV band 3	Near-infrared	0.79–0.89	–0.82	–0.41	–0.42 ^d	–0.41 ^d

Sources

^aRipple et al. (1991)^bBrockhaus and Khorram (1992)^cNilsson (1997)^dDanson (1987)

been reported by numerous researchers (e.g. Horler and Ahern 1986; Danson 1987; Poso et al. 1987; Ripple et al. 1991; Ardö 1992; Brockhaus and Khorram 1992; Asari et al. 2017; Mohsin et al. 2021). Regression functions are often used to relate these variables to the satellite data (e.g. Franklin 1986; Ahern et al. 1991; Ripple et al. 1991; Ardö 1992; Brockhaus and Khorram 1992; Trotter et al. 1997; Suratman et al. 2004). This requires that the correlation between the variables and the satellite data be sufficiently strong. The regression models used in many studies relate different stand variables to functions of spectral band, band products, band ratios, and band transformations (Jakubauskas and Price 1997; Scheer et al. 1997; Asari et al. 2017; Tengku Hashim et al. 2020; Mohsin et al. 2021).

A study conducted in the boreal forest by Ardö (1992) showed that field plots established for forest planning in Sweden could be used to construct regression models that predict wood volume. The correlation value between the observed and the estimated volume was 0.83 and the standard error of estimate was 46.5 m^3/ha . Ardö concluded that there was a stronger relationship between spectral radiance and volume for compartments with small volumes than for compartments with large volumes. This agrees with Franklin (1986), who suggested that when the vegetation cover approaches 100%, the basal area continues to increase as the stand grows

older. However, the remotely sensed signal is not affected by the increase because it is most sensitive to the degree of crown closure.

An alternative to regression technique is the k nearest neighbour (kNN) estimation method, in which forest variables are calculated as weighted means of spectrally nearby samples (Muinonen and Tokola 1990; Tomppo 1990). The method has been used operationally in the Finnish National Forest Inventory (NFI) since 1990. According to Tomppo (1990), among the advantages of this estimation method is that a vector consisting of all variables that are measured or registered in the NFI can be estimated. However, lack of or a low number of sample plots in certain forest types might lead to unreliable estimates (Moeur 1987). kNN estimates are unreliable at a pixel level, but reliable when aggregated to a community level (Tomppo 1990). For example, a study by Tokola et al. (1996) in the south of Finland with primary species of Scots pine (*Pinus sylvestris*), Norway spruce (*Picea abies*) and birch (*Betula* spp.) found that the standard error of estimates for wood volume on a pixel level was approximately 68–77 m³/ha.

7 Summary

It is essential to gain information about forest condition via forest inventory to achieve an effective planning and management of forest resources. A reliable forecast is required in managing forest activities from all the managed stands. This accurate information is vital to strategise decision related to forest policies in order to achieve the management objectives. This review summarises sampling techniques and the development of remote sensing and gave examples of remote sensing forestry applications in the tropics. It shows that remote sensing has evolved through black-and-white aerial photography into a complex process, using satellites, thermal scanning, and radar. In terms of applications, it has evolved from the realm of pure research to that of worldwide day-to-day application. Many previous studies have reported that several forest parameters can be related to satellite imageries from spectral radiance recorded by remotely sensed data. As the need for more and better information arises, new sensor systems are being developed from time to time and put into orbit.

References

- Ahem FJ, Erdle T, MacLean DA, Knepeck ID (1991) A quantitative relationship between forest growth rates and Thematic Mapper reflectance measurements. *Int J Remote Sens* 12(3):387–400
- Aldrich RC (1979) Remote sensing of wild land resource: a state-of-art review. USDA Forest Service, Rocky Mountain Forest and Range Experiment Station, Fort Collins, CO, General Technical Report RM-71, 56 pp
- Ardö J (1992) Volume quantification of coniferous forest compartments using spectral radiance recorded by Landsat Thematic Mapper. *Int J Remote Sens* 13(9):779–786

- Asari N (2017) Modelling and monitoring of stand volume, above ground biomass and carbon stocks of oil palm (*Elaeis guineensis*) plantations using landsat thematic mapper in Malaysia. PhD dissertation, 256 pp (unpub.)
- Asari N, Suratman MN, Jaafar J (2017) Modelling and mapping of above ground biomass (AGB) of oil palm plantations in Malaysia using remotely-sensed data. *Int J Remote Sens* 38(16): 4741–4764. <https://doi.org/10.1080/01431161.2017.1325533>
- Baltsavias E, Pateraki M, Zhang L (2001) Radiometric and geometric evaluation of IKONOS geo images and their use for 3D building modelling (Web page). Available at: http://www.photogrammetry.ethz.ch/general/persons/jana/isprs/tutmapup/ISPRS_tutorial_Baltsavias_hannover.pdf
- Bickford CA (1961) Stratification for timber cruising. *J For* 59:761–763
- Bickford CA, Meyer CE, Ware KD (1963) An effective sampling design for forest inventory: The northeastern forest resurvey. *J For* 61(11):826–833
- Bolstad PV, Lillesand TM (1992) Improved classification of forest vegetation in northern Wisconsin through a rule-based combination of soils, terrain, and Landsat Thematic Mapper data. *For Sci* 38:5–20
- Bong PP (1991) Application of remote sensing techniques to study the changes of mangrove forest at Canau Peninsula, South Vietnam. In *Application of remote sensing in Asia and Oceania—environ change monitoring*, pp 282–285
- Bowden DC et al (1979) Multilevel sampling designs for resource inventories. Department of Forest and Wood Sciences, Colorado State University
- Brockhaus JA, Khorram S (1992) Comparison of SPOT and Landsat-TM data for forest inventories. *Int J Remote Sens* 13(16):3035–3043
- Cochran WG (1977) *Sampling techniques*, 3rd edn. Wiley, 428 pp
- Czaplewski RL (1999) Multistage remote sensing: toward an annual national inventory. *J For* 97(12):44–48
- Danson FM (1987) Preliminary evaluation of the relationships between SPOT-1 HRV data and forest stand parameters. *Int J Remote Sens* 8(10):1571–1575
- Darus A (1989) Application of Landsat MSS data in land use mapping: a Malaysian experience. In *Proceedings of the 10th Asian Conference on Remote Sensing, Malaysia, Kuala Lumpur*, 23–29 Nov, 1989, pp 81–88
- Euroimage (2002) QuickBird: the world's highest resolution commercial satellite (Web page). Available at: http://www.euroimage.com/Products/product_pdf/qb.pdf. Accessed date 25 Apr 2022
- European Space Agency (2022) Earth online (Web page). Available at <https://earth.esa.int/eogateway/missions/spot>. Accessed date 25 Apr 2022
- FAO (1995) *Forest resources assessment 1990: global synthesis*. FAO Forestry Paper 125, Rome
- FAO (1996) *Forest resources assessment 1990: survey of tropical forest cover and study of change processes*. FAO Forestry Paper 130, Rome
- FAO (1998) The status of the forest resources assessment in the South-Asia sub-region and the country capacity building needs. In *Proceedings GCP/RAS/162/JPN Regional Workshop, Dehradun*
- Faridah-Hanum I, Mohamad AL, Hakeem K, Ozturk KR (2014) *Mangrove ecosystems of Asia, status, challenges and management strategies*. Springer, New York, NY
- Franklin J (1986) Thematic Mapper analysis of coniferous forest structure and composition. *Int J Remote Sens* 7(10):1287–1301
- Frayer WE (1981) Multilevel designs for resource inventories. In *XVII IUFRO World Congress Proceedings Division 9*, pp 169–173
- Freese F (1962) *Elementary forest sampling*. Agriculture handbook 232, USDA, 91 pp
- FSI (1997) *Forest survey of India*. Ministry of Environment and Forest, Dehra Dun
- Guidon B, Edmonds CM (2002) Large-area land-cover mapping through scene-based classification compositing. *Photogram Eng Remote Sens* 68(6):589–596

- Hamilton R, Megown K, Ellenwood J, Lachowski H, Maus P (2010) Assessing insect-induced tree mortality across large areas with high-resolution aerial photography in a multistage sample. In: Pye JM, Rauscher HM, Sands Y, Lee DC, Beatty JS (eds) *Advances in threat assessment and their application to forest and rangeland management*. General Technical Report PNW-GTR-802. Portland, OR
- Hartono H (1994) The use of SPOT image for mangrove inventory in Cimanuk delta West Java, Indonesia. *Indonesian J of Geogr* 26(68):11–26
- Hartono H, Muljosukojo B (1990) Monitoring disappearance of mangrove by remote sensing. *Indonesian J of Geogr* 20(60)
- Heller RC, Ulliman JJ (1983) Forest resource assessments. In *Man of remote sensing*, 2nd ed, vol 2, pp 2229–2324
- Hildebrant G (1989) Inventory and monitoring extended forest lands by remote sensing. In *Proceedings of the Remote Sensing and the Earth's Environment*, Alpbach, pp 87–94
- Holmgren P, Masakha EJ, Sjöholm H (1994) Not all-African land is being degraded: a recent survey of trees on farms in Kenya reveals rapidly increasing forest resource. *Ambio* 23(7):390–395
- Horler DNH, Ahern FJ (1986) Forestry information content of Thematic Mapper data. *Int J Remote Sens* 7(3):405–428
- Hutchinson ID (1978) An example of the use of two-phase sampling design for reconnaissance inventory in tropical forest. *NZJ For* 23(1):95–106
- Hwai YY (2006) Monitoring forest using remote sensing (Web page). Available at www.fao.org/forestry/10966-0b15189db8b2e3fa909e0d67b6f6d3b01.pdf
- IUFRO (1994) International guideline for forest monitoring. IUFRO world series, vol 5
- Jakubauskas ME, Price KP (1997) Empirical relationships between structural and spectral factors of Yellowstone lodgepole pine forests. *Photogram Eng Remote Sens* 63(12):1375–1381
- Kamaruzaman J, D'Souza G (1996) Quantifying disturbed hill dipterocarp forest lands in Ulu Tembeling, Malaysia with HRV/SPOT images. *Photogram Remote Sens* 51:39–48
- Kamaruzaman J, Hasssan HM (1996) Forest recreation planning in Langkawi Island, Malaysia, using landsat TM. *Int J Remote Sens* 18:3599–3613
- Kamaruzaman J, Mohd Rasol RAF (1995) Satellite remote sensing of deforestation in the Sungai Buloh forest reserve, Peninsular Malaysia. *Int J Remote Sens* 16(11):1981–1997
- Kätsch C, Vogt H (1999) Remote sensing from space – present and future applications in forestry, nature conservation, and landscape management. *Southern Afr For J* 185:14–27
- Keiner LE, Yah XH (1998) A neural network model for estimating sea surface chlorophyll and sediments from Thematic Mapper imagery. *Remote Sens Environ* 66(2):153–165
- Kohl M, Kushwaha SPS (1994) A four-phase sampling method for assessing standing volume using Landsat-TM data, aerial photography and field assessments. *Commonwealth For Rev* 73(1): 35–53
- Kohl M, Sutter R (1991) Application of aerial photographs in the estimation of standing volume in the Swiss NFI. In Kohl M, Pelz DR (eds) *Forest inventories in Europe with special reference to statistical methods*. In *Proceedings of the International IUFRO S.4.02 and S.6.04 Symposium*, May 14–16, 1990, Birmensdorf, pp 176–191
- Kushwaha SPS (1987) Remote sensing of shifting cultivation on North-Eastern India. In *Application of remote sensing in Asia and Oceania—environmental change monitoring*, pp 61–77
- LaBau VJ, Schreuder HT (1983) A multiphase, multiresource inventory procedure for assessing renewable resource and monitoring change. In *proceedings of the International Conference on Renewable Resource Inventories for Monitoring Change and Trends*, Corvallis, OR, pp 456–459
- Lachowski HM, Dietrich DL (1978) *Forest inventory of the Philippines using satellite imagery*. General Electric Company, Beltsville, MD, 116 pp
- Lal JB, Singh J, Gulati AK, Projapati RC (1990) Deforestation study in Kodagu district of Karnataka using Landsat MSS data. *Indian For* 116(6):487–493
- Leckie DG (1990) Advances in remote sensing technologies in forest surveys based on satellite imagery. *Can J For Res* 20(4):464–483

- Leckie DG (1998) Forestry applications using imaging radar. In: Henderson FM, Lewis AJ (eds) *Man of remote sensing*, vol 2, 3rd edn. Wiley, New York, pp 435–519
- Leckie DG, Gillis MD (1995) Forest inventory in Canada with emphasis on map production. *For Chron* 71(1):74–88
- LeMay V, Marshall PL (1990) *Forest mensuration. FRST238 Course Manual*. University of British Columbia, 213 pp
- Lidov L (1999) IKONOS satellite launches into space: News releases (Web page). Available at: <http://www.spaceimaging.com/newsroom/releases/1999/inorbit.htm>.
- Lillesand TM, Kiefer RF (2000) *Remote sensing and image interpretation*, 4th edn. John Wiley and Sons, NY, p 724
- Lindgren DT (1985) *Land use planning and remote sensing*. Martinus Nijhoff, Dordrecht, 176 pp
- Mahmood NN, Bruneau M, Lemen H (1983) A pilot study on the use of satellite remote sensing data for agroecological mapping in Peninsular Malaysia. *MARDI Special Report 2*, 31 pp
- Malingreau JP (1986) Global vegetation dynamics: satellite observation over Asia. *Int J of Remote Sens* 7:1121–1146
- Marco O, Kuenzer C (2020) Spaceborne L-band synthetic aperture radar data for geoscientific analyses in coastal land applications: a review. *Remote Sens* 12(14):2228. <https://doi.org/10.3390/rs12142228>
- Miller LD, Nualchawee K, Tom C (1978) Analysis of the dynamics of shifting cultivation in the tropical forests of northern Thailand using landscape modelling and classification of Landsat Imagery; NASA Technical Memorandum 79545, Greenbelt, MD
- Moerur M (1987) Nearest neighbour inference for correlated multivariate attributes. In *Proceeding of the IUFRO Conference on Forest Growth Modelling and Prediction*, Minneapolis, MN, 23–27 Aug 1987. USDA Forest Service General Technical Report NC-120, pp 716–723
- Mohsin AF, Suratman MN, Yamani SAK (2021) Modelling of stand volume of eucalyptus plantations using worldview-2 imagery in Sabah, Malaysia. *ASM Sci J* 14:18–125
- Morain SA, Klankamsoon B (1978) Forest mapping and inventory techniques through visual analysis of Landsat imagery: examples from Thailand. In *Proceedings of the 12th International Symposium for Remote Sensing of Environment*, Ann Arbor, MI, pp 417–426
- Moreau N, Vercesi L (1989) *Cartographie des mangrove de guinea a l'aide du satellite SPOT 1*, in photo-interpretation No. 1989–1 fascicule 4, Janvier Fervier 1989 (as cited)
- Muinonen E, Tokola T (1990) An application of remote sensing for communal forest inventory. In *Proceeding of the Usability of Remote Sensing for Forest Inventory and Planning SNS/IUFRO Workshop Umeå, Sweden*, 26–28 Feb 1990, pp 35–42
- Nilsson M (1997) *Estimation of wood volume using satellite spectral data: a simulation study*. Ph.D. dissertation, Swedish University of Agricultural Sciences, Umeå, 54 pp
- NRSA (1983) *Nation-wide mapping of forest and non-forest areas using Landsat false colour composites for the periods 1972–1975 and 1980–82*. Project Report, National Remote Sensing Agency, Hyderabad
- Poso S, Paananen P, Samila M (1987) Forest inventory by compartments using satellite imagery. *Silva Fennica* 21:69–94
- Rao PPN, Jayaraman V, Chandrasekhar MG (1991) Remote sensing applications to natural resources development in India. In *Application of remote sensing in Asia and Oceania—environmental change monitoring*, Asian Association on Remote Sensing, Tokyo, pp 131–138
- Ripple WJ, Wang S, Isaacson DL, Paine DP (1991) A preliminary comparison of Landsat TM and SPOT-1 HRV multispectral data for estimating coniferous forest volume. *Int J Remote Sens* 12(9):1971–1977
- Salas WA, Ducey MJ, Rignot E, Skole D (2002) Assessment of JERS-1 SAR for monitoring secondary vegetation in Amazonia: II. Spatial, temporal, and radiometric considerations for operational monitoring. *Int J Remote Sens* 10(23):1381–1399
- Salleh MW (1976) Preliminary interpretation of ERTS imagery of Peninsular Malaysia. *Malaysian For* 39:13–16

- Scheer L, Acka A, Feldkotter C (1997) Efficient growing stock estimation from satellite data employing two-phased sampling with regression. *Geo Inform Sys* 10(3):22–25
- Suratman MN, Ahmad S (2012) Multi temporal landsat TM for monitoring mangrove changes in Pulau Indah, Malaysia. In: Proceedings IEEE Symposium on Business, Engineering and Industrial Applications (ISBEIA2012). <https://doi.org/10.1109/ISBEIA.2012.6422861>
- Suratman MN, Bull GQ, Leckie DG, LeMay V, Marshall PL (2002) Modelling attributes of rubberwood (*Hevea brasiliensis*) stands using spectral radiance recorded by landsat thematic mapper in Malaysia. In: Proceedings 2002 IEEE International Geoscience of Remote Sensing Symposium (IGARSS 2002) and the 24th Canadian Symposium on Remote Sensing
- Suratman MN, Bull GQ, LeMay VM, Leckie DG, Marshall PL, Mispan MR (2004) Prediction models for estimating volume, age and predicting area of rubber plantations in Malaysia using landsat TM data. *Int For Rev* 6(1):1–13
- Sylvander R, Bystrom M, Hogberg P (1988) The use of satellite imagery for delineation of vegetation types in eastern Tanzania. Section of Forest Mensuration and Management Report No. 17
- Temu AB (1981) Double sampling with aerial photographs in estimating wood volumes in miombo woodlands. Division of Forestry Record No. 22. Morogoro
- Temu AB, Phillip MS (1981) Sampling woodland for fuel wood. In Proceedings of the Forest Inventory Growth Models, Management Planning and Remote Sensing. XVII World Congress, IUFRO, pp 272–279
- Tengku Hashim TMZ, Suratman MN, Singh HR, Jaafar J, Bakar AN (2020) Predictive model of mangroves carbon stocks in Kedah, Malaysia using remote sensing. *IOP Conference Series, Earth Environ Science* 540 012033, 1–10 pp
- Thompson MD, MacDonald BC, Jefferies WC (1993) Progress in operational forest mapping using airborne radar in tropical regions. International Symposium on Operationalization of Remote Sensing, pp 163–175
- Toan LT (1995) Assessment of ERS-1 SAR data for forest studies in Southeast Asia. *Earth Observ Quart* 48:16–20
- Tokola T, Pitkänen J, Partinen S, Muinonen E (1996) Point accuracy of a non-parametric method in estimation of forest characteristics with different satellite materials. *Int J Remote Sens* 17(12): 2333–2351
- Tomppo E (1990) Designing a satellite image-aided national forest survey in Finland. In Proc. in the Usability of Remote Sensing for Forest Inventory and Planning. SNS/IUFRO Workshop in Umeå, 26–28 Feb, 1990, pp 43–47
- Toutin T, Cheng P (2000) Demystification of IKONOS. *Earth Observation Magazine* (Web page). Available at: <http://www.eomonline.com/Common/Archives/July00/toutin.htm>
- Trotter CM, Dymond JR, Goulding CJ (1997) Estimation of timber volume in a coniferous plantation forest using Landsat TM. *Int J Remote Sens* 18(10):2209–2223
- USGS (2000) Satellite image of environmental change: remote sensing before Landsat 1 (Web page). Available at: <http://edc.usgs.gov/earthshots/slow/Help-GardenCity/remotesensing>
- Wacharakitti S, Morain SA (1978) Procedures for land-use analysis in developing countries: example for Southeast Asia. In Proceedings of the 12th International Symposium on Remote Sensing of Environment, Manila, the Philippines. Environmental Research Institute of Michigan, Ann Arbor MI, vol 1, pp 587–595
- Wilkie DS, Finn JT (1996) Remote sensing imagery for natural resources monitoring. Columbia University Press, New York, 295 pp
- Zahriah A, Cheah H, Layden D (1989) Forest mapping and change detection using satellite data. In Proceedings of the 10th Asian Conference of Remote Sensing (ACRS), Kuala Lumpur

Part II

Overview of Remote Sensing



Multiple Sensors and Platforms for Biophysical and Biochemical Characterisations of Various Ecosystem Types of Tropical Forests in Malaysia: Advance, Limitation, and Opportunity

Hamdan Omar

Abstract

Malaysia with a landmass of about 32.9 million ha has about 18.2 million ha of forest cover. This covers three major types of forest ecosystems, which are tropical inland, peat swamp, and mangrove forests with the extents of about 16.94, 0.67, and 0.63 million ha, respectively. Malaysia pledged to the world that it will maintain is forest cover by 50%. These forests house thousands of flora and fauna species and Malaysia is known as the top 12 megadiversity country in the world. Sustainable forest management (SFM) is being the pillar for the management of forest resources that balance between protection, conservation, production, and consumption of resources and forest products in Malaysia. Various technologies are used as tools in the management as well as research and development (R&D) in forestry sector to ensure that these resources are sustained. Remote sensing is one of the famous technologies that is utilised to understand and characterise the biophysical and biochemical properties of forests in Malaysia at varying scales and spatial, radiometric, and temporal resolutions. This technology is also adopted in tailoring management prescriptions as well as a tool for monitoring and enforcement. This chapter highlights recent advancements in remote sensing methodology and applications in the perspective of multiple platform types including spaceborne, airborne, and unmanned aerial vehicle (UAV) and sensor types, i.e. optical (multispectral and hyperspectral), synthetic aperture radar (SAR), and light detection and ranging (LiDAR). This chapter also identifies advances and limitations of the applied methodology and

H. Omar (✉)

Geoinformation Programme, Division of Forestry and Environment, Forest Research Institute Malaysia (FRIM), Kepong, Selangor, Malaysia
e-mail: hamdanomar@frim.gov.my

© The Author(s), under exclusive license to Springer Nature Singapore Pte Ltd. 2022

M. N. Suratman (ed.), *Concepts and Applications of Remote Sensing in Forestry*, https://doi.org/10.1007/978-981-19-4200-6_2

opportunities for future improvements in remote sensing technology applications in the forestry sector in Malaysia.

Keywords

Remote sensing · Forestry · Biophysical and biochemical · Malaysia

1 Introduction

Malaysia has roughly 18.2 million ha of forest cover, with a landmass of about 32.9 million ha. This includes three primary forest ecosystems: tropical inland dipterocarp, peat swamp, and mangrove forests, which span approximately 16.94, 0.67, and 0.63 million ha, respectively. Malaysia has promised the world that it will maintain a 50% forest cover. The Malaysian tropical rainforest is one of the world's most complicated ecosystems. It has one-of-a-kind natural heritage, which includes a diverse range of plant and animal species that have evolved over millions of years. Malaysia's flora is estimated to contain at least 8000 kinds of flowering plants, with roughly 2500 of these being tree species. As a result, depending on edaphic conditions, drainage, and height, there are many diverse rainforest formations.

Lowland dipterocarp forest, hill dipterocarp forest, upper hill dipterocarp forest, oak-laurel forest, montane ericaceous forest, peat swamp forest, and mangrove forest are the major forest types in Malaysia. Smaller sections of freshwater swamp forest, melaleuca forest, heath forest, limestone forest, and quartz ridge forest are also present. Considering the composition of these forests in Malaysia, the types can be generalised into three types, which are inland, peat swamp, and mangroves.

In Malaysia, sustainable forest management (SFM) is the pillar for forest resource management that strikes a balance between resource protection, conservation, production, and consumption. To guarantee that these resources are sustained, many technologies are utilised as management and research and development (R&D) instruments in the forestry sector. Remote sensing is a well-known technique for determining and characterising the biophysical and biochemical aspects of Malaysian forests at various sizes and geographical, radiometric, and temporal resolutions. This technology is also used to customise management prescriptions and as a monitoring and enforcement tool.

Remote sensing has made it possible to monitor forest characteristics consistently and repeatedly in qualitative and quantitative ways. Such data collection and reporting are a significant factor that assists in research and development processes. It also makes it easier to integrate forestry with other agencies. Nowadays, remote sensing is applied in different areas of forest management.

It is also desirable to use remote sensing data to monitor forests consistently and repeatedly over large areas, and automated image analysis techniques. Several types of remote sensing data, including optical multispectral scanner, synthetic aperture radar (SAR), light detection and ranging (LiDAR), aerial photography, and unmanned aerial vehicle (UAV) data, have been used by forest research and

operational agencies to detect, identify, classify, evaluate, and measure various forest cover types and their changes. Over the past decades tremendous progress has been made in demonstrating the potentials and limitations of the applications of remote sensing in forestry.

In both qualitative and quantitative methods, remote sensing can detect, identify, classify, evaluate, and measure many forest properties. Forest cover types can be classified qualitatively as coniferous and deciduous forest, mangrove forest, marsh forest, forest plantations, and so on using remote sensing. Quantitative analysis can quantify or estimate forest metrics such as density, height, basal area, number of trees per unit area, timber volume, and woody biomass, as well as floristic composition, life forms, and structure. Users of forest data are looking for new sensors and platforms for a variety of remote sensing applications in forestry in certain locations of the world, such as tropical areas. An inventory of all remote sensing applications in the forestry sector in Malaysia is required to determine what kind of information we can extract from current remote sensing sensors and platforms, as well as how accurate that information is.

This chapter highlights recent advancements in remote sensing methodology and applications in the perspective of multiple platform types including spaceborne, airborne, and UAV, and sensor types, i.e. optical (multispectral and hyperspectral), SAR, and LiDAR. This chapter also identifies limitations of applied methodology and opportunities for future improvements in remote sensing technology applications in the forestry sector in Malaysia.

2 Remote Sensing as Tool for Forest Mapping and Inventory

Forestry was one of the first disciplines in Malaysia to identify the importance of remote sensing in acquiring timely and accurate data, which is critical for long-term forest management and tracking trends in forest land use (Kamaruzaman and Souza 1997). Among the first attempts that were made to use remote sensing data in forestry are Thang (1983), Thang et al. (1987), and Wan Yusoff (1988). But that time, the applications were concentrated only on classification methods for forest cover mapping. In the case of forest inventories and practices, the role of remote sensing technology has grown significantly because it can provide enhanced information directly or indirectly, as well as collect forest resource information with high spatial accuracy, allowing tactical, strategic, and operational forest planning and management. Since the early 1990s optical remote sensing has been widely used also for forest inventory parameter assessment (Wulder 1998). Government agencies in Malaysia, such as the Forestry Department of Peninsular Malaysia (FDPM), have been using remote sensing technology for nearly two decades to plan, manage, and monitor their forest areas (Wan Abd Rahman 2016).

Factors to consider when selecting remote sensing products include spatial resolution, spectral resolution, radiometric resolution, and temporal resolution. Spatial resolution refers to the size of the smallest object that can be detected on an image. There are also some common considerations that need to be taken into

Fig. 1 Common considerations in forest assessment using remote sensing



Fig. 2 The trade-offs between cost and accuracy of using remotely sensed data in assessing forests

Cost ↑ High	Not recommended	Budget oriented (Optional)
	Objective oriented (Optional)	Most recommended
Low	Accuracy → High	

account when using remote sensing in various applications in forestry. The most common are cost of data acquisition, scale of the studied areas, attainable accuracies, time to process the data, and the rapidity and replicability of the end products (Fig. 1).

Depending on the objectives of the studies, remote sensing offers some trade-offs between cost and accuracy. It is often that the higher the resolution of the data, the higher the cost. And this can be directly related to the scale or size of the study area. Figure 2 illustrates how cost and accuracy are related to each other and how these factors can influence the selection of remotely sensed data in specific study area with justified objectives.

There are several studies that used remote sensing data for forest mapping and inventory in Malaysia. Mohd Najib and Kanniah (2019) employed the Carnegie Landsat Analysis System-Lite (CLASlite) algorithm to determine forest cover using Landsat satellite data in Peninsular Malaysia. The goal of this project was to create a

map of forest cover in Peninsular Malaysia. The study's findings reveal that the CLASlite algorithm incorrectly identified some oil palm, rubber, and urban areas as forest vegetation. By integrating Landsat and Advance Land Observation Satellite, Phased-Array type L-Band Synthetic Aperture Radar (ALOS PALSAR) images to detect oil palm, rubber, and urban areas and then eliminating them, a valid forest cover map was created. The ALOS PALSAR (threshold technique) data on horizontal-horizontal (HH) and horizontal-vertical (HV) polarisations could detect oil palm plantations with an overall accuracy of 85%. With an overall classification accuracy of 94.5%, these techniques generated a forest cover reading of 5,914,421 ha.

Landsat missions have been producing a consistent dataset over Malaysia regions since year 1978 (Fig. 3). It is the only satellite that can provide historical data on forest cover and other land uses. Hamdan et al. (2021) utilised Landsat-5 Thematic Mapper TM and Landsat-7 Enhanced Thematic Mapper (ETM+) and Landsat-8-Operational Land Imaging (OLI) to map the forest cover and changes from 2005 to 2020. The study found that forest cover in Malaysia has declined from about 19.3 million ha (in 2005) to 18.2 million ha in year 2020 (Table 1). The study found that the deforestation from 2005 to 2020 amounted to the loss of 1,087,030 ha (5.6%) of its year 2005 forest cover, with the annual rate of deforestation at 0.37% year⁻¹.

Hamdan et al. (2020a) also conducted a study to map mangroves at national level using Landsat-8 OLI data. To create a mosaic that covers the entirety of Malaysia, at least 29 scenes of Landsat images are required. However, due to its location in the tropics, Malaysia is constantly shrouded in clouds that are very impossible to remove completely. To produce a cloudless image, many images taken at different times over the same spot are required. For further processing, the study has set a restriction of five top photographs of the same scenes taken within 3 years of the targeted year. These photos must have a cloud cover of less than 30% and be taken between the specified time frames. Even with Landsat's 16-day repetition cycle, which produces around 22 scenes over the same coverage in a year, finding the best image is still challenging. This is owing to the dense cloud cover in Malaysia's atmosphere, particularly in hilly areas and during the monsoon season (October to February). Cloud covers in most settings range from 10 to 90%; thus, the chances of getting a cloud cover of 30% are slim. To obtain cloud-free images over Malaysia for a one-time observation, at least 145 scenes of Landsat-8 datasets are required. This problem was remedied, though, by having many high-quality sequences. The Fmask method was used to detect and mask the clouds in these images (Fig. 4). About 629,038 ha of mangroves cover in the whole country for the year 2017 was mapped from this study. The accuracy was verified by using ground truthing points, which attained at least 85% (Fig. 5).

About similar study was conducted by Kanniah et al. (2015) in Iskandar Malaysia (IM), the fastest growing national special economic region located in southern Johor, Malaysia. The Maximum likelihood classification (MLC) was adopted, and the technique provided significantly higher accuracies compared to the support vector machine (SVM) technique. The classified satellite images using the MLC technique

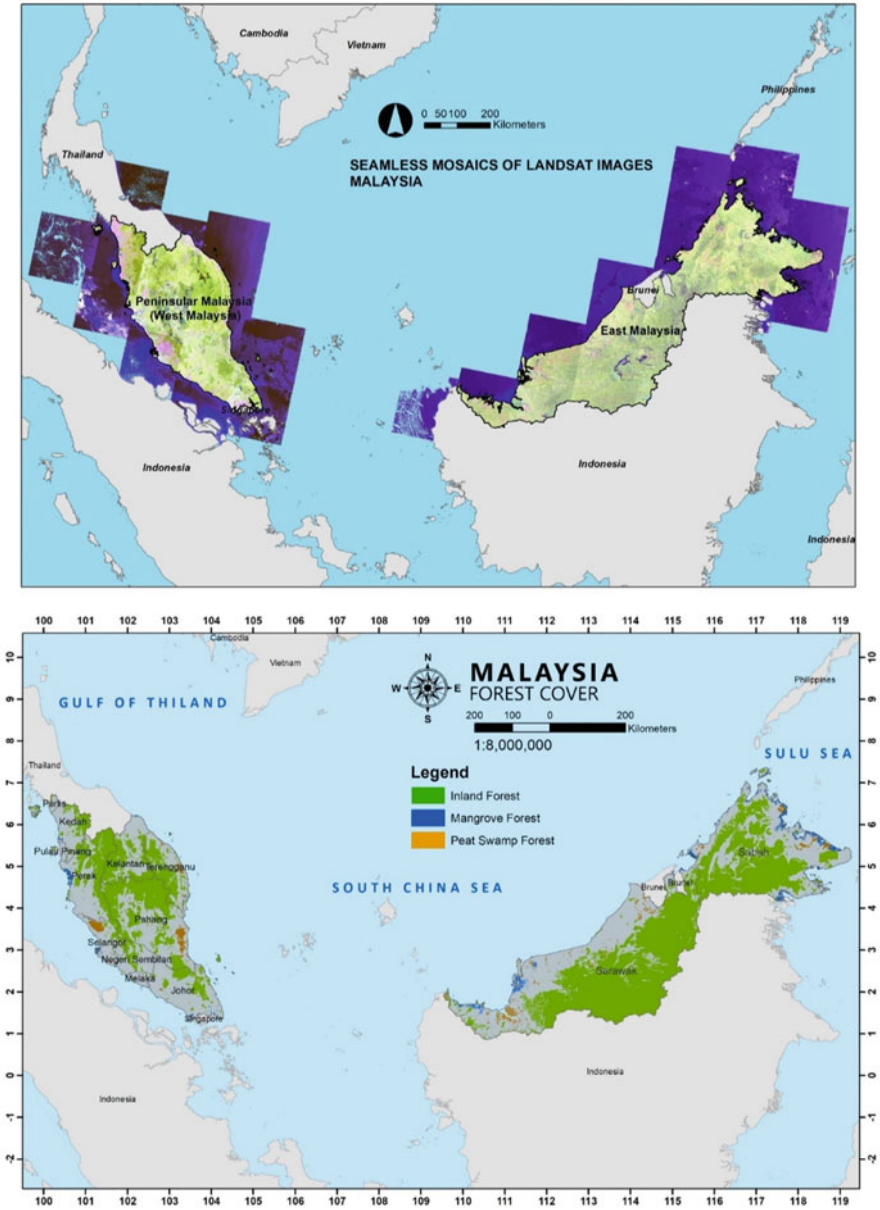


Fig. 3 The Landsat datasets (top) and the produced forest cover map (bottom)

showed that IM lost 6740 ha of mangrove areas from 1989 to 2014. Nevertheless, a gain of 710 ha of mangroves was observed in this region, resulting in a net loss of 6030 ha. Earlier, a study was conducted within the same study area at the Sungai

Table 1 Forest cover in Malaysia (2020)

Region	Forest cover (ha)				Total forest cover (ha) (d) = (a) + (b) + (c)	Land area ^a (ha) (e)	Percentage (%) (f) = (d)/(e) * 100
	Inland forest (a)	Peat swamp forest (b)	Mangrove forest (c)				
Peninsular Malaysia	5,338,082	243,504	110,953	5,692,539	13,100,367	43.5	
Sarawak	7,328,029	320,207	139,890	7,788,126	12,444,951	62.6	
Sabah	4,273,536	97,276	378,195	4,749,007	7,390,224	64.3	
Total	16,939,647	660,987	629,038	18,229,673	32,935,542	55.3	

^aSources: Department of Survey and Mapping Malaysia, Lands and Surveys Department, Sabah and Department of Land and Survey, Sarawak

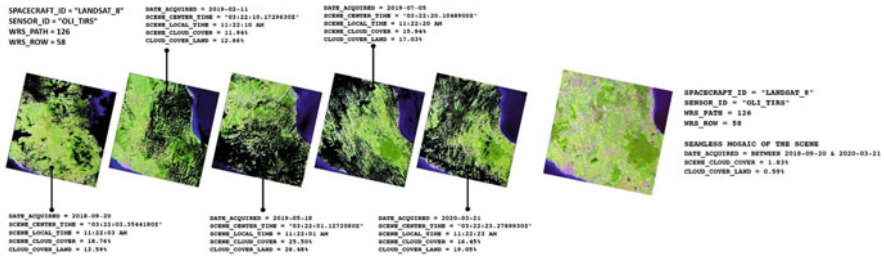


Fig. 4 Cloud masking process and the final product of a scene of Landsat

Pulai RAMSAR site and its surrounding areas. This study was carried out to identify and map land cover types using SPOT-4 imagery. Through unsupervised classification technique a total of seven classes of land cover type were mapped, where the accuracy was attained at about 90%. Later, vegetation densities were classified into five levels, namely, very high, high, medium, low, and very low, based on crown density scale using vegetation indices such as normalized difference vegetation index (NDVI), advance vegetation index (AVI), and optimized soil adjusted vegetation index (OSAVI) (Ismail et al. 2011).

Moving to the lesser-known wetland ecosystem type, Melaleuca forest, known as Gelam forest, a study was conducted to identify its coverage and locality. Hamdan et al. (2020b) used optical images from Landsat-8 OLI as primary input for this study. Spectral characteristic from visible and infrared channels was derived from the images to produce a specific vegetation index, i.e. NDVI, land surface water index (LSWI) (also known as normalized difference infrared index (NDII)), soil-adjusted vegetation index (SAVI), and enhanced vegetation index (EVI), which were used for recognising Melaleuca forest on the images. The study demonstrated that the Melaleuca forest covered about 23,000 ha in Peninsular Malaysia (Fig. 6). It also demonstrated that the use of Landsat-8 OLI satellite images was good at delineating Melaleuca forest. The integration of multispectral bands and VIs has improved the classification accuracy from 72.3 to 93.7%. Green and near-infrared (NIR) bands together with soil-adjusted vegetation index (SAVI) were the most important input for the classification.

3 Remote Sensing for Biomass Carbon Assessment

Remotely sensed data is currently being extensively used for estimating forest biomass. Satellite-based estimates of carbon stock are likely to become more accessible over the next few years (Vashum and Jayakumar 2012). Remote sensing data does not directly determine the quantity of biomass present in the forest. It only analyses biomass-related factors such as tree height, crown size, forest density, forest type, forest volume, leaf area index, and so on. The above-ground biomass (AGB) is estimated using remote sensing data combined with field-based forest measurements. Field measurements are frequently used to create predictive models

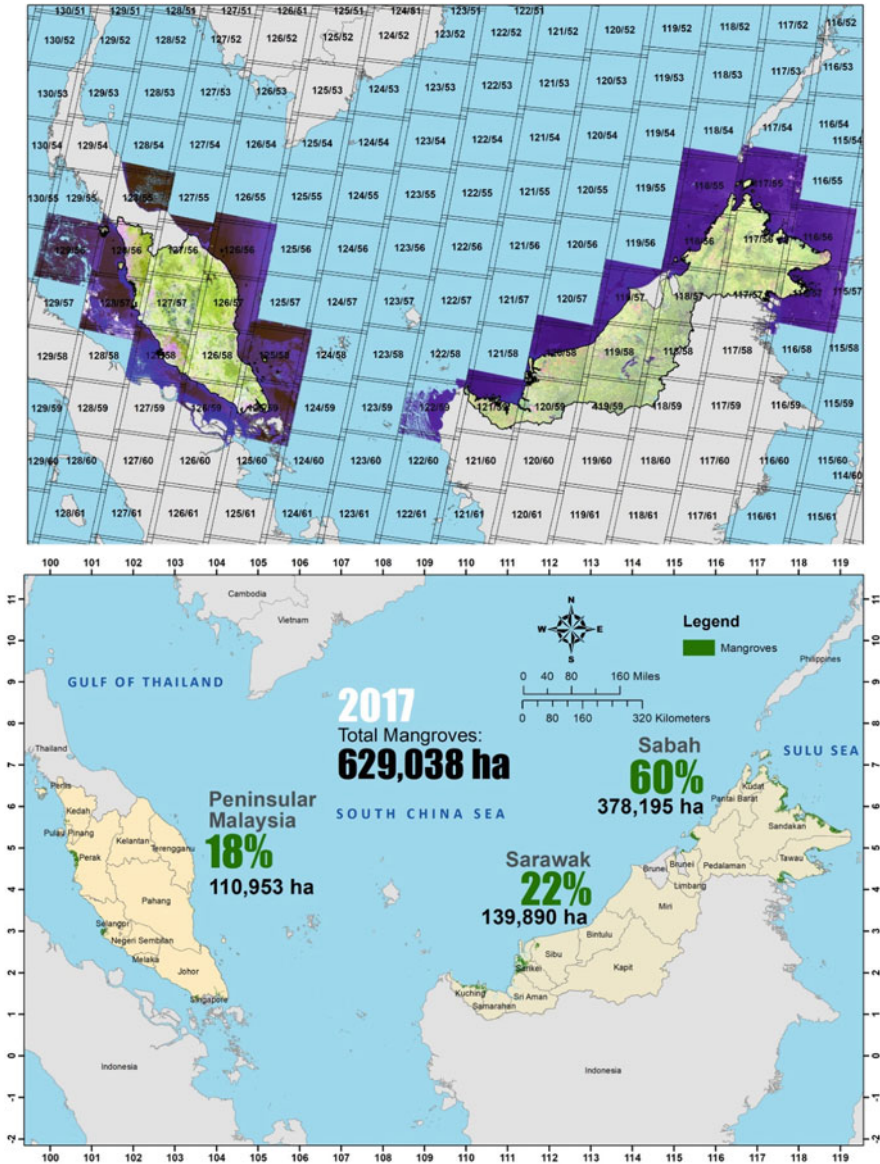


Fig. 5 The Landsat datasets (top) and the produced mangroves cover map (bottom)

or allometric equations for biomass and to verify remotely sensed data results. Once validated, remotely sensed data can be used to estimate forest biomass for a larger area where field measurement data is few or not existent.

Generally the source of remote sensing data, sensor type, algorithm employed, processing technique, bioclimatic conditions, and forest types all influence the

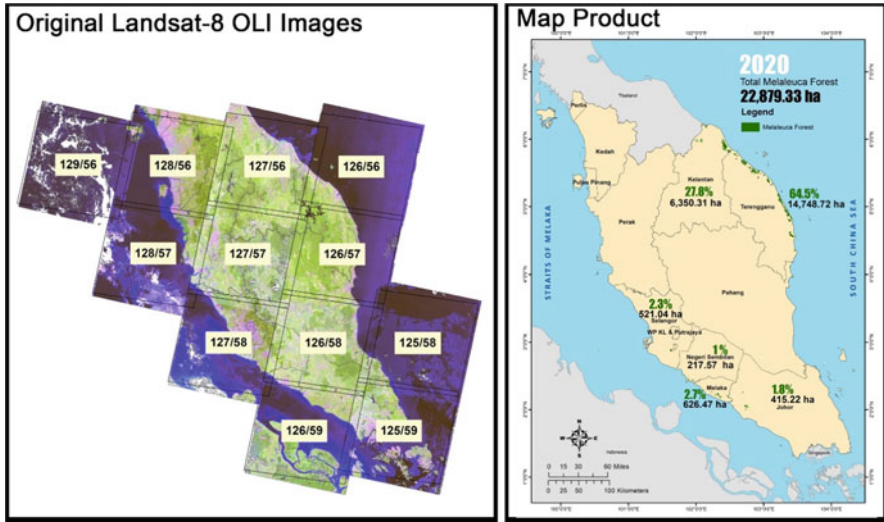


Fig. 6 The Landsat datasets (left) and the produced Melaleuca forest cover map (right)

reliability estimation of AGB using a remote sensing technique. Developing modelling regression to obtain the best AGB prediction would be a new approach, especially in terms of comprehending the integration of allometric equations and remote sensing modelling (Mohd Zaki and Abd Latif 2017). Malaysia with variety of forests, various stand conditions, and management practices would offer different challenges in AGB estimations using remote sensing. The users need to be very selective in the applied methodologies, field survey protocols, allometric equations, and the sensor type used to quantify AGB in the forests of Malaysia.

Optical and SAR (and the combination of both) systems are utilised widely for biomass assessment in Malaysia since the last two decades at different scales and forest types. To some extent where more accurate results are required, high-resolution images and LiDAR are engaged by adopting various processing techniques. Seo et al. (2014) estimated the AGB and distribution of tropical forest in a production forest reserve in Tangkulap Forest Reserve (FR), Sabah, using k-NN method in combination with field survey data, Landsat TM-5 image spectral bands, and GIS data. The k-NN method was used to determine the number of reference plots. Common NDVI with 3×3 texture measure was found to be the best indicator for estimating AGB as compared to the original digital number without filtering.

Another study to estimate AGB was conducted by Langnera et al. (2012) at Tangkulap and Deramakot FR, Sabah. They identified that the mid-infrared band of Landsat-8 OLI, which is sensitive to soil components and vegetation moisture content, was the best at representing the crown cover condition and forest status. High reflectance values indicate openings in the crown cover. Younger vegetation and regrowth and characteristic successional land cover types with intermediate reflectance values can be separated from pristine forests, which show lower

reflectance values. Crown cover and forest status (CCFS) index is derived as the reciprocal of the illumination and atmosphere-corrected reflectance values ($\text{MidIR}(b7)_{\text{corr}}$). A haze correction was done by using the reflectance values of the blue band. The resulting modified bands ($\text{Blue}(b1)_{\text{mod}}$) were finally used to correct the CCFS index:

$$\text{CCFS}_{\text{corr}} = \frac{1}{\text{MidIR}(b7)_{\text{corr}} - 0.3 \times \text{Blue}(b1)_{\text{mod}}}$$

Two models to estimate AGB in the study area were proposed, which are:

$$\text{Model 1: } \text{AGB}_{\text{Landsat}} = \text{CCFS}_{\text{corr}}^2 + \text{CCFS}_{\text{corr}}$$

$$\text{Model 2: } \text{AGB}_{\text{Landsat}} = \text{CCFS}_{\text{corr}}^2$$

Aster and SPOT satellites were also considered in developing alternative methods for biomass estimation. A similar study was conducted by Abd Latif et al. (2015) at Besul FR, Terengganu, to detect the impact of logging operations to the forest loss using SPOT-5 satellite imagery. The data was used to detect forest canopy loss and to extract parameters for estimating biomass loss between years 2012 and 2014. Forest AGB was estimated at 259.1 Mg ha^{-1} by using original digital number from individual bands without filtering and 263.4 Mg ha^{-1} estimated from NDVI. Slightly lower estimates were produced when 3×3 filtering was applied, with the estimated AGB being 248.1 and 257.3 Mg ha^{-1} from the individual bands and NDVI, respectively.

Focusing more on the image-processing method, Tangki and Chappell (2008) used a total of 50 sampling plots of 0.1 ha to quantify mean tree biomass in different conditions of forest, i.e. virgin and logged forests at Ulu Segama RF, Sabah. These data were then correlated with the spectral radiance of individual Landsat-5 TM bands over the $15 \text{ km} \times 15 \text{ km}$ study area. At this scale, a two-parameter linear model of Landsat TM radiance in the NIR band explained 76% of the variation in biomass. The differences in mean radiance may be related to a change in the proportion of emergent tree canopy compared to a cover of either pioneer trees or ginger/shrubs, according to the local-scale measurements; the canopies of emergent trees have the lowest NIR radiance of the vegetation characteristic of selectively logged forest.

On the other hand, Minerva et al. (2014) developed a novel Fourier transform textural ordination (FOTO) method, which involves the combination of 2D fast Fourier transform (FFT) and ordination through principal component analysis (PCA) for characterising the structural and textural properties of vegetation. In the context of tropical forest in Sabah, this research shows the potential of Fourier transform approaches in estimating different forest types, their stand structure, and biomass dynamics. The approach was used to record the research area's very-high-resolution (VHR) Satellite Pour l'Observation de la Terre (SPOT) imagery. The method was effective in discriminating between forest types and constructing distinct biomass estimation models for different forest types. The FOTO approach correctly resolves high AGB values of diverse forest types, according to the results.

Table 2 Summary of the correlations between AGB and backscatter of HV polarization

Year	Sensor	Prediction equation	R^2	Number of samples (n)	RMSE (Mg ha ⁻¹)
2010	PALSAR	$y = 2182.9e^{0.1442x}$	0.2735	254	115.89
2016	PALSAR-2	$y = 8665e^{0.2535x}$	0.5581	80	117.45
2010 and 2016	PALSAR + PALSAR-2	$y = 3166.7e^{0.1744x}$	0.3541	334	116.91

Backscatter is in gamma nought (γ^0 , dB) and AGB in (Mg ha⁻¹). All correlations are significant at $p < 0.05$

An alternative to the optical satellite systems, spaceborne SAR data have become one of the primary sources for AGB estimation. Radar is well known for its capability to penetrate cloud cover and it has been recognised as the most significant advantage compared to optical sensor systems. The possibility of obtaining cloud-free, wall-to-wall images is higher for a tropical region, especially Malaysia. Moreover, long wavelength SAR such as L-band is more reliable for AGB estimation in various forest ecosystems. However, studies demonstrated signal saturation at certain biomass level. This has become another constraint for estimating AGB in Malaysia's forests. Hamdan et al. (2015) confirmed that the L-band SAR backscatter started to saturate at AGB of 200 Mg ha⁻¹. A direct approach may not be appropriate to address this limitation and some indirect approaches are needed to produce accurate estimate of very high levels of biomass. Hamdan et al. (2014a) also indicated that the saturation occurred in mangrove forest when the biomass level reached at 100 Mg ha⁻¹. The errors associated with the prediction model were also observed to increase largely as the AGB exceeded 150 Mg ha⁻¹. However, the use of L-band SAR can provide an alternative that allows rapid assessment of AGB in large areas where access is limited.

Understanding and identifying major uncertainties caused by different stages of the AGB estimation procedure and devoted efforts to reduce these uncertainties are critical. Hamdan et al. (2014b) did a review on the use of L-band SAR data primarily from ALOS PALSAR for AGB assessments in tropical regions including Malaysia. Issues related to approaches, methodologies, advancements, limitations, and options for AGB estimation by using L-band SAR data are also elaborated. Example uses of L-band PALSAR and PALSAR-2 data for AGB estimation in Malaysia were presented by Hamdan and Muhamad Afizzul (2018). Predictive models were derived from these systems as summarised in Table 2. Since the sample plots covered only lowland, hill, and hill dipterocarp forests, the equation produced is only valid for these forests and not accurate for other types of vegetation. This equation is also valid only for PALSAR and PALSAR-2 datasets.

When the use of a single system portrays some issues, synergetic use or attempts to combine multiple sensors then came into the picture to address these issues. The synergy of the prediction has been obtained when the variables were integrated into an empirical prediction equation derived from multiple line regression. This method was applied to the single PALSAR-2, to Sentinel-1A polarisation, and also to the

Table 3 The best correlations derived from multiple regression from a single sensor and combination of sensors

Sensor	Prediction equation	R^2
PALSAR-2	$146.90HH + 169.78HV - 7.03(HH \times HV) + 416.96(HH \times HV)^{1/2} + 227.07$	0.342
Sentinel-1A	$-17.040VH - 2.344(VV \times VH) + 24.327(HH \times HV)^{1/2} + 181.918$	0.138
Combination	$-10.877VH - 13.292(HH \times HV)^{1/2} + 139.702HH + 162.287HV - 6.526(HH \times HV) + 394.502(HH \times HV)^{1/2} + 238.524$	0.356

All polarizations are in sigma nought (σ^0 , dB). All correlations are significant at $p < 0.05$

variables from the combination of both PALSAR-2 and Sentinel-1A. The best three models have been produced as summarised in Table 3. Evidently the combination of PALSAR-2 L-band and Sentinel-1A is able to strengthen the relationship between AGB and the polarisation, thus improving the accuracy of estimates (Hamdan et al. 2017). Both data have complemented each other that eliminated the effects of backscattering diffusion.

This effort was also demonstrated by Cutler et al. (2012), where multispectral Landsat TM and Japan Earth Resources Satellite (JERS-1) SAR data were used together to estimate tropical forest biomass at three separate geographical locations: Brazil, Malaysia, and Thailand. Texture measures were derived from JERS-1 SAR data using wavelet analysis and grey level co-occurrence matrix methods, then combined with multispectral data to provide inputs to artificial neural networks that were trained under four different raining scenarios and validated using biomass data from 144 field plots. The addition of SAR texture to multispectral data revealed good relationships with above-ground biomass when trained and tested with data taken from the same site ($r = 0.79, 0.79, \text{ and } 0.84$ for Thailand, Malaysia, and Brazil, respectively). Furthermore, the level of correlation ($r = 0.55$) was stronger when networks were trained and evaluated with data from all three locations than previously reported results from the same sites using only multispectral data.

Laser instruments, namely, LiDAR and terrestrial laser scanner (TLS), are another popular sensor type that is currently used for AGB estimation in tropical forest with high density and complex stand structures. An intensive investigation of the relationship between LiDAR properties with the AGB was carried out by Hamdan et al. (2020c) in 50 ha Pasoh Dynamic Plot (PDP) by using airborne LiDAR and a comprehensive census data. PDP is situated on a 50 ha dynamic plot in the Pasoh Forest Reserve in Negeri Sembilan, which is a lowland dipterocarp forest, a type of evergreen tropical forest. The LiDAR metrics have generated a lot of variables. These factors were compared to AGB calculated from census data. The CHM and a few matrices were determined to be the best predictors of AGB and were thus utilised to estimate AGB across the study area. The estimated AGB ranged from 52 to 718 Mg ha⁻¹, with a root mean square error (RMSE) of about 59 Mg ha⁻¹, with an accuracy of 83.36%. The study also demonstrated that estimating AGB in tropical forest by using waveform LiDAR can be improved by reducing RMSE up to 40 Mg ha⁻¹ as compared with other estimates from satellite imagery data.

Meanwhile, Solomon et al. (2020) explored the viability of terrestrial laser scanning (TLS) in the tropical forest of Malaysia for forest inventory and AGB estimate. Manual and automatic detection methods were used to identify individual trees. The manual and automatic detection methods produced an average tree detection rate of 99.6% and 93.8%, respectively. Using field diameter at breast height (DBH) as reference, the accuracy measured from TLS was confirmed. For manually and automatically measured TLS DBH, the root mean square error (RMSE) was 1.37 cm (6.6%) and 2.36 cm (11.5%), respectively. TLS-based tree height was also evaluated using the height of an airborne laser scanner (ALS) as reference, yielding RMSE of 1.74 m (9.30%) and 3.17 m (17.40%) for the manual and automatic methods, respectively. Finally, the variables extracted from the TLS data were used to calculate AGB. The R^2 value was 0.98, and the RMSE was 0.08 Mg. The findings of this study showed that TLS, as a nondestructive method, can accurately estimate forest characteristics and AGB under dense tropical forest circumstances. This suggestion was supported earlier by Abd Rahman et al. (2017). These instruments were not used alone or separately. An attempt to combine both ALS and TLS that was made by Muluken et al. (2018) found the integrative use of ALS and TLS can enhance the capability of estimating more accurately AGB or carbon stock of the tropical forests.

The selection of sensor systems, method, and techniques varied between geographical regions and the forest types being studied. High-resolution images were not missed in this application. Ahmad et al. (2021) conduct a thorough assessment of the literature on AGB estimation and mapping using high-resolution optical satellite images (with a spatial resolution of 5 m) from around the world. In 15 years (2004–2019), 44 peer-reviewed journal articles were published, according to the literature review. Asia had 21 studies, North America and Africa had 8, South America had 5, and Europe had 4. The published approaches for AGB prediction modelling and validation are examined in this review study. According to the literature review, QuickBird, WorldView-2, and IKONOS satellite photos were the most extensively employed for AGB estimations, with higher estimated accuracies, along with the integration of other sensors.

4 Remote Sensing for Tree Species Recognition

Forest trees species recognition and identification are among remote sensing applications that are being used and explored in the forestry sector in Malaysia. Various platforms including spaceborne and airborne, and multiple sensor systems are used to venture this application. The high diversity in species composition and distribution will definitely add to the complexity of the classification. Despite the fact that numerous methods have been used to identify tree species in forests, the challenges remain unanswered, and this application has yet to mature.

Ruhasmizan et al. (2013) used an airborne hyperspectral data to identify several timber species in Balah Forest Reserve, Kelantan. Spectral Angle Mapper (SAM) technique was applied and found that the highest spectral signature in NIR range was

Kembang semangkok (*Scaphium macropodum*), followed by Meranti sarang punai (*Shorea parvifolia*) and Chengal (*Neobalanocarpus heimii*). Meanwhile, the lowest spectral response was Kasai (*Pometia pinnata*), Kelat (*Eugenia* spp.), and Merawan (*Hopea beccariana*), respectively. The overall accuracy obtained was 79%. Another attempt was made by Misman et al. (2021) to use UAV-based OCITM-F hyperspectral imager sensor in identifying six tree species on the campus of Forest Research Institute Malaysia (FRIM). To find the best strategy to identify tree species, this study investigated different data formats and classification approaches. A log of spectral reflectance (LogR) and derivative of the log of spectral reflectance (DLogR) were evaluated using random forest (RF) and support vector machine (SVM) classifiers in addition to reflectance (R) and derivative (D) spectra. The Boruta approach was also utilised to minimise the data input's dimensionality. The results showed that the performance varied depending on the data input and classifier used. Reflectance spectra identified with the SVM classifier had the best accuracy of 72.6%, while the combination of derivative spectra and RF classifier had the lowest accuracy of 52.9%. Based on this study, the UAV-based OCITM-F hyperspectral imager sensor has the potential to be used to identify forest tree species in a tropical forest with acceptable accuracy.

This kind of study was also conducted in mangrove forest. Zulfa et al. (2020) measured in situ spectral signatures of 19 mangrove species to investigate whether mangrove species could be discriminated through spectral reflectance data. The research was carried out at the Matang Mangrove Forest Reserve, and the spectral signatures were captured with a handheld spectroradiometer. The study successfully distinguished 7 visible wave bands (400–700 nm), 9 NIR wave bands (701–1000 nm), 16 SWIR-1 wave bands (1001–1830 nm), and 19 SWIR-2 wave bands (1831–2500 nm) in the visible area. The study found that mangrove species' leaf spectral reflectance is low in the visible region (400–700 nm) due to excessive chlorophyll concentration. The most essential component in this variance seems to be leaf surface reflectance. Further, Zulfa et al. (2021) spectral information divergence (SID) algorithm was compared with that derived from the Landsat 8 using the SAM algorithm for the species. They found that the two methods offered different but complementary information with different rates of accuracy. The observed levels of classification accuracy for SID and SAM algorithm were at 84.95% and 85.21%, respectively.

Similar to the AGB studies, species recognition can also be conducted by using combination of sensors. Using aerial hyperspectral data, Nik Effendi et al. (2021) used a comparison classification strategy to investigate multiple classifiers. In addition, hyperspectral data was used to extract the crown of individual tree species for classification and estimate using the object-based image analysis (OBIA) approach. To decrease the data dimensionality and diverse training samples from the numerous species employed in this study, the minimum noise fraction transform (MNF) was used. When compared to other classifiers in the tropical forest, SVM and RF achieved the highest overall accuracy above 50%.

5 Remote Sensing for Forest Structure

Forest structure is the three-dimensional arrangement of trees and other plants, in combination with nonliving spatial elements such as soils, slopes, and hydrology. In short, structure is the physical geography of the forest, considered at a range of spatial scales. Remote sensing has been used for such assessments of forest structure in various ways. Satyanarayana et al. (2011) assessed the mangrove vegetation at Delta Kelantan based on ground-truth and remote sensing measurements. The mangroves are composed of several species including *Nypa fruticans*, *Sonneratia caseolaris*, *Avicennia alba*, *Rhizophora apiculata*, *R. mucronata*, and *Bruguiera gymnorhiza*, in order of dominance. The stem density and basal area were estimated using the point-centred quarter method (PCQM) at various ground locations. Land-use/cover classification and normalized differential vegetation index (NDVI) mapping for the delta were created using recent high-resolution multispectral satellite data (QuickBird 2006, 2.4 m spatial resolution of the multispectral images). The study found that there was a relationship between the (mean) NDVI and stem density.

Phua et al. (2014) used IKONOS image to delineate tree crown with dark object subtraction and topographic effect correction prior to watershed segmentation. The overall segmentation accuracy was 64% when compared to the field observation. The detection of crowns revealed a strong relationship with tree density. Furthermore, the satellite-based crown area exhibited the best association with the DBH observed in the field. They created a DBH allometric model that explained 74% of the variance in the data. The IKONOS-2 image was segmented to provide two crown variables: crown perimeter and crown area. By assuming a circular shape, the crown diameter was derived from the crown area. The DBH and thus AGB of the individual trees measured on the ground were then linked with these variables.

Focusing on the Matang Mangrove Forest Reserve (MMFR) in Perak Province, Malaysia, Otero et al. (2018) investigated the use of UAV imagery for retrieving structural information (i.e. height and AGB) on mangroves. The study suggested that UAV data are viable for retrieving canopy height and biomass from forests that were relatively homogeneous and with a single dominant layer. More advance assessments on tree crowns were made by Wan-Mohd-Jaafar et al. (2017, 2018) and Nordin et al. (2018) by using LiDAR and UAV hyperspectral data, respectively. The method, namely, individual tree crown (ITC) segmentation, was developed from the studies. The studies isolated successfully individual trees from the background vegetation and precisely delineate the crown boundaries by using separate processing methods for LiDAR and hyperspectral.

Coarser image resolution from Moderate Resolution Imaging Spectroradiometer (MODIS) was also used in vegetation structure assessment. A study conducted by Kanniah et al. (2021) used the leaf area index (LAI) and gross primary productivity (GPP) produced by MODIS to inspect the impact of fragmentation on the mangrove ecosystem process in Iskandar Malaysia, Johor. The impact on LAI and GPP due to fragmentation was found to rely on the patch characteristics, i.e. size, edge, and shape complexity.

Another attempt was made by Charissa et al. (2020) to use SRTM data to estimate growth progress of mangrove in Sabah. A tree-level approach was developed to deal with the substantial temporal discrepancy between the SRTM data and the mangrove's field measurements. A canopy height model (CHM) was derived by correcting the SRTM data with ground elevation and the annual growth of diameter at breast height was predicted from the CHM, while in Berkelah FR, Pahang, a study was carried out by Rozali et al. (2020) to extract feature changes in tropical rainforest cover using Landsat image and airborne LiDAR (ALS). Disturbance index (DI) derived from Landsat-8 OLI images was used together with an ALS height by using object-based segmentation process. The accuracy increased with the integration of ALS in Landsat image.

Looking at a larger scale with attention to the management practices in Matang Mangrove Forest Reserve (MMFR), Otero et al. (2019) used a time series (1988–2015) of Landsat data to (1) detect clear-felling events that take place in the reserve as part of the local management and (2) trace back and quantify the early regeneration of mangrove forest patches after clear-felling. From this series, they found that the average period mangroves recover after the clear-felling event was 5.9 ± 2.7 years. Continually Lucas et al. (2020a) used Japanese Earth Resources Satellite (JERS-1) SAR, ALOS PALSAR, PALSAR-2, and WorldView-2 to produce thematic and continuous environmental descriptors, including lifeform, forest age, canopy cover, AGB, and relative amounts of woody debris. The work was carried out under the framework of the Earth Observation Data for Ecosystem Monitoring (EODESM). In addition to the earth imaging satellites, topographic data from NASA Shuttle RADAR Topography Mission (SRTM) and TanDEM-X data were also obtained for the MMFR and the surrounding landscapes. The study was then supported by Lucas et al. (2020b) with additional UAV images as the high-resolution images' input to the structural characterization of mangrove stands in MMFR.

6 Limitation and Advancement in Remote Sensing

Tropical forests in Malaysia, with dense trees and canopies, various types and geomorphology of forest, various levels of horizontal and vertical strata, complex canopy structure, different management perspectives at various growth conditions, undulating topography, and cloudy atmosphere, always offer greater challenges as compared to the other forest types in the world. These to some extent hinder the assessments of certain biophysical properties of forests. However, with the recent advancements in sensor development, some of the challenges can be addressed. Additional spectral bands on board satellites with optical sensors, longer wavelength on SAR sensors (e.g. L-band and P-band), and more high-resolution satellites launched to the space will open wider windows for forestry applications, especially in Malaysia. Latest upgrades on UAV sensor system such as hyperspectral, multi-spectral, thermal, LiDAR waveform, and even close-range TLS with a mobile

capability will ensure that the measurement of biophysical and biochemical of trees can be conducted with zero contact to the trees.

The combination of multiple sensors such as optical with SAR and LiDAR with hyperspectral and UAV photogrammetry seems, in many cases, although cannot fully address some issues, to complement each other. Optical or synthetic aperture radar (SAR) system has its own potential in retrieving forest attributes, but several issues remain unaddressed. While optical remote sensing is often hindered by cloud, SAR systems are always limited by signal saturation and demanding in data processing. Besides, development of new and improvement on algorithms in image processing such as SVM, random forest, and artificial neural network (ANN) can provide alternatives to the analysis. The emerging new remote sensing data processing software, especially open source, also offers solutions for specific applications.

7 Opportunity

This review of remote sensing image analysis techniques, with reference to forest structural parameters, illustrates the dependence of spatial resolution to the level of detail of the parameters which may be extracted from remotely sensed imagery. As a result, the scope of a particular investigation will influence the type of imagery required and the limits to the detail of the parameters that may be estimated (Indu et al. 2019). The complexity of parameters that may be extracted can be increased through combinations of image-processing techniques. For example, multitemporal analysis of image radiance values or multispectral image classification maps may be analysed to undertake the assessment of such forest characteristics as area of forest disturbances, forest succession and development, or sustainability of forest management practices. Further, the combination of spectral and spatial information extraction techniques shows promise for increasing the accuracy of estimates of forest inventory and biophysical parameters.

It was clear from the review that the limitations of the traditional techniques lead to the development of most advanced technologies including remote sensing. The integration of the advanced technologies along with conventional field measurements can also be used for the accurate and effective measurement of the forest parameters. For example, the limitations of optical remote sensing in the estimation of forest structural parameters lead to the advancement of active remote sensing, e.g. LiDAR and SAR for forest mensuration. Dealing with large forest landscapes, upscaling concept might provide opportunities in forestry research (Rasib et al. 2018). It involves the combination of data sources at different spatial and temporal scales to produce accurate information at large coverage (Fig. 7).

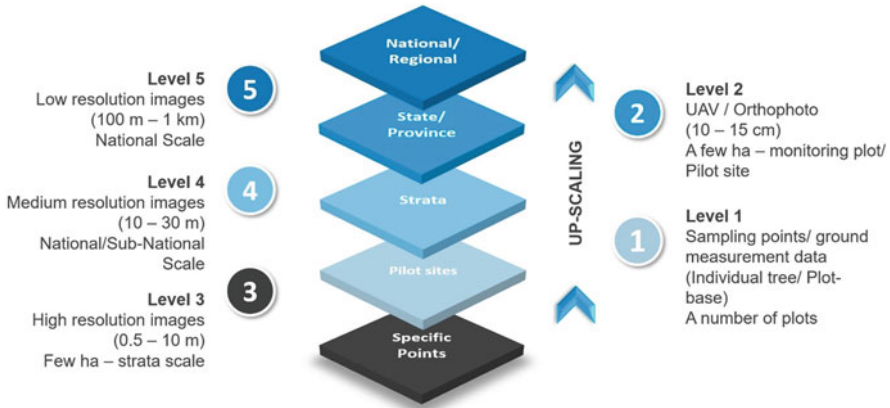


Fig. 7 The concept of upscaling in remote sensing

8 Conclusion

Although remote sensing technology has long been introduced in Malaysia, its application in forestry is still limited to mapping and monitoring functions. Even though there are studies on the assessment on various forest attributes, the scales are relatively confined to a small area and not ready for operational level. In addition, lack of exposure, expertise, and high cost are among the main challenges that need to be addressed to achieve the objectives of sustainable forest management and planning. Remote sensing can not only be used for obtaining information on forested land but also can be expanded for planning, logging operation, biodiversity assessment, and even wildlife beneath the forest canopies. The forestry sector in Malaysia is expected to last forever since the importance of forest ecosystem for the people is borderless. Remote sensing technology is also expected to become more advance in the near future along with the developments of the country. These advances in sensor technology are occurring concurrently with changes in forest management practices, requiring detailed measurements intended to enable ecosystem-level management in a sustainable manner. The use of this technology benefits the management of the area and encourages savings to the cost of labour, as well as benefits the storage of more efficient information for a long period of time. The accuracy of the data containing the information of forest areas is very important to determine the sustainability of both forestry and remote sensing sectors.

References

Abd Latif Z, Zaqwan HM, Saufi M, Adnan NA, Omar H (2015) Deforestation and carbon loss estimation at tropical forest using multispectral remote sensing: case study of besul tambahan

- permanent forest reserve. In: Proceeding of IEEE International Conference on Space Science and Communication (IconSpace), 10–12 Aug 2015, Langkawi
- Abd Rahman AR, Abu Bakar MA, Razak KA, Rasib AW, Kanniah KD, Wan Kadir WH, Omar H, Faidi MA, Kassim AR, Abd Latif Z (2017) Non-destructive, laser-based individual tree aboveground biomass estimation in a tropical rainforest. *Forests* 8(86):1–22
- Ahmad A, Gilani H, Ahmad SR (2021) Forest aboveground biomass estimation and mapping through high-resolution optical satellite imagery—a literature review. *Forests* 12:914
- Charissa JW, James D, Besar NA, Kamlun KU, Tangah J, Tsuyuki S, Phua MH (2020) Estimating mangrove above-ground biomass loss due to deforestation in Malaysian Northern Borneo between 2000 and 2015 using SRTM and landsat images. *Forests* 11:1018
- Cutler MEJ, Boyd DS, Foody GM, Vetrivel A (2012) Estimating tropical forest biomass with a combination of SAR image texture and Landsat TM data: an assessment of predictions between regions. *ISPRS J Photogramm Remote Sens* 70:66–77
- Hamdan O, Muhamad Afizzul M (2018) Time series maps of aboveground biomass in dipterocarps forests of Malaysia from PALSAR and PALSAR-2 polarimetric data. *Carbon Balance Manag* 13:19
- Hamdan O, Mohd Hasmadi I, Khali Aziz H, Helmi Zulhaidi MS, Norizah K (2014a) Forest biomass assessment with special reference to L-band alos palsar data. *Malays For* 77(1):1–18
- Hamdan O, Mohd Hasmadi I, Khali Aziz H, Norizah K, Helmi Zulhaidi MS (2014b) Factors affecting L-band Alos Palsar backscatter on tropical forest biomass. *Global J Sci Front Res* 14(3):51–63
- Hamdan O, Mohd Hasmadi I, Khali Aziz H, Norizah K, Helmi Zulhaidi MS (2015) Determining L-band saturation level for aboveground biomass assessment of dipterocarp forests in Peninsular Malaysia. *J Trop For Sci* 27(3):388–399
- Hamdan O, Muhamad Afizzul M, Kassim AR (2017) Synergetic of PALSAR-2 and sentinel-1A SAR polarimetry for retrieving aboveground biomass in dipterocarp forest of Malaysia. *Appl Sci* 7:675
- Hamdan O, Muhamad Afizzul M, Ismail P (2020a) Extents and distribution of mangroves in Malaysia. In: Hamdan O, Tariq Mubarak H, Ismail P (eds) Status of mangroves in Malaysia. FRIM special publication no. 50. Forest Research Institute Malaysia, pp 1–42
- Hamdan O, Muhamad Afizzul M, Siti Yasmin Y (2020b) Vegetation indices for identifying melaleuca forest from multispectral satellite sensors. *IOP Conf Ser Earth Environ Sci* 540: 012009
- Hamdan O, Muhamad Afizzul M, Leong YZ (2020c) Quantifying aboveground biomass over 50-Ha tropical forest dynamic plot in Pasoh, Malaysia using LiDAR and census data. *Borneo Sci* 41(2):30–40
- Hamdan O, Thirupathi RN, Norsheilla MJC, Nur Atikah AB, Muhamad Afizzul M (2021) Utilization of remote sensing technology for carbon offset identification in Malaysian forests. IntechOpen, London
- Indu I, Nair HMV, Nair JR, Nidamanuri RR (2019) Optical remote sensing for biophysical characterisation in forests: a review. *Int J Appl Eng Res* 14(2):344–354
- Ismail MH, Pakhriazad HZ, Norlida K (2011) Remote sensing for mapping RAMSAR heritage site at sungai pulai mangrove forest reserve, Johor, Malaysia. *Sains Malays* 40(2):83–88
- Kamaruzaman J, Souza GD (1997) Use of satellite remote sensing in Malaysian forestry and its potential. *Int J Remote Sens* 18(1):57–70
- Kanniah KD, Sheikhi A, Cracknell AP, Goh HC, Tan KP, Ho CS, Rasli FN (2015) Satellite images for monitoring mangrove cover changes in a fast-growing economic region in Southern Peninsular Malaysia. *Remote Sens* 7(11):14360–14385
- Kanniah KD, Kang CS, Sharma S, Amir AA (2021) Remote sensing to study mangrove fragmentation and its impacts on leaf area index and gross primary productivity in the South of Peninsular Malaysia. *Remote Sens* 13:1427

- Langnera A, Samejima H, Ong RC, Titin J, Kitayama K (2012) Integration of carbon conservation into sustainable forest management using high resolution satellite imagery: a case study in Sabah, Malaysian Borneo. *Int J Appl Earth Obs Geoinf* 18:305–312
- Lucas R, Otero V, Kerchove RV et al (2020a) Monitoring matang's mangroves in Peninsular Malaysia through earth observations: a globally relevant approach. *Land Degrad Dev* 32:1–20
- Lucas R, Kerchove RVD, Otero V, Lagomasino D, Fatoyinbo L, Omar H, Satyanarayana B, Guebas FD (2020b) Structural characterisation of mangrove forests achieved through combining multiple sources of remote sensing data. *Remote Sens Environ* 237:111543
- Minerva S, Malhi Y, Bhagwat S (2014) Biomass estimation of mixed forest landscape using a Fourier transform texture-based approach on very-high resolution optical satellite imagery. *Int J Remote Sens* 35(9):3331–3349
- Misman MA, Omar H, Yaakub SY, Ayop N, Musadad AAA, Shari NHZ (2021) UAV-based hyperspectral imaging system for tree species identification in tropical forest of Malaysia. *J Adv Geospat Sci Technol* 1(1):145–162
- Mohd Najib NE, Kanniah KD (2019) Optical and radar remote sensing data for forest cover mapping in Peninsular Malaysia. *Singap J Trop Geogr* 40(2):272–290
- Mohd Zaki NA, Abd Latif Z (2017) Carbon sinks and tropical forest biomass estimation: a review on role of remote sensing in aboveground-biomass modelling. *Geocarto International* 32(7):701–716
- Muluken NB, Hussin YA, Kloosterman EH (2018) Integrating airborne LiDAR and terrestrial laser scanner forest parameters for accurate above-ground biomass/carbon estimation in Ayer Hitam tropical forest, Malaysia. *Int J Appl Earth Obs Geoinf* 73:638–652
- Nik Effendi NAF, Mohd Zaki NA, Abd Latif Z, Suratman MN, Bohari SN, Zainal MZ, Omar H (2021) Unlocking the potential of hyperspectral and LiDAR for above-ground biomass (AGB) and tree species classification in tropical forests. *Geocarto International* 1990419
- Nordin SA, Abd Latif Z, Omar H (2018) Individual tree crown segmentation in tropical peat swamp forest using airborne hyperspectral data. *Geocarto International* 1475511
- Otero V, Kerchove RVD, Satyanarayana B, Columba ME, Fisol MA, Ibrahim MR, Sulong I, Mohd-Lokman H, Lucas R, Guebas FD (2018) Managing mangrove forests from the sky: forest inventory using field data and Unmanned Aerial Vehicle (UAV) imagery in the Matang Mangrove Forest Reserve, peninsular Malaysia. *For Ecol Manag* 411(2018):35–45
- Otero V, Kerchove RVD, Satyanarayana B, Mohd-Lokman H, Lucas R, Guebas FD (2019) An analysis of the early regeneration of mangrove forests using landsat time series in the matang mangrove forest reserve, Peninsular Malaysia. *Remote Sens* 11:774
- Phua MH, Ling ZY, Wong W, Korom A, Ahmad B, Besar NA, Tsuyuki S, Ioki K, Hoshimoto K, Hirata Y, Saito H, Takao G (2014) Estimation of above-ground biomass of a tropical forest in Northern Borneo using high-resolution satellite image. *J For Environ Sci* 30(2):233–242
- Rasib AW, Mohd Ali H, Alvin LMS, Kanniah KD, Idris NH, Omar H, Faidi MA, Dollah R, Ahmad MA (2018) Upscaling aboveground biomass estimation at low-land royal belum forest reserve using unmanned aerial vehicle image. *Int J Integr Eng* 10(4):140–150
- Rozali S, Abd Latif Z, Adnan NA, Hussin Y, Blackburn A, Pradhan B (2020) Estimating feature extraction changes of Berkelah Forest, Malaysia from multisensor remote sensing data using and object-based technique. *Geocarto Int* 37:3247–3326
- Ruhasmizan MZ, Ismail MH, Pakhriazad HZ (2013) Classifying forest species using hyperspectral data in Balah Forest Reserve, Kelantan, Peninsular Malaysia. *J For Sci* 29(2):131–137
- Satyanarayana B, Mohamad KA, Idris F, Mohd-Lokman H, Guebas FD (2011) Assessment of mangrove vegetation based on remote sensing and ground-truth measurements at Tumpat, Kelantan Delta, East Coast of Peninsular Malaysia. *Int J Remote Sens* 32(6):1635–1650
- Seo HS, Phua MH, Ong RC, Choi B, Lee JS (2014) Determining aboveground biomass of a forest reserve in Malaysian borneo using K-nearest neighbour method. *J Trop For Sci* 26(1):58–68
- Solomon MB, Hussin YA, Kloosterman HE, Ismail MH (2020) Forest inventory and aboveground biomass estimation with terrestrial LiDAR in the tropical forest of Malaysia. *Can J Remote Sens* 46(2):130–145

- Tangki H, Chappell NA (2008) Biomass variation across selectively logged forest within a 225-km² region of Borneo and its prediction by Landsat TM. *For Ecol Manag* 256:1960–1970
- Thang HC (1983) Application of remote sensing in agriculture and forestry in Malaysia. Paper presented at the Second Asian Agriculture Symposium, Manila, Philippines, 28 Feb–3 Mar 1983
- Thang HC, Tay YC, Cheong EC (1987) Remote sensing in forestry in Malaysia. Paper presented at the meeting of the Technical Working Group on Remote Sensing and Information System, Bangkok, Thailand, 13± 16 Aug 1987
- Vashum KT, Jayakumar S (2012) Methods to estimate above-ground biomass and carbon stock in natural forests—a review. *J Ecosyst Ecogr* 2:116
- Wan Abd Rahman WAHS (2016) Comparison results of forest cover mapping of Peninsular Malaysia using geospatial technology. *IOP Conf Ser Earth Environ Sci* 37:012027
- Wan Yusoff WA (1988) Application of landsat/SPOT digital and visual analysis as a tool for forest classification and mapping in lesong forest reserve, Peninsular Malaysia. ASEAN Institute of Forest Management Fellowship Report, 15 Mar–31 Dec 1988
- Wan-Mohd-Jaafar WS, Woodhouse IH, Silva CA, Omar H, Hudak AT (2017) Modelling individual tree aboveground biomass using discrete return lidar in lowland dipterocarp forest of Malaysia. *J Trop For Sci* 29(4):465–484
- Wan-Mohd-Jaafar WS, Woodhouse IH, Silva CA, Omar H, Abdul MK, Hudak AT, Mohan M, Klauber C (2018) Improving individual tree crown delineation and attributes estimation of tropical forest using airborne LiDAR data. *Forests* 9:759
- Wulder M (1998) Optical remote-sensing techniques for the assessment of forest inventory and biophysical parameters. *Prog Phys Geogr* 22(4):449–476
- Zulfa AW, Norizah K, Hamdan O, Zulkifly S, Faridah-Hanum I, Rhyma PP (2020) Discriminating trees species from the relationship between spectral reflectance and chlorophyll contents of mangrove forest in Malaysia. *Ecol Indic* 111:106024
- Zulfa AW, Norizah K, Hamdan O, Faridah-Hanum I, Rhyma PP, Fitrianto A (2021) Spectral signature analysis to determine mangrove species delineation structured by anthropogenic effects. *Ecol Indic* 130:108148



A Review on the Use of LiDAR Remote Sensing for Forest Landscape Restoration

Siti Munirah Mazlan, Wan Shafrina Wan Mohd Jaafar, Aisyah Marliza Muhmad Kamarulzaman, Siti Nor Maizah Saad, Norzalyta Mohd Ghazali, Esmaeel Adrah, Khairul Nizam Abdul Maulud, Hamdan Omar, Yit Arn Teh, Dzaeman Dzulkifli, and Mohd Rizaludin Mahmud

Abstract

Forest landscape restoration (FLR) is the process where vegetation is recovering in terms of its forest traits, ecosystem functionality, climate change mitigation, building up human livelihoods, and well-being in deforested and degraded forest landscapes by promoting accelerated forest regrowth. Several countries within the Global Partnership of FLR have made ambitious pledges to promote FLR

S. M. Mazlan · W. S. Wan Mohd Jaafar (✉) · A. M. Muhmad Kamarulzaman · E. Adrah
Earth Observation Centre, Institute of Climate Change, Universiti Kebangsaan Malaysia, Bangi, Selangor, Malaysia
e-mail: p113604@siswa.ukm.edu.my; wanshafrina@ukm.edu.my; p103420@siswa.ukm.edu.my; p113998@siswa.ukm.edu.my

S. N. M. Saad
Earth Observation Centre, Institute of Climate Change, Universiti Kebangsaan Malaysia, Bangi, Selangor, Malaysia

Universiti Teknologi MARA, Cawangan Perlis, Arau, Perlis, Malaysia
e-mail: p95200@siswa.ukm.edu.my

N. Mohd Ghazali
Faculty of Science and Technology, Universiti Kebangsaan Malaysia, Bangi, Selangor, Malaysia
e-mail: p106873@siswa.ukm.edu.my

K. N. Abdul Maulud
Earth Observation Centre, Institute of Climate Change, Universiti Kebangsaan Malaysia, Bangi, Selangor, Malaysia

Faculty of Engineering and Built Environment, Department of Civil Engineering, Universiti Kebangsaan Malaysia, Bangi, Selangor, Malaysia
e-mail: knam@ukm.edu.my

H. Omar
Forest Research Institute Malaysia, Kepong, Selangor Darul Ehsan, Malaysia
e-mail: hamdanomar@frim.gov.my

© The Author(s), under exclusive license to Springer Nature Singapore Pte Ltd. 2022

M. N. Suratman (ed.), *Concepts and Applications of Remote Sensing in Forestry*, https://doi.org/10.1007/978-981-19-4200-6_3

globally and to restore at least 350 million ha of degraded and deforested lands by 2030 worldwide. FLR accountability has been limited to the schematic quantification of how much the land area in the forest has been restored and how many trees have been replanted for conservation purposes. Natural regeneration, old-growth forests, and mixed-species plantations of different types of species are some of the FLR strategies. Monitoring the outcome of complex forest restoration efforts requires appropriate methods and sophisticated tools. The logical procedures are by distinguishing the different forest cover types across different forest landscapes and second by identifying their respective values to ecosystem services and biodiversity conservation. Canopy structural attributes are one of the most important parameters that can act both, distinguishing the forest cover types and indicator to the forest respective values. Traditional assessments rely heavily on field-based inventory, which is cost-prohibitive and difficult to track a million hectares scale progress. Light detection and ranging (LiDAR) remote sensing has emerged as a great alternative to monitoring forest structure, function, and composition. With the ability to penetrate the forest canopy it allows an accurate measurement of structural canopy parameters along with the vertical profile. This paper will review the trends of FLR and the use of LiDAR remote sensing technology to monitor forest restoration outcomes towards achieving sustainable forest management practices.

Keywords

Forest landscape restoration · LiDAR · Forest type · Forest structure · Structural attributes

1 Introduction

The area of tropical forests has been drastically changing over the last several decades, with forest cover declining by 2101 square kilometres every year (Hansen 2013). Massive climate change consequences have resulted in increasingly one of the biggest carbon dioxide emissions across Southeast Asian nations, as a result of

Y. A. Teh

School of Natural and Environmental Sciences of Newcastle University, Newcastle upon Tyne, UK
e-mail: YitAm.Teh@newcastle.ac.uk

D. Dzulkifli

Tropical Rainforest Conservation and Research Centre, Kuala Lumpur, Wilayah Persekutuan Kuala Lumpur, Malaysia
e-mail: dzaeman@trcrc.org

M. R. Mahmud

Geoscience & Digital Earth Centre, Faculty of Built Environment & Surveying, Universiti Teknologi Malaysia, Skudai, Johor, Malaysia
e-mail: rizaludin@utm.my

excessive deforestation. Malaysia's progress and economic development activities also contribute to increased carbon emissions through land clearance and conversion of forested areas to other residential and commercial usage sectors such as farming, habitation, quarrying, and fishery (Begum et al. 2020).

Issues and local efforts have generated democratic influence for the restoration of 150 million ha of forest landscapes by 2020 and 350 million ha by 2030. The Bonn Challenge is based on the forest landscape restoration (FLR) concept, which varies from more efficient ecological restoration in that human livelihoods and biodiversity protection are given equal importance (Stanturf et al. 2017). Ecological restoration approaches vary, from singular or mixture plantings for storing carbon (Nave et al. 2019), to focused species selection to meet animal habitat needs (Hale et al. 2020). Therefore, assessing the efficiency of ecological restoration in restoring the desired ecological resources and activities is a significant difficulty.

Both biodiversity protection and human livelihoods are top priorities for FLR. It involves planting new trees, protecting wildlife reserves, regenerating forests, creating ecological corridors, agroforestry, riverbank plantings to preserve streams, managed plantations, and agriculture. Within and across whole landscapes, this pattern of communicating land cover begins – a level whereby ecological, social, as well as economic goals maybe harmonised (Matrushka 2020). FLR is a method for regaining, improving, and maintaining vital ecological and social services in a degrading or deforested landscape over time, as well as increasing the resilience against ecological and societal transformations.

Monitoring is a key aspect of determining the efficacy of restoration efforts. It is critical to approach assessment in order to advise future efforts and prevent restoration failures (Zhang et al. 2019). Key response qualities must be defined in order to quantify the short- and long-term efficacy of restoration operations (Maginel et al. 2016). In many situations, indicator species are employed to assess the progress of the ecological restoration in comparison to a reference system. In a broader sense, the structural complexity of an ecosystem, such as a forest, is regarded as a reliable and repeatable indicator of biodiversity and can reflect an ecosystem's health and function (Hao et al. 2021) and also has provided a reference condition against which to guide (and assess) the efficiency of restoring a decreased environment (Perring et al. 2015). Field data normally monitor forest restoration results by assessing the forest structure parameters, such as canopy gap, the diameter of the trees and the height (estimates of biomass and carbon stocks are possible), as well as diversity factor. Furthermore, restoring spatial structure has advantages that are connected to a variety of ecosystem services. The abundance of deadwood and coarser deadwood, for example, has a direct impact on ecosystem functions and animal habitats (Camarretta et al. 2020). In reality, canopy layers have a positive impact on bird populations and the mix of tree species (Viani et al. 2017). Aboveground biomass (AGB) is a significant variable to monitor in restoration efforts since it is among the most essential restoration results in tropical forest areas (Aragón et al. 2021). This is a good proxy for a variety of other variables related to tropical forest succession (Chazdon 2014). Another important ecological indicator in restoration plantations is

canopy openness, which is linked to the reduction of grasslands and natural forest regrowth (Viani et al. 2017).

Remote sensing is being effectively utilised to obtain forest structural information that might aid decision-making. Nevertheless, the direct carbon storage estimate in moderate to high biomass forests continues to be significantly difficult for remote sensing. While it has been very effective in quantifying the biophysical properties of vegetation in places with low plant canopy cover, quantifying vegetation structure in areas with a leaf area index (LAI) more than three seems to be less successful.

LiDAR (light detection and ranging) is a relatively new sensor technology gaining considerable interest in the forestry sector as a speedy and effective method for forest inventories. In contrast to passive remote sensing techniques such as photogrammetric mapping, active remote sensing techniques such as airborne LiDAR may immediately capture precise three-dimensional point cloud data to describe the earth's geomorphologic profile (Hui et al. 2019). Typically, airborne LiDAR scanners can classify first/last or numerous returns. Furthermore, because they may both be georeferenced using the same direct exterior orientation (direct EO) methods, LiDAR scanners can be coupled by a different camera system to assist in interpreting LiDAR returns. There are also full-waveform aerial LiDAR systems available, albeit the usage in forestry can be limited to the research community (van Leeuwen and Nieuwenhuis 2010). Models constructed utilising ALS data were the most exact, while incorporating information from various sources resulted in a negligible improvement in structure prediction (Dash et al. 2016).

2 Forest Landscape Restoration

2.1 Definition

Modern commercialisation by humans and modification of the world's ecosystems have resulted in extensive habitat extinction and reductions in ecosystem conditions, resulting in decreased ecosystem production (Bullock et al. 2011; Muhmad Kamarulzaman et al. 2022). Although recent data reveal that deforestation is now starting to decrease, the overall amount of deforestation remains high (OECD-FAO 2021). In Southeast Asia, for example, Fox and Vogler (2005) stated that up to 49% of these additional agricultural areas have been subsequently developed, abandoned, and become shrub, bush, or other types of secondary forest. Unplanned deforestation has resulted in several social, economic, and environmental issues (Chomitz 2007; Wan Mohd Jaafar et al. 2020a, b). In the tropics, this is particularly true. Despite the riches created by cutting tropical forests, many local people live mainly around these settings, and biodiversity and soil have suffered significant losses (Saad et al. 2020). However, several developments are currently taking place that will impact the amount towards which existing forest areas are preserved and the chance of deforested areas being restored.

Restoration ecology has made great progress in recent years, both as a scholarly field and as useful management of environmental management. Significantly,

restoration ecology has improved the environmental management system since it can enhance human livelihoods and biodiversity. Chazdon (2008) gives a present overview of forest ecological restoration, emphasising the work done in many nations to reverse current forest degradation and loss. However, as noted by Newton and Tejedor (2011) the effects of bigger-scale forest restoration along with future landscape’s composition and function, as well as the species that populate them, are still unknown. There is also limited research on the consequences of various restoration procedures of the restoration of ecosystem services and their connections to biodiversity. Traditional techniques have been site-based, focusing on a few forest products, relying primarily on non-native tree planting, and failing to deal with the core causes of forest loss and degradation. Forest landscape restoration is one of the restoration approaches examined in this research (FLR). In response to the widespread inadequacy of more traditional techniques for forest restoration, the World Wildlife Fund (WWF), as well as the International Union for the Conservation of Nature (IUCN), devised the FLR idea during a workshop in 2000 (Mansourian et al. 2005a). Therefore, the outcome resulted in several principles of forest landscape restoration.

2.2 Principles of Forest Landscape Restoration

An effective FLR, according to Mansourian et al. (2005a, b) and Newton and Tejedor (2011), is forward-looking and dynamic, focusing on building landscape resilience and developing future choices to modify and further optimise ecosystem products and services when societal requirements change or new obstacles emerge. It integrates a number of guiding of six principles of forest landscape restoration (Fig. 1).



Fig. 1 Principles of forest landscape restoration (Source: IUCN)

2.2.1 Focus on Landscape

The landscape is a human construct that can have a variety of interpretations according to whoever is saying. A conservation effort will generally operate within a predetermined ‘conservation landscape’, which is frequently based on considerations such as the amount of land required to preserve functioning ecosystems and species. It’s also essential to identify any ‘culture landscapes’ nested inside or overlapped with the restoration landscape, in addition to picking the conservation landscape. A cultural landscape is described as an area of particular importance to people who live in or visit the landscape often, such as a community, a strip of land utilised by nomadic people, or a forestry concession (Maginnis and Jackson 2002).

FLR occurs throughout and across landscapes, rather than specific locations, and represents mosaics of overlapping land cover and management methods under multiple ownership and governance regimes. Ecological, social, and economic interests can be synchronised at this scale. The WWF has several Ecoregion Action Programs, many of which are in forest ecoregions (Bowling 2004). The WWF’s six worldwide Target Driven Programs (on forests, marine and freshwater species, climate change, and toxics) aim to complement efforts in key conservation ecoregions while also having global scope. In the case of forests, the link may be described as in Fig. 2.

The forest program is trying to improve the integration of its goals and ecoregion programs. It has focused on priority landscapes in key ecoregions identified through the ecoregion conservation process. Each priority region, or priority conservation landscape, will comprise several sites that form a landscape mosaic. Conservation landscapes range in size from a few tens of thousands of hectares to a million hectares or more, and techniques must adapt to account for these differences. In theory, a program like this could be implemented across an entire ecoregion.

When considering landscape-scale advantages, it is necessary to pay greater attention to the aggregate worth of numerous sites rather than individual sites. One possibility is a woodland patchwork similar to the ones in Fig. 3 comprises a scattering of protected areas of multiple IUCN categories (and thus various management regimes) for forests with the most significant conservation efforts; some handled native woodland to provide a mix of biodiversity and human benefits; some replanned wood products and fibre plantations; forests controlled for environmental consequences such as watershed protection; and careful restoration is

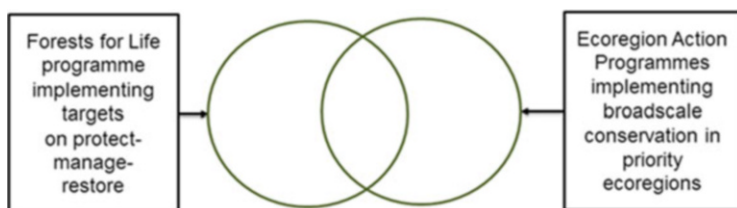


Fig. 2 The link between Forest for Life and Ecoregion Action (Source: Bowling 2004)

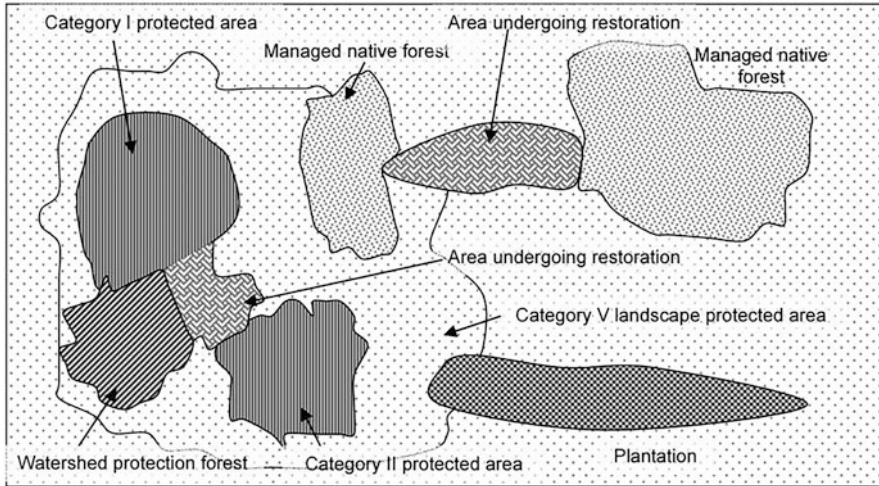


Fig. 3 Scattering of protected areas of multiple IUCN categories (Source: Bowling 2004)

planned at the landscape scale to achieve maximum efficiency. Tropical forests would also need to coexist towards other land uses such as farming and population.

The specific combination would vary depending on location, forest type, and biome and would most likely appear considerably different in a region that still included vast tracts of natural woods. However, the notion of pursuing a balanced combination of preservation, management, and restoration that provides biological, ecological, economic, and social advantages while opposing harmful change remains unchanged.

2.2.2 Preservation and Enhancing Natural Ecosystems Within Landscapes

Tropical forests and other ecosystems are not converted or destroyed as a result of FLR. This principle relates to preserving and restoring the dynamic behaviour and interconnectivity of all forms of tropical forest, meadows, scrublands, and swamps within a landscape to increase economy, ecosystem functions, and biomass production. It helps to improve forest and other ecosystem conservation, recovery, and long-term management (Chazdon et al. 2019). Several tropical forests are decreased—but not damaged—due to human activity and conservation areas, including trees and timber harvesting, hunting, crop production, and mining. It is critical to consider this degradation as a type of bad forest ecosystem that may be corrected and restored in order to properly address it. The intention or duty to maintain ecological and related cultural traditions of such landscape areas (Higgs and Hobbs 2010) related towards the structural and functional of ecosystems will promote ecological restoration inside such conservation zones.

2.2.3 Work Collaboratively with the Stakeholders and Participate in Government

To have the impact that's required, FLR requires very well-organised and scheduled participation of stakeholders. This principle emphasises the engagement of all relevant stakeholders—including women, young people, and vulnerable groups—in planning and decision-making processes, including setting goals and strategies, deciding on implementation and benefit-sharing methods, and carrying out monitoring, assessment, and review. FLR success is built on long-term engagement and participation between members and stakeholders (Egan et al. 2011), especially when protected areas include permanent or native indigenous populations. Some nations have a legal responsibility to consult traditional and indigenous peoples and informed permission should always be acquired for projects on their land. Engaging stakeholders in preparation, implementation, and mutual learning may promote communication of ownership and loyalty, as well as a population of supports (Hill et al. 2010) for forest restoration. Awareness of forest landscape restoration can provide useful experience and knowledge (Berkes et al. 2000). Paying attention and being willing to act on what is heard may assist in optimising community benefits, uncovering possible concerns, effectively engaging in restoration, observations, and reuniting communities with nature. Hence, FLR can help prevent degradation and assist in attaining larger reserved territory and biodiversity environmental conservation by encouraging people, especially visitors, to protect areas.

2.2.4 Adapt to the Local Environment Through a Variety of Methods

Every community, landscape, and ecosystem are different, and FLR interventions need to take this into account to succeed. The best way to ensure that FLR is well adapted to local conditions is for local stakeholders to be fully involved in its development, implementation, monitoring, and assessment. They were generating local benefits, including opportunities to increase incomes and develop sustainable supply chains. Residents and stakeholders, travellers, and staff of the protected area who interact with the public are the major targets of communication initiatives. When different methods and techniques are used to target different audiences, communication and learning become more successful. Local gatherings, guided tours, talks, exhibitions, and the utilisation of a variety of media were established as communication and learning choices. They were given to a varied audience in a variety of locations (Keenleyside et al. 2012).

2.2.5 Restore Multiple Functions for Multiple Benefits

Successful FLR uses locally based expertise to restore a wide variety of economic, social, and ecological processes within such a landscape and provide environmental products and solutions that appropriately benefit stakeholders. According to the handbook by (Keenleyside et al. 2012), many environmental functionalities also at landscape scale are strongly related to the existence of forest resources that can be managed or regenerated to satisfy many complementary purposes. Although the multifunctional organisation is not a dominant approach in the forest sector, in

reality, examples are developing via FLR spanning from the local level, such as community forestry systems, to the large scale, including such jurisdictional programmes to implement REDD+ techniques.

2.2.6 Manage Adaptively for Long-Term Resilience

The ability of a system to absorb disturbance and reorganise while experiencing a change in order to keep the same function, structure, identity, and feedback is referred to as resilience (Walker et al. 2004a, b). An ecosystem's resistance to change is a key component of its resilience. FLR actions such as implementing an adaptive management system and re-establishing natural stream flow, removing invasive species, and providing migration/dispersal corridors between protected areas contribute to resilience by maintaining diversity, continuously measuring the biophysical dimensions of the landscape, and periodically assessing vulnerability to climate change and evolving gene pools over time (Elmqvist et al. 2003; Walker et al. 2004a, b). Factors such as ecologically effective population sizes, genetic and functional diversity, densities of highly interactive species, ecological community tolerance to extreme events, and microtopographic diversity are also important considerations in restoration strategies aimed at maintaining or restoring resilience and encouraging open access to and sharing of information and knowledge (Gilman et al. 2010).

3 Understanding Forest Types

The three main forest biome categories found throughout the world are boreal, temperate, and tropical forests. Forest biomes are classified into broad categories based on their distribution by latitude, starting with the most northern (boreal) and progressing through the temperate and tropical zones (Landsberg and Waring 2014). Figure 4 shows the distribution of the main forest biome around the world.

Boreal forest, also known as taiga, is characterised by evergreen coniferous trees with needle-like leaves. Boreal forests cover a large area of Eurasia and North America, with two-thirds of them in Siberia and the remainder in Scandinavia, Alaska, and Canada. Temperate forest is made up of broad-leaved plants that are leafless during winter. This forest type is found only in Europe, eastern Asia, and eastern North America in the northern hemisphere. Closer to the equator, tropical forest is a lush forest found in wet tropical in both uplands and lowlands. It is one of the world's biggest biomes characterised by a dense upper canopy of broad-leaved trees (layer of foliage) and supports an abundance of vegetation and other life (Armstrong 2018).

Forests are shelters to the million flora and fauna species in this world, supplying ecosystem services essential to agriculture, communities, and humans. Forests are identified as ground spanning more than 0.5 ha with trees above 5 m and with a cover for the canopy higher than 10%, or trees able of reaching these threshold limits in their natural environment. There are some exceptions, such as land that is mainly used for agricultural or municipal purposes. Forests cover 31% or 4.06 billion ha of

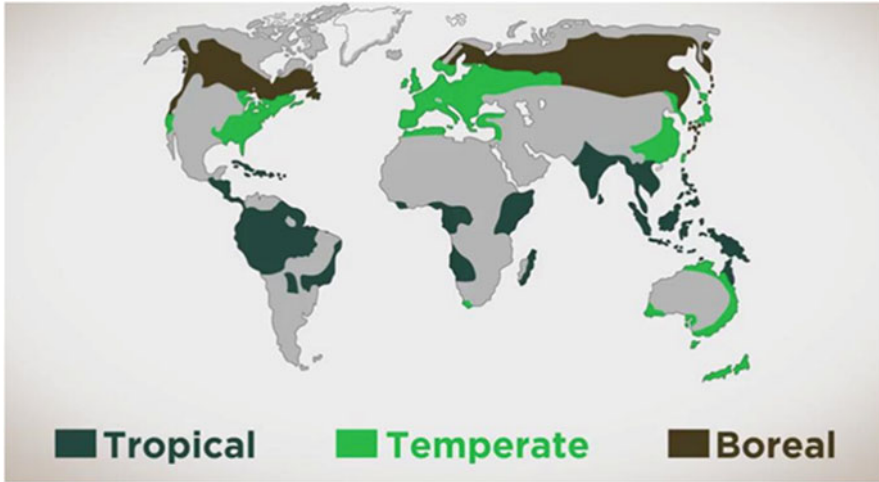


Fig. 4 The distribution of the main forest biome around the world (Source: plantlet.org)

the global land area. About half of the forest area is relatively undisturbed, and more than a third is primary forest (FAO 2020).

While forest cover on a global scale decreased, forest cover is rising in several regions as a result of the expansion of ‘new forests’ (i.e., secondary forests, plantations, and other woody vegetation). In this context, forest land has been categorised as primary forest, secondary forest, and restored forest (Fig. 5).

3.1 Primary Forest

Primary forests are recognised as having an aesthetic, cultural, and natural conservation value due to their content. It has become a diverse host to a variety of magnificent flora and fauna and is critical for maintaining biodiversity as well as ecological processes. The concepts of primary forest which are also known as old-growth forest or virgin forest was described as a forest land with naturally regenerated forest growth of a native species and not facing any obvious or visible human activities and any significant disturbance to the forest ecology process (FAO 2015). The ecosystem of primary forests is dominated by large, aged forest trees of mixed-species forest community and uneven-aged population distribution. According to the World Resources Institute (2021), it is estimated that only 21% of forest distribution around the world is categorised as remaining primary forest; 35% of these intact landscapes are found in South America, specifically in Brazil’s

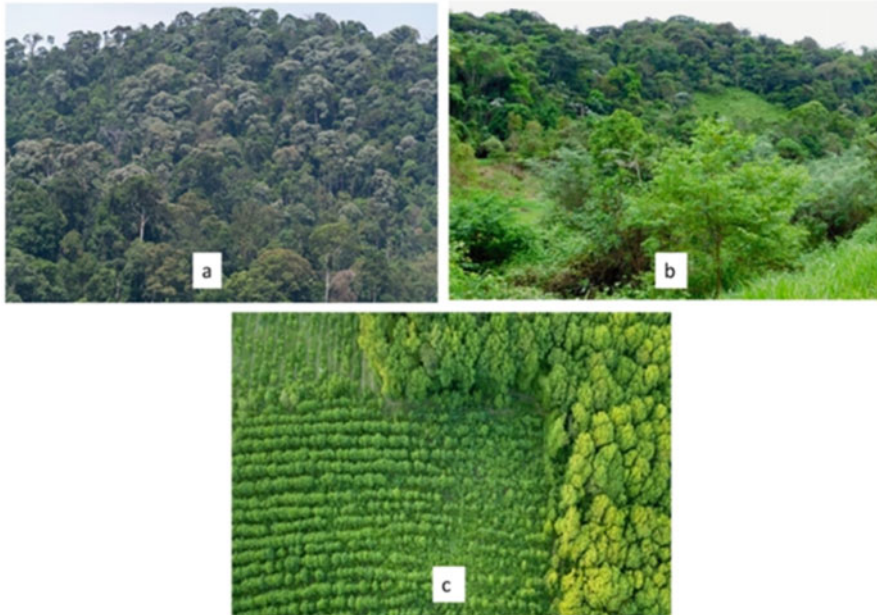


Fig. 5 (a) Primary Forest (source: rainforestjournal.com), (b) Secondary Forest (Source: oneearth.org) and (c) Restored Forest (source: europeanscientist.com)

Amazon rainforest; 28% in North America, particularly Canada and Alaska; and 19% in North Asia (world's largest boreal forest) and South Africa accounting for around 8% of the total. South Asia Pacific has only 7% of intact virgin forest left all over the world and merely about 3% of the world's remaining primary forests exist in Europe, and more than 150 km² is removed each year (Worldatlas 2021).

The nature of the primary forest is determined by its characteristic and natural coverage. This forest stands with a complex structure such as multiple horizontal layers, gaps of foliage within the canopies, massive standing dead plants, and logs laying on the forest ground. The topography of the primary forest can be described as pit and mound, and in a tropical region, it lies on peak and valley ground structure. The nature of forest trees in primary forest landscapes is massive, tall, and aged and they may have similar species with secondary forests (Kormos et al. 2016). The Food and Agriculture Organization of the United Nations FAO (2015) had underlined the main characteristics of primary forest or old-growth as the forested landscape which displays a natural forest-growing process, such as natural species formation, the existence of deadwood, age structure, and natural growth of forest regeneration. The landscape of primary forest is sufficiently wide to preserve its natural composition, without any sign of substantial human interference, or if any, it occurred a long time ago which allowed the forest structure and its composition to be re-constructed and regenerated.

The primary forest ecosystem is an ecological unique landscape that offers significant value that is needed to be maintained and managed for a variety of purposes due to its importance towards the overall forest ecosystem. This complex structure supports a variety of wildlife, plants, and endangered species (Gilhen-Baker et al. 2022), and decaying woods and forest residue play a significant influence on the composition of its habitats and nutrient cycle (Hilbert and Wiensczyk 2007). Due to its aged and undisturbed condition, primary forests retain more carbon than other forest types which help in stabilising the earth's climate and are usually irreplaceable in a biodiversity context. Even if forest regrowth occurs, the recovered secondary forest will not be able to equal the carbon and biodiversity values of a primary forest for several decades or longer (Hilbert and Wiensczyk 2007). The destruction of these forests causes carbon to be emitted into the atmosphere and causes greenhouse gas (GHG) emission, leading to the risk of global climate change (Wan Mohd Jaafar et al. 2020a, b). In addition, primary forest helps protect communities and the environment from natural disasters including forest fires, landslides, and floods and simultaneously acts as a natural water reservoir for the needs of life (Kormos et al. 2016). For indigenous people and local people who live in or near them, primary forest is equally essential because of their enormous biological productivity. The forest provides shelter as well as essential resources such as food, medicine, and freshwater (Kormos et al. 2016).

Primary forest had faced great challenges and threats including human disturbances, natural disasters including forest fire, landslides, species, and plant disease, and forest conversion to agriculture. Consequently, vast species of plants and wildlife were threatened (Betts et al. 2017), and the forest landscape was exposed to massive damage and altered the forest biodiversity and global climate. Logging and forest clearing also become major factors of the challenge to sustain the primary forest. As a result, the primary forest was declining all over the world due to the difficulties in maintaining and replacing the forest cover.

3.2 Secondary Forest

More than 50% of the global tropical forests are not primary forests but naturally regenerating forests, also known as secondary forests. In the next few decades, secondary forests will account for a significant portion of the global total forest area (FAO 2010). A secondary forest is a forest that regenerates largely naturally or unnaturally following disturbances caused by humans or nature. The main contributor to forest transition from primary to secondary forest is agriculture. Agriculture remains the primary driver of global deforestation, and agricultural, forestry, and land policies frequently conflict (FAO 2016).

Secondary forests mainly regenerated naturally after significant disruption of the primary forests exhibits significant forest structure and/or species composition differences compared to pristine primary forests (FAO 2003). Secondary forest vegetation is grown through either natural or artificial regeneration. Regeneration occurs naturally when seeds are dispersed without human intervention. The process

regenerates forests through self-sowing seeds, root suckers, or coppicing, while artificial regeneration involves direct seeding and planting (Huss 2004).

Secondary forests differ significantly from the nearby primary forest in terms of forest structure and/or canopy species composition, goods, and services. However, compared to plantation forests, naturally regenerating forests make a greater contribution to biodiversity conservation and offer a wide range of advantages and certain ecosystem services (Brockhoff et al. 2017). Secondary forests are also viewed as having greater potential than primary forests in some ways. For instance, it has been demonstrated secondary forests sequester tenfold the amount of atmospheric carbon as CO₂ as primary forests (Poorter et al. 2016).

3.3 Restored Forest

The restored forest is where the forest area has been restored from degradation and deforestation. In the context of forest restoration, this refers to restoring the ecological functions through the assisted or unassisted process of natural regeneration of the area to benefit humans (contribute to rural economies and livelihoods), wildlife, and the environment (Chazdon et al. 2020).

Restoration goals may be classified broadly into diverse strategies such as *rehabilitation reconstruction*, *reclamation*, and *replacement*. The term *rehabilitation* refers to the process of re-establishing a damaged ecosystem's desired species composition, structure, or processes. *Reconstruction* is the process of re-establishing native plant communities on land previously used for another purpose, such as crop production or pasture. *Reclamation* describes seriously degraded land that is generally empty of vegetation and is frequently the result of extraction of underground resources, such as mining or oil and gas drilling work platforms, and *replacement* will involve replacing species that are being moved in changes of the climate resulting in the emergence of previously unknown species or genotypes of familiar species for an extended period.

Given the active human activities and natural disasters, many forest areas are extremely disturbed resulting in their ecological function being in doubt. Hence, forest restoration is urgently needed as a sustainable plan to recover the forest function and improve the quality of community well-being in this degraded forest (Mansourian et al. (2005a, b); César et al. 2021). Restored forests offer many benefits to the forest landscape ecology and human society. According to César et al. (2021), restored forest benefits can be categorised into several aspects: (1) ecology benefit, (2) economic benefit, (3) socio-economic benefit, and (4) human aspect. For the ecology aspect, forest restoration may generate carbon sequestration towards climate change mitigation and biodiversity conservation and serves to protect water and soil (Báez et al. 2011; de Souza et al. 2016). In economic aspect, restoration of the forest is believed to help enhance the productivity of the forest land, help in food security issues since forests become the sources of food to certain communities, able to generate new jobs and income for the community, and increase the forest-related product for trading purposes (Adams et al. 2016). Forest restoration is offering a

great benefit to the improvement of human well-being as well as socio-economic outcome through its non-material benefits. The well-restored forest landscapes can enhance the quality of the environment and create a potential recreational site for eco-tourism (Chadourne et al. 2012; Adams et al. 2016) as well promote the improvement of physical health (César et al. 2021).

Monocultures may be an option in a forest restoration context, where fast-growing tree species with worldwide demand potential for timber are readily available (Cummins et al. 2012), where it is advantageous to generate rapid revenue for the local community. However, the planting of multiple species, on the other hand, is also necessary since different species frequently affect distinct ecosystem functions; focusing exclusively on a single function will grossly underrate the biodiversity necessary to sustain an ecosystem with various purposes at numerous times and locations in an altering environment (Isbell et al. 2011).

4 Light Detection and Ranging (LiDAR)

4.1 An Overview of LiDAR

There has been a growing interest in using light detection and ranging (LiDAR) in forestry applications for measuring forest characteristics in the last two decades. LiDAR is an accurate distance measurement technology based on measuring the travelling time of laser pulses between the instrument and the target. This measurement is enabled by sending narrow beams of near-infrared light and recording the return time. LiDAR instruments are primarily mounted on airborne platforms where a LiDAR system registers the instrument position and orientation for the returned pulses using a GPS interior measurement unit (IMU) in order to determine the target coordinates. In a forest environment, LiDAR penetrates the forest canopy and records different reflections from different parts of the plants describing the vertical structure of the forest canopy. These multiple returns per pulse energy are stored either as discrete points or as a full waveform.

In a discrete LiDAR, a system predefined threshold is used to distinguish a true return from noise and the true discrete returns are recorded as coordinates and intensity when the return energy exceeds the predefined threshold. Common current systems record multiple returns including the first (top of canopy), last (ground surface), and three other intermediate returns. In the case of the full-waveform LiDAR, the entire energy pulse responses are stored as a function of time. This waveform characterises the multiple targets' vertical structure from the upper canopy to the ground surface within individual pulses.

LiDAR systems in forestry are also classified as small- or large-footprint LiDAR. Small-footprint LiDAR is usually operated on low-flying altitude air platforms with a scanning instrument that goes back and forth with a beam diameter at intersecting surfaces of less than 1 m (5–30 cm). It records the returned signal as discrete points at high sampling densities, while the flying speed and altitude determine the number of shots per square meter according to the intended application. The large-footprint

LiDAR is commonly seen as a full waveform. In these instruments, a larger beam diameter (between 5 and 25 m) at intersecting surfaces is used in a cross-track scanning system where the signal is averaged across the footprint and used to sample the vegetation cover (Dubayah and Drake 2000; Drake et al. 2002).

Through enabling the direct measurements of the top of canopy elevation, ground topography, and vertical distribution, a wide range of forest characteristics can be derived (Dubayah and Drake 2000). Forest canopy height can be typically calculated directly by subtracting a digital elevation model (DEM) fitted to the return classified as ground points from other returns. Other characteristics can be modelled or inferred based on these directly measured attributes either in a plot scale or individual tree scale analysis (e.g. aboveground biomass could be derived based on individual tree dimensions and existing metrics or using multiple regression analysis between LiDAR-derived attributes and field data to derive biomass at plot scale).

5 LiDAR in Monitoring the Effectiveness of Forest Restoration

Forest structural attribute is a crucial factor in the estimation of aboveground biomass. Therefore, many studies have been conducted to find the best finding and give the best improvement and new technologies. In a nutshell, precise and consistent assessments of planted forest structural characteristics are critical for forest managers to make long-term sustainable forest management choices (Ozdemir and Karnieli 2011). On the other hand, remote sensing imaging is more useful when assessing forest restoration due to its capacity to identify variations in locations that are difficult to analyse from the ground (Liu 2019). Light detection and ranging (LiDAR) is one of the current active remote sensing technologies that can penetrate the vegetation canopy (Asner and Mascaro 2014) and describe the three dimensions of forest structure (Almeida et al. 2016) allowing for AGB assessment and canopy openness over enormous regions (Almeida et al. 2019).

6 LiDAR in Quantifying Structural Attributes

6.1 Tree Dimensions

Tree species are classified based on the shape and geometry of their branches (Koenig and Höfle 2016). As well as height information, multiplex geometric metrics extracted from LiDAR which captures tree spatial neighbourhood data in 3D or 2D (two-dimensional)—such as grid, raster, voxel, or height layers—are beneficial. Utilising LiDAR-derived data, we quantified the 3D texture, leaf clustering degree, foliage clustering scale, and gap distribution of a single tree in horizontal and vertical directions. The approach attained an overall accuracy of 77.5% ($k = 0.7$) for the categorisation of four species. According to Li et al. (2013) tree extraction should be improved to further improve the classification accuracy. A method for

categorising conifer species according to their inside and outside crown structure was proposed by Harikumar et al. (2017). Using 3D region growth and key element analysis, this model accurately describes the branch structure. 94.7% accuracy was achieved for species categorisation using the proposed method, and its usefulness was proven for recognising the species of conifers. It is important to test the recommended modelling method more extensively to study the influences of crown overlap and understory vegetation, as well as the impact of damaged trees with missing branches and trees with asymmetrical crowns. Feature representations of the internal structure of the crown are useful in tree species classification (Li et al. 2013; Lin and Hyyppä 2016). LiDAR data with an extremely dense resolution is needed for identifying such features.

6.2 Aboveground Biomass

Aboveground biomass (AGB) from forests is critical for monitoring the global carbon cycle and reducing climate change's consequences (Ghosh and Behera 2018). Although aboveground biomass comprises both alive and dead plant material, current research on biomass measurement has concentrated somewhat on the 'active' component (live trees) due to its significance. To better understand the consequences of deforestation and environmental degradation on climate change, accurate biomass calculations are necessary. Aboveground biomass measurement provides the foundation for carbon inventories and the bulk of global discussions on carbon trading regimes. Carbon markets need continuing data on carbon stocks, especially the aboveground 'living' biomass, which is the most dynamic, changeable, and manipulable of all biomass pools. This is the component of biomass that is 'merchantable' (Kumar and Mutanga 2017). Since the early 1970s, remote sensing technology has been used (Ghosh and Behera 2018) to estimate biomass, and several approaches have been developed, either in terms of model complexity (Becknell et al. 2018) or through the use of an unmanned aerial vehicle (UAV), which provided a novel solution (Zheng et al. 2019) for biomass estimation. The AGB value can be determined using existing biomass allometric equations (O'Brien et al. 2019). This was accomplished using cross-validation against an AGB subset of a vast worldwide dataset of on-the-ground measured stem diameters, heights, and crown widths (Camarretta et al. 2020).

6.3 Deadwood

Coarse woody debris (CWD) and deadwood are seen by forest managers as unnecessary consequences. Sustainability in forest management must not be ignored. Additionally, deadwood contributes to the ecosystem by replenishing soil nutrients and establishing microsites where plants and trees may grow. Nowadays, there is some study that helps on detecting the CWD by remote sensing technologies such as a high-resolution terrestrial laser scanner (TLS), an unoccupied aerial vehicle (UAV)

laser scanner (ULS), and a combination of data from both sensors (Shokirov et al. 2021). However, a random forest (RF) classification algorithm was used and accuracy was very varied, depending on the data and ground vegetation cover, and ranged between 20% and 86%, and 12% and 96%, respectively, when compared to field data. The accuracy of CWD identification varied according to plant type, the quantity of ground vegetation cover, and LiDAR data. The density of ground cover had a significant detrimental effect on accuracy, notably for TLS and FLS data.

Other studies are using optical imagery and multispectral aerial LiDAR (Queiroz et al. 2020) and airborne laser scanning (ALS) (Joyce et al. 2019; Jarron et al. 2021). The use of optical imagery and multispectral aerial LiDAR with the chosen models achieved high predictive accuracy (0.623 R^2 and 0.224 root mean square error in cross-validation; 0.721 R^2 and 0.198 root mean square error in the verification area) but required a sophisticated set of inputs, including high-resolution aerial images, dense LiDAR point clouds, and machine learning point clouds.

As for the ALS, The accuracy of CWD detection is then evaluated at the individual log level, and CWD volume is predicted at the plot level. The volume totals of CWD predicted by ALS were compared to field-measured CWD and found to be highly correlated ($R = 0.81$ by Jarron et al. (2021) and $R = 0.96$ by Joyce et al. (2019)), allowing to expand the methodology and map CWD over a larger region. LiDAR-based CWD identification and mapping will be beneficial for applications that concentrate on bigger and longer pieces of CWD or applications focused on total CWD volume.

6.4 Canopy Structure and Layering

A rainforest's overstory, canopy, understory, shrub layer, and ground level are only a few of its features. The canopy refers to the dense canopy of leaves and tree branches formed by densely packed forest trees. The upper canopy rises 100–130 ft above the forest floor, with the overstory made primarily of irregular emergent trees 130 ft or higher. In contrast, the understory comprises leaf and branch layers under the canopy ceiling. The shrub layer is the understory's lowest layer, rising 5–20 ft (1.5–6 m) above the ground, and consists of shrubby plants and tree seedlings. Field-based observations of vertical forest structures over huge regions are time intensive and complex, limiting the data's use when applied to larger areas (Whitehurst et al. 2013).

Consequently, LiDAR remote sensing is an excellent technology for detecting layers inside the vertical canopy structure. However, it is capable of providing exceedingly detailed vertical and horizontal information (Camarretta et al. 2020). Compared to LiDAR, structure from motion can have poor ground-level penetration because canopy openings are too small to allow for equivalent illumination of the ground and canopy, resulting in underexposure in imagery, and to be viewed at the oblique angles required triangulation of position (Zarco-Tejada et al. 2014; Dandois et al. 2017). It might, however, be enhanced by including terrestrial laser scanning (TLS) (Fig. 6) and structure from motion (SfM) (Fig. 7). Both of these developing

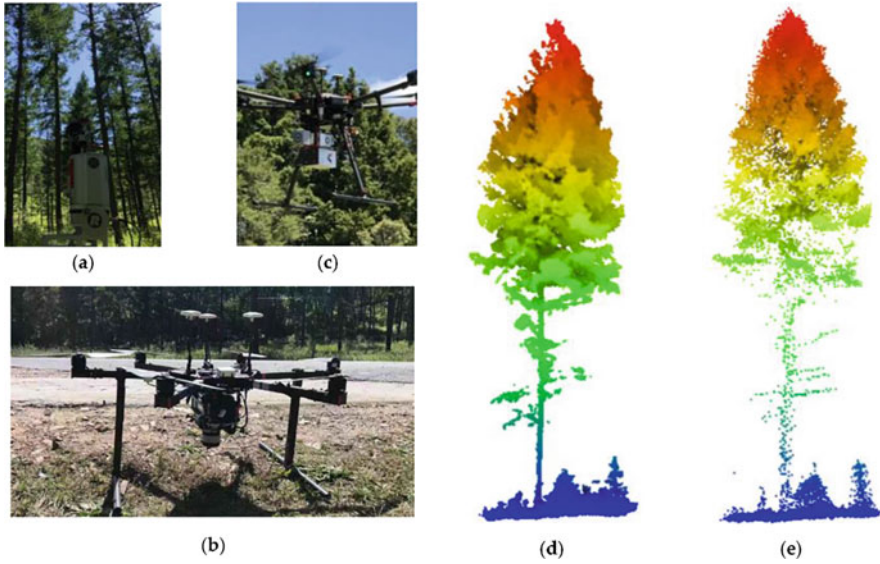


Fig. 6 Various platforms and examples of a single tree point cloud: (a) represents the terrestrial laser scanning (TLS) platform, (b) represents the unmanned aerial vehicle (UAV) LiDAR platform, and (c) represents the unmanned aerial vehicle (UAV) platform equipped with a digital camera. (d, e) represent the TLS and UAV LiDAR point clouds of a single tree, respectively (Source: Zhang et al. 2021)

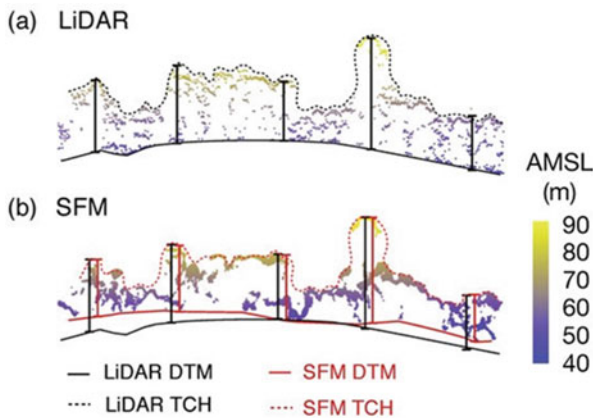


Fig. 7 Cross-sections of the same forest area at Hutun Harapan obtained using (a) LiDAR (airborne laser scanning) and (b) Structure from Motion (SfM) point clouds: The points are shaded based on their unnormalized height above mean sea level (AMSL). The solid black and red lines represent the digital terrain models created using LiDAR and SfM measurements, respectively (DTM). Despite the fact that SfM generates much greater point densities, its inability to identify ground points results in an overestimation of the ground location and, thus, an underestimate of the top-of-canopy height (TCH; dashed lines) as compared to LiDAR. The vertical bars represent tree heights, which are skewed downward when assessed with SfM (Source: Swinfield et al. 2019)

technologies can collect the information below the canopy (Zhang et al. 2021) and enhance ground position (Swinfield et al. 2019). These technologies can significantly increase the value of UAV surveys for monitoring forest health changes and direct restoration despite requiring wall-to-wall LiDAR coverage.

6.5 Vegetation Cover

The traditional way to identify vegetation cover is by remote sensing systems utilising active and passive optical image sensors used in conjunction with one another (Moorthy et al. 2011). As opposed to passive optical imaging sensors, which can only provide comprehensive measurements of horizontal distributions in vegetation canopies, LiDAR systems are capable of producing more accurate data in both the horizontal and vertical dimensions (Lim et al. 2003; Vazirabad and Karslioglu 2011), allowing for the creation of high-resolution (Asner and Mascaro 2014) digital elevation models (DEMs). Fisheye photography is a typical strategy that may provide precise results, but it is inefficient when used in a small area since it requires several sample locations and takes too much time. In contrast, high-resolution aerial images, satellites, and their integration with LiDAR data are the only options available for large areas.

6.6 Tree Species Composition

Accurate estimation of the tree species composition in forest contexts would benefit forest ecologists, land managers, and commercial harvesters. Additionally, it may be used to monitor biodiversity trends (Shen and Cao 2017), predict wood stocks, and enhance forest fire risk assessments (Fricker et al. 2019). In remote sensing technology for tree species composition, the first application was manually interpreting the aerial photograph. However, the consequences of this technique are slow, costly in money, and very dependent on the knowledge of researchers towards tree species (Wang et al. 2018). Therefore, initiatives have adopted various remote sensing data sources and classification methods to overcome these concerns. Tree species can be distinguished by high-resolution multispectral satellite remote sensing (Immitzer et al. 2012), hyperspectral airborne imaging (Martin et al. 1998; Clark et al. 2005), and even non-spectral airborne light detection and ranging (Holmgren and Persson 2004). In addition, there are numerous approaches for classifying using a data fusion strategy, integrating LiDAR with multispectral (Dalponte et al. 2012), airborne hyperspectral, or hyperspectral images (Asner et al. 2012; Marrs and Ni-Meister 2019). However, there are a few methods to evaluate the various techniques. For example, Chauhan et al. evaluated classification performance by using random forest (RF), while Shen and Cao (2017) used LiDAR metrics which were extracted and selected by the indices of principal component analysis (PCA) and the mean decrease in Gini index (MDG) from random forest (RF). Other studies have used different ways to classify the tree by (Fricker et al. 2019) using a convolutional neural network classifier

(CNN). Since many research reveal the capability of RS applications to classify vegetation types and species, significant challenges remain in increasing the overall diversity of species spotted and in enhancing the excellent magnification details needed for morphological characteristics over vast areas without sacrificing the required level of resolution (Camarretta et al. 2020).

6.7 Structural Complexity

A researcher from the University of Connecticut, Virginia Commonwealth University, and Purdue University prove for the first time that the structural complexity of a forest is a more prominent predictor of carbon sequestration potential than tree species variation (Elaina Hancock 2019). The classification of forest tree species utilising RS systems has been studied using ALS data and remotely sensed pictures. Therefore, many studies have been conducted to detect the structural complexity of forests.

A study by Jayathunga et al. (2018) investigated airborne LiDAR data and aerial photography to derive structural complexity forest by integrating multiple forest structural attributes. First, the capacity of each plot to represent vertical and horizontal differences in forest structure was determined, and second, plot-level metrics were generated by field measurement and remote sensing data. A multivariate collection of forest structural variables was utilised to categorise forest structure into structural complexity classes. The canopy height, canopy density, and surface area ratio will be measured using LiDAR and the percentage of broadleaf cover by one image metric. The findings indicate a strong connection where the measurements have a similar structural pattern between the different measurements.

Another research by LaRue et al. (2018) employs terrestrial LiDAR measurements of structural complexity to characterise the organisation of plants in the canopy and might be connected with Landsat-derived metrics via their effect on energy and light. Connecting Landsat to terrestrial LiDAR may allow for a more nuanced interpretation of Landsat-derived metrics and a broader spatial scale for evaluating structural complexity. The results indicated a correlation between canopy reflectance, greenness, and brightness and numerous indices of canopy structure. Greenness was more correlated in stands with a higher canopy, a higher leaf area density and diversity, and a less open and porous canopy. The result shows NDVI had the strongest correlation with (adj. $R^2 = 0.52-0.62$) of all greenness indicators for the six metrics.

Acknowledgement The authors gratefully acknowledge the source of the funding of this research work supported under the Fundamental Research Grant Scheme with grant no: FRGS/1/2020/WAB03/UKM/02/1

References

- Adams C, Rodrigues ST, Calmon M, Kumar C (2016) Impact of large scale forest restoration on socioeconomic status and local livelihoods: what we know and do not know. *Biotropica* 48(6):731–744
- Almeida DRA et al (2016) Contrasting fire damage and fire susceptibility between seasonally flooded forest and upland forest in the Central Amazon using portable profiling LiDAR. *Remote Sens Environ* 184:153–160. <https://doi.org/10.1016/j.rse.2016.06.017>
- Almeida DRA et al (2019) Monitoring the structure of forest restoration plantations with a drone-lidar system. *Int J Appl Earth Obs Geoinf* 79:192–198. <https://doi.org/10.1016/j.jag.2019.03.014>
- Aragón S, Salinas N, Quispe AN, Qqueillon VH, Paucar GR, Huaman W, Porroa PC, Olarte JC, Cruz R, Muniz JG, Yupayccana CS, Espinoza TEB, Tito R, Cosio EG, Cuesta RMR (2021) Aboveground biomass in secondary montane forests in Peru: slow carbon recovery in agroforestry legacies. *Glob Ecol Conserv* 28:e01696. <https://doi.org/10.1016/j.gecco.2021.e01696>
- Armstrong AH (2018) Tropical rainforest ecosystems. In: International encyclopedia of geography, pp 1–16. <https://doi.org/10.1002/9781118786352.wbieg0644.pub2>
- Asner GP, Mascaro J (2014) Mapping tropical forest carbon: calibrating plot estimates to a simple LiDAR metric. *Remote Sens Environ* 140:614–624. <https://doi.org/10.1016/j.rse.2013.09.023>
- Asner GP et al (2012) Carnegie Airborne Observatory-2: increasing science data dimensionality via high-fidelity multi-sensor fusion. *Remote Sens Environ* 124:454–465. <https://doi.org/10.1016/j.rse.2012.06.012>
- Báez S, Ambrose K, Hofstede R (2011) Ecological and social bases for the restoration of a high andean cloud forest: preliminary results and lessons from a case study in northern Ecuador. *Tropical montane cloud forests*. In: Science for conservation and management. Cambridge University Press, Cambridge, pp 628–643. <https://doi.org/10.1017/CBO9780511778384.068>
- Becknell JM et al (2018) Landscape-scale lidar analysis of aboveground biomass distribution in secondary Brazilian Atlantic Forest. *Biotropica* 50(3):520–530. <https://doi.org/10.1111/btp.12538>
- Begum RA, Raihan A, Said MNM (2020) Dynamic impacts of economic growth and forested area on carbon dioxide emissions in malaysia. *Sustainability (Switzerland)* 12:1–15. <https://doi.org/10.3390/su12229375>
- Berkes F, Colding J, Folke C (2000) Rediscovery of traditional ecological knowledge as adaptive management. *Ecol Appl* 10:1251–1262. [https://doi.org/10.1890/1051-0761\(2000\)010\[1251:ROTEKA\]2.0.CO;2](https://doi.org/10.1890/1051-0761(2000)010[1251:ROTEKA]2.0.CO;2)
- Betts MG, Wolf C, Ripple WJ, Phalan B, Millers KA, Duarte A, Butchart SHM, Levi T (2017) Global forest loss disproportionately erodes biodiversity in intact landscapes. *Nature* 547:441–444. <https://doi.org/10.1038/nature23285>
- Bowling J (2004) Integrating forest protection, management and restoration at a landscape scale (March)
- Brockerhoff EG, Barbaro L, Castagneyrol B, Forrester DI, Gardiner B, González-Olabarria JR, Lyver POB, Meurisse N, Oxbrough A, Taki H, Thompson ID, van der Plas F, Jactel H (2017) Forest biodiversity, ecosystem functioning and the provision of ecosystem services. *Biodivers Conserv* 26(13):3005–3035. <https://doi.org/10.1007/s10531-017-1453-2>
- Bullock JM, Aronson J, Newton AC, Pywell RF, Benayas JM (2011) Restoration of ecosystem services and biodiversity: conflicts and opportunities. *Trends Ecol Evol* 26:541–549. <https://doi.org/10.1016/j.tree.2011.06.011>
- Camarretta N, Harrison PA, Bailey T, Potts B, Lucieer A, Davidson N, Hunt M (2020) Monitoring forest structure to guide adaptive management of forest restoration: a review of remote sensing approaches. *New For* 51:573–596. <https://doi.org/10.1007/s11056-019-09754-5>
- César RG, Belei L, Badari CG, Viani RAG, Gutierrez V, Chazdon RL, Brancalion PHS, Morsello C (2021) Forest and landscape restoration: a review emphasizing principles, concepts, and practices. *Land* 10:1–22. <https://doi.org/10.3390/land10010028>

- Chadourne MH, Cho SH, Roberts RK (2012) Identifying priority areas for forest landscape restoration to protect ridgelines and hillsides: a cost-benefit analysis. *Can J Agric Econ* 60: 275–294. <https://doi.org/10.1111/j.1744-7976.2012.01252.x>
- Chazdon RL (2008) Beyond deforestation: restoring forests and ecosystem services on degraded lands. *Science* 320:1458–1460. <https://doi.org/10.1126/science.1155365>
- Chazdon RL (2014) Second growth the promise of tropical forest regeneration in an age of deforestation. Retrieved from <http://www.myilibrary.com?id=600216>
- Chazdon RL, Gutierrez V, Brancalion P, Laestadius L, Guariguata MR (2019) Co-creating conceptual and working forest and landscape restoration frameworks based on core principles. *Forest and Landscape Restoration Standards Taskforce (FLoRES)*
- Chazdon RL, Lindenmayer D, Guariguata MR, Crouzeilles R, Rey Benayas JM, Lazos Chavero E (2020) Fostering natural forest regeneration on former agricultural land through economic and policy interventions. *Environ Res Lett* 15(4). <https://doi.org/10.1088/1748-9326/ab79e6>
- Chomitz KM (2007) At loggerheads? Agricultural expansion, poverty reduction, and environment in the tropical forests. World Bank, Washington, DC. <https://doi.org/10.1596/978-0-8213-6735-3>
- Clark ML, Roberts DA, Clark DB (2005) Hyperspectral discrimination of tropical rain forest tree species at leaf to crown scales. *Remote Sens Environ* 96(3–4):375–398. <https://doi.org/10.1016/j.rse.2005.03.009>
- Cummings JA, Parker IM, Gilbert GS (2012) Forest restoration, biodiversity and ecosystem functioning. *Plant Ecol* 213(12):29–1989. <https://doi.org/10.1111/j.1526-100X.1994.tb00054.x>
- Dalponte M, Bruzzone L, Gianelle D (2012) Tree species classification in the Southern Alps based on the fusion of very high geometrical resolution multispectral/hyperspectral images and LiDAR data. *Remote Sens Environ* 123:258–270. <https://doi.org/10.1016/j.rse.2012.03.013>
- Dandois JP et al (2017) What is the point? Evaluating the structure, color, and semantic traits of computer vision point clouds of vegetation. *Remote Sens* 9(4). <https://doi.org/10.3390/rs9040355>
- Dash JP et al (2016) Characterising forest structure using combinations of airborne laser scanning data, RapidEye satellite imagery and environmental variables. *Forestry* 89(2):159–169. <https://doi.org/10.1093/forestry/cpv048>
- de Souza SEXF, Vidal E, de Freitas CG, Elgar AT, Brancalion PHS (2016) Ecological outcomes and livelihood benefits of community-managed agroforests and second growth forests in Southeast Brazil. *Biotropica*:868–881. <https://doi.org/10.1111/btp.12388>
- Drake JB et al (2002) Estimation of tropical forest structural characteristics using large-footprint lidar. *Remote Sens Environ* 79:305–319
- Dubayah RO, Drake JB (2000) Lidar remote sensing for forestry. *J For* 98:44
- Egan D, Hjerpe E, Abrams J (2011) In: Higgs E (ed) Human dimensions of ecological restoration integrating science, nature, and culture. Island Press
- Elaina Hancock BM (2019) Structural complexity in forests improves carbon capture. Available at: <https://today.uconn.edu/2019/08/structural-complexity-forests-improves-carbon-sequestration/#>
- Elmqvist T, Folke C, Nyström M, Peterson G, Bengtsson J, Walker B (2003) Response diversity, ecosystem change, and resilience. *Front Ecol Environ* 1:488–494. [https://doi.org/10.1890/1540-9295\(2003\)001\[0488:RDECAR\]2.0.CO;2](https://doi.org/10.1890/1540-9295(2003)001[0488:RDECAR]2.0.CO;2)
- FAO (2003) Workshop on tropical secondary forest management in Africa: reality and perspectives. Available at: <https://www.fao.org/3/j0628e/J0628E00.htm>
- FAO (2010) Food and Agriculture Organization of the United Nations. Global forest resources assessment. FAO Forestry Paper 163 Available at: <https://www.fao.org/3/i1757e/i1757e.pdf>
- FAO (2015) Global forest resource assessment 2015: country profile—Malaysia
- FAO (2016) Forests and agriculture: land-use challenges and opportunities, State of the World's Forests. Available at: <http://ccafs.cgiar.org/news/press-releases/agriculture-and-food-production-contribute-29-percent-global-greenhouse-gas>.

- FAO (2020) Global forest resources assessment 2020: terms and definitions. Forest Resources Assessment Working Paper 32. Available at: <http://www.fao.org/forestry/58864/en/>
- Fox J, Vogler JB (2005) Land-use and land-cover change in montane mainland southeast, pp 394–403. <https://doi.org/10.1007/s00267-003-0288-7>
- Fricker GA et al (2019) A convolutional neural network classifier identifies tree species in mixed-conifer forest from hyperspectral imagery. *Remote Sens* 11(19). <https://doi.org/10.3390/rs11192326>
- Ghosh SM, Behera MD (2018) Aboveground biomass estimation using multi-sensor data synergy and machine learning algorithms in a dense tropical forest. *Appl Geogr* 96:29–40. <https://doi.org/10.1016/j.apgeog.2018.05.011>
- Gilhen-Baker M, Roviello V, Beresford-Kroeger D, Roviello GN (2022) Old growth forests and large old trees as critical organisms connecting ecosystems and human health. A review. *Environ Chem Lett*. <https://doi.org/10.1007/s10311-021-01372-y>
- Gilman SE, Urban MC, Tewksbury J, Gilchrist GW, Holt RD (2010) A framework for community interactions under climate change. *Trends Ecol Evol* 25:325–331. <https://doi.org/10.1016/j.tree.2010.03.002>
- Hale R, Blumstein DT, Nally RM, Swearer SE (2020) Harnessing knowledge of animal behavior to improve habitat restoration outcomes. *Ecosphere*. <https://doi.org/10.1002/ecs2.3104>
- Hansen MC (2013) High-resolution global maps of 21st-century forest cover change. *Science* 342 (November):850–854. <https://doi.org/10.1126/science.1244693>
- Hao Z, Wang C, Sun Z, Zhao D, Sun B, Wang H, Konijnendijk VDBC (2021) Vegetation structure and temporality influence the dominance, diversity, and composition of forest acoustic communities. *For Ecol Manag*. <https://doi.org/10.1016/j.foreco.2020.118871>
- Harikumar A et al (2017) An internal crown geometric model for conifer species classification with high-density LiDAR data, pp 1–17
- Higgs ES, Hobbs R (2010) Wild design: principles to guide interventions in protected areas. In: Dlm. Cole (pnyt.), Yung (pnyt.). Beyond naturalness, hlm Island Press.
- Hilbert J, Wiensczyk A (2007) Old-growth definitions and management: a literature review. *BC J Ecosyst Manag* 8:15–31
- Hill C, Lillywhite S, Simon M (2010) Guide to free prior and informed consent. In: Talia Eilon MB (ed) hlm, 1st edn. Oxfam Australia, Victoria. Retrieved from www.oxfam.org.au
- Holmgren J, Persson Å (2004) Identifying species of individual trees using airborne laser scanner. *Remote Sens Environ* 90(4):415–423. [https://doi.org/10.1016/S0034-4257\(03\)00140-8](https://doi.org/10.1016/S0034-4257(03)00140-8)
- Hui Z et al (2019) An active learning method for DEM extraction from airborne LiDAR point clouds. *IEEE Access* 7:89366–89378. <https://doi.org/10.1109/ACCESS.2019.2926497>
- Huss J (2004) Natural stand regeneration. *Encyclopedia of forest sciences*, pp 1017–1033
- Immitzer M, Atzberger C, Koukal T (2012) Tree species classification with Random forest using very high spatial resolution 8-band worldView-2 satellite data. *Remote Sens* 4(9):2661–2693. <https://doi.org/10.3390/rs4092661>
- Isbell F, Calcagno V, Hector A, Connolly J, Harpole WS, Reich PB, Scherer-Lorenzen M, Schmid B, Tilman D, Van Ruijven J, Weigelt A, Wilsey BJ, Zavaleta ES, Loreau M (2011) High plant diversity is needed to maintain ecosystem services. *Nature* 477(7363):199–202. <https://doi.org/10.1038/nature10282>
- Jarron LR et al (2021) Detection and quantification of coarse woody debris in natural forest stands using airborne LiDAR. *For Sci* 67(5):550–563. <https://doi.org/10.1093/forsci/fxab023>
- Jayathunga S, Owari T, Tsuyuki S (2018) Analysis of forest structural complexity using airborne LiDAR data and aerial photography in a mixed conifer–broadleaf forest in northern Japan. *J For Res* 29(2):479–493. <https://doi.org/10.1007/s11676-017-0441-4>
- Joyce MJ et al (2019) Forest ecology and management detection of coarse woody debris using airborne light detection and ranging (LiDAR). *For Ecol Manag* 433(October 2018):678–689. <https://doi.org/10.1016/j.foreco.2018.11.049>
- Keenleyside K, Dudley N, Cairnes S, Hall C, Stolton S (2012) Ecological restoration for protected areas principles, guidelines and best practices. In: Valentine P (ed) IUCN, Gland, Switzerland in

- collaboration with Parks Canada, the Society for Ecological Restoration, and the Secretariat of the Convention on Biological Diversity
- Koenig K, Höfle B (2016) Full-waveform airborne laser scanning in vegetation studies—a review of point cloud and waveform features for tree species classification. *Forests* 7:1–22. <https://doi.org/10.3390/f7090198>
- Kormos CF, Mittermeier RA, Jaeger T, Mackey B (2016) A geography of hope: saving the last primary forests. *Earth in focus*, Qualicum Beach
- Kumar L, Mutanga O (2017) Remote sensing of above-ground biomass. *Remote Sens.* <https://doi.org/10.3390/rs9090935>
- Landsberg J, Waring R (2014) Forest types around the world. *Forests in our changing world*, pp 21–46. https://doi.org/10.5822/978-1-61091-497-0_2
- LaRue EA et al (2018) Linking Landsat to terrestrial LiDAR: vegetation metrics of forest greenness are correlated with canopy structural complexity. *Int J Appl Earth Obs Geoinf* 73:420–427. <https://doi.org/10.1016/j.jag.2018.07.001>
- Li J, Hu B, Noland TL (2013) Agricultural and forest meteorology classification of tree species based on structural features derived from high density LiDAR data. *Agric For Meteorol* 171–172:104–114. <https://doi.org/10.1016/j.agrformet.2012.11.012>
- Lim K et al (2003) Lidar remote sensing of biophysical properties of tolerant northern hardwood forests. *Can J Remote Sens* 29(5):658–678. <https://doi.org/10.5589/m03-025>
- Lin Y, Hyypä J (2016) A comprehensive but efficient framework of proposing and validating feature parameters from airborne LiDAR data for tree species classification. *Int J Appl Earth Observ Geoinf* 46:45–55
- Liu CC (2019) Assessment of forest restoration with multitemporal remote sensing imagery. *Sci Rep* 9(1). <https://doi.org/10.1038/s41598-019-43544-5>
- Maginel CJ, Knapp BO, Kabrick JM, Olson EK, Muzika RM (2016) Floristic quality index for woodland ground flora restoration: utility and effectiveness in a fire-managed landscape. *Ecol Indic* 67:58–67. <https://doi.org/10.1016/j.ecolind.2016.02.035>
- Maginnis S, Jackson W (2002) Restoring forest landscapes. ITTO tropical forest update, pp 9–11
- Mansourian S, Vallauri D, Dudley N (2005a) Forest restoration in landscapes: beyond planting trees. <https://doi.org/10.1007/0-387-29112-1>
- Mansourian S, Vallauri D, Dudley N (2005b) Overview of forest restoration strategies and trends. In: *Forest restoration in landscapes: beyond planting trees*. Springer, New York, pp 8–13. <https://doi.org/10.1007/0-387-29112-1>
- Marrs J, Ni-Meister W (2019) Machine learning techniques for tree species classification using co-registered LiDAR and hyperspectral data. *Remote Sens* 11(7). <https://doi.org/10.3390/rs11070819>
- Martin ME, Newman SD, Aber JD Congalton RG (1998) Determining forest species composition using high spectral resolution remote sensing data. Available at: <http://www-eosdis.ornl.gov>
- Matrushka (2020) The bonn challenge. International Union for Conservation of Nature (IUCN). <https://www.bonnchallenge.org/>
- Moorthy I et al (2011) Field characterization of olive (*Olea europaea* L.) tree crown architecture using terrestrial laser scanning data. *Agric For Meteorol* 151(2):204–214. <https://doi.org/10.1016/j.agrformet.2010.10.005>
- Muhammad Kamarulzaman AM, Wan Mohd Jaafar WS, Abdul Maulud KN, Saad SNM, Omar H, Mohan M (2022) Integrated segmentation approach with machine learning classifier in detecting and mapping post selective logging impacts using UAV imagery. *Forests* 13:48. <https://doi.org/10.3390/f13010048>
- Nave LE, Walters BF, Hofmeister KL, Perry CH, Mishra U, Domke GM, Swanston CW (2019) The role of reforestation in carbon sequestration. *New For* 50:115–137. <https://doi.org/10.1007/s11056-018-9655-3>
- Newton AC, Tejedor N (2011) Principles and practice of forest landscape restoration case studies from the drylands of Latin America. *Principles and practice of forest landscape restoration: case*

- studies from the drylands of Latin America, p 412. Retrieved from <http://eprints.bournemouth.ac.uk/18729/>
- O'Brien MJ et al (2019) Positive effects of liana cutting on seedlings are reduced during El Niño-induced drought. *J Appl Ecol* 56(4):891–901. <https://doi.org/10.1111/1365-2664.13335>
- OECD-FAO (2021) OECD-FAO agricultural outlook 2021–2030. OECD-FAO Agricultural Outlook 2021–2030. Retrieved from <https://doi.org/10.1787/agr-outl-data-%0Ahttp://www.fao.org/documents/card/en/c/cb5332en>
- Ozdemir I, Karnieli A (2011) Predicting forest structural parameters using the image texture derived from worldview-2 multispectral imagery in a dryland forest, Israel. *Int J Appl Earth Observ Geoinf* 13(5):701–710. <https://doi.org/10.1016/j.jag.2011.05.006>
- Perring MP, Standish RJ, Price JN, Craig MD, Erickson TE, Ruthrof KX, Whiteley AS, Valentine LE, Hobbs RJ (2015) Advances in restoration ecology: rising to the challenges of the coming decades. *Ecosphere*. <https://doi.org/10.1890/ES15-00121.1>
- Poorter L, Bongers F, Aide TM, Almeyda Zambrano AM, Balvanera P, Becknell JM, Boukili V, Brancalion PHS, Broadbent EN, Chazdon RL, Craven D, De Almeida-Cortez JS, Cabral GAL, De Jong BHI, Denslow JS, Dent DH, DeWalt SJ, Dupuy JM, Durán SM, Espírito-Santo MM, Fandino MC, César RG, Hall JS, Hernandez-Stefanoni JL, Jakovac CC, Junqueira AB, Kennard D, Letcher SG, Licona JC, Lohbeck M, Marín-Spiotta E, Martínez-Ramos M, Massoca P, Meave JA, Mesquita R, Mora F, Munõz R, Muscarella R, Nunes YRF, Ochoagaona S, De Oliveira AA, Orihuela-Belmonte E, Penã-Claros M, Pérez-García EA, Piotto D, Powers JS, Rodríguez-Velázquez J, Romero-Pérez IE, Ruíz J, Saldarriaga JG, Sanchez-Azofeifa A, Schwartz NB, Steininger MK, Swenson NG, Toledo M, Uriarte M, Van Breugel M, Van Der Wal H, Veloso MDM, Vester HFM, Vicentin A, Vieira ICG, Bentes TV, Williamson GB, Rozendaal DMA (2016) Biomass resilience of neotropical secondary forests. *Nature* 530(7589):211–214. <https://doi.org/10.1038/nature16512>
- Queiroz GL et al (2020) Estimating coarse woody debris volume using image analysis and multispectral LiDAR
- Saad SNM, Abdul Maulud KN, Wan Mohd Jaafar WS, Muhmad Kamarulzaman AM, Omar H (2020) Tree stump height estimation using canopy height model at tropical forest in Ulu Jelai Forest Reserve, Pahang, Malaysia. *IOP Conf Ser Earth Environ Sci*. <https://doi.org/10.1088/1755-1315/540/1/012015>
- Shen X, Cao L (2017) Tree-species classification in subtropical forests using airborne hyperspectral and LiDAR data. *Remote Sens* 9(11). <https://doi.org/10.3390/rs9111180>
- Shokirov S et al (2021) Multi-platform LiDAR approach for detecting coarse woody debris in a landscape with varied ground cover. *Int J Remote Sens* 42(24):9324–9350. <https://doi.org/10.1080/01431161.2021.1995072>
- Stanturf JA, Mansourian S, Kleine M (2017) Implementing forest landscape restoration: a practitioner's guide
- Swinfield T et al (2019) Accurate measurement of tropical forest canopy heights and aboveground carbon using structure from motion. *Remote Sens* 11(8). <https://doi.org/10.3390/rs11080928>
- van Leeuwen M, Nieuwenhuis M (2010) Retrieval of forest structural parameters using LiDAR remote sensing. *Eur J For Res* 129(4):749–770. <https://doi.org/10.1007/s10342-010-0381-4>
- Vazirabad YF, Karşlioglu MO (2011) Lidar for biomass estimation. In: Matovic D (ed) *Biomass*. IntechOpen, Rijeka. <https://doi.org/10.5772/16919>
- Viani RAG, Holl KD, Padovezi A, Strassburg BBN, Farah FT, Garcia LC, Chaves RB, Rodrigues RR, Brancalion PH (2017) Protocol for monitoring tropical forest restoration: perspectives from the atlantic forest restoration pact in Brazil. *Trop Conserv Sci*. <https://doi.org/10.1177/1940082917697265>
- Walker B, Holling CS, Carpenter SR, Kinzig A (2004a) Ecological Restoration—a means of conserving biodiversity and sustaining livelihoods International and the IUCN Commission on Ecosystem Management. *Ecol Soc*. Retrieved from <http://www.ecologyandsociety.org/vol9/iss2/art5>

- Walker B, Holling CS, Carpenter SR, Kinzig A (2004b) Resilience, adaptability and transformability in social-ecological systems
- Wan Mohd Jaafar WS, Abdul Maulud KN, Muhmad Kamarulzaman AM, Raihan A, Md Sah S, Ahmad A, Saad SNM, Mohd Azmi AT, Jusoh Syukri NKA, Khan WR (2020a) The influence of deforestation on land surface temperature—a case study of Perak and Kedah, Malaysia. *Forests* 11:1–27. <https://doi.org/10.3390/F11060670>
- Wan Mohd Jaafar WS, Said NFS, Abdul Maulud KN, Uning R, Latif MT, Muhmad Kamarulzaman AM, Mohan M, Pradhan B, Saad SNM, Broadbent EN, Cardil A, Silva CA, Takriff MS (2020b) Carbon emissions from oil palm induced forest and peatland conversion in Sabah and Sarawak, Malaysia. *Forests* 11:1–22. <https://doi.org/10.3390/f11121285>
- Wang K, Wang T, Liu X (2018) A review: individual tree species classification using integrated airborne LiDAR and optical imagery with a focus on the urban environment, vol 10, *Forests*, p 1. <https://doi.org/10.3390/f10010001>
- Whitehurst AS et al (2013) Characterization of canopy layering in forested ecosystems using full waveform lidar. *Remote Sens* 5(4):2014–2036. <https://doi.org/10.3390/rs5042014>
- World Resource Institute (2021) Forest pulse: the latest on the world's forests. *Glob For Rev*:1–18. Available at: <https://research.wri.org>
- Worldatlas (2021) Old-growth forests contents, pp 1–9. Available at: <https://www.worldatlas.com/articles/old-growth-forests.html>
- Zarco-Tejada PJ et al (2014) Tree height quantification using very high resolution imagery acquired from an unmanned aerial vehicle (UAV) and automatic 3D photo-reconstruction methods. *Eur J Agron* 55:89–99. <https://doi.org/10.1016/j.eja.2014.01.004>
- Zhang Y, Wu H, Yang W (2019) Forests growth monitoring based on tree canopy 3D reconstruction using UAV aerial photogrammetry. *Forests* 10:1–16. <https://doi.org/10.3390/F10121052>
- Zhang W et al (2021) Automated marker-free registration of multisource forest point clouds using a coarse-to-global adjustment strategy. *Forests* 12(3):1–17. <https://doi.org/10.3390/f12030269>
- Zheng H et al (2019) Improved estimation of rice aboveground biomass combining textural and spectral analysis of UAV imagery. *Precis Agric* 20(3):611–629. <https://doi.org/10.1007/s11119-018-9600-7>



Assessment and Modelling of Forest Biomass and Carbon Stock and Sequestration Using Various Remote Sensing Sensor Systems

Yousif Ali Hussin

Abstract

The global climatic crisis along with the threat to the forests has increased the need to research for more accurate and accessible methods and techniques to quantify biomass and carbon in forest while supporting the REED+ and other world objectives. With the aim of reaching zero net deforestation, all participant countries of the United Nation Framework Convention on Climate Change (UNFCCC) have to present an up-to-date report of their carbon balance periodically, as well as compensation actions of REDD+ programme. In the 2020s, REDD+ compensation payments should start to be implemented along with the compensation actions in which money from emission countries should be paid to carbon stock countries. Therefore, accuracy, transparency and accessibility of the carbon quantification processes are essential to achieve REDD+ objectives and ultimately the conservation and enhancement of forest carbon stocks. Measurement, Recording and Verification (MRV) is the mechanism to make sure that the claim of countries that they have more carbon stock than emitted is correct.

For ages, assessment of forest aboveground biomass (AGB) and aboveground carbon (AGC) or carbon stock has relied on the classical forest inventory approach. Usually, DBH and tree height are measured in the field to assess forest AGB using an allometric equation. Although forest inventory data provide the needful information, it is time-consuming and less accessible, and datasets are often limited to a small area. Therefore, having a robust method using remote sensing technology to assess AGB and AGC is essential in monitoring forest biomass and carbon stock. This technology is reasonably accurate, economical

Y. Ali Hussin (✉)

Department of Natural Resources, Faculty of Geo-information Science and Earth Observation,
University of Twente, Enschede, The Netherlands

e-mail: y.a.hussin@utwente.nl

© The Author(s), under exclusive license to Springer Nature Singapore Pte Ltd. 2022

M. N. Suratman (ed.), *Concepts and Applications of Remote Sensing in Forestry*,
https://doi.org/10.1007/978-981-19-4200-6_4

and operational along with the complement of field measurement. This chapter will review several latest remote sensing sensor systems (e.g. VHRS, Airborne RGB, SAR, Airborne LiDAR, terrestrial laser scanner and UAV RGB and MSS images) and analysis techniques and their applications in the assessment of AGB and carbon stock and sequestration.

Keywords

Forest AGB · Carbon stock · Carbon sequestration · Remote sensing · LiDAR · SAR · TLS · UAV

1 Introduction

The current climate change crisis is caused by the effects of global warming, which is produced by the increment in the concentration of greenhouse gases (GHG) in the atmosphere (IPCC 2018). Carbon dioxide is one of the main GHGs which resulted from land use changes, e.g. deforestation and forest degradation. The Intergovernmental Panel on Climate Change (IPCC) reported that the amount of carbon dioxide in the atmosphere is increasing by 1.4 ppm per year and this will contribute to the increase in temperature by 1.8–4 °C by the end of the century (IPCC 2007). Dramatic increase of CO₂ concentration is highly related to human activities. Over the past 20 years, about 75% of the anthropogenic emissions of CO₂ to the atmosphere are due to fossil fuel burning (IPCC 2007). The rest is mostly due to land use change, especially deforestation. Reducing carbon emissions from deforestation and forest degradation in developing countries is important to combat global warming. A tonne of carbon in trees is the result of the removal of 3.67 tonnes of carbon dioxide from the atmosphere; thus, the world's forest 'sink' holds more carbon than the atmosphere. Maintenance of existing forests as well as increasing forest area can contribute highly to the mitigation of global climate change.

Aboveground biomass (AGB) estimation is a key for quantifying carbon stocks in forests. The carbon stored in the aboveground living biomass of trees is the largest pool and the most directly impacted by deforestation and forest degradation (Gibbs et al. 2007). Thus, estimation of the AGB with sufficient accuracy to analyse carbon stored in the forest is important for recently emerging policies like REDD+. However, the most accurate method for the estimation of biomass is through cutting of trees and weighing of their parts, which is time consuming and expensive for large areas. This destructive method is often used to validate other less invasive and cheaper methods, such as the estimation of carbon stock using non-destructive in-situ measurements and remote sensing. The aim of this chapter is to assess the accuracy of various remote sensing sensor system data to estimate and model forest AGB and AGC.

2 Remote Sensing and AGB/Carbon Stock Assessment

Remote sensing technology is widely used in forestry to retrieve forest parameters, e.g. DBH, trees and stand height, trees and stand BA, trees and stand volume, aboveground biomass (AGB) and carbon stock. Remote sensing has the advantage of acquiring spatial data over a larger area that is not accessible to traditional field survey. Remote sensing techniques, through different sensors and methods, offer means for estimating AGB. The advantage of using remote sensing data is that spatial distribution of forest biomass can be obtained at reasonable cost and with acceptable accuracy. Moreover, attempts have been made to estimate forest biomass and carbon stock using different platforms (airborne and space-borne) and sensors (optical, radar and LiDAR). However, some of these remotely sensed images and data tend to be inaccurate or very costly for AGB estimation in tropical forest (Gibbs et al. 2007). Furthermore, several methods have been proposed for estimating forest biomass using remote sensing techniques that make use of a combination of regression models, vegetation indices and canopy reflectance models.

Very high-resolution satellite (VHRS) images in the early 2000s together with object-based image analysis (OBIA) techniques have started providing opportunities to improve AGB estimation analysis through assessing tree crown projection area (CPA) using OBIA and image segmentation techniques. The relationship between stem diameter at breast height (DBH) and CPA of a tree opens a possibility to calculate AGB using high-resolution optical imagery where every tree is identifiable.

Crown area or crown projection area is defined as the proportion of the forest floor that is covered by the vertical projection of the tree crowns (Jennings et al. 1999) as shown in Fig. 1. CPA is calculated from the maximum crown diameter assuming a circular crown projection.

During the 2010s, LiDAR (light detection and ranging) or ALS (airborne laser scanner) becomes more accurate in assessing tree height. ALS uses its laser beams which are sent from aircraft to the forest canopy, and through the technique the canopy height model (CHM) or tree height can be calculated by subtracting DTM (digital terrain model) from DSM (digital surface model) as seen in Fig. 2. The

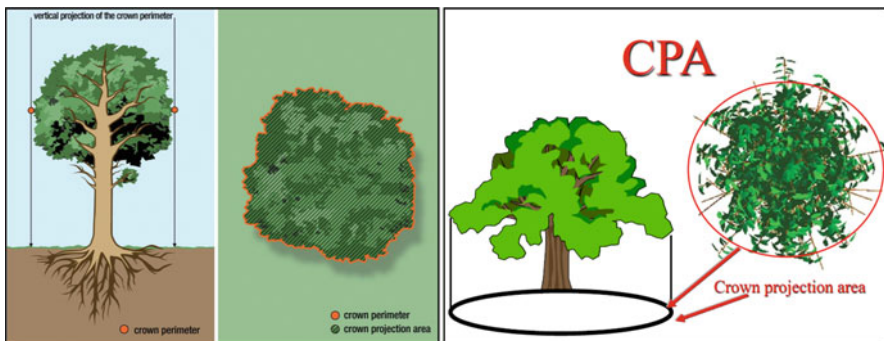


Fig. 1 Crown projection area, after (Gschwantner et al. 2009)

Fig. 2 Canopy height model
 $CHM = DSM - DTM$

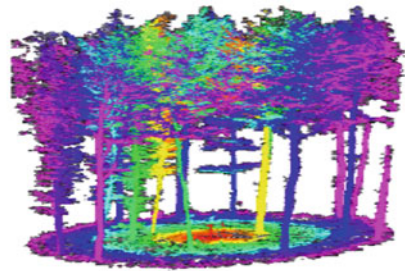
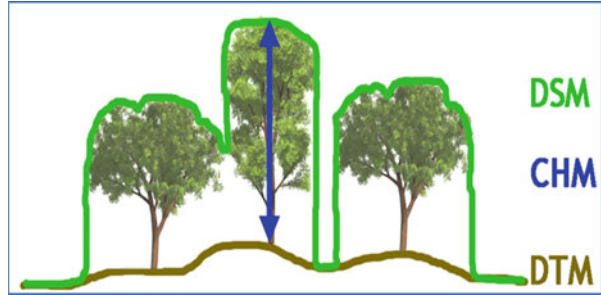


Fig. 3 TLS measurements and output in a forest circular sample

presentation of the ALS data is 3D point clouds, which is considered as the most accurate remotely sensed data in terms of geometry and coordinates.

The density of point clouds would make the shape of the object (tree). The higher the number of point clouds per square meter, the better the representation of the object. Hence, high density, e.g. 30–40 point clouds per square meter, can show much higher details of the object, while low point cloud density would poorly represent the object. Combining CPA measured from VHRS images and tree height measured using ALS has improved the AGB estimation using regression models.

Terrestrial laser scanning (TLS) is also known as ground-based LiDAR. It uses a laser and a scanning system to automatically measure the surrounding environment during a very short timeframe. The TLS is typically mounted on a tripod over a ground position specified by a certain application (Fig. 3). The objects around the static scanning position are captured by 3-D points reflected by the nearest object surfaces in the direction of the laser beams. The scanner measures the surrounding environment in horizontal and vertical directions stepwise, with a fast vertical mirror rotation and a slower horizontal instrument rotation. The output of multiple scanning of a circular plot in forest is a group of hundreds of thousands of point clouds and a very accurate 3D presentation of trees.

From TLS data DBH, height, stem and canopy volume can be measured.

SAR or synthetic aperture radar is a type of radar sensor that has been widely used to monitor land surfaces due to its characteristics of using its own illumination energy, penetration of earth superficial materials and night imaging and

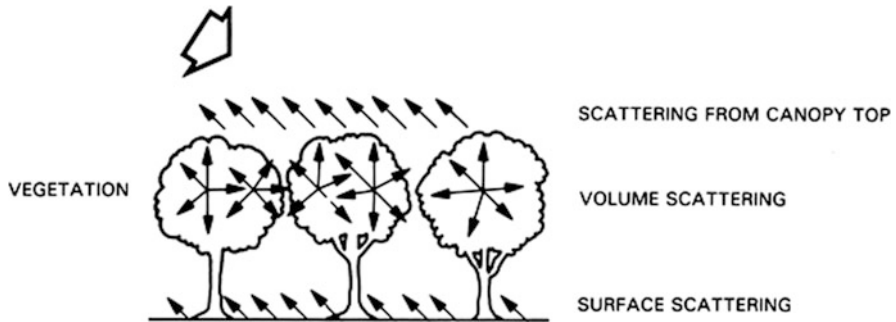


Fig. 4 Scattering contribution from the forest [Images adapted from Carver (1988)]

all-weather imaging capability. SAR as an active sensor is a side looking system: It transmits electromagnetic pulses as it moves along its path and sequentially records the backscattered signal. The received backscatter results in the detection of object and determination of its position. In forestry, the penetration properties of the radar image are of significance to model forest AGB. The pulse penetration has a significant influence on the choice of a wavelength and polarisation channel for forest biomass estimation. The wavelength bands from X, C, S, L, P and polarisation channels of the radar system determine the penetration ability of the electromagnetic pulses and scattering mechanisms of signals received by the radar sensor. Wavelength bands L and P together with cross-polarisation VH and HV are known for their penetration characteristics within the forest layer which in turn results in three types of radar pulse scattering mechanisms. The mechanisms are surface scattering or single bounce, double bounce or ground and tree trunk and volume scattering. The volume scattering from forest canopy is of importance for forest AGB estimation. Figure 4 shows an example of the volume scattering of L-band cross-polarisation as adapted from Carver (1988).

Data acquisition using unmanned aerial vehicle (UAV)-based platform has high operational flexibility in terms of cost, time, platforms, place and repeatability compared to the satellite-based platform and traditional manned photogrammetric operations. UAV has the capability of providing high spatial and temporal resolution data which is useful in assessing AGB and carbon stock (Fritz et al. 2013). UAV platform can capture high-resolution images that can be used effectively and efficiently to generate the digital terrain model (DTM), digital surface model (DSM) and orthomosaic image (Stöcker et al. 2017). Moreover, conventional remote sensing techniques can provide horizontal forest structure accurately rather than vertical forest structure. On the contrary, UAV is capable of providing horizontal and vertical forest structure. Therefore, more accurate estimation of forest stand parameters, e.g. CPA, height and AGB, can be assessed from 3D orthomosaic UAV images (Fig. 5).

The captured images from the UAV platform are used to generate DSM, DTM and orthomosaic based on structure from motion (SfM) technique. Structure from motion (SfM) represents the process to obtain a three-dimensional structure of a

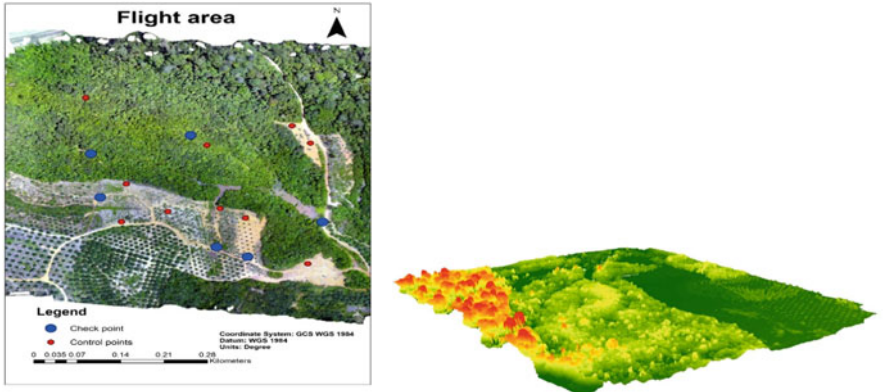


Fig. 5 UAV orthomosaic image (left) and CHM or trees height image (right)

scene of an object from a series of digital images (Micheletti et al. 2015). SfM photogrammetry is cost- and time-effective to estimate forest AGB and carbon stock. SfM uses a sequence of overlapping images to produce a sparse 3D model of the scene. SfM photogrammetry approach is capable of generating a digital surface model, reflecting the top of the canopy in the case of a forest and a digital terrain model. Canopy height model (CHM) can be generated from DSM and DTM. From CHM, the tree height can be extracted that would be the input for allometric equations to assess biomass and carbon.

Among all biophysical parameters of the tree, diameter at breast height (DBH) is one of the essential variables to assess the biomass and carbon because it explains more than 95% variation in biomass (Gibbs et al. 2007). Studies have proved that there is a significant relationship between CPA and DBH (Anderson et al. 2000; Hussin et al. 2014). The correlation was demonstrated between CPA and all parts of trees such as foliage mass, branch mass and stem mass for biomass. Tree height can be estimated using CHM. Thus, aboveground biomass and carbon stock can be assessed based on the relationship between CPA and DBH and CHM using regression model and allometric equations.

3 Key Literatures of Remote Sensing Applications in Forest AGB and Carbon Stock Estimation

The following are samples of key development in research work using different remote sensing sensor systems to assess forest AGB and carbon stock in this decade.

3.1 Very High-Resolution Satellite (VHRS) Image Applications

Hussin et al. (2014) have reported that the methods of forest carbon estimation using remote sensing data and techniques are evolving within a short timeframe as compared to traditional forest inventory methods. Object-based image analysis (OBIA) provided new opportunities to improve biomass and carbon stock estimation and mapping by delineating and classifying crown projection area (CPA) of individual trees. In this paper, image segmentation techniques of OBIA (region growing and valley following) are being applied on GeoEye-1 satellite data and compared in terms of accuracy in Ludhikhola watershed in the Gorkha District of Nepal. Accuracy assessment of tree crown delineation of both segmentation approaches was analysed using accuracy measures of D and one-to-one (1:1) correspondence. The combination of over-segmentation and under-segmentation, D is interpreted as the 'closeness' measure to an ideal segmentation, results in relation to a predefined reference set. Region growing and valley following segmentation with 68% and 58% accuracy, respectively, were achieved and linear regression model was developed for carbon stock for *Shorea robusta* which resulted into a coefficient of determination value of 0.67 at 95% confidence level and the coefficient of determination resulted into a value of 0.70 for other species. The research concluded that region growing approach showed better delineation as compared to valley follow approach, since it used both features of local maxima and local minima.

A study by Karna et al. (2015) in which they aimed to develop species-specific regression model using canopy projection area (CPA) and LiDAR (ALS) derived tree height as predictor variables for accurate estimation and mapping of carbon stock in tropical forests of Chitwan, Nepal. In this study WorldView-2 image was co-registered to airborne LiDAR data. LiDAR data was further processed to obtain the canopy height model (CHM) by subtracting digital terrain model (DTM) from digital surface model (DSM). Both the pan-sharpened image and CHM layers were used for tree crown delineation to extract CPA and height of the individual trees. Aboveground carbon stock was calculated from field-measured DBH and height using species-specific allometric equation and a conversion factor. Species-wise multiple regression models were developed using CPA, LiDAR height and field-measured carbon stock for carbon mapping of the study area. Shannon diversity index of each community forest (CF) was calculated to find out the relationship between tree species diversity and carbon stock of CF.

LiDAR or ALS-derived height showed overestimation of field height with RMSE of 3.84 m and was able to explain 76% of variability in height measurement. Multi-resolution segmentation resulted with overall accuracy of 75% in 1:1 correspondence and 67% segmentation accuracy (33% error) was observed from goodness of fit (D value). Transformed divergence indicated a good separation among different tree species with best average separability of 1970.99. NIR1, NIR2 and Red-Edge of WorldView-2 image were found to be the best bands for spectral separability. Tree species classification resulted in overall accuracy of 58.06% and Kappa statistics 0.47 for classifying six tree species. On average correlation coefficients of CPA and carbon, height and carbon and CPA and height were found to be 0.73, 0.76 and 0.63,

respectively, and indicated significant relationship for five dominant tree species. Species-wise multiple regression models were able to explain 94%, 78%, 76%, 84% and 78% of variation in carbon estimation using CPA and LiDAR height for *Shorea robusta*, *Lagerstroemia parviflora*, *Terminalia tomentosa*, *Schima wallichii* and others, respectively. A total of 188,485 Mg C carbon stock was estimated with an average of 216 MgCha⁻¹. The relationship between tree diversity and carbon stock at CF level was not significant and indicated weak correlation. They concluded that WorldView-2 satellite imagery and airborne LiDAR data are very promising remote sensing sources for estimating and mapping species-wise aboveground carbon stock of tropical forests.

3.2 Airborne Laser Scanner (ALS) Applications

A study by Bazezew et al. (2018) presents an approach for accurate assessment of AGB of tropical rainforest of Ayer Hitam, Malaysia, by integrating airborne laser scanner (ALS) and terrestrial laser scanner (TLS). Integrative use of ALS and TLS of modern remote sensing technologies has enabled to detect a comparable number of manually recorded trees. ALS and TLS were used to detect and extract upper and lower canopies tree parameters, respectively. About 62% of trees were detected by ALS, while the remaining 38% were detected by TLS. The height of upper and lower canopy trees was then measured from the corresponding ALS and TLS point cloud data. Diameter at breast height (DBH) of all trees was measured by TLS, and ALS detected trees were matched and linked with the corresponding tree stems detected by TLS for DBH use. DBH derived from TLS was validated using manually measured field DBH. On the other hand, two ways of tree height validation were implemented: upper canopy and lower canopies tree height. Upper canopy tree height measured from ALS was used as a ground-truth reference to validate corresponding field-based tree heights.

For lower canopy trees height measurement validation, controlled field experiment was performed to assess the accuracy and height measurement variation of the TLS and handheld laser instruments (Leica DISTO 510, TruPulse and Forestry Laser Rangefinder). Height measurements were done in the known height of the windowsills and selected solitary and complex cluster of trees. The result showed TLS provides highly accurate height approaching to the actual heights of the windowsills with root mean square (RMSE) of 5 cm, while Leica DISTO 510, TruPulse and Forestry Laser Rangefinder provided RMSE of 60, 73 and 85 cm, respectively. Height measurement with handheld laser instruments showed deviations from regression line with increasing distance and height of the object. On the other hand, handheld laser instrument height measurement of selected trees showed significant differences among observers and distances to the tree.

Coefficient of determination (R^2) and RMSE between field and TLS-based DBH were 0.989 and 1.30 cm (6.52%), respectively. The R^2 and RMSE between upper canopy tree field-based height and the corresponding heights identified by ALS were 0.61 and 3.24 m (20.18%), respectively. On the other hand, R^2 of 0.69 and RMSE of

1.45 m (14.77%) were found for lower canopy tree heights when field-based height was validated with TLS-measured tree heights. The AGB calculated from the combination of ALS- and TLS-derived parameters was compared with the traditional field-based AGB at the plot level, and R^2 of 0.966 and RMSE of 0.62 Mg (7.64%) were achieved.

Wassihun et al. (2019) have investigated the effect of forest stand density on the estimation of AGB/carbon stock using ALS- and TLS-derived tree parameters in Berkelah tropical rainforest, Malaysia. Purposive sampling approach was adopted for the selection of the unit of analysis. Results are based on data collected from 32 sample plots measured and scanned in the field. ALS was used to derive upper canopy tree height, while TLS was used to derive the height of lower canopy trees and DBH of all scanned trees in all sampled plots. DBH measured in the field was used to validate the DBH manually derived from TLS (terrestrial laser scanner) point cloud data and it was also used to compute the stand basal area of field-measured trees and extracted from TLS point cloud data. The DBH manually derived from TLS point cloud was used to estimate AGB of the sampled plots for both upper and lower canopy trees. Descriptive statistics, linear regression and correlation analysis were used to answer the research questions of this study.

The coefficient of determination (R^2) and RMSE of the DBH manually derived from TLS point cloud data validated by field-measured DBH were 0.99 and 1.37 cm, respectively. This result revealed the existence of almost one-to-one relationship, and based on the statistical test undertaken, there is no statistically significant difference between the two DBH measurements. Out of 1033 trees measured and scanned in the field, 855 trees (82.7%) were extracted from TLS point cloud data and 178 trees (17.3%) were missed. The Pearson's correlation coefficient (r) between total number of trees measured and scanned in the field and total number of trees extracted from TLS point cloud was 0.95. R^2 of 0.89 and 0.15 was found to explain the relationship between the number of missed trees per plot against number of trees measured in the field and number of missed trees against forest stand density, respectively, per plot regardless of the size of missed trees. On the other hand, R^2 of 0.912 and 0.179 was found for forest stand density against aboveground biomass and number of trees per plot against aboveground biomass, respectively. Furthermore, for AGB sensitivity analysis, when TLS tree height was validated by corresponding trees height from ALS, 0.72 and 2.42 m were found for R^2 and RMSE, respectively, and AGB was not sensitive to TLS tree height measurement variation. Finally, based on the findings, forest stand density significantly affects the estimation of aboveground biomass at alpha equal to 0.01 significance level.

Ojoatre et al. (2019) in a study aimed at assessing the uncertainty of tree height and aboveground biomass from terrestrial laser scanner (TLS) and hypsometer using airborne laser scanner (ALS) data in tropical rainforests of Ayer Hitam, Malaysia. Then they assess the effects of tree height accuracy on the forest biomass and carbon stock through sensitivity analysis of the error in height measurement and how it affects the accuracy of tree biomass/carbon stock. Field height measurement using Leica DISTO 510 showed underestimation of tree height with RMSE of 4.07 m, while TLS showed underestimation of height with RMSE 1.33 m when airborne

LiDAR was used as a standard to validate the field and TLS measurements. There was significant difference in the amount of AGB and carbon stock from the three (3) different measurements notably 146.33 Mg of AGB and 68.77 Mg of carbon from field measurements, 170.86 Mg of AGB and 80.31 Mg of carbon from TLS and 179.85 Mg of AGB and 84.53 Mg of carbon from the airborne LiDAR. Considering the airborne LiDAR measurement as the most accurate, the AGB and carbon stock from field represent 85.55% of respective total AGB and carbon stick estimation from airborne LiDAR. Meanwhile TLS measurements reflect 95.02% of respective AGB and carbon stock estimated using airborne LiDAR as a standard measurement. The results have shown that the amount of AGB and carbon stocks is sensitive to height measurement errors resulting from the various methods used to undertake the measurements and the forest conditions; airborne LiDAR measures tree height more accurately compared to field measurements using Leica DISTO 510 and TLS as they are terrestrially based and cannot accurately capture the top of trees as airborne LiDAR.

Kumar et al. (2012) have reported that light detection and ranging (LiDAR), a relatively recent active remote sensing technology, can provide accurate appraisal of vertical forest canopy structure. Individual tree and stand-level physical attributes such as height, vertical structure, canopy closure and density can be retrieved from LiDAR data. In their research they present a novel method to precisely detect individual trees from high-density airborne LiDAR point cloud data. Tree canopies are delineated using object-based image analysis and a new approach of Thiessen polygons. Further an array of important tree parameters such as tree height, canopy projection area (CPA), canopy base height, canopy volume, canopy density, canopy gaps, local tree density and canopy inclination have been extracted from the LiDAR point cloud data to prepare geospatial forest inventory. The research also deals with tree species classification based on query method on structural tree parameters in inventory database. Lastly, the sequestered forest carbon in the study area has been assessed by developing regression equation from the extracted parameters. Tree peaks were detected with high accuracy of 96%, while best crown segmentation accuracy for region growing segmentation approach was 84% with 93.5% one-to-one (1:1) correspondence. Thiessen polygon segmentation approach proved to be a good estimator of CPA with 94.2% 1:1 correspondence and it could explain reference CPA with $R^2 = 0.90$, $RMSE = 3.2 \text{ m}^2$. Tree height was extracted with $R^2 = 0.86$, $RMSE = 0.86 \text{ m}$, while canopy base height was extracted with an accuracy of $R^2 = 0.73$, $RMSE = 0.86 \text{ m}$. Species classification was achieved with an overall accuracy of 97%. The best carbon model using extracted parameters had accuracy of $R^2 = 0.78$, $RMSE = 0.23 \text{ kg}$. In this research, LiDAR has emerged as a potential technology to fulfil the needs of precision forestry.

3.3 Terrestrial Laser Scanner (TLS) Applications

In a study by Kalwar et al. (2021), they assessed forest inventory parameters (species, position, diameter at breast height (DBH), tree height, etc.) in tropical

rainforest of Royal Belum State Park of Malaysia using TLS. Data on these parameters were collected from field observations to be used as ground truth. TLS data of the sample plot were acquired through multiple scanning using a Riegl VZ-400 scanner. Pre-processing and registration of multiple scans were done in RSCAN PRO software. After that all sampled trees within the inventory plots of 500 m² were extracted manually in RiSCAN PRO. Then DBH and tree height were measured manually in RiSCAN PRO and CloudCompare software. Automatic derivation of DBH and tree height was also computed using Computree algorithms. The inventory parameters derived from different methods were compared to analyse the relationships between them. Aboveground biomass (AGB) stocks of the sample plots were estimated based on both the field-measured and TLS-derived DBH and tree height using an allometric equation. A conversion factor (0.47) was used to convert AGB stocks to aboveground carbon (AGC) stocks.

Plot-wise average manual and automatic detection rate of tree was 80 and 90 % achieved with respect to field observations. The average of plot values of R^2 and RMSE was 0.95, 2.7 cm and 0.93, 2.29 cm, respectively, for manual and automatic computation of DBH. Similarly, the average of plot values of R^2 and RMSE for manual measurement and automatic derivation of tree height was 0.77, 2.96 m and 0.04 and 5.35 m, respectively.

The average stocks of AGB and AGC estimated from field-measured DBH and tree height were 286 Mg ha⁻¹ and 134 Mg ha⁻¹, respectively, while the average stocks of AGB and AGC estimated from manually measured DBH and tree height from TLS data were 278 Mg ha⁻¹ and 130 Mg ha⁻¹, respectively. Similarly, the R^2 values for the estimated AGB and AGC from manually measured DBH and tree height from T-LiDAR data were 0.93 and the corresponding RMSE values were 42.4 Mg ha⁻¹ and 19.9 Mg ha⁻¹. The RMSE% value for AGB and AGC was 14.8%, i.e. AGB and AGC can be estimated with 14.8 accuracy with respect to field-measured DBH and tree height.

Thus, this study suggests that TLS technology has potential to derive forest plot inventory parameters (stem detection, BDH and tree height) for AGB and AGC estimation in tropical forest. Compared with field measurement, these parameters were manually measured with reasonable accuracy from TLS data. Automatic derivation of these parameters was not very successful. There is a need to develop robust algorithms for automatic derivation of forest inventory parameters.

Another study on TLS applications by Beyene et al. (2020) aimed at the assessment of the effect of scanning positions of TLS on derivation of tropical forest inventory parameters and aboveground biomass estimation in the tropical rainforest of Ayer Hitam, Malaysia.

Therefore, for this study, four and five scanning positions were used to derive forest inventory parameters and aboveground biomass or carbon stock estimation. A total of ten sample plots were established to collect validation data from field. Concurrently with the field data collection, the sample plot was scanned with TLS using four and five scanning positions. The point cloud data was then processed using manual and automatic extraction method in RiSCAN PRO and Computree software. Thus, the individual trees were extracted manually and automatically from

the point cloud. Respectively, the overall manual extraction percentage of trees was 97.99 and 99.55% for the four and five scanning positions. Similarly, the automatic extraction of individual trees was analysed with respect to the collected field data and the result showed that 91% and 93.75% of the trees were extracted from the four and five scanning positions, respectively. Moreover, the accuracy of the automatic and manually measured TLS DBH was validated using the field-measured DBH as independent variable.

The root mean square error (RMSE) for the manually derived DBH from the four and five scanning positions was 1.66 cm (8.06%) and 1.37 cm (6.60), respectively. Similarly, the RMSE for the automatically derived DBH from the four and five scanning positions was 3.12 cm (14.57%) and 2.36 cm (11.47%), respectively. The RMSE for the automatically measured height from the five and four scanning positions was 3.17 m (17.40%) and 3.68 m (19.97%). The result also showed R^2 value of 0.98 and RMSE of 0.077 Mg for above ground biomass calculated from five scanning positions. There was no significant difference of AGB 84.65 Mg and 39.78 Mg of carbon from manually measured parameters and AGB of 77.24 Mg and 36.31 Mg of carbon measured from automatically measured parameters with four scanning positions. Similarly, the result of the aboveground biomass and carbon was calculated manually and automatically from the five scanning positions and they did not show a significant difference with a value of 101.2 Mg AGB and 47.48 Mg of carbon and 83.75 Mg of AGB and 39.36 Mg of carbon, respectively. The result has shown that increasing the number of scanning position from four to five did not have any effect both in the derivation of parameters and aboveground biomass or carbon stock estimation. However, it has an effect on the extraction of individual trees from the point cloud data since increasing the number of scanning positions has the potential to capture all the trees within the sample area.

In other study by Muumbe et al. (2021) they explored the feasibility of using terrestrial laser scanner and quantitative structure modelling (QSM) to assess AGB in a tropical rainforest of Ayer Hitam Forest Reserve, Malaysia. In this study point clouds were acquired from 26 circular plots of 500 m² using a RIEGL VZ 400 terrestrial laser scanner. Registration, extraction of individual trees and measurement of DBH and height were conducted in RISCAN PRO v 2.1. One hundred (100) trees were selected for the QSM reconstruction based on extraction quality and DBH distribution. TLS-derived DBH and height with wood density were used to calculate AGB from allometric equations. AGB was calculated from the QSM-derived volume and wood density. The DBH and height derived from the TLS were compared to the DBH and height measured from the field. The AGB biomass derived from allometric equations was compared with the AGB derived from QSM and the distribution of AGB along the different parts of the trees was assessed. Sensitivity analysis was carried out on parameters that affect the volume reconstruction. These parameters are the number of runs, cover set diameters and nmin values. Above-ground carbon (AGC) per tree was calculated by using a conversion factor of 0.47 to convert the AGB/tree into AGC/tree.

Field-measured DBH with TLS-derived DBH showed a high correlation with an R^2 of 0.993 and an RMSE of 1.1 cm, while field height and TLS height showed a low

correlation with an R^2 of 0.589 and an RMSE of 3.4 m. Of the 100 trees, 29 observations had trunk biomass greater than canopy and 71 observations had canopy biomass greater than trunk biomass. Of the 29 observations, there was a strong relationship between AGB from allometric equations and from QSM. An R^2 of 0.968 with an RMSE of 120 kg/tree was observed when using the FAO default wood density value for Asia (0.57 g/cm^3) and an R^2 of 0.934 and an RMSE of 131.61 kg/tree were obtained using species-specific wood density. The 71 observations showed a slightly lower relationship with an R^2 of 0.817 and an RMSE of 163 kg/tree using 0.57 g/cm^3 wood density and an R^2 of 0.797 with an RMSE of 198 kg/tree using species-specific wood density. Compared to the allometry reference AGB was overestimated by 47% for 100 trees. No statistically significant difference was observed in using either the FAO default wood density value or species-specific wood density in calculating AGB. The average AGC per tree was 294 kg/tree using species-specific wood density values and 281 kg/tree using the FAO default wood density value.

This study shows the potential of TLS and QSM in estimating AGB but further work is needed for accurate reconstruction of trees in a heterogeneous forest. Reconstruction of the trees was not very successful as many factors play a role in producing a robust reconstruction. There is a need to develop algorithms that properly extract individual trees from point clouds, accurately separate the branches and leaves before reconstruction and also automate the process of finding optimum modelling parameters to suit the variety of species.

3.4 Synthetic Aperture Radar (SAR) Applications

The first study on SAR application in assessing AGB is by Masolele et al. (2019), which examined the application of L-band ALOS-2 PALSAR-2 SAR data to model the AGB/carbon stock and carbon sequestration of the tropical rainforest. The SAR parameters were evaluated on the basis of the single SAR backscatter image and time series analysis of SAR backscatter, together with an analysis of the influence of combined HV and HH backscatter on AGB estimation. Also, the saturation effect of radar backscatter for AGB estimation was established by determining the saturation level at which AGB prediction tends to level off. The seasonal (moist, dry) dependence of SAR backscatter for AGB estimation was also analysed. The satellite SAR data used for this study were represented by a time series of SAR images acquired in three-time periods: September 2006, January 2017 and September 2017 by the ALOS-2 PALSAR-2 sensor. The study area is in the tropical rainforest Berkelah, Malaysia, and represented a typically managed complex tropical rainforest land. The relationship of different L-band SAR parameters and their temporal stability was studied along with reference field AGB data calculated from forest DBH and tree height measurements. Further, two polarimetric parameters, cross-polarisation and co-polarisation backscatter, were chosen for further investigation and AGB retrieval.

A relationship between forest AGB and L-band SAR parameters was established using the linear, logarithmic and multiple regression approaches. Ways of obtaining

the optimal combination of L-band SAR images were evaluated as well. For a single scene, the best results were observed with HV-polarised backscatter ($R^2 \approx 0.82$, RMSE ≈ 79 tons ha^{-1}) and ($R^2 \approx 0.87$, RMSE ≈ 68 tons ha^{-1}) using logarithmic regression for scenes acquired in September 2016 and September 2017 conditions, respectively. SAR backscatter saturation was estimated at 270 tons ha^{-1} , the point at which SAR backscatter response to AGB started to decrease by 0.02dB. At the same time, AGB validation result with an ($R^2 \approx 0.8$, RMSE ≈ 84 tons ha^{-1}) and ($R^2 \approx 0.78$, RMSE ≈ 88 tons ha^{-1}) was achieved for logarithmic and linear regression analysis of HV backscatter, respectively. Hence, logarithmic regression was a better predictor of AGB than using linear regression. Multiple aggregations of HV and HH did not significantly improve the AGB estimates for both studied SAR parameters with p -value > 0.05 . The stronger achievement was observed in the estimation of the amount of carbon sequestration between September 2016 and September 2017. An estimated total of 3.62 tons ha^{-1} of carbon was sequestered in Berkelah forest in 1 year. This study proved that combining temporal series of SAR scenes could be a better estimator of carbon sequestration.

In general L-band, SAR backscatter has proved to have a significant potential for AGB/carbon stock estimation and carbon sequestration. It provides an opportunity for climate change programmes (REDD+) to engage more in using SAR data for forest carbon monitoring. However, challenges of SAR backscatter saturation, moisture effect on SAR backscatter and accurate forest height estimation for AGB estimation using SAR data still need to be addressed.

However, when using SAR data to assess AGB in mangrove forest, the accuracy estimation is relatively low according to the literatures. In this context, Nesha et al. (2020) study was carried out to estimate AGB/carbon stock using backscatter coefficients of ALOS-2 PALSAR-2 in the part of the mangrove forest at Mahakam Delta, East Kalimantan, Indonesia. The forest parameters (DBH and tree height) were collected from a total of 71 sampling plots in October 2018. The forest parameters were used to calculate the field-based AGB using an allometric equation for the mangrove forests. PALSAR-2 data with level 1.1 fine beam dual (FBD) polarisation was obtained from JAXA. A linear regression model was applied to estimate AGB in the study area (105 ha) using HV and HH polarisation backscatter of PALSAR-2. The accuracy of the AGB estimation was assessed in terms of R^2 , RMSE and p -value. The results of the linear regression models revealed that HV backscatter coefficients estimate AGB with high accuracy at R^2 of 0.89, RMSE of 23.16 tons ha^{-1} and p -value < 0.01 . The accuracy of the model validation was also high at R^2 of 0.89, RMSE of 22.69 tons ha^{-1} and p -value < 0.01 . This implied that HV backscatter coefficients of PALSAR-2 predicted AGB in the mangrove forest with 89% accuracy in our study. Therefore, the equation derived from the simple linear regression model was used to map the AGB and carbon stock in the study area. The estimated AGB in the study area of the mangrove forest ranged from 1 to 350 tons ha^{-1} with an average of 181 tons ha^{-1} , and the total AGB accounted for 13,719 tons.

The findings of our study showed a promising accuracy in estimating AGB using HV-polarised ALOS-2 PALSAR-2 backscatter coefficients in the mangrove forest.

Therefore, our study concluded that L-band ALOS-2 PALSAR-2 data has a great potential to estimate AGB with high accuracy in the mangrove forest as in the inland forest in the tropics. Thus, the findings of our study can contribute to the MRV mechanism of UN-REDD+ programme for monitoring the carbon emission reduction in the mangrove forests in the tropics.

Sumareke (2016) in her study model and map AGB and carbon stock of Ayer Hitam Rainforest Reserve in Malaysia using ALOS PalSAR images, data from 27 plots were assessed. Out of these data, 17 plots were used for developing the model and other 10 plots were retained for model validation. AGB was obtained based on plot level using the improved allometric equation developed by Chave et al. (2015). Meanwhile, backscatter coefficient from HH and HV polarisation was retrieved and converted to sigma nought. Besides, total stand BA, average DBH and height were also obtained.

Correlation and simple linear regression analyses were done separately between observed AGB and backscatter coefficient of ALOS-2 PALSAR, HH and HV polarisation. Results of the analysis showed a positive and strong relationship ($R^2 = 0.817$) between AGB and HV-polarised backscatter. About 82% of the variability in AGB was explained by the HV backscatter coefficient. The ten independent data were used to validate the model. The predicted AGB was plotted against the observed AGB. A strong correlation was identified with R^2 of 0.796. The correlation was significant at 99 and 95% confidence level. The AGB of the study area was estimated using the simple linear regression developed with HV backscatter and AGB. The AGB and carbon stock map of the Ayer Hitam Forest Reserve were produced. Carbon stock values were calculated using 0.5 conversion factor.

The observed amount of AGB of AHFR obtained from the measured data using the allometric equation ranges from 60.17 to 367.07, while the estimated AGB using the simple linear model with HV SAR data ranges from 20 to 576.42 tons ha⁻¹. The average AGB for observed and estimated was 208.79 tons ha⁻¹ and 257.98 tons ha⁻¹, respectively. The total estimated AGB of the whole study area of AHFR derived from HV backscatter is. 321,966.28 tons, while the total AGB observed is about 260,574.27 tons. Average estimated carbon stock of AHFR is 128.99 tons ha⁻¹ and the total estimated carbon stock is 160,983.14 tons.

The present study found that the average value of AGB per ha⁻¹ obtained in AHFR agrees with several similar studies which were carried out in tropical countries as well in Malaysia using ALOS PALSAR. This indicates that ALOS-2 PALSAR-2 is able to estimate AGB accurately in tropical countries. Further study is needed to be undertaken in saturation sensitivity analysis of ALOS-2 PALS-2 in tropical forest with high density of biomass.

3.5 Unmanned Aerial Vehicle (UAV) Applications

Reuben et al. (2017) have investigated the accuracy of tree height derived from point clouds of UAV compared to airborne laser scanner and its effect on estimating biomass and carbon stock in a part of tropical rainforest of Ayer Hitam, Malaysia.

The accuracy of photogrammetry (structure from motion (SfM)) image matching DTM of UAV and that of LiDAR was assessed by using height (z value) recorded by differential global positioning system (DGPS), and it was revealed that RMSE of UAV DTM was 3.84 m or 7.96% and $R^2 = 0.96$, while the same measures for LiDAR RMSE, RMSE% and R^2 were 1.25 m, 2.75% and 0.99. Then the accuracy of the DTM of UAV was assessed by comparison to the DTM of ALS in all six flights of UAV, and the results revealed that RMSE, RMSE% and R^2 were 0.31–1.49 m, 1.57–8.34% and 0.53 to 0.82, respectively. The accuracy assessment went further and assessed DTM generated from photogrammetry image matching of UAV in the area which shows small difference between UAV and LiDAR DTM. In this case the RMSE was 0.19 m, RMSE% = 0.5%, and R^2 was 0.99, while at the same area, the estimated tree height of UAV images compared to tree height from airborne LiDAR showed RMSE of 1.56 m and RMSE% of 8.7 with R^2 of 0.80.

Tree height measurements were conducted by using three main methods: field measurement using Leica DISTO, UAV and ALS. The accuracy of estimating tree height of the field and UAV was validated by using the tree height derived from ALS. The validation of field-measured tree height revealed that the RMSE was 2.55 m RMSE% of 15.25 and R^2 of 0.62. When the estimated tree height of UAV was regressed with derived tree height from ALS, R^2 was 0.78, while RMSE was 1.7 m and RMSE% was 9.63. Furthermore, the AGB and carbon stock were computed using an allometric equation which utilised diameter at breast height (DBH), tree height and wood density. The AGB and carbon stock did not show statistically significant difference, and the total biomass computed was 189.48 Mg, 177.13 Mg and 172.97 Mg for ALS, UAV and field, respectively. The accuracy assessment revealed that 97% of field biomass was accurately modelled by ALS computed biomass, with RMSE of 0.11 Mg (24%), while 99% of calculated UAV biomass was accurately predicted by ALS computed biomass, with RMSE of 0.06 Mg and RMSE % of 13. The measured tree heights were later adjusted to reveal its influence on the calculated AGB and carbon stock. The field tree height was adjusted based on RMSE of 3 m, while tree height derived from photogrammetry image matching of UAV was adjusted by RMSE = 4 m.

Kustiyanto et al. (2019) have assessed aboveground biomass (AGB)/carbon stock using UAV images of 2017 and 2018 as well as calculate carbon sequestration over a 1-year period in a part of mangrove forest in Mahakam Delta, East Kalimantan, Indonesia. Fieldwork was done to collect biometric mangrove tree parameters such as diameter at breast height (DBH) and tree height to calculate aboveground biomass/carbon stock and carbon sequestration using UAV images of October 2017 and December 2018. These results were compared with biometric data collected in the field to assess its accuracy.

The results show that there was a significant relationship between crown diameter derived from crown projection area of UAV images and the ground-truth DBH of both 2017 and 2018. The results reveal that there was a strong relationship between tree height derived from canopy height model (CHM) of UAV images and tree height derived from terrestrial laser scanner (TLS) data in 2017 and 2018. The AGB modelled from UAV images was 102 Mg/ha and 112 Mg/ha in 2017 and 2018, while

the AGB from biometric (i.e. ground truth) data in 2017 was 104 Mg/ha and in 2018 was 114 Mg/ha. According to the results from UAV images in the period from October 2017 to December 2018, sequestered carbon was 6 Mg/ha/year compared to 5 Mg/ha/years of carbon sequestration assessed using biometric ground-truth data.

Hashem et al. (2019) have investigated the assessment of forest aboveground biomass/carbon stock and carbon sequestration using high-resolution UAV images in tropical forest of Kebun Raya Samarinda, East Kalimantan, Indonesia. The DSM, DTM and orthomosaic were generated based on structure from motion (SfM) and 3D point cloud filtering techniques. The canopy height model (CHM) was generated from the DSM and DTM. The height extracted from the CHM and the predicted DBH calculated from the CPA based on the quadratic model were used as input in the generic allometric equation to estimate AGB and carbon stock.

The *F*-test and *t*-test revealed that the tree height extracted from CHM and the field-measured tree height had no significant difference. The relationship between field DBH and manually delineated CPA was made and showed the highest coefficient of determination and lowest RMSE for the quadratic model. The model validation also performed and showed a strong correlation between observed DBH and predicted DBH. The results of the *F*-test and *t*-test revealed that there was no statistically significant difference between field-based AGB and UAV-based AGB. The total amount of sequestered carbon for 1 year was assessed at 6.32 Mg ha⁻¹. The difference of UAV-based AGB with and without inflated/deflated height was found to be 21.66 Mg ha⁻¹ which is equivalent to 8.73% of original estimated UAV-based AGB without inflation and deflation of height. The single factor/one-way ANOVA test revealed that there was a statistically significant difference between estimated UAV-based AGB with 8.94% inflation and deflation of height and UAV-based AGB without inflation/deflation of height. The average variation of biomass due to 1% inflation and deflation of CPA was 2.47 Mg ha⁻¹ and showed statistically insignificant influence on biomass estimation. For 5% inflation and deflation of CPA, the average variation of biomass was estimated to be 12.37 Mg ha⁻¹. Despite its large variation, it had no statistically significant difference from original biomass, but the amount of AGB was observed very much close to the estimated amount of sequestered biomass for 1 year. On the other hand, the average variation of biomass 24.70 Mg ha⁻¹ was estimated to be 10% inflated and deflated CPA that showed a statistically significant difference and it affected 9.96% variation of AGB from the original biomass. The estimated amount of carbon due to CPA error was double compared to the amount of sequestered carbon for 1 year. To summarise, this study showed a novelty by assessing carbon sequestration using UAV images for 2 consecutive years.

Gaden et al. (2022) have assessed the potential of UAV multispectral imagery over the UAV RGB images for estimation of AGB and carbon stock in coniferous forest of Haagse Bos, Netherlands.

Tree parameters derived from UAV multispectral and RGB imagery to estimate aboveground biomass or carbon (AGB/AGC) were evaluated in a temperate conifer forest of the Netherlands. A total of 650 trees measured in 35 plots were employed as a reference parameter to assess the accuracy of UAV-estimated parameters through

linear regression using statistical indicators such as correlation (r), determination of coefficient (R^2), the slope of the regression (β) line, RMSE and bias (%). The results demonstrate the potentiality of UAV multispectral images with SfM algorithm to retrieve tree parameters to estimate AGB/AGC.

Tree crown diameter (CD) was derived from canopy projection area (CPA) manually digitised from multispectral (MS) and RGB orthomosaic. The comparison of crown diameter from MS CPA showed higher ($r = 0.98$) agreement with RGB CPA. However, a paired t -test showed a significant difference in mean tree crown diameter ($t = -7.94$, $df = 629$, $p < 0.05$).

The tree height (TH) in this study was extracted from the canopy height model (CHM) produced from a digital surface model (DSM) and digital terrain model (DTM). The study found that MS-derived tree height ($R^2 = 0.72$, RMSE = 2.6 m) was less accurate than RGB-derived tree height ($R^2 = 0.75$, RMSE = 2.2 m). One-way ANOVA F -test showed a significant difference between the group means of tree height ($F(2, 1887) = 36.95$, $p < 0.05$). The follow-up Tukey post hoc test showed a significant difference between all group means of tree height ($p < 0.05$).

A set of regression models were compared to determine how accurately the tree diameter at breast height (DBH) can be estimated using UAV-derived parameters. Among the models, tree height and crown diameter ($TH \times CD$) were better in predicting DBH compared to TH , CPA and CD as an independent predictor. The model validation using independent dataset showed MS model ($R^2 = 0.82$; RMSE = 4.39 cm) performing better than RGB model ($R^2 = 0.79$; RMSE = 4.65 cm) in estimating DBH. However, the one-way ANOVA F -test showed no significant difference in a group means of DBH ($F(2, 747) = 0.01$, $p > 0.05$).

The species-specific allometric equation was used in this study to estimate the AGB. At the plot level, the mean AGB estimated from field-measured parameters was 9.02 Mg plot⁻¹, while the mean AGB estimated from MS and RGB imagery was 8.50 and 9.10 Mg plot⁻¹, respectively. Since half of the AGB was considered as a carbon conversion factor, the mean AGB estimated from the field, MS and RGB parameters were 4.50, 4.24 and 4.54 Mg plot⁻¹, respectively. One-way ANOVA F -test showed no significant difference between the group means of AGB estimates ($F(2, 1887) = 0.76$, $p > 0.05$).

The accuracy of AGB estimates was assessed both at a tree and hectare level by extrapolating the plot-wise AGB estimates. At tree level, the accuracy of MS AGB estimates ($R^2 = 0.89$; RMSE = 166.96 kg) was higher than RGB AGB estimates ($R^2 = 0.86$; RMSE = 193.29 kg). Similarly, at hectare level, the accuracy of MS AGB estimates ($R^2 = 0.93$, RMSE = 25.40 Mg) was higher than RGB AGB estimates ($R^2 = 0.89$, RMSE = 31.83 Mg). Simple t -test showed that the slope of regression line between field and UAV-based AGB estimates was significantly different from one ($\beta \neq 1$, $p < 0.05$).

4 Conclusions

The following conclusive remarks can be made:

- VHRS images can be used to assess AGB and carbon stock with reasonable accuracy based on the identification of canopy projection area (CPA).
- Airborne laser scanner (ALS) or airborne LiDAR can be used to assess tree height with high accuracy. It also can detect and delineate CPA accurately. However, when ALS height is used together with CPA from VHRS, a good accuracy can be achieved for AGB and carbon stock.
- High-density point clouds (35/m² or more) from ALS can assess AGB and carbon stock very accurately.
- L-band cross-polarised radar backscatter can model AGB, carbon stock and carbon sequestration with good accuracy.
- Terrestrial laser scanner data can be used to assess AGB and carbon stock with good accuracy only on plot basis.
- Very high-resolution unmanned airborne vehicle (UAV) RGB or MSS images can be used to assess AGB, carbon stock and carbon sequestration with good accuracy.

References

- Anderson SC, Kupfera JA, Wilsonb RR, Cooper RJ (2000) Estimating forest crown area removed by selection cutting: a linked regression-GIS approach based on stump diameters. *For Ecol Manag* 137(2000):171–177. [https://doi.org/10.1016/S0378-1127\(99\)00325-4](https://doi.org/10.1016/S0378-1127(99)00325-4)
- Bazewew MN, Hussin YA, Kloosterman EH (2018) Integrating airborne LiDAR and terrestrial laser scanner forest parameters for accurate above-ground biomass/carbon estimation in Ayer Hitam tropical forest, Malaysia. *Int J Appl Earth Obs Geoinf* 73:638–652. <https://doi.org/10.1016/j.jag.2018.07.026>
- Beyene SM, Yousif AH, Kloosterman HE, Ismail MN (2020) Forest inventory and aboveground biomass estimation with terrestrial LiDAR in the tropical forest of Malaysia. *Canadian J Remote Sens* 46:2. <https://doi.org/10.1080/07038992.2020.1759036>
- Carver K (1988) SAR synthetic aperture radar—earth observing system. NASA National Aeronautics & Space Administration. Instrument Panel Report, vol Iif, Radar Imaging From Space, 233 pp
- Chave J et al (2015) Improved allometric models to estimate the aboveground biomass of tropical trees. *Glob Chang Biol* 20:3177–3190. <https://doi.org/10.1111/gcb.12629>
- Fritz A, Kattenborn T, Koch B (2013) UAV-based photogrammetric point clouds- tree stem mapping in open stands in comparison to terrestrial laser scanner point clouds. *ISPRS Int Arch Photogramm Remote Sens Spat Inf Sci XL-1/W2*(September):141–146. <https://doi.org/10.5194/isprsarchives-XL-1-W2-141-2013>
- Gaden K, Hussin YA, Van Leeuwen LM (2022) Assessing potential of UAV Multispectral imagery for Estimation of AGB and Carbon stock in conifer forest over the RGB imagery. The 43rd Asian Conference on Remote Sensing, 3–7 Oct 2022, Ulaanbaatar
- Gibbs HK, Brown S, Niles JO, Foley JA (2007) Monitoring and estimating tropical forest carbon stocks: Making REDD a reality. *Environ Res Lett* 2(4):045023. <https://doi.org/10.1088/1748-9326/2/4/045023>

- Gschwantner T, Schadauer K, Vidal C, Lanz A, Tomppo E, di Cosmo L, Robert N, Englert Duursma D, Lawrence M (2009) Common tree definitions for national forest inventories in Europe. *Silva Fenn* 43(2):303–321
- Hashem MDA, van Leeuwen L, Hussin YA, Sulistioadi YB (2019) Estimation of Aboveground biomass/ carbon stock and carbon sequestration using UAV images at Kebun Raya Unmul Samarinda (KRUS) education forest, East Kalimantan, Indonesia. ICORS 2019, Proceedings of the 5th International Conference of Indonesian Society of Remote Sensing and Mapping Congress. National Institute of Technology Bandung, Indonesia, vol 2, 17–20 Sept 2019, 170–186 pp
- Hussin YA, Gilani H, van Leeuwen L, Murthy MSR, Shah R, Baral S, Tsendbazar NE, Shrestha S, Kumar Shah S, Qamer FM (2014) Evaluation of object—based image analysis techniques on very high—resolution satellite image for biomass estimation in a watershed of hilly forest of Nepal. *Appl Geom* 6(1):59–68. <https://doi.org/10.1007/s12518-014-0126-z>
- IPCC (2007) Climate change 2007 synthesis report. Retrieved from https://www.ipcc.ch/site/assets/uploads/2018/02/ar4_syr_full_report.pdf
- IPCC (2018) In: Masson-Delmotte V, Zhai P, Pörtner H-O, Roberts D, Skea J, Shukla PR, Pirani A, Moufouma-Okia W, Péan C, Pidcock R, Connors S, Matthews JBR, Chen Y, Zhou X, Gomis MI, Lonnay E, Maycock T, Tignor M, Waterfield T (eds) Global warming of 1.5°C. An IPCC Special Report on the impacts of global warming of 1.5°C above pre-industrial levels and related global greenhouse gas emission pathways, in the context of strengthening the global response to the threat of climate change, sustainable development, and efforts to eradicate poverty
- Jennings SB, Brown ND, Sheil D (1999) Assessing forest canopies and understorey illumination: canopy closure, canopy cover and other measures. *Forestry* 72(1):59–74
- Kalwar OPP, Hussin YA, Michael JC, Weir CA, de Bie JM, Yogendra K (2021) Deriving forest plot inventory parameters using terrestrial laser scanning in the tropical rainforest of Malaysia. *Int J Remote Sens* 42(3):884–901. <https://doi.org/10.1080/01431161.2020.1817606>
- Karna YK, Hussin YA, Gilani H, Bronsveld MC, Murthy MSR, Qamer FM, Karky BS, Bhattarai T, Aigong X, Baniya CB (2015) Integration of WorldView-2 and airborne LiDAR data for tree species level carbon stock mapping in Kayar Khola watershed, Nepal. *Int J Appl Earth Observ Geoinform* 38:280–291. <https://doi.org/10.1016/j.jag.2015.01.011>
- Kumar V, Hussin Y, van Gils H (2012) Fusion of LiDAR data with high resolution optical image for biomass and carbon estimation in Bois Noir forests in the French Alps. XXII ISPRS Congress, Technical Commission VIII (vol XXXIX-B8) 25 Aug–1 Sept 2012, Melbourne
- Kustiyanto E, Hussin YA, van Duren I, Sulistioadi YB (2019) Estimating aboveground biomass/ carbon stock and carbon sequestration using UAV (Unmanned Aerial Vehicle) images in the Mangrove Forests Mahakam Delta, East Kalimantan, Indonesia. In ICORS 2019, Proceedings of the 5th International Conference of Indonesian Society of Remote Sensing and Mapping Congress. National Institute of Technology Bandung, Indonesia, vol 2, 17–20 Sept 2019, 206–222 pp
- Masolele RN, Hussin YA, Kloosterman H, Latif ZA (2019) ALOS-2 PALSAR-2 L-band cross-polarized data analysis for the assessment of carbon sequestration of tropical rainforest, Berkelah, Malaysia. In: IUFRO XXV World Congress 2019. International Union of Forest Research Organization XXV Congress, 29 Sept–5 Oct 2019, Curitiba, 8 pp
- Micheletti N, Chandler JH, Lane SN (2015) Structure from motion (SfM photogrammetry). *Br Soc Geomorphol Geomorphol Tech* 2(2):1–12. <https://doi.org/10.5194/isprsarchives-XL-5-W4-37-2015>
- Mumbe TP, Tagwireyi P, Mafuratiidze P, Hussin Y, van Leeuwen L (2021) Estimating above-ground biomass of individual trees with terrestrial laser scanner and 3D quantitative structure modelling. *South For* 83(1):56–68. <https://doi.org/10.2989/20702620.2020.1818535>
- Nesha MK, Hussin YA, van Leeuwen LM, Sulistioadi YB (2020) Modeling and mapping above-ground biomass of the restored mangroves using ALOS-2 PALSAR-2 in East Kalimantan,

- Indonesia. *Int J Appl Earth Obs Geoinf* 91(2020):102158. <https://doi.org/10.1016/j.jag.2020.102158>
- Ojoatre S, Zhang C, Hussin YA, Kloosterman HE, Ismail MH (2019) Assessing the uncertainty of tree height and aboveground biomass from terrestrial laser scanner and hypsometer using airborne LiDAR data in tropical rainforests. *IEEE J Sel Top Appl Earth Obs Remote Sens* 12(10):4149–4159. <https://doi.org/10.1109/JSTARS.2019.2944779>
- Reuben J, Hussin YA, Kloosterman H, Ismail MH (2017) Tree height derived from point clouds of UAV compared to airborne laser scanning and its effect on estimating biomass and carbon stock in tropical rain forest of Malaysia. In: 38th Asian Conference on Remote Sensing, 23–27 Oct 2016, New Delhi, 8 pp
- Stöcker C, Bennett R, Nex F, Gerke M, Zevenbergen J (2017) Review of the current state of UAV regulations. *Remote Sens* 9(5). <https://doi.org/10.3390/rs9050459>
- Sumareke AM (2016) Modelling and mapping aboveground biomass and carbon stock using ALOS-2 PALSAR-2 data in Ayer Hitam tropical rainforest reserve in Malaysia. Faculty of Geo-information Science and Earth Observation, University of Twente, NRS Department MSc Thesis
- Wassihun AN, Hussin YA, Van Leeuwen LM, Latif ZA (2019) Effect of forest stand density on the estimation of above ground biomass/carbon stock using airborne and terrestrial LIDAR derived tree parameters in tropical rain forest, Malaysia. *Environ Syst Res* 8:27. <https://doi.org/10.1186/s40068-019-0155-z>

Part III

Modelling and Monitoring



Spatial Modeling of Transport and Resources Accessibility for Protecting Forest Ecosystems Against Forest Fires

Abdullah Emin Akay, Ekaterina S. Podolskaia, and Burak Aricak

Abstract

Forest fires are inevitable events that cause negative impacts on forests and threaten the sustainability of forest resources. For effective combating against forest fires, the ground teams should arrive at the fire scene in critical response time in which the possibility of extinguishing the fire is very high. Road networks, including public and forest roads, are the main structures that ensure ground access to the forest resources for management and protection purposes. A network analysis method is effectively used to solve complex transportation problems. Most recent advances in computer technology and geographical information system (GIS) tools with network analysis-based modules have made it possible to develop GIS-based decision support system (DSS) for solving such transportation problems. Network analysis features of proprietary and open source software provide managers with effective methods to define the fastest fire-access route and accessible forested areas by ground teams considering the critical response time. The new route and closest facility methods under Network Analyst tool of ArcGIS software assist fire managers to search for the optimum route that minimizes the travel time of the ground team to the fire. A new service area, which is a well-known method under Network Analyst, is used to evaluate accessibility of the forest areas by the ground teams. This chapter provides a comprehensive review of the previous studies, conducted on the spatial modeling

A. E. Akay (✉) · B. Aricak

Faculty of Forestry, Forest Engineering Department, Bursa Technical University, Bursa, Turkey
e-mail: abdullah.akay@btu.edu.tr

E. S. Podolskaia

Laboratory of Forest Ecosystems Monitoring, Center for Forest Ecology and Productivity of the Russian Academy of Sciences, Moscow, Russian Federation

© The Author(s), under exclusive license to Springer Nature Singapore Pte Ltd. 2022

M. N. Suratman (ed.), *Concepts and Applications of Remote Sensing in Forestry*,
https://doi.org/10.1007/978-981-19-4200-6_5

of transport and accessibility for the forest resources based on the specific GIS modules.

Keywords

Forest fires · Fire-access route · GIS-based DSS · GIS tools · Closest facilities · New service area

1 Introduction

The public pressure and demands on forest products have increased the pressure on forest resources. The most obvious reflections of the pressure on forest resources are manifested as opening up of forests, illegal cutting, and forest fires. Forest fires are as one of the top severe factors damaging forest resources in many regions in the world due to the existence of fire-sensitive plant species and the arid climatic conditions in summer (Haska et al. 2021). Forest fires lead to reduction in the economic values of the trees, which become more susceptible to insects and fungus after fire damages.

The efficiency of the firefighting activities is of great importance in reducing possible volume and value losses of forest resources due to forest fires. To effectively respond to forest fires, especially in fire-sensitive forests, the transportation time of the ground team to the fire scenes should not exceed the critical response time. For this reason, the optimum route that will enable the ground team to arrive at the fire areas in the shortest time possible after the fire announcement is received should be determined. The network analysis method is widely preferred in solving transportation problems involving the determination of the optimum route that minimizes the travel time of a vehicle between two know points. The advances in computer programming and GIS technology make it possible to use network analysis-based GIS techniques to solve transportation problems. Particularly, the new route, new closest facility, and new service area methods under Network Analyst tool of ArcGIS software provide fire managers with effective tools to search for the optimum route to the fire areas and to determine the forest areas that can be reached within the critical response time (Akay et al. 2012).

The GIS-based DSS using the new route and new closest facilities methods has been examined to determine the most appropriate route that allows firefighting teams to reach the fire areas in the shortest time (Dimitrakopoulos et al. 2011; Akay et al. 2012; Podolskaia et al. 2019a, 2020a, b). In such studies, the effects of variables such as road type, road condition, and population density on the solution phase were evaluated. The decision support systems using new service area have been also used to determine where fire trucks should be placed to maximize firefighting efficiency (Akay et al. 2018; Akay and Taş 2020). In this chapter, a broad overview on spatial modeling of transport and resources accessibility for protecting forest ecosystems against forest fires was presented by reviewing previously conducted studies. Firstly, the studies on the optimum ground access route to forest fires, accessible forest lands

by firefighting teams, and their optimal locations are provided, and then the studies on the forest roads as effective infrastructures for fire protection are reviewed.

2 The Optimum Ground Access Route to Forest Fires

For effective firefighting activities, it is crucial that the ground team should arrive at the fire scene within the critical response time. In a study conducted by Bilici (2009), the effects of forest roads along with fires firebreaks and fireline on early access of ground teams to the fire areas were investigated by using the GIS-based network analysis method. Gallipoli National Park in the city of Çanakkale in Turkey was selected as the study area. The network analysis method was used in order to compare the road network without fires firebreaks and fireline and the road network with fires firebreaks and fireline in terms of the fastest access to fire. With this method, it was found that in 27 of 30 inquiries made for 10 potential fire points, the route in the road network with fires firebreaks and fireline was shorter than the route on the road network where fires firebreaks and fireline were not considered. In addition, it has been revealed in the study that the walking distance from the end of the road to the fire point on the route formed as a result of an inquiry was shorter in the road network with fires firebreaks and fireline. When the results of the inquiry were examined, it was determined that fires firebreaks and fireline contributed positively to forest fires at the point of early intervention, and it was revealed that forest roads should be planned together with fires firebreaks and fireline.

Akay et al. (2012) developed a GIS-based DSS to find the optimum route which minimized the transportation time of the ground team from stations to the potential forest fire locations. The application area of the project consists of six forest enterprise directorates located in Regional Forestry Directorate of Kahramanmaraş in Turkey. These Enterprises were classified as sensitive to forest fire and there were 20 fire stations available in the region. In the study, firstly, the digital layers for the road networks (forest roads, rural roads, highways), the fire stations, and previous fire areas (15 fires) were produced by using ArcGIS. Then, network database was generated based on the road layer where travel time of fire truck was assigned to each road section. The travel time was a function of the section length and average truck speed, which varied based on road type and condition. Finally, the optimum route from each ground team to the potential fire areas was found by the new closest facility method (Fig. 1). Besides, inaccessible roads, closed due to fire or some other reasons, were eliminated in the network database, so that the optimum route also provided the safest path. The results indicated that ground teams could not reach 7 out of 15 potential fire areas on time. When the barriers were placed in the database, inaccessible fires increased to eight fires. To increase the efficiency of the ground teams in the study area, it was suggested to locate new fire station, increase the road density, and improve the road standards.

In a study conducted by Podolskaia et al. (2019a), the traveling time of special vehicles (fire trucks, tank trucks, etc.) and the distance from the nearest fire station to a forest fire were estimated using the regional transport model, generated by the

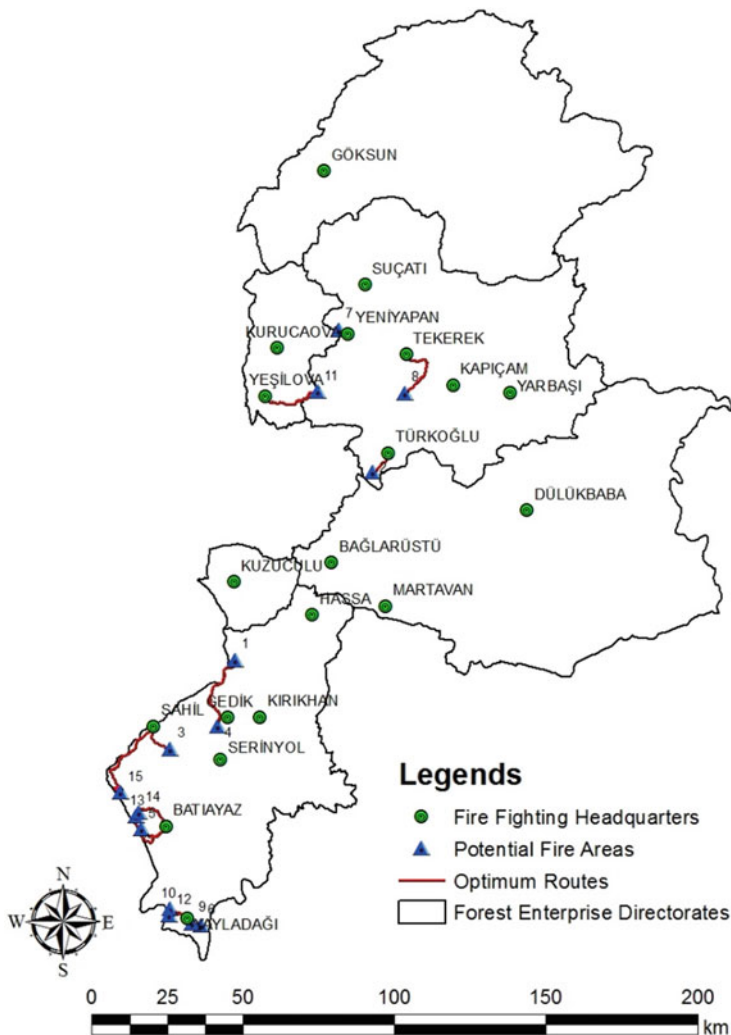


Fig. 1 Optimum routes to potential fire areas (Akay et al. 2012)

Network Analyst tool in ArcGIS (Fig. 2). Based on the dataset of 16 years (2002–2017), the study was conducted in Irkutsk region of Russian Federation where forests are highly sensitive to fires (Goldammer et al. 2003). The GIS dataset was developed to have digital data of necessary layers such as road network, forest glades, fire stations, and forest fire locations. Then, the travel time of the vehicle was computed based on average speed and distance data and then it was assigned to each road section in road network layer. The vehicle speed was computed for each road section based on the road types, elevation data, and terrain slope. The forest fire data detected by MODIS (Moderate Resolution Imaging Spectroradiometer) satellite

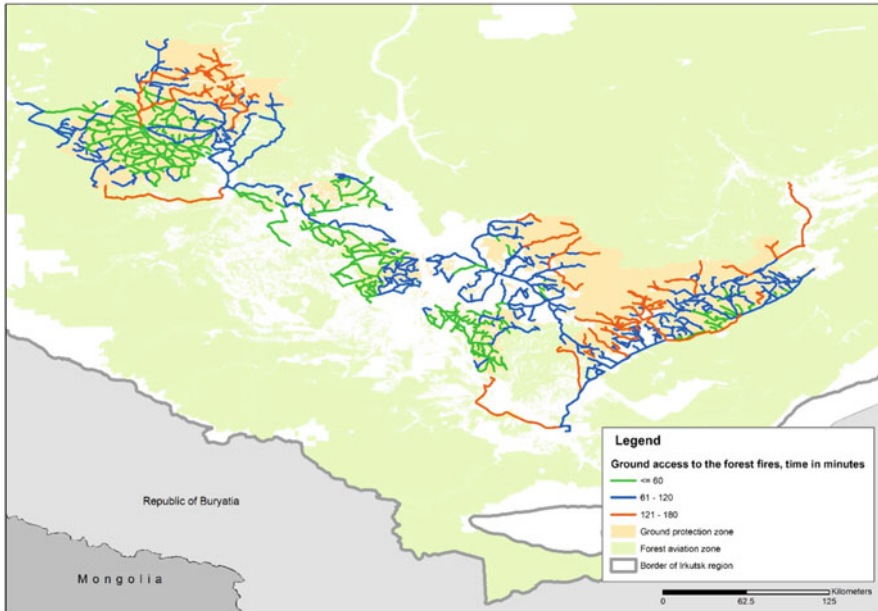


Fig. 2 Optimum routes to forest fires according to travelling time classes (Podolskaia et al. 2019a)

system (2006–2012) was used for model validation. The digital layers for fire protection zones were generated to evaluate the accessibility of ground teams for three time periods (i.e., 1, 2, and 3 h) recommended by the guidelines to ensure the prompt response to forest fires based on the fire danger classes of the forests (Classes I, II, and III). It was found that forest fires are mostly located within the zones of 1 (68.2%) and 2 h (24.3%) availability, while almost all of the fires (98.5%) were accessible in 3 h. The results revealed that the ground protection zone was designed by considering the arrival time of the ground team to the forest fire within 3 h. It was emphasized that the success of the transport value depends on up-to-date spatial data on the road networks and forest glades.

Podolskaia et al. (2020a) developed a GIS technology to determine the optimum ground access routes for special fire vehicles departing from fire-chemical stations and arriving at the detected fire areas. The study was implemented in the central part of the Siberian Federal District in Russian Federation. In the study, the digital data layers for public roads, forest glades, locations of the fire-chemical stations, and forest fires detected by MODIS satellite system (2002–2019) were generated in ArcGIS. Then, a GIS technology consisted of a Python-based set of programs was developed to generate a thematic map of road accessibility to forest fires based on key elements including access time (in hours), road length (in kilometers), and average vehicle speed (in kilometers per hour). The results indicated that most of forest fires recorded in 2002–2019 were accessible by the ground team. However, forest fires located away from the center of the Siberian District were not well

accessed by the ground teams. It was also pointed out that forest fires become less accessible when the forest areas get larger.

Some current experience in solving the transport modeling tasks for ground access, mainly in the Russian forestry, is described in a study conducted by Podolskaia (2021a). The geodata sources, data services, and Open Source developments, as well as using various remote sensing data and spatial resolution for the transport modeling, were noted. The projects were done by the scientific and educational institutions in Russia on forest transport accessibility which is a complex issue accenting on the environment and economy. It was suggested that the work should be continued to determine the optimum location for the fire stations, cutting areas, and forest warehouses considering different regions and forest infrastructures. Other potential future studies provided in the study were developing new methods to balance the infrastructural load and natural stability of forest ecosystems.

3 Accessible Forest Lands by Firefighting Teams and Their Optimal Locations

The term “transport accessibility” is widely used in different applications. In the modern forest management worldwide transport logistics of technical means and human resources along the roads to timely reach a place of forest fire or a forest area are among the most challenging ones for forest ecosystem protection and use. Relevant geospatial data for public roads of seasonal and off-seasonal use as well as forest roads and their volume and quality remain essential for the forestry projects (Podolskaia 2021b). From the data management point of view, spatial modeling of transport and resources accessibility depends on the continuous increase of geodata archives and complexity of their practical use.

Implementation of GIS for the ground and aviation transport accessibility and links between fire stations and destinations in the forests at the regional and country levels have been among the research topics already for certain years, especially in the countries covered by forests and having strong and constant forest fire periods. Russia and Turkey are two country examples with such forest fire activity in their warm respective seasons of the year, mainly from spring to autumn.

Ground transport accessibility relates with a question of placing a fire station (a fire-chemical station in Russian forestry terminology) or a logistical center in a particular region. According to the Russian forestry regulations, fire stations and their firefighting brigades are putted in place in the regions to prevent, detect, and limit the spread of forest fires in a timely manner. They are located mainly in the settlements, make a forest fire regional protection network, and include forest enterprises, national parks, and state nature reserves. They have special firefighting equipment, heavy vehicles, and staff.

A research undertaken by Akay et al. (2018) showed that about 1/3 of forest land (Mustafakemalpaşa, Bursa, Turkey) was reachable from presently located fire stations in a time frame regulated by the forestry in Turkey. Forest accessibility increased up to 72% when the authors applied a scenario with new fire station

location. This scenario includes implementation of GIS-based decision support system (Akay et al. 2012). Fire risk degrees for the fire-sensitive areas have been considered and presented in the cartographic form, including accessibility maps for forest areas with a system of access time frames in the paper (Akay and Taş 2020) for the Yenikoy Forest Enterprise Chief which is closed to the Karacabey Forest Enterprise Directorate (Bursa, Turkey). An important study's output states that about 24% of forest areas were accessible for fire extinguishing works within 30 min.

In Russian Federation forestry transport modeling is a research area for educational and scientific institutions. At the Center for Forest Ecology and Productivity of the Russian Academy of Sciences (CEPF RAS), there is a "Transportation Task" research group which is a part of the Laboratory of Forest Ecosystems Monitoring. Its ongoing activities and projects include the implementation of Open Data and Open Source GIS tools, globally known datasets of OSM and QGIS (Podolskaia 2020, 2021c). In the paper of Podolskaia et al. (2020a), they did a quality control of existing transport systems' datasets by road type (public, forest road, forest glades) and made a comparison with the archived road data.

One of the recent studies was a work done by Podolskaia et al. (2019b) for the large territories of Siberia, the Russian Federation. In order to estimate the spatial location of fire stations the authors suggest three data groups, namely: presence of road network (length, density, and configuration), forest fires detected by satellites, and fire station service areas. GIS analysis with its buffering, allocation, density, as well as geographic and directional distribution, was used as method. The researchers noted that there are other factors and data, and they can certainly influence the fire station's location (access regime of protected areas, use of road depending on the season, zones of protection against forest fires, placement of stations in the most populated areas, etc.). It was advisable to make a fire station placement analysis before and after the fire hazardous season; its results would be of help for retrospective evaluation and forecasting of forest firefighting events.

Accessibility of forest resources presented in the work of Podolskaia et al. (2020c) uses a scenario approach for the territory of regional scale in Russia. A general scheme of methodology including brief data description and operations with data is presented in Fig. 3; it consists of the steps of scenario's preparation, then mapping and analysis.

Novosibirsk region, located in the southwest of the Siberian Federal district of Russian Federation, has been chosen as a key research area because of its developed infrastructure in combination with constant annual forest fire activity; according to the MODIS data it is classified by mixed broadleaf-coniferous forests and non-forest vegetation (Fig. 4). In the study (Podolskaia et al. 2020c) the authors have moved from the previous estimations of forest fires' accessibility (Podolskaia et al. 2019b, 2020b) to the accessibility of forest areas and their resources (Podolskaia et al. 2020c). Spatial transport modeling included creation and use of transport model for two forest management scenarios, namely: without any barriers and with forestries (unit of forestry management in Russia) as barriers; this second one is

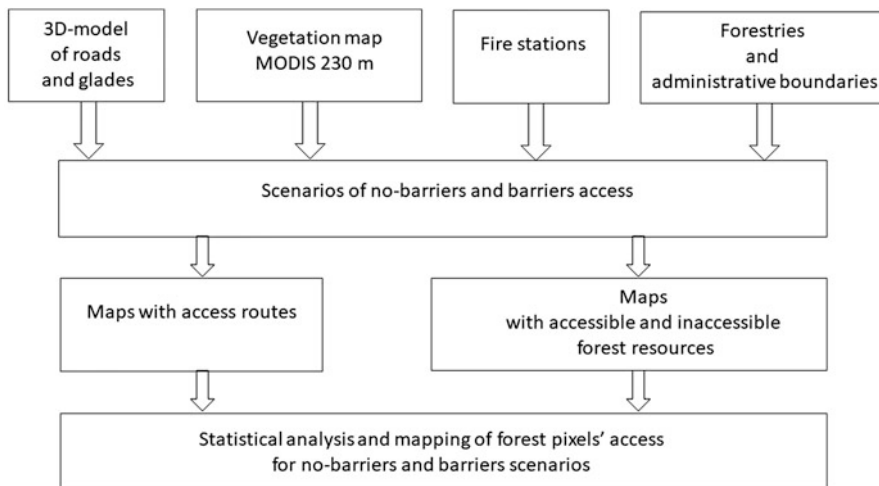


Fig. 3 General scheme of methodology (Podolskaia et al. 2020c)

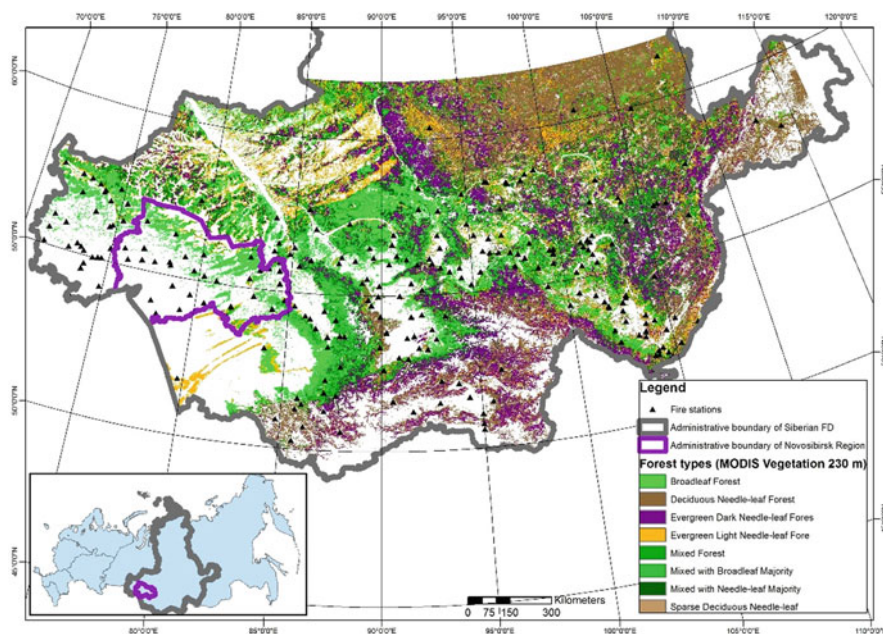


Fig. 4 Key area (Podolskaia et al. 2020c)

spatially presented in Fig. 5. As we can see on the map, the majority of forestries have at least one fire station within their borders.

In that study, the location of existing fire stations has been evaluated under the 3 h condition which is an actual critical response time to access forest fires by ground

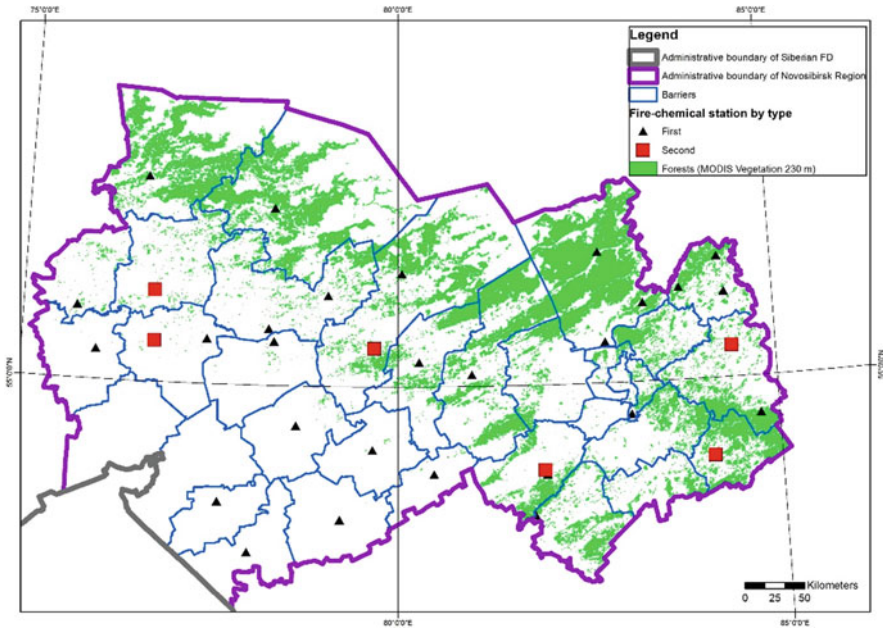


Fig. 5 Fire stations and forests as barriers within Novosibirsk region (Podolskaia et al. 2020c)

technical means in Russian forestry. Fire stations were used as starting points of move along the roads. By implementing this relatively strict time limit for the “no-barriers” scenario, the authors noted that there were about 17% of inaccessible forest areas (namely, forest pixels of MODIS satellite coverage); about 14% of areas were reachable within more than 3 h and 20%—within an hour (Fig. 6). Quantitative results confirmed that forest management scenario of “no barriers” is more promising than a scenario with barriers. The authors detailed that up to 83% of forests (MODIS pixels) of Novosibirsk region were reachable by moving along the roads of different types in “no-barriers” scenario.

Along with the proprietary GIS software like ArcGIS from ESRI, Open Source tools nowadays are of great importance in the geoinformation research. A review of Open Source QGIS forestry plugins done in the study conducted by Podolskaia (2021c) described plugins for the tasks of forest fire and forest resources monitoring and management. Plugin analysis done in this work was aimed to help future researchers by providing them with a list of QGIS plugins compatible to QGIS version 3.18 (as an example of version available for the users in 2021) for a forestry GIS project. An option for future research subjects may be a development of plugins with available data in the form of cartographic services for territories of different spatial coverage, taking into account that archived data and their accessibility is a key asset in the forestry. Subject-related forest scope in the present-day repository of QGIS plugins tends to be relatively limited. Such review of plugin functionality has to be performed repeatedly, following the QGIS developments and trends. Overall,

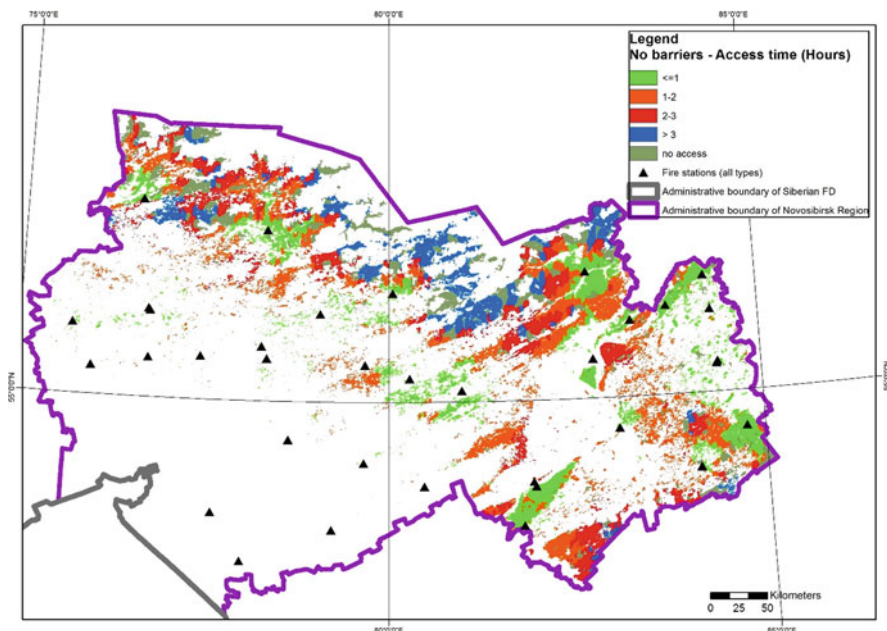


Fig. 6 Transport accessibility of forest resources in Novosibirsk Region. No-Barriers scenario classified by time, in hours (Podolskaia et al. 2020c)

the role of Open Geodata and Open Source GIS instruments will be stably very important in the forestry industrial and scientific projects.

4 Forest Roads as Effective Infrastructures for Fire Protection

Forest fire is recognized as one of the most detrimental natural disasters damaging forest resources. Aricak et al. (2014) facilitated high-resolution GeoEye satellite images and GIS data to investigate the potential fire risk zones in the forest area based on stand characteristics (age, crown closure, tree species). The flowchart of the implemented methodology is given in Fig. 7. In the study, the road networks in the forest area located in the Central District of the Kastamonu Regional Forest Directorate in Turkey were also included in the database. The fire trucks used during extinguishing of forest fires were able to spray water and chemicals with the pressure of 40 bars. Thus, in spite of ground slope steepness, a fire truck can intervene in an area with a minimum diameter of 400 m. Then, a buffer zone with the width of 400 m was generated for both sides of the roads using proximity tool in ArcGIS. Finally, the areas that can and cannot be intervened in the potential fire risk areas from the existing roads have been effectively determined by using GIS techniques. In a similar study conducted by Drosos et al. (2014), a model was developed to optimize opening ups in forest lands by primarily considering the fire prevention and

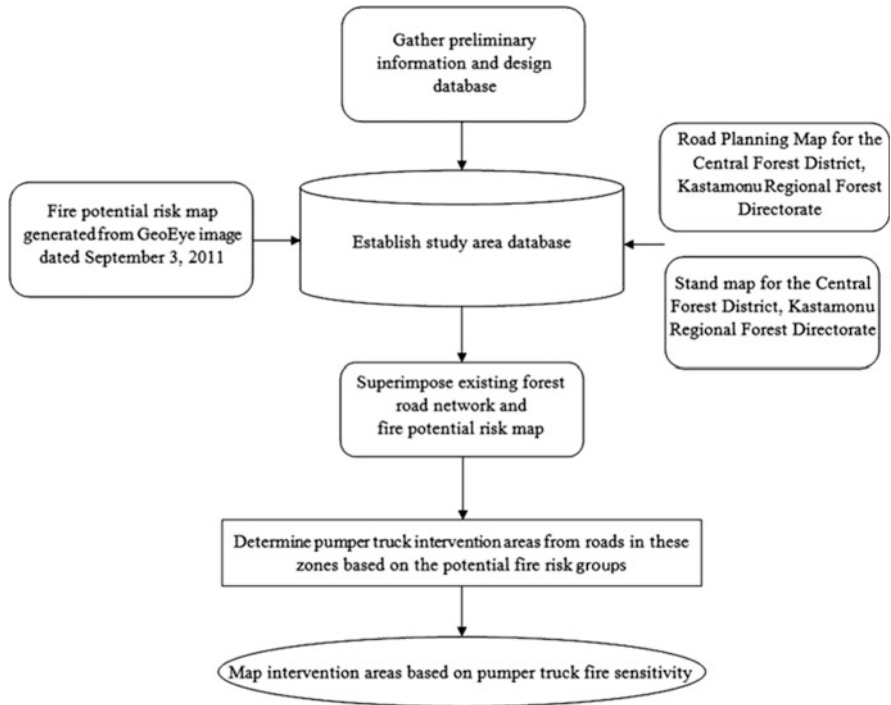
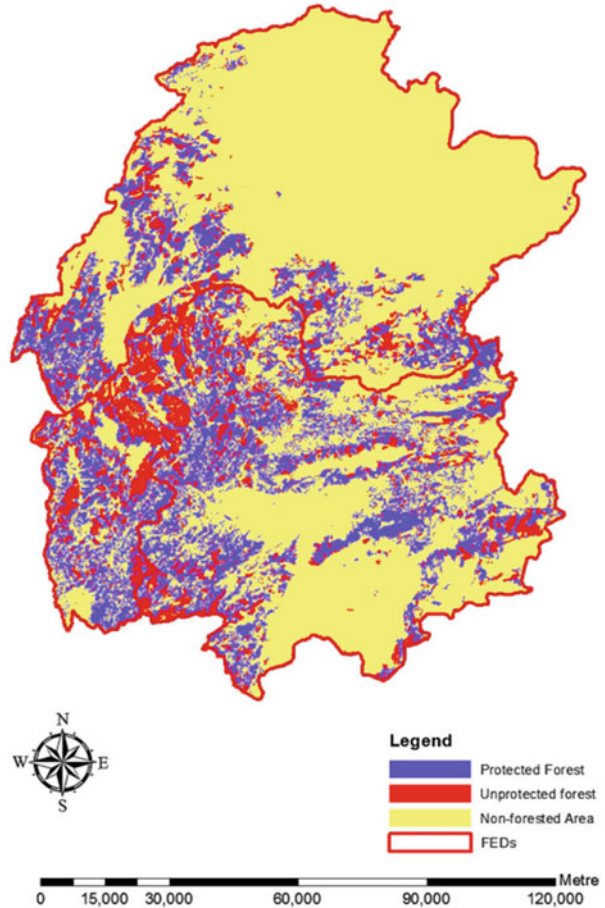


Fig. 7 Work flow of the study (Aricak et al. 2014)

suppression. The fire-suppression buffer zones were generated based on topography to define the lands being reached by the hoses of fire trucks. In the study, the buffer widths were considered as 150–300 m for uphill and 250–500 m for downhill from a location where the fire trucks are located.

Akay et al. (2017) searched for the fire-access zones by fire trucks in forested areas located in Kahramanmaraş where forests are sensitive to forest fires because of high temperatures and low humidity in summer season. In the study, GIS techniques were used to determine fire-access zones in forested areas by using the reach distance of the water sprayed by the fire hoses of fire trucks. The accessible buffer zones were defined from both sides of the roads, while taking into account ground slope, terrain structures (uphill, downhill, and flat), and the capabilities of the fire trucks. In the first stage, GIS database was generated to produce necessary data layers including road network map, forest land map, and fire sensitivity map. The ground slope map was produced using the Digital Elevation Model (DEM) derived from an ASTER satellite image. Then, the terrain structure of the study area was produced by considering the road network as the reference surface. For the locations over the reference surface, the terrain structure was determined as uphill, while it was downhill when they are under the reference surface. The locations that were at the same elevation with the reference surface were defined as flat areas. In the study,

Fig. 8 The accessible and inaccessible forest areas



specific formulas were developed to determine the fire-access zone widths for downhill, uphill, and flat areas, considering the maximum water pressure at the pump, the minimum water pressure at the nozzle, the water pressure loss for each 10 m distance from the fire truck due to friction, and the ground slope. The areas with very high slope (more than 60%) were excluded from the fire-access zones since it could be unsafe and not applicable to conduct firefighting on steep slopes. Finally, the fire-access zone map was generated, indicating protected and unprotected forest areas (Fig. 8). The results indicated that the accessible forests, sensitive to fire with the first, second, and third degrees, were 69.59%, 69.96%, and 67.16%, respectively. The results revealed that determining the areas outside of reach distance of the hoses can provide an important information to evaluate the capabilities of the road network in firefighting activities.

Forest road networks are the most important infrastructures that provide access to forest areas for the protection and operation of forest resources. Increasing vehicle speed by improving road standards, especially in forests with high fire risk, will

make a significant contribution to the expansion of accessible forest areas within the critical response time. Therefore, the improvement of road standards and the effectiveness of firefighting activities should be evaluated together. Akay et al. (2021) used GIS techniques to search for the potential contribution of improving road standards on expanding the forest areas that can be reached by the ground team within the critical response time. The study was implemented in the first-degree fire-sensitive forests located in Mediterranean city of Kahramanmaraş in Turkey. In the study, primarily the forest areas that can be reached by the firefighting team (six available teams in the region) within the critical response time were determined by considering the existing road network in the study area. Then, the possible increase in the accessible forest areas with high fire risk was investigated considering the improved road standards with higher vehicle speed on forest roads. In the solution process, the new service area method of Network Analyst tool in ArcGIS was used to determine the forest areas that firefighting team can reach within the critical response time. The results indicated that the accessible forested areas in critical response time increased by 19% by considering improved road standards (Fig. 9). They emphasized that increasing the design speed of the forest roads minimizes the arrival time of ground teams to the fire, which increases the accessible forest areas in critical response time.

In a study conducted in Tirana Albania, Haska et al. (2021) generated digital data layers for the locations of fire stations and road networks using ArcGIS 10.4 software. They determined the forest areas that firefighters could reach within the critical response time to the fire using Network Analyst. According to result of the study, it was found that 27% of the forest areas in the study area at Tiran was accessed by the ground team within the critical response time. In the application, an optimal location was suggested for the additional station which potentially increased the accessible forest areas up to 65%. In a similar study, Laschi et al. (2019) emphasized the essential rules for planning efficient forest road network in fire-sensitive forest lands. They suggested that the functions of forest roads should be analyzed in fire prevention and suppression and the importance of forest roads for protecting forests against fires should be considered in planning and building stages. Besides, the construction and maintenance characteristics should be considered for building and maintaining an efficient forest road network against fires. As a concluding remark, it was emphasized that road maintenance activities should be performed appropriately to have efficient transportation accessibility to potential forest fire areas.

5 Conclusion

This chapter described three topical directions of international research in the forestry spatial modeling indicating the optimality of access routes to forest fires and accessibility of forest resources and forest fires and highlighting the forest roads as a key element of forestry infrastructure. Ground transport features are regularly changing geometrically and attributively and becoming just more complex from

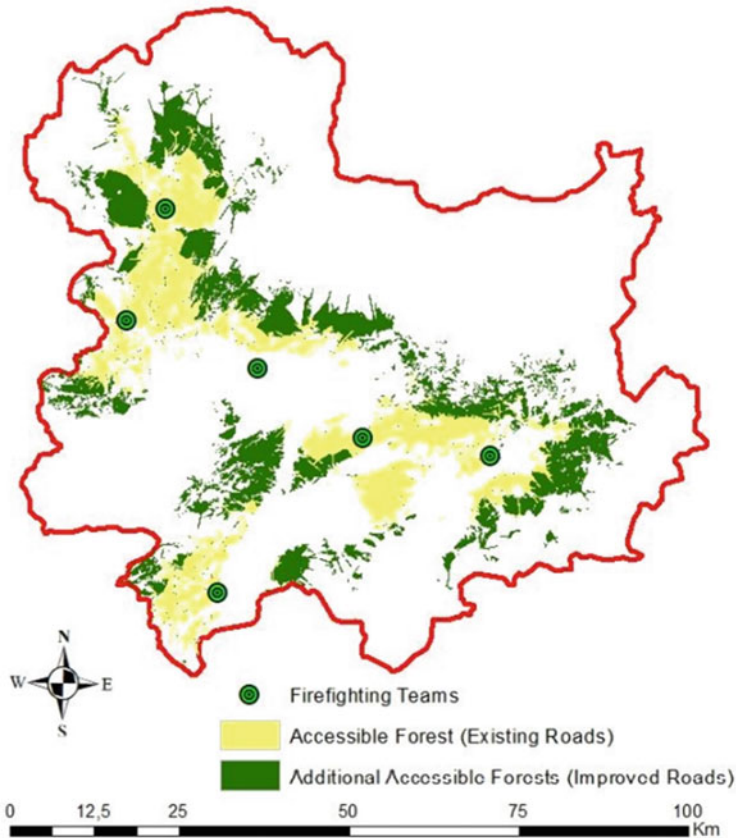


Fig. 9 The accessible forest areas for existing roads and improved roads

their technical maintenance, data management, and data analysis points of view. Forestry as industry uses a mixed network consisting of public off-seasonal and seasonal roads as well as of special forest roads used for logging purposes mainly.

Experience of two countries with different geographical location, state forestry situation, rules in the forest management, as well as spatial extents of key areas gave an opportunity to find the commonalities and differences in the undertaken studies. For example, research done by Turkish scientists confirmed by calculations that improved road standards and timely and appropriate maintenance of forest roads would improve the accessibility to the forest resources and forest fires.

The presented examples also show that current and future research directions are undoubtedly based on the combination of network analysis, decision support systems, and forest management scenarios with the help of modern GIS, namely, extensions and plug-ins of proprietary and Open Source software. Supporting cartographic materials with research key areas included in the chapter served as spatial modeling results' visualization.

Authors' Contributions All authors performed the same effort in this study. They all wrote, read, reviewed, and decided to submit a chapter of a book.

Conflict of Interest No conflict of interest.

References

- Akay AE, Taş İ (2020) Using GIS techniques for assessment of accessible forest lands by firefighting teams considering fire risk degrees. *Eur J For Eng* 6(2):87–95
- Akay AE, Wing GM, Sivrikaya F, Sakar D (2012) A GIS-based decision support system for determining the shortest and safest route to forest fires: a case study in Mediterranean Region of Turkey. *Environ Monit Assess* 184(3):1391–1407
- Akay AE, Wing MG, Zengin M, Köse O (2017) Determination of fire-access zones along road networks in fire sensitive forests. *J For Res* 28(3):557–564
- Akay AE, Karas IR, Kahraman I (2018) Determining the locations of potential firefighting teams by using GIS techniques. *Int Arch Photogramm Remote Sens Spat Inf Sci* 42(4):83–88
- Akay AE, Podolskaia ES, Uçar Z (2021) Effects of improving forest road standards on shortening the arrival time of ground-based firefighting teams accessing to the forest fires. *Eur J For Eng* 7(1):32–38. <https://doi.org/10.33904/ejfe.952174>
- Aricak B, Kucuk O, Enez K (2014) Determination of pumper truck intervention ratios in zones with high fire potential by using geographical information system. *J Appl Remote Sens* 8(1):083598. <https://doi.org/10.1117/1.JRS.8.083598>
- Bilici E (2009) A study on the integration of firebreaks and fireline with forest roads networks and it's planning and construction (A case study of Gallipoly National Park) Istanbul University. *Fac For J Ser A* 59(2):86–102
- Dimitrakopoulos AP, Vlahou M, Anagnostopoulou CG, Mitsopoulos IJCC (2011) Impact of drought on wildland fires in Greece: implications of climatic change? *Clim Change* 109(3–4): 331–347
- Drosos VC, Giannoulas VJ, Stergiadou A, Daoutis C (2014) Forest construction infrastructures for the prevision, suppression, and protection before and after forest fires. Second International Conference on Remote Sensing and Geoinformation of the Environment (RSCy2014), 7–10 Apr, Paphos
- Goldammer JG, Sukhinin A, Csizsar I (2003) Current fire situation in the Russian Federation: implications for enhancing international and regional cooperation in the UN Framework and the global programs on fire monitoring and assessment, GFMC contribution to the International Workshop “New Approaches to Forest Protection and Fire Management at an Ecosystem Level”, Khabarovsk, pp 1–24
- Haska H, Akay AE, Ergin H (2021) Forest road networks-effective infrastructures for extinguishing forest fires. 3rd International Conference on Agriculture and Life Sciences, 1–3 Nov, Tirana
- Laschi A, Foderi C, Fabiano F, Neri F, Cambi M, Mariotti B, Marchi E (2019) Forest road planning, construction and maintenance to improve forest fire fighting: a review. *Croat J For Eng* 40(1): 207–219
- Podolskaia E (2020) Basics of working in Open Source QGIS: geodata, coordinates, functionality, data quality control, map design and web-publishing. Manual Lab Publisher, p 52
- Podolskaia ES (2021a) Review of experience in solving the transport modeling tasks in the forestry. *For Sci* 4(4):1–32
- Podolskaia ES (2021b) Analysis of infrastructural forest data with GIS-tools. *Abst Int Cartogr Assoc* 3:243. <https://doi.org/10.5194/ica-abs-3-243-2021>
- Podolskaia ES (2021c) Review of open source QGIS forestry plugins. *For Sci* 4(2):1–11

- Podolskaia ES, Kovganko KK, Ershov DV, Shulyak PP, Suchkov AI (2019a) Using of transport network model to estimate travelling time and distance for ground access a forest fire. *For Sci Issues* 2(1):1–24. <https://doi.org/10.31509/2658-607x-2019-2-2-1-22>
- Podolskaia E, Ershov D, Kovganko K (2019b) GIS-analysis of ground transport accessibility of fire stations at regional scale. *Abst Int Cartogr Assoc* 1:301. <https://doi.org/10.5194/ica-abs-1-301-2019>
- Podolskaia E, Ershov D, Kovganko K (2020a) Comparison of data sources on transport infrastructure for the regional forest fire management. Book of abstracts *Managing forests in the 21st century*. Conference at the Potsdam Institute for Climate Impact Research (Potsdam 2020), p 59. <https://doi.org/10.2312/pik.2020.002>
- Podolskaia E, Ershov D, Kovganko K (2020b) Automated construction of ground access routes for the management of regional forest fires. *J For Sci* 66:329–338. <https://doi.org/10.17221/59/2020-JFS>
- Podolskaia E, Ershov D, Kovganko K (2020c) GIS-Approach to estimate ground transport accessibility of forest resources (Case Study: Novosibirsk Region, Siberian Federal District, Russia). *J Geogr Inf Syst* 12:451–469. <https://doi.org/10.4236/jgis.2020.125027>



Assessment of Forest Aboveground Biomass Estimation from SuperView-1 Satellite Image Using Machine Learning Approaches

Nurul Ain Mohd Zaki, Azinuddin Mohd Asri,
Nur Ilyani Mohd Zulkiflee, Zulkiflee Abd Latif, Tajul Rosli Razak,
and Mohd Nazip Suratman

Abstract

Tropical forests play the main role in the earth's carbon cycle sources. Nowadays, the study for conservation and management of forest restoration is increasingly needed to preserve the biodiversity of forests and retain the valuable species of tropical forest for the next generation. The accurate tropical tree species recognition is one of the important issues in forest management that have relation to the

N. A. Mohd Zaki (✉)

Centre of Studies for Surveying Science and Geomatics, Faculty of Architecture, Planning and Surveying, Universiti Teknologi MARA, Perlis Branch, Arau, Perlis, Malaysia

Institute for Biodiversity and Sustainable Development (IBSD), Universiti Teknologi MARA, Shah Alam, Selangor, Malaysia

e-mail: nurulain86@uitm.edu.my

A. Mohd Asri · N. I. Mohd Zulkiflee

Faculty of Architecture, Planning and Surveying, Centre of Studies for Surveying Science and Geomatics, Universiti Teknologi MARA, Arau, Perlis, Malaysia

Z. Abd Latif

Institute for Biodiversity and Sustainable Development (IBSD), Universiti Teknologi MARA, Shah Alam, Selangor, Malaysia

Faculty of Architecture, Planning and Surveying, Centre of Studies for Surveying Science and Geomatics, Universiti Teknologi MARA, Shah Alam, Selangor, Malaysia

T. R. Razak

Faculty of Computer and Mathematical Science, Universiti Teknologi MARA, Arau, Perlis, Malaysia

M. N. Suratman

Faculty of Applied Sciences and Institute for Biodiversity and Sustainable Development, Universiti Teknologi MARA (UiTM), Shah Alam, Malaysia

increasing need to better understand the role of the forest ecosystem. It is essential and valuable information towards an understanding of the ecosystem biodiversity and its function over large spatial scales. Information such as the tree species and location of the trees is crucial for species regeneration and ecological purposes. Currently, machine learning (ML) has been shown a remarkable efficient evolution utilized in artificial intelligence along with the inclination of deep learning (DL) usage in many research, and this includes tropical forest carbon stocks. Therefore, this study aimed to classify the forest aboveground biomass by estimating crown projection area using object-based image analysis (OBIA) and to determine the accuracy assessment for estimating forest aboveground biomass using an artificial neural network (ANN) and random forest (RF). This study involved the use of the object-based technique by fusing SuperView-1 imagery and airborne LiDAR to estimate the aboveground biomass using RF and ANN algorithm. Statistical tools from open-source R will help bridge the gap between analysis and implementation. This study hopes to solve the fundamental issues of forest inventories and carbon stock modeling and will help several organizations for estimating carbon stocks and forest fluxes.

Keywords

Machine learning · Tropical forest · Aboveground biomass · Carbon stocks

1 Introduction

The ecosystem of the forest is the biggest and the terrestrial environment's most significant natural ecosystem, which has a significant impact on global ecological balancing, global biological evolution, and society's succession (Li et al. 2020). One of the most well-known ecosystem services that are supplied by trees is atmospheric carbon (CO₂) absorption and storage (Chazdon et al. 2016). Carbon (C) was kept in both the aboveground and underground parts of the tree. Aboveground biomass consists of stems, stumps, branches, bark, seeds, and leaves, while underground biomass consists entirely of living biomass in the form of live roots. Aboveground biomass in the forest is a major factor in tracking the carbon cycle on a global scale and reducing climate change's effects (Ghosh and Behera 2018).

In the study conducted by Urbazaev et al. (2018), the entire amount of aboveground live organic matter in plants is referred to as aboveground biomass. It is measured per unit area of oven-dry tons. Aboveground biomass in forests is an essential variable for determining the ecological system of the forest structure and function (Gao et al. 2018). Forest biomass estimation is important for accounting for carbon budgets, monitoring carbon fluxes, and studying the forest ecosystem's reaction to climatic changes (Nandy et al. 2019). Therefore, estimating plant biomass/carbon reserves helps with REDD (reducing emissions from deforestation and forest degradation) and long-term forest conservation (Hussin et al. 2014).

According to Vafaei et al. (2018), the main weakness of the AGB estimate in terms of optical data is due to forest features such as a tight canopy, high variety, and other complicated structures. As a result, optical data may become saturated and less sensitive in high-biomass locations, making it difficult to estimate the AGB accurately. However, AGB estimation is inaccurate due to data constraints (e.g., data saturation for optical and radar data and spectral and spatial resolution limits) and complicated connections between AGB and spectral variables (Gao et al. 2018).

According to most previous studies, the best method for estimating forest AGB is to combine field measurements and remotely sensed datasets. However, current AGB estimations are still subject to significant uncertainty due to inaccuracies in the allometric equations that were utilized to estimate aboveground biomass, as well as uncertainties in remote sensing datasets and algorithms used to estimate AGB.

Previous researchers used pixel-based methods to link AGB to environmental and remote sensing data at the plot level. However, if compared to the object-based image analysis classification, the majority estimation by pixel-based techniques has some weaknesses (Silveira et al. 2019). For example, a field plot is more likely to be found in an object than in a single pixel. Employing object-based image analysis could decrease the unpredictability of positioning mismatch between field and image data and using a “pure” object can successfully minimize local noise and heterogeneity (Zhang et al. 2018; Addink et al. 2007).

Machine learning approaches have been utilized since they successfully estimate forest AGB in several previous studies (Vafaei et al. 2018). Although the benefits of applying nonparametric and machine learning approaches to estimate AGB were acknowledged, the accuracy of their estimate is highly dependent on the parameter optimization employed in appropriate algorithms and the data’s representativeness (Gao et al. 2018). Algorithms either learn from data or are “fit” to a collection of data. Random forest and artificial neural network are the algorithms which have proven the best performance in previous research. Algorithms such as artificial neural network (ANN), random forest (RF), and support vector machine (SVM) are widely being utilized to predict biomass by combining remote sensing and field data in recent years (Dhanda et al. 2017; Pandit et al. 2018; Wu et al. 2016).

Previous studies have shown the importance of remote sensing technology in accurately estimating forest aboveground biomass, even at the regional scale. In Hunan Province’s subtropical forests, Li et al. (2020) utilized remote sensing datasets which were combined with machine learning approaches like extreme gradient boosting (XGBoost), linear regression, and random forest. XGBoost is a tree-boosting algorithm that is a scalable framework common among data scientists that produces cutting-edge results for a variety of issues. Data compression, data fragmentation, and the usage of certain cache access patterns are all used to analyze billions of samples in a whole dataset with just a small number of computational resources. Previous research has also shown that decision tree-based methods, such as gradient boosting (GB) and random forest (RF), perform very well in biomass estimation models.

The types of remote sensing data, combined with appropriate selection algorithms, play an important role in accurately estimating biomass. The previous studies showed the datasets that have been used by Li et al. (2020) were the Landsat 8 Operational Land Imager and Sentinel-1A satellites, as well as data from China's National Forest Continuous Inventory, which were combined with three algorithms. Landsat, SPOT, WorldView-2, and Sentinel-2 optical remotely sensed data, as well as their outputs, such as vegetation indices and texture pictures, have also been found to be strongly connected to biomass (Li et al. 2020), while Vafaei et al. (2018) used ALOS-2 PALSAR-2 and Sentinel-2A images to increase the accuracy of forest aboveground biomass estimation. ALOS-2 PALSAR-2 data that has been combined with Sentinel-2 MSI data has been the choice of use because the Sentinel-2A sensor contains multispectral bands that depict different types of canopy cover reflections, whereas the long wavelengths of the ALOS-2 PALSAR-2 sensor allow it to penetrate dense forest canopy. Meanwhile, Gao et al. (2018) used various datasets and modeling methods (e.g., ALOS PALSAR L-band data, Landsat Thematic Mapper (TM), and their mergers).

Several machine learning approaches were chosen and evaluated, such as support vector regression (SVR), Gaussian processes (GP), random forest (RF), and multi-layer perceptron neural networks (MPL neural nets) (Vafaei et al. 2018). These algorithms were chosen because they've been shown to be successful in estimating forest aboveground biomass for many types of studies. Meanwhile, Gao et al. (2018) used several algorithms, such as random forest (RF), linear regression (LR), k-nearest neighbor (kNN), support vector regression (SVR), and artificial neural network (ANN) to estimate stratification and non-stratification of forest categories in a subtropical area. Machine learning techniques and nonparametric such as RF, SVR, kNN, and ANN can manage nonlinear connections in this situation. As a result, throughout the last decade, these algorithms have gotten a lot of attention.

Therefore, this study intends to analyze the capability of the OBIA technique and the machine learning approach using SuperView-1 imagery to improve the accuracy of estimation of forest aboveground biomass.

2 Study Area

The Forest Research Institute Malaysia (FRIM) was selected as the study area due to its closed forest canopies, diverse tree species composition, and structural variety. This area's coordinates are 3° 14' 13'' N, 101° 38' 16'' E, and it is located at Kepong, Selangor Darul Ehsan, Malaysia. FRIM is one of the world's foremost research institutes on tropical forests and is classified as a lowland dipterocarp forest. According to Nik Effendi et al. (2021), this location was chosen since it encompasses around 545 ha and has approximately 2500 tree species. Figure 1 displays the study area map for this research.

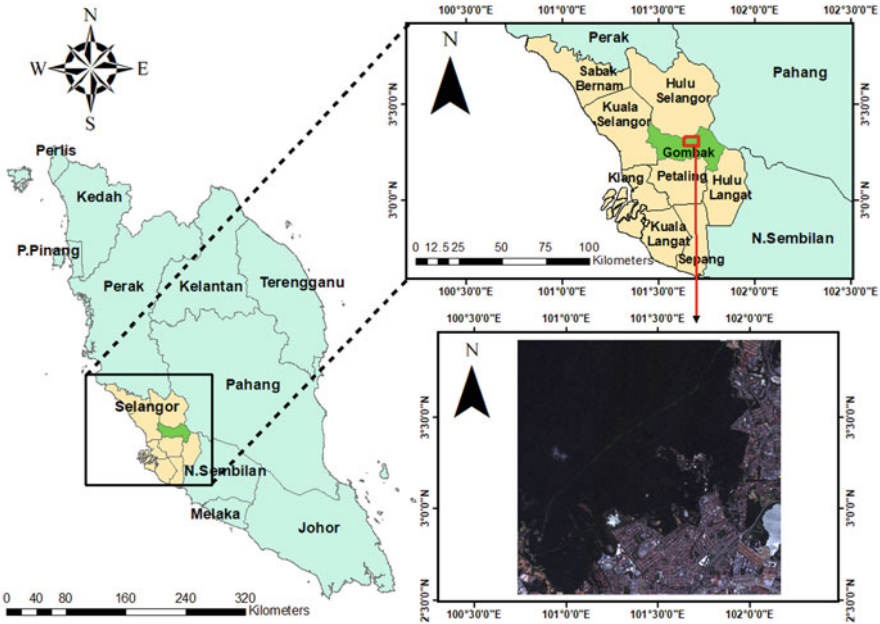


Fig. 1 Study area at Forest Research Institute Malaysia (FRIM), Kepong, Selangor, Malaysia

3 Research Methodology

There are several data processes carried out in order to accomplish the aims and objectives of the research work. The methodology of this project was divided into four main phases, such as: (1) data collection, (2) preprocessing, (3) post-processing, and (4) machine learning processing. The first phase project was data collection. The datasets used in this study were tree inventory data, the SuperView-1 satellite, and LiDAR data. The second phase project was preprocessing. The methods used in this phase were georeferencing, orthorectification, and LAS tool processes. Then, the third phase project was post-processing, which uses SuperView-1 satellite image and LiDAR data to produce the accuracy assessment. The fourth phase project was machine learning (ML) processing, which used an ANN and RF algorithm.

4 Forest Inventory, SuperView-1 Satellite Image, and LiDAR Data

Forest inventory is referred to as the systematic acquisition of data on forest resources within a certain region. Tree data in this study were tree ID, coordinates for horizontal point (x) and vertical point (y), DBH (cm), CBH (cm), CD (m), Ht (m), family, species, common name, and status or remarks. SuperView-1 is a

high-resolution satellite which has 0.5 m panchromatic band and four multispectral bands. The multispectral bands for SuperView-1 are blue, green, red, and near-infrared (NIR). Airborne LiDAR data has been used in this study to estimate the canopy height model (CHM) of the FRIM forest. Airborne Airborne LiDAR data was acquired in 2013, and projected to the Malayan Rectified Skew Orthomorphic (MRSO) system.

5 Georeferencing and Orthorectification

Georeferencing involves the ability of digital maps or aerial photos' internal coordinate system to be matched to a ground system of geographic coordinates. The georeferencing process was performed in this study using ArcGIS software. A total of ten GCPs were chosen based on permanent benchmarks such as road corners, automobile parking, and buildings on the ground, which was modified from GPS data and then detected in the LiDAR point cloud on the ground (Nik Effendi et al. 2021). The projection coordinate system employed in this study was the Malayan Rectified Skew Orthomorphic (MRSO). The orthorectification was accomplished, and the total root mean square error (RMSE) that has been achieved was 0.249 m.

6 Segmentation and Classification Process of Tropical Forest

In order to decide the size of the objects, the algorithm must specify a scale parameter, as well as color, shape, and smoothness/compactness weights, with a small value creating more objects and a high value generating fewer objects (Zhang et al. 2018). In this study, multi-resolution segmentation was performed using 27 scale parameters with 0.9 for shape and 0.8 for compactness based on trial and error. This study used normalized difference vegetation index (NDVI) as the statistical classification algorithms.

The range for tree classification is less than or equal to 0.41–0.86. This study used mean value of brightness to find a suitable min and max range for masking the shadow in SuperView-1 image. The range for shadow classification is less than or equal to 310–380. While the value of max different has been used to classify the building and road, the range that has been selected for building classification is less than or equal to 0.2–1. Morphological methods are important for determining the prevailing crown sizes through the geometric and structural information of tree crowns (Jaafar et al. 2018). This study used close image objects for operator and mask size for width value was 17. The width value that has been selected was size 13, and the circle mask.

7 Tree Classification

This study used NDVI as the statistical classification algorithm. This algorithm has been chosen because it can measure plants by calculating the differences between near-infrared light that represents the vegetation strongly reflects and red light that indicates the vegetation absorbs calculated as follows:

$$\text{NDVI} = (\text{NIR} - \text{Red}) / (\text{NIR} + \text{Red}) \quad (1)$$

The NDVI values always vary from -1 to $+1$. For example, if the NDVI value is negative, that means the feature is water. If an NDVI value is close to $+1$, there could be dense green leaves, and when NDVI is close to zero, there are not green leaves, or it could be an urbanized region. When compared to other wavelengths, vegetation chlorophyll reacts or reflects more near-infrared (NIR) and green light. However, it absorbs more red and blue light. That's why human eyes can detect vegetation in green and near-infrared colors. This study used NDVI resolution to classify the tree crown of tropical forest at the Forest Research Institute Malaysia (FRIM). The range for tree classification is less than or equal to $0.41-0.86$ with a small value creating more objects and a high value generating fewer objects (Zhang et al. 2018).

8 Shadow Masking and Building Classification

The shadow was masked out of the image to outline the tree canopy using numerous rulesets. This study used mean value of brightness to find a suitable min and max range for masking the shadow in SuperView-1 image. The range for shadow classification is less than or equal to $310-380$. While the value of max different has been used to classify the building and road, the range that has been selected for building classification is less than or equal to $0.2-1$.

9 Morphology

Morphological methods are important for determining the prevailing crown sizes through the geometric and structural information of tree crowns (Jaafar et al. 2018). Morphological operators have two types of operators, which are closing and opening, that have been used to improve the shape of the segmented results' margins. Furthermore, the morphology parameters were adjusted to modify the mask value depending on the appropriateness of the tree crown. The width value that has been selected was size 13, and the circle mask. Each of the sizes should be trial and error, based on the type of satellite image. This study used close image objects for operator and mask size for width value was 17.

10 Accuracy Assessment of Segmentation Output

The concepts of under-segmentation and over-segmentation have been created in order to evaluate the multi-resolution segmentation outcome. Under-segmentation occurs when the training sample is smaller than the segmentation output, while over-segmentation occurs when the training sample is larger than the segmentation result.

$$\text{Under-segmentation} = 1 - \text{area}((xi \cap yj)) / (\text{area}(yj)) \quad (2)$$

$$\text{Over-segmentation} = 1 - \text{area}((xi \cap yj)) / (\text{area}(xi)) \quad (3)$$

According to Eqs. 2 and 3, xi is defined as a training sample, while yj is defined as a segmentation polygon. The over- and under-segmentation, which requires the area of the training sample (xi), the segmentation output (yj), and the intersect area, were used to calculate the distance index (D).

$$D = \sqrt{(\text{Over Segmentation}^2 + \text{Under Segmentation}^2) / 2} \quad (4)$$

The distance index has been used to show the ideal segmentation or closeness of the space. The accuracy of segmentation is evaluated using a distance index (D), which varies from 0 to 1, with 0 indicating an ideal match between xi and yj and 1 indicating the smallest discrepancy (Mohd Zaki et al. 2015).

11 Allometric Equation for AGB and Carbon Stock Estimation

This study has chosen Kenzo et al. (2009) and Mohd Zaki et al. (2018) allometric equations for estimating forest aboveground biomass and carbon stock using a fieldwork approach.

$$\text{AGB}_{\text{est}} = 0.0829 \times \text{DBH}^{2.43} \quad (5)$$

$$\ln \text{Sc} = -4.092 + 0.898 \ln h_L + 2.073 \ln \text{DBH} - 0.058 \ln \text{CPA} \quad (6)$$

where AGB_{est} is the aboveground estimation and DBH is the diameter at breast height (cm), Sc is for carbon stock (kg), h_L is the height of the tree from the LiDAR, and CPA is in (m).

12 Artificial Neural Network (ANN) and Random Forest (RF)

The data used in this study consists of two types which were dependent variables and independent variables. Dependent variable data was carbon stock (CS), while independent variables are diameter breast height (DBH), crown projection area (CPA), total height of tree measured in the field (h_F), and height extracted from LiDAR (h_L).

The independent variables (i.e., DBH, h_L , and CPA) were used to estimate carbon stock (dependent variable) using machine learning algorithms. Multiple linear regression was used to estimate dependent variables. Before implementing at the landscape level, it is vital to develop a regression model for AGB estimate at the stem level in order to identify the most essential LiDAR metrics that correlate with field AGB.

The Excel data in CSV (comma delimited) format was imported into RStudio through the import dataset. The data entered were shown in the RStudio Interface's R-Environment. Specific scripts were utilized in conjunction with the artificial neural network and random forest model for processing, and the packages used were defined in the code editor to ensure that the scripts ran smoothly. The packages, such as the "neuralnet" and "randomForest" packages used in this study, have been installed in the graphical output of the RStudio Interface to ensure that the scripts can be launched. The R-Console displayed the scripts that have been run. If an error occurs when running the scripts, the errors were presented on the R-Console so that the parts of the scripts that exhibit the issue may be rectified. The methods involved in carbon stock prediction were data normalization, training and test sets, model fitting, and model validation, which comprised prediction and correct computation.

To reduce the impact of a very significant predictor, two significant training parameters were defined in RF modeling: Ntree, which is recognized as the number of trees to be developed in the forest, and Mtry, which appears to be the number of randomly selected variables for each node of the tree—or Ntree (number of trees grown) or Mtry (number of predictors sampled for splitting at each node) (López-Serrano et al. 2020).

An artificial neural network has two types of hidden layer, which are one hidden layer and two hidden layers. In random forest, Ntree is the number of trees to be developed in the forest, and Mtry appears to be the number of randomly selected variables for each node of the tree, or Ntree (number of trees grown) or Mtry (number of predictors sampled for splitting at each node) (López-Serrano et al. 2020). The data had been split into training set (70%) and testing set (30%). Data normalization was done after done the splitting dataset using minimum and maximum normalization. Next, the model was fit using neural network or random forest algorithm. Prediction of the independent variable and model validation was done after the process was done.

13 Regression Model Evaluation

The following equation represents the difference between the original and predicted values extracted by averaging the absolute difference over the dataset.

$$\text{MAE} = \frac{1}{N} \sum_{i=1}^N (y - \hat{y}) \quad (7)$$

The below equation represents the difference between the original and predicted values extracted by squaring the average difference over the dataset.

$$\text{MSE} = \frac{1}{N} \sum_{i=1}^N (y - \hat{y})^2 \quad (8)$$

This equation represents the error rate by the square root of MSE.

$$\text{RMSE} = \sqrt{\text{MAE}} = \sqrt{\frac{1}{N} \sum_{i=1}^N (y - \hat{y})^2} \quad (9)$$

The R^2 refers to the multiple coefficient of determination which measures how well the values fit compared to the original values. The values range from 0 to 1 and are interpreted as percentages. The higher the value, the better the model.

$$R^2 = 1 - \frac{\sum (y - \hat{y})^2}{\sum (\bar{y})^2} \quad (10)$$

where:

\bar{y} = mean value of y
 \hat{y} = predicted value of y

An artificial neural network consists of two types of hidden layer, which are one hidden layer and two hidden layers.

14 Results and Analysis

14.1 Description of Statistical Values of Dependent and Independent Variables

This study applied a variety of datasets from different years, such as field data, SuperView-1, and LiDAR dataset. Table 1 represents the statistical values of variables that have been collected using field and remote sensing approaches.

The main objective of this study was to assess the tropical forest aboveground biomass from SuperView-1 satellite image using machine learning (ML) approaches of an ANN and RF. Field observation data has been used to calculate diameter breast

Table 1 Statistical values of variables (number of trees = 279)

	Carbon stock (kg/tree)	DBH (cm)	h_L (m)	CPA (m ²)
Min	4.891	6.015	-0.283	-0.135
Max	8407.818	10.169	3.541	0.345
Mean	1442.423	7.902	3.246	0.236
Standard dev.	1411.788	0.880	0.335	0.063

height (DBH), while LiDAR data has been used to estimate height from LiDAR (h_L) by producing a canopy height model (CHM), and SuperView-1 image has been used to calculate crown projection area (CPA). These values were vital in order to estimate the carbon stock of tropical forests at the Forest Research Institute Malaysia (FRIM).

Table 1 represents statistical values for variables from field and remote sensing data. The statistical values for the carbon stock (kg/tree) were 4.891 min, 196.250 max, 101.142 mean, and 46.340 standard deviation. There were 6.015 min for DBH (cm), 10.169 max, 7.902 mean, and 0.880 standard deviation. The statistical values for h_L (m) were -0.283 min, 3.541 max, 3.246 mean, and 0.335 standard deviation. For CPA (m^2) the values were -0.135 min, 0.345 max, 0.236 mean, and 0.063 standard deviation.

14.2 Analysis of Statistical Value and Accuracy Assessment of OBIA Output

The data for crown delineation that has been segmented in eCognition software should be overlaid with manual digitizing in ArcMap software to get the best accuracy. Figure 2 shows four categories of tree crown segmentation that have been processed in this study, which are: (a) perfect match, (b) mismatch segmentation, (c) over-segmentation, and (d) under-segmentation. The red line in Fig. 2 represents automatic segmentation, while the yellow line represents manual digitization.

Table 2 represents statistical values for crown delineation reference polygons. The statistical values for the manual digitizing output were 3034.250 m^2 total area, 36 m min, 196.250 m max, 101.142 m mean, and 46.340 m standard deviation.

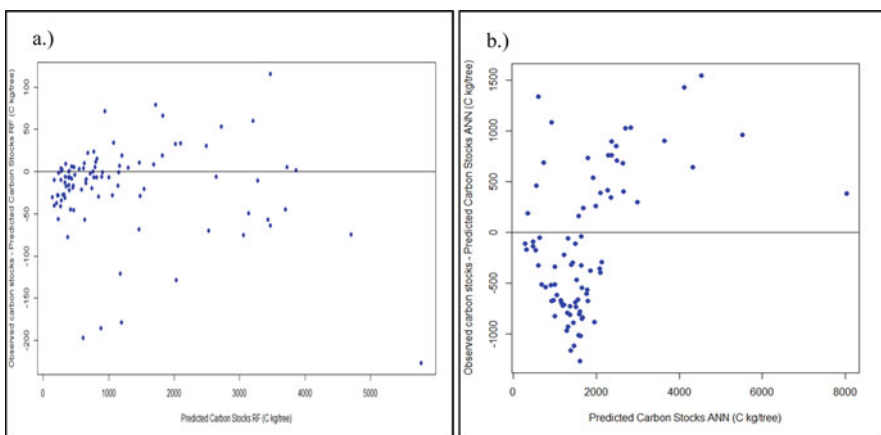


Fig. 2 Tree crown segmentation. (a) Perfectly match (b) Not match (c) Over-segmentation (d) Under-segmentation

Table 2 Statistical values for crown delineation reference polygons

Reference polygon (30)	Manual digitizing output (x_i)	Segmentation output (y_j)	Intersection area between x_i and y_j
Total area (m ²)	3034.250	2791.051	2791.051
Min	36.000	35.695	35.695
Max	196.250	171.729	171.729
Mean	101.142	93.035	93.035
Standard deviation	46.340	38.614	38.614

Table 3 Accuracy assessment of OBIA output

Table	Accuracy segmentation				
	Total reference polygon	Total 1:1 match	Over-segmentation	Under-segmentation	D
1:1	30	29			
Goodness of fit			0.000	0.080	0.040
Total accuracy		96.6%			96%

There were 2791.051 m² total area for segmentation output, 35.695 m min, 171.729 m max, 93.035 m mean, and 38.614 m standard deviation. The statistical values for the intersection area between x_i and y_j were the same as the segmentation output, which had 2791.051 m² total area, 35.695 m min, 171.729 m max, 93.035 m mean, and 38.614 m standard deviation.

Table 3 represents accuracy assessment of OBIA output. This study chose thirty (30) total reference polygons to get the accuracy assessment output of OBIA. Based on the results of Eqs. 2–4, the goodness of fit (D value) was calculated to be 96% segmentation accuracy with 4% error. In a 1:1 match, the overall accuracy of multi-resolution segmentation was 96.6%. The total accuracy of segmentation in this study was more accurate than in previous studies by Nik Effendi et al. (2021) which were 86% and 0.14 for the distance index (D). As a result, the accuracy of the segmentation output in this study is acceptable and can be applied for further investigation.

14.3 The Accuracy Assessment for Estimating Forest Aboveground Biomass Using an Artificial Neural Network (ANN) and Random Forest (RF)

Tables 4 and 5 show the accurate assessment of the model using the artificial neural network algorithm with different layers. The accuracy of the prediction model was evaluated using conventional validation indices such as MAE, MSE, RMSE, and R^2_{adj} (López-Serrano et al. 2020). Two types of hidden layers have been tested to obtain the accuracy value in order to estimate the carbon stocks by using one hidden

Table 4 Accuracy assessment of one hidden layer

No.	Model candidates	One hidden layer	MAE	MSE	RMS E	R-squared	Data sources
1	DBH + h_L – CPA	1	750.781	1,117,711	1057.219	0.565	Field, LiDAR, SVI
2	DBH + h_L – CPA	2	3960.773	17,770,124	4215.462	-5.908	Field, LiDAR, SVI
3	DBH + h_L – CPA	3	1603.529	3,375,286	1837.195	-0.312	Field, LiDAR, SVI

DBH diameter at breast height, h_L height extracted from LiDAR, CPA crown projection area, SVI SuperView-1

Table 5 Accuracy assessment of two hidden layers

No.	Model candidates	Two hidden layer	MAE	MSE	RMS E	R-squared	Data sources
1	DBH + h_L - CPA	c (1,3)	709.906	654,261	808.864	0.745	Field, LiDAR, SVI
2	DBH + h_L - CPA	c (2,2)	1041.939	1,346,346	1160.321	0.476	Field, LiDAR, SVI
3	DBH + h_L - CPA	c (3,1)	617.628	493,600.5	702.567	0.808	Field, LiDAR, SVI

DBH diameter at breast height, h_L height extracted from LiDAR, *CPA* crown projection area, *SVI* SuperView-1

layer and two hidden layers. Based on the table, Model 3 shows the lowest accuracy (RMSE = 702.567 Mg ha⁻¹ and $R^2 = 0.808$) obtained by using two hidden layers c (3, 1) followed by model 1 with (RMSE = 808.864 Mg ha⁻¹ and $R^2 = 0.745$). The less accurate result based on the table was Model 2 with (RMSE = 1160.321 Mg ha⁻¹ and $R^2 = 0.476$). From the table, all the accuracy assessments of the model that used one hidden layer had shown higher in error compared with two hidden layers. From this, it can be concluded that using two hidden layers for prediction was better than using one hidden layer (Thomas et al. 2017).

Table 6 shows the three variable results that been processed using a random forest algorithm in RStudio software. In order to increase the accuracy, the model differs based on the *Mtry* value obtained using the tested methods of $m = P/3$, ($m = \sqrt{P}$) and $m = P$, where *P* is the number of independent variables (López-Serrano et al. 2020). According to the table, Model 2 has the greatest accuracy assessment (RMSE = 55.067 Mg ha⁻¹ and $R^2 = 0.998$), followed by Model 3 (RMSE = 67.390 Mg ha⁻¹ and $R^2 = 0.998$), and finally Model 1 (RMSE = 141.326 Mg ha⁻¹ and $R^2 = 0.992$).

14.4 Plot the Graph and Evaluation Model of ANN and RF Algorithms

In this study, two algorithms of machine learning approaches (ANN and RF) were used to estimate the carbon stocks of tropical forest at FRIM by integrating field data combined with remote sensing data such as LiDAR data and SuperView-1 image. Figure 3 represents an accuracy graph for Model 3 of the artificial neural network (ANN), and for Model 2 of the random forest (RF). The data for crown delineation that has been segmented in eCognition software should be overlaid with manual digitizing in ArcMap software to get the best accuracy.

Table 7 represents the comparison and evaluation model using ANN and RF algorithms that have been used with the same three variable data sources. Based on

Table 6 Model validation of random forest model based on $Mtry$ value

No.	Model candidates	$Mtry$	$Ntree$	MAE	MSE	RMS E	R-squared	Data sources
1	DBH + h_L - CPA	1	500	87.700	19,973.05	141.326	0.992	Field, LiDAR, SVI
2	DBH + h_L - CPA	2	500	34.051	3032.437	55.067	0.998	Field, LiDAR, SVI
3	DBH + h_L - CPA	3	500	34.777	4541.437	67.390	0.998	Field, LiDAR, SVI

DBH diameter at breast height, h_L height extracted from LiDAR, CPA crown projection area, SVI SuperView-1

Fig. 3 Accuracy graph: (a) Model 3 of the artificial neural network (ANN) (b) Model 2 of the random forest (RF)

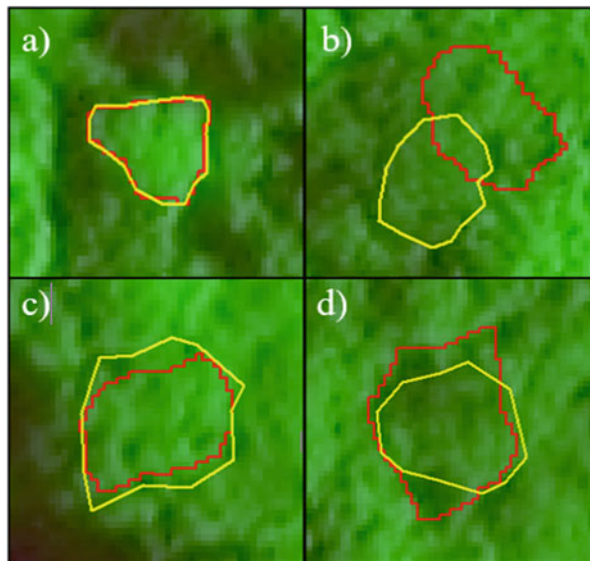


Table 7 Comparison and evaluation model using ANN and RF algorithms

No.	Algorithms	MAE	MSE	RMS E	R-squared	Data sources
3	ANN	617.628	493,600.5	702.567	0.808	Field, LiDAR, SV1
2	RF	34.051	3032.437	55.067	0.998	Field, LiDAR, SV1

the validation result obtained, Model 2 that used RF algorithm represented the most accurate accuracy assessment with an R^2 value (0.998) and lower RMSE (55.067 Mg ha⁻¹) compared to Model 3 that used ANN algorithm which obtains the result of R^2 value (0.808) with the highest RMSE value (702.567 Mg ha⁻¹). Higher R^2 and lower RMSE values show that the model's estimating accuracy is better (López-Serrano et al. 2020; Li et al. 2020). Based on the previous study by Nik Effendi et al. (2021), the multiple coefficient of determination (R^2) between AGB predicted and observed using hL , CPA, and DBH was 0.949. It was possible to conclude that a combination of LiDAR, hyperspectral data, and field observations can be applied to estimate AGB in a tropical forest. Overall, random forest (RF) was more suitable to estimate carbon stock compared to an artificial neural network (ANN), and the coefficient of determination (R^2) that using random forest (RF) for Model 2 represented the independent variables (hL , DBH, and CPA) was suitable to estimate the dependent variable (Sc).

15 Conclusion

Natural forests represent areas of different species of flora and fauna. Trees are vital elements for ecosystem balance that supply the storage of oxygen to humans and store carbon dioxide. Many effects can happen if the value of carbon dioxide is higher, such as green house, climate change, thinning of the ozone layer, global warming, and others. This study has been conducted to estimate the carbon stock in the tropical forest in order to maintain the terrestrial ecosystem balance for the Malaysian community, especially at FRIM Forest, Kepong, Selangor.

The first objective of this study was to classify the forest aboveground biomass by estimating crown projection area (CPA) using object-based image analysis (OBIA). This study used three combinations of data which were field observation, LiDAR data, and SuperView-1 image in order to estimate the carbon stock in tropical forests. LAS tool has been used in order to obtain canopy height model value. An OBIA approach has been applied in this to classify the tree crown using automatic segmentation and manual digitize. The OBIA approach had more advantages compared to pixel-based classification, which can classify the object through its shape and can save time without classifying the object by pixel.

The second objective was to determine the accuracy assessment for estimating forest aboveground biomass using an artificial neural network (ANN) and random forest (RF). This study used artificial neural network (ANN) and random forest (RF) algorithms for machine learning approach in order to calculate the accuracy of assessment of dependent and independent variables. Three independence variables (DBH, h_L , and CPA) have been applied in this study in order to calculate the dependent variable (carbon stock). The random forest algorithm was more suitable to calculate the accuracy assessment of dependent variables (S_c) and independent variables (h_L , DBH, and CPA) since it can obtain higher R^2 and lower RMSE values. The number of observation values and the number of independent variables are crucial in obtaining an accurate and low-error validation value and ensuring that the findings produced are neither over- nor underfitting. This study was successfully proven by Mohd Zaki et al. (2018) since the independent variable can be used to estimate carbon stock. In conclusion, the objectives of this study have been successfully achieved.

Acknowledgment We would like to acknowledge the Forest Research Institute Malaysia (FRIM) for granting access to the study area. We thank the team of research expedition from Universiti Teknologi MARA, Perlis Branch, and Institute for Biodiversity and Sustainable Development (IBSD) for their assistance in the field data collection.

References

Addink EA, De Jong SM, Pebesma EJ (2007) The importance of scale in object-based mapping of vegetation parameters with hyperspectral imagery. *Photogramm Eng Remote Sens* 73:905–912

- Chazdon RL, Broadbent EN, Rozendaal DMA, Bongers F, Zambrano AMA, Aide TM, Balvanera P, Becknell JM et al (2016) Carbon sequestration potential of second-growth forest regeneration in the Latin American tropics. *Sci Adv* 2:5
- Dhanda P, Nandy S, Kushwaha SPS, Ghosh S, Murthy YVKN, Dadhwa VK (2017) Optimizing spaceborne LiDAR and very high resolution optical sensor parameters for biomass estimation at ICESat/GLAS footprint level using Optimizing spaceborne LiDAR and very high resolution optical sensor parameters for biomass estimation at ICESat. *Prog Phys Geogr* 41:1–21
- Gao Y, Lu D, Li G, Wang G, Chen Q, Liu L, Li D (2018) Comparative analysis of modeling algorithms for forest aboveground biomass estimation in a subtropical region. *Remote Sens* 10:4
- Ghosh SM, Behera MD (2018) Aboveground biomass estimation using multi-sensor data synergy and machine learning algorithms in a dense tropical forest. *Appl Geogr* 96:29–40
- Hussin YA, Gilani H, Van Leeuwen L, Murthy MSR, Shah R, Baral S, Tsendbazar NE, Shrestha S, Shah SK, Qamer FM (2014) Evaluation of object-based image analysis techniques on very high-resolution satellite image for biomass estimation in a watershed of hilly forest of Nepal. *Appl Geom* 6:59–68
- Jaafar WSWM, Woodhouse IH, Silva CA, Omar H, Maulud KNA, Hudak AT, Klauber C, Cardil A, Mohan M (2018) Improving individual tree crown delineation and attributes estimation of tropical forests using airborne LiDAR data. *Forests* 9:1–23
- Kenzo T, Furutani R, Hattori D, Kendawang JJ, Tanaka S, Sakirai K, Ninomiya I (2009) Allometric equations for accurate estimation of above-ground biomass in Allometric equations for accurate estimation of above-ground biomass in logged-over tropical rainforests in Sarawak. *J For Res* 14:365–372
- Li Y, Li M, Li C, Liu Z (2020) Forest aboveground biomass estimation using Landsat 8 and Sentinel-1A data with machine learning algorithms. *Sci Rep* 10:1
- López-Serrano PM, Domínguez JLC, Corral-Rivas JJ, Jiménez E, López-Sánchez CA, Vega-Nieva DJ (2020) Modeling of aboveground biomass with landsat 8 OLI and machine learning in temperate forests. *Forests* 11:1–18
- Mohd Zaki NA, Abd Latif Z, Zainal MZ, Zainuddin K (2015) Individual tree crown (ITC) delineation using watershed transformation algorithm for tropical lowland dipterocarp. *International Conference on Space Science and Communication, IconSpace, 2015 Sept (October)*, pp 237–242
- Mohd Zaki NA, Abd Latif Z, Suratman MN (2018) Modelling above-ground live trees biomass and carbon stock estimation of tropical lowland Dipterocarp forest: integration of field-based and remotely sensed estimates. *Int J Remote Sens* 39:2312–2340
- Nandy S, Ghosh S, Kushwaha SPS, Kumar S (2019) *Remote Sensing of Northwest Himalayan Ecosystems*. Springer Nature Singapore, Singapore
- Nik Effendi NAF, Mohd Zaki NA, Abd Latif Z, Suratman MN, Bohari SN, Zainal MZ, Omar H (2021) Unlocking the potential of hyperspectral and LiDAR for above-ground biomass (AGB) and tree species classification in tropical forests. *Geocarto Int* 42:1–26. <https://doi.org/10.1080/10106049.2021.1990419>
- Pandit S, Tsuyuki S, Dube T (2018) Estimating above-ground biomass in sub-tropical buffer zone community forests, nepal, using sentinel 2 data. *Remote Sens* 10:1–18
- Silveira EMO, Silva SHG, Acerbi-Junior FW, Carvalho MC, Carvalho LMT, Scolforo JRS, Wulder MA (2019) Object-based random forest modelling of aboveground forest biomass outperforms a pixel-based approach in a heterogeneous and mountain tropical environment. *Int J Appl Earth Obs Geoinf* 78:175–188
- Thomas AJ, Petridis M, Walters SD, Gheytsi SM, Morgan RE (2017) Two hidden layers are usually better than one. *Commun Comput Inf Sci* 744:279–290

- Urbazaev M, Thiel C, Cremer F, Dubayah R, Migliavacca M, Reichstein M, Schmullius C (2018) Estimation of forest aboveground biomass and uncertainties by integration of field measurements, airborne LiDAR, and SAR and optical satellite data in Mexico. *Carbon Balance Manag* 13:1
- Vafaei S, Soosani J, Adeli K, Fadaei H, Naghavi H, Pham TD, Bui DT (2018) Improving accuracy estimation of Forest Aboveground Biomass based on incorporation of ALOS-2 PALSAR-2 and Sentinel-2A imagery and machine learning: a case study of the Hyrcanian forest area (Iran). *Remote Sens* 10:2
- Wu C, Shen H, Shen A, Deng J, Gan M, Zhu J, Xu H, Wang K (2016) Comparison of machine-learning methods for above-ground biomass estimation based on Landsat imagery. *J Appl Remote Sens* 10:3
- Zhang C, Denka S, Cooper H, Mishra DR (2018) Quantification of sawgrass marsh aboveground biomass in the coastal Everglades using object-based ensemble analysis and Landsat data. *Remote Sens Environ* 204:366–379



Potential Tree Species Distribution Modelling Using MaxEnt Model for Resource Partitioning in Azad Jammu and Kashmir (AJK), Pakistan

Adeel Ahmad , Sajid Rashid Ahmad, and Hammad Gilani

Abstract

This chapter aims to spatially predict the potential distribution of four native tree species (*Abies pindrow*, *Olea ferruginea*, *Pinus roxburghii*, and *Pinus wallichiana*) using 21 bioclimatic, 2 biophysical, and 3 topographical remotely sensed variables through MaxEnt modelling in the region of Azad Jammu and Kashmir (AJK), Pakistan. In the MaxEnt model, a total of 739 tree occurrence from 45 circular plots of selected species were used with selected variables, filtered through multicollinearity tests. The jackknife test showed different essential variables influencing the prediction of species distribution, including elevation, vegetation indices, temperature, and precipitation. For all the tree species distributions, satisfactory results were achieved with area under ROC (receiver operating characteristic) curve (AUC) testing and training values greater than 0.74 and 0.88, respectively. Based on the 10-percentile training presence threshold-dependent values, the True Skill Statistic (TSS) test attained at least 76% overall accuracy for tree species distribution. *Abies pindrow* covered 429.58 km², *Pinus wallichiana* 346.28 km², *Pinus roxburghii* 341.93 km², and *Olea ferruginea* 27.53 km² area within the very highly suitable category of

Supplementary Information The online version contains supplementary material available at https://doi.org/10.1007/978-981-19-4200-6_7.

A. Ahmad

College of Earth and Environmental Sciences, University of the Punjab, Lahore, Pakistan

Department of Geography, University of the Punjab, Lahore, Pakistan

S. R. Ahmad

College of Earth and Environmental Sciences, University of the Punjab, Lahore, Pakistan

H. Gilani (✉)

Department of Space Science, Institute of Space Technology, Islamabad, Pakistan

© The Author(s), under exclusive license to Springer Nature Singapore Pte Ltd. 2022

M. N. Suratman (ed.), *Concepts and Applications of Remote Sensing in Forestry*, https://doi.org/10.1007/978-981-19-4200-6_7

predicted potential distribution. The results also showed that the Himalayan subtropical pine forest ecoregion has the highest tree species diversity. The resulted resource partitioning of the selected tree species can be considered as recommended hotspots for management and conservation activities by the local stakeholders and government agencies to make informed decisions.

Keywords

Tree distribution · Bioclimatic · Topographical · MaxEnt · True Skill Statistic (TSS) · Ecoregion · Resource partitioning

1 Introduction

A habitat is an integral part of the environment and home to several diverse animal and plant species. Different species are products of the same or different habitats for fulfilling their needs like food requirements, shelters, space occupation, and other survival needs (Qamar et al. 2011). These species are the building blocks of a geographic region (Chetan et al. 2014). For ecologists and conservationists, it is vital to understand a specific species relationship with its surrounding climate and biophysical environment (Kaky et al. 2020). To conserve and manage various plant and animal species, reliable and accurate information on their respective habitats is of key importance (Qamar et al. 2011).

Ecological niche models (ENMs) or species distribution models (SDMs) are algorithmic tools that attempt to relate a geographic area's environmental, climatic, and other biophysical characteristics with the distribution and occurrence of a particular species (Jaryan et al. 2013). ENMs or SDMs are extremely important to predict the potential geographic zones of species when limited occurrence data is available (Zhang et al. 2019). The distribution and diversity maps generated through the ENMs or SDMs are used to design scientific surveys for scheming management and conversation activities by related departments and authorities (Kumar et al. 2014). There are many SDMs that are being used by researchers, including generalized linear model (GLM) (Guisan et al. 2016), multivariate adaptive regression splines (MARS) (Quirós et al. 2009), boosted regression trees (BRTs) (Becker et al. 2020), domain environmental envelope (DOMAIN) (Carpenter et al. 1993), ecological niche factor analysis (ENFA) (Basille et al. 2008), generic algorithm for rule-set production (GARP) (Yang et al. 2020), and maximum entropy modelling (MaxEnt) (Jaryan et al. 2013). Among all these SDMs, MaxEnt is particularly endorsed and used widely by the scientific community as it produces more accurate predictions (Gilani et al. 2020; Kaky et al. 2020). SDMs primarily rely on the presence-only occurrence data of species for their potential spatial distribution modelling (Bobrowski et al. 2017; Gilani et al. 2020). However, presence-absence occurrence records of species from the field produce more certain distributions than occurrence-only data if available (Gilani et al. 2020).

In Pakistan, different studies reported biodiversity analysis, some of which have used SDMs, to assess the potential distribution of animal and plant species (Qamar et al. 2011; Khanum et al. 2013; Ali et al. 2014; Kazim et al. 2015; Ashraf et al. 2016; Zaidi et al. 2016; Fatima et al. 2016; Kabir et al. 2017; Gilani et al. 2020; Hameed et al. 2020; Khalil et al. 2021). For instance, Qamar et al. (2011) focused on distribution modelling of different mammal species (snow leopard, common leopard, musk deer, wolf, long-tailed marmot, etc.) in Pakistan's three national parks in the Western Himalayas. They used mammal occurrence data along with digital elevation model (DEM), land use and land cover (LULC) maps, and other topographical information in GIS to generate habitat maps of these animal species. The following study by Khanum et al. (2013) used MaxEnt to assess the spatial distribution of medicinal Asclepiad species (*Pentstemon spiralis*, *Tylophora hirsuta*, and *Vincetoxicum arnotianum*) in Pakistan. They used field-based occurrence information of these species for 2010 and 2011 to run the model. The study by Ali et al. (2014) also used MaxEnt for predicting the present and future distribution of *Abies pindrow* (tree species) in Swat district in Khyber Pakhtunkhwa (KP) province of Pakistan. Kazim et al. (2015) reported 29 species (from 17 families under 25 genera) of spider fauna in the Gilgit-Baltistan (GB) administrative area of Pakistan. They reported spiders' biodiversity using literature and extensive field surveys. The study by Zaidi et al. (2016) used MaxEnt modelling to predict the distribution of screw-worm larvae (a fly species) in the northwest region of Pakistan. Among the four eco-zones of the study area, the species preferred zones with more moisture content in the climate. The subsequent study by Ashraf et al. (2016) predicted the potential distribution of *Olea ferruginea* (tree species) in Pakistan. They used MaxEnt to predict the distribution of *Olea ferruginea* for future climatic scenarios. Fatima et al. (2016) used MaxEnt for modelling the spatial distribution of mosquitoes (*Aedes aegypti*) in the Lahore district of Punjab, Pakistan. They related this distribution with the spatial spread of dengue fever in the study area. The study by Kabir et al. (2017) focused on assessing habitat suitability and movement corridors of grey wolf (*Canis lupus*) in northern Pakistan. They also utilized MaxEnt for this purpose.

Similarly, Hameed et al. (2020) identified priority landscapes for snow leopard conservation in Pakistan using MaxEnt modelling. They used 98 presence points and 11 environmental variables to achieve their objectives. The study by Gilani et al. (2020) predicted six native tree species (*Abies pindrow*, *Betula utilis*, *Cedrus deodara*, *Picea smithiana*, *Pinus wallichiana*, and *Quercus ilex*) in GB, Pakistan, under a climate change scenario. They used 21 bioclimatic and three topographic variables to perform this spatial prediction using MaxEnt. The latest study in this regard by Khalil et al. (2021) used MaxEnt to map the potential distribution of potato (*Solanum tuberosum*) crop cultivation in Pakistan. This study utilized 19 bioclimatic variables, covariates (soil type, elevation, and irrigation), and 58 occurrence points for modelling the distributions under climate change scenarios.

Keeping in view the discussed literature, the objectives of this study are i) predicting the potential spatial distribution of four native tree species (*Abies pindrow*, *Olea ferruginea*, *Pinus roxburghii*, and *Pinus wallichiana*) of Azad Jammu and Kashmir (AJK), ii) assessing the tree species diversity in AJK, and iii)

identifying the most diversified ecoregion based on these four native tree species distributions.

2 Study Area

The region of AJK lies in the northeast of Punjab province, east of Islamabad Capital Territory (ICT), east of Khyber Pakhtunkhwa (KP) province, and south of Gilgit-Baltistan (GB) territory in Pakistan. The geographical extent of AJK lies between 32.767283° north to 35.154967° north latitude and 73.395781° east to 75.465172° east longitude (Fig. 1). The study area is comprised of ten districts. The elevation variation of the region ranges between 225 meters (m) to 6000 m. As a part of the Western Himalayas, the region received rainfall in winters and summers with annual precipitation exceeding 1300 millimetres (mm). The region is classified as subtropical, temperate, and alpine forests with dominant native conifer species of *Pinus roxburghii*, *Pinus wallichiana*, *Abies pindrow*, and *Cedrus deodara* (Khan et al. 2020). Among important native broadleaved species, one is *Olea ferruginea*. The leave extracts of *Olea ferruginea* are used for treating skin disease in the study area, *Pinus roxburghii* is used for firewood and furniture (Azeem et al. 2020), and *Pinus wallichiana* and *Abies pindrow* are used for medicinal purposes as well as for construction, fuel, and exporting (Ishtiaq et al. 2012). Some of these tree species are endangered and can become extinct if no conservation measures are taken soon (Azeem et al. 2020).

3 Materials and Methods

The methodology is broadly split into (i) data preparation and processing (ii) MaxEnt model calibration and evaluation (iii) tree species diversity maps. Figure 2 presents a systematic flow chart of the detailed methodology adopted to achieve the research objectives.

3.1 Data Preparation and Processing

For this study, 739 trees species records were used for the potential spatial distribution and mapping over the entire region of AJK (Fig. 3). Geographically well-distributed 45 circular plots (~1 ha or 0.01 km² area) were measured.

The circular plots with specific dominant species were selected for modelling (Table 1). For the tree species distribution, four important tree species were selected based on their respective importance. Three (*Abies pindrow*, *Pinus roxburghii*, and *Pinus wallichiana*) out of four species belong to the conifer tree species group, while one (*Olea ferruginea*) belongs to the broadleaved tree species group.

Landsat-8 OLI (Operational Land Imager) 30 m cloud-free satellite data was used to extract two biophysical variables using Google Earth Engine (GEE) cloud-

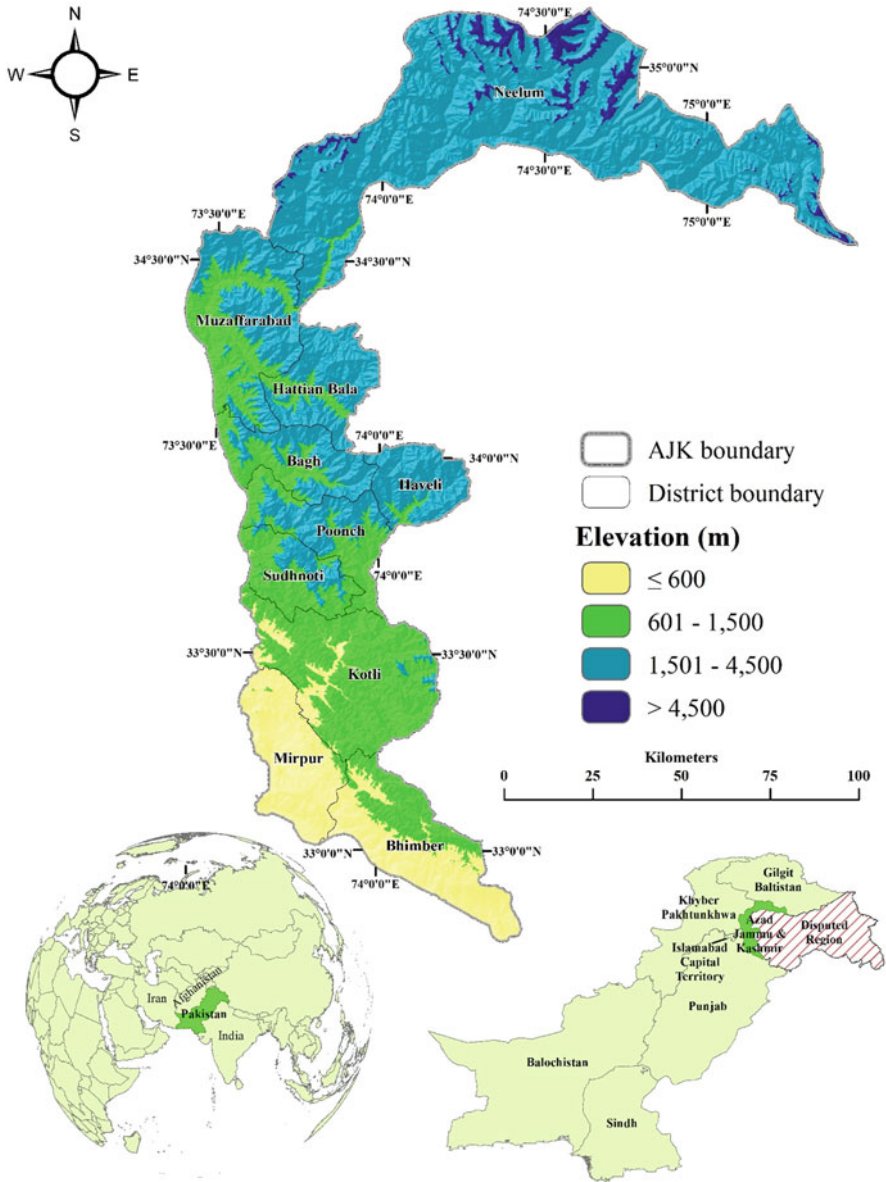


Fig. 1 The topography and districts of Azad Jammu and Kashmir (AJK), Pakistan

computing platform. We used normalized difference normalized vegetation index (NDVI) and enhanced vegetation index (EVI) as biophysical variables in MaxEnt modelling. These remote sensing-based vegetation indices strongly correlate with the changes in the chlorophyll content of tree species (Gu et al. 2007).

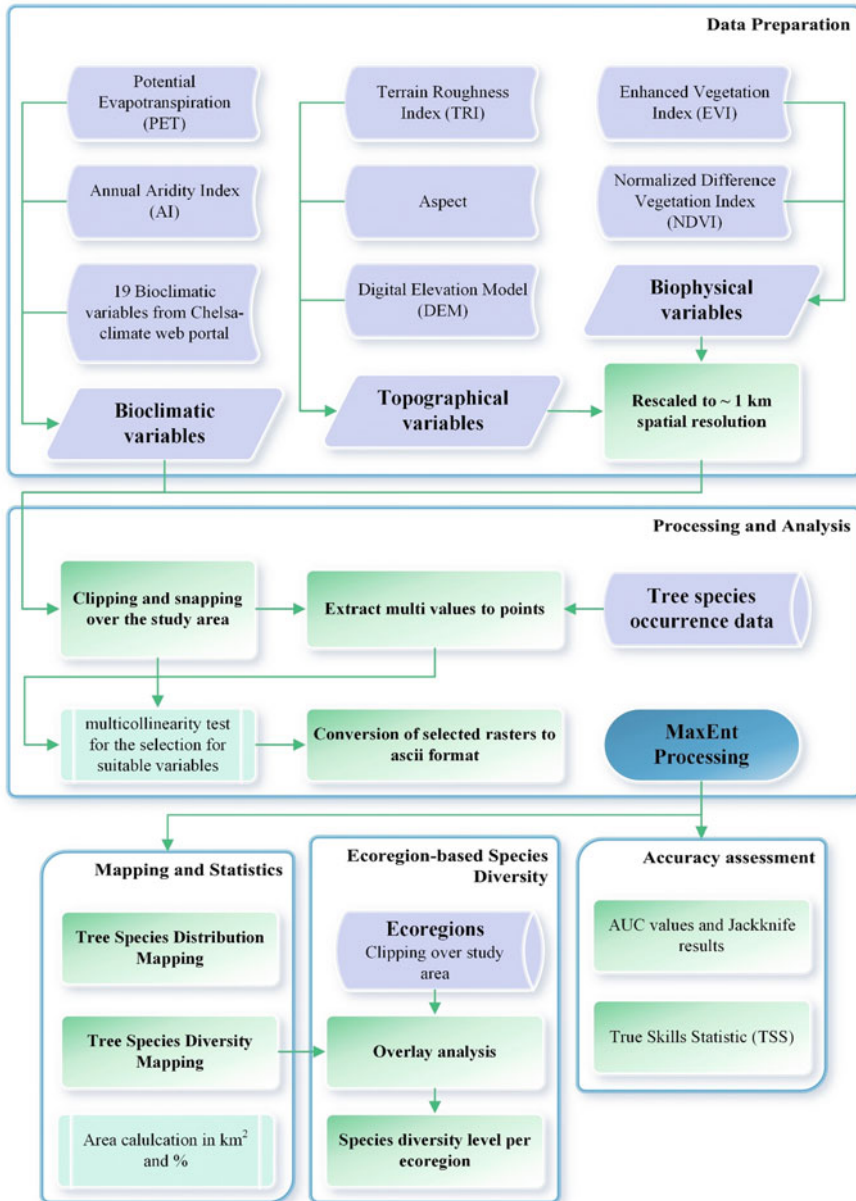


Fig. 2 Systematic flow diagram of the adopted methodology

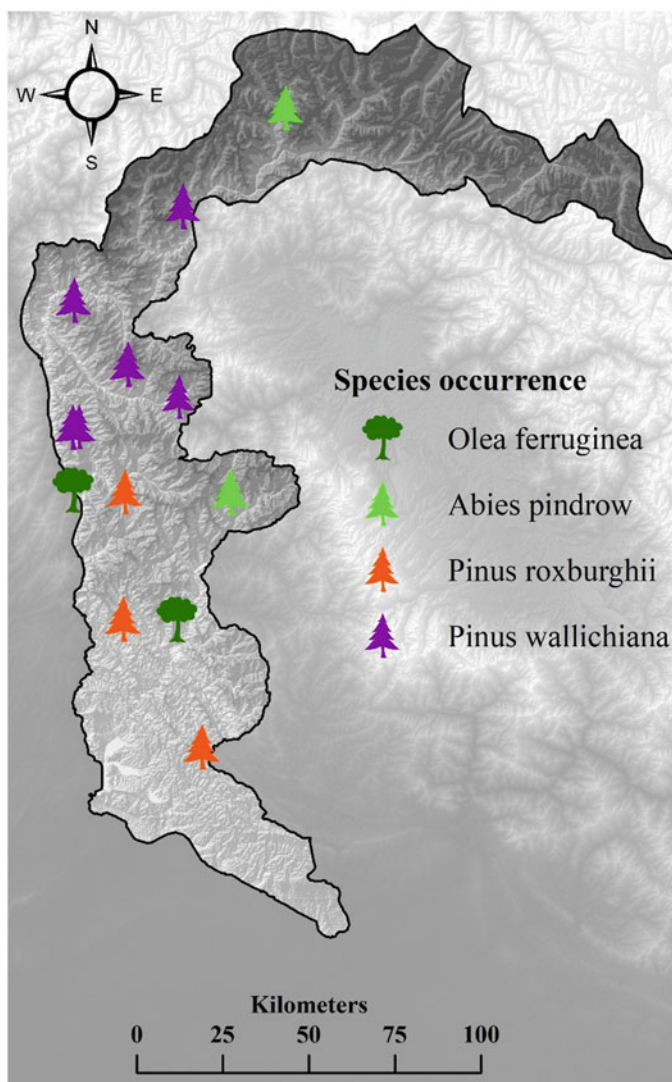


Fig. 3 Spatial occurrence of four tree species used in distribution modelling

Table 1 Selected four native trees species for distribution modelling in AJK

The scientific name of the tree species	Vernacular/local name of the tree species	Number of plots	Tree counts
<i>Abies pindrow</i>	Fir	9	120
<i>Olea ferruginea</i>	Kahu	7	221
<i>Pinus roxburghii</i>	Chir pine	11	102
<i>Pinus wallichiana</i>	Blue pine	18	296

Through GEE 30 m Shuttle Radar Topography Mission (SRTM), DEM was extracted over the study area. The DEM generated the aspect and TRI over the AJK region. These independent topographic variables were selected as they greatly influence the species distribution (Wang et al. 2009).

This study included 21 readily available bioclimatic variables with ~1 kilometre (km) spatial resolution at the equator from the Chelsa-climate web portal (<https://chelsa-climate.org/bioclim/>). These bioclimatic products consist of temperature and precipitation datasets averaged annually, quarterly, and seasonally (Table S1). The annual aridity index (AI) and potential evapotranspiration (PET) global products were accessed and downloaded from the CGIAR-CSI web portal (<https://cgiarcsi.community/data/global-aridity-and-pet-database/>).

The global ecoregion datasets produced by Dinerstein et al. (2017) were used for tree species diversity assessment over ecoregions lying within the study area. The dataset was downloaded from the RESOLVE web portal (<https://ecoregions.appspot.com/>).

All datasets, including bioclimatic, biophysical, and topographical variables, were clipped over the study area i.e. AJK administrative boundary. The biophysical and topographical 30 m variables were rescaled to ~1 km to match the resolution of the bioclimatic variables. All variables were projected to the geographic coordinate system (WGS84) and, after analysis, reprojected to the UTM 43N zone for area calculation. Final rasters were converted into ASCII format as this is the format that MaxEnt desktop software takes as input.

Multicollinearity is one of the communal problems when a high association among variables exists, leading to unfavourable and unreliable regression evaluations (Gilani et al. 2020). A multicollinearity test was performed among all 26 variable values, extracted against each occurrence point of each tree species. Pearson's correlation, one of the most widely used correlation coefficients, was used to perform this test (Table S2). Highly correlated variables ($r \geq \pm 0.9$) against each tree species were disregarded for processing in MaxEnt model (Graham 2003).

3.2 MaxEnt Model Calibration and Evaluation

Out of all the tree species occurrence data, 75% points were used to train the model, while the remaining 25% were used for 10-percentile training presence threshold-dependent cross-validation. Only for *Olea ferruginea*, 35% occurrence points were used for model validation as 25% were insufficient given the low number of occurrence points compared to other tree species. The resultant output raster of the MaxEnt model ranges between 0 and 1, with 0 referring to the lowest possible occurrence space for selected species and 1 referring to the highest potential space of selected species occurrence (Phillips and Dudík 2008). To generate absence or background points, 10,000 randomly distributed points were generated in MaxEnt model, which helped to calculate the reliability and accuracy of the species prediction modelling.

The area under the ROC curve AUC is primarily used to evaluate the performance of the MaxEnt model (Phillips et al. 2004; Gilani et al. 2020). The AUC score of 0.7–0.9 range shows that the model achieved adequate accuracy, while a score of >0.9 represents the very high accuracy of the model (Gilani et al. 2020). However, the AUC alone is inadequate to show the accuracy of a model because it does not use a threshold approach for explaining predictive accuracy (Allouche et al. 2006). Therefore, a threshold-dependent error matrix was generated to measure the values of sensitivity, specificity, overall accuracy, kappa statistic, maximum kappa, and True Skill Statistic (TSS). This error matrix correlated observed and predicted values and evaluates the performance of the species prediction modelling. A 10-percentile training presence threshold was used in this study to calculate these values, with kappa values ranging from -1 (poor performance) to $+1$ (best performance) (Allouche et al. 2006).

The resultant output raster of MaxEnt of each tree species was regrouped into five classes, as Gilani et al. (2020) proposed. The prediction values were classified as (1) least potential (0–0.2), inadmissible natural surroundings; (2) less potential (0.2–0.4), scarcely reasonable living space; (3) moderate potential (0.4–0.6), appropriate territory; (4) high potential (0.6–0.7), an exceptionally appropriate environment; and (5) very high potential (0.7–1), profoundly reasonable living space. The area in km^2 and the percentage of each regrouped class against each species were calculated and reported.

3.3 Tree Species Diversity Maps

A tree species diversity map was generated using equally weighted overlay analysis of output rasters of all four potential species distributions (Ranjitkar et al. 2016). The tree species diversity map was categorized into five classes: (1) very low, (2) low, (3) moderate, (4) high, and (5) very high. Class 1 refers to a low to no species diversity, and class 5 to pixels with the richest tree species diversity.

Six ecoregions: (1) Himalayan subtropical pine forests, (2) western Himalayan broadleaf forests, (3) western Himalayan subalpine conifer, (4) Aravalli west thorn scrub forests, (5) Karakoram-West Tibetan plateau, and (6) northwestern Himalayan alpine shrub and meadows were laid over tree species diversity raster to identify the ecoregion with the least to highest diversity.

4 Results

The Results sections are divided into five sections: (1) selected independent variables for MaxEnt modelling, (2) model calibration and evaluation, (3) tree species distribution maps, and (4) tree species diversity maps.

4.1 Selected Independent Variables for MaxEnt Modelling

Using multicollinearity test, 10 independent variables for *Abies pindrow*, 11 for *Olea ferruginea* and *Pinus roxburghii* each, and 9 for *Pinus wallichiana* were selected (Table 2). Among all these independent variables, AI, Aspect, DEM, EVI, NDVI, TRI, Bio02, Bio07, and Bio15 were commonly used for all four tree species prediction in the MaxEnt model. Bio04 independent variable was only used for predicting *Apies pindrow*, while Bio12 and Bio14 were used for predicting *Olea ferruginea* and *Pinus roxburghii*, in addition to common independent variables. All other independent variables showed a strong Pearson correlation ($r \geq \pm 0.9$) and were eliminated accordingly.

4.2 Model Calibration and Evaluation

The AUC values attained using MaxEnt (Table 3) show that the highest training accuracy (0.9963) was achieved for *Olea ferruginea* and the lowest (0.8776) for *Abies pindrow*. On the other hand, the test accuracy showed the highest value (0.9873) for *Pinus wallichiana* and the lowest value (0.7389) for *Olea ferruginea*. All these values were satisfactory if it ranged from adequate to very high accuracy.

The jackknife test (Fig. 4) showed different important variables influencing the prediction of species distribution, including elevation, vegetation indices, temperature, and precipitation. AI and DEM showed prediction importance for *Abies pindrow*, *Olea ferruginea*, and *Pinus roxburghii*; NDVI for *Olea ferruginea*, *Pinus roxburghii*, and *Pinus wallichiana*; and Bio12 and Bio15 (temperature products) for all selected tree species. All remaining independent variables showed the importance for relative tree species.

Based on 10-percentile training presence threshold-dependent, more than 80% accuracy was achieved except *Pinus roxburghii* (Table 3). TSS values of >0.8 were achieved for *Abies pindrow* and *Pinus wallichiana*. A very low TSS (0.33) was achieved for *Olea ferruginea*, while a moderate TSS (0.60) was achieved for *Pinus roxburghii*.

4.3 Tree Species Distribution Maps

The tree species distribution maps show that the northeastern and southwestern part of the study area lies within inadmissible natural surroundings for any of the selected

Table 2 Area under the ROC (receiver operating characteristic) curve (AUC) values attained using MaxEnt for each tree species by partitioning tree species data into training (75%) and test (25%)

	<i>Abies pindrow</i>	<i>Olea ferruginea</i>	<i>Pinus roxburghii</i>	<i>Pinus wallichiana</i>
Training	0.8776	0.9963	0.9387	0.9215
Test	0.8389	0.7389	0.7826	0.9873

tree species (Fig. 5). *Abies pindrow* and *Pinus wallichiana* are distributed on the higher elevations of the study area, while *Olea ferruginea* and *Pinus roxburghii* were predicted on lower elevations.

The area graph (Fig. 6 and Table S3) shows that *Abies pindrow* occupies the highest area (3.23%) within the profoundly reasonable living space category, followed by *Pinus wallichiana* (2.60%), *Pinus roxburghii* (2.57%), and *Olea ferruginea* (0.21%).

4.4 Tree Species Diversity Maps

Figure 7 shows the spatial distribution of the tree species diversity in the study area based on the four selected tree species (*Abies pindrow*, *Olea ferruginea*, *Pinus roxburghii*, and *Pinus wallichiana*). Most of the northern and southern latitudes of the study area possess the least diverse region that also corresponds to high elevation—snow areas above tree line and low elevation areas—agricultural and settlements areas, respectively. In the middle latitudes of the study area, tree species diversity hotspots or corridors can be observed clearly.

Out of the six ecoregions laid over the study area, ecoregions 3 (western Himalayan subalpine conifer), 4 (Aravalli west thorn scrub forests), and 5 (Karakoram-West Tibetan plateau) possess the least diverse tree species covering more than 90% area under the very low to low diversity category (Fig. 8). This is followed by ecoregion 6 (northwestern Himalayan alpine and meadows), covering only 3.1% area under high diversity. Ecoregion 1 (Himalayan subtropical pine forests) is the highest diverse ecoregion in terms of very high diversity class, covering an area of 2.8%, followed by ecoregion 2 (western Himalayan broadleaf forests) covering an area of 1.6% in the same class. Overall, ecoregion 2 possesses 36.5% area within high to very high diversity class, the highest among all other ecoregions in the study area.

Table 3 Result evaluation of MaxEnt model through 10-percentile training presence-threshold-dependent True Skill Statistic (TSS), specificity, sensitivity, kappa statistics, and overall accuracy values

	<i>Abies pindrow</i>	<i>Olea ferruginea</i>	<i>Pinus roxburghii</i>	<i>Pinus wallichiana</i>
10-percentile training presence-threshold-dependent	0.54	0.651	0.323	0.476
Sensitivity	1.00	0.33	0.83	1.00
Specificity	0.86	1.00	0.76	0.82
TSS	0.86	0.33	0.60	0.82
Kappa	0.01	0.048	0.00	0.01
Kappa maximum	0.44	0.15	0.32	0.44
Overall accuracy	0.86	1.00	0.76	0.82

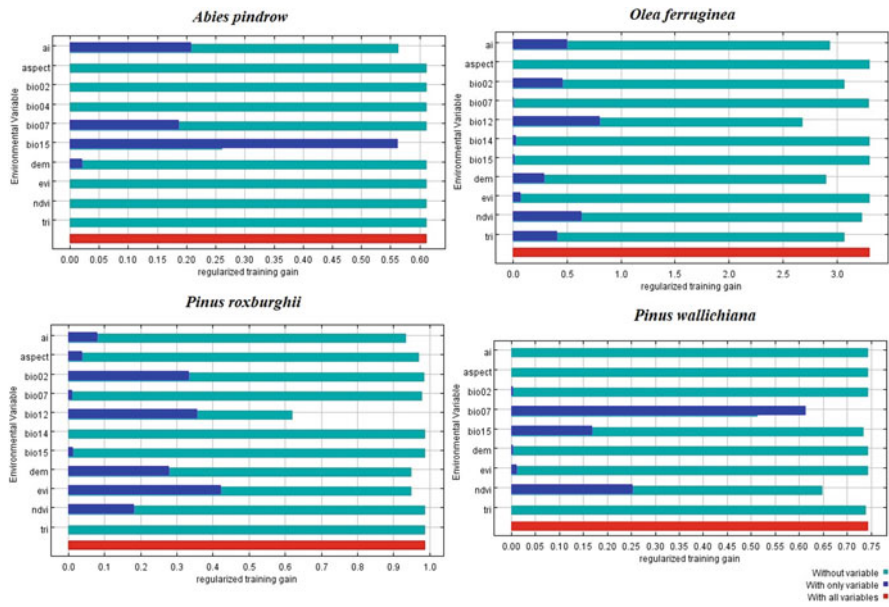


Fig. 4 The evaluation of relative importance of independent variables for each species using the jackknife test

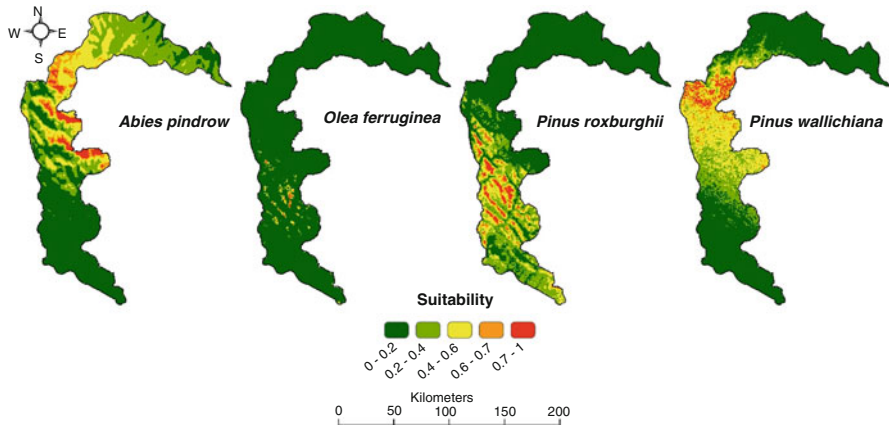


Fig. 5 Potential spatial distribution of four tree species (*Abies pindrow*, *Olea ferruginea*, *Pinus roxburghii*, and *Pinus wallichiana*) in AJK

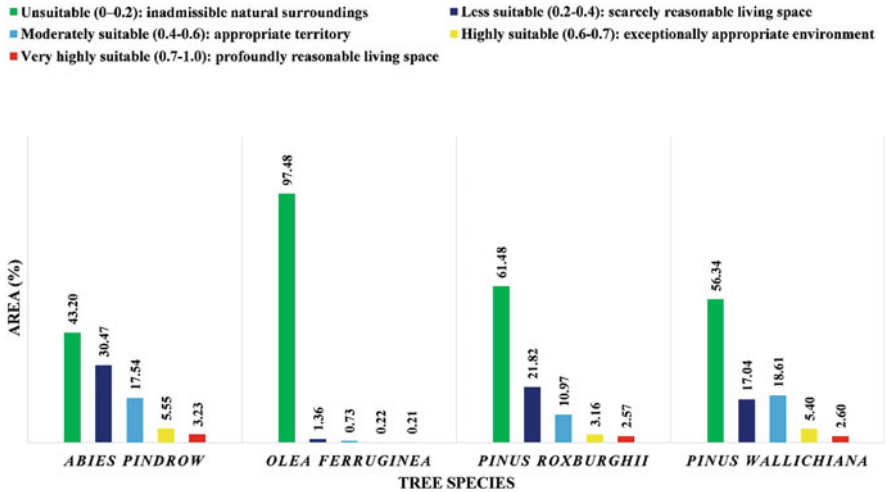


Fig. 6 The area (%) occupied by each suitability category against each tree species

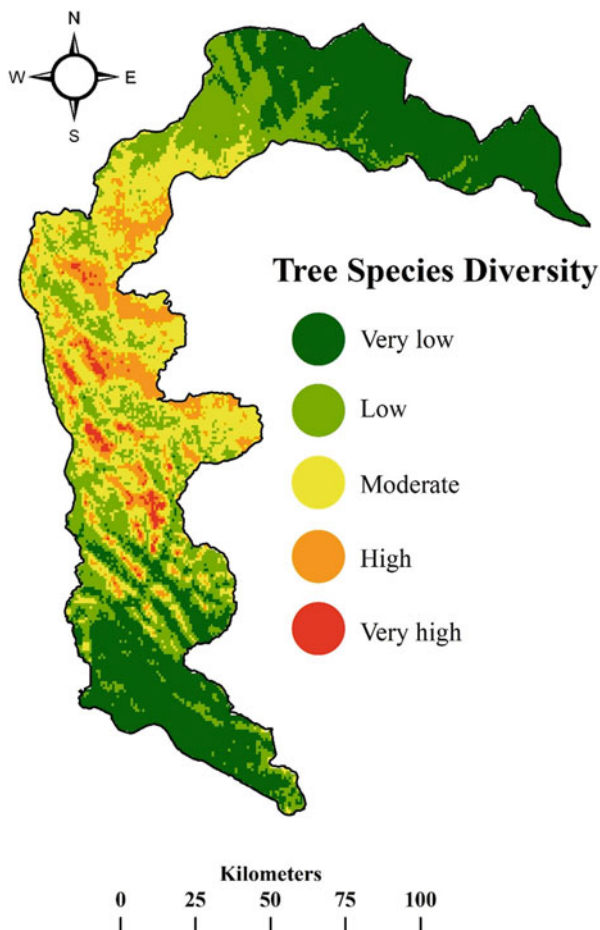
5 Discussion

Using MaxEnt model, the potential distribution of four tree native species in the region of AJK was spatially predicted. The independent variables (bioclimatic, biophysical, and topographical) were processed at ~1 km spatial resolution. A very few studies in Pakistan have used SDMs for assessing the potential distribution of plants and animals, and out of these studies, only five studies focused on plant species distribution. Different factors contribute towards the low tendency of literature available in Pakistan, including the unavailability of tree species occurrence data, financial constraints to design extensive field surveys, and difficult terrain (especially in the northern Himalayan region of Pakistan).

The studies in Pakistan on tree species diversity mainly used only bioclimatic variables as independent variables for modelling in MaxEnt. The studies by Ashraf et al. (2016) and Gilani et al. (2020) incorporated topographical variables in modelling tree species distribution along with bioclimatic variables. This study incorporated biophysical (NDVI and EVI) variables with bioclimatic and topographical variables. The jackknife test shows that these biophysical variables influence the distribution of *Abies pindrow*, *Olea ferruginea*, *Pinus roxburghii*, and *Pinus wallichiana* tree species in AJK. Chhetri et al. (2018) also reported a greater influence of biophysical variables than other variables used in the prediction modelling in the Himalayan region.

The study by Qamer et al. (2016) reported deforestation and forest degradation in the western Himalayan region of Pakistan. They reported that AJK has the highest percentage of forest cover compared to other administrative areas of Pakistan, with

Fig. 7 Spatial distribution of tree species diversity in AJK



Abies pindrow and *Pinus wallichiana* among the dominating tree species. Our study authorizes this information as the same two species reported falling under a profoundly reasonable living space class.

The tree species diversity is an indicator of the overall biodiversity of a region. To manage, protect, or regenerate biodiversity, the idea of ecoregion-based identification of tree species diversity hotspots is more focused and narrowed down. This is because biodiversity is not merely a varied life form but should be discussed under the arena of ecological complexes (Wang et al. 2010).

This study used a very limited number of tree species occurrence points for the prediction modelling in MaxEnt. This resulted in a very low TSS score for *Olea ferruginea* because this tree species also had the lowest number of circular plots compared to other tree species predicted in this study. The field surveys designed for collecting such field data also have some limitations, including collecting samples from steep slopes, narrow valleys, unfavourable weather, positional accuracy issue

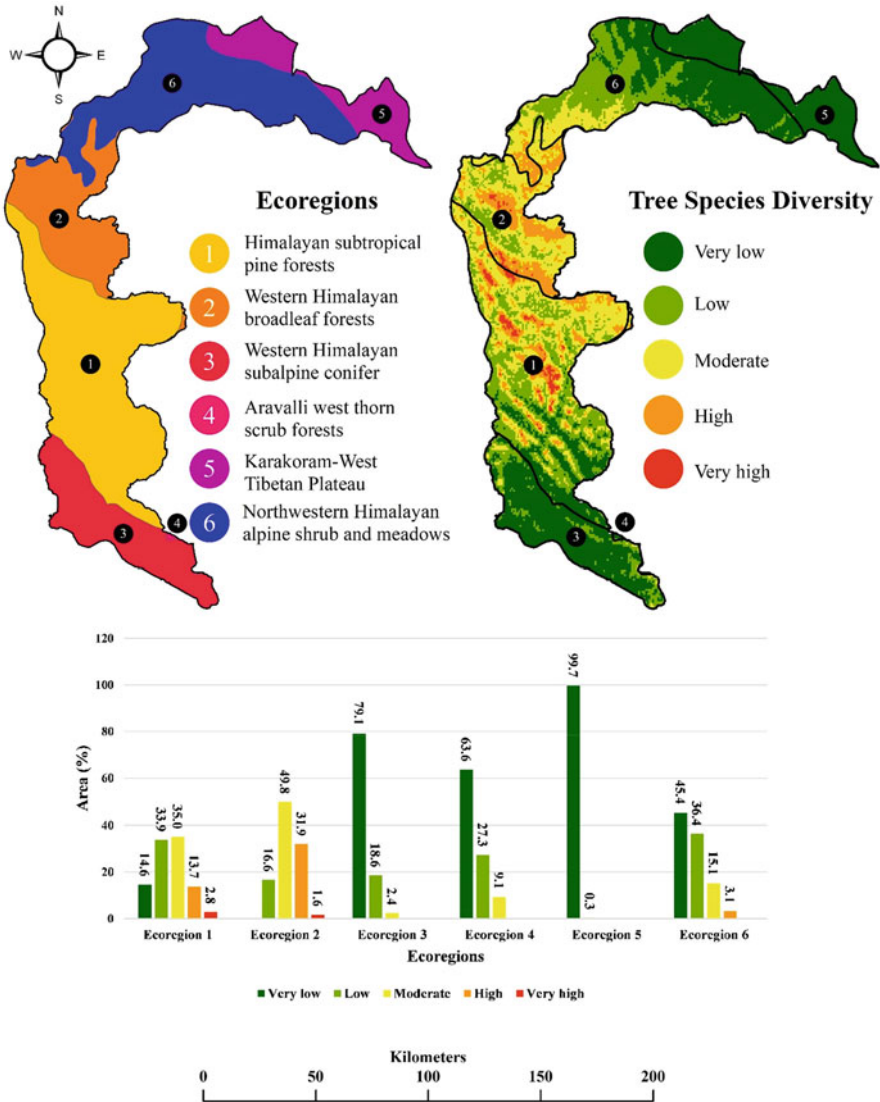


Fig. 8 Ecoregion-based spatial distribution of tree species diversity and statistics

of locational devices, etc. All independent variables were rescaled to $\sim 1 \times 1$ km spatial resolution because the bioclimatic variables are available in this spatial resolution. This is a coarse resolution for extracting values of topographical and biophysical variables.

6 Conclusion

This study attempted to predict the spatial distribution of four native tree species (*Abies pindrow*, *Olea ferruginea*, *Pinus roxburghii*, and *Pinus wallichiana*) in AJK, Pakistan, using MaxEnt model. Through a multicollinearity test, the prediction modelling involved selected bioclimatic and remote sensing-based (biophysical and topographical) independent variables. The role of remotely sensed datasets and their products is of fundamental importance for such prediction modelling. Introducing more related independent variables in modelling tree species in such environments can produce more reliable results. Integration of long-term satellite-based and ground-based bioclimatic information can also help to produce better results. Along with MaxEnt, other SDMs can also produce potential distribution scenarios for the same tree species. The results from these ENMs can be spatially overlaid and produce interesting results.

The introduction of ecoregion-based tree species diversity opens up a new horizon of linking tree species diversity intensity with specific ecoregions. The ecoregion zones and their link with overall tree species diversity or potential distribution of a specific tree species enhance our understanding of diversity and distribution behaviour. On a regional scale, the results of this study can be used to design conservation corridors for these tree species in AJK and help stakeholders and other agencies to plan plantation activities in suitable areas.

Acknowledgement We would like to express our thanks to the management of the Institute of Space Technology (IST), Islamabad, and University of the Punjab, Lahore, Pakistan. We are thankful to REDD+, Ministry of Climate Change, Pakistan for providing tree species occurrence data.

References

- Ali K, Ahmad H, Khan N, Jury S (2014) Future of *Abies pindrow* in Swat district, northern Pakistan. *J For Res* 25:211–214. <https://doi.org/10.1007/s11676-014-0446-1>
- Allouche O, Tsoar A, Kadmon R (2006) Assessing the accuracy of species distribution models: Prevalence, kappa and the true skill statistic (TSS). *J Appl Ecol* 43:1223–1232. <https://doi.org/10.1111/j.1365-2664.2006.01214.x>
- Ashraf U, Ali H, Chaudry MN et al (2016) Predicting the potential distribution of *Olea ferruginea* in Pakistan incorporating climate change by using Maxent Model. *Sustainability* 8:1–11. <https://doi.org/10.3390/su8080722>
- Azeem A, Zeb A, Umer S et al (2020) Ethno botanical studies of Tatta Pani Valley, Kotli, Azad Jammu and Kashmir (AJK) Pakistan. *J Med Plants Stud* 8:14–20
- Basille M, Calenge C, Marboutin É et al (2008) Assessing habitat selection using multivariate statistics: some refinements of the ecological-niche factor analysis. *Ecol Modell* 211:233–240. <https://doi.org/10.1016/j.ecolmodel.2007.09.006>
- Becker EA, Carretta JV, Forney KA et al (2020) Performance evaluation of cetacean species distribution models developed using generalized additive models and boosted regression trees. *Ecol Evol* 10:5759–5784. <https://doi.org/10.1002/ece3.6316>
- Bobrowski M, Gerlitz L, Schickhoff U (2017) Modelling the potential distribution of *Betula utilis* in the Himalaya. *Glob Ecol Conserv* 11:69–83. <https://doi.org/10.1016/j.gecco.2017.04.003>

- Carpenter G, Gillison AN, Winter J (1993) DOMAIN: a flexible modelling procedure for mapping potential distributions of plants and animals. *Biodivers Conserv* 2:667–680. <https://doi.org/10.1007/BF00051966>
- Chetan N, Praveen KK, Vasudeva GK (2014) Delineating ecological boundaries of hanuman langur species complex in peninsular India using MaxEnt modeling approach. *PLoS One* 9:1–11. <https://doi.org/10.1371/journal.pone.0087804>
- Chhetri B, Badola HK, Barat S (2018) Predicting climate-driven habitat shifting of the near threatened Satyr Tragopan (*Tragopan Satyra*; Galliformes) in the Himalayas. *Avian Biol Res* 11(4):221–230. <https://doi.org/10.3184/175815618X15316676114070>
- Dinerstein E, Olson D, Joshi A et al (2017) An ecoregion-based approach to protecting half the terrestrial realm. *Bioscience* 67:534–545. <https://doi.org/10.1093/biosci/bix014>
- Fatima SH, Atif S, Rasheed SB et al (2016) Species distribution modelling of *Aedes aegypti* in two dengue-endemic regions of Pakistan. *Trop Med Int Heal* 21:427–436. <https://doi.org/10.1111/tmi.12664>
- Gilani H, Goheer MA, Ahmad H, Hussain K (2020) Under predicted climate change: distribution and ecological niche modelling of six native tree species in Gilgit-Baltistan, Pakistan. *Ecol Indic* 111:106049
- Graham MH (2003) Confronting multicollinearity in ecological. *Ecology* 84:2809–2815
- Gu Y, Brown JF, Verdin JP, Wardlow B (2007) A five-year analysis of MODIS NDVI and NDWI for grassland drought assessment over the central Great Plains of the United States. *Geophys Res Lett* 34:1–6. <https://doi.org/10.1029/2006GL029127>
- Guisan A, Edward TC Jr, Hastie T (2016) Generalized linear and generalized additive models in studies of species distributions: setting the scene. *Ecol Modell* 157:89–100
- Hameed S, ud Din J, Ali H et al (2020) Identifying priority landscapes for conservation of snow leopards in Pakistan. *PLoS One* 15:1–20. <https://doi.org/10.1371/journal.pone.0228832>
- Ishtiaq M, Mumtaz AS, Hussain T, Ghani A (2012) Medicinal plant diversity in the flora of Leepa Valley, Muzaffarabad (AJK), Pakistan. *Afr J Biotechnol* 11:3087–3098. <https://doi.org/10.5897/ajb11.2711>
- Jaryan V, Datta A, Uniyal SK et al (2013) Modelling potential distribution of *Sapium sebiferum*—an invasive tree species in western Himalaya. *Curr Sci* 105:1282–1287
- Kabir M, Hameed S, Ali H et al (2017) Habitat suitability and movement corridors of grey wolf (*Canis lupus*) in Northern Pakistan. *PLoS One* 12:1–17
- Kaky E, Nolan V, Alatawi A, Gilbert F (2020) A comparison between Ensemble and MaxEnt species distribution modelling approaches for conservation: a case study with Egyptian medicinal plants. *Ecol Inform* 60:101150. <https://doi.org/10.1016/j.ecoinf.2020.101150>
- Kazim M, Perveen R, Zaidi A et al (2015) Biodiversity of spiders (Arachnida: Araneae) fauna of Gilgit Baltistan Pakistan. *Int J Fauna Biol Stud* 2:77–79
- Khalil T, Asad SA, Khubaib N et al (2021) Climate change and potential distribution of potato (*Solanum tuberosum*) crop cultivation in Pakistan using Maxent. *AIMS Agric Food* 6:663–676. <https://doi.org/10.3934/AGRFOOD.2021039>
- Khan IA, Khan MR, Baig MHA et al (2020) Assessment of forest cover and carbon stock changes in sub-tropical pine forest of Azad Jammu & Kashmir (AJK), Pakistan using multitemporal Landsat satellite data and field inventory. *PLoS One* 15:1–19. <https://doi.org/10.1371/journal.pone.0226341>
- Khanum R, Mumtaz AS, Kumar S (2013) Predicting impacts of climate change on medicinal asclepiads of Pakistan using Maxent modeling. *Acta Oecol* 49:23–31. <https://doi.org/10.1016/j.actao.2013.02.007>
- Kumar S, Graham J, West AM, Evangelista PH (2014) Using district-level occurrences in MaxEnt for predicting the invasion potential of an exotic insect pest in India. *Comput Electron Agric* 103:55–62. <https://doi.org/10.1016/j.compag.2014.02.007>
- Phillips SJ, Dudík M (2008) Modeling of species distributions with Maxent: new extensions and a comprehensive evaluation. *Ecography* 31:161–175. <https://doi.org/10.1111/j.0906-7590.2008.5203.x>

- Phillips SJ, Dudík M, Schapire RE (2004) A maximum entropy approach to species distribution modeling. In: Proceedings, Twenty-First Int Conf Mach Learn ICML 2004, pp 655–662. <https://doi.org/10.1145/1015330.1015412>
- Qamar FM, Ali H, Ashraf S et al (2011) Distribution and habitat mapping of key fauna species in selected areas of Western Himalaya, Pakistan. *J Anim Plant Sci* 21:396–399
- Qamer FM, Shehzad K, Abbas S et al (2016) Mapping deforestation and forest degradation patterns in Western Himalaya, Pakistan. *Remote Sens* 8:1–17. <https://doi.org/10.3390/rs8050385>
- Quirós E, Felicísimo ÁM, Cuartero A (2009) Testing multivariate adaptive regression splines (MARS) as a method of land cover classification of TERRA-ASTER satellite images. *Sensors* 9:9011–9028. <https://doi.org/10.3390/s91109011>
- Ranjitkar S, Sujakhu NM, Merz J et al (2016) Suitability analysis and projected climate change impact on banana and coffee production zones in nepal. *PLoS One* 11:1–18. <https://doi.org/10.1371/journal.pone.0163916>
- Wang Z, Ye W, Cao H et al (2009) Species-topography association in a species-rich subtropical forest of China. *Basic Appl Ecol* 10:648–655. <https://doi.org/10.1016/j.baae.2009.03.002>
- Wang K, Franklin SE, Guo X, Cattet M (2010) Remote sensing of ecology, biodiversity and conservation: a review from the perspective of remote sensing specialists. *Sensors* 10:9647–9667
- Yang A, Gomez JP, Blackburn JK (2020) Exploring environmental coverages of species: a new variable contribution estimation methodology for rulesets from the genetic algorithm for rule-set prediction. *PeerJ* 8:e8968. <https://doi.org/10.7717/peerj.8968>
- Zaidi F, Fatima SH, Khisroon M, Gul A (2016) Distribution Modeling of three screwworm species in the ecologically diverse landscape of North West Pakistan. *Acta Trop* 162:56–65. <https://doi.org/10.1016/j.actatropica.2016.06.015>
- Zhang K, Zhang Y, Tao J (2019) Predicting the potential distribution of *Paeonia veitchii* (Paeoniaceae) in China by incorporating climate change into a maxent model. *Forests* 10(2): 190. <https://doi.org/10.3390/f10020190>



Application of Remote Sensing Vegetation Indices for Forest Cover Assessments

Weeraphart Khunrattanasiri

Abstract

Forests are an indispensable foundation of life for humans. They fulfil multiple functions in a single area: they are a source of income to many; they provide wood, an environmentally compatible, renewable resource, as well as foodstuffs and many other basic commodities; they protect the soils from erosion and stabilize the water table; they stabilize the climate on a regional and global level and they offer humans numerous opportunities for recreation and relaxation. These functions have different levels of significance in the various regions of the earth. For the past 20 years, increases in the produce and income generated resulted from the increase of the agricultural area rather than that of products per unit area due to the high rate of population growth correlated with a limited area of land available for cropping and housing. Situations such as poverty and a scarcity of food have forced villagers to migrate into the forest reserves, where they subsequently destroy the forests through shifting cultivation, especially in the watershed areas.

Remote sensing using satellites can make a significant contribution to regional and global forest cover assessment. Satellite images permit the observation of large geographical areas and can be repeated at short time intervals and the costs are reasonable. The basic forest cover information that can be obtained from satellite images at different spatial resolutions relates to the area and spatial distribution of broad forest cover types, to the degree of canopy fragmentation and to the forest cover changes occurring. Recent research papers show that remotely sensed data are well correlated with forest stand parameters. Vegetation index is a spectral transformation of at least two optical bands to obtain the

W. Khunrattanasiri (✉)

Department of Forest Management, Faculty of Forestry, Kasetsart University, Bangkok, Thailand
e-mail: fforwpk@ku.ac.th

© The Author(s), under exclusive license to Springer Nature Singapore Pte Ltd. 2022

M. N. Suratman (ed.), *Concepts and Applications of Remote Sensing in Forestry*,
https://doi.org/10.1007/978-981-19-4200-6_8

vegetation properties. Normalized difference vegetation index (NDVI), green normalized difference vegetation index (GNDVI) and soil-adjusted vegetation index (SAVI) were cited in numerous research papers and they have been widely used in the forest researches to investigate the relationship between forest parameters such as diameter at breast height (DBH), per cent crown cover, tree age class, tree height, basal area, tree volume and aboveground living biomass. Nowadays it has been possible for researcher worldwide to access the satellite data with free download, for example, Landsat 8, Landsat 9 or Sentinel-2. The use of vegetation index is necessary for understanding the forest area in a global level and the greater efficiency of sustainable forest management.

Keywords

Vegetation index · Forest parameter · Satellite image

1 Introduction

After the 26th UN Climate Change Conference in November 2021 the member states are expected to fulfil responsibilities to mitigate climate change, cooperating in preparing for adaptation measures to deal with the impact of climate change, as well preparing public awareness material to promote education and training material related to combatting climate change. Some countries set the goal to accelerate the phase-out of coal, curtail deforestation, speed up the switch to electric vehicles and encourage investment in renewables. Climate change is already affecting every region on earth. Due to climate change issues nowadays it turns the public interest in the state of the world's forest resources because the forest areas are an important part of the global carbon cycle. They contain the largest store of terrestrial carbon and continuously transfer carbon between the terrestrial biosphere and the atmosphere.

The Food and Agriculture Organization (FAO) of the United Nations has been monitoring the world's forests at 5- to 10-year intervals since 1946 and the latest information about the status of global forest resources was reported in Global Forest Resources Assessment 2020 (FAO 2020). The world has a total forest area of 4.06 billion ha, which is 31% of the total land area. This area is equivalent to 0.52 ha per person. The tropical domain has the largest proportion of the world's forests (1834.14 million ha or 45%), followed by the boreal, temperate and subtropical domains. More than half (2188.63 million ha or 54%) of the world's forests is in only five countries such as the Russian Federation, Brazil, Canada, the United States of America and the Republic of China (FAO 2020).

Most of the spatial data explaining the status of global forest resources in FRA report were normally derived not only from field observation or forest inventory but also from satellite remote sensing technology. Field measurement has been laboured-intensive and expensive and the time required for field data measurements was long. Remote sensing using satellites can make a significant contribution to

regional and global forest cover assessment. Satellite images permit the observation of large geographical areas and can be repeated at short time intervals and the costs are reasonable. Remote sensing models can be divided into two categories: passive or optical remote sensing and active or microwave remote sensing. Passive remote sensing measures the electromagnetic radiation reflected by or emitted from the earth, while active remote sensing satellites use their own energy sources to illuminate the earth and detect and measure the reflected radiation. Although both types of remote sensing can produce high-quality information over the large area at a low cost, for the forestry research passive remote sensing had been widely chosen to investigate the stand parameters because of the high number of spectral bands including visible light, near-infrared and short-wave infrared. The basic forest cover information that can be obtained from satellite images at different spatial resolutions relates to the area and spatial distribution of broad forest cover types, to the degree of canopy fragmentation and to the forest cover changes occurring. Recent papers show that remotely sensed data are well correlated with forest stand parameters such as diameter at breast height (DBH), per cent crown cover, tree age class, tree height, basal area and volume.

The most frequently used remote sensing products continue to be from optical sensors with a moderate spatial resolution (10–30 m). Examples include Thematic Mapper (TM) of Landsat 5, Enhanced Thematic Mapper Plus (ETM+) of Landsat 7 and Operational Land Imager (OLI) and Thermal Infrared Sensor (TIRS) of Landsat 8 and Multispectral Scanner of Thaichote (Thailand First Observation Satellite), which are all multispectral sensors with 3–11 broad spectral bands. Presently, the satellite image is widely used in scientific research due to the free access data of Sentinel-2 satellite by the Copernicus programme of the European Space Agency (ESA) with 10 m spatial resolution in visible and near-infrared band of MSI sensor and the newest generation of Landsat programme “Landsat 9” satellite, which is designed and operated to repeatedly observe the global land surface at a moderate scale and to reduce the build time and a risk of a gap in earth observations. Landsat 9 data bring the research interest back to analyse the free of charge dataset. However, Sentinel-2 Landsat 8 and Landsat 9 are suggested, because they were developed to support vegetation, land cover and environmental monitoring.

2 Spectral Reflectance of Vegetation

To understand the forest status, a graph of the spectral reflectance is used to explain the object area or phenomena on the earth surface. A graph of the spectral reflectance of an object as a function of wavelength is termed a spectral reflectance curve. The configuration of spectral reflectance curves gives us insight into the spectral characteristics of an object and has a strong influence on the choice of wavelength regions in which remote sensing data are acquired for a particular application. The vegetation reflectance is used to synthesize the index from satellite image data.

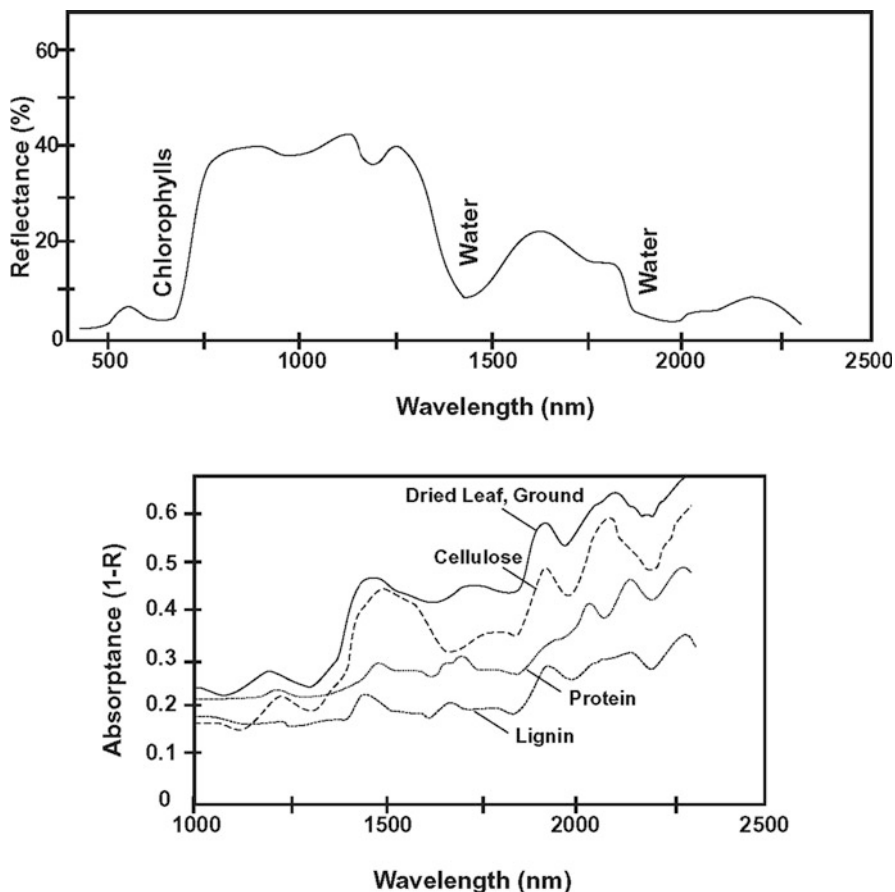


Fig. 1 Spectral reflectance curves of some typical objects (Peterson et al. 1988)

Figure 1 shows that the reflectance of healthy vegetation increases dramatically in the region from the visible to the near-infrared portion of the spectrum at about 0.7 μm . In the range from 0.7 to 1.3 μm , a plant leaf typically reflects 40–50% of the energy incident upon it. Most of the remaining energy is transmitted, since absorption in this spectral region is minimal (less than 5%). Plant reflectance in the range 0.7–1.3 μm results primarily from the internal structure of plant leaves. This structure varies greatly between plant species. Because the position of the red edge and the magnitude of the near-IR reflectance beyond the red edge are highly variable among plant species, reflectance measurements in these ranges often permit us to discriminate between species, even if they look the same in visible wavelengths (Lillesand and Kiefer 2015). In general, in the visible region, leaf pigments govern the leaf spectrum. The normal chlorophyll-pigmented leaf has a minor but characteristic green reflection peak. In the anthocyanin-pigmented leaf, the green reflection is absent and there is greater reflection in the red wavelength, giving a red.

3 Vegetation Index

Forest is a type of vegetation cover over the land, and it can automatically classify from satellite image by using pixel-based techniques. Basically, the value stored in each pixel is digital number (DN) which is normally in the form of integer in the range of satellite sensor bit depths. For example, OLI-2 sensor on board Landsat 9 was designed to store the range of energies examined in 16 bits (0–65,535). During the 1980s and 1990s, most classification techniques employed the image pixel as the basic unit of analysis, in which each pixel is labelled as a single land-use land cover class. With the pixel as the basic analysis unit, a series of classification techniques, such as unsupervised, supervised (i.e. maximum likelihood, artificial neural network, decision tree, support vector machine, random forests) and hybrid classification (i.e. semi-supervised and fusion of supervised and unsupervised learning), is still an active classification technique in the areas of multispectral and hyperspectral remote sensing image analysis (Li et al. 2014). With the improvement of spatial resolution of remote sensing images, remote sensing image classification gradually formed three parallel classification branches at different levels: pixel-level, object-level and scene-level classification (Cheng et al. 2020). However, the latter considerations demonstrate that the quantitative interpretation of remote sensing information from vegetation is a complex task. Many studies have limited this interpretation by extracting vegetation information using individual light spectra bands or a group of single bands for data analysis (Xue and Su 2017). Remote sensing of vegetation is mainly performed by obtaining the electromagnetic wave reflectance information from canopies using passive sensors. It is well known that the reflectance of light spectra from plants changes with plant type, water content within tissues and other intrinsic factors (Chang et al. 2016). Vegetation indices are frequently used to characterize spatial and temporal trends in vegetation richness or productivity. Vegetation indices are based on mathematical calculations of canopy reflectance at specific visible and near-infrared wavelengths. Two or more spectral bands need to be combined in mathematical formulas. Many vegetation indices have been used in agricultural and ecological research; however, four widely cited indices are chosen to show an example.

3.1 Ratio Vegetation Index

A very useful image processing technique used to describe the vegetation richness of a specific area is band rationing. A ratio of different spectral bands from the same image is useful in reducing the effect of topography, as a vegetation index, and for enhancing subtle differences in the spectral characteristics for rocks and soils. Although the ratio image is a concept of image enhancement, it can well explain the vegetation status over the land also. Four spectral bands such as blue, green, red and near-infrared bands that are sensitive to plant biomass and vigour are mostly selected to analyse the ratio image and also other following vegetation indices. Within these four bands the reflectance of the vegetation showed significant

difference with soil and clear water bodies especially in near-infrared band. An example of ratio vegetation index is near-infrared band divided by red band.

3.2 Normalized Difference Vegetation Index

The normalized difference vegetation index (NDVI) was developed in the 1970s (Rouse et al. 1973) when a research team at Texas A & M University studied data beamed back from earth observation satellites. The NDVI, one of the earliest remote sensing analytical products used to simplify the complexities of multispectral imagery, is now the most popular index used for vegetation assessment (Huang et al. 2021). The ratio of the difference of the red and infrared radiances over their sum uses to adjust or “normalize” the effects of the solar zenith angle. Originally, they called this ratio the *vegetation index*. The NDVI is one of the oldest vegetation indices and the most widely used because of the simplicity of its calculation, and this is the reason why all sensors have bands on red and NIR. The explanation of results is easy, and most publications have used it in a supportive way in the research (Giovos et al. 2021).

$$\text{NDVI} = \frac{\text{NIR} - \text{RED}}{\text{NIR} + \text{RED}}$$

The development of NDVI (which more strongly relates to reflectance as measured in the image to forest conditions) was instrumental in showing that useful information can be extracted from remote sensing imagery, and once the forest information content of the NDVI was determined, it became more obvious which applications would be worthwhile. The NDVI is based on the use of a near-infrared (IR) band and a red (R) band.

The NDVI is a dimensionless index, so its values range from -1 to $+1$. In a practical sense, the negative values corresponded to water bodies and the values close to 0 are bare soil, while higher values are indicators of high photosynthetic activity linked to scrub land, agricultural area, temperate forest and evergreen forest. Areas of barren rock, sand or snow usually show very low NDVI values (e.g. 0.1 or less). Sparse vegetation such as shrubs and grasslands or senescing crops may result in moderate NDVI values (approximately 0.2 – 0.5). High NDVI values (approximately 0.6 – 0.9) correspond to dense vegetation such as that found in temperate and tropical forests or crops at their peak growth stage (Brown 2018). Although the extraction of NDVI from imagery is straightforward, the interpretation of NDVI values for different forest types has sometimes been problematic (Franklin 2001). Normally, one would expect a high NDVI to be found where there’s a high leaf area. Foliage reflects little energy in the red portion of the spectrum because most of the near infrared is reflected by foliage (Gausman 1977).

3.3 Green Normalized Difference Vegetation Index

The green normalized difference vegetation index (GNDVI) was introduced by Gitelson et al. (1996). It has a similar formation to NDVI except that it measures the green spectrum band from 540 to 570 nm instead of the red spectrum band. This index is more sensitive to chlorophyll concentration than NDVI. The GNDVI is used for estimating the photosynthetic activity of the vegetation cover, and it is most often used in assessing the moisture content and nitrogen concentration in plant leaves according to multispectral data which do not have an extreme red channel. The formation of GNDVI is similar to NDVI except that instead of the red spectrum band, it measures the green spectrum band in the range from 0.54 to 0.57 μm .

$$\text{GNDVI} = \frac{\text{NIR} - \text{GREEN}}{\text{NIR} + \text{GREEN}}$$

Compared to the NDVI index, GNDVI is more sensitive to chlorophyll concentration. It is used in assessing depressed and aged vegetation, assessing the moisture content and nitrogen concentration in plant leaves according to multispectral data which do not have an extreme red channel.

3.4 Soil-Adjusted Vegetation Index

In areas where vegetative cover is low and the soil surface is exposed, the reflectance of light in the red and near-infrared spectra can influence vegetation index values. Huete (1988) proposed the soil-adjusted vegetation index (SAVI) to correct NDVI from the influence of soil brightness in satellite images where sparse vegetative cover occurs. The NDVI is successfully used to investigate the vegetation richness above ground; however, the use of NDVI in some satellite images which appear just few percent of vegetation cover is not recommended. In the SAVI the red and NIR spectral wavelengths are used. The SAVI can nearly eliminate the soil influences in vegetation indices. It was developed as a modification of the NDVI with the addition of soil brightness correction factor (L).

$$\text{SAVI} = \frac{\text{NIR} - \text{RED}}{\text{NIR} + \text{RED}} \times 1 + L$$

The L value varies by the amount or cover of green vegetation: in very high vegetation areas, L value is set to 0 (SAVI value same as NDVI), and in areas with no green vegetation, L value is set to 1. Generally, 0.5 of L value works fit for the area with intermediate level of vegetation cover and this value is used most widely in ecological and agricultural research. The soil factor of 0.2, 0.5 and 0.9 was comparable to NDVI result when 0.5 is best suited with vegetation and 0.9 is the best suited soil factor for the land where the soil influence is more. The SAVI is the best suited vegetation index in semi-arid areas (Vani and Mandla 2017).

4 Use of Vegetation Indices for Forest Cover Assessments

Forests are changing in response to climate, with potentially important feedbacks to regional and global climate through altered carbon cycle. In the assessment of forest cover by means of remote sensing, numerous vegetation indices are usually extracted from the scene classification of remote sensing images. The most applied technique for forest assessment is vegetation index because the output index values can well use to explain the forest status worldwide. The relationship between vegetation index values and measured property is nonlinear which makes the use of vegetation index somewhat difficult. Weeraphart Khunrattanasiri (2007) investigated the potential of Landsat 5 TM image to estimate forest parameters to supplement the forest inventory data in a dry evergreen forest of Khao Ang Runai Wildlife Sanctuary. Different forest parameters derived from forest inventory sample plots were investigated and compared with the reflectance values of Landsat 5 TM. The results of the study showed that middle infrared band (band 5) minus red band (band 3) of the Landsat 5 TM provided a useful technique to establish the connection between the pixel values and the per cent crown cover—percentage of the plot area covered by the vertical projection of all of the visible crowns of trees and shrubs on the plot—derived from forest inventory plots, better than for the other forest parameters. The internal structure of leaves absorbs the spectral bands and reflects them back to the detectors. It is impossible in this case for the spectral bands to penetrate the top layer. In some places where the crown cover is less dense, the reflectance can penetrate the crown to the level of other parameters and the correlation in such cases relates with other attributes such as basal area and tree volume. Loranty et al. (2018) found also that the NDVI is related to forest cover.

Carmen Lourdes Meneses Tovar (2009) attempted to establish relations between forest usage and the NDVI estimated from satellite imagery. The study showed a disturbance in a vegetation community was reflected in a corresponding fall in the value of NDVI. The greater the NDVI contrast between vegetated and water areas, the higher the spatial variability of Landsat 8 OLI NDVI, indicating that the new sensor has better capability in land surface process monitoring, such as land cover mapping, spatiotemporal dynamics of vegetation growth and drought assessment (Ke et al. 2015).

The Royal Forest Department (RFD), Ministry of Natural Resources and Environment of Thailand, has the main responsibility of analysing the forest status from satellite image since 1973. At the beginning satellite imageries from Landsat 5 Thematic Mapper (TM) were used for forest status classification with visual interpretation techniques until 2008. The forest assessment using visual interpretation of large-scale image (1:50,000) and using GIS to calculate forest land-use areas is more reliable and accurate than small-scale image (1:250,000) (Ongsomwang 2003). Following the launching of Thailand's Thaichote satellite (former name THEOS), in 2012 RFD together with the Faculty of Forestry, Kasetsart University (KUFF), used Thaichote satellite images to replace the Landsat 5 TM data because of the better spatial resolution from 30 m of Landsat 5 TM down to 15 m of Thaichote MS sensor. Because of change in spatial resolution, the concept of segmentation based

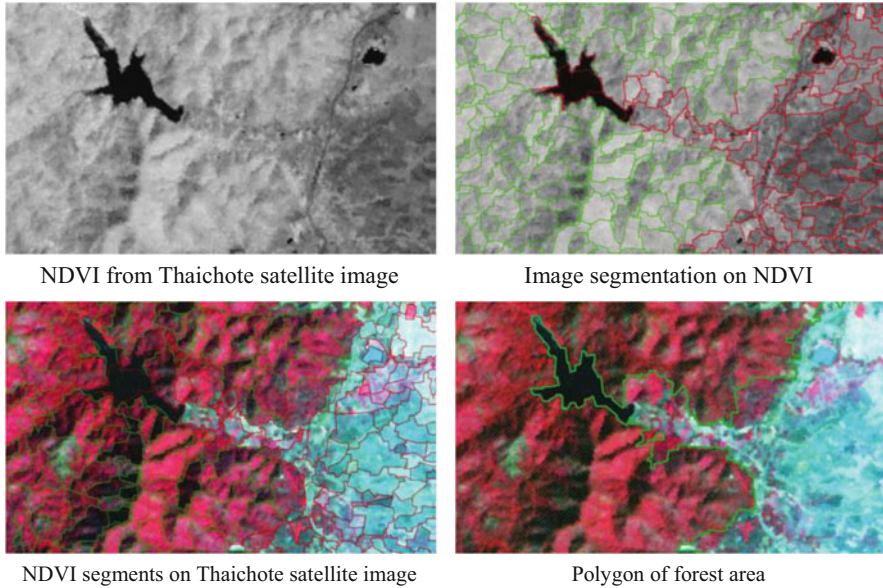


Fig. 2 Use of NDVI and Thaichote satellite image segmentation technique for forest cover assessment

on NDVI dataset was suggested to be used for forest area analysis (Fig. 2). The percent of total accuracy was 98.56% calculated from 862 ground verification points.

The potential of NDVI and SAVI-based classification for detection of forest cover changes in comparison to supervised classification showed that the NDVI performed better in forest cover change detection than the SAVI (Islam et al. 2021). A joint research in 2018 between the KUFF and Double A (1991) Public Company Limited aimed to investigate the efficiency of various vegetation indices such as the NDVI, GNDVI, infrared percentage vegetation index (IPVI), SAVI and transformed vegetation index (TVI) calculated from Landsat 8 OLI sensor with 30 m spatial resolution for the detection of eucalyptus plantation in Prachin Buri Province, Thailand. The results showed that the SAVI with L factor equal to 0.5 was the best vegetation index for eucalyptus detection and volume estimation. The linear regression is used to explain the relationship with coefficient of determination equal to 0.80 and the error of estimation equal to 0.93 (Weeraphart Khunrattanasiri 2018).

5 Use of Vegetation Indices for Forest Type Classification

Vegetation index is highly related to leaf area index, absorbed photosynthetically active radiation and vegetation cover. Vegetation index reflects photosynthesis intensity of plants and manifests different forest types (Jinguo and Wei 2013). In Thailand, the first GIS dataset of national forest types was firstly created in 2000 by

the Royal Forest Department. A visual interpretation based on Landsat 5 TM satellite imageries at 1:50,000 map scale was used as the main technique together with ground verification for the entire country (Royal Forest Department 2021). The second dataset of GIS national forest types is ready for use since 2018. The NDVI dataset derived from Sentinel-2 MSI sensor with 10 m resolution of blue, green, red and near-infrared spectrum band was used together with the Global Digital Elevation Model (GDEM) to improve the first national forest type dataset. The specific range of elevation calculated from GDEM was used as a parameter to group forest types, because most of the forest types appear in specific elevation. A total of 741 ground verification points were used for an accuracy assessment task, and they were located in the entire country. An overall accuracy was 80.43%.

Klaydach and Khunrattanasiri (2012) studied the reflection of light derived from multispectral instrument on board Thaichote satellite. The NDVI, ratio vegetation index (RVI), difference vegetation index (DVI), infrared percentage vegetation index (IPVI), transformed normalized difference vegetation index (TNDVI) and SAVI were utilized to investigate the relationship between forest types and vegetation index in Doi Luang national park, Thailand. Mixed deciduous forest, dry evergreen forest and deciduous forest can be well classified by using NDVI with 65.25% accuracy.

The NDVI, TVI and GNDVI and the various vegetation indices based on the simple mathematical operations of four-band (blue, green, red and near-infrared bands) data from Thaichote satellite were used for forest type classification. The results showed the vegetation index of $R - NIR/B + G$ has the highest overall accuracy with 60.51%. The ratio of $R - NIR/B + R$, GNDVI, NIR/G , NDVI, NIR/B and TVI appeared to have the overall accuracy of 55.90%, 54.87%, 52.82%, 52.31%, 52.31% and 37.97%, respectively. It can be concluded that the vegetation index calculated by dividing the difference in the red bands and near infrared by the sum of the blue and green bands is the best appropriate index for Thailand forest type classification. Nguyen Trong et al. (2020) found the possibility of using random forest algorithm with Sentinel-2 in forest type classification in line with vegetation index application.

6 Recommendation Before Using Vegetation Index for Forest Assessment

Firstly, a misregistration of the ground data in the satellite imagery is always a serious problem when satellite images are applied in ecological research. A position accuracy assessment process was necessary to relate the ground truth and remote sensing data, to be sure that both datasets could be overlaid onto the same geographical position. Under the tree cover in natural forest, the detection of a desired weak GPS signal is often problematic because the strong signal is not adequately attenuated by the receiver processing. Forest canopy affects the GPS signals due to obstruction, attenuation and reflection (Pirtti 2008). The misregistration causes an important error when terrain variables are correlated with remotely sensed data. It

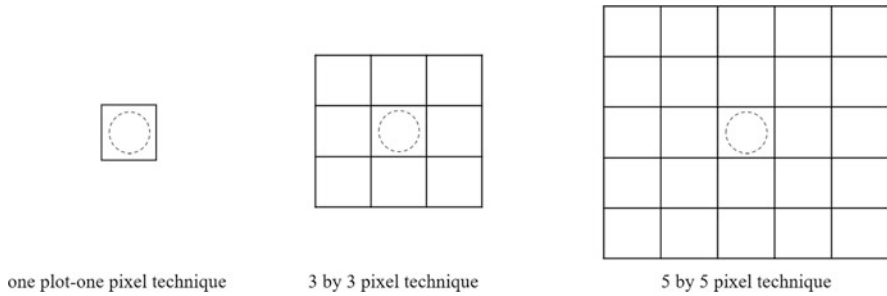


Fig. 3 Three techniques for matching sample plot to image

can occur during the analysis process, when the ground truth data is being laid onto the satellite image and through the distortion of the satellite image during geometric correction. The misregistration of ground truth data occurring in satellite imagery was calculated by position accuracy assessment. Therefore, three ground plot-to-pixel matching approaches have been developed to compensate for positional errors, namely, the one plot-one pixel technique, the 3 by 3 pixel technique and the 5 by 5 pixel technique. Basically, one plot-one pixel was the first technique used, with a single sample plot laid directly over a single pixel with the same geographic location after the geometric correction process of satellite image. The second technique employed a 3 by 3 pixel window overlay over a plot centre to guarantee that if misregistration appears, the plots will as a result be shifted inside the specific window area. The pixel windows were created around the plot location (Fig. 3) to solve the misregistration aspect. The new pixel value was calculated by the mean of all pixels in a window size covering the location. The correlation coefficient was used to determine the precision of forest parameters derived from ground sample plots and vegetation values. It is, therefore, essential to make a measurement on homogeneous areas of at least 3 by 3 pixels. Finally, a 5 by 5 pixel window was built around a plot centre.

Secondly, the absence of radiometric correction process in satellite data can create a course of unexpected results. The radiometric correction involves subtracting the background signal and dividing the gain of the satellite sensor, which converts the raw sensor output (in digital number, DN) to a radiance. Satellite image with radiometric corrected is suggested to calculate various vegetation indices because the conversion of DN into apparent reflectance is the most important step for vegetation index correction (Guyot and Gu 1994). Gu et al. (2011) reported that the use of vegetation indices from multiple radiometric correction images can better exploit the capabilities of remote sensing information, thus improving the accuracy of LAI estimating. Different radiometric correction levels of remote sensing image could help mine valuable information from remote sensing image and thus improve the accuracy of vegetation fractional coverage estimation (Gu et al. 2008). The proper use of atmospheric correction methods is crucial and has a significant impact on NDVI estimation (Moravec et al. 2021). Dewa and Danoedoro (2017) tried to investigate the influence of various radiometric correction levels of Landsat 8 OLI

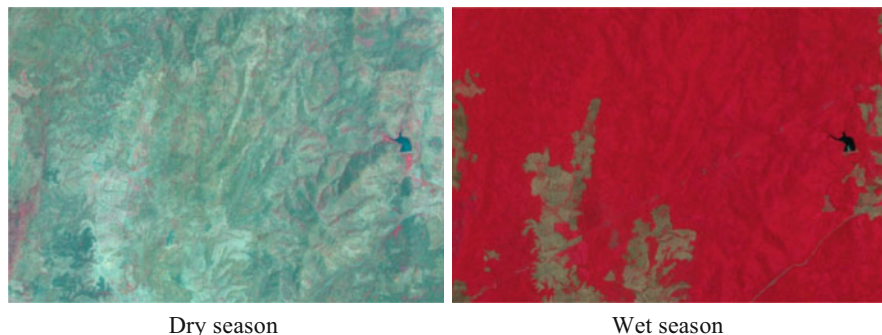


Fig. 4 Sentinel-2 satellite images of mixed deciduous forest in wet and dry seasons

and the number of vegetation strata on the accuracy of vegetation density estimates. It found that different radiometric correction methods resulted in canopy density estimates with different accuracies. The number of canopy strata also played an important role. Every vegetation index transformation performed its best accuracy by using different radiometric correction method and different number of canopy layers.

Finally, the researcher needs to understand the forest stand characteristics. Forest types are often classified according to topographical characteristics and species compositions of the forests. For example, forests in Thailand can be classified into two main types: namely, evergreen forest and deciduous forest. In the areas of evergreen forest, vegetation index can be used effectively without any consideration, because the evergreen tree retains its leaves through the year and into the following growing season. In contrast, for deciduous forests, the trees shed all their leaves during the dry season and they regrow new foliage during the next suitable growing season. In this case the selection of satellite image data should be highly considered. The periods when the deciduous trees remain to have complete leaf are the first criteria for satellite dataset query. Figure 4 illustrates the Sentinel-2 satellite images of mixed deciduous forest comparing the dry season on 25 March 2021 and wet season on 3 June 2021. The area of mixed deciduous trees that appeared in satellite images is red colour. Another interesting point when using vegetation index for time-series analysis is that a set of satellite images for the same months are needed as a preliminary data for yearly analysis to prevent the seasonal errors of tree cover.

7 Conclusion

With the high rate of deforestation in tropical forests in most countries over the last decade, the rapid collection of information on the status of forests is vital in order to assist governments and landowners in monitoring the forest area. Detection of vegetation dense can be used as a tool for monitoring the dynamics of ecosystem. Forest assessments using remote sensing techniques have become an important

component of ecological research, due to the lack of detailed spatial information on forest resources. Spatial resolution improvement through several decades of development and rapidly temporal resolution of the new earth observation satellites will play important roles for researchers to produce more effective vegetation index datasets. Numerous advantages of vegetation indices in remote sensing also help improve the useful data in ecological research together with the AI-based classification. Consequently, positive vegetation index trends may be associated with declines in terrestrial carbon storage. Moreover, vegetation indices calculated from satellite image can be used to monitor the long-term ecological changes such as large changes in forest density or variable forest parameters.

Techniques to assess the carbon sequestration of the trees or the forest areas from vegetation index will lead the research direction because they provide quick answers related to global climate change. Machine learning, which is a part of artificial intelligence, will become a useful algorithm to forecast several environmental indicators, including vegetation indices. Development of machine learning will be a useful indicator for monitoring and mitigating forest changes on the earth's surface in the future.

References

- Brown J (2018) NDVI, the Foundation for Remote Sensing Phenology. <https://www.usgs.gov/special-topics/remote-sensing-phenology/science/ndvi-foundation-remote-sensing-phenology#overview>
- Carmen Lourdes Meneses Tovar (2009) Analysis of the Normalized Differential Vegetation Index (NDVI) for the detection of degradation of forest cover in Mexico 2008–2009. FAO, Rome
- Chang LIU, Peng-Sen SUN, Shi-Rong LIU (2016) A review of plant spectral reflectance response to water physiological changes. *Chin J Plant Ecol* 40(1):80–91. <https://doi.org/10.17521/cjpe.2015.0267>
- Cheng G, Xie X, Han J, Li K, Xia GS (2020) Remote sensing image scene classification meets deep learning: challenges, methods, benchmarks, and opportunities. *IEEE J Sel Top Appl Earth Obs Remote Sens* 13:3735–3756. <https://doi.org/10.1109/JSTARS.2020.3005403>
- Dewa R, Danoedoro P (2017) The effect of image radiometric correction on the accuracy of vegetation canopy density estimate using several Landsat-8 OLI's vegetation indices: a case study of Wonosari area, Indonesia. *IOP Conf Ser Earth Environ Sci* 54:012046. <https://doi.org/10.1088/1755-1315/54/1/012046>
- FAO (2020) Global forest resources assessment 2020: main report
- Franklin SE (2001) Remote sensing for sustainable forest management. CRC Press LLC, Florida, 407 p
- Gausmann H (1977) Reflectance of leaf components. *Remote Sens Environ* 6:1–9
- Giovas R, Tassopoulos D, Kalivas D, Lougkos N, Priovolou A (2021) Remote sensing vegetation indices in viticulture: a critical review. *Agriculture* 11(5):457. <https://www.mdpi.com/2077-0472/11/5/457>
- Gitelson AA, Kaufman YJ, Merzlyak MN (1996) Use of a green channel in remote sensing of global vegetation from EOS-MODIS. *Remote Sens Environ* 58:289–298
- Gu Z, Zeng ZY, Shi XZ, Yu D, Zheng W, Zhang Z, Hu ZF (2008) Estimation models of vegetation fractional coverage (VFC) based on remote sensing image at different radiometric correction levels. *Ying yong sheng tai xue bao (J Appl Ecol)* 19:1296–1302
- Gu Z, Shi X, Li L, Yu D, Liu L, Zhang W (2011) Using multiple radiometric correction images to estimate leaf area index. *Int J Remote Sens* 32:9441–9454. <https://doi.org/10.1080/01431161.2011.562251>

- Guyot G, Gu XF (1994) Effect of radiometric corrections on NDVI-determined from SPOT-HRV and Landsat-TM data. *Remote Sens Environ* 49(3):169–180. [https://doi.org/10.1016/0034-4257\(94\)90012-4](https://doi.org/10.1016/0034-4257(94)90012-4)
- Huang S, Tang L, Hupy JP, Wang Y, Shao G (2021) A commentary review on the use of normalized difference vegetation index (NDVI) in the era of popular remote sensing. *J For Res* 32(1):1–6. <https://doi.org/10.1007/s11676-020-01155-1>
- Huete A (1988) A soil-adjusted vegetation index. *Remote sensing of environment*, p 27
- Islam MR, Khan MNI, Khan MZ, Roy B (2021) A three decade assessment of forest cover changes in Nijhum dwip national park using remote sensing and GIS. *Environ Chall* 4:100162. <https://doi.org/10.1016/j.envc.2021.100162>
- Jinguo Y, Wei W (2013) Identification of forest vegetation using vegetation indices. *Chin J Popul Resour Environ* 2:12–16. <https://doi.org/10.1080/10042857.2004.10677383>
- Ke Y, Im J, Lee J, Gong H, Ryu Y (2015) Characteristics of Landsat 8 OLI-derived NDVI by comparison with multiple satellite sensors and in-situ observations. *Remote Sens Environ* 164:298–313. <https://doi.org/10.1016/j.rse.2015.04.004>
- Khunrattanasiri W (2007) Application of LANDSAT-5 thematic mapper in forest inventory. Paper presented at the National Mapping and Geoinformatics 2007 Congress, Bangkok
- Khunrattanasiri W (2018) Detection of eucalyptus plantation using satellite imagery in Prachin Buri Province. Retrieved from Bangkok
- Klaydach T, Khunrattanasiri W (2012) Using of vegetation indices from THAICHOTE satellite data for forest types classification in Doi luang national park, Chiang Rai province. Paper presented at the 33rd Asian conference on remote sensing 2012, 26–30 November 2012, Pattaya, Thailand
- Li M, Zang S, Zhang B, Li S, Wu C (2014) A review of remote sensing image classification techniques: the role of spatio-contextual information. *Eur J Remote Sens* 47(1):389–411. <https://doi.org/10.5721/EuJRS20144723>
- Lillesand TM, Kiefer RW (2015) *Remote sensing and image interpretation*, 7th edn. Wiley
- Loranty MM, Davydov SP, Kropp H, Alexander HD, Mack MC, Natali SM, Zimov NS (2018) Vegetation indices do not capture forest cover variation in upland siberian larch forests. *Remote Sens* 10(11):1686. <https://www.mdpi.com/2072-4292/10/11/1686>
- Moravec D, Komarek J, Lopez-Cuervo Medina S, Molina I (2021) Effect of atmospheric corrections on NDVI: intercomparability of Landsat 8, Sentinel-2, and UAV sensors. *Remote Sens* 13:1–14. <https://doi.org/10.3390/rs13183550>
- Nguyen Trong H, Nguyen TD, Kappas M (2020) Land cover and forest type classification by values of vegetation indices and forest structure of tropical lowland forests in Central Vietnam. *Int J For Res* 2020:8896310. <https://doi.org/10.1155/2020/8896310>
- Ongsomwang S (2003) *Forest assessment and conservation in Thailand*. Forest Resources Assessment Division, Royal Forest Department
- Peterson DL, Aber JD, Matson PA, Card DH, Swanberg N, Wessman C, Spanner M (1988) Remote sensing of forest canopy and leaf biochemical contents. *Remote Sens Environ* 24
- Pirtti A (2008) Accuracy analysis of GPS positioning near the forest environment. *Croat J For Eng* 29
- Rouse JW, Haas RH, Schell JA, Deering DW (1973) Monitoring vegetation systems in the great plains with ERTS (Earth Resources Technology Satellite). Paper presented at the Proceedings of 3rd Earth Resources Technology Satellite Symposium, 10–14 December 1973, Greenbelt
- Royal Forest Department (2021) Final report of forest area status data in 2021. Retrieved from Bangkok
- Vani V, Mandla V (2017) Comparative study of NDVI and SAVI vegetation indices in Anantapur district semi-arid areas. *Int J Civil Eng Technol* 8:559–566
- Xue J, Su B (2017) Significant remote sensing vegetation indices: a review of developments and applications. *J Sens* 2017:1–17. <https://doi.org/10.1155/2017/1353691>



Rainforest Assessment in Brunei Darussalam Through Application of Remote Sensing

Shafi Noor Islam and Surayah Banu Syed Hussain Haroon Rasheed

Abstract

Remote sensing application has advanced over the decades from primarily aerial photography to detection and measurement of energy patterns from different portions of the electromagnetic spectrum to obtain information of an area or phenomenon on the earth surface or near environmental surface to study the physical and chemical characteristics from a distance. This is common and ideal in the forest sector study particularly in monitoring and assessment of forest cover changes. These interrelated disciplines have succeeded to observe the changing patterns of the rainforest in Brunei Darussalam from the year 1990–2015 based on primary and secondary sources relative to Brunei Darussalam. The annual deforestation rate used to estimate the net loss of forest cover is the contributory factor. The monitoring and assessment of Bruneian forest using remote sensing technique has been suggested for this investigation. The monitoring and assessment of rainforest cover with more than 90% accuracy using multitemporal Landsat images deduced the trend of forest cover change in Brunei Darussalam with 46% non-forest expansion, 27% forest conversion, and 12% forest regeneration in 25 years. Relatively, health, safety, and environmental (HSE) procedure; statistical data for non-wood forest products; recognition of the shared indigenous culture in Brunei in relation to Borneo; and sustainable development are suggested to supplement rainforest sustainability through the application of remote sensing for comprehensive rainforest resources monitoring and assessment in Brunei Darussalam.

S. N. Islam (✉) · S. B. Syed Hussain Haroon Rasheed
Department of Geographical and Environmental Studies, Faculty of Arts and Social Sciences (FASS), Universiti Brunei Darussalam, Jalan Tungku Link, Bandar Seri Begawan, Brunei Darussalam
e-mail: shafi.islam@ubd.edu.bn

© The Author(s), under exclusive license to Springer Nature Singapore Pte Ltd. 2022

M. N. Suratman (ed.), *Concepts and Applications of Remote Sensing in Forestry*, https://doi.org/10.1007/978-981-19-4200-6_9

Keywords

Rainforest · Remote sensing · Forest cover · Monitoring · Assessment and sustainability

1 Introduction

The tropical rainforest's significance in the global environmental and economic role beyond boundaries (Maini 1992). This should increase demand for forest and agricultural products as well as settlement development and construction for urban development and economic growth and uneven distribution of forest resources (Schaller 2005). This highly bio-diverse tropical rainforest with 80% biodiversity has been deforested up to 40 million ha approximately since 2000 (FAO 2010) distinctively in the Amazon, Congo Basin, far East Russia, Borneo and Sumatra.

The science of remote sensing developed 150 years ago has advances to sense and quantifies energy representations of the electromagnetic spectrum (Lira and Tabora 2014) for environmental properties and processes (Zheng et al. 2004). The application through multitemporal change detection analysis technique using Landsat images is common in forestry studies to assess forest depletion in a large spatial and temporal scale and capable of deducing different types of forest cover (Becek 2008). Rapid data acquisition (Soon 2011) and high re-visitation frequencies over large areas of interest (Zheng et al. 2004) are among the advantages of remote sensing application using Landsat images. Nevertheless, noises in the Landsat images could hinder Landsat signal from the earth surface (Surayah 2018).

In the tropical region about 27 million ha of forest has been removed from 2000 to 2005 mainly for timber or plantation, while another 398 million ha allotted for the timber industry (Bryan et al. 2013) notably in SEA and South America (Becek and Odihi 2008). Particularly, Borneo states of Sabah and Sarawak are renowned deforestation hotspots with unsustainable harvesting practices of oil palm and logging industries (Bryan et al. 2013; Gaveau et al. 2013). The main cause is believed to be due to the leading species of Dipterocarpaceae tree family for its marketable timber and non-timber forest products (Chandra 2011) and the introduction of mechanized harvesting such as chainsaw and caterpillar in the 1950s which speeded land clearance after the Second World War (Haase and Camphausen 2007) whereas infrastructural development, poor forest management, encroachment, shifting cultivation, and illegal logging are the major interlinked factors [8]. Air pollution, groundwater level change, drought, and global warming are the large-scale slow degrading factor (Becek and Odihi 2008). In addition to the small temperature range of the natural thermal regime of tropical vegetation of 10% (24–34 °C) compared to the temperate region, which is 70% (–30 °C) to 40 °C (Becek and Odihi 2008).

Brunei has the highest proportion of intact forest cover area (56.9%) compared to other states in Borneo, Kalimantan (39.6%), Sabah (19.1%), and Sarawak (14%) (Gaveau et al. 2013). The slow rate of annual forest depletion of about (0.8%) on

average (Becek and Odihi 2008) ranked as the lowest proportion of degraded forest area, with an estimated decrease of growing stock of 2598 ha (0.9%) per year, but increase by 1297 ha per year (0.82%) in the secondary forest in the 14 years from 1990 (Hunting Technical Services Ltd 1969). The change is derived from national development, mineral exploitation, urbanization, forest exploitation, forest development, agriculture activities (Hunting Technical Services Ltd 1969), and settlement (Pescott and Durst 2010).

Tropical forests were converted into percentages by giving a value of 0.58 each. 50 out of 57 indicators were satisfied with the total value of 29, aligned with index 4 from the index-weighting matrix, reflecting a well-managed forest contributing to sustainable conditions (Surayah 2018). This is owing to centralized forest management, dominance of the oil and gas industry, change in people's lifestyle within interior regions to urban areas along the coastlines, preference of involvement with formal sectors, and awareness of the importance of education in Brunei (Surayah 2018).

While the other component is image processing by Multispec 2.12.15 for multitemporal change detection analysis of forest and non-forest cover by the supervised reclassification of Landsat 4-5 TM (1990), 7 TM+ (2001), and 8 OLI (2015) derived from USGS. In addition to Google Earth for desk-ground throthing and image layering apart for using GIMP 2.8.1.4 application for the processed image masking. The image analysis portrayed patches of non-forest in the interior parts of Brunei in 1990 and spreads into the surrounding forest cover through 2015, segregating large forest cover block. This situation is deduced from the increasing non-forest expansion from 33% to 40% and forest conversion from 14% to 27% with extension of tracks linking most of the identified areas together with a decrease in both shift deforestation from 3% to 0% and forest regeneration from 19% to 12% between 2001 and 2015 resulting in forest cover changes within the 25 years period (Surayah 2018).

This study aimed to measure tropical forest sustainability in Brunei, with reference to the existing forest initiatives and forest cover progression from the past until the present years through three objectives: (1) defining a logical framework of Brunei's forestry by outlining forestry initiatives in Brunei and delineating it to the International Tropical Timber Organization Criteria and Indicator of Sustainable Forest Management (ITTO C & I of SFM) for Tropical Forests (ITTO 2005); (2) determining past and present Brunei's tropical forest cover through remote sensing application using Landsat images for a real visualization of Brunei forest cover extent; and (3) recommending forest sustainability initiatives through the identified loose factor based on this research findings.

2 Physical Characteristic of Case Study Area

Brunei is covered with tropical forests that comprise the dominant Mixed Dipterocarp forests (MDF) and the less dominant Peat Swamp, Mangrove, Mixture, Freshwater Swamp, Montane, and Heath forests (Anderson and Marsden 1984). MDF

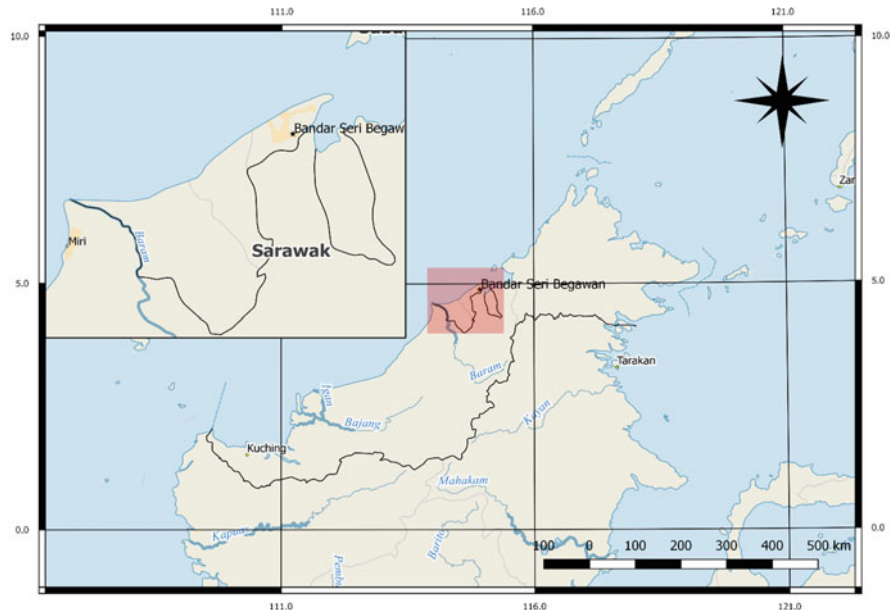


Fig. 1 Map of Brunei Darussalam (Map Source: Kaffli 2017, Retrieved on 23 July 2017)

comprises >200 species of Dipterocarpaceae family (Engbers 1998) including the marketable wood species for timber such as Meranti (*Shorea* spp.), *Urat mata* (*Parashorea* spp.), Resak (*Vatica* spp.), and Kapur (*Dryobalanops* spp.) (Engbers 1998). The total land area of the country is 5,765.32 km² occupies 1% of Borneo Island in the north west coast facing the South China Sea within the Southeast Asian region, surrounded by the Malaysian states of Sarawak and Sabah and the Indonesian state of Kalimantan (Forestry Department 2011). Brunei's geographical location of 443 km ahead of the Equator on the longitude between 114° 23' and 115° 23' east and latitudes of 4° 00' and 5° 05' north (Becek 2008; Forestry Department 2011) influenced experiencing tropical climates (Fig. 1).

The maximum and minimum mean temperatures are between 32 and 28 °C with mean annual rainfall approximately 2300 mm to over 4000 mm (Becek 2008) and high humidity of about 82% (FAO 2012). The seasonal variations are influenced by monsoon winds of Northeast Monsoon from December to March and Southwest Monsoon from May to October (Engbers 1998). Mainly, low relief topography is observable in both coastal areas and in Belait and Tutong river basins. Also in Brunei bay, flat alluvial swamp deposits are common (Surayah 2018) which was formed after the last significant sea level subsidence 500–600 years ago (Surayah 2018). Flat alluvial swamp deposits are common in Brunei bay (Engbers 1998; Becek 2008). The islands are drained by four major rivers, namely the Belait River, Tutong River, Temburong River, and Brunei River which collectively account for about 15 Km² (Becek 2008). This influences the vegetation cover where rainforests persist in the

interior part, peat swamps on the alluvial plains (Engbers 1998), mangrove on the brackish wetlands near riverbanks, and heaths on the sandy deposits (Engbers 2010, 1998; Forestry Department 2011)

3 Data and Methodology

This study adopts a mixed method that synchronously runs both qualitative and quantitative methods through exploratory and experimental design. This ought to be the nature of both qualitative and quantitative methods, which comes hand in hand in order to gain a better understanding of the phenomena. The main materials used for this research are the revised International Tropical Timber Organization Criteria and Indicators of Sustainable Forest Management (ITTO C & I of SFM) for Tropical Forests which was published by the ITTO (2005) and the Landsat 4-5 TM, 7 ETM+ and 8 OLI images derived from the USGS online in 2015. The ITTO C & I of SFM [16] are delineated to Brunei forestry and evaluated into simplified numerical output using an arithmetical approach, which are then keyed into “Criteria and Indicators Analytical Framework” (CIAF). The CIAF consists of a total of 7 criteria and 57 indicators that are converted into percentage form giving the value of 0.57 to each indicator. From the working of the CIAF, 50 out of 57 indicators were satisfied leaving 7 indicators unsatisfied identified as loose factors prevalence from its inapplicability to the country and unavailability of data and information. The sum of the satisfied indicators is multiplied with 0.57 and rounded off giving the final value of 29 whereas the criteria and indicators are listed in the summary of the CIAF’s Table 1 as follows.

$$N = \sum(C1 + C2 + C3 + C4 + C5 + C6 + C7) \times 0.57 \tag{1}$$

On the remote sensing component of multitemporal change detection analysis, supervised classification based on >90% accuracy for each raw Landsat 4-5 TM and 8 OLI images was performed using Multispec 2.12.15 software from the year 1990 to 2015 acquired from USGS (2015).

Table 1 Summary of criteria and indicators analytical framework (CIAF)

No.	Criteria	Indicator	Satisfied	Unsatisfied
C1	Enabling condition	11	10	1
C2	Extent of forest condition	6	5	1
C3	Forest ecosystem health	2	1	1
C4	Forest production	12	11	1
C5	Biological diversity	7	7	0
C6	Soil and water productivity	5	5	0
C7	Economy, social and cultural aspects	14	11	3
	Total	57	50	7

The classification is based on the principle of spectral signature produced by unique spectral reflectance properties of each land use and land cover types through recorded spectral reflectance on radiometric band into seven classes and further summarized into two main thematic classes of forest and non-forest areas. Amid the classifications process, Google Earth was applied as a desk ground-truth map for image-to-image referencing for higher image accuracy and image layering for national border identification between Brunei and the neighboring states. Successively GIMP 2.8.14 application was used to mask the classified image.

The extent of harvested compartments according to the harvesting plans is not confirmed with the prevalence of information that starting about 40,000 ha of forest was logged but remains without silvicultural treatment (Yussof 2000). However, compartment system was observed as the forest reserves are divided into compartments or known as logging management unit, ranging from 200 to 400 ha for each component. The components are further divided into smaller manageable logging blocks ranging between 50 and 70 ha each where a compartment applies to only one logging license or permit (Yussof 2000). Another is the acknowledgement of the ratification of 7 permit types as a key to enter and allow activities within the restricted forest reserves as stated under the Forest Act (1934) Chapter 46, revised in 2002 Amended in 2007 (Attorney General Chambers 2009).

4 Results and Discussion

The role of tropical rainforest in the global environment (Surayah 2018) is seen through ecosystem services that are experienced beyond boundaries despite their static location (Maini 1992). The ecosystem services are the condition and process where the ecosystem could naturally withstand and satisfy human needs (Daily 1997; Kremen and Ostfield 2005 in Gonzales Inca 2009). It resulted from physical, chemical, and biological processes of ecosystem functioning for self-maintenance (King and Mazzotta 2000). Soil erosion prevention, air purity, filtered water, climate change mitigation, and essential timber, food, and medicine resources supports the indigenous community and adverse diversity. The ecosystem services are identified as provisioning services, regulating services, cultural and amenity services, and supporting services (Gonzales Inca 2009). Figure 2 provides a general overview and rainforest characters in Brunei Darussalam in 2020. The figure shows that the scenario of rainforest areas in 2016 and 2020 is degrading.

Figure 2 shows a major category of forest which is mixed dipterocarp which covers 38% of the land base (Islam et al. 2019). The lowest category of forest is montane forest that covers 1.2% of total forest area in Brunei Darussalam. The deforestation rate in Brunei is 34.5% in the recent tenant and it is gradually increasing. In 1990 104,277 ha (18%) of forest areas are cleared whereas 200,893 ha (34.5%) were cleared in 2016. This has occurred within 40 years in Brunei Darussalam. A detailed classification of forest status is shown in Table 2. Seven major forest classifications have been recognized in Brunei Darussalam (Islam et al. 2018).

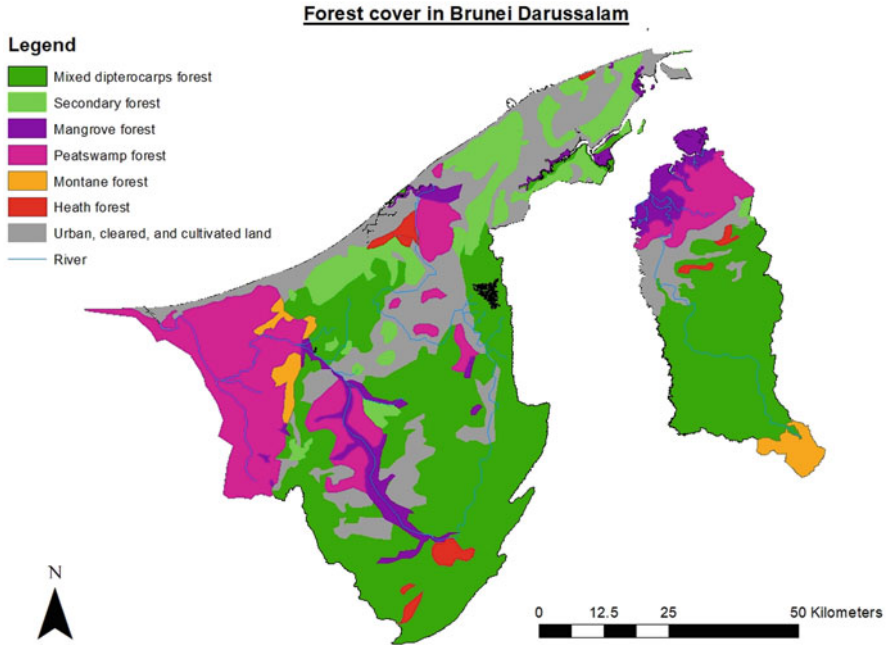


Fig. 2 General overview of land cover and rainforest areas in Brunei Darussalam in 2020

Table 2 Extent of forest in Brunei Darussalam in 1980 (Source: Anderson and Marsden 1984)

Forest types	Area (ha in 1980)	% of Forest areas	Area (ha in 2000)	Total (5) of forest areas
Mangrove	18,487	3.2	12,633	2.2
Freshwater Swamp	13,656	2.3	12,001	2.1
Peat Swamp	105,994	18.2	78,269	13.4
Kerangas	9506	1.6	7453	1.3
Mixed dipterocarps	226,159	45.7	221,414	38.0
Montane	7100	1.2	7160	1.2
Secondary	56,958	9.8	42,374	7.3
Total	477,920	82.0	381,304	65.5
Cleared and cultivation	104,277	18.0	200,893	34.3
Grand Total	582,197	100.0	382,197	100.0

However, continuous illegal logging activities, poor management practices, and increasing demands of forest and agricultural products enabled accessibility, settlement, and land conservation in the forest, thus allowing forest exploitation. There are grounded on a combination of factors of demographic increase (Surayah 2018).

They are grounded in a combination of factors: demographic increase (Surayah 2018). Deforestation is severe in the highly bio-diverse ecosystem with 80% of the

world biodiversity in the tropical region. Approximately 40 million ha has been deforested since 2000 (FAO 2010) notably in the Amazon, Congo Basin, Far East Russia, Borneo and Sumatra (Surayah 2018). For instance, the Borneo Island holds more than 600 bird species, 15,000 plant types, and hundreds of indigenous forest-dependent communities for food and shelter, while in its fragmented form, 25 acres of tropical forest hold over 700 species of trees, equivalent to the North American tree diversity (Surayah 2018).

4.1 The Status of the Tropical Rainforest in Brunei Darussalam

Brunei's economic developments are mainly generated by the natural resources of the oil and gas industry since 1929, which allowed the preservation of the country's tropical rainforest. A study by Gaveau et al. (2013) found that Brunei has the highest proportion of intact forest cover area of 56.9% compared to other states in Borneo with 39.6% in Kalimantan, 19.1% and 14% in Sabah and Sarawak, respectively (Engbers 2010; Islam et al. 2019). This is related to the FRA estimation of growing stock in 2014 where the primary forest decreases from 70,403 to 59,045 m³ while secondary forest increases from 11,176 to 213,215 m³ from 1990 to 2010. Despite the increase in the forest cover and growing stock within the secondary forest, the reduced primary forest values are however irreplaceable (Surayah 2018).

4.2 The Management of Rainforest

From the working of the CIAF, it resulted that criteria 1 weighted 6.0, criteria 2 weighted 3.0, criteria 3 weighted 1.0, criteria 4 weighted 6.0, criteria 5 weighted 4.0, criteria 6 weighted 3.0, and criteria 7 weighted 6.0. These weights are summed up producing a total value of 29 with most of the indicators accomplished albeit several unaccomplished indicators.

Through the CIAF working, it is found that 10 indicators out of 11 are satisfied under criteria 1, 5 out of 6 indicators are satisfied under criteria 2; 1 out of 2 indicators are satisfied under criteria 3; 11 out of 12 indicators are satisfied under criteria 4; 11 out of 14 indicators are satisfied under criteria 7, whereas 7 and 5 indicators under the respective criteria of 5 and 6 were all satisfied. Altogether, 50 indicators out of 57 indicators were satisfied leaving 7 indicators, a summary of which is presented in Table 3.

Subsequently, prior to the acquired result from the CIAF operationalization, an index-weighting matrix is applied, where forest management is categorized into poorly managed, moderately managed, and well managed which reflect the forest sustainability conditions of unsustainable, marginally sustainable, or sustainable as presented in Table 4. The resulted CIAF value of 29 is grouped into a built index matrix for forestry sustainability status that stood between 25 and 32 aligned with index 4 under well-managed category that indicates sustainable condition, which

Table 3 Summary of criteria and indicators analytical framework (CIAF)

Criteria	Indicators	Satisfied	Unsatisfied
Condition of SFM	11	10	1
Extent of forest condition	6	5	1
Forest ecosystem health	2	1	1
Forest production	12	11	1
Biological diversity	7	7	0
Soil and water productivity	5	5	0
Economy, social, and cultural aspects	14	11	3
Total	57	50	7

Table 4 Index-weighting matrix

Weighting	Index	Categories	Condition
1–8	1	Poorly managed	Unsustainable
9–16	2	Moderately managed	Marginally sustainable
17–24	3		
25–32	4	Well managed	Sustainable

reflects sustainable condition of Brunei forest under well management practice as presented in Table 4.

4.3 Monitoring and Changing Pattern of Rainforest

Land use and land cover transition relative to forest cover changes from 1990 to 2015 were observed. In 1990, the intact forest cover areas especially in the interior Tutong and Belait district were partly converted into built, plantation and sparse vegetation as non-forest, distinctive along the coastline (Engbers 2010) (Fig. 3). The spreading inwards leads to the detachment of forest areas in the interior region. The horizontal and vertical stretch of non-forest cover from east to west and southwards is presented in Fig. 4.

Over time, the forest is divided into north and south due to sparse vegetation extension over the areas observed in 2015 (Fig. 5) whereas Temburong district showed undistinguishable changes over the 25 years period. From the multi-temporal change detection technique of the Landsat images, the trend of forest cover change in Brunei was deduced to be driven by (1) non-forest expansion from its focal point (Surayah 2018); (2) forest conversion into non-forest for built areas, plantation that overtime partially generate into sparse vegetation; (3) shift deforestation of forest regeneration and forest conversion on side to side; (4) incomparable forest regeneration, (5) tracks development; and (6) water body as development of reservoir. The extent and trend of the forest and non-forest cover changes over the years is presented in Figs. 5 and 6.

Figure 5 shows existing forest area (43%), existing non-forest area (53%), and missing data area (5%) in 1990. By 2015 (Fig. 6), the existing forest area had

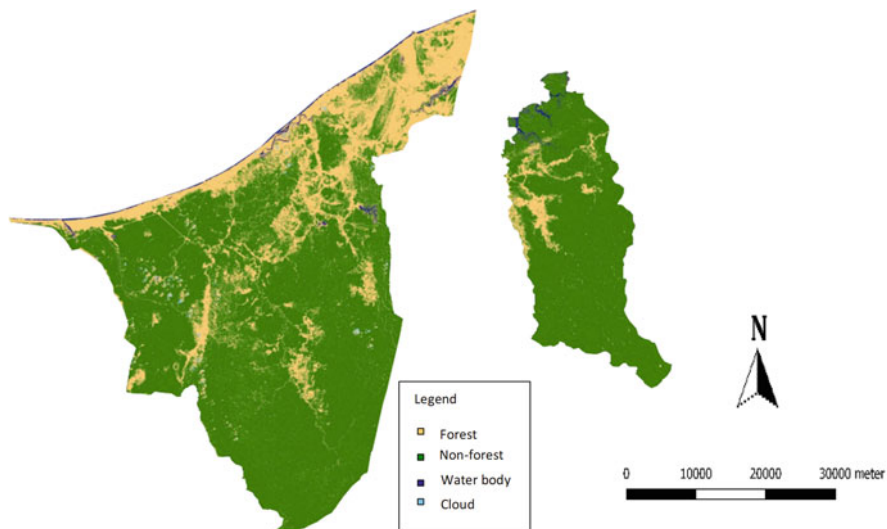


Fig. 3 The supervised image re-classification of forest and non-forest cover in 1990

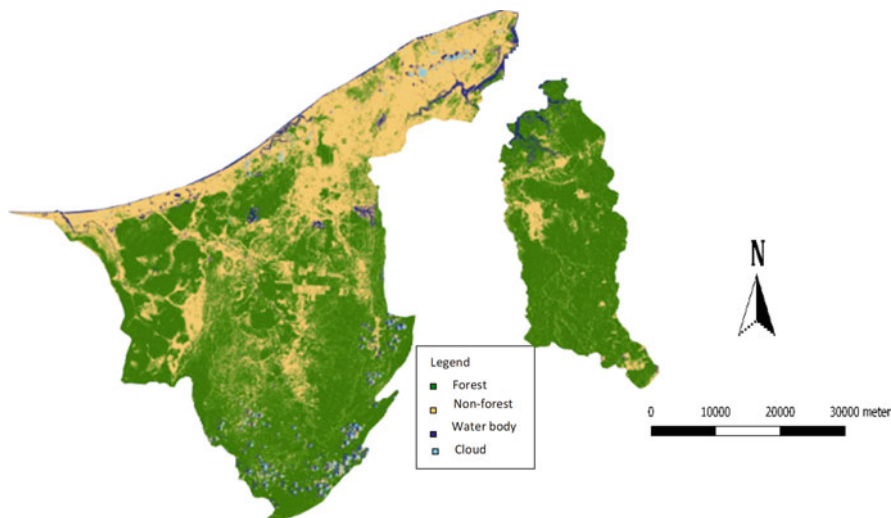


Fig. 4 Supervised image re-classification of forest and non-forest cover in 2015

undergone changes which detects increasing non-forest expansion (46%), forest conversion (27%), decreased forest regeneration (12%), tracks development (6%), and newly covered water body (6%) leaving shift deforestation and existing forest area 0% whereas the missing data areas have newly gained coverage identified as existing non-forest areas (3%). Therefore, the adoption of both ITTO C & I and remote sensing application in this research has perceived tropical forest

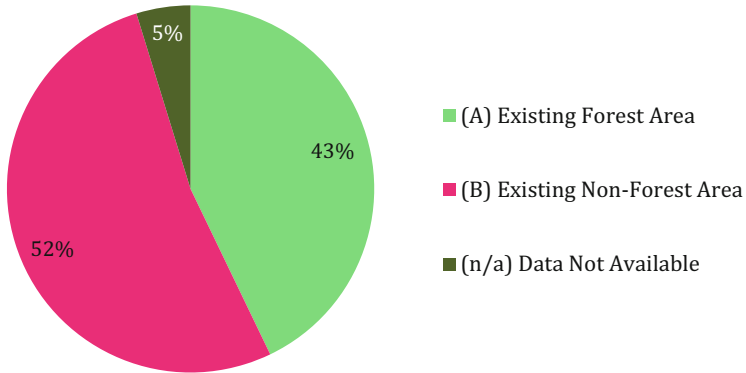


Fig. 5 Forest and non-forest cover trend of changes in 1990

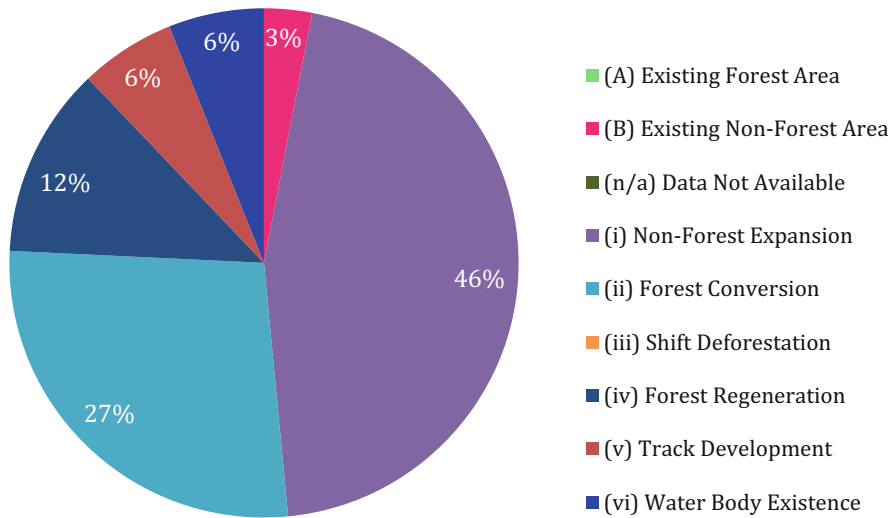


Fig. 6 Forest and non-forest cover trend of changes in 2015

sustainability and visualized the progress of forest cover change in the frame of development, urbanization, and economic demand.

These forest changes leave only 6% of the existing forest areas (A), none or 0% of the existing non-forest areas (B), and 3% of uncovered areas (n/a). Through 14 years, which is by 2015, non-forest expansion increased to 46% (1), forest conversion increased to 27% (2), There was no new or shifting deforestation (3), and forest regeneration accounted for 12% of the total. Tracks also dropped to 6%, indicating that much of it has expanded and become non-forest areas. Water body is just discovered which accounts for 6% (6) of the identified areas. These again leave

Table 5 Summary of the forest trends of changes in 1990, 2001, and 2015

Year/trend of changes	A	B	n/a	i	ii	iii	iv	v	vi
1990	43%	54%	5%						
2001	6%	0%	3	33	14%	3	19	22	0
2015	0%	3%	0%	46%	27%	0 %	12%	6%	6%

none or 0% of both the identified existing forest (A) and uncovered areas (n/a), where 3% of the missing areas has newly gained coverage identified as existing non-forest areas (B). These outcomes are assembled in Table 5.

Through this it is analyzed that the existing forest areas are reducing, in contrast to the increasing existing non-forest over the years. Through this research, it is inferred that the sustainability of the global tropical rainforest is mainly challenged by the continuous demographic increase in economic growth and uneven distribution of forest resources, combined with increasing demand for forest and agricultural products. This results in forest exploitation through logging, encroachment, and land conservation for development, plantation, and also settlement leading to accessibility. Especially to Brunei, the erosion proneness of Brunei's sedimentation and alluvial in Brunei Muara, Tutong and Temburong districts, and the largely peat swamp cover in Belait district support regional diverse and complex tropical rainforest bio-ecology. However, continuous challenges from the industrial development, urbanization, mineral exploitation, forest exploitation and forest development, agricultural activities, and settlement affect the country's forest cover as recorded from 81% in 1979 (Ryni 2014) to 65.5% in 2000 (Becek 2008; Becek and Odihi 2008), which is a concern for the present sustainability of the country's forest cover.

5 Conclusions

Through this research, it is inferred that the sustainability of the global tropical rainforests is mainly challenged by the continuous demographic increase and economic growth as well as uneven distribution of forest resources, combined with an increasing demand for forest and agricultural products. This results in forest exploitation through logging encroachment and land conversion for development, plantation, and also settlement leading to accessibility. Specifically, to Brunei, the erosion proneness of Brunei's sedimentation and alluvial in Brunei Muara, Tutong and Temburong districts, and the largely peat swamp cover in Belait district support regional diverse and complex tropical rainforest bio-ecology.

Through the provisions of this research methodology, we have therefore recognized the adaption of the mixed method within research, involving few research designs and approaches under the qualitative and quantitative methods. This allowed for the identification of several research materials, including ITTO C and I of SFM for tropical forest and Remote Sensing application of multi-temporal change detection analysis, which have measured and comprehended Brunei

tropical forest sustainability. The centralized forest management practices that are accompanied by active forest cover change in Brunei are contributed to by the centralized forest management practices (Abee 2000), the oil and gas industry (Pescott and Durst 2010), traditional lifestyle evolution in modern form (Faisal 2009), the preference for involvement in the formal sector and an understanding of the value of formal education (Gira 2003).

Nevertheless, in association with the loose factors, relative initiatives to supplement forest sustainability in Brunei are suggested for instance: (1) a set of detailed HSE procedures to guide forest workers, forest environment, forest industry, and environmental forestry including educational or recreational forestry; (2) consideration of the non-wood forest products statistical data and harvests in the informal market as its myriad products are used or consumed in everyday life, hence would be beneficial and significant resources; (3) recognition of the regionally shared unique indigenous culture of Brunei with the neighboring states would be an added value to both forestry and eco-tourism industry hence to the national economy; and (4) relevant sustainable development initiative (CATIE 2012) to support sustainable forest cover of the country in the long run such as co-finance investment between government and investors for certain land use or promotion of production practices in afforestation, sustainable forest management, and sustainable land management, as well as subsidies provision for sustainable land management practice; green technology (water treatment plants, soil conservation equipment, energy-efficient light bulbs); or non-monetary provision of technical assistance, seeds and plants.

Therefore, it is deduced that the adoption of C & I for SFM in this study would be able to strengthen efficacy of forest management as it could identify looseness or development relevant to further enhance the country's forest sustainability systematically. Furthermore, the application of the remote sensing approach would be an advantage for forest monitoring and assessment timelessly; this is seen to be an effective mechanism to achieve full equilibrium of SFM for forest sustainability, as it is capable of distinguishing the Brunei's forest cover extent in 25 years period in a short time. In addition to extraction of the forest cover within the frame of development, urbanization and economic demand coincides with the increasing population within the limited land supply. It is also vital to be aware of the extent of forest cover in the country considering forest contribution to the country's environmental, economic, and social functions and services.

References

- Abee A (2000) Sustainable forest management: the application of criteria and indicator measurements in the unites states forest service. In: *Int. Persp. on Stream. Local-Level Info. for Sust. Forest Manag.*, Vancouver, Canada, British Columbia, August 2000, pp 17–30
- Anderson, Marsden (Forestry Consultant) Ltd. (1984) *The forest resources in Negara Brunei Darussalam, Brunei forest resources and strategic planning study final report, vol 1*
- Attorney General Chambers (2009) *Musing from the Chambers Report published by Attorney General Chambers of the Government of Brunei Darussalam, Bandar Seri Begawan, Brunei Darussalam*, pp 1–64. <http://www.agc.gov.bn>

- Becek K (2008) Detection of tropical forest depletion by exploring second-degree moment of its spectral profile, 2008, pp 1–11
- Becek K, Odihi JO (2008) Identification and assessment of factors affecting forest depletion in Brunei Darussalam. In: Proceeding of the international archives of the photogrammetry, remote sensing and spatial information sciences, 37, (B2). Beijing, China, 3rd July–11th July 2008, pp 209–213. BRN//BRN-CP-eng.pdf
- Bryan JE, Shearman PL, Asner GP, Knapp DE, Aoro G, Barbara L (2013) Extreme differences in forest degradation in Borneo: comparing practices in Sarawak, Sabah, and Brunei, pp 1–6
- CATIE (Tropical Agricultural Research and Higher Education Center) (2012) The Global mechanism and the united nation convention to combat desertification (GM-UNCCD). Incentive and market-based mechanism to promote sustainable land management, framework and tool to assess applicability, pp 25–30
- Chandra RPP (2011) Ecological analysis of Dipterocarpaceae of North Andaman forest, India. *J Plant Dev* 18:135–149
- Daily GC (1997) Introduction: what are ecosystem services. *Nature's Services: societal dependence on natural ecosystems* 1(1)
- Engbers P (1998) Wildlife watch in Brunei Darussalam. Syabas Publisher, Brunei Darussalam, pp 1–13
- Engbers P (2010) Forest cover of Borneo and Brunei. In: Focus on forest. Panaga natural history, pp 3–29
- Faisal M (2009) Diversification through forest conservation with climate change context: Brunei Darussalam's perspectives. Master's thesis, University of Glasgow, Scotland, United Kingdom, pp 13–49
- Food and Agriculture Organization of the United Nations (FAO) (2010) Global forest resources assessment (GFRA) 2010. Country report, Brunei Darussalam, Rome, Italy, pp 5.6, 10,15–42. <http://www.fao.org/docrep/013/al466E/al466E.pdf>
- Food and Agriculture Organization of the United Nations (FAO) (2012) Brunei Darussalam. In: Fenken K (ed) Irrigation in southern and eastern Asia in figures-AQUASTAT survey 2011, FAO water reports 37. Food and Agriculture Organizations of the United Nations, Rome, Italy, pp 107–204
- Forestry Department (2011) Sustainable Forestry in Brunei Darussalam Report, Forestry Department, Ministry of Forestry Industry and Primary Resources, Bandar Seri Begawan, Brunei Darussalam, pp 1–5
- Gaveau DLA, Sloan S, Molidena E, Yaen H, Sheil D (2013) Four decades of forest persistence, clearance and logging on Borneo. *PLoS One* 9(7):1–11
- Gira H (2003) Puak– Puak Negara Brunei Darussalam: Kes Kajian orang Iban daerah Belait dari perspektif sejarah 1946-1996. Master's thesis, Universiti Brunei Darussalam, pp 22–67
- Gonzales Inca CA (2009) Assessing the land cover and land use change and its impact on watershed service in a tropical Andean watershed of Peru. Master Thesis at University of Jyväskylä, Finland
- Haase G, Camphausen A (2007) Best practices for sustainable forest management in Southeast Asia. In: Göhler D, Greiner-Mann V (eds) Sunset media creative studio, pp 7–13 <http://www.fao.org/nr/water/aquastat/countries/regions/>
- Hunting Technical Services Ltd (1969) Land capability study. Government of the State of Brunei 1: 1–24
- Islam SN, Jenny YSL, Mamit NABH, Matusin AMB, Bakar NSBA, Suhaini MHB (2018) GIS application in detecting forest and bush fire risk areas in Brunei Darussalam: case analysis on Muara and Belait Districts. IET Digital Library, UK, pp 1–4
- Islam SN, Mohamad SMBH, Azad AK (2019) Acacia: invasive trees along the Brunei Coast, Borneo (Chapter 14). In: Makowski C, Finkl CW (eds) Impacts of invasive species in coastal environment, Coastal Research Library, vol 29. Springer, Switzerland, pp 455–476

- ITTO (International Tropical Timber Organization) (2005) Revised ITTO criteria and indicators for the sustainable forest management of tropical forest including reporting format. ITTO Policy development series 15. Yokohama, Japan, pp 7–33
- Kaffi NE (2017) Map of Brunei Darussalam. Environmental studies. Universiti Brunei Darussalam
- King DM, Mazzotta MJ (2000) Contingent valuation in ecosystem valuation. In: Ecosystem valuation methods, Section 6. http://www.ecosystemvaluation.org/Contingen_C
- Kremen C, Ostfield RS (2005) A call to ecologists: measuring, analyzing, and managing ecosystem services. In: *Frontiers in ecology and the environment*, vol 3, no 10. Wiley, pp 540–548
- Lira C, Taborda R (2014) Advances in applied remote sensing to coastal environments using free satellite imagery. In: Frikle C, Makowski C (eds) *Remote sensing and modelling advances in coastal and marine resources*, Coastal Library, vol 9. Springer, pp 77–102
- Maini JS (1992) Sustainable development of forest. In: Dembner SA (ed) *An International Journal of Forestry and Forest Industries Unasylva*-No 169 sustainability. Vol 43 (1992/2). FAO. Retrieved on 4th March 2015. <http://www.fao.org/docrep/u6010e/u6010e03.htm>
- Pescott MJ, Durst PB (2010) Reviewing FLEG progress in Asia and the Pacific. In: Pescott MJ, Durst PB, Leslie RN (eds) *Asia Pacific Forestry Commission forest law enforcement and governance: progress in Asia and The Pacific*. RAP Publication, Bangkok), p 8
- Ryni S (2014) Forest Resource Assessment (FRA) in Brunei Darussalam. In: *National Forest Resources Assessment (NFRA) Seminar The Way forward*, organised by Forestry Department Brunei Darussalam and AFOCO.: Bandar Seri Begawan, Brunei Darussalam, 23rd October 2014
- Schaller M (2005) Brunei. In: *Important bird's areas in Asia, key sites for conservation*. Birdlife International, (Birdlife conservation series no 13), Cambridge, UK, pp 45–46
- Soon JYK (2011) Forest management in Brunei Darussalam: assessment of principles and policies and feasible forest assessment tool. Master's thesis, Universiti Brunei Darussalam, pp 6–52
- Surayah, BBHR (2018) The tropical rainforest sustainability in brunei darussalam: an application of criteria and remote sensing, MA. Thesis in Environmental Studies. Dept. Geography and Environmental Studies, Faculty of Arts and Social Sciences, Universiti Brunei Darussalam, Brunei Darussalam, pp 1–131
- United States Geological Survey (USGS) (2015) LT51190571990169BKT00; LT41180571990170XXX06; LC81190572015078LGN00; LC81180572015231LGN00 Earth Explorer, U.S Department of The Interior. <https://earthexplorer.usgs.gov>
- Yussof M (2000) Forest harvest planning for mixed dipterocarp forest in Brunei Darussalam, Master's Thesis at the Australian National University, Canberra, Australia
- Zheng D, Rademacher J, Chen J, Crow T, Breese M, Le Moine J, Ryu SR (2004) Estimating aboveground biomass using Landsat 7 ETM+ data across a management landscape in Northern Wisconsin, USA. *Remote Sens Environ* 93(3):402–411

Part IV

Remote Sensing of Agricultural Tree Crops



Rubber Trees and Biomass Estimation Using Remote Sensing Technology

Mohd Hasmadi Ismail, Iqbal Putut Ash Shidiq,
Mohammad Firuz Ramli, Norizah Kamarudin,
Pakhriazad Hassan Zaki, and Rokhmatuloh

Abstract

In Southeast Asia, rubber plantation is considered the second largest main crop after oil palm. Hence, it also becomes more critical when seeing rubber as part of the forest ecosystem that possesses an essential biomass and carbon sequestration source. In general, the changes in carbon stocks of the terrestrial ecosystem may have direct implications on the socioeconomics of local communities and biodiversity. However, the process of measuring carbon stock over time is essential to complement climate change mitigation needs. Therefore, there are several numbers or errors in estimating the given carbon pools. It varied from sampling error in the number of plots within the tree's population, error in measuring soil carbon and stem diameter, and error when applying regression using inventory data or biomass conversion. Unfortunately, the estimation of biomass and carbon fluxes from rubber plantations has been rarely studied. This chapter mainly elaborates the related studies and discussions towards biomass, specifically above-ground biomass (AGB), the accretion of biomass utilization since it was first discovered, the benefit for renewable energy intervention, and the significant role in sequestering the atmospheric carbon. More importantly, several studies refer to remote sensing applications for biomass quantifications that engage different

M. H. Ismail (✉) · N. Kamarudin · P. H. Zaki
Department of Forestry Science & Biodiversity, Faculty of Forestry and Environment, Universiti Putra Malaysia, Serdang, Selangor, Malaysia
e-mail: mhasmadi@upm.edu.my

I. P. A. Shidiq · Rokhmatuloh
Department of Geography, Faculty of Mathematics & Natural Sciences, University of Indonesia, Jakarta, Indonesia

M. F. Ramli
Department of Environment, Faculty of Forestry and Environment, Universiti Putra Malaysia, Serdang, Selangor, Malaysia

remote sensing systems. This paper's main perspective is to give insight into the ability and potential of remote sensing for delivering an efficient spatial approach as the primary tool for rubber plantation biomass estimates.

Keywords

Rubber tree · Biomass · Allometric equation · Remote sensing · Spatial techniques

1 Introduction

Global warming caused by greenhouse gasses (GHCs), primarily carbon dioxide (CO₂), is one of the most urgent global contributors. The uncontrolled emission of CHGs can potentially cause irreversible and disastrous damage to the whole biosphere if it is not managed appropriately. Among anthropogenic CHGs, CO₂ is the most abundant and is responsible for more than half the radiation associated with the greenhouse effect (Solomon and Srinivasan 1996). In order to utilize the mitigation program towards global warming, recent studies have shown the significant impact of using biomass for both alternative renewable fuel and the source of carbon sequestration that are critically important in maintaining the global climate (Gao and Zhang 2021). According to FAO (2005), global forest ecosystems store more than 638 Gt carbon (Egbe et al. 2012), which is essential to control atmospheric carbon. The ability of vegetation and soil organic matter to sequester atmospheric CO₂ has recently received much attention. Two management options for enhancing carbon sequestration include tropical forest conservation and plantations (Yang et al. 2004). Both of these options have a similar intention to optimize the carbon concentration within the biomass.

Rubber tree, or *Hevea brasiliensis*, is a major world crop cultivated for natural rubber production. It is mainly grown in tropical areas and has an economic lifespan of 30–35 years. It occupies more than 11 million ha of agricultural land globally. Approximately 9.2 million ha (78%) of total rubber is planted in Southeast Asia, with about 3.67 million ha (31%) in Indonesia and 3.23 million ha (27%) in Thailand (FAO 2020). Rubber trees are typically grown for approximately 25–35 years before being felled for timber production. Therefore, the total carbon stock of rubber in plantations has been estimated to be higher than many tropical forestry and agroforestry systems (Brahma et al. 2016). The time-averaged carbon stock of lowland and highland rubber plantations is estimated to be 58 and 28 MgC/ha, respectively (Yang et al. 2016). In addition, the role of rubber in mitigating climate change has been recognized globally (Verchot et al. 2007; Fox et al. 2014; Min et al. 2020). Therefore, the accurate estimation of biomass and carbon stock in rubber plantations has become more critical than previously.

Remote sensing is considered the best approach in biomass estimates at a regional level, where field data are scarce or difficult to collect. Almost two decades have passed since pioneers such as Tucker et al. (1985) and Sader et al. (1989) studied the relationship between biomass and the reflectance value recorded at the sensor. Since

then, many studies in different regions have found strong correlations between biomass and reflectance at different wavelengths. Several review papers have been conducted on biomass estimation in the past few years. However, most of them have described remote sensing-based estimates for forest biomass (Lu 2006; Goetz et al. 2009; Song 2013; Lu et al. 2016). This current review incorporates remote sensing-based biomass estimation for three major vegetation ecosystems: forest, grassland and rangelands, and tropical savanna, which covers around 80% of earth's vegetations (FAO 2005, 2012). These vegetative surfaces on earth are more "natural" ecosystems without much human disturbance, unlike agricultural lands, which are heavily dependent on cropping management, and thus provide an opportunity to the reader to assess the challenges and differences in remote sensing-based biomass estimations for these ecosystems (Kumar et al. 2015).

This paper mainly elaborates the related studies and discussions towards biomass, specifically above-ground biomass (AGB), the accretion of biomass utilization since it was first discovered, and the significant role in sequestering atmospheric carbon. More importantly, several studies refer to remote sensing applications for biomass quantifications that engage different remote sensing systems. This paper's main perspective is to give insight into the ability and potential of remote sensing for delivering an efficient spatial approach as the primary tool for rubber plantation biomass estimates.

2 Biomass at a Glance

In the mid-1800, biomass had dominated the primary world's energy supplies. However, it decreases with the invention of fossil fuel, which is later intensely implemented in industrialized countries. When the world hit the First Oil Shock in mid-1970, biomass was realized again by many countries to support the viability of energy supplies. It was also believed to help reduce oil consumption that caused some severe national deficit by dependency on imported oil (Klass 1998).

Biomass is considered the most developed renewable energy source, which provides 35% of the primary energy needs in developing and industrialized countries. It has more flexibility as an energy resource than other sources such as wind and sunlight (Li et al. 2020). The technology development in harvesting biomass for energy supplies is not as progressive as other energy sources. Biomass can be used for direct heating in industrial or domestic applications, steam production for electricity generation, or gaseous or liquid fuels. Among the policymakers, biomass is gaining considerable interest in electricity production, which utilized direct heating as the most widespread application (Boyle 1996; Wereko-Brobby and Hagan 1996).

Besides its advantage as the energy source, biomass has taken a significant role in the terrestrial carbon cycle. Almost half of the biomass content is counted for carbon. Although biomass carbon is considered a tiny fraction, it is significant. It helps maintain the delicate balance among the atmosphere, hydrosphere, and biosphere to

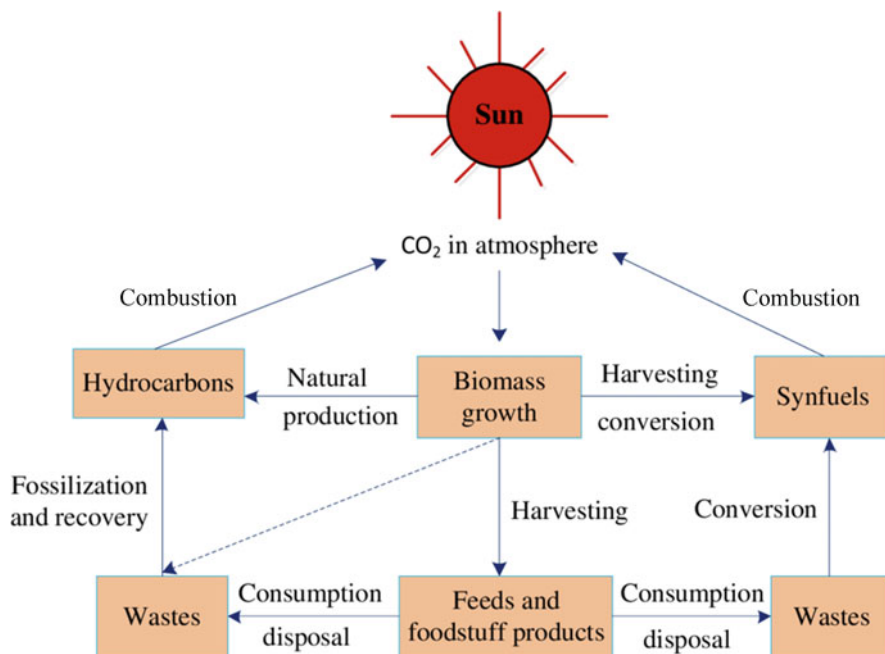


Fig. 1 Features in biomass energy. (Source: Klass 1998)

support all life forms essential to species diversity that inhabit the earth and sustain their gene pools (Klass 1998).

Originally, biomass resources could be grouped into several formations. Wood residues are generated from wood product industries; agricultural residues generated from crops, agro-industries and animal farms, energy crops, trees dedicated to energy production such as rubber plantation, municipal solid waste, and also, tropical forest as the vast virgin biomass that is available naturally (Easterly and Burnham 1996). Meanwhile, the largest reservoir of biomass carbon resides in life forest biomass. This is because it fixes atmospheric CO_2 during most of its life cycle.

Forest biomass dominates the carbon stocks and has more carbon than the total carbon stock in the atmosphere. Among the different biomass, only the tropical forest holds as much carbon in its vegetation carpet. Despite only covering 28% of the land surface, tropical forests contain 80% of the terrestrial carbon and net primary production (Wright 2010) and are stored as biomass and soil organic carbon (Voivontas et al. 2001; FAO 2005).

In a conventional method, biomass is harvested for feed, food, fiber, and construction materials or left in the growth areas where natural decomposition occurs. The waste products from harvesting and processing biomass disposed of inland can theoretically be recovered after a long time as fossil fuels (Fig. 1). Alternatively, biomass and any wastes from the process could be converted directly into synthetic organic fuels if suitable conversion processes were available. The energy content of

biomass could be diverted to direct heating applications or electricity production by combustion. Moreover, biomass can also be harvested by growing certain species of vegetation that store significant biomass sources, such as the rubber tree. In this case, biomass serves the dual role of carbon fixing apparatus and a continuous source of hydrocarbons without being consumed in the process (Klass 1998).

Forest biomass is considered a key variable in annual and long-term changes in the terrestrial carbon cycle. It is substantial to have a standardized carbon estimation modeling to describe the uptake and redistribution process of the carbon cycle within the ecosystem (Houghton 2005). However, the estimations of global terrestrial biomass remain uncertain and are still being studied in line with understanding the global carbon cycle (Gibbs et al. 2007). The dynamic anthropological activities and the increasing population continuously disturb the sustainability of the world's biomass growth areas. It has been estimated that tropical forest is disappearing at a rate of tens of thousands of square miles per year and contributes about a fifth of total anthropogenic carbon dioxide (CO₂) emissions to the atmosphere (Gibbs et al. 2007). Deforestation counts for 40% of the total CHG emissions (IPCC 2007). Most of those contributors come from tropical countries (Houghton 1991). Due to this high carbon content of vegetation biomass, it is essential to acquire accurate quantification and monitoring of forest biomass to reduce carbon emissions from changes in the forest area.

Consequently, the forest plays the most significant role among different terrestrial ecosystems in mitigating climate change impacts and controlling the global carbon balance (Houghton 2005 in Hamdan et al. 2014). Therefore, quantifying carbon in a forest is crucial for monitoring and reporting the changes in the global environmental condition. Since this issue has reached a wide range of interest in many countries and regional levels, the quantification method should be arranged within comprehensive guidance and proper legal binding. These include assigning forest carbon to suit previous land use analysis, such as determining whether the carbon was caused by afforestation or deforestation, and a consistent scaling procedure through a large area where it could produce a reliable estimation (Zheng et al. 2008).

3 Carbon Sequestration

Carbon dioxide (CO₂) is the major greenhouse gasses from the land-use sector, particularly forests and grasslands. Besides being caused by the burned fossil fuel from industrial activities and transportation, it is also caused by the conversion of forests (tropical deforestation), loss of soil, forest degradation due to non-sustainable logging and fuelwood collection, and forest fire. The process of producing, emitting carbon through the surrounding environment, and then sequestered by natural livings is described as the carbon cycle. It explains the movement of carbon within the biosphere, atmosphere, geosphere, and oceans. Carbon, notably carbon dioxide (CO₂), is cycled between different system components. For example, green plants absorb CO₂ from the atmosphere during photosynthesis (also called primary production) and release CO₂ back into the atmosphere during respiration. Two critical

anthropogenic processes that contribute to CO₂ emission into the atmosphere are burning fossil fuels and changes in land use. Fossil fuels are burned in industries, power plants, and automobiles. Land-use change is a broad term that encompasses a host of essentially human-induced activities, including the conversion of natural ecosystems such as forests and grasslands into managed systems such as cropland, grazing land, and settlements (Ravindranath and Ostwald 2008).

In addition, trees act as a sink for the carbon stored by fixing carbon during photosynthesis and storing excess carbon as biomass. The net long-term carbon source or sink dynamics of forests change through time as trees grow, die, and decay. Human influences on forests can further affect the carbon dynamics through fossil fuel emissions and harvesting or utilization of biomass (Crane and Novak 2001). The efforts to sequester more carbon through trees and forests are widely emphasized as a necessary climate change mitigation.

Above-ground biomass is the most significant form of carbon sequestration compared to other parts like soil carbon. According to Houghton (1995), carbon sequestration estimation is half of the amount of AGB. However, it is more challenging to evaluate the amount of carbon sequestered over time than the overall potential sequestered due to the high uncertainty of parameters. Many factors influence the process of accumulation which affects the nonlinear increase of carbon sequestration. Although there is prominent literature debate regarding the functional form of carbon sequestration in biomass, the linear increase is wisely chosen to simplify the calculation (Yang et al. 2003).

In the end, the management for carbon sequestration in the tropical area means increasing the amount of carbon stored in vegetation such as living above- and below-ground biomass, dead organic matter, and soil that includes litter, deadwood, and mineral soil. In order to increase the capacity of the carbon pool, silvicultural treatments can be attempted in the existing forest by protecting the secondary forest and other degraded forests where carbon and biomass were accumulated less than their maximum capacity. In addition, the forest can be encouraged to sequester more carbon by natural or artificial regeneration or increase the tree cover on the agricultural forest for environmental protection and local need (Yang et al. 2003).

4 Application of Remote Sensing for Rubber

The remote sensing technique provides spatial information and temporal data of a specific place in the world. The complementary functions between GIS and remote sensing techniques have been increasingly used for planning, decision-making, and environmental management. GIS and remote sensing are also often combined with environmental or ecosystem modeling in many applications such as forest-degradation analysis, biomass analysis, and terrestrial carbon cycle (Skidmore 2002; Turner et al. 2004). In particular, remote sensing was explicitly designed to capture spatiotemporal information on landscape and vegetation reflectance properties, while models focus on the underlying biogeochemical process (Turner et al. 2004).

Monitoring by using remote sensing plays an essential role in agricultural management and production. Through practical and intensive monitoring, producers can identify corrective and preventive steps to optimize input while maximizing production. Traditionally, rubber tree monitoring is time-consuming and labor-intensive. The collection of ground data relies heavily on conventional monitoring methods. It has played a vital role in mapping rubber trees at local and regional scales and has facilitated understanding of changes in spatial patterns of rubber plantations over time. For rubber tree biomass and carbon and leaf area index estimation, most studies develop models to establish relationships between remote sensing data and biophysical parameters. Examples of model inputs include spectral bands, vegetation indices, and tree growth data.

There are several ways remote sensing imagery can estimate carbon density and changes in carbon density. It can be estimated directly based on quantifiable relationships between biomass and spectral responses. Also, it can be estimated based on classification techniques, indices, and regression equations or models developed through research pairing measurements with remote sensing reflectance measurements. This study mainly discusses the utilization of various remote sensing data and techniques to obtain feasible biomass estimation and carbon stock in rubber plantations. The apparent reason is to tackle the time- and labor-consuming problem due to the significant spatial locus and the need for continuous temporal data.

5 Vegetation Indices for Biomass Calculation

Vegetation indices feature the extraction operations designed to yield the estimation of vegetative cover from an image. These indices are based on the fact that vegetation absorbs well in the visible and reflects very efficiently in the near-infrared spectrum of electromagnetic waves. Numerous spectral vegetation indices (VIs) have been developed to characterize vegetation canopies for retrieving vegetation structure from optical remote sensing. These indices are well correlated with vegetation parameters, including green leaf area, biomass, percent green cover, productivity, and photosynthetic activity (Asrar et al. 1984; Hatfield et al. 1984; Sellers 1985).

Another reason for applying remote sensing is to utilize the excellence of remote sensors that are sensitive to capture the earth's surface features, especially vegetation characteristics. Various types of vegetation indices such as NDVI (normalized difference vegetation index), LAI (leaf area index), EVI (enhanced vegetation index) from LANDSAT, and MODIS have been used by many researchers to analyze vegetation features like phenology, biomass, and forest carbon cycle (Turner et al. 2004; Anaya et al. 2009; Gasparri et al. 2010; Morel et al. 2011; Tian et al. 2012; Shidiq and Ismail 2016). Retrospectively, remote sensing sensors could capture the radiative process in plant canopies, which was further used as input information for biomass modeling (Zheng et al. 2007). For instance, LAI which is generated from several vegetation indices is often used to calculate biomass. It is

usually combined with other parameters such as stand age and forest type to produce high accuracy of biomass calculation.

6 Rubber Tree Biomass as a Carbon Sink

Since the invention of latex for the manufacturing sector, the demand for rubber production has increased vastly, pushing countries with suitable climate conditions like China, Malaysia, Thailand, and Indonesia to expand the rubber plantation area extensively. Besides being planted in 20 countries for many latex productions, rubber is primarily planted in Southeast Asian countries which became a world leader for natural rubber production. More than 70% of rubber world is cultivated in Indonesia, Thailand, and Malaysia (Shigematsu et al. 2011).

In addition to its benefit as the primary crop tree production, rubberwood also holds promising gains in biomass production, thus becoming a renewable energy source. Alternative renewable energy is turning into such an important issue in the global discussion. Many parties have realized that the over-dependency only on fossil fuel is entirely unsustainable and risky against global dynamics. Biomass offers one alternative solution which relates to the natural environment provided within the country. It has been studied that a standing tree can produce biomass from different sources, including the trunk, branches, twigs, and leaves (Ratnasingam and Scholz 2009).

Moreover, Lim et al. (2000) mentioned that the energy content of rubberwood reaches up to 68.61 GJ per year or 40.04 GJ per hectare per year. The amount of this estimation is quite considerable to be applied for alternative energy compliance. The conversion technologies including combustion, pyrolysis (Shaaban et al. 2013), and gasification (Kaewluan and Pipatmanomai 2011; Adisurjosatyo and Nugroho 2012) have been used to generate energy from rubberwood biomass.

Apart from storing biomass for alternative energy, a forest plantation, including rubber plantation, can be a significant carbon sink, which is important to control global climate change. Studies show that the average carbon concentration for trees components was 48.7% (Wauters et al. 2008), and some are nearly 50% (IPCC 2004). Therefore, preserving forest plantations, mainly rubber plantations, becomes an essential climate change mitigation and sustainable development strategy. In tropical countries, forest plantation serves as a tool of carbon credits utilized by countries worldwide. The carbon sink in countries like Malaysia and Indonesia are that much important for countries in Europe and America, where emissions from industrial activities are the main contributors to climate change (Houghton 2005; Vieira et al. 2005; Shin et al. 2007; Egbe and Tabot 2011). Since the carbon sink from the forest plantation ecosystem is quite significant for maintaining the environment, the addition of a carbon sink could be very favorable by utilizing the deforested land. It creates new carbon sinks which complement prior sinks from other natural forests (Garrity et al. 2006; Serigne et al. 2006).

7 Remote Sensing for Biomass Estimation

The distribution of global biomass has a unique pattern determined by the geographical characteristics of a particular area. The suitability and also the site-specific characteristic highly relate to the spatial aspect upon its availability. This makes biomass estimation challenging, especially in areas with complex forest stand structures and environmental conditions requiring accurate and consistent measurement methods (Thenkabail et al. 2004a; Lu 2006). Hence, remote sensing is considered the best approach to estimate biomass at a regional level where field data are difficult to collect (Kumar et al. 2015). It becomes the most prominent and feasible approach for generating information for biomass estimation at a reasonable cost and acceptable accuracy. It is also considered the most feasible effort because of the benefit of repeated data collection, multispectral and multi-temporal images, synoptic view, fast digital processing of large quantities of data, and compatibility with GIS (Lu et al. 2004).

Studies on biomass estimation have been published in the past few years, and most of them have described remote sensing-based estimation for forest biomass (Foody et al. 2003; Zheng et al. 2007; Goh et al. 2014; Koju et al. 2019; Kashongwe et al. 2020). In addition, the studies vary among different types of remotely sensed data and various forest locations. The distinct types of forest, such as a mature forest with the high complexity of vegetation texture up to degraded forest that changes into secondary forest planted with crop plantation, also determine these studies' results. Several types of research have explored the estimation of above-ground estimation in tropical regions based on Landsat Thematic Mapper (TM) (Sader et al. 1989; Lucas et al. 1998; Boyd 1999; Nelson et al. 2000; Steininger 2000; Foody et al. 2001, 2003) or synthetic aperture radar data (SAR) (Rignot et al. 1995; Luckman et al. 1997, 1998; Santos et al. 2002, 2003). Those have shown the difficulty of AGB estimation based only on spectral responses from optical sensor data or backscatter data. Lucas et al. (2004) comprehensively reviewed SAR data for AGB estimation in tropical forests and indicated the difficulty and data saturation problem in AGB estimation. Along with the progress of biomass estimation performance, other studies also examined the roles of textures in improving the relationship between remotely sensed data and biomass estimation (Smith et al. 2002; Zhang et al. 2003; Lu et al. 2004). They have shown that textures are also valuable for improving land cover and vegetation classification (Franklin et al. 2001; Podest and Saatchi 2002; Zhang et al. 2003). However, it is still challenging to properly select suitable textures that effectively improve the biomass estimation performance due to various attributes and site-specific characteristics.

Since it is impossible to directly measure tree crown in the middle and lower layer of multilayer forest stands, estimating biomass starts with measuring tree crown diameters on aerial photographs or high-resolution satellite images. Then, using those values to estimate tree biomass because the biomass of each tree increases as its crown size (diameter and area) increases. However, the main requirement to successfully apply this method is that the individual crown must be visible. The most suitable forest is the open forest with large crown trees where remote sensing sensors

can capture the tree's information individually. The secondary or bamboo forest is less suitable for utilizing this method because of the probability of misdetection through similar tree crowns (Hirata et al. 2012).

Although the biomass of an individual tree increases predictably with the tree crown size, which consists of diameter and area of tree cover (Kiyono et al. 2011), the measurable diameter of a tree crown depends on the ground resolution of the remote sensing imagery being used. The crown diameter of an upper layer tree can be measured on an aerial photograph or a satellite image with high ground resolution. In addition, the measurement of tree crown diameters is influenced by the availability of color information, the data acquisition time, and whether a stereo pair of images makes it easier to discriminate tree stratum and adjacent tree crowns using height information (Hirata et al. 2012). In their paper, Kumar et al. (2015) have comprehensively described the application of three different types and methods of remote sensing in forest biomass estimation.

8 Optical Remote Sensing for Biomass Estimation

Optical remote sensing data have been widely used for biomass estimation using different types of spatial and temporal resolution as well as a variety of image processing technologies (Zheng et al. 2004; Lu 2005; Muukkonen and Heiskanen 2005; Rahman et al. 2005; Li et al. 2008; Song 2013; Koju et al. 2019). The most commonly used approaches are multiple regression analysis, *k*-nearest neighbor, and neural network (Steininger 2000; Foody et al. 2003; Zheng et al. 2004; Halme et al. 2019). Optical data can be used to perform vegetation classification from the particular area where biomass is predictably generated. On the other hand, for indirect biomass estimation, optical remote sensing data are relatively used to determine vegetation parameters such as tree canopy or crown diameter using multiple regression analysis or canopy reflectance models (Phua and Saito 2003; Popescu et al. 2003). Different types of vegetation indices and band ratios derived from optical data can also be obtained to extract biomass estimation by correlating vegetation index values or band ratio values with field biomass quantification (Dong et al. 2003).

According to previous studies, at least three different spatial resolutions of optical remote sensing data can be attempted as particular tools in forest biomass estimation. First, the high-resolution data from range sensors can be applied to generate tree parameters of forest canopy structures (Kumar et al. 2015). High-resolution data from IKONOS and QuickBird have been used for generating tree crown size (Song et al. 2010) and estimate biomass as well as carbon calculation conducted in secondary forest oil palm plantation (Thenkabail et al. 2004b). These applications of high-resolution data reveal large-scale photographs and photo mensuration methods that can be used to obtain forest characteristics such as tree height, crown diameter, crown closure, and stand area (Bertolette et al. 1999; Clark et al. 2005). However, there are some limitations from this type of resolution related to the aspect of shadows and spectral separability. A study from Hirschmugl et al. (2007) suggests

that spectral variance between tree crowns creates some distress in developing expected biomass estimation models.

Furthermore, the substantial need for more extensive storage also becomes a primary issue when using high spatial resolution data, especially if the estimation model required massive broad areas with various land covers surrounding the forest. Moreover, the vegetation classifications become more complex when using the traditional pixel-based spectral classifiers (Kumar et al. 2015). However, some studies have found that integrating textual information and object-based method has successfully addressed this problem (Blaschke and Strobl 2001; Blaschke 2010). It is supported by extracting such variables of statistic spectral band, geometric features, and texture features. It has been strengthened by a study from Lu and Batistella (2005) that used variables of GLCM texture (mean, median, homogeneity, contrast, dissimilarity, entropy, second moment, and correlation) with Landsat TM bands 2–5 and 7, which found a strong relationship between textural images and biomass for a mature forest with complex vegetation structure. However, the result showed a weak relationship for a secondary forest with a simple stand structure.

Second, the medium spatial resolution also has been frequently used in biomass estimation. Linear or nonlinear regression models, k -nearest neighbors, neural networks, and vegetation canopy models are several methods that are mainly applied when using this type of resolution. Landsat TM was used to estimate tree volume and biomass using the k -nearest neighbor estimation method (Franco-Lopez et al. 2001; Halme and Tomppo 2001; Tomppo et al. 2002), whereas SPOT 5 was used to estimate above-ground forest biomass from canopy reflectance model inversion (Ghasemi et al. 2011). Some limitations related to the application of medium spatial resolution are visible when estimating the tropical area. Previous studies revealed that spectral reflectance and vegetation indices were not reliable to act as biomass predictors and the low sensitivity through the biomass changes (Steininger 2000; Foody et al., 2003). However, advanced studies have successfully added significant factors to improve sensitivity performance. The use of texture information in the change analysis process by Lu (2005) and Nichol and Sarker (2011) has favorably improved biomass estimation results in the tropical forest. In other cases, incorporating spectral variables with age into Landsat TM of the forest also positively influenced estimating forest biomass. Additionally, vegetation indices have been advantageous in minimizing spectral variability when measuring biophysical properties for biomass estimation, especially in complex vegetation stand structures. The utilization of vegetation indices strengthened the combination of image texture and spectral reflectance for improving biomass estimation performance.

Lastly, coarse-spatial resolution AVHRR NDVI data have been used to estimate biomass in temperate woody biomass in Canada, Finland, Norway, Russia, Sweden, and the USA (Dong et al. 2003). Numerous spectral types from MODIS data have successfully improved biomass estimation accuracy at the continental or global scale. For example, a recent study in the Amazon basin conducted by Saatchi et al. (2007) and in the USA by Blackard et al. (2008) used MODIS data to compose tree-based models and metrics combined with radar data, climate, topography, and vegetation maps. MODIS data also shows positive performance for biomass

estimation when integrated with precipitation, temperature, and elevation in the national forest of California, USA. On the other hand, compared to the other two kinds of spatial resolution, this type of optical sensor has more complex limitations due to the occurrence of the mixed pixel, a saturation of spectral data at high biomass density, and the mismatch between the size of plots and pixel (Kumar et al. 2015). As a result, some studies utilized coarse and medium resolution combined with different modeling approaches to attain preferable biomass estimation results for more expansive areas (Hame et al. 1997; Tomppo et al. 2002).

In general, optical sensor data in 2D types are considered more appropriate for extracting vegetation structure such as vegetation types and canopy cover but less effective for estimating vertical aspects such as canopy height, which become essential predictors for biomass estimation (Kumar et al. 2015). Studies found these optical sensor data have prospected opportunity to improve the viewing capability, hence establishing more accurate canopy height estimation (St-Onge et al. 2008; Ni et al. 2014). More accuracy has been shown from 3D data generated from SPOT 5, which adequately mapped the tree height, stem diameter, and forest tree volume (Reinartz et al. 2005; Wallerstein et al. 2010). Therefore, it can be concluded that high-resolution data can be used extensively as an alternative to deriving height vegetation information compared to other types of data.

9 Radar Remote Sensing for Biomass Estimation

Recently, the use of synthetic aperture radar (SAR) data for biomass estimation has been rapidly increasing, especially in the area where frequent cloud cover is clearly discovered. It results in the difficulty of the optical sensor to obtain high-quality images. SAR sensors can catch various data within all weather and light conditions, penetrating through vegetation in different degrees and generating information of structure distribution in 3D format (Zhou et al. 2009). Several studies have shown that the utilization of SAR data mainly focuses on developing algorithms for classification and biomass estimation in the closed-canopy forest (Lucas et al. 2006, 2010) and complex subtropical forest (Sarker et al. 2012). The available SAR sensors widely used for remote sensing studies are TerraSAR-X, and the Advanced Land Observing Satellite and Phased Array L-band SAR (ALOS-PALSAR). Those SAR data can be retrieved to examine the relationship between ground-based biomass estimation and single-channel data (Zhou et al. 2009).

SAR is an active sensor that transmits microwave pulses to the earth's surface and then detects the reflected pulses back from the earth's surface. The backscattering coefficient is derived from the reflected signals (Shimada 2010). The correlation between the backscattering coefficient and biomass is high for long-wavelength (L band, about 23 cm, but saturation occurs at a biomass of about 100 t/ha³). For comparison, the above-ground biomass of mature tropical forests can be as high as 400–500 t/ha and usually exceeds 200 t/ha. For this reason, it is not easy to estimate the biomass of a mature forest. However, the method is suitable for mapping biomass changes over a large forest area, recovering from some large-scale disturbance (e.g.,

slash-and-burn or plantation agriculture). In hilly terrain, topographic distortion should be corrected (Hirata et al. 2012).

Since the SAR sensor can detect both horizontal (H) and vertical (V) components from backscatter radiation, four possible polarization configurations are applied within this sensor system. First, HH consists of horizontal transmit and horizontally received, which are available on ERS satellite. Vertical transmit and vertically received is called VV that belongs to the RADARSAT satellite. The other is a combination of previous polarization: HV from the horizontal transmission and vertical reception, and VH from the vertical transmission and horizontal reception. The pattern of those polarization components depends on the states from detected radar signals (Kumar et al. 2015). The backscatter radar of P and L bands has particularly shown a positive correlation with various primary forest parameters such as tree age, tree height, DBH, basal area, and above-ground dry biomass (Imhoff et al. 2000; Castel et al. 2002; Santos et al. 2002; Sun et al. 2002).

Studies have discovered that L-band is the most useful for forest biomass estimation (Le Toan et al. 1992). However, those SAR bands still showed the correlation between biomass and forest parameters. For instance, a study conducted by Harrell et al. (1997) used SAR C and L band multi-polarization for biomass estimation in the southern USA and found L band HH data is essentially significant to obtain accurate estimation. Furthermore, they also found that the addition of C band HH and HV significantly improves the estimation performance. For the area of after-logged forest, JERS-1/JERS is found useful to conduct forest biomass estimation (Kuplich et al. 2000) and in the mountainous area (Santos et al. 2002). While in the tropical forest, RADARSAT has been tested for biomass estimation and yielded satisfactory results, although there are some problems in data saturation, especially when reaching complex forest stand structures (Sarker et al. 2012). Lastly, PALSAR data indicate a promising ability to map forest with encouraging results in a more complex forest area like Amazon and Siberia (Lucas and Armston 2007).

According to Zhou et al. (2009), there are several advantages of using radar compared to optical sensors for biomass estimation. Radar sensor performs freely from solar radiation variations caused by high penetration through cloud and haze. It is essential when applied in tropical areas. Furthermore, it can actively manage the sensors and power outlet, thus ensuring consistent transmit and return rates. However, radar data are less applicable in regional studies due to the small swath width, high costs of airborne acquisitions, and limited coverage (Lucas et al. 2010).

10 LiDAR Remote Sensing for Biomass Estimation

LiDAR is a relatively advanced new technology developed to resolve spatial analysis limitations using previous 2D remote sensing. It can transform two-dimensional into third-dimensional data, which simplifies the analytical process of remote sensing. LiDAR instruments can detect the vertical distribution and canopy surface (Dubayah and Drake 2000; Harding et al. 2001), which has become the most efficient technology for structural assessment since it can capture landscape

structural data for more accurate biomass estimation (Zhao et al. 2009). Previous studies have shown a robust relationship between LiDAR metrics and above-ground biomass that enhance the ability to estimate forest biomass (Lefsky et al. 1999; Means et al. 1999). Moreover, LiDAR also gained more sophisticated technology in waveform digitizing sensors, increasing the image quality captured in a more complex forest structure (Lefsky et al. 1999, 2002; McGlinchy et al. 2014). However, some restrictions have also been adhered to when using LiDAR for field application: (1) fewer simple data analysis that requires advanced image processing knowledge and skill and (2) more expensive data acquisition process which covers smaller detection areas. Due to these restrictions, few and very specific studies can be conducted using this type of sensor, and hence it is not widely applied for biomass estimation in a larger area (Kumar et al. 2015).

As mentioned in study results from passive sensors, the problem of attaining optimum detection emerges severely in mature and complex structure forests. Most of the sensors failed to correlate the forest structure and biomass variables (Lu 2006). However, LiDAR data can estimate structure variables such as height, crown size, and stem volume through vertical appearance. There are two types of LiDAR for conducting sensor operations. Todd et al. (2003) mention that the first type is discrete return LiDAR (small footprint), and the second is full-waveform LiDAR (large footprint). Both are calibrated to operate in the 900–1064-nm wavelengths where vegetation reflectance is the highest. The discrete return LiDAR has two approaches: (1) area-based and (2) individual tree-based methods (Chen 2013). Area-based methods develop statistical models to relate biomass with metrics derived from a LiDAR point cloud at the plot or stand level. This model is subsequently applied to accurately estimate the entire study area (Thomas et al. 2006; Gleason and Im 2012). Height metrics are the most frequently utilized parameter implemented in area-based LiDAR, which can be computed from different variables such as the first and all returns or by a grid of the canopy heights (Lim et al. 2003; Asner et al. 2009).

On the other hand, the individual tree-based method applies the approach by identifying the individual tree crown then generating the information from the LiDAR point cloud. The biomass estimation can be attained by processing the tree height or crown size information related to the amount of biomass within the forest. Both the area-based and individual-based approaches need calibration and field validation, but the individual approach requires less validation because the data needed are only for a few numbers of the tree for data sampling.

Like other sensors, the biomass estimation generated from LiDAR is also derived from some structure variables. The most widely used is tree height which several studies have utilized to obtain biomass estimation. García et al. (2010) conducted a biomass model based on LiDAR height or intensity, both used separately or combined. They found that the normalized intensity-related variables are more helpful in explaining the biomass estimation than the other variables. Other studies from Lefsky et al. (2005) and Popescu et al. (2011) revealed the broad application of space-borne LiDAR for accurate biomass estimation. A summary of the remote

sensing methods, data types, and some examples for forest biomass estimation is shown in Table 1.

11 The Allometric Equation for Biomass Estimations

Scaling equations that relate to the sizes of different parts of a tree are called allometric equations. Recently, the allometric equation has been considered a powerful tool for assessing tree weight from independent forest variables. The equations are developed through destructive methods and field sampling that applied trunk diameter, age, type of species, wood density, and total height assessment. Several cut-down trees were taken and dried up to a certain temperature to attain dry weight. This dry weight is considered as an actual biomass amount. The following step uses the data sampling from the forest site to be statistically analyzed, thus obtaining the needed equation (Sone et al. 2014). The results will be varied across the site-specific or species-specific up to different climate, forest types, and methods to execute the field sampling.

However, there is some limitation when applying allometric equations, especially when encountering various variables with different site condition. The results often show several types of relationships among the variables, hence generating less general interpretation to be applied in other common studies. It is important to choose an allometric equation suitable for the region's environmental conditions and the forest type, such as evergreen or deciduous (Cairns et al. 1997; Mokany et al. 2006). Furthermore, it is also too complicated and costly to utilize a series of allometric equations for each tree species and forest site. Therefore, it is essential to develop a general allometric equation that can be applied in various forest site conditions and geographical locations. Eventually, the general equation can be obtained using common predictors of tree structure based on biological or physical theories (Komiyaama et al. 2005).

One of the most referred biomass estimations for tropical trees is the allometric equation developed by Chave et al. (2005), updated in Chave et al. (2014). They mainly analyzed the global database of directly harvested trees at 58 sites, spanning a wide range of climatic conditions and vegetation types, with the indictable effect of the region or environment factors. According to Chave (2005), the most critical AGB predictors are trunk diameter (D), wood specific gravity or wood density, total height (H), and forest type (dry, moist, or wet). Since, in particular conditions, total height data is challenging to obtain, or the availability is less accurate to reveal the actual conditions of tree's height, Chave's equations focused on two conditions of height data availability, with or without height data. In a particular situation, tree height may improve the model's quality but ignore the total height and might be helpful when predicted to cause some bias. In addition, when utilizing the equations into a much broader range of vegetation, wood density is a significant predictor for AGB estimation (Chave et al. 2014). Chave's model restricts the model only for the tropical forest with broadleaf tree species, excluding plantations or other manageable forests.

Table 1 Summary of the remote sensing methods, data types, and some examples for forest biomass estimation

No.	Methods	Data used	Characteristics	Examples
1	Methods based on the spatial resolution data (<5 m) (parametric classifiers, MLC, MDM, etc.; nonparametric classifiers, ISODATA, <i>k</i> -means)	Aerial photographs, IKONOS, QuickBird, GeoEye, WorldView	Per-pixel level	Asner et al. (2002), de Jong et al. (2003), Thenkabail et al. (2004b), Song et al. (2010)
2	Methods based on medium-spatial resolution data (10–100 m) (linear, exponential, and multiple regression analysis, neural network, <i>k</i> -nearest neighbor method, productivity model)	Landsat 4 5 7 TM/enhanced TM+, Systeme Probatoire D'Observation de la Terre (SPOT)	Per-pixel level	Franco-Lopez et al. (2001), Foody et al. (2001), Halme and Tomppo (2001), Tomppo et al. (2002), Soenen et al. (2010)
3	Methods based on coarse-spatial resolution data (>100 m) (regression models and artificial neural network (ANN), <i>k</i> -nearest neighbor, statistical model)	IRS-1C WiFS, AVHRR, MODIS, SPOT, vegetation	Per-pixel level	Hame et al. (1997), Barbosa et al. (1999), Tomppo et al. (2002), Dong et al. (2003), Baccini et al. (2004), Saatchi et al. (2007), Baccini et al. (2008)
4	Methods based on radar data (regression model, canopy height model, multiplicative models)	SIR-C, SAR-L JERS-1 SAR-L, AeS-1 SAR-P, InSAR, airborne laser, large and small footprint LiDAR	Per-pixel level	Le Toan et al. (1992), Santos et al. (2003), Lefsky et al. (2005), Asner et al. (2009), Popescu et al. (2011), Gleason and Im (2012), Chen (2013)
5	Methods based on image fusion techniques (intensity hue and saturation (HIS), Brovey, PCA)	Multispectral and panchromatic		Chen and Stow (2003), Amarsaikhan and Douglas (2004), Choi et al. (2005)
6	Vegetation index-based method (NDVI, ratio)		Object-level	Elvidge and Chen (1995), Blackburn and Steele (1999), Lu et al. (2004), Mutanga and Skidmore (2004)

(continued)

Table 1 (continued)

No.	Methods	Data used	Characteristics	Examples
7	Object-based (segmentation and classification, ANNs, <i>k</i> -nearest neighbor, statistical models, random forest)		Object-level	Blaschke and Strobl (2001), Lu and Batistella (2005), Goodchild et al. (2007), Blaschke (2010)
8	Advanced classifiers spectral mixture analysis (SVM), random forest, support vector machine (SVM)	Multispectral	Per-pixel level	Dennison and Roberts (2003), Lu et al. (2004), Calvao and Palmeirim (2004), Lu and Batistella (2005)

Adapted from Kumar et al. (2015)

Unlike the tropical forest, which contains hundreds of tree species, and diverse trees' physical appearance, plantation or manageable forest has a similar condition for tree age, type of species, and forest management practice. Thus, the appropriate model will be slightly or much different from biomass equations for tropical forests (Brown 1997; Chave et al. 2005, 2014; Houghton 2005). Previous studies upon biomass estimation with and carbon sequestration have been conducted in mangroves (Sherman et al. 2003; Komiyama et al. 2005), oil palm (Asari et al. 2013), and rubber plantations (Yang et al. 2005; Wauters et al. 2008; Sone et al. 2014). Specific allometric equations also have been developed from those types of plantations. Biomass estimation in rubber plantations strongly engages the tree age as an important variable since it determines the trunk diameter and total height (Wauters et al. 2008; Sone et al. 2014). Results from Sone et al. (2014) show that the biomass estimation relationship with tree age increased consistently from 5% at the age of 3 years to 40% at the age of 20 years in rubber tree.

A biomass expansion factor converts the trunk volume into the volume of the whole tree, including branches, leaves, and roots. This factor depends on the tree species and the forest stand age. That value is converted to carbon stocks by multiplying it by 0.5. Since species, forest age, and forest management practices are constant in the case of a plantation, it can be assumed that tree size and growth conditions are also constant. In this case, the biomass expansion factor can be used as follows:

$$C = [V \times WD \times BEF]^* (1 + R) \times CF$$

Here, *C* is carbon stock per unit area (t-C/ha), *V* is stand volume (m³/ha), *WD* is wood density (t/m³), *BEF* is the biomass expansion factor, and *CF* is the carbon content ratio (t-C/m³).

Table 2 lists the most commonly used biomass allometric equations based on a destructive method. Some of them were conducted by taking the area of tropical forest in Southeast Asian countries and focusing on primary and secondary forest.

Table 2 List of most common used biomass allometric equations cased on destructive method

No.	Source	Allometric equations	Site
1	Kato et al. (1978)	$1/H = 1/(2.0 * D) + 1/61$	Primary forest, Peninsular Malaysia
		From the values of D and H the dry mass of stem, branches, and leaves of the tree is estimated	
		$M_s = 0.0313 * (D^2 H)^{0.9733}$	
		$M_b = 0.136 * M_s^{1.070}$	
		$1/M_1 = 1/(0.124 M_s^{0.794}) + 1/125$	
2	Ketterings et al. (2001)	$\ln(Wt) = 2.59 \times \ln(D) - 2.75$	Secondary forest, Sumatera, Indonesia
3	Chave et al. (2005)	$Wt = \rho * \exp(-1499 + 2.148 * \ln(D) + 0.207 * (\ln(D))^2 - 0.0281 * (\ln(D))^3)$	Pasoh 50 ha plots and other Center for Tropical Forest Science (CTFS) plots
4	Basuki et al. (2009)	$\ln(Wt) = 2.196 \times \ln(D) - 1.201$	Secondary forest, Kalimantan, Indonesia
		$\ln(M_s) = -1.472 + 2.180 * \ln(D)$	
		$\ln(Wt) = -0.097 + 1.361 * \ln(D)$	
		$\ln(Wt) = -1.392 + 1.250 * \ln(D)$	
5	Kenzo et al. (2009)	$Wt = 0.0829 \times D^{2.43}$	Secondary forest, Sarawak, Malaysia
6	Sone et al. (2014)	$Wt = 0.144 \times D^{2.40}$	Rubber plantation forest, north Sumatera, Indonesia
		$Wt = 279 \times (D^2 \times H)^{0.867}$	
7	Wauters et al. (2008)	$\frac{\exp(-6.748 + 2.723 \times \ln(C_{170}))}{0.487}$	Rubber tree plantation in Western Ghana and Brazil
8	Asari et al. (2013)	$71.797 H_{palm} - 7.0872$	Oil palm plantations in south Sumatera, Indonesia
		$\pi r^2 H_{palm} \rho$	
9	Tang et al. (2003)	$Wt = 0.1190219 \times (D^2 H)^{0.6052483}$	Secondary tropical forest, Xishuangbanna
10	Brown (1997)	$Wt = \exp(-2.134 + 2.530 \times \ln(D))$	Tropical forest
11		$C \text{ stocks: } W \times Fc$	
		Fc is a standard conversion factor of 0.5 kg C kg^{-1}	

Note: H is the total tree height; D is the stem diameter at breast height (dbh); M_s , M_b , and M_1 denote the dry mass of stem, branches, and leaves, respectively; Wt is the above-ground biomass of standing trees, and ρ is the wood density. (Adapted from Hamdan et al. 2014)

However, the recently updated models have been elaborated on the plantation forest, which possesses different tropical primary and secondary forest characteristics.

Finally, there are some critical reviews for forest biomass estimation models, common mistakes, and corrective. A large degree of uncertainty exists in estimated forest biomass, carbon stocks, and fluxes (Somogyi et al. 2007; van Breugel et al. 2011; Clark and Kellner 2012; Ahmed et al. 2013; Molto et al. 2013). Lack of consensus on definitions, methodological inconsistencies, and assumptions also lead

to widely differing results even among similar studies (Somogyi et al. 2007; Clark and Kellner 2012). In addition, Sileshi (2014) explained that the common mistake in developing biomass allometric equations was the arbitrary choice of analytical methods, inadequate model diagnosis, ignoring collinearity, uncritical use of model selection criteria, and uninformative reporting of results. In other cases, errors in parameter estimates were not checked, and model uncertainty was ignored when interpreting and explaining the results. It is crucial to choose a reasonably simple functional expression that involves less non-interpretable parameters, to minimize the risks of mistakes when applying or developing allometric equations. It can be simpler equations with fewer parameters and “independent” predictors and without polynomial terms. As expected, by alerting those common mistakes, the far-reaching consequences of biomass allometric equations will be more accountable.

12 Remote Sensing for Rubber Trees Above-Ground Biomass (AGB)

There is a limited number of studies focusing on remote sensing for rubber tree AGB estimation. Most of the studies elaborate primary tropical forest, consisting of mixed vegetation, broader leaves, and different tree ages. On the other hand, the rubber tree biomass estimation is discussed through allometric equations generated from destructive sampling in several forest types (Brown 1997; Wauters et al. 2008; Basuki et al. 2009; Sone et al. 2014). Yasen and Koedsin (2015) had precisely elaborated this topic in Thailand. They used the multispectral bands of high spatial resolution satellite imagery for estimating rubber tree biomass at Phuket, Thailand. The multispectral bands of WorldView-2 are used as the input variables for multiple linear regression and artificial neural network to construct the model of rubber tree AGB.

The application of remote sensing for capturing forest structure extensively depends on spectral bands combinations that formed vegetation indices. It is also applied when performing specifically for rubber tree plantations. A previous study (Yakham et al. 2012) reported that normalized difference vegetation index (NDVI) derived from SMMS satellite images could classify the rubber stand age with reasonable accuracy. Likewise, Sopharat (2009) found that soil-adjusted vegetation index (SAVI) derived from SPOT-5 was strongly related to the leaf area index (LAI) of the rubber tree. Several studies of other vegetation types found that vegetation index such as NDVI correlates with biomass and LAI (Wang et al. 2005; Heiskanen 2006; Devagiri et al. 2013).

Besides, Lu (2005) has clearly explained the AGB model and vegetation indices based on his study. The TM spectral responses are more suitable for AGB estimation in sites with relatively simple forest stand structures than sites with complicated forest stand structures. On the other hand, textures appear more critical than spectral responses, and textures improve AGB estimation performance. Biophysical conditions are largely affecting AGB estimation performance. Therefore, many remote sensing variables, including spectral signatures, vegetation indices,

transformed images, and textures, may become potential variables for AGB estimation. However, not all variables are required because some are weakly related to AGB or highly correlated. Hence, selecting the most relevant variables is critical for developing the AGB estimation model. In general, vegetation indices can partially reduce the impacts on reflectance caused by environmental conditions and shadows, thus improving the correlation between AGB and vegetation indices, especially in those sites with complex vegetation stand structures (Lu et al. 2004). Since rubber tree plantation has a less complex structure, it is expected to be more straightforward in identifying suitable textures that are strongly related to AGB but weakly related to each other.

Not only important to generate a comprehensive rubber plantation map, an evident and reliable vegetation structure that is strongly related to AGB estimation might also be discovered from a remote sensing approach. The difficulty of mapping rubber plantations from optical images mainly focuses on the effect of frequent cloud cover on tree delineation and the similarity of spectral characteristics between rubber trees and another forest type. Compared to an optical sensor, SAR can successfully penetrate clouds above the tropical forest through tree canopies, especially for longer wavelengths (L-band SAR) (Baghdadi et al. 2009). When the SAR sensor transmits the radar pulse, the transmitted energy is called forward scattering, and the returned signal after interacting with the forest is called backscatter. It is much influenced by the electric and structural properties of the forest structure, consisting of canopy, leaves, branches, and trunk of the tree. In addition, the forest medium can be considered a homogenous medium containing a large number of scatters of a single category. The backscatter value depends mainly on the backscatter and forward scatter function's orientation, size, and dielectric constant (Chen et al. 2009). In addition, Dong et al. (2012) found that the use of cloud-free PALSAR data supported robust mapping, and the integration of PALSAR 50-m forest maps and 250-m MODIS NDVI phenology can map fractional cover of rubber plantation extent accurately.

Two groups of studies have used optical remote sensing data to delineate rubber plantations. The first group focuses on using spectral signatures with cluster analysis and traditional classifiers to identify and map rubber plantations, such as Mahalanobis classifier (Li and Fox 2011, 2012). The challenge from this group is that rubber trees have similar spectral characteristics with the natural tropical forests, mainly secondary forests, as observed by single-date multispectral data during peak growing season (Li and Fox 2011). The second group of studies relies on the temporal signals of optical images to delineate rubber trees. Recently Chen et al. (2010) and Tan et al. (2010) utilized the intra-annual temporal profile of rubber plantations to delineate them in Hainan, China. This approach relied on phenological features of rubber plantations. However, the spatial resolution from low-res imageries sometimes limits its suitability for rubber plantation mapping in fragmented landscapes. In addition, the frequent cloud cover in tropical regions makes it challenging to construct consistent year-long time series with reliable data quality.

On the other hand, the allometric equation faces some challenges in estimating the rubber tree biomass appropriately. As Wauters et al. (2008) explained, site-specific allometric equations were used to estimate the carbon content of the tree's components correctly. The inclusion of the clone type and total height only slightly improved the model. The comprehensive understanding of tree components yet vegetation structure becomes the substantial basis for constructing the fit model. It is also reported by Sone et al. (2014) in their study toward rubber tree AGB in Sumatera, Indonesia, that emphasizes the critical role of stand parameter and tree age as significant input variables that are strongly related to AGB biomass. Estimation AGB is based on the volume and structure of the trees, which considered the diameter at the breast height (DBH) and height of the tree (H) as the significant parameters. The absence of the tree species-specific biomass equation will be addressed by applying the wood density parameter, which considers the species-specific volume equation with the forest type developed by Chave et al. (2005) for moist forest stands. As supported by Komiyama (2005), the measurement of trunk diameter or girth is more practical than other parameters, especially for those working in closed and tall canopies where tree height is difficult to measure accurately.

13 Conclusion

Comprehensive studies on the uses of remote sensing and allometric equation have been conducted to highlight the existence of crop plantations for biomass contribution to the carbon cycle. However, the absence of similar previous research realizes the current study is the prior work in developing such an inventory for both rubber tree biomass models combined with remote sensing techniques. As elaborated among the literature and research questions, the missing elements are expected to be found in further study. It is also attributed to the other focuses and methodologies, which eventually fill the gaps in this present work.

In fact, the combination of variables developed by previous allometric models and remote sensing approaches is aimed to generate updated studies that reveal the biomass estimation using remote sensing technique, specifically for rubber tree plantations in tropical areas. Several inevitable challenges, such as site-specific or species-specific characteristics, remote sensing imagery availability, limited field sampling data, and un-fitted allometric equation, may have hindered the AGB estimation performance. However, comprehensive elaboration through some studies and previous research highlights the stand parameters like trunk diameter and height, age tree from vegetation structure combined with spectral bands, backscattered signal, and vegetation indices, to be appropriately applied as biomass predictors and input variables. Remote sensing data will support land management decisions and land-use policies. The information retrieved from remotely sensed data not just become an essential indicator for monitoring plantation areas and observing biomass, assessing carbon stocks, and predicting yield gain or loss. Remote sensing is

expected to grow and continue to play an important role in managing global rubber plantations in the future.

References

- Adisurjosatyo F, Nugroho YS (2012) Performance gasification per batch rubber wood in conventional updraft gasifier. *J Eng Appl Sci* 7:494–500
- Ahmed R, Siqueira P, Hensley S, Bergen K (2013) Uncertainty of forest biomass estimates in north temperate forests due to allometry: implications for remote sensing. *Remote Sens* 5:3007–3036
- Amarsaikhan D, Douglas T (2004) Data fusion and multisource image classification. *Int J Remote Sens* 25:3529–3539
- Anaya JA, Chuvieco E, Palacios-Orueta A (2009) Aboveground biomass assessment in Colombia: a remote sensing approach. *For Ecol Manag* 257:1237–1246
- Asari N, Suratman MN, Jaafar J, Khalid MM (2013) Estimation of aboveground biomass for oil palm plantations using allometric equations. In: 4th interence conference on biology, environment and chemistry, Singapore, IPCBEE
- Asner GP, Palace M, Keller M, Pereira R Jr, Silva JN, Zweede JC (2002) Estimating canopy structure in an Amazon Forest from laser range finder and IKONOS satellite observations. *Biotropica* 34:483–492
- Asner GP, Hughes RF, Varga TA, Knapp DE, Kennedy-Bowdoin T (2009) Environmental and biotic controls over aboveground biomass throughout a tropical rain forest. *Ecosystems* 12:261–278
- Asrar GQ, Fuchs M, Kanemasu ET, Hatfield JL (1984) Estimating absorbed photosynthetic radiation and leaf area index from spectral reflectance in wheat. *Agron J* 76:300–306
- Baccini A, Friedl MA, Woodcock CE, Warbington R (2004) Forest biomass estimation over regional scales using multisource data. *Geophys Res Lett* 31:L10501
- Baccini A, Laporte N, Goetz SJ, Sun M, Dong H (2008) A first map of tropical Africa's above-ground biomass derived from satellite imagery. *Environ Res Lett* 3:045011
- Baghdadi N, Boyer N, Todoroff P, El Hajj M, Bégué A (2009) Potential of SAR sensors TerraSAR-X, ASAR/ENVISAT and PALSAR/ALOS for monitoring sugarcane crops on Reunion Island. *Remote Sens Environ* 113:1724–1738
- Barbosa PM, Stroppiana D, Grégoire JM, Cardoso Pereira JM (1999) An assessment of vegetation fire in Africa (1981–1991): burned areas, burned biomass, and atmospheric emissions. *Global Biogeochem Cycles* 13:933–950
- Basuki TM, van Laake PE, Skidmore AK, Hussin YA (2009) Allometric equations for estimating the above-ground biomass in tropical lowland Dipterocarp forest. *For Ecol Manag* 257:1684–1694
- Bertolette DR, Spotskey DB, Gollberg, GE (1999) Fuel model and forest type mapping for FARSITE input. In: The joint fire science conference and workshop. University of Idaho and International Association of Wildland Fire, Boise
- Blackard JA, Finco MV, Helmer EH, Holden GR, Hoppus ML, Jacobs DM, Lister AJ, Moisen GG, Nelson MD, Riemann R, Ruefenacht B, Salajano D, Weyermann DL, Winterberger KC, Brandeis TJ, Czaplowski RL, McRoberts RE, Patterson PL, Tymcio RP (2008) Mapping US forest biomass using nationwide forest inventory data and moderate resolution information. *Remote Sens Environ* 112:1658–1677
- Blackburn GA, Steele CM (1999) Towards the remote sensing of matorral vegetation physiology: relationships between spectral reflectance, pigment, and biophysical characteristics of semiarid bushland canopies. *Remote Sens Environ* 70:278–292
- Blaschke T (2010) Object based image analysis for remote sensing. *ISPRS J Photogramm Remote Sens* 65:2–16

- Blaschke T, Strobl T (2001) What's wrong with pixels? Some recent developments inter-facing remote sensing and GIS. *GeoBIT/GIS* 6:12–17
- Boyd DS (1999) The relationship between the biomass of Cameroonian tropical forests and radiation reflected in middle infrared wavelengths (3.0–5.0 μm). *Int J Remote Sens* 20:1017–1023
- Boyle G (1996) *Renewable energy: power for a sustainable future*, vol 2. Oxford University Press, Oxford
- Brahma B, Nath AJ, Das AK (2016) Managing rubber plantations for advancing climate change mitigation strategy. *Curr Sci* 110:2015
- Brown S (1997) Estimating biomass and biomass change of tropical forests: a primer, vol 134. Food & Agriculture Organization, Rome
- Cairns MA, Brown S, Helmer EH, Baumgardner A (1997) Root biomass allocation in the world's upland forests. *Oecologia* 111:1–11
- Calvao T, Palmeirim JM (2004) Mapping Mediterranean scrub with satellite imagery: biomass estimation and spectral behaviour. *Int J Remote Sens* 25:3113–3126
- Castel T, Guerra F, Caraglio Y, Houllier F (2002) Retrieval biomass of a large Venezuelan pine plantation using JERS-1 SAR data. Analysis of forest structure impact on radar signature. *Remote Sens Environ* 79:30–41
- Chave J, Andalo C, Brown S, Cairns MA, Chambers JQ, Eamus D, Fölster H, Fromard F, Higuchi N, Kira T, Lescure JP, Nelson BW, Ogawa H, Puig H, Riéra B, Yamakura T (2005) Tree allometry and improved estimation of carbon stocks and balance in tropical forests. *Oecologia* 145:87–99
- Chave J, Réjou-Méchain M, Búrquez A, Chidumayo E, Colgan MS, Delitti WB, Duque A, Eid T, Fearnside PM, Goodman RC, Henry M, Martínez-Yrizar A, Mugasha WA, Muller-Landau HC, Mencuccini M, Nelson BW, Ngomanda A, Nogueira EM, Ortiz-Malavassi E, Péliissier R, Ploton P, Ryan CM, Saldarriaga JG, Vieilledent G (2014) Improved allometric models to estimate the aboveground biomass of tropical trees. *Glob Change Biol* 20:3177–3190
- Chen Q (2013) LiDAR remote sensing of vegetation biomass. In: Weng Q, Wang G (eds) *Remote sensing of natural resources*. CRC Press, Boca Raton, pp 399–420
- Chen D, Stow D (2003) Strategies for integrating information from multiple spatial resolutions into land-use/land-cover classification routines. *Photogramm Eng Remote Sens* 69:1279–1287
- Chen E, Li Z, Ling F, Lu Y, He Q, Fan F (2009) Forest volume density estimation capability of ALOS PALSAR data over hilly region. In: *Proceedings of the international workshop on science and applications of SAR polarimetry and polarimetric interferometry, PollinSAR*, 26–30 January 2009, Frascati, Italy
- Chen H, Chen X, Chen Z, Zhu N, Tao Z (2010) A primary study on rubber acreage estimation from MODIS-based information in Hainan. *Chin J Trop Crops* 31:1181–1185
- Choi M, Kim RY, Nam MR, Kim HO (2005) Fusion of multispectral and panchromatic satellite images using the curvelet transform. *IEEE Geosci Remote Sens Lett* 2:136–140
- Clark DB, Kellner JR (2012) Tropical forest biomass estimation and the fallacy of misplaced concreteness. *J Veg Sci* 23:1191–1196
- Clark ML, Roberts DA, Clark DB (2005) Hyperspectral discrimination of tropical rain forest tree species at leaf to crown scales. *Remote Sens Environ* 96:375–398
- Crane CE, Novak JT (2001) Carbon addition reduced lag time for 2,4,6-trichlorophenol degradation. *J Environ Eng* 127:760–763
- De Jong SM, Pebesma EJ, Lacaze B (2003) Above-ground biomass assessment of Mediterranean forests using airborne imaging spectrometry: the DAIS Payne experiment. *Int J Remote Sens* 24:1505–1520
- Dennison PE, Roberts DA (2003) End member selection for multiple end member spectral mixture analysis using end member average RMSE. *Remote Sens Environ* 87:123–135
- Devagiri GM, Money S, Singh S, Dadhawal VK, Patil P, Khaple A, Devakumar AS, Hubballi S (2013) Assessment of above ground biomass and carbon pool in different vegetation types of south western part of Karnataka, India using spectral modeling. *Trop Ecol* 54:149–165

- Dong J, Kaufmann RK, Myneni RB, Tucker CJ, Kauppi PE, Liski J, Buermann W, Alexeyev V, Hughes MK (2003) Remote sensing estimates of boreal and temperate forest woody biomass: carbon pools, sources, and sinks. *Remote Sens Environ* 84:393–410
- Dong J, Xiao X, Sheldon S, Biradar C, Xie G (2012) Mapping tropical forests and rubber plantations in complex landscapes by integrating PALSAR and MODIS imagery. *ISPRS J Photogramm Remote Sens* 74:20–33
- Dubayah RO, Drake JB (2000) Lidar remote sensing for forestry. *J For* 98:44–46
- Easterly JL, Burnham M (1996) Overview of biomass and waste fuel resources for power production. *Biomass Bioenergy* 10:79–92
- Egbe AE, Tabot PT (2011) Carbon sequestration in eight woody non-timber forest species and their economic potentials in southwestern Cameroon. *Appl Ecol Environ Res* 9:369–385
- Egbe AE, Tabot PT, Fonge BA, Bechem E (2012) Simulation of the impacts of three management regimes on carbon sinks in rubber and oil palm plantation ecosystems of South-Western Cameroon. *J Ecol Nat Environ* 4:154–162
- Elvidge CD, Chen Z (1995) Comparison of broad-band and narrow-band red and near-infrared vegetation indices. *Remote Sens Environ* 54:38–48
- FAO (2005) Grasslands of the world plant production and protection series. Food and Agriculture Organization of the United Nations, Rome
- FAO (2012) State of the World's forests, 10th edn. Food and Agriculture Organization of the United Nations, Rome
- FAO (2020) FAOSTAT statistical database 2020. <http://www.fao.org/faostat/en/?#data/QC>. Accessed 11 Mar 2022
- Foody GM, Cutler ME, Mcmorrow J, Pelz D, Tangki H, Boyd DS, Douglas I (2001) Mapping the biomass of Bornean tropical rain forest from remotely sensed data. *Glob Ecol Biogeogr* 10:379–387
- Foody GM, Boyd DS, Cutler ME (2003) Predictive relations of tropical forest biomass from Landsat TM data and their transferability between regions. *Remote Sens Environ* 85:463–474
- Fox J, Castella JC, Ziegler AD, Westley SB (2014) Expansion of rubber mono-cropping and its implications for the resilience of ecosystems in the face of climate change in Montane Mainland Southeast Asia. *Glob Environ Res* 18:145–150
- Franco-Lopez H, Ek AR, Bauer ME (2001) Estimation and mapping of forest stand density, volume, and cover type using the k-nearest neighbors' method. *Remote Sens Environ* 77: 251–274
- Franklin J, Simons DK, Beardsley D, Rogan JM, Gordon H (2001) Evaluating errors in a digital vegetation map with forest inventory data and accuracy assessment using fuzzy sets. *Trans GIS* 5:285–304
- Gao J, Zhang L (2021) Does biomass energy consumption mitigate CO₂ emissions? The role of economic growth and urbanization: evidence from developing Asia. *J Asian Pac Econ* 26:96–115
- García M, Riaño D, Chuvieco E, Danson FM (2010) Estimating biomass carbon stocks for a Mediterranean forest in central Spain using LiDAR height and intensity data. *Remote Sens Environ* 114:816–830
- Garrity D, Okono A, Grayson M, Parrott S (2006) World agroforestry into the future. World Agroforestry Centre, Nairobi. 196 p
- Gasparri NI, Parmuchi MG, Bono J, Karszenbaum H, Montenegro CL (2010) Assessing multi-temporal Landsat 7 ETM+ images for estimating above-ground biomass in subtropical dry forests of Argentina. *J Arid Environ* 74:1262–1270
- Ghasemi N, Sahebi MR, Mohammadzadeh A (2011) A review on biomass estimation methods using synthetic aperture radar data. *Int J Geomat Geosci* 1:776–788
- Gibbs HK, Brown S, Niles JO, Foley JA (2007) Monitoring and estimating tropical forest carbon stocks: making REDD a reality. *Environ Res Lett* 2:045023
- Gleason CJ, Im J (2012) Forest biomass estimation from airborne LiDAR data using machine learning approaches. *Remote Sens Environ* 125:80–91

- Goetz SJ, Baccini A, Laporte NT, Johns T, Walker W, Kellndorfer J, Houghton RA, Sun M (2009) Mapping and monitoring carbon stocks with satellite observations: a comparison of methods. *Carbon Balance Manag* 4:2
- Goh J, Miettinen J, Chia AS, Chew PT, Liew SC (2014) Biomass estimation in humid tropical forest using a combination of ALOS PALSAR and SPOT 5 satellite imagery. *Asian J Geoinformatics* 13:1–10
- Goodchild MF, Yuan M, Cova TJ (2007) Towards a general theory of geographic representation in GIS. *Int J Geogr Inf Syst* 21:239–260
- Halme M, Tomppo E (2001) Improving the accuracy of multisource forest inventory estimates to reducing plot location error—a multicriteria approach. *Remote Sens Environ* 78:321–327
- Halme E, Pellikka P, Möttöus M (2019) Utility of hyperspectral compared to multispectral remote sensing data in estimating forest biomass and structure variables in Finnish boreal forest. *Int J Appl Earth Obs Geoinf* 83:101942
- Hamdan O, Aziz HK, Hasmadi IM (2014) L-band ALOS PALSAR for biomass estimation of Matang mangroves, Malaysia. *Remote Sens Environ* 155:69–78
- Hame T, Salli A, Andersson K, Lohi A (1997) A new methodology for the estimation of biomass of conifer-dominated boreal forest using NOAA AVHRR data. *Int J Remote Sens* 18:3211–3243
- Harding DJ, Lefsky MA, Parker GG, Blair JB (2001) Laser altimeter canopy height profiles: methods and validation for closed-canopy, broadleaf forests. *Remote Sens Environ* 76:283–297
- Harrell PA, Kasischke ES, Bourgeau-Chavez LL, Haney EM, Christensen NL Jr (1997) Evaluation of approaches to estimating aboveground biomass in southern pine forests using SIR-C data. *Remote Sens Environ* 59:223–233
- Hatfield JL, Asrar G, Kanemasu ET (1984) Intercepted photosynthetically active radiation estimated by spectral reflectance. *Remote Sens Environ* 14:65–75
- Heiskanen J (2006) Estimating aboveground tree biomass and leaf area index in a mountain birch forest using ASTER satellite data. *Int J Remote Sens* 27:1135–1158
- Hirata Y, Takao G, Sato T, Toriyama J (2012) REDD-plus Cookbook. REDD Research and Development Center, Forestry and Forest Products Research Institute, Tsukuba
- Hirschmugl M, Ofner M, Raggam J, Schardt M (2007) Single tree detection in very high-resolution remote sensing data. *Remote Sens Environ* 110:533–544
- Houghton RA (1991) Releases of carbon to the atmosphere from degradation of forests in tropical Asia. *Can J For Res* 21:132–142
- Houghton RA (1995) Land-use change and the carbon cycle. *Glob Change Biol* 1:275–287
- Houghton RA (2005) Above ground forest biomass and the global carbon balance. *Glob Change Biol* 11:945–958
- Imhoff ML, Johnson P, Holford W, Hyer J, May L, Lawrence W, Harcombe P (2000) BioSAR/sup TM: an inexpensive airborne VHF multiband SAR system for vegetation biomass measurement. *IEEE Trans Geosci Remote Sens* 38:1458–1462
- IPCC (2004) Good practice guidance. Cambridge University Press, Cambridge
- IPCC (2007) Climate change 2007: synthesis report. Contribution of working group I, II and III to the fourth assessment report of the intergovernmental panel on climate Change. IPCC, Geneva
- Kaewluan S, Pipatmanomai S (2011) Gasification of high moisture rubber woodchip with rubber waste in a bubbling fluidized bed. *Fuel Process Technol* 92:671–677
- Kashongwe HB, Roy DP, Bwagoy JRB (2020) Democratic Republic of the Congo tropical Forest canopy height and aboveground biomass estimation with Landsat-8 operational land imager (OLI) and airborne LiDAR data: the effect of seasonal Landsat image selection. *Remote Sens* 12:1360
- Kato R, Tadaki Y, Ogawa H (1978) Plant biomass and growth increment studies in Pasoh forest. *Malay Nat J* 30:211–224
- Kenzo T, Ichie T, Hattori D, Itioka T, Handa C, Ohkubo T, Kendawang JJ, Nakamura M, Sakaguchi M, Takahashi N, Okamoto M, Tanaka-Oda A, Sakurai K, Ninomiya I (2009) Development of allometric relationships for accurate estimation of above- and below-ground biomass in tropical secondary forests in Sarawak, Malaysia. *J Trop Ecol* 25:371–386

- Ketterings QM, Coe R, van Noordwijk M, Ambagau' Y, Palm CA (2001) Reducing uncertainty in the use of allometric biomass equations for predicting above-ground tree biomass in mixed secondary forests. *For Ecol Manag* 146:199–209
- Kiyono Y, Saito S, Takahashi T, Toriyama J, Awaya Y, Asai H, Furuya N, Ochiai Y, Inoue Y, Sato T, Sophal C, Sam P, Tith B, Ito E, Siregar CA, Matsumoto M (2011) Practicalities of non-destructive methodologies in monitoring anthropogenic greenhouse gas emissions from tropical forests under the influence of human intervention. *Jpn Agric Res Q* 45:233–242
- Klass DL (1998) Biomass for renewable energy, fuels, and chemicals. Elsevier, Amsterdam
- Koju UA, Zhang J, Maharjan S, Zhang S, Bai Y, Vijayakumar DB, Yao F (2019) A two-scale approach for estimating forest aboveground biomass with optical remote sensing images in a subtropical forest of Nepal. *J For Res* 30:2119–2136
- Komiyama A, Pongpam S, Kato S (2005) Common allometric equations for estimating the tree weight of mangroves. *J Trop Ecol* 21:471–477
- Kumar L, Sinha P, Taylor S, Alqurashi AF (2015) Review of the use of remote sensing for biomass estimation to support renewable energy generation. *J Appl Remote Sens* 9:097696
- Kuplich TM, Salvatori V, Curran PJ (2000) JERS-1/SAR backscatter and its relationship with biomass of regenerating forests. *Int J Remote Sens* 21:2513–2518
- Le Toan T, Beaudoin A, Riom J, Guyon D (1992) Relating forest biomass to SAR data. *IEEE Trans Geosci Remote Sens* 30:403–411
- Lefsky MA, Cohen WB, Acker SA, Parker GG, Spies TA, Harding D (1999) Lidar remote sensing of the canopy structure and biophysical properties of Douglas-fir western hemlock forests. *Remote Sens Environ* 70:339–361
- Lefsky MA, Cohen WB, Harding DJ, Parker GG, Acker SA, Gower ST (2002) Lidar remote sensing of above-ground biomass in three biomes. *Glob Ecol Biogeogr* 11:393–399
- Lefsky MA, Harding DJ, Keller M, Cohen WB, Carabajal CC, Del Bom E-SF, Hunter MO, de Oliveira JR (2005) Estimates of forest canopy height and aboveground biomass using ICESat. *Geophys Res Lett* 32:L22S02
- Li Z, Fox JM (2011) Integrating Mahalanobis typicalities with a neural network for rubber distribution mapping. *Remote Sens Lett* 2:157–166
- Li Z, Fox JM (2012) Mapping rubber tree growth in mainland Southeast Asia using time-series MODIS 250 m NDVI and statistical data. *Appl Geogr* 32:420–432
- Li M, Tan Y, Pan J, Peng S (2008) Modeling forest aboveground biomass by combining spectrum, textures and topographic features. *Front For China* 3:10–15
- Li M, Lenzen M, Yousefzadeh M, Ximenes FA (2020) The roles of biomass and CSP in a 100% renewable electricity supply in Australia. *Biomass Bioenergy* 143:105802
- Lim KO, Alaudin ZAZ, Quadir GA, Mohd ZA (2000) Energy potential and utilization of plantation crops in Malaysia. *ASEAN J Sci Technol Dev* 17:1–16
- Lim K, Treitz P, Wulder M, St-Onge B, Flood M (2003) LiDAR remote sensing of forest structure. *Prog Phys Geogr* 27:88–106
- Lu D (2005) Aboveground biomass estimation using Landsat TM data in the Brazilian Amazon. *Int J Remote Sens* 26:2509–2525
- Lu D (2006) The potential and challenge of remote sensing-based biomass estimation. *Int J Remote Sens* 27:1297–1328
- Lu D, Batistella M (2005) Exploring TM image texture and its relationships with biomass estimation in Rondônia, Brazilian Amazon. *Acta Amazon* 35:249–257
- Lu D, Mausel P, Brondizio E, Moran E (2004) Relationships between forest stand parameters and Landsat TM spectral responses in the Brazilian Amazon Basin. *For Ecol Manag* 198:149–167
- Lu D, Chen Q, Wang G, Liu L, Li G, Moran E (2016) A survey of remote sensing-based aboveground biomass estimation methods in forest ecosystems. *Int J Digit Earth* 9:63–105
- Lucas RM, Armston JD (2007) ALOS PALSAR for characterizing wooded savannas in Northern Australia. In: 2007 IEEE international geoscience and remote sensing symposium, pp 3610–3613

- Lucas RM, Honzak M, do Amaral I, Curran P, Foody GM, Amaral S (1998) The contribution of remotely sensed data in the assessment of the floristic composition, total biomass and structure of tropical regenerating forests. In: Gascon C, Moutinho P (eds) *Regeneracao Florestal: Pesquisas na Amazonia*. Inpa Press, Manaus, pp 61–82
- Lucas RM, Moghaddam M, Cronin N (2004) Microwave scattering from mixed-species forests, Queensland, Australia. *IEEE Trans Geosci Remote Sens* 42:2142–2159
- Lucas RM, Cronin N, Lee A, Moghaddam M, Witte C, Tickle P (2006) Empirical relationships between AIRSAR backscatter and LiDAR-derived forest biomass, Queensland, Australia. *Remote Sens Environ* 100:407–425
- Lucas RM, Lee AC, Armston J, Carreiras JM, Viergever KM, Bunting P, Clewley D, Moghaddam M, Siqueira P, Woodhouse I (2010) Quantifying carbon in savannas: the role of active sensors in measurements of tree structure and biomass. In: *Ecosystem function in Savannas*. CRC Press, Boca Raton, pp 195–214
- Luckman A, Baker JR, Kuplich TM, Yanasse CCF, Frery AC (1997) A study of the relationship between radar backscatter and regenerating forest biomass for space borne SAR instrument. *Remote Sens Environ* 60:1–13
- Luckman A, Baker J, Honzák M, Lucas R (1998) Tropical forest biomass density estimation using JERS-1 SAR: seasonal variation, confidence limits, and application to image mosaics. *Remote Sens Environ* 63:126–139
- McGlinchy J, van Aardt JA, Erasmus B, Asner GP, Mathieu R, Wessels K, Kennedy-Bowdoin T, Rhody H, Kerekes JP, Ientilucci EJ, Wu J, Sarrazin D, Cawse-Nicholson K (2014) Extracting structural vegetation components from small-footprint waveform lidar for biomass estimation in savanna ecosystems. *IEEE J Sel Top Appl Earth Obs Remote Sens* 7:480–490
- Means JE, Acker SA, Harding DJ, Blair JB, Lefsky MA, Cohen WB, Harmon ME, McKee WA (1999) Use of large-footprint scanning airborne lidar to estimate forest stand characteristics in the Western Cascades of Oregon. *Remote Sens Environ* 67:298–308
- Min S, Wang X, Jin S, Waibel H, Huang J (2020) Climate change and farmers' perceptions: impact on rubber farming in the upper Mekong region. *Clim Chang* 163:451–480
- Mokany K, Raison RJ, Prokushkin AS (2006) Critical analysis of root: shoot ratios in terrestrial biomes. *Glob Change Biol* 12:84–96
- Molto Q, Rossi V, Blanc L (2013) Error propagation in biomass estimation in tropical forests. *Methods Ecol Evol* 4:175–183
- Morel AC, Saatchi SS, Malhi Y, Berry NJ, Banin L, Burslem D, Nilus R, Ong RC (2011) Estimating aboveground biomass in forest and oil palm plantation in Sabah, Malaysian Borneo using ALOS PALSAR data. *For Ecol Manag* 262:1786–1798
- Mutanga O, Skidmore AK (2004) Narrow band vegetation indices overcome the saturation problem in biomass estimation. *Int J Remote Sens* 25:3999–4014
- Muukkonen P, Heiskanen J (2005) Estimating biomass for boreal forests using ASTER satellite data combined with stand wise forest inventory data. *Remote Sens Environ* 99:434–447
- Nelson RF, Kimes DS, Salas WA, Routhier M (2000) Secondary forest age and tropical forest biomass estimation using thematic mapper imagery: single-year tropical forest age classes, a surrogate for standing biomass, cannot be reliably identified using single-date tm imagery. *Bioscience* 50:419–431
- Ni W, Ranson KJ, Zhang Z, Sun G (2014) Features of point clouds synthesized from multi-view ALOS/PRISM data and comparisons with LiDAR data in forested areas. *Remote Sens Environ* 149:47–57
- Nichol JE, Sarker MLR (2011) Improved biomass estimation using the texture parameters of two high-resolution optical sensors. *IEEE Trans Geosci Remote Sens* 9:930–948
- Phua H, Saito H (2003) Estimation of biomass of a mountainous tropical forest using Landsat TM data. *Can J Remote Sens* 29:429–440
- Podest E, Saatchi S (2002) Application of multiscale texture in classifying JERS-1 radar data over tropical vegetation. *Int J Remote Sens* 23:1487–1506

- Popescu SC, Wynne RH, Nelson RF (2003) Measuring individual tree crown diameter with lidar and assessing its influence on estimating forest volume and biomass. *Can J Remote Sens* 29: 564–577
- Popescu SC, Zhao K, Neuenschwander A, Lin C (2011) Satellite lidar vs. small footprint airborne lidar: comparing the accuracy of aboveground biomass estimates and forest structure metrics at footprint level. *Remote Sens Environ* 115:2786–2797
- Rahman MM, Csaplovics E, Koch B (2005) An efficient regression strategy for extracting forest biomass information from satellite sensor data. *Int J Remote Sens* 26:1511–1519
- Ratnasingam J, Scholz F (2009) Rubberwood an industrial perspective, vol 68. World Resource Institute, Washington, DC, p 115
- Ravindranath NH, Ostwald M (2008) Methods for estimating above-ground biomass. Carbon inventory methods handbook for greenhouse gas inventory, carbon mitigation and roundwood production projects. Springer, Berlin, pp 113–147
- Reinartz P, Müller R, Hoja D, Lehner M, Schroeder M (2005) Comparison and fusion of DEM derived from SPOT-5 HRS and SRTM data and estimation of forest heights. In: Proceedings EARSeL workshop on 3D-remote sensing, Porto, vol 1
- Rignot EJ, Zimmermann R, van Zyl JJ (1995) Spaceborne applications of P band imaging radars for measuring forest biomass. *IEEE Trans Geosci Remote Sens* 33:1162–1169
- Saatchi SS, Houghton RA, Dos Santos Alvala RC, Soares V, Yu Y (2007) Distribution of aboveground live biomass in the Amazon basin. *Glob Change Biol* 13:816–837
- Sader SA, Waide RB, Lawrence WT, Joyce AT (1989) Tropical forest biomass and successional age class relationships to a vegetation index derived from Landsat TM data. *Remote Sens Environ* 28:143–198
- Santos JR, Lacruz MP, Araujo LS, Keil M (2002) Savanna and tropical rainforest biomass estimation and spatialization using JERS-1 data. *Int J Remote Sens* 23:1217–1229
- Santos JR, Freitas CC, Araujo LS, Dutra LV, Mura JC, Gama F, Soler LS, Sant’Anna SJ (2003) Airborne P-band SAR applied to the aboveground biomass studies in the Brazilian tropical rainforest. *Remote Sens Environ* 87:482–493
- Sarker MLR, Nichol J, Iz HB, Ahmad BB, Rahman AA (2012) Forest biomass estimation using texture measurements of high-resolution dual-polarization C-band SAR data. *IEEE Trans Geosci Remote Sens* 51:3371–3384
- Sellers PJ (1985) Canopy reflectance, photosynthesis and transpiration. *Int J Remote Sens* 6:1335–1372
- Serigne TK, Verchot LV, Mackensen J, Boye A, Van Noordwijk M, Tomich TP, Ong C, Allbrecht A, Palm C (2006) Opportunities for linking climate change adaptation and mitigation through agroforestry systems. In: Garrity D, Okono A, Grayson M, Parrott S (eds) World agroforestry into the future. World Agroforestry Centre, Nairobi, pp 113–123
- Shaaban A, Se SM, Mitan NMM, Dimin MF (2013) Characterization of biochar derived from rubber wood sawdust through slow pyrolysis on surface porosities and functional groups. *Procedia Eng* 68:365–371
- Sherman RE, Fahey TJ, Martinez P (2003) Spatial patterns of biomass and aboveground net primary productivity in a mangrove ecosystem in the Dominican Republic. *Ecosystems* 6: 384–398
- Shidiq PA, Ismail MH (2016) Stand age model for mapping spatial distribution of rubber tree using remotely sensed data in Kedah, Malaysia. *J Teknol* 78(5):5-2016
- Shigematsu A, Mizoue N, Kajisa T, Yoshida S (2011) Importance of rubberwood in wood export of Malaysia and Thailand. *New For* 41:179–189
- Shimada M (2010) Ortho-rectification and slope correction of SAR data using DEM and its accuracy evaluation. *IEEE J Sel Top Appl Earth Obs Remote Sens* 3:657–671
- Shin DW, Cocke S, LaRow E (2007) Diurnal cycle of precipitation in a climate model. *J Geophys Res Atmos* 112(D13)
- Sileshi GW (2014) A critical review of forest biomass estimation models, common mistakes and corrective measures. *For Ecol Manag* 329:237–254

- Skidmore AK (2002) Taxonomy of environmental models in the spatial sciences. *Environmental modelling with GIS and remote sensing*, pp 8–25
- Smith AMS, Wooster WJ, Powell AK, Usher D (2002) Texture based feature extraction: application to burn scar detection in earth observation satellite sensor imagery. *Int J Remote Sens* 23:1733–1739
- Soenen SA, Peddle D, Hall RJ, Coburn CA, Hall FG (2010) Estimating aboveground forest biomass from canopy reflectance model inversion in mountainous terrain. *Remote Sens Environ* 114:1325–1337
- Solomon S, Srinivasan J (1996) Radiative forcing of climate change. In: Watson RT, Zinyowera MC, Moss RH (eds) *Climate change 1995*. Cambridge University Press, Cambridge, pp 108–118
- Somogyi Z, Cienciala E, Mäkipää R, Muukkonen P, Lehtonen A, Weiss P (2007) Indirect methods of large-scale forest biomass estimation. *Eur J For Res* 126:197–207
- Sone K, Watanabe N, Takase M, Hosaka T, Gyokusen K (2014) Carbon sequestration, tree biomass growth and rubber yield of PB260 clone of rubber tree (*Hevea brasiliensis*) in North Sumatra. *J Rubber Res* 17:115–127
- Song C (2013) Optical remote sensing of forest leaf area index and biomass. *Prog Phys Geogr* 37:98–113
- Song C, Dickinson MB, Su L, Zhang S, Yaussey D (2010) Estimating average tree crown size using spatial information from Ikonos and QuickBird images: across-sensor and across-site comparisons. *Remote Sens Environ* 114:1099–1107
- Sopharat J (2009) Application of SPOT-5 image to assess leaf area index of rubber tree: case study of namon district songkhal province. Doctoral dissertation, MS thesis. Prince of Songkla University, Songkla, Thailand
- Steininger MK (2000) Satellite estimation of tropical secondary forest above-ground biomass: data from Brazil and Bolivia. *Int J Remote Sens* 21:1139–1157
- St-Onge B, Hu Y, Vega C (2008) Mapping the height and above-ground biomass of a mixed forest using lidar and stereo Ikonos images. *Int J Remote Sens* 29:1277–1294
- Sun G, Ranson KJ, Kharuk VI (2002) Radiometric slope correction for forest biomass estimation from SAR data in the Western Sayani Mountains, Siberia. *Remote Sens Environ* 79:279–287
- Tan Z, Yang X, Ou Z, Sun H, Chen H, Xi G (2010) The extraction of rubber spatial distributing information in Hainan province based on FY-3a satellite data. In: *World automation congress proceedings (WAC)*, pp 25–29
- Tang Y, Carmichael GR, Woo JH, Thongboonchoo N, Kurata G, Uno I, Streets DG, Blake DR, Kondo Y (2003) Influences of biomass burning during the transport and chemical evolution over the Pacific (TRACE-P) experiment identified by the regional chemical transport model. *J Geophys Res Atmos* 108:8824
- Thenkabail PS, Enclona EA, Ashton MS, Van Der Meer B (2004a) Accuracy assessments of hyperspectral waveband performance for vegetation analysis applications. *Remote Sens Environ* 91:354–376
- Thenkabail PS, Stucky N, Griscom BW, Ashton MS, Diels J, Van der Meer B, Enclona E (2004b) Biomass estimations and carbon stock calculations in the oil palm plantations of African derived savannas using IKONOS data. *Int J Remote Sens* 25:5447–5472
- Thomas V, Treitz P, McCaughey JH, Morrison I (2006) Mapping stand-level forest biophysical variables for a mixed wood boreal forest using lidar: an examination of scanning density. *Can J For Res* 36:34–47
- Tian XF, Fang Z, Guo F (2012) Impact and prospective of fungal pre-treatment of lignocellulosic biomass for enzymatic hydrolysis. *Biofuels Bioprod Biorefin* 6:335–350
- Todd KW, Csillag F, Atkinson PM (2003) Three-dimensional mapping of light transmittance and foliage distribution using lidar. *Can J Remote Sens* 29:544–555
- Tomppo E, Nilsson M, Rosengren M, Aalto P, Kennedy P (2002) Simultaneous use of Landsat-TM and IRS-1C WiFS data in estimating large area tree stem volume and aboveground biomass. *Remote Sens Environ* 82:156–171

- Tucker CJ, Vanpraet CL, Sharman MJ, Van Ittersum G (1985) Satellite remote sensing of total herbaceous biomass production in the Senegalese Sahel: 1980–1984. *Remote Sens Environ* 17: 233–249
- Turner DP, Guzy M, Lefsky MA, Ritts WD, Van Tuyl S, Law BE (2004) Monitoring forest carbon sequestration with remote sensing and carbon cycle modeling. *Environ Manag* 33:457–466
- Van Breugel M, Ransijn J, Craven D, Bongers F, Hall JS (2011) Estimating carbon stock in secondary forests: decisions and uncertainties associated with allometric biomass models. *For Ecol Manag* 262:1648–1657
- Verchot LV, Van Noordwijk M, Kandji S, Tomich T, Ong C, Albrecht A, Mackensen J, Bantilan C, Anupama KV, Palm C (2007) Climate change: linking adaptation and mitigation through agroforestry. *Mitig Adapt Strateg Glob Chang* 12:901–918
- Vieira S, Trumbone S, Carnargo PB, Sethorst D, Chambers JQ, Higuchi N, Martinelli LA (2005) Slow growth rates of Amazonian trees: consequences for carbon cycling. *Proc Natl Acad Sci U S A* 102:18502–18507
- Voivontas D, Assimacopoulos D, Koukios EG (2001) Assessment of biomass potential for power production: a GIS based method. *Biomass Bioenergy* 20:101–112
- Wallerman J, Fransson JE, Bohlin J, Reese H, Olsson H. (2010) Forest mapping using 3D data from SPOT-5 HRS and Z/I DMC. In: 2010 IEEE international geoscienc remote sensing symposium, pp 64–67
- Wang Q, Adiku S, Tenhunen J, Granier A (2005) On the relationship of NDVI with leaf area index in a deciduous forest site. *Remote Sens Environ* 94:244–255
- Wauters J, Coudert S, Grallien E, Jonard M, Ponette Q (2008) Carbon stock in rubber tree plantations in Western Ghana and Mato Grosso (Brazil). *For Ecol Manag* 255:2347–2361
- Wereko-Brobby C, Hagan EB (1996) *Biomass conversion and technology*. Wiley, Chichester, p 10
- Wright SJ (2010) The future of tropical forests. *Ann N Y Acad Sci* 1195:1
- Yakham P, Nontananandh S, Methakullachat D (2012) Study on relation between vegetation index and range of rubber age using SMMS satellite imagery. In: 50 Kasetsart University annual conference, Bangkok (Thailand), 31 Jan-2 Feb 2012
- Yang XM, Zhang XP, Fang HJ (2003) Importance of agricultural soil sequestering carbon to offsetting global warming. *Sci Geogr Sin* 23:101–106
- Yang JC, Huang JH, Pan QM, Tang JW, Han XG (2004) Long-term impacts of land-use change on dynamics of tropical soil carbon and nitrogen pools. *J Environ Sci* 16:256–261
- Yang JC, Huang JH, Tang JW, Pan QM, Han XG (2005) Carbon sequestration in rubber tree plantations established on former arable lands in Xishuangbanna, SW China. *Chin J Plant Ecol* 29:296–303
- Yang X, Blagodatsky S, Lippe M, Liu F, Hammond J, Xu J, Cadisch G (2016) Land-use change impact on time-averaged carbon balances: rubber expansion and reforestation in a biosphere reserve, south-West China. *For Ecol Manag* 372:149–163
- Yasen K, Koedsin W (2015) Estimating aboveground biomass of rubber tree using remote sensing in Phuket Province, Thailand. *J Med Biol Eng* 4:451–456
- Zhang X, Friedl MA, Schaaf CB, Strahler AH, Hodges JC, Gao F, Reed BC, Huete A (2003) Monitoring vegetation phenology using MODIS. *Remote Sens Environ* 84:471–475
- Zhao K, Popescu N, Nelson R (2009) Lidar remote sensing of forest biomass: a scale-invariant estimation approach using airborne lasers. *Remote Sens Environ* 113:182–196
- Zheng D, Rademacher J, Chen J, Crow T, Bresee M, Le Moine J, Ryu SR (2004) Estimating aboveground biomass using Landsat 7 ETM+ data across a managed landscape in northern Wisconsin, USA. *Remote Sens Environ* 93:402–411
- Zheng G, Chen JM, Tian QJ, Ju WM, Xia XQ (2007) Combining remote sensing imagery and forest age inventory for biomass mapping. *J Environ Manag* 85:616–623
- Zheng S, Shi WZ, Liu J, Tian J (2008) Remote sensing image fusion using multiscale mapped LS-SVM. *IEEE Trans Geosci Remote Sens* 46:1313–1322
- Zhou F, Xing M, Bai X, Sun G, Bao Z (2009) Narrow-band interference suppression for SAR based on complex empirical mode decomposition *IEEE Geosci Remote Sens Lett* 6:423–427



The Use of Landsat TM Imagery for the Application of Rubber Tree Area and Stand Volume Predictive Models in Rubber Plantations in Selangor, Malaysia

Mohd Nazip Suratman, Gary Bull, Valerie LeMay, Peter Marshall, and Donald G. Leckie

Abstract

The requirement for information of the spatial distribution of forest resources has increased rapidly in recent years. Integration of remote sensing data with Geographical Information System (GIS) hold the keys to contribute to effective mapping and monitoring of forest resources. Globally, there have been tremendous efforts of mapping of forest resources, agroforestry, forest plantations, and agricultural tree crops at regional and local scales. Rubber tree (*Hevea brasiliensis*) is one of the important agricultural tree crops which plays roles as the main sources of natural rubber and wood products not only in Malaysia but also in other countries such as Indonesia, Thailand, India, Vietnam, and China. Effective management and appropriate policy for this tree crop require reliable information on resource dynamics and forecasts of resource availability. The need for inventories and effective monitoring prompted this study into utilising Landsat Thematic Mapper (Landsat TM) for the application of rubber tree area and stand volume predictive models which was previously developed by Suratman et al. (Int For Rev 6(1):1–13, 2004). In this study, the application of predictive models has produced thematic maps of spatial distribution of rubber tree areas and stand volume for a case study area of rubber tree plantations in

M. N. Suratman (✉)

Faculty of Applied Sciences and Institute for Biodiversity and Sustainable Development, Universiti Teknologi MARA (UiTM), Shah Alam, Malaysia

e-mail: nazip@uitm.edu.my

G. Bull · V. LeMay · P. Marshall

Department of Forest Resources Management, Faculty of Forestry, University of British Columbia, Vancouver, BC, Canada

D. G. Leckie

Pacific Forestry Centre, Canadian Forest Service, Victoria, BC, Canada

© The Author(s), under exclusive license to Springer Nature Singapore Pte Ltd. 2022

215

M. N. Suratman (ed.), *Concepts and Applications of Remote Sensing in Forestry*, https://doi.org/10.1007/978-981-19-4200-6_11

Selangor, Malaysia. The work in this study has demonstrated the development of methods for mapping rubber plantation by linking ground information with model projections based on satellite data. Additionally, the maps produced in this work demonstrates a spatial distribution and availability of rubber tree resources across landscapes. This information is needed for effective resource planning aimed at maximizing the potential benefits of rubber tree crops for wood and natural rubber supply in Malaysia.

Keywords

Rubber tree · Landsat TM · Predictive models · Model application · Regression analysis

1 Introduction

The total natural forest area in Malaysia is 18.3 million ha, or 55.3% of the total land base. Of this total, 10.9 million ha has been set aside for a permanent forest reserve to be managed sustainably (Ministry of Energy and Natural Resources 2022). From this area, about 4.1 million ha is state land production forests and 3.1 million ha is protection forests. An additional more than two million ha of forest area is known as conversion forest, which in due time, will be converted to other uses to meet the needs of population growth and balanced economic development. In addition to natural forests, the country has established about 0.25 million ha of forest plantations consisting of fast-growing tree species such as *Acacia* (*Acacia mangium*), *Batai* (*Albizia falcataria*), *Yamane* (*Gmelina arborea*), and *Eucalyptus* (*Eucalyptus* spp.). Additionally, Malaysia has 5.27 million ha of agricultural tree crops which are mainly rubber, oil palm, coconut, and cocoa (FAO 2002).

Rubber tree crops play pivotal roles in providing natural rubber, sources of wood products, and other benefits that support basic human needs and economic development (Killmann and Hong 2000; Suratman et al. 2004; Suratman 2011). Despite their importance, little attention has been given to inventory, mapping, and monitoring the crops. This could be because government agencies are often under-funded; thus data on tree crop resource monitoring tend to be sporadic. In spite of the country's awareness of the socio-economic roles of rubber plantations, a decline in the total area of rubber plantations in Malaysia occurred throughout the 1990s. At the beginning of the decade, Malaysia had about 1.84 million ha of rubber plantations compared to 1.43 million ha in 2000, representing about a 22% reduction (MRB 2002). At present, the planted area of rubber estates and small holdings in the country is 1.14 million ha (MRB 2022).

Rubberwood timber from rubber tree plantation is available at the time of replanting. The properties and utilisation of rubberwood have been studied since the 1950s, but the commercial utilisation of the wood only began in the late 1970s. The main utilisation of rubberwood before the development of the rubber industry was fuelwood, which was estimated to be 67% of the total rubberwood annual consumption. The other 33% were used as reconstituted products, charcoal, sawlogs,

and plywood/veneer (Hong and Sim 1999). During the late 1970s, there was an urgent need to find new raw materials to satisfy the demand for depleting light-coloured timber species such as Ramin (*Gonystylus bancanus*) and Damar minyak (*Agathis borneensis*). Rubberwood was identified as one of the promising materials to be developed due to many similarities in characteristics between these species (Abdul Razak and Hoi 1988). After many years of research, a number of inherent weaknesses (e.g., susceptibility to fungal and insect attacks) have been identified, and methods to overcome these problems have been determined (Mohd Dahlan et al. 1999). Research and development to broaden the utilisation of rubberwood has now ventured into value-added products (Hong and Sim 1999).

Remote sensing technology offers potential gains in inventory efficiency based on its ability to quantitatively characterise stand canopies through spectral reflectance (Ahern et al. 1991; Lillesand and Kiefer 2000). At the regional level, the potential advantages of using satellite images for mapping forest resources include cost-effectiveness, broad coverage, and the ability to reveal landscape processes at large areas (Wilkie and Finn 1996). While many studies have been conducted looking at land use/cover changes, very little is understood at a local level about the complex relationship between specific resource availabilities and the factors that drive such changes (Mertens and Lambin 1997).

The need for effective inventories and mapping of rubber tree resources was the impetus for this study into applying previously developed rubber tree area and stand volume predictive models into an independent area of rubber plantations with information from satellite remote sensing. The thematic maps produced from this work may be used to serve the needs of rubber plantation agencies, owners, and land use planners in their goal of characterising the existing condition of the rubber tree resources as a baseline for later research and as a starting point for the development of future scenarios. This point is particularly important, because in order to focus policy interventions geographically, one needs to measure the resource availability in relation to their spatial distribution at the landscape level. Such information is essential to support the implementation of appropriate responses to forecast of landscape-resource changes to ensure the sustainability of essential resources.

2 Materials and Methods

The predictive model application area chosen was located about 20 km south of Kuala Lumpur in the State of Selangor, Malaysia, between 101° 25' and 101° 45' E latitudes and 2° 50' and 3° 05' N longitudes, covering about 250 km² (Fig. 1). The region has a tropical climate characterised by a dry season (March to May) and a wet season (November to January), with a mean annual precipitation of 2178 mm. Daytime mean temperature ranges from 22.9 to 27.7 °C (Meteorological Service 2022). The selected area consists of rubber small holders and plantations in three districts, namely Petaling, Sepang, and Kuala Langat. The topography in the area is predominantly flat, with altitudes ranging from 5 to 80 m above sea level (ASL), with the highest point at Permatang Kuang of 213 m above sea level. The area

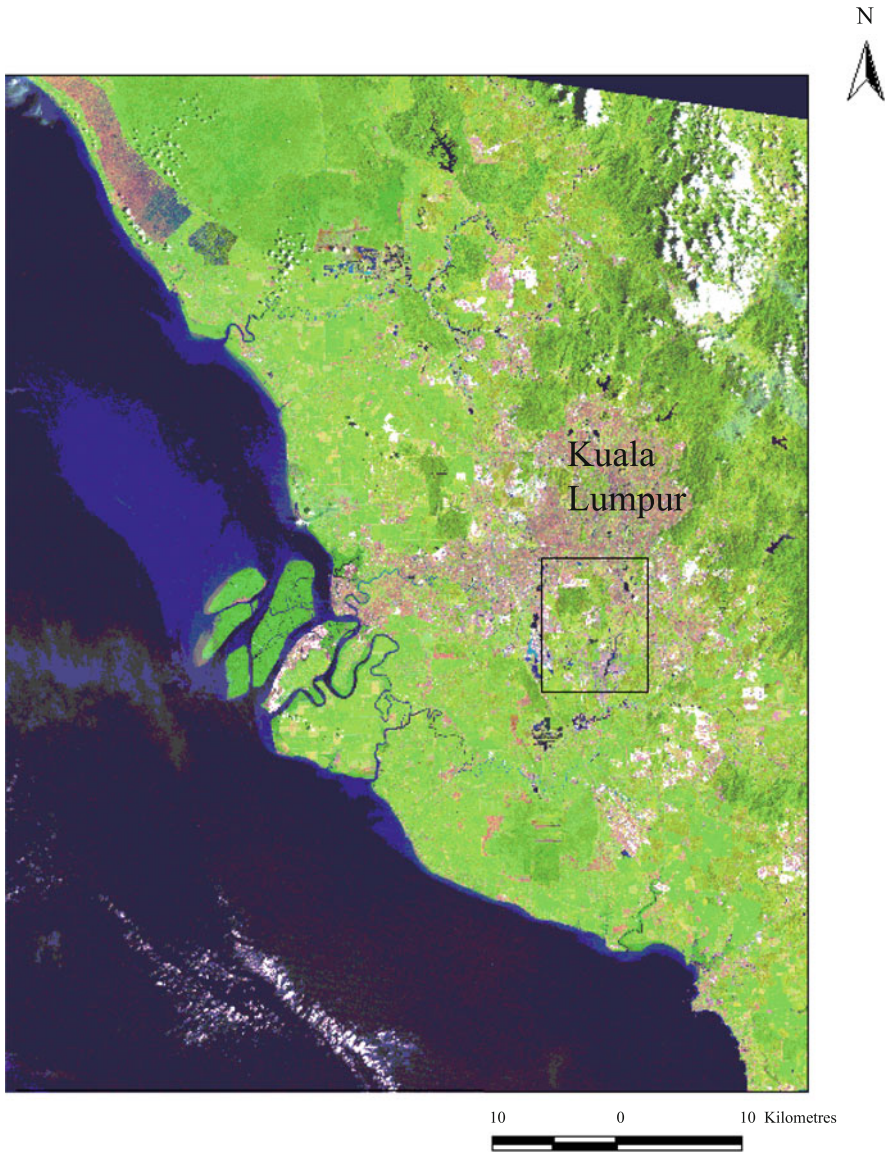


Fig. 1 Predictive model application area (in the box) in south of Kuala Lumpur, Malaysia. The full scene is a pseudocolour composite (TM bands 5, 4, and 3) image of the State of Selangor (path 127, row 58) acquired on 1999/06/11

includes the Ayer Hitam Forest which was selectively logged several times between 1936 and 1965 (Faridah-Hanum 1999). According to Faridah-Hanum (1999), this forest is one of the few remaining forests in the Klang Valley, along with the Bukit Nanas Forest in Kuala Lumpur. The forest has been leased to the Universiti Putra

Malaysia (UPM) for 80 years from the Government of Selangor as a facility for research, demonstration, and education in the field of forestry. It is located 25 km from the university campus. Other than rubber small holders and plantations, other crop types include oil palm plantations, as well as varying sizes of mixed crops. The mixed crops are characterised by diverse intercropping of traditional homegarden systems, with a mixture of coffee, cocoa, coconut, banana, shrubs, and herbaceous plants (Suratman et al. 2000). The grasslands in the study area are characterised by a high percentage of grasses (e.g., *Imperata cylindrica*, *Paspalum conjugatum*, and *Axonopus compressus*), which occur with scattered herbaceous plants and shrubs (e.g., *Melastoma malabathricum*) (Chee and Ahmad 1990). This area is representative of the ecological and land use/cover conditions throughout the State of Selangor.

The area has been a focus of large-scale changes in land use over the last decade. Rapid rates of land cover changes and land use conversions were due to the development of the new Federal Government Administration Centre (previously in Kuala Lumpur) known as Putrajaya started in 1994, covering an area about 4400 ha. This resulted in the development of townships, residential and industrial estates, and man-made lakes surrounding the site. The nearby town to the west is Cyberjaya, where a new construction, Multimedia City, which covers 75,000 ha was completed in 2011. This makes land use planning in this area one of most important issues for the State of Selangor.

2.1 Satellite Image Acquisition and Reference Data

The remote sensing imagery acquired on 11 February 2009 was the full scene image of the State of Selangor, Malaysia, from the TM sensor on Landsat-5 (Fig. 1). Due to security reasons, attempts to obtain complete aerial photographic coverage of the area from the Department of Survey and Mapping, Malaysia, were unsuccessful. Available reference data to support this work consisted of ground truth data, a 1999 State of Selangor map at a scale of 1:125,000 (series 9101), and 1990 topographic maps at a scale of 1:50,000 (sheet numbers 3756 and 3757) and a 1966 soil map at a scale of 1:253,440 were used. All topographic and soil maps were obtained from the Department of Agriculture, Malaysia. Together, the maps provided information on Universal Transverse Mercator (UTM) coordinates, state and district boundaries, contour lines, general land use/cover, soil types, village and built-up area, and infrastructures.

2.2 Image Pre-processing

PCI Geomatics software was used to perform all image-processing functions required to complete the land use/cover classification and change analyses. ArcView GIS software was used to carry out data management and a spatial analysis. Geometric correction is critical for producing spatially corrected maps of land use/cover. Therefore, the scene acquired in 1999 was converted to UTM projected

to the Zone 47 coordinate system. GCPs were extracted from topographic maps at the scale of 1:50,000 based on easily identifiable points such as intersections, bridges, and other landmarks. The RMSE of the registration process was less than 0.5 pixels.

2.3 Application of the Predictive Rubber Area and Stand Volume Models

The following rubber area model developed using logistic regression model by Suratman et al. (2004) was applied to the 1999 Landsat TM imagery using the MODEL command in 'Xspace' utilities of PCI Geomatics software;

$$\hat{p} = \frac{\exp(14.86 - 0.57 \times B2 - 0.33 \times B3 - 0.32 \times B4 + 0.47 \times B5 - 0.05 \times B7)}{1 + \exp(14.86 - 0.57 \times B2 - 0.33 \times B3 - 0.32 \times B4 + 0.47 \times B5 - 0.05 \times B7)}$$

where \hat{p} is predicted probability of being rubber areas and B2, B4, B5, and B7 are TM bands 2, 4, 5, and 7, respectively.

Output bitmaps of predicted rubber pixels were produced where the probability of rubber was ≥ 0.5 and displayed on the imagery. The output bitmaps of rubber area predicted by area model using a logistic regression was compared to the thematic map of rubber area produced by a supervised classification.

Application of the volume model was based on a segmentation technique which allows partitioning of an image into spatially continuous and homogeneous polygons (Makela and Pekkarinen 2001). For this purpose, an eCognition software was used to automatically segment the pixels of the 1999 Landsat TM image. The rubber stands volume model predictive model developed by Suratman et al. (2004) using multiple regression was applied to the mean values of all pixels classified as rubber through a supervised classification process. The rubber tree stand volume was estimated using the following equation:

$$\text{Rubber tree stand volume : } \hat{V} = -2413.13 + 11.79 \times B1 + 158,296 \times B5^{-1} \\ - 19,439 \times B7^{-1} + 2843.55 \times GI1 + 2180.16 \times VCI4$$

where \hat{V} , predicted rubber tree stand volume; B1, TM band 1; B5, TM band 5; B7, TM band 7; GI, Greenness Index I; and VCI, Vegetation Condition Index 4.

This step has produced the predicted rubber volume for the segment. Rubber pixels within the segment area were then exported into a shape file (.shp) in ArcView GIS, and the estimated rubber volume for each polygon was categorized into six classes and superimposed on the pseudocolour composite image of Landsat TM to display the volume spatial distribution.

2.4 Supervised Image Classification

The Landsat TM image was classified for general land use/cover and rubber volume classes. This operation produced a thematic map with 12 classes which include 5 rubber tree stand volume categories. For methodological consistency, all images were classified using supervised classification based on the maximum likelihood algorithm. The selected training areas were digitised on the image. They were selected to obtain adequate representation of land/use cover types. To ensure a good sampling of land use/cover types, training areas were chosen from across the full extent of the image, rather than in just a localised region. These training areas were chosen from the images on the basis of a priori knowledge from reference data. Twelve land use/cover and rubber tree stand volume classes were identified. These were water, forest, oil palm, mixed crop, grasslands, cleared areas, urban areas, and five rubber tree stand volume classes. The inclusion of rubber stand volume classification was performed to evaluate the capability of the classifier to categorize rubber stand volume measured from the field in combination with other land use/cover classes. Training and testing areas for rubber volume classes were based on the delineated rubber volume polygons. The 76 field measured stands were sorted according to field volume measurements (m^3/ha) and split into training and testing areas. Splitting was done by matching cases in pairs of similar volume classes and placing one of each pair into one of the two data sets. Volume class 1 ranged from 0 to $75 \text{ m}^3/\text{ha}$, class 2 ranged from 76 to $150 \text{ m}^3/\text{ha}$, class 3 ranged from 151 to $225 \text{ m}^3/\text{ha}$, class 4 ranged from 226 to $300 \text{ m}^3/\text{ha}$, and class 5 was greater than $300 \text{ m}^3/\text{ha}$. The training signatures for the training areas of each volume class were determined for supervised image classification using satellite data.

For each cover type, fairly large and homogeneous training areas were selected. These areas covered 18,502 pixels and incorporated a representative example of each of the 12 classes. Pixels were extracted from five to ten independent sites for each class. From a statistical standpoint, the more pixels delineated, the greater the accuracy in the calculation of means and covariance data required for the signature construction stage (Lillesand and Kiefer 2000; Tole 2002). After the training areas had been digitised, signature files were created. A histogram for each signature was evaluated for normality.

The Jeffries-Matusita (J-M) Distance was calculated to test signature separability between pairs of classes (Richards and Jia 1999). Signature separability is a statistical measure of the distance between two signatures (Bourne and Graves 2001) and was calculated for each pair of land use/cover classes. A total of five to ten testing areas containing representative examples of each land use/cover class were digitised for estimating the accuracy of each classification. The test areas for the image incorporating a representative example of each of the 12 classes. These areas were chosen in areas of known land use/cover types identified from reference data and were different from the training areas used in the classifier.

2.5 Accuracy Assessment of the Land Use/Cover Classification

The accuracy of the classified products was assessed in comparison with independent test areas using the standard procedures (Congalton 1991). This created error matrices, which encompassed reference pixels with classified pixels. Four criteria were used to assess the accuracy of the classifications: (1) overall accuracy; (2) user's accuracy or commission error; (3) producer's accuracy or omission error; and (4) Kappa coefficient = $[(\text{overall accuracy} - \text{expected accuracy}) / (1 - \text{expected accuracy})]$. The Kappa coefficient is an analytical way to evaluate the total accuracy of the classification because it takes the contribution of uncertainty into account (Rosenfield and Fitzpatrick-Lins 1986). Essentially, the Kappa coefficient answers the question of how much better the overall classification is compared to the classification if one randomly assigned class values to each pixel (Verbyla 1995).

3 Results and Discussion

3.1 Rubber Area Model Application

Investigation was carried out to decide whether to use the area model developed from logistic regression or supervised classification for producing rubber area masks for the volume model application. For this purpose, the output rubber bitmaps and classification accuracies produced from both techniques were evaluated (Fig. 2). Comparison of rubber area bitmaps produced from these techniques indicated some spatial agreements, although, when applied to the full scene image, the rubber area produced from a supervised classification was 10% higher than that produced from the area model. In terms of accuracy, it was found that the supervised classification using the maximum likelihood algorithm was superior to the area model. When refitted with the entire data set, overall, the area model correctly assigned 94.5% of the pixels. However, the model did a better job in predicting non-rubber (96.3%) than that of rubber (87%) (Table 1). The supervised classification produced a higher accuracy of classifying rubber at 96.9%. Therefore, it was decided that the rubber area map produced from supervised classification would be used for the volume model application.

3.2 Rubber Tree Stand Volume Model Application

With an image segment-based approach, the application of the rubber stand volume model in classified rubber pixels was demonstrated. The mean of spectral radiance of rubber stands were extracted by segments, and then the equation was applied to each segment. The image segmentation technique resulted in 812 rubber segments, with segment area ranging from 1.5 to 14 ha. The mean area of the segments was 3.3 ha, and the estimated mean of rubber volume derived from the model was 237 m³/ha.

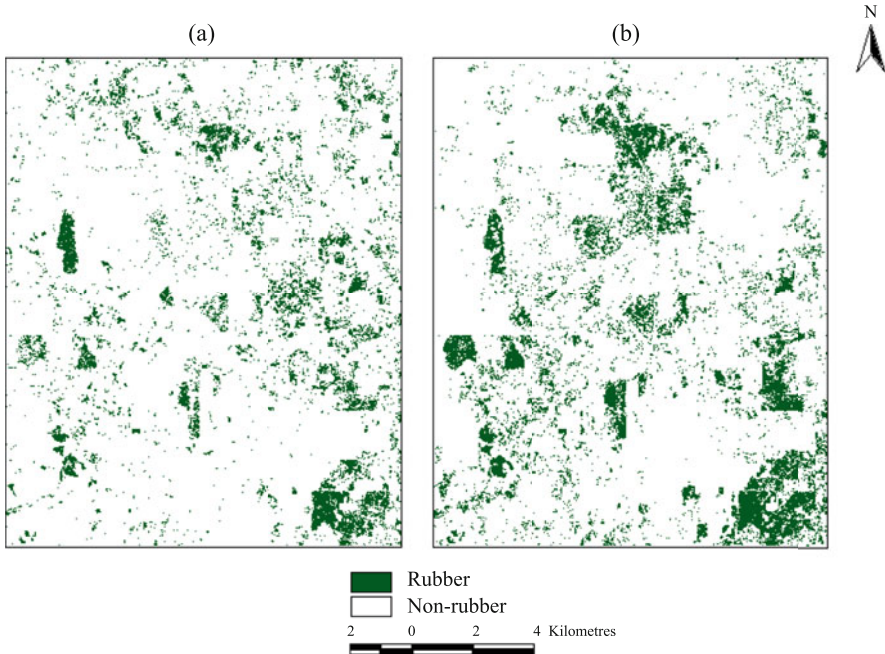


Fig. 2 Rubber area maps from the 1999 Landsat TM image of the demonstration area: (a) output bitmaps of rubber area predicted by area model using a logistic regression, and (b) thematic map of rubber area produced by a supervised classification

Table 1 Classification accuracy of logistic regression model for predicting rubber areas

		Training (<i>n</i> = 33,473 pixels)			Validation (<i>n</i> = 16,794 pixels)		
		Predicted		Percent correct	Predicted		Percent correct
		0	1		0	1	
Observed	0	25,905	979	96.4	13,027	509	96.2
	1	846	5743	87.2	409	2849	87.4
Overall				94.5			94.5

Notes: 0 denotes “non-rubber”, 1 denotes “rubber”

Prior to the image segmentation analysis, an attempt was made to apply the volume model to the scene at the pixel level. This experiment was attempted despite the fact that the model was built at the stand level. In an ideal case, the application of the model should also be at the stand level. As expected, the pixel-level model application resulted in high estimation errors, as they were developed with stand means. The presence of spectral variability among pixels within the rubber areas resulted in errors.

Applying the model at the stand level allowed for the extraction of spectral features to be carried out by segments, which are homogenous in the sense of their spectral and stand characteristics. In the context of rubber management planning, the

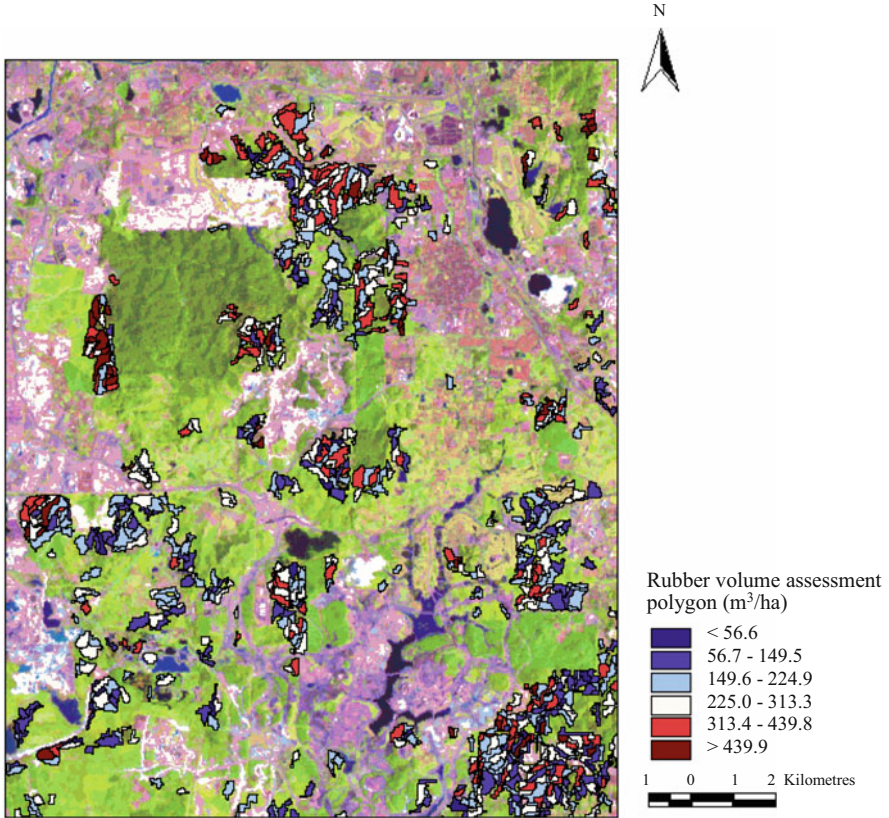


Fig. 3 Rubber volume assessment polygon produced from an application of volume model and an image segmentation technique superimposed on the 1999 Landsat TM pseudocolour composite (RGB = bands 5, 4, 3) image of the demonstration area

segments could be referred to as rubber estates or rubber small landholding units. The resulting rubber assessment polygons with five volume classes (m^3/ha) estimated from the model are shown in Fig. 3.

Although the stand-based model application performed much better than the pixel-based approach, there were minor exceptions. For example, of 812 rubber segments, 14 segments gave negative volume estimates, and 5 segments gave volume estimates greater than $600 \text{ m}^3/\text{ha}$, which was an overestimation of stand volume for rubber plantations. Negative volume estimations could have been avoided if the exponential shape of the model ($\hat{y} = x^a b^x$) had been used, as this function will not allow for them. However, during the initial stage of the model building process, this function was tested and found to be less promising than others that were applied in terms of the trend of residuals and goodness of fit.

Besides these minor problems, the analysis demonstrated that the stand attribute model derived from satellite data could be applied using the image segmentation

technique. This provides a useful tool for estimating average volume within localised areas, plantations, or segments.

3.3 Land Use/Cover Classification

Preliminary examination of the data set revealed a wide range of spectral contrasts among land use/cover types. Spectral separability was analysed using J-M Distance. Measured values were between 0 and 2, where '0' indicated a complete overlap between the signatures of two classes and '2' indicated a complete separation. An analysis of the land use/cover class signatures suggested good spectral separability among the different classes, with an average separability of 1.93. Spectrally, rubber was fairly well separated from other classes, with separability ranging from 1.85 to 2.00. Spectral separability between classes was weakest in the case of grasslands and mixed crops (1.41) which recorded user's accuracy of 60.9% (Table 2). With the exception of mixed crops and grasslands, each class exhibited over 90% producer's accuracy. The user's accuracies for each class were all over 80% (Table 2).

The land use/cover map yielded an overall classification accuracy of 88.3% (Kappa coefficient of 0.86) (Table 2). With the exception of mixed crops and grasslands, the producer's and user's accuracies for each class were over 80%. Overall, all maps met the minimum accuracy value of 85%, which is the basic requirement for digitally classified images (Anderson 1971; Paul 1991; Wulder et al. 2002). The Kappa coefficient was 0.86 indicated that the classification achieved an accuracy that is 86% better than what would be expected from random assignment of pixels to the land use/cover types in the study area. This range of Kappa coefficients represented a high accuracy and was well within the range of good classification performance of 0.61–0.80 specified by Landis and Koch (1977). The overall accuracy indicated that these digitally classified images are useful in mapping the land use/cover of the study area. The high accuracy may be partly attributed to the simple classes used.

As expected, the main source of error in classification was in separating mixed crops and grasslands and vice versa. The difficulty in separating mixed crops and grasslands is evident from the confusion matrix. For example, the error matrix was comprised of 6159 classified pixels, with 719 pixels in the mixed crop class: of which 554 were correctly classified (user's accuracy = 77.1%); 282 pixels (16 + 74 + 187 + 5) were excluded (omission errors = 33.7%); and 187 were erroneously classified as grasslands. On the other hand, 165 pixels (1 + 75 + 82 + 7) were included in this class (commission errors = 22.9%), and 82 of these belonged to grasslands. Similarly, 599 pixels were classified as grasslands, of which 365 were correctly classified (user's accuracy = 60.9%). Of 104 pixels (20 + 82 + 2) excluded (omission errors = 22.2%), 82 pixels were misclassified as mixed crops, and 234 (3 + 25 + 187 + 4 + 15) were incorrectly included (commission errors = 39.1%), 187 of which belonged to mixed crops. These errors could be due to the training areas containing internal variability within each class. Variability (e.g., in canopy cover, density, and structure) increased the variance of the Gaussian distributions

Table 2 Confusion matrix of land use/cover classification accuracy defined by the number of pixels of the test sites classified correctly in the thematic map of 1999 Landsat TM

Land use/cover classes	Pixels classified by class										Total	User's accuracy
	Water	Forest	Oil palm	Mixed crops	Grasslands	Rubber	Cleared areas	Urban				
Water	664										664	100.0
Forests	11	1080	34	16		79					1222	88.4
Oil palm		29	732	74	20	1				4	860	85.1
Mixed crops		1	75	554	82	7					719	77.1
Grasslands	3		25	187	365	4	15				599	60.9
Rubber	3	21		5	2	1039	2			2	1075	96.6
Cleared areas								637			637	100.0
Urban									15		383	96.1
Total	681	1132	866	836	469	1130	669	669	376	98.0	6159	
Producer's accuracy	97.5	95.5	84.5	66.3	77.8	91.9	95.2					

Note: The bold values show the correctly classified pixels in each category

$$\text{Overall accuracy} = \frac{(664+1080+732+554+365+1039+637+368)}{6159} \times 100 = 88.3\%$$

Overall Kappa coefficient = 0.86

assumed for each class type and derived from the training data sets (Saatchi et al. 2000). The increase in the variance increased the confusion in choosing the class label using the maximum-likelihood classifier. Another potential source of error was because mixed crops containing ground vegetation may be similar to grasslands. To some extent, grasslands and croplands may be interchangeable in the sense that at certain times the croplands can be left fallow and become grasslands (Indrabudi et al. 1998).

Another area of misclassification is the minor confusion of forest as oil palm, mixed crops, and rubber (Table 2). The misclassification of forests could be due to the presence of some amount of low density or disturbed areas in the forests that may have similar spectral responses with the latter classes. In tropical forests, the spectral response of vegetation on satellite images is inevitably dominated by canopy cover (Myers 1988).

In some areas, rubber and oil palm plantations were confused with forests. These areas were probably unmanaged plantations that sometimes show similar reflectance to logged-over forests. This could be explained by the similarity in the presence of pioneer tree species that dominated the canopy of secondary forests and/or abandoned rubber and oil palm plantations such as Mahang (*Macaranga* spp.), Balik angin (*Mallotus* spp.), and Sesenduk (*Endospermum malaccense*) (Kueh and Lim 1999).

From the classified image, rubber exhibited user's accuracy 96.6% and producer's accuracy of 91.9% (Table 2). In previous studies, rubber plantations have been classified using Landsat TM with varying degrees of accuracy. For example, in a study monitoring deforestation in Sungai Buloh, Malaysia, Kamaruzaman and Mohd Rasol (1995) reported that rubber had 79% classification accuracy with 21% confusion with forests and 5% with grasslands. In mapping land use/cover distribution in mountainous Langkawi Island, Malaysia, Baban and Kamaruzaman (2001) achieved 74% classification accuracy for rubber, where major misclassification was reported between rubber and forests (13%). This was attributed to the topographic shadow effects on the island forest, with elevation rising to 870 m ASL in some areas.

For this study, misclassification between rubber and forests was found to be less than 7%. This confusion may be attributed to minor shadow effects due to relatively flat topography in this area. In addition to misclassification of forests and mixed crops as rubber, there was an additional confusion with oil palm and grasslands classed as rubber. This could be because of rubber test areas containing young rubber stands with ground vegetation cover which show a similar signature response to grasslands, mixed crops, and understory vegetation of open (young) oil palm stands.

Water and cleared areas were the most accurately identified categories (Table 2). They exhibited the similar highest user's accuracies of 100%. This could be due to their easy isolation with respect to other classes and to their homogeneity. Also, because of the relatively higher reflectance of water in the visible region and almost total absorption in the mid-infrared region of the electromagnetic radiation (EMR) spectrum, enough contrast between water and other land features was observed. As mentioned, the two least accurate classes were grasslands and mixed crops. Lower

error could probably be achieved if these classes were simplified to broader cover types, which probably are more suitable to TM capabilities. For example, in mapping land use/cover in Georgia using Landsat TM imagery, Yang and Lo (2002) combined grasslands, croplands, and other herbaceous vegetation as a single class and achieved 96% user's accuracy.

The mixed crop class is diverse and includes a variety of different crop types. In North America, farms generally are large in size with single crop production (USDA 2001). In Malaysia and other tropical countries, croplands generally occur at a much smaller area and can be likened to gardening with respect to the small size of plots and variety of crops produced. Multi-crop fields and small field sizes produce texture and tones that can be difficult to differentiate. Mixed crops are generally small, less than 0.5 ha, but plots for a village are usually adjacent to each other (Suratman et al. 2000). The smaller plots and the variety of crop types within plots create heterogeneous surfaces, which are more difficult to characterise than larger plots with a single crop. Cultivation of mixed crops and grasses grown for livestock often adjoin each other, giving images a heterogeneous texture that is difficult to characterise.

With the exception of mixed crops and grasslands, the remaining vegetated classes (i.e., forest and oil palm) achieved high individual accuracies (>85%) for both user's and producer's accuracies for each classification. This could be due to their spectrally homogenous characteristics, allowing easy definition using the classification algorithm.

Positional errors from the map scale are often of concern in mapping since it effects the information on a thematic map. The accuracy and precision are a function of the scale at which a map is created. In this study, the use of topographic maps at a scale of 1:50,000 and a land use map at a scale of 1:125,000 to aid in the selection of training and testing areas resulted in positioning errors of ± 25.4 m and ± 65.5 , respectively.

3.4 Rubber Tree Stand Volume Classification

A good signature separation between the five rubber volume classes and the five-land use/cover types (i.e., water bodies, forests, cleared areas, and urban) with an average J-M Distance separability of 1.98 was obtained (table not shown). With the exception of volume classes 4 and 5, the signature separability between the volume classes and the two vegetation covers (i.e., mixed crops and oil palm) was moderate, with an average of 1.73. Grasslands and mixed crops had lower separability with volume class 1 (1.55 and 1.47, respectively). Among all volume classes, classes 4 and 5 were the two most well separated with the seven-land use/cover categories (separability ranged 1.85–2.00).

3.5 Signature Separability Between Rubber Volume Classes

There were spectral overlaps in signatures between rubber volume classes that were from poor to moderate separability for all combination pairs of volume classes. Average spectral separability between rubber volume classes was 1.08, with a range of 0.51–1.79. Volume class 1 had moderately good separability with volume classes 4 and 5 (1.62 and 1.79), but poor separability with classes 2 and 3 (1.40 and 1.47). Volume class 2 had very poor separability with volume class 3 (0.73). Also, volume class 4 had very poor separability with volume 5 (0.51). This indicated that signature separation of rubber volume generally could be grouped into two broad categories, the first category consisting of volume classes 1–3 (0–225 m³/ha, young stands) and the second category consisting of volume classes 4 and 5 (≥226 m³/ha, mature stands).

3.6 Rubber Volume Classification Accuracy

Supervised classification resulted in a thematic map (Fig. 4) and error matrix table (Table 3) consisting of seven land use/cover-class categories combined with five rubber stand volume classes. The overall accuracy and Kappa coefficient values were 67.7% and 0.64%, respectively. While water bodies, forests, cleared areas, and urban areas were displayed without much confusion, mixed crops, grasslands, and all rubber volume classes showed high amounts of misclassification. The low accuracy was attributed to the difficulty in separating grasslands from rubber volume class 1. In particular, 72% (430) pixels belonging to grasslands were misclassified as volume class 1. Only 18.2% of the pixels (user's accuracy) were correctly classified. Major confusion was also observed between mixed crops and volume class 1. About 58% (417) of pixels belonging to mixed crops were confused with volume class 1, which resulted in a user's accuracy of 27.1% (Table 3). These confusions can be observed visually by analysing the resulting maps derived from the 1999 Landsat TM (Fig. 3 vs. Fig. 4), where the majority of the area of grasslands and mixed crops in Fig. 3 were occupied by rubber volume class 1 (0–75 m³/ha) in Fig. 4. Again, this result can be attributed to the existence of ground vegetation and low rubber crown closure in young rubber plantations (3–8 years of age for volume class 1), resulting in similar signatures to grasslands and the undergrowth components of mixed crops. As expected, due to poor separability, each of the volume classes recorded only poor to moderately good classification accuracies. The user's accuracy ranged from 18.2% (volume class 3) to 71.0% (volume class 1) (Table 3).

Rubber volume class 1 was clearly associated with grasslands and mixed crops, and there was confusion among the five rubber volume classes. However, it is also interesting to explore how well the classification with multiple volume classes performed for just separating rubber from non-rubber classes and broader volume class of rubber. Three approaches were used to investigate these questions.

The first approach was to reclassify the image by omitting volume class 1 from the classification, reducing the number of classes to 11 classes. While this resulted in

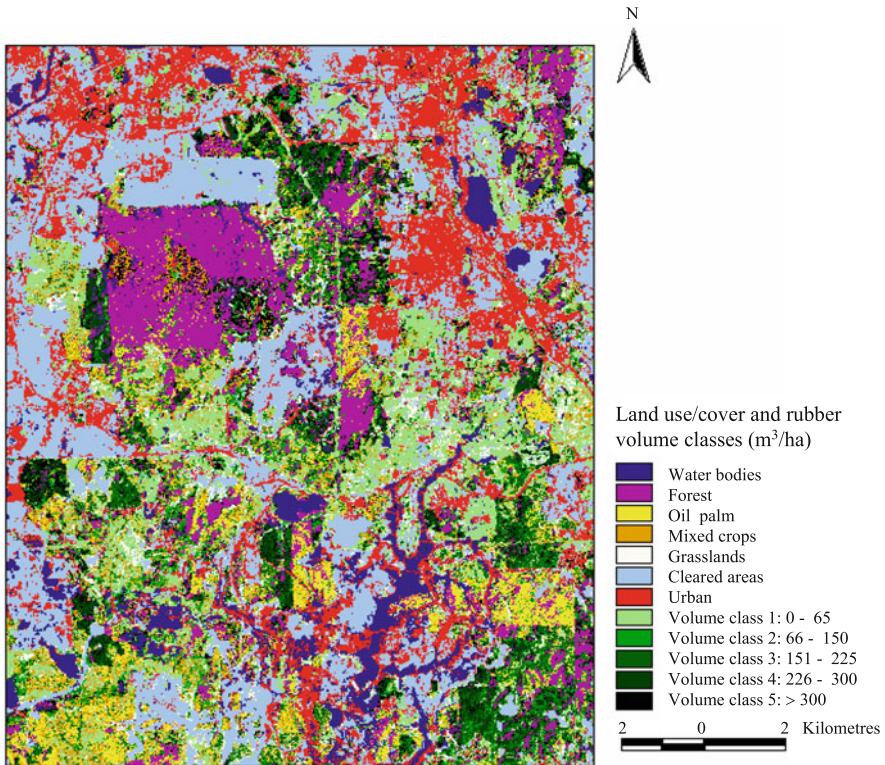


Fig. 4 Land use/cover thematic map combined with rubber volume class map produced by a supervised classification of the 1999 Landsat TM image

improvements in the overall classification accuracy (67.7–76.7%), the user's accuracies of mixed crops (27.1–69.3%), and grasslands (18.2–57.8%), it did not result in an appreciable increase in all rubber volume class accuracies (table not shown).

The second approach involved comparing overall rubber volume classification accuracy to general land use/cover classification (see grey boxes in Table 3). Results from these analyses indicated that combining all rubber volume classes together produced an overall user's accuracy of 91.0% $((980/1078) \times 100)$ and producer's accuracy of 47.8% $((980/2051) \times 100)$. The poor overall producer's accuracy was attributed to the association of mixed crops and grasslands with rubber volume class 1. Combining all classes together except volume class 1 produced 89.2% user's accuracy $((839/941) \times 100)$ and 78.1% producer's accuracy $((839/1074) \times 100)$ overall. The main source of error was in separating oil palm and rubber volume class 2. Subsequently, combining all classes together except volume classes 1 and 2 produced an overall user's accuracy of 78.6% $((608/774) \times 100)$ and producer's accuracy of 75.1% $((608/810) \times 100)$.

Table 3 Confusion matrix of land use/cover and rubber volume classification accuracy by the number of pixels classified correctly in the Thematic Map of the 1999 Landsat TM

Land use/cover and rubber volume classes	Pixels classified by class											User's accuracy		
	Water	Forest	Oil palm	Mixed crops	Grasslands	Cleared areas	Urban	Vol. class 1	Vol. class 2	Vol. class 3	Vol. class 4		Vol. class 5	Total
Water	664												664	100.0
Forest	10	1058	24	11			1						1222	86.6
Oil palm		26	685	69	4			46	9	15			860	79.7
Mixed crops		1	52	195	26			60	1				718	27.1
Grasslands	2		8	34	109			10	18				599	18.2
Cleared areas						637		430	3	3			637	100.0
Urban						15	368						383	96.1
Vol. class 1			5	9	4	1		96	9	9		2	135	71.0
Vol. class 2		10	1	7	1	1		13	38	10	32	54	167	22.8
Vol. class 3		1	23	6				7	20	16	3	12	88	18.2
Vol. class 4	1	1	1	11	1	2		4	54	62	232	53	422	55.1
Vol. class 5		3	4	2		1		1	23	37	124	69	264	26.1
Total	676	1100	803	344	145	667	374	977	264	164	406	240	6159	
Producer's accuracy	98.2	96.2	85.3	56.7	75.1	95.5	98.5	9.8	14.4	9.7	57.2	28.8		

Notes: The bold values show the correctly classified pixels in each category. Numbers of pixel in the grey boxes were used to highlight accuracy comparison between general land use/cover and rubber volume classes

$$\text{Overall accuracy} = \left(\frac{664+1058+685+195+109+637+368+96+38+16+232+69}{6159} \right) \times 100 = 67.7\%$$

$$\text{Overall Kappa coefficient} = 0.64$$

The third approach was comparing general land use/cover classification with rubber volume classification (12 classes) accuracy (Table 3) to a rubber class using rubber volume classes as test areas as presented in an 8 × 5 confusion matrix table (8 classes) in Table 4.

Using the 12-class category, of 135 pixels belonging to rubber volume class 1, only 9.7% (13) of pixels were misclassified as mixed crops and grasslands (see Table 3). On the other hand, if the 8 classes were used, 67.4% (91) of rubber volume class 1 pixels were incorrectly classified as mixed crops and grasslands (Table 4). For the 12 classes, about 26.2% (23) of 88 pixels belonging to rubber volume class 3 were confused as oil palm, and 6.8% (6) pixels as mixed crops. However, using the 8 classes, 31.8% (28) and 22.7% (20) of rubber volume class 3 pixels were misclassified as oil palm and mixed crops, respectively. About 89.3% (377) of 422 pixels belonging to rubber volume class 4 and 86.7% (299) of 264 pixels belonging to rubber volume classes 5 were correctly classified as rubber (Table 4). Therefore, the general land use/cover classification seemed to underestimate rubber if it is young. From these approaches, it can be seen that rubber was fairly well separated from the rest of the classes if young stands (i.e., volume classes 1–3) were excluded.

Generally, errors from rubber volume classification were resulted from high natural variability within volume classes. Also, the high error was likely due to the volume classes used for the classification being too fine. This caused an overlap of spectral signatures because the spectral characteristics of the volume classes were not distinctive enough to be used for the identification and separation of individual

Table 4 Confusion matrix of rubber volume classes versus general land use/cover classes using rubber volume class as test areas of the 1999 Landsat TM

Rubber volume class	Pixels classified by class										Total
	Water	Forest	Oil palm	Mixed crops	Grasslands	Rubber	Cleared areas	Urban			
Vol. class 1	0	0	7	39	52	34 (25%)	3	0	135		
Vol. class 2	0	14	8	21	6	117 (70%)	1	0	167		
Vol. class 3	0	4	28	20	0	35 (40%)	1	0	88		
Vol. class 4	2	2	2	16	3	377 (89%)	20	2	422		
Vol. class 5	1	6	5	2	0	229 (86%)	21	1	264		

Note: The bold values show the number and percent of pixels belonging to rubber volume classes correctly classified as a rubber class

rubber volume classes. Also, the volume classes are a continuum with transition zones between them. A combination of these factors, in part, may have contributed to the confusion in determining the volume classes using the maximum-likelihood classifier.

The preceding analyses showed a comparison of two approaches for predicting rubber stand volume in the demonstration area. They are (1) the use of a supervised classification to delineate a rubber map for an application to rubber volume model and (2) the use of ground information to provide training areas for a combined supervised classification of land use/cover and volume classes. The first approach resulted in 11.7% overall classification error with eight land use/cover as compared to an overall classification error of 32.3% for the 12 classes in the second approach. The classification errors using the first approach was 3.6% as compared to a classification error of 29.0–81.8% (Tables 3 and 4) for the 5 rubber volume classes in the second approach. Therefore, for the purpose of predicting rubber volume classes within a spatial unit, the first approach was preferred.

4 Conclusions

The study presented in this chapter has demonstrated the usefulness of satellite remote sensing for the application of rubber tree area and stand volume models across landscape and in producing reasonable land use/cover and rubber tree resource maps for the area south of Kuala Lumpur, Malaysia. The value of the maps is a function of the accuracy of the classification. Accuracy assessments confirmed the image processing procedures were useful in extracting land use/cover and planted rubber tree areas, stand volume maps, and statistics for the areas. The methodology used was based on an understanding of landscape features, sensor characteristics, and the information extraction techniques employed.

In this study, the use of supervised image classification for rubber area delineation and subsequent volume model application was a better procedure for rubber stand volume prediction than the classification of a combined land use/cover and volume classification. Eight categories of land use/cover of area south of Kuala Lumpur were classified for 1999, with overall classification accuracy of 88.3%, respectively. Rubber stand volume classification indicated low overall accuracy mainly due to confusion between lower volume classes and grasslands and mixed crops.

The extent and nature of land use/cover that were identified can provide a useful indicator of overall landscape in the area. The extent of land use/cover can also act as an indicator for general land use planning. Studies such as this can assist decision-makers in assessing the resource condition, availability, and dynamics of land use/cover change in addressing the broader requirements of land use policy development and planning.

References

- Abdul Razak MA, Hoi WK (1988) Rubberwood: a new timber resource. *Malays For* 51(3):155–163
- Ahern FJ, Erdle T, MacLean DA, Knepeck ID (1991) A quantitative relationship between forest growth rates and Thematic Mapper reflectance measurements. *Int J Remote Sens* 12(3):387–400
- Anderson JR (1971) Land use classification schemes used in recent applications of remote sensing. *Photogramm Eng* 37(4):379–387
- Baban SMJ, Kamaruzaman WY (2001) Mapping land use/cover distribution on a mountainous tropical island using remote sensing and GIS. *Int J Remote Sens* 22(10):1909–1918
- Bourne SG, Graves MR (2001) Classification of land-cover types for the Benning ecoregion using enhanced Thematic Mapper data. In: Strategic environmental research and development program (SERDP), ERDC/EL TN-ECMI-01-01, 9 pp
- Chee YK, Ahmad F (1990) Sheep grazing reduces chemical weed control in rubber. In: Proceedings forage for plantation crops, Bali, Indonesia, 27–29 June 1990, pp 120–123
- Congalton RG (1991) Review of assessing the accuracy of classifications of remotely sensed data. *Remote Sens Environ* 37:35–46
- FAO (2002) An overview of forest products statistics in South and Southeast Asia (web page). <https://www.fao.org/3/ac778e/AC778E00.htm#TOC>. Accessed 24 Apr 2022
- Faridah-Hanum I (1999) Plant diversity and conservation value of Ayer Hitam Forest, Selangor, Peninsular Malaysia. *Pertanika J Trop Agric Sci* 22(2):73–83
- Hong LT, Sim HC (1999) Products from rubberwood—an overview. In: Hong LT, Sim HC (eds) *Rubberwood: processing and utilisation*. FRIM, Kuala Lumpur, pp 177–186
- Indrabudi H, De Gier A, Fresco LO (1998) Deforestation and its driving forces: a case study of Riam Kanan watershed, Indonesia. *Land Degrad Dev* 9:311–322
- Kamaruzaman J, Mohd Rasol RAF (1995) Satellite remote sensing of deforestation in the Sungai Buloh forest reserve, Peninsular Malaysia. *Int J Remote Sens* 16(11):1981–1997
- Killmann W, Hong LT (2000) Rubberwood—the success of an agricultural by-product. *Unasylva* 201(51):66–72
- Kueh RJH, Lim MT (1999) Forest biomass estimation in Ayer Hitam Forest Reserve. Paper presented at the Management and Ecology of Ayer Hitam Forest Reserve, 12–13 Sep 1999, 7 pp
- Landis JR, Koch GG (1977) The measurement of observed agreement for categorical data. *Biometrics* 33:159–174
- Lillesand TM, Kiefer RW (2000) *Remote sensing and image interpretation*, 4th edn. Wiley, New York. 724 pp
- Makela H, Pekkarinen A (2001) Estimation of timber volume at the sample plot level by means of image segmentation and landsat TM imagery. *Remote Sens Environ* 77:66–75
- Mertens B, Lambin EF (1997) Spatial modelling of deforestation in Southern Cameroon. *Appl Geogr* 17(2):143–162
- Meteorological Service (2022) Annual climate statistics (web page). http://www.kjc.gov.my/main_e.html. Accessed 24 Apr 2022
- Ministry of Energy and Natural Resources (2022) Total forested areas in Malaysia (1990–2018) (web page). <https://www.ketsa.gov.my/en-my/KetsaCore/Forestry/Pages/Total-Forested-Areas-in-Malaysia.aspx>. Accessed 24 Apr 2022
- Mohd Dahlan J, Hong LT, Azlan M, Wong AHH (1999) Preservation of rubberwood. In: Hong LT, Sim HC (eds) *Rubberwood: processing and utilisation*. FRIM, Kuala Lumpur, pp 91–109
- MRB (2002) Malaysian rubber boards rubber statistic (web page). <http://www.lgm.gov.my>
- MRB (2022) Natural rubber statistics (Jan–Dec 2021) (web page). <https://www.lgm.gov.my/webv2/pdfViewer/nrStatistic>. Accessed 24 Apr 2022
- Myers N (1988) Tropical deforestation and remote sensing. *For Ecol Manage* 23:215–225
- Paul M (1991) *Computer processing of remotely sensed images: an introduction*. Biddley Ltd., London. 352 pp
- Richards JA, Jia X (1999) *Remote sensing digital image analysis: an introduction*, 3rd edn. Springer-Verlag, New York. 363 pp

- Rosenfield G, Fitzpatrick-Lins K (1986) A coefficient of agreement as a measure of thematic classification accuracy. *Photogramm Eng Remote Sens* 48(1):131–137
- Saatchi S, Agosti D, Alger K, Delabie J, Musinky J (2000) Examining fragmentation and loss of primary forest in the southern Bahian Atlantic forest of Brazil with radar imagery. *Conserv Biol* 15(4):867–875
- Suratman MN (2011) Satellite imagery for rubber plantation monitoring. UiTM Press, Universiti Teknologi MARA, Shah Alam. 250 pp
- Suratman MN, Muhammed S, Abd Rahman MN, Jiwan D (2000) A preliminary survey of agroforestry systems in Malaysia. In: Proceedings of the fourth conference on forestry and forest products research. FRIM, Malaysia, pp 497–507
- Suratman MN, Bull GQ, LeMay VM, Leckie DG, Marshall PL, Mispan MR (2004) Prediction models for estimating volume, age and predicting area of rubber plantations in Malaysia using Landsat TM Data. *Int For Rev* 6(1):1–13
- Tole L (2002) An estimate of forest cover extent and change in Jamaica using Landsat MSS data. *Int J Remote Sens* 23(1):91–106
- USDA (2001) Major world crop areas and climatic profiles (web page). <http://www.usda.gov/oce/waob/jawf/profiles/mwcap2.htm>
- Verbyla DL (1995) Satellite remote sensing of natural resource. Lewis Pub, Boca Raton. 198pp
- Wilkie DS, Finn JT (1996) Remote sensing imagery for natural resources monitoring. Columbia University Press, New York. 295 pp
- Wulder M, Cranny M, Dechka J (2002) An illustrated methodology for land cover mapping of forests with Landsat-7 ETM+ data: methods in support of EOSD land cover, version 2 methods. Can. For. Serv., Pac. For. Cen, Victoria. 39 pp
- Yang X, Lo CP (2002) Using time series of satellite imagery to detect land use and land cover changes in the Atlanta, Georgia metropolitan area. *Int J Remote Sens* 23(9):1775–1798



Using Historical Disturbance Identified with LandTrendr in Google Earth Engine for Land Cover Mapping of Oil Palm Landscapes

Daniel Platt, Reza Azmi, Ahimsa Campos-Arceiz, Michelle Li Ern Ang, Darrel Tiang, Badrul Azhar, Hoong Chen Teo, Simon Jones, and Alex M. Lechner

Abstract

In Malaysia, land under oil palm plantation has been steadily increasing. Meanwhile voluntary measures to improve sustainability of palm oil production have been introduced including regulation of land conversion to oil palm plantations.

D. Platt · M. L. E. Ang · D. Tiang

School of Environmental and Geographical Sciences, University of Nottingham Malaysia, Semenyih, Malaysia

R. Azmi

Wild Asia, Kuala Lumpur, Malaysia

A. Campos-Arceiz

Southeast Asia Biodiversity Research Institute, Chinese Academy of Sciences and Center for Integrative Conservation, Xishuangbanna Tropical Botanical Garden, Chinese Academy of Sciences, Mengla, Yunnan, China

B. Azhar

Department of Forestry Science and Biodiversity, Faculty of Forestry and Environment, Universiti Putra Malaysia, Serdang, Selangor, Malaysia

Institute of Tropical Forestry and Forest Products, Universiti Putra Malaysia, Serdang, Selangor, Malaysia

H. C. Teo

Department of Biological Sciences, National University of Singapore, Singapore, Singapore

S. Jones

School of Mathematical and Geospatial Sciences, RMIT University, Melbourne, Australia

A. M. Lechner (✉)

School of Environmental and Geographical Sciences, University of Nottingham Malaysia, Semenyih, Malaysia

Monash University Indonesia, Tangerang, Banten, Indonesia

e-mail: Alex.Lechner@Monash.edu

The objective of this study is to assess the utility of Google Earth Engine with the LandTrendr algorithm for classifying land cover, as a first step towards developing a tool for land cover change detection in Peninsular Malaysia to support Roundtable on Sustainable Oil Palm (RSPO) certification. Ground validation data on land cover and disturbance events from satellite imagery were used to calibrate LandTrendr to detect and map change from forest to oil palm, other vegetation or urban; other vegetation to oil palm; and oil palm to oil palm (replanting). The resulting disturbance rasters were then used with a 2019 multispectral Landsat mosaic in a random forests supervised classification. The classified maps of 2019 land cover showed a small improvement in accuracy with the addition of LandTrendr rasters over using only Landsat imagery. Our results suggest that disturbance history may provide useful ancillary information to support remote sensing mapping and LandTrendr could potentially become a useful tool for detecting land cover change in the tropics. In many cases the maps performed better with the addition of LandTrendr rasters; however, the resulting difference was small in overall accuracy. The method improved the accuracy of oil palm, rubber, forest and urban land covers, while it decreased the accuracy for other land cover classes. Vegetation classes such as oil palm, rubber and forest were often confused and remain challenging to map.

Keywords

LandTrendr · Oil palm · Remote sensing · Historical land cover · Google Earth Engine

1 Introduction

Operationalising the monitoring of oil palm using remote sensing is perhaps one of the most critical applications for remote sensing of the environment in Southeast Asia. The oil palm is a tree that grows within tropical regions, was traditionally planted in smallholder groves in Africa, but in the early 1900s, oil palm was planted on an industrial scale across the world. Since the 1980s, there has been a growing awareness of the environmental impacts caused by oil palm expansion, as these estates are being developed in tropical regions which are dominated by natural forests (Miettinen et al. 2016; Tang and Al Qahtani 2020). By the early 2000s, the oil palm industry and NGOs had developed a certification system for oil palm growers which was believed to be the answer to halting deforestation of critical natural habitats (Omont 2005; RSPO 2015), known as the *Roundtable for Sustainable Palm Oil* (RSPO). In order to qualify for RSPO certification, plantation owners must conduct a Land Use Change Analysis (LUCA) to show that no virgin forest was cleared for establishing the plantation.

The aim of this study is to improve the monitoring of deforestation by developing a method for mapping land cover in tropical Southeast Asia using multi-temporal Landsat data to characterise historical disturbance patterns. The focus is on

deforestation driven by expansion of oil palm plantations. We first created multi-date satellite image composites to address cloud cover issues. Then we used the image time series with LandTrendr pixel-based trajectory analysis to analyse the temporal characteristics of different land covers in order to differentiate between land covers with similar spectral characteristics but different land cover change patterns. Finally, raster outputs from LandTrendr and a Landsat mosaic are combined then classified using supervised random forests to produce a land cover map. We used a case study in Peninsular Malaysia to test and develop the remote sensing approach. We concluded by discussing the results, limitations and application of the novel approach for multi-temporal remote sensing in the tropics and suggestions for further research, especially within the context of mapping oil palm to support RSPO certification.

By investigating the utility of LandTrendr for land cover mapping, this project contributes towards developing a tool to more efficiently carry out LUCA for RSPO certification. This study provides a novel demonstration of LandTrendr to mapping oil palm. LandTrendr was expected to improve the classification accuracy of oil palm, forest and rubber by providing additional historical disturbance information which is useful to help the random forest classifier to differentiate similar vegetation classes. This is one of the first studies to apply such a novel approach.

2 Background to Remote Sensing Methods for Mapping Oil Palm in Insular Southeast Asia

Land Use Change Analysis (LUCA) is an approach used by the RSPO for tracking the success of conservation planning and natural resource management activities at site, regional and national scales (RSPO 2015). Globally freely available spatial data products (e.g. global forest watch forest change) and remote sensing imagery (Landsat, MODIS and Sentinel) are increasing in quantity and quality, making the provision of land cover and land use data no longer the sole responsibility of the government (Lechner et al. 2020). In addition, a huge step change in the provision and application of remote sensing is taking place due to the development of the Google Earth Engine (GEE) where data is provided and analysed on the cloud, dramatically reducing processing and development times (Kennedy et al. 2018, Mutanga and Kumar 2019).

Remote sensing of land cover and land use in tropical Southeast Asian countries such as Malaysia and Indonesia is challenging due to high incidence of cloud cover and rapid changes in vegetation cover due to regrowth and conversion to other land uses. The most dominant form of land conversion in Southeast Asia is for oil palm (Kanniah et al. 2019; Stibig et al. 2014; Tang et al. 2019; Trisasongko and Paull 2020). However, clear felling and selective logging, shifting agriculture and rubber plantations as well as urbanisation and mining are also common (Razali et al. 2014).

Remote sensing has been used for mapping oil palm for various purposes, including plantation management and carbon stock auditing (Chong et al. 2017; Trisasongko and Paull 2020), classification of oil palm extent and other land covers

(Deilmai et al. 2014) and change detection (Pittman et al. 2013). Daliman et al. (2014) classified oil palm at the plantation scale using GLCM-SVM and NDVI from Worldview-2 imagery. Pittman et al. (2013) studied the expansion of oil palm across Borneo by decade using Landsat imagery. The differentiation of oil palm from other land covers was achieved at plantation scale by Kamiran and Sarker (2014) and at subnational level by Deilmai et al. (2014) and Razali et al. (2014). Studies using multitemporal data include Razali et al. (2014) who classified land cover in several different years based on MODIS satellite imagery. Razak et al. (2018) used Landsat time series to differentiate rubber from oil palm and other land covers. Oon et al. (2019a, b) discriminated between large-scale and smallholding oil palm on tropical peatlands using LANDSAT-8 and ALOS-2 PALSAR-2 L-band and Sentinel-1 C-band SAR.

For the purposes of long-term monitoring of land cover change in oil palm landscapes, Landsat and MODIS are the only freely available datasets which go back far enough to be useful for conducting LUCA for RSPO certification. Studies that attempted to differentiate oil palm, rubber and/or forest used MODIS (Razali et al. 2014; Senf et al. 2013), Landsat (Beckschäfer 2017; Deilmai et al. 2014; Lee et al. 2016; Razak et al. 2018; Sun et al. 2017), SAR (Trisasongko et al. 2017) and other satellites (Kamiran and Sarker 2014; Razali et al. 2014). To tackle spectral similarity between rubber and forest, Razak et al. (2018), Beckschäfer (2017) and Senf et al. (2013) used seasonal differences in rubber spectral data and vegetation indices caused by defoliation of rubber trees to differentiate them from other land covers and specifically from forest and oil palm. A variety of classifiers (CART, RF, Minimum Distance, Maximum Likelihood, SVM) have been used with Landsat imagery (Deilmai et al. 2014; Lee et al. 2016). Sun et al. (2017) used Landsat with a decision tree classifier (C5.0 adaptive boosting algorithm) and additional filtering to remove speckling. Problems included excessive cloud cover (Lee et al. 2016; Razali et al. 2014; Sun et al. 2017), similarity between plantations and forest (Razali et al. 2014; Sun et al. 2017), mixed land cover pixels (Deilmai et al. 2014; Sun et al. 2017) and difficulty gathering historical ground truth from satellite imagery (Beckschäfer 2017; Razak et al. 2018; Sun et al. 2017). Due to the lack of imagery due to cloud cover, Sun et al. (2017) used a mixture of imagery from different seasons which introduced spectral variability, but did not choose imagery based on rubber phenology, making it more difficult to differentiate.

A key challenge for remote sensing in this region is associated with similarity in spectral properties between woody vegetation, for example, agricultural land uses such as palm oil and rubber being confused with natural forest (Miettinen et al. 2018). While the spectral signatures of these land covers are relatively similar, the temporal change and multitemporal profiles of clearance, disturbance and regrowth (natural and through plantations) can potentially be used in analyses such as with LandTrendr (Kennedy et al. 2010).

Several change detection algorithms have been developed for use with spectral time series, including LandTrendr, BFAST and VCT, using a range of active and passive sensors (Boriah 2010). LandTrendr is used for disturbance and recovery detection, whereas VCT only detects disturbance and BFAST is used for

drought-related vegetation disturbance (Zhu 2017). For example, annual oil palm extent in Malaysia and Indonesia has been mapped for 2001–2016 by Xu et al. (2020), using ALOS PALSAR, ALOS PALSAR-2 and MODIS NDVI data, with extent mapped using BFAST for those years in which high-resolution imagery is not available. On the other hand, the LandTrendr algorithm is dependent on Landsat imagery (Kennedy et al. 2010). LandTrendr has been used for land cover classification (Zhu et al. 2019) and change tracking (Bartz et al. 2015), change agent detection (Kennedy et al. 2015), tracking of insect damage (Liang et al. 2014) and monitoring of forest health and extent (Hudak et al. 2013; Wang et al. 2016), among other applications (Zhu 2017).

LandTrendr is an algorithm for “generating trajectory-based spectral time series data” from Landsat imagery (Kennedy et al. 2010). It operates on a pixel-by-pixel basis on annual mosaic stacks and returns simplified trajectories and segment information. Unlike single image approaches to LUCA, LandTrendr uses satellite data across a broad time period. This allows detection of both long-term and short-term change while reducing inter-annual signal noise (Kennedy et al. 2010). A variety of methods have been used with LandTrendr, including correlation with ground-based measurements (Meigs et al. 2011; Pflugmacher et al. 2012), magnitude and relative magnitude threshold (Kennedy et al. 2012), sliding threshold (Grogan et al. 2015), change characterization (Zhu et al. 2019), image stabilization (Bartz et al. 2015) and classification of disturbance rasters (Hislop et al. 2019; Rathnayake et al. 2020). While most applications have focused on North America, studies targeting the tropics and Southeast Asia in particular have used LandTrendr for studying forest disturbance related to rubber and timber plantations (Grogan et al. 2015; Shen et al. 2017; Tang et al. 2019), forest cover change (Fragal et al. 2016; Wang et al. 2016; Ye et al. 2021), mining disturbance (Wang et al. 2020), clearance of savannahs (Almeida de Souza et al. 2020), land cover change (Rathnayake et al. 2020) and cultivation patterns in smallholdings (Schneibel et al. 2017). LandTrendr has been integrated with Google Earth Engine, making it widely available, allowing for processing very large datasets on the cloud and convenient for carrying out and sharing methods of land cover analysis (Kennedy et al. 2018).

This study is the first to use LandTrendr in Malaysia or at a national scale and the first to study oil palm using LandTrendr. It adds to the small body of work on LandTrendr which has been conducted in the tropics (Fragal et al. 2016; Grogan et al. 2015; Schneibel et al. 2017; Shen et al. 2017; Shen and Li 2017; Tang et al. 2019; Yang et al. 2018), which have specific challenges associated with the region including high cloud cover (Fragal et al. 2016; Shen et al. 2017; Tang et al. 2019), spectral similarity between dominant tree-based land covers (forests and plantations) (Mohd Najib et al. 2020) and rapid vegetation regrowth after clearance (Shen et al. 2017). LandTrendr was employed to help overcome some of these issues as it utilizes the entire historical Landsat record to analyse both long-duration and abrupt change and so helps to identify disturbance events and differentiate similar land covers by characteristics of their spectral history (Kennedy et al. 2010; Zhu et al. 2019). Lack of imagery due to cloud cover was tackled by constructing annual image mosaics from imagery taken from all seasons. LandTrendr with GEE makes it

possible to develop a tool which can be easily shared for use by non-specialists in GIS for conducting LUCA (Kennedy et al. 2018).

3 Methods

3.1 Study Area

Malaysia comprises two parts, East Malaysia, consisting of Sarawak and Sabah on the island of Borneo, and Peninsular Malaysia, connected to mainland Southeast Asia by the Kra Isthmus. Peninsular Malaysia, excluding surrounding islands, lies between 1°15′–6°44′N and 100°7′–104°18′E and has an area of 132,090 km² (Swee-Hock 2018). It has a tropical equatorial climate influenced largely by the southwestern and north-eastern monsoons (Tangang et al. 2012) and an annual average rainfall of 2420 mm (Ahmad et al. 2017). In 2020, 58% of land in Malaysia was occupied by forests (FAO 2020); however, deforestation is a major issue, with a reduction in tree cover of 81,200 km² between 2002 and 2019 (Global Forest Watch n.d.).

The population of Peninsular Malaysia is concentrated in coastal cities, particularly in the metropolitan areas of Kuala Lumpur, Penang and Johor Bahru (Department of Statistics 2017). Human land use is dominated by oil palm plantations and urban areas, followed by rubber plantations, rice paddies and other agriculture (Olaniyi et al. 2013; Samat et al. 2020). Land conversion to oil palm plantations has been steadily increasing since 1974, with a rise in the area of land under oil palm plantation from 5657.66 to 59,001.57 km² between 1974 and 2019 (Department of Statistics 2017). Oil palm plantations currently make up about 21% of the total land area in Peninsular Malaysia (Malaysian Palm Oil Board 2019).

3.2 Overview of Methods

In this study we used historical disturbance identified with LandTrendr to map land cover for Peninsular Malaysia using a method compatible with RSPO Land Use Change Assessment (LUCA) (RSPO 2015) which is used to assess compliance for certification. There were four steps to the processing (see Fig. 1):

1. LandTrendr disturbance rasters were extracted along with a 2019 multispectral Landsat mosaic and SRTM elevation data to construct raster stacks.
2. Create LandTrendr disturbance rasters using sliding thresholds to optimize LandTrendr parameters for each of five change patterns (see Table 1—Change Pattern Macroclass). Some potential change patterns (such as ‘oil palm to urban and other brown’) were not included in the study as there was not sufficient ground truth data available for these land covers to accurately conduct the analysis:
 - (a) ‘Forest to oil palm’
 - (b) ‘Oil palm to oil palm’ (replanting)

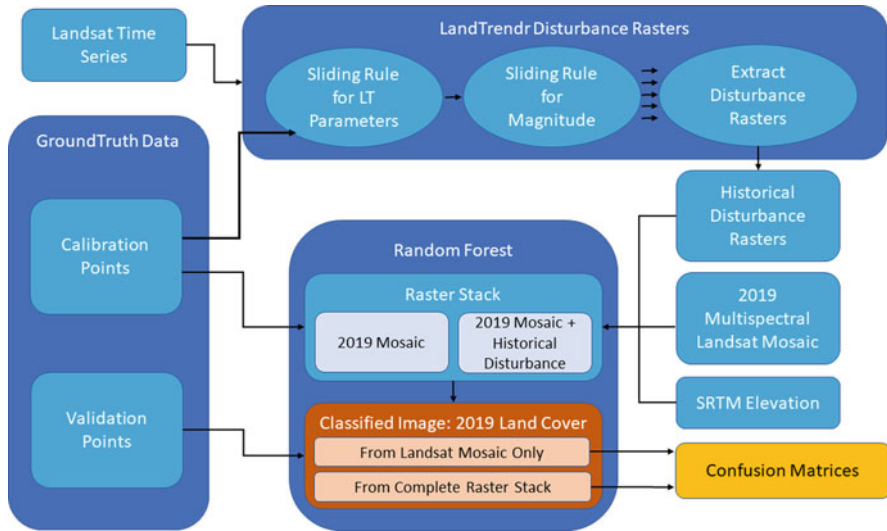


Fig. 1 Flowchart of the process of gathering ground truth data (3.5), calibrating LandTrendr using sliding rules (3.6), extracting disturbance rasters, assembling raster stacks and running Random Forest classification (3.7) and conducting accuracy assessment (3.8)

- (c) 'Forest to urban and other brown'
 - (d) 'Forest to other green'
 - (e) 'Other green to oil palm'
3. Land cover maps of Peninsular Malaysia were produced using a supervised classification with the random forest algorithm.
 4. Confusion matrices were produced to compare accuracies for the land cover maps.

3.3 Image Preparation

The GEE platform was used to build stacks of Surface Reflectance Tier 1 Landsat TM/ETM+/OLI (Landsat 5, 7 and 8) images from 1988 to 2019 from the USGS free Landsat archive. An image collection was created using the Peninsular Malaysia boundary as the region of interest, from across 12 Landsat path/row numbers. The Normalized Burn Ratio (NBR) was chosen as the index for LandTrendr to work on (Grogan et al. 2015; Schneibel et al. 2017; Senf et al. 2015) as qualitative trials found it to be more responsive to clearance events and to track the year of disturbance onset more accurately than other bands and indices during the preliminary calibration. Although NBR is used for detecting fires, it is also excellent at detecting small changes in vegetation intensity (Schneibel et al. 2017). It is calculated from near infrared and short-wave infrared as follows:

Table 1 Idealized land cover classes, RSPO vegetation coefficient, relevant change patterns and land cover macroclasses used for change detection and supervised classification in this study

Macroclass	Land cover class	RSPO vegetation coefficient	Relevant change pattern	Change pattern macroclass	2019 class
Forest	Undisturbed rainforest	1	Forest	Forest	Forest
	Lightly logged/lightly disturbed forest	1	Forest	Forest	Forest
	Mature secondary forest	1	Forest	Forest	Forest
	Secondary forest	0.7	Forest	Forest	Forest
Wetlands	Marsh	1	OtherGreen	OtherGreen	OtherVegetation
	Swamp	1	Forest	Forest	Forest
	Mangroves	1	Forest	Forest	Forest
	Polycultural orchards and agroforestry	0.4	OtherGreen	OtherGreen	OtherAgriculture
Agriculture	Oil palm	0	Oil palm	Oil palm	Oil palm
	Rubber	0	OtherGreen	OtherGreen	Rubber
	Rice	0	OtherGreen	OtherGreen	Rice
	Monocultural orchards	0	OtherGreen	OtherGreen	OtherAgriculture
	Tea plantation	0	OtherGreen	OtherGreen	–
	Vegetable farms	0	OtherGreen	OtherGreen	–
	Other agriculture	0	OtherGreen	OtherGreen	OtherAgriculture
	River	–	–	–	–
	Lake	–	–	–	–
	Pond farms/aquaculture	–	–	–	–
Degraded	Bare ground/cleared	0	UrbanOtherBrown	UrbanOtherBrown	Bare ground
	Grassland	0	OtherGreen	OtherGreen	OtherVegetation
	Scattered trees	0	OtherGreen	OtherGreen	OtherVegetation
	Sand/mud	0	UrbanOtherBrown	UrbanOtherBrown	Bare ground

$$\text{NBR} = \frac{\text{NIR} - \text{SWIR}}{\text{NIR} + \text{SWIR}}$$

Due to the scarcity of cloud-free images in Peninsular Malaysia, annual median mosaics were created using multispectral images from across the whole year. All 30-m bands were used. Trials with shorter collection periods (i.e. less than 1 year) resulted in large areas with no data. The biannual monsoon and significant regional differences in the timing of the monsoon season (Hashim et al. 2016) also made it challenging to use a single collection period which would capture sufficient imagery for all years and across the whole study area. However, Malaysia's equatorial monsoon climate means that it has little deciduous forest (Zakaria et al. 2019) and so relatively small seasonal variation in phenology of forest vegetation. The collection was masked in GEE for clouds, cloud shadow and water with the CFmask prior to mosaicking. The CFmask uses decision trees and scene-wide statistics to label pixels in the scene and identify cloud cover and iteratively estimates cloud heights and projects them onto the ground to identify cloud shadow (CFMask Algorithm n.d.). The CFmask was found to be the most accurate out of several cloud detecting algorithms by Foga et al. (2017), including for detecting cloud and cloud shadow over regions of brightness when thermal data is available. In addition, multi-temporal rasters were derived by compositing several images using the median method which discards the most extreme pixel values such as temporary excessive brightness due to water.

3.4 Land Cover Classification Scheme

The land cover classification scheme was designed to represent the key land cover classes found in Malaysia (Yoshino et al. 2010), with consideration for distinctions in spectral appearance and structural differences. Two schemes were employed (1) for the land cover classification for 2019 (9 classes—see Table 1: 2019 Class) and (2) for the classification of historical disturbance patterns (5 classes—see Table 1: Change Pattern Macroclass). We first started by identifying a set of idealized land cover classes (Table 1) and from that identified a subset of classes based on the remote sensing limitations and usefulness for RSPO mapping. Forest was further split according to vegetation coefficient as described in the RSPO guidelines (RSPO 2015) and disturbance history. Fine land cover classes were grouped thematically into coarse Macro land cover classes (Table 1).

Different schemes were used for the land cover mapping and for use in change detection to create the historical land cover change raster (Table 1). Classes for the supervised classification were grouped together by assumed spectral similarity. For example, bare ground and sand/mud were grouped together as 'bare ground' as they have similar spectral characteristics, but 'urban' was not included as it was assumed to show more permanent characteristics. For the change detection, only the classes relevant to the major change patterns being studied were included, namely, *forest, oil palm, other green* and *urban and other brown* (Table 2). We used a smaller number

Table 2 Number of points used for optimizing parameters per change pattern

	Forest to oil palm	Oil palm to oil palm (replanting)	Forest to urban and other brown	Forest to other green	Other green to oil palm
Change	88	310	24	54	25
No change	126	26	126	126	33
Total	214	336	150	180	58

for the change detection as other classes were not sufficiently represented in the ground truth data.

3.5 Ground Truth Data for Calibration and Accuracy Assessment

Reference data was gathered in three batches using visual assessment of high-resolution Google Earth Pro historical imagery (commonly World View), Landsat imagery, World View Imagery in ArcGIS Pro, Google Timelapse (Gorelick et al. 2017) and land cover maps from Malaya Landuse, iPlan and an existing historical Oil Palm mapping product by WRI (Harris et al. 2019). The data was digitised by several interpreters, with the bulk of the points digitized by the same independent interpreter. All reference points used a homogenous area of 90 m² centred around each point as the relevant area for inspection, equal to the 3 × 3 pixel window used by the LandTrendr algorithm to reduce the effect of localized abnormalities in spectral value and spectral trajectory, and geometric error between the Landsat pixel and the reference data. Accordingly, the minimum distance allowed between points was set at 180 m.

The LandTrendr algorithm was used with default LandTrendr parameters to produce a raster showing year of disturbance. The default parameters were used for maximum segments (6), spike threshold (0.9), vertex count overshoot (3), prevent 1-year recovery (false), recovery threshold (0.25), *p*-value threshold (0.1), best model proportion (1.25) and minimum observations needed (6). The index selected was NBR. However, the annual date range for image compositing was extended to cover the whole year from 01–01 to 12–31. Vegetation change type was kept as ‘loss’ and sorted by ‘greatest’ disturbance. All filters were set to ‘false’ except for minimum mappable unit = 11 pixels.

The resulting raster was used for stratifying 2000 random points equally according to year of change (including *no change*) between 2001 and 2019 (Table 3). Data was recorded regarding current land cover, land cover in the year 2000, occurrence of change prior to the year 2000 and year of disturbance onset and ‘before’ and ‘after’ land cover class for any changes taking place after the year 2000.

To examine the satellite imagery, ground truth points were imported into Google Earth Pro and Google Earth Engine. The annual historical imagery in Google Earth and the high-resolution historical imagery were examined at each point, as well as that of the surrounding landscape for context. An example of the use of context is

Table 3 Calibration and validation points for each class

Class	Calibration	Validation	Total
Forest	241	219	460
Other vegetation	64	73	137
Oil palm	443	456	899
Rubber	100	104	204
Rice	58	52	110
Other agriculture	78	70	148
Bare ground	35	34	69
Urban	50	59	109
Water	12	104	116
Total	1081	1171	2252

assessing whether an area of dark green vegetation is surrounded by similar land cover with no roads or settlements or if it is in an agricultural region near to towns and villages—the former would indicate it is likely forest, whereas the latter would suggest it could be oil palm plantation. The original land cover in the year 2000 was examined, with comparison to previous years to determine if it was previously disturbed—particularly important in differentiating primary and secondary forest and in differentiating forest from plantation. The imagery was also examined up to the present, noting the current land cover as of the year 2019 and any disturbances to the land cover, such as forest clearance, plantation replanting, conversion to built-up areas, flooding which destroys vegetation, extreme drought or draining of land, conversion between different types of agriculture, damming of rivers, erosion and change of river courses and forest regrowth. The type of change was not explicitly recorded, but the time of disturbance onset was recorded, along with both the land cover present before the disturbance occurred and the stable land cover which the land cover became after recovery from the disturbance. If multiple disturbance events occurred, each disturbance was recorded separately. Google Earth Engine was used for viewing customized Landsat composites when a closer view of the pixels was required or for inspecting a more specific time period to determine whether a disturbance occurred in a certain year or in the following year.

Of the points examined, 172 were discarded due to falling on areas with heterogeneous land cover or with extremely complicated land cover histories, while 1828 points were kept for use in the analysis. Heterogeneous land cover included areas of part forest mixed with oil palm, rubber or agriculture or oil palm mixed with rubber or agriculture, as well as some points located on the edge of water bodies. Complicated land cover histories generally involved areas which were cleared or disturbed by flooding or drought multiple times to the point where individual disturbance events could not be clearly differentiated by the interpreter and where an area of otherwise homogeneous forest was cleared in sections with several years gap between clearance events. As some land cover classes were under-represented, to supplement these points for training and validation, a further 424 points were created and labelled with current land cover only.

An additional set of 333 points targeted towards the ‘other vegetation’, ‘rice’, ‘other agriculture’ and ‘bare ground’ land cover classes were created by digitizing polygons in areas dominated by those land cover classes. Points were created randomly within those polygons, maintaining a distance of 180 m from each other and all existing points. They were labelled with current land cover only. Points were discarded which fell on mixed land cover (‘other vegetation’, ‘rice’ or ‘other agriculture’ mixed with each other, ‘forest’, ‘oil palm’ or ‘urban’ and ‘bare ground’ mixed with vegetation classes) or on other land cover classes. Once sufficient points had been digitized for each class, any remaining unlabelled points were discarded. A further set of 91 points covering the ‘water’ class were gathered with current land cover to be used for validation only. These points were created manually, making sure to keep a distance of at least 180 m between points. A total of 2252 ground truth points were collected of which 1081 were used for calibration/training and 1171 were used in the accuracy assessment.

3.6 LandTrendr Historical Disturbance Mapping

3.6.1 Sliding Rule

We used sliding thresholds to optimize LandTrendr for each of five key land cover change patterns that dominate Malaysia (Grogan et al. 2015; Kennedy et al. 2010) (Table 2). One of the key challenges with applying LandTrendr to a new location is the need to parameterise the LandTrendr model, and unlike many LandTrendr studies, we used training data to systematically identify the best parameterisation for running LandTrendr. As LandTrendr only identifies disturbance patterns (i.e. magnitude, length of disturbance and date of disturbance onset), we calibrated LandTrendr separately for each coarse-scale land cover change pattern (Table 2). Calibration points for each change pattern were assigned to a reference and classified dataset values as either change or no change (i.e. disturbance) based on the ground truth data and the LandTrendr greatest disturbance segment data, respectively. The reference and classified values were then compared and used to calculate overall accuracy for four LandTrendr parameters (i.e. 1-year recovery, recovery threshold and p -value) to identify the best combination of LandTrendr parameterization which resulted in the most accurate detection of change for a period from 2000 to 2019.

The number of points per change lists produced from the reference data are summarized in Table 2.

3.6.2 Calibration Points

The ground truth data were converted into change lists for each change pattern, summarized in Table 2. Points were only included in a change list if the original land cover in the year 2000 was of the relevant class. Points were assigned reference values of either ‘Change’ if they subsequently underwent change to the relevant land cover class or ‘no change’ if they remained unchanged with no disturbance having occurred.

3.6.3 LandTrendr Parameters

The LandTrendr algorithm was run iteratively with a sliding range of values for each of four LandTrendr parameters: maximum segments, 1-year recovery, recovery threshold and p -value. The remaining LandTrendr parameters were kept at conservative values as they were determined during preliminary calibration to have little effect. The range of values used are summarized in Table 4. A brief description of each parameter is given below:

- Spike threshold—A sudden spike in spectral value may indicate false changes, for example, due to clouds. LandTrendr removes spikes where the difference in spectral values before and after the spike is less than a chosen percentage of the magnitude of the spike itself.
- Pval threshold—If the p -of- F value is greater than the chosen threshold, the pixel is considered no change.
- Maximum segments—The maximum number of segments allowed for the final trajectory.
- Recovery threshold—Rapid recovery after disturbance may be an illusion caused by cloud cover. A segment will be removed if it's rate of recovery relative to the total spectral range is less than $1/\text{recoveryThreshold}$.
- Vertex count overshoot—The initial model is created with a greater number of segments before undergoing simplification. This number is maximum segments + vertex count overshoot.
- Prevent 1-year recovery—Complete recovery within a year after vegetation disturbance is considered unlikely in many ecosystems but does occur in Malaysia. Setting this parameter to *true* will remove those recovery segments.
- Best model proportion—After undergoing simplification, the model is chosen which has the most vertices but with a p value no more than a certain proportion from that of the model with the lowest p value.
- Minimum observations needed—If there are fewer than this number of annual images in a pixel's time series, then it will not be analysed by LandTrendr and no output will be given.

A sample of some of the LandTrendr parameters used to run LandTrendr for the parameterization is given in Table 5.

Table 4 List of variables used for LandTrendr parameter

Parameter	Value(s)
maxSegments	2, 4, 6, 8
spikeThreshold	0, 9
vertexCountOvershoot	3
preventOneYearRecovery	TRUE, FALSE
recoveryThreshold	0, 0.33, 0.67, 0.99, 1
pvalThreshold	0.01, 0.05, 0.1
bestModelProportion	0.75
minObservationsNeeded	6

For each iteration of LandTrendr, disturbance rasters were sampled using the calibration points and values for magnitude and year of disturbance onset were extracted. These data were filtered to include only disturbances beginning after the year 2000.

3.6.4 Magnitude Threshold

Each point was assigned a classified value of ‘change’ or ‘no change’ based on a sliding threshold for magnitude, from 0 to 500 at intervals of 10. Magnitude refers to the change in spectral value, which has a possible range of 0–1000. If the magnitude of disturbance was greater than the threshold value, then it was counted as ‘change’, and if it was less than or equal to the threshold value, then it was counted as ‘no change’. Given the average NBR value of forest and oil palm, and that of bare ground, it is unlikely for small disturbances with magnitude of up to 100 or 200 to represent true clearance. However, disturbances may show lower magnitudes if the post-disturbance imagery does not capture the bare ground signature due to rapid regrowth.

3.6.5 Accuracy Estimation

For each set of LandTrendr parameters and each magnitude threshold value, user’s and producer’s accuracy for change detection was estimated (Grogan et al. 2015). The equations for calculating accuracy are given below. nA is the number of points where both the reference value and the classified value are ‘Change’. nB is the number of points where the classified value is ‘Change’. nC is the number of points where the reference value is ‘Change’.

User’s accuracy was calculated as:

$$UA = \frac{nA}{nB}$$

Producer’s accuracy was calculated as:

$$PA = \frac{nA}{nC}$$

Overall accuracy was calculated as:

$$OA = \frac{UA + PA}{2}$$

The maximum overall accuracy at any magnitude threshold was extracted for each parameterization and was averaged across all change patterns and the best parameterization was used to make the disturbance rasters.

3.7 Supervised Random Forest Classification of Land Cover for 2019

A random forest supervised classification was conducted using a raster stack which included the disturbance rasters from LandTrendr, a Landsat multi-date 2019 mosaic and SRTM elevation data. The final method was identified from an iterative process which included combining ancillary data to achieve the best classification. In addition, we compared classification results with and without the disturbance rasters. Initially several iterations of the classification were conducted to attempt to improve the accuracy of the output maps, which mainly proved to make little improvement to the overall accuracy. The more useful measures attempted included using a water mask to map the water class and including an elevation layer in the raster stack. These were implemented in the final iteration of the classification. The elevation layer was included as many land covers are spatially concentrated by altitude, such as oil palm and rice in lower elevations and higher elevations dominated by forest (Jarvis et al. 2008).

The random forest classification was conducted on two image stacks. One stack consisted of a multispectral annual Landsat mosaic for the year 2019 with SRTM elevation data. Seven 30-m resolution Landsat bands were used, including visible light, ultrablue, near infrared and short-wave infrared. The second stack contained additional LandTrendr disturbance rasters representing greatest disturbance segment information extracted for each of the parameterizations chosen in the parameter optimization step. The disturbance rasters consisted of seven raster layers representing year of disturbance onset, end year, pre-disturbance NBR value, post-disturbance NBR value, magnitude of change in NBR, duration of disturbance and annual rate of disturbance (Hudak et al. 2013).

The calibration points used to train the random forest classifier were the same points used for the parameter optimization step. Each point was assigned a current land cover value. Points assigned to the 'water' class were removed, as were points which fell on areas with no 2019 Landsat imagery available. The supervised classification was run with 300 trees and a total of 1068 training points. After classification, the JRC-GSW layer was used to map areas of the 'water' class (Pekel et al. 2016). The 'transition' layer was used, and pixels labelled 'permanent', 'new permanent' or 'season-to-permanent' were masked as water. (We found that the seasonal and ephemeral JRC water classes overlapped with rice paddy.)

3.8 Validation

The resulting land cover maps were assessed using a separate set of 1171 validation points to produce confusion matrices. Percentage values for user's, producer's and overall accuracy were produced. The matrices for the two land cover maps were compared (with and without the inclusion of the LandTrendr disturbance rasters), and areas of confusion between particular land cover classes were identified.

4 Results

4.1 Optimal Parameters

The optimum parameters are presented in Table 6. These parameters were used in producing the LandTrendr disturbance rasters for the raster stack. Table 7 presents the maximum Overall accuracy values obtained with the optimal magnitude threshold along with the User's and Producer's accuracies. Note also that although optimal magnitude threshold values are presented, no magnitude filter was used in producing the disturbance rasters for the supervised classification.

For comparison, the optimal overall accuracy for each individual change pattern when optimized separately is presented in Table 8 and the raw accuracy values for some of the tested iterations of LandTrendr in Table 9. The overall accuracy of detection of each change pattern is slightly lower using the chosen parameters (except for 'other green to oil palm' which remains the same) than if the change pattern were optimized separately. However, as using multiple LandTrendr outputs adds a large number of bands to the raster stack and so reduces accuracy, it is

Table 6 Optimum LandTrendr parameters chosen for extracting disturbances rasters

Parameter	Value
maxSegments	8
spikeThreshold	0.9
vertexCountOvershoot	3
preventOneYearRecovery	FALSE
recoveryThreshold	1
pvalThreshold	0.1
bestModelProportion	0.75
minObservationsNeeded	6

Table 7 Optimal magnitude threshold and accuracy values for detection of each change pattern when chosen LandTrendr parameters are used

Change pattern	Forest to oil palm	Oil palm to oil palm (replanting)	Forest to urban and other brown	Forest to other green	Other green to oil palm
Magnitude threshold	290	≤110	310	150	≤140
User's accuracy (%)	72.41	96.94	44.83	58.90	60.00
Producer's accuracy (%)	71.59	81.61	54.17	79.63	60.00
Overall accuracy (%)	72.00	89.27	49.50	69.27	60.00

Table 8 Optimal overall accuracies for detection of individual change patterns separately

	Overall accuracy (%)
Forest to oil palm	72.78
Oil palm to oil palm (replanting)	89.29
Forest to urban and other brown	50.30
Forest to other green	71.70
Other green to oil palm	60.00

necessary to compromise and use a parameterization that works reasonably well with all five land cover change patterns.

4.2 Land Cover Maps

Figures 2 and 3 show the classified maps of land cover using Landsat, elevation and LandTrendr data and using only Landsat and elevation data.

In Tables 10 and 11 are the confusion matrices for the land cover maps which were classified using raster stacks of LandTrendr disturbance rasters, Landsat and elevation data and Landsat and elevation data without LandTrendr disturbance rasters. As can be seen from the last columns of Tables 10 and 11, the number of points varies greatly between land cover classes. Oil Palm and Forest, as the dominant land covers in Malaysia, have the most points. This imbalance affects the classification, skewing the output map to favour oil palm, as shown by the high number of points misclassified as oil palm among other classes.

4.3 Accuracy Assessment

User's, Producer's and Overall accuracy were calculated for both land cover maps (Table 12).

The map produced using Landsat, elevation data and LandTrendr disturbance rasters had an Overall accuracy of 60.45%, with User's and Producer's accuracy of 63.72% and 57.17%, respectively. User's, Producer's and Overall accuracy was calculated for each land cover class. Water had the highest accuracy for all measures. After Water, the class with the highest overall accuracy was Oil Palm (79.53%), followed by Rice (77.89%) and Forest (70.08%). The same pattern was followed for Producer's Accuracy, with 89.25%, 80.77% and 69.27%, respectively. User's accuracy was highest for Rice (75.00%), then Forest (70.89%) and Oil Palm (69.81%). Bare Ground scored the lowest overall, with 30.00%, 36.36% and 33.18% User's, Producer's and Overall accuracy, respectively. However, Rubber and Other Vegetation had the lowest Producer's Accuracies at 15.39% and 24.66%.

In the map produced using only Landsat and elevation data, the relative accuracies of the classes were about the same, although User's accuracy was considerably lower for Rubber (45.95%) and Forest (65.76%). The Overall accuracy

Table 9 An example of some of the accuracy values obtained for various iterations of LandTrendr, using different magnitude thresholds

Overall accuracy of ‘forest to oil palm’									
Parameter ID		1	2	3	4	5	6	7	8
Magnitude threshold	0	13.24	14.20	22.07	22.07	24.49	23.67	24.49	20.45
	100	13.24	14.20	22.07	22.07	24.49	23.67	24.49	20.45
	200	14.20	15.34	22.07	22.07	24.49	23.67	24.49	20.45
	300	15.34	16.70	23.67	23.67	27.27	25.57	27.27	22.27
	400	7.71	8.90	13.64	13.64	17.80	17.80	17.80	15.42
500	10.57	10.57	10.57	13.07	17.23	25.57	17.23	17.23	
Parameter ID		9	10	11	12	13	14	15	16
Magnitude threshold	0	14.20	14.20	23.67	23.67	24.49	27.84	24.49	25.57
	100	14.20	14.20	23.67	23.67	24.49	27.84	24.49	25.57
	200	15.34	15.34	23.67	23.67	24.49	27.84	24.49	25.57
	300	15.34	16.70	23.67	23.67	27.27	30.62	27.27	27.84
	400	7.71	8.90	15.42	15.42	21.14	21.14	21.14	17.80
500	10.57	10.57	10.57	13.07	17.23	25.57	17.23	17.23	
Parameter ID		17	18	19	20	21	22	23	24
Magnitude threshold	0	14.20	14.20	20.45	25.57	21.14	38.56	21.14	34.09
	100	14.20	14.20	20.45	25.57	21.14	38.56	21.14	34.09
	200	15.34	15.34	20.45	25.57	21.14	38.56	21.14	34.09
	300	16.70	16.70	20.45	25.57	21.14	38.56	21.14	34.09
	400	8.90	8.90	15.42	17.80	26.14	34.47	26.14	26.14
500	10.57	10.57	10.57	13.07	17.23	25.57	17.23	17.23	
Parameter ID		25	26	27	28	29	30	31	32
Magnitude threshold	0	12.84	10.97	66.54	64.70	67.88	67.59	68.34	69.55
	100	12.84	10.97	66.35	65.24	69.35	69.02	69.43	70.59
	200	11.80	12.27	64.02	62.83	67.43	67.05	69.67	70.03
	300	14.04	14.77	59.38	57.20	64.89	64.39	68.66	68.92
	400	5.11	5.57	45.45	44.69	53.13	52.42	54.89	53.32
500	6.82	7.71	38.40	36.82	43.66	42.35	42.42	41.09	
Parameter ID		33	34	35	36	37	38	39	40
Magnitude threshold	0	12.84	10.97	65.78	63.94	66.38	66.84	69.09	70.29
	100	12.84	10.97	65.59	64.48	67.52	67.94	69.85	71.02
	200	11.80	12.27	64.02	62.83	66.68	67.05	70.41	70.77
	300	14.04	14.77	59.38	57.20	64.12	64.39	70.13	70.40
	400	5.11	5.57	45.45	44.69	52.22	51.52	55.75	54.20
500	6.82	7.71	38.40	36.82	42.42	41.09	42.42	41.09	

of Bare Ground, while remaining amongst the lowest two classes, was much higher at 36.36%, as was Rice at 81.59%.

Tables 13 and 14 show the confusion matrices with percentages instead of number of points for the map which used LandTrendr data in the input raster stack. Percentages are calculated for Table 13 based on the total number of reference points for each land cover class, while percentages for Table 14 are calculated based

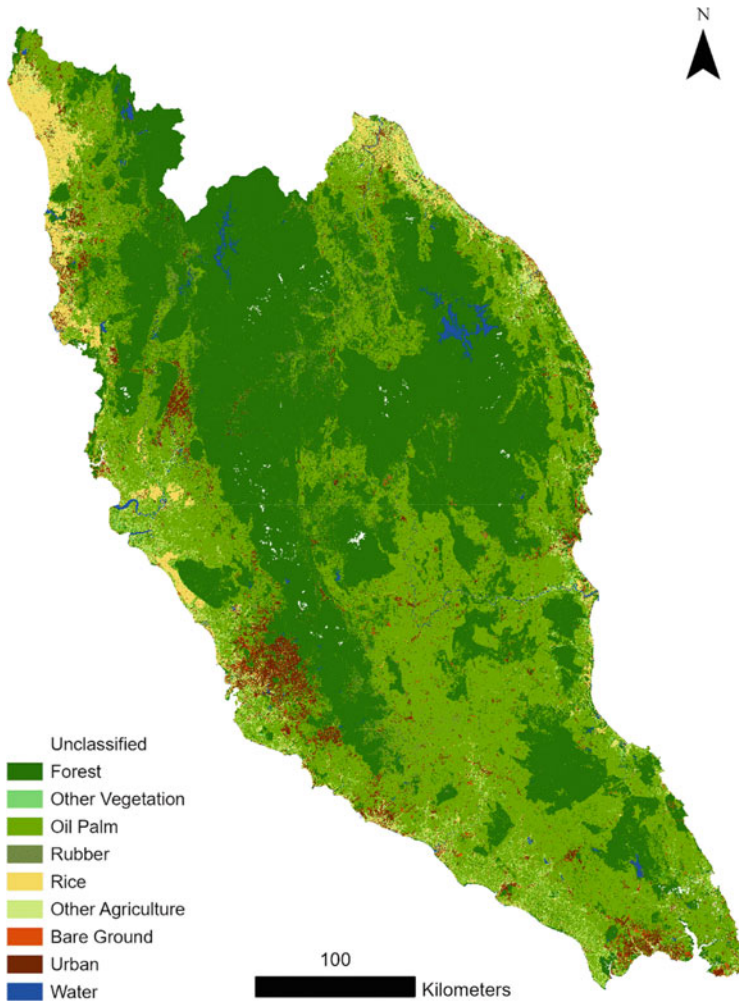


Fig. 2 Land cover map classified with LandTrendr disturbance rasters, Landsat and elevation data

on the total number of classified points for each land cover. The totals calculated under ‘omission error’ and ‘commission error’ are the sum of percentages for each column/row excluding correctly classified points. The bolded values running diagonally from top-left to bottom-right are the percentage of correctly classified points. In Table 13 these values represent producer’s accuracy, while in Table 14 they represent user’s accuracy.

The highest source of omission error is from misclassification as oil palm for all other classes except bare ground and rice. This is partly due to the over-representation of oil palm in the training data and also due to the similarity between oil palm and rubber, other vegetation and forest, which were the classes that were

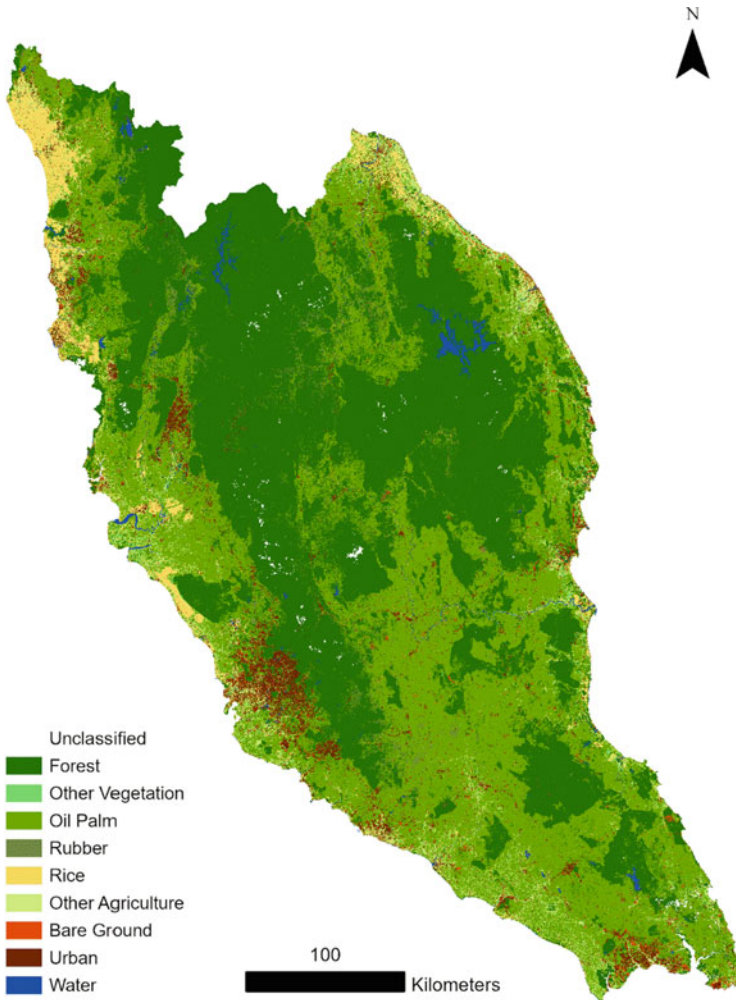


Fig. 3 Land cover map classified with Landsat and elevation data

most often misclassified as oil palm. The highest sources of commission error are from confusion between ‘other agriculture’ and ‘other vegetation’ and confusion between ‘urban’ and ‘bare ground’. The confusion between these classes is likely caused by the similarity in their spectral appearances.

Tables 15 and 16 show confusion matrices with percentages for the map produced without LandTrendr data. The main difference in commission error was in rubber—commission went from 54% down to 41% with the addition of LandTrendr data. When LandTrendr was added, user’s accuracy improved for forest, other vegetation, rubber and urban. It remained the same for oil palm and decreased for rice, other agriculture and bare ground. Producer’s accuracy averaged across all land covers

Table 10 Confusion matrix for image classified with LandTrendr disturbance rasters, Landsat and elevation data

Reference	Classified										Total
	Forest	Other vegetation	Oil palm	Rubber	Rice	Other agriculture	Bare ground	Urban	Water	Total	
Forest	151	1	57	3	2	0	2	1	1	218	
Other vegetation	4	18	27	1	3	16	1	3	0	73	
Oil palm	30	1	407	3	1	9	4	1	0	456	
Rubber	20	0	62	16	0	0	4	2	0	104	
Rice	1	1	2	0	42	4	0	2	0	52	
Other agriculture	2	9	16	0	5	31	6	1	0	70	
Bare ground	2	2	3	3	0	4	12	7	0	33	
Urban	0	0	9	1	3	1	10	35	0	59	
Water	3	1	0	0	0	0	1	0	99	104	
Total	213	33	583	27	56	65	40	52	100	1069	

Table 11 Confusion matrix for image classified with Landsat and elevation data

Reference	Classified										Total
	Forest	Other vegetation	Oil palm	Rubber	Rice	Other agriculture	Bare ground	Urban	Water	Total	
Forest	144	2	56	11	1	0	2	1	1	218	
Other vegetation	3	21	28	0	3	14	1	3	0	73	
Oil palm	29	0	399	8	2	12	2	4	0	456	
Rubber	28	0	54	17	0	0	2	3	0	104	
Rice	0	1	5	0	44	2	0	0	0	52	
Other agriculture	3	11	13	0	5	32	5	1	0	70	
Bare ground	4	2	4	1	0	5	12	5	0	33	
Urban	6	1	9	0	1	0	9	33	0	59	
Water	3	1	0	0	0	0	0	1	99	104	
Total	220	39	568	37	56	65	33	51	100	1169	

Table 12 Accuracy values by land cover class and general for both classified images

	With LandTrendr			Without LandTrendr		
	UA (%)	PA (%)	OA (%)	UA (%)	PA (%)	OA (%)
Forest	70.89	69.27	70.08	65.46	66.06	65.76
Other vegetation	54.55	24.66	39.60	53.85	28.77	41.31
Oil palm	69.81	89.25	79.53	70.25	87.50	78.87
Rubber	59.26	15.39	37.32	45.95	16.35	31.15
Rice	75.00	80.77	77.89	78.57	84.62	81.59
Other agriculture	47.69	44.29	45.99	49.23	45.71	47.47
Bare ground	30.00	36.36	33.18	36.36	36.36	36.36
Urban	67.31	59.32	63.32	64.71	55.93	60.32
Water	99.00	95.19	97.10	99.00	95.19	97.10
Total	63.72	57.17	60.45	62.60	57.39	59.99

decreased slightly but improved for forest, oil palm and urban. It remained the same for bare ground and decreased for other vegetation, rubber, rice and other agriculture.

Overall accuracy improved for the land covers of interest for mapping oil palm—forest, oil palm and rubber (as it is spectrally similar). Therefore, while overall accuracy for the map as a whole was only minimally affected by addition LandTrendr data, it has made a larger improvement to differentiation of these key land covers.

4.4 LandTrendr

Using LandTrendr disturbance rasters for supervised classification increased overall accuracy by 0.45 percentage points. This suggests that historical disturbance data from LandTrendr may be of some value for land cover change mapping in Malaysia. Preliminary analysis showed that LandTrendr is capable of detecting disturbance due to several different change patterns. However, the small change is also attributed to the percentage area which is covered by oil palm. It is too soon to say conclusively that it is feasible to use LandTrendr to differentiate types and timing of change in Malaysia. However, it will certainly require further research before LandTrendr can be used to this purpose.

A key challenge for historical land use and land cover change analysis using only Landsat historical satellite imagery is developing accurate training and validation data. The low resolution of the satellite imagery, high variation in appearance within land cover classes and high similarity in appearance between certain land covers makes it difficult to say with certainty what class of land cover is present and what change has taken place. However, with time and experience, a human interpreter could probably make a reasonable attempt to digitize land use and land cover change using the available Landsat bands and supplementary data (Cohen et al. 2010). But

Table 13 The percentages of validation points by reference class for the map using LandTrendr data. The last column shows the total percentage of misclassified points for that class (omission error)

	Classified										Omission error (%)	
	Forest (%)	Other vegetation (%)	Oil palm (%)	Rubber (%)	Rice (%)	Other agriculture (%)	Bare ground (%)	Urban (%)	Water (%)			
Reference												
Forest	69	0	26	1	1	0	1	0	0	0	0	31
Other vegetation	5	25	37	1	4	22	1	4	0	0	0	75
Oil palm	7	0	89	1	0	2	1	0	0	0	0	11
Rubber	19	0	60	15	0	0	4	2	0	0	0	85
Rice	2	2	4	0	81	8	0	4	0	0	0	19
Other agriculture	3	13	23	0	7	44	9	1	0	0	0	56
Bare ground	6	6	9	9	0	12	36	21	0	0	0	64
Urban	0	0	15	2	5	2	17	59	0	0	0	41
Water	3	1	0	0	0	0	1	0	0	0	95	5

Table 14 The percentages of validation points by classified map class for the map using LandTrendr data. The last row shows the total percentage of validation points which were misclassified as a certain land cover (commission error)

	Classified									
	Forest (%)	Other vegetation (%)	Oil palm (%)	Rubber (%)	Rice (%)	Other agriculture (%)	Bare ground (%)	Urban (%)	Water (%)	
Reference	71	3	10	11	4	0	5	2	1	
Other vegetation	2	55	5	4	5	25	3	6	0	
Oil palm	14	3	70	11	2	14	10	2	0	
Rubber	9	0	11	59	0	0	10	4	0	
Rice	0	3	0	0	75	6	0	4	0	
Other agriculture	1	27	3	0	9	48	15	2	0	
Bare ground	1	6	1	11	0	6	30	13	0	
Urban	0	0	2	4	5	2	25	67	0	
Water	1	3	0	0	0	0	3	0	99	
Commission error	29	45	30	41	25	52	70	33	1	

Table 15 The percentages of validation points by reference class for the map without LandTrendr data. The last column shows the total percentage of misclassified points for that class (omission error)

	Classified										Omission error (%)	
	Forest (%)	Other vegetation (%)	Oil palm (%)	Rubber (%)	Rice (%)	Other agriculture (%)	Bare ground (%)	Urban (%)	Water (%)			
Reference												
Forest	66	1	26	5	0	0	1	0	0	0	0	34
Other vegetation	4	29	38	0	4	19	1	4	0	0	0	71
Oil palm	6	0	88	2	0	3	0	1	0	0	0	13
Rubber	27	0	52	16	0	0	2	3	0	0	0	84
Rice	0	2	10	0	85	4	0	0	0	0	0	15
Other agriculture	4	16	19	0	7	46	7	1	0	0	0	54
Bare ground	12	6	12	3	0	15	36	15	0	0	0	64
Urban	10	2	15	0	2	0	15	56	0	0	0	44
Water	3	1	0	0	0	0	0	1	95	0	0	5

Table 16 The percentages of validation points by classified map class for the map without LandTrendr data. The last row shows the total percentage of validation points which were misclassified as a certain land cover (commission error)

	Classified									
	Forest (%)	Other vegetation (%)	Oil palm (%)	Rubber (%)	Rice (%)	Other agriculture (%)	Bare ground (%)	Urban (%)	Water (%)	
Reference	65	5	10	30	2	0	6	2	1	
Other vegetation	1	54	5	0	5	22	3	6	0	
Oil palm	13	0	70	22	4	18	6	8	0	
Rubber	13	0	10	46	0	0	6	6	0	
Rice	0	3	1	0	79	3	0	0	0	
Other agriculture	1	28	2	0	9	49	15	2	0	
Bare ground	2	5	1	3	0	8	36	10	0	
Urban	3	3	2	0	2	0	27	65	0	
Water	1	3	0	0	0	0	0	2	99	
Commission error	35	46	30	54	21	51	64	35	1	

this would be difficult to scale to the national level without losing spatial resolution or taking a very long time.

5 Discussion

5.1 Overview

The method used in this study for mapping land cover LandTrendr to study land use and land cover change. However, these previous studies have mostly focused on a limited range of land cover classes or types of change, such as disturbances affecting forest (Hislop et al. 2019) or abandonment of cropland (Dara et al. 2018). They also tend to have already identified land cover distribution in the base year (Zhu et al. 2019) or restrict the study to an area with a narrow range of land cover change patterns present (Grogan et al. 2015; Kennedy et al. 2012). In addition, LandTrendr applications in the tropics for detecting disturbance (Grogan et al. 2015) and recovery (Shen et al. 2017) in forests and timber plantations and conversion to rubber plantations (Tang et al. 2019).

Other studies used LandTrendr output rasters for supervised classification; however, they used them to identify specific land covers or change patterns, rather than for general land cover classification—or else they targeted a much smaller study area (Rathnayake et al. 2020). In this thesis the method was also modified to suit the tropics—utilizing full-year image collections for creating annual mosaics to reduce cloud cover without affecting coverage, following Grogan et al. (2015), and calibrating LandTrendr to change patterns prevalent in the region.

The results in this thesis did not show a clear advantage in using LandTrendr over using only Landsat and elevation data nor did it show conclusive evidence that LandTrendr is a viable tool for land cover change mapping. However, it does suggest that LandTrendr has potential to be developed into such a tool. The use of LandTrendr improved overall accuracy for oil palm, rubber and forest detection, and specifically user's accuracy improved for forest and rubber, while producer's accuracy improved for forest and oil palm. This means that use of LandTrendr improves differentiation of these three very similar land covers and therefore careful use of LandTrendr could have a positive impact on attempts to map change from forest to oil palm. In contrast there was unexpected decreases in accuracy for certain land covers when LandTrendr was used, such as increased confusion between bare ground and rubber and bare ground and urban, decrease in producer's accuracy for rubber and the overall decrease in accuracy for rice and other agriculture. It may be that LandTrendr outputs may have more relevance to the change patterns being targeted.

5.2 Parameterization

The parameters used were found to have a large effect on the accuracy of change detection, with overall accuracy values ranging from below 10% for some change patterns up to above 80% depending on the parameters and magnitude threshold used. The overall accuracy under optimal conditions varied from 50.30% for 'forest to urban and other brown' to 89.29% for 'oil palm to oil palm' (replanting). Lower accuracy may reflect a lack of calibration points as the change patterns with the three lowest overall accuracy values were also those with the fewest calibration points. The variability in change events may also be a factor, with forest clearance and replanting of oil palm widely following standard patterns of management, whereas urban development may have a variety of time periods and spectral appearances following clearance.

Only one LandTrendr parameter was used for producing disturbance rasters, as it was found that including additional parameterizations had a negative impact on map accuracy, likely due to having too many bands with too few training points. Therefore, the algorithm hasn't been able to detect each type of change equally well. In choosing the optimum parameters, each change pattern was weighted equally even though 'forest to oil palm' and 'oil palm to oil palm' (replanting) are both the most prevalent change patterns and the patterns being studied. However, a compromise seems better as it allows detection of all change patterns and reduces the complexity of the classification. It would be useful in further studies to know in which years conversion to oil palm is most prevalent. However, from the ground truth data, we cannot accurately determine an overall temporal pattern in forest to oil palm conversion.

5.3 Mapping

The two land cover maps produced with and without LandTrendr didn't appear very noticeably different from each other, with major areas of land cover remaining largely the same in both. Out of 145.9 million total pixels, only 7.5% (10.9 million pixels) differed between the two land cover maps. This is approximately 9913 km². Most of the differences were due to differences in the classification of oil palm and forest. Only 1.7 million pixels (1563 km²) represented net differences between the two methods. At a smaller scale, differences are visible in small groups of pixels with differences between similar land cover classes and in mixed landscapes. Two examples are given in Fig. 4 from Negeri Sembilan and the coast of Pahang.

The scene from Negeri Sembilan (a) shows a linear settlement with agriculture that runs parallel to a highway with forest in the north-eastern corner. The two images differ in their distribution of 'forest' and 'oil palm' pixels in the transition zone, and the image with LandTrendr (a1) shows a section of road ('urban') misclassified as 'rice'. The scene from Pahang shows rice and oil palm fields (b), with an area of denser vegetation between them and paths. The two images show

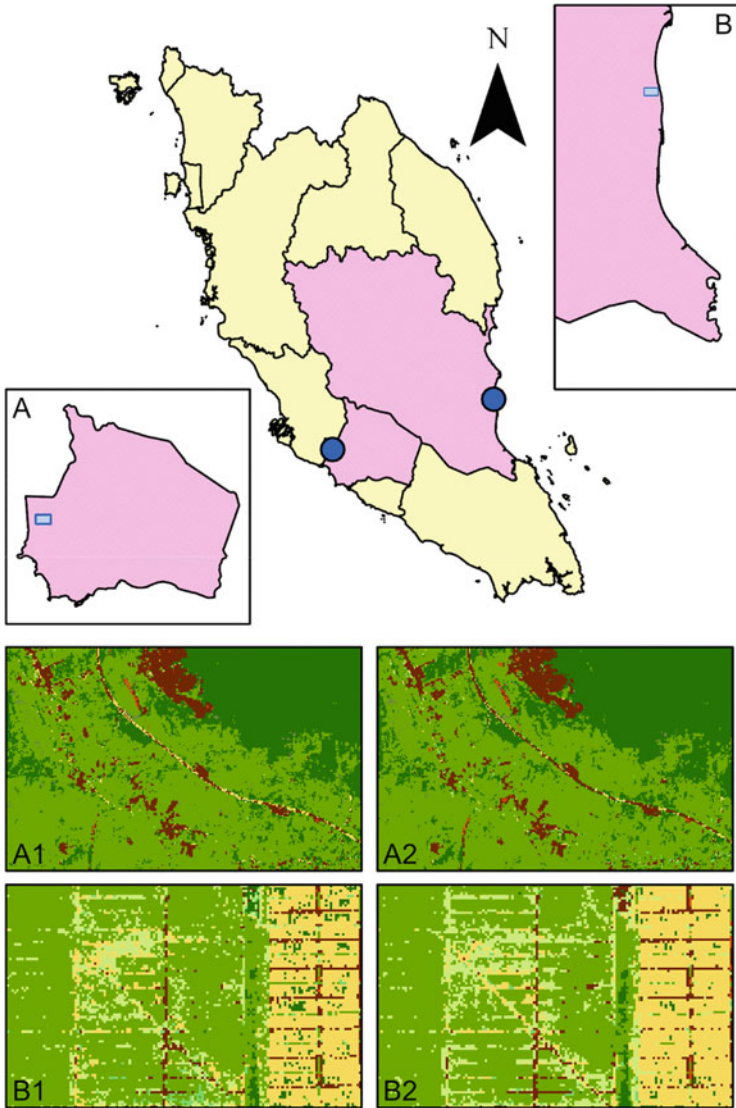


Fig. 4 Examples of areas which show differences between land cover maps classified from an input raster stack consisting of Landsat imagery, elevation data and LandTrendr outputs (a1, b1) and produced from a raster stack consisting of only Landsat imagery and elevation data (a2, b2). The locations are in Negeri Sembilan (a) and Pahang (b)

differences in distribution of the pixels making up the paths (classified as ‘urban’) between rows of vegetation.

For the map classified using LandTrendr, the greatest sources of confusion were between ‘other vegetation’ and ‘other agriculture’ (orchards and miscellaneous other

types of agriculture such as large home gardens and banana fields—see Table 1: 2019 Land Cover) and between ‘bare ground’ and ‘urban’. In terms of the number of misclassified points, the most frequently confused land covers were ‘rubber’, ‘oil palm’ and ‘forest’ as also found in previous studies (Mohd Najib et al. 2020). A major source of commission errors for ‘forest’ and ‘oil palm’ were ‘oil palm’ or ‘rubber’ being classified as ‘forest’ and ‘rubber’ or ‘forest’ being classified as ‘oil palm’. Other sources of error were ‘other agriculture’ being classified as ‘bare ground’. The greatest source of omission was misclassification of land covers as ‘oil palm’, particularly misclassification of ‘rubber’, ‘other vegetation’ and ‘forest’. While ‘oil palm’ and ‘forest’ maintained accuracy values all above 69%, ‘rubber’ had a poor producer’s accuracy at only 15%. This may be due to the difficulty encountered during ground truthing as rubber was difficult to differentiate from forest and oil palm, while being less common than either class.

The map classified using LandTrendr data is slightly more accurate than the one using only Landsat and elevation data, although producer’s accuracy decreased slightly. There was a large increase in overall accuracy for ‘rubber’ and ‘forest’ and a smaller increase for ‘oil palm’ and ‘urban’ but a decrease in overall accuracy for ‘other vegetation’, ‘rice’, ‘other agriculture’ and ‘bare ground’. As LandTrendr detects disturbance by analysing temporal change, the improvement in detection of rubber and forest may be attributed to the ability to detect past clearance and differentiate it from undisturbed forest. The decrease in accuracy of detecting bare ground may be due to associating recent disturbance with a bare ground signal, whereas vegetation in the tropics may recover rapidly, hiding the bare ground signal in as little time as a year. Likewise, detection of rice may have been confounded by temporary changes in spectral value due to seasonal flooding and harvest patterns being interpreted as change by LandTrendr.

5.4 Limitations and Future Research

While the results indicate that LandTrendr is useful for helping to map land cover and investigating historical land cover change, the accuracy of the land cover map is still quite low and will require further research to potentially improve it. The results might be improved by increasing the number and quality of training points (Kanniah et al. 2015; Li et al. 2014; Shaharum et al. 2020). The ground truth data may not have been labelled accurately, as some land covers are difficult to differentiate from satellite imagery, and high-resolution imagery is not uniformly available for all areas and time periods. The constraints in selecting more numerous, reliable training points for this study were time and cost and difficulty of reliably interpreting historical satellite imagery. As high-quality imagery over the complete time period is scarce and land covers are difficult to differentiate, it requires an expert interpreter with experience in the task and in the land cover patterns present in the target area.

The similarity of many common land covers in Malaysia is partly due to the domination of the landscape by trees, including natural forest and oil palm and rubber plantations, which share similar spectral appearances. These classes are

difficult to differentiate visually or using random forests as they are spectrally similar. We found from a small sample of points for bare land, forest, oil palm, water and urban that the NDVI and NBR of forest, oil palm and bare land overlapped with each other. The large study area and fine level of land cover classes used in the analysis were also limiting as it increased the potential variability in land cover patterns. To simplify the study, land covers were not differentiated into different stages of growth, despite vast differences in appearance and spectral value between newly planted and mature oil palm and between dry and flooded rice fields.

Other challenges encountered were due to the local climate. Located in the equatorial region, Malaysia experiences high rainfall and cloud cover. The tropical climate means that vegetation may change appearance rapidly after rainfall, especially after a dry period; and rapid vegetation regrowth may obscure disturbance signals from being detected by LandTrendr, which operates at a temporal scale of 1 year.

One of the limitations of using LandTrendr is that disturbance data only applies to a small proportion of the whole study area. Furthermore, we have not identified which LandTrendr outputs are most important for identifying land cover. Further research to investigate the significance of individual segment characteristics and spectral bands or indices (Hudak et al. 2013), and the use of recovery information and data from multiple disturbances (Kennedy et al. 2012) per pixel may help to develop LandTrendr for land use and land cover change mapping for tropical Southeast Asia.

6 Conclusion

This study is the first to use LandTrendr in Malaysia and the first use it for mapping land cover classes in Southeast Asia. While the method demonstrated only small improvements in overall accuracies, such an approach needs further research to assess the capability for mapping land conversion to oil palm plantation, conducting LUCA assessments and for conservation planning. We believe that a key challenge for land cover mapping of oil palm can be solved through the application of temporal information, providing extra information required for differentiating between woody vegetation in the tropics than using spectral differences alone.

References

- Ahmad F, Ushiyama T, Sayama T (2017) Determination of Z-R relationship and inundation analysis for Kuantan River. Research publication no. 2, pp 1–39. http://www.met.gov.my/data/research/researchpapers/2017/researchpaper_201702.pdf
- Almeida de Souza A, Galvão LS, Korting TS, Prieto JD (2020) Dynamics of savanna clearing and land degradation in the newest agricultural frontier in Brazil. *GIScience Remote Sens* 57(7): 965–984. <https://doi.org/10.1080/15481603.2020.1835080>
- Bartz KK, Ford MJ, Beechie TJ, Fresh KL, Pess GR, Kennedy RE, Rowse ML, Sheer M (2015) Trends in developed land cover adjacent to habitat for threatened salmon in Puget Sound, Washington, U.S.A. *PLoS One* 10(4):e0124415. <https://doi.org/10.1371/journal.pone.0124415>

- Beckschäfer P (2017) Obtaining rubber plantation age information from very dense Landsat TM and ETM + time series data and pixel-based image compositing. *Remote Sens Environ* 196:89–100. <https://doi.org/10.1016/j.rse.2017.04.003>
- Boriah S (2010) Time series change detection: algorithms for land cover change. [University of Minnesota]. <https://conservancy.umn.edu/handle/11299/90706>
- CFMask Algorithm (n.d.) USGS. <https://www.usgs.gov/core-science-systems/nli/landsat/cfmask-algorithm>. Accessed 26 May 2021
- Chong KL, Kanniah KD, Pohl C, Tan KP (2017) A review of remote sensing applications for oil palm studies. *Geo-Spatial Inform Sci* 20(2):184–200. <https://doi.org/10.1080/10095020.2017.1337317>
- Cohen WB, Yang Z, Kennedy R (2010) Detecting trends in forest disturbance and recovery using yearly Landsat time series: 2. TimeSync—tools for calibration and validation. *Remote Sens Environ* 114(12):2897–2910. <https://doi.org/10.1016/j.rse.2010.07.010>
- Daliman S, Rahman SA, Bakar SA, Busu I (2014) Segmentation of oil palm area based on GLCMSVM and NDVI. In: IEEE TENSYP 2014–2014 IEEE region 10 symposium. <https://doi.org/10.1109/tenconspring.2014.6863113>
- Dara A, Baumann M, Kuemmerle T, Pflugmacher D, Rabe A, Griffiths P, Hölzel N, Kamp J, Freitag M, Hostert P (2018) Mapping the timing of cropland abandonment and recultivation in northern Kazakhstan using annual Landsat time series. *Remote Sens Environ* 213:49–60. <https://doi.org/10.1016/j.rse.2018.05.005>
- Deilmai BR, Ahmad B, Zabihi H (2014) Comparison of two classification methods (MLC and SVM) to extract land use and land cover in Johor Malaysia. *IOP Conf Ser Earth Environ Sci* 20(1):012052. <https://doi.org/10.1088/1755-1315/20/1/012052>
- Department of Statistics (2017) Malaysia economics statistics—time series 2016. https://www.dosm.gov.my/v1/index.php?r=column/ctimeseriesandmenu_id=NHJlaGc2Rlg4ZXlGTjh1SU1kaWY5UT09
- FAO (2020) Global Forest Resources Assessment (FRA) 2020 Malaysia. <http://www.fao.org/3/cb0033en/cb0033en.pdf>
- Foga S, Scaramuzza PL, Guo S, Zhu Z, Dilley RD, Beckmann T, Schmidt GL, Dwyer JL, Joseph Hughes M, Laue B (2017) Cloud detection algorithm comparison and validation for operational Landsat data products. *Remote Sens Environ* 194:379–390. <https://doi.org/10.1016/j.rse.2017.03.026>
- Fragal EH, Silva TSF, Novo EMLM (2016) Reconstrução histórica de mudanças na cobertura florestal em várzeas do baixo amazonas utilizando o algoritmo landtrendr. *Acta Amazonica* 46(1):13–24. <https://doi.org/10.1590/1809-4392201500835>
- Global Forest Watch (n.d.) Tree cover loss in Malaysia. www.globalforestwatch.org. Accessed 30 Jan 2021
- Gorelick N, Hancher M, Dixon M, Ilyushchenko S, Thau D, Moore R (2017) Google Earth Engine: planetary-scale geospatial analysis for everyone. *Remote Sens Environ* 202:18–27
- Grogan K, Pflugmacher D, Hostert P, Kennedy R, Fensholt R (2015) Cross-border forest disturbance and the role of natural rubber in mainland Southeast Asia using annual Landsat time series. *Remote Sens Environ* 169:438–453. <https://doi.org/10.1016/j.rse.2015.03.001>
- Harris N, Dow Goldman E, Gibbes S (2019) Spatial database of planted trees version 1.0. Technical note. World Resources Institute, Washington, DC
- Hashim M, Reba N, Nadzri M, Pour A, Mahmud M, Mohd Yusoff A, Ali M, Jaw S, Hossain M (2016) Satellite-based run-off model for monitoring drought in Peninsular Malaysia. *Remote Sens* 8(8):633. <https://doi.org/10.3390/rs8080633>
- Hislop S, Jones S, Soto-Berelov M, Skidmore A, Haywood A, Nguyen TH (2019) A fusion approach to forest disturbance mapping using time series ensemble techniques. *Remote Sens Environ* 221:188–197. <https://doi.org/10.1016/j.rse.2018.11.025>
- Hudak AT, Bright BC, Kennedy RE (2013) Predicting live and dead basal area from LandTrendr variables in beetle-affected forests. In: MultiTemp 2013—7th international workshop on the analysis of multi-temporal remote sensing images: “our dynamic environment”, proceedings. <https://doi.org/10.1109/Multi-Temp.2013.6866024>

- Jarvis A, Reuter HI, Nelson A, Guevara E (2008) Hole-filled SRTM for the globe Version 4. <https://srtm.csi.cgiar.org>
- Kamiran N, Sarker MLR (2014) Exploring the potential of high resolution remote sensing data for mapping vegetation and the age groups of oil palm plantation. *IOP Conf Ser Earth Environ Sci* 18(1):012181. <https://doi.org/10.1088/1755-1315/18/1/012181>
- Kanniah KD, Sheikhi A, Cracknell AP, Goh HC, Tan KP, Ho CS, Rasli FN (2015) Satellite images for monitoring mangrove cover changes in a fast growing economic region in southern Peninsular Malaysia. *Remote Sens* 7(11):14360–14385. <https://doi.org/10.3390/rs71114360>
- Kanniah KD, Cracknell AP, Yu L (2019) Preface. *Int J Remote Sens* 40(19):7287–7296. <https://doi.org/10.1080/01431161.2019.1613069>
- Kennedy RE, Yang Z, Cohen WB (2010) Detecting trends in forest disturbance and recovery using yearly Landsat time series: 1. LandTrendr—temporal segmentation algorithms. *Remote Sens Environ* 114(12):2897–2910. <https://doi.org/10.1016/j.rse.2010.07.008>
- Kennedy RE, Yang Z, Cohen WB, Pfaff E, Braaten J, Nelson P (2012) Spatial and temporal patterns of forest disturbance and regrowth within the area of the Northwest Forest Plan. *Remote Sens Environ* 122:117–133. <https://doi.org/10.1016/j.rse.2011.09.024>
- Kennedy RE, Yang Z, Braaten J, Copass C, Antonova N, Jordan C, Nelson P (2015) Attribution of disturbance change agent from Landsat time-series in support of habitat monitoring in the Puget Sound region, USA. *Remote Sens Environ* 166:271–285. <https://doi.org/10.1016/j.rse.2015.05.005>
- Kennedy RE, Yang Z, Gorelick N, Braaten J, Cavalcante L, Cohen WB, Healey S (2018) Implementation of the LandTrendr algorithm on Google Earth Engine. *Remote Sens* 10(5):691. <https://doi.org/10.3390/rs10050691>
- Lechner AM, Foody GM, Boyd DS (2020) Applications in remote sensing to forest ecology and management. *One Earth* 2(5):405–412. <https://doi.org/10.1016/j.oneear.2020.05.001>
- Lee JSH, Wich S, Widayati A, Koh LP (2016) Detecting industrial oil palm plantations on Landsat images with Google Earth Engine. *Remote Sens Appl Soc Environ* 4:219–224. <https://doi.org/10.1016/j.rsase.2016.11.003>
- Li C, Wang J WL, Hu L, Gong P (2014) Comparison of classification algorithms and training sample sizes in urban land classification with Landsat thematic mapper imagery. *Remote Sens* 6(2):964–983. <https://doi.org/10.3390/rs6020964>
- Liang L, Hawbaker TJ, Chen Y, Zhu Z, Gong P (2014) Characterizing recent and projecting future potential patterns of mountain pine beetle outbreaks in the Southern Rocky Mountains. *Appl Geogr* 55:165–175. <https://doi.org/10.1016/j.apgeog.2014.09.012>
- Malaysian Palm Oil Board (2019) Oil palm planted area 2019. http://bepi.mpob.gov.my/images/area/2019/Area_summary.pdf
- Meigs GW, Kennedy RE, Cohen WB (2011) A Landsat time series approach to characterize bark beetle and defoliator impacts on tree mortality and surface fuels in conifer forests. *Remote Sens Environ* 115(12):3707–3718. <https://doi.org/10.1016/j.rse.2011.09.009>
- Miettinen J, Shi C, Liew SC (2016) Land cover distribution in the peatlands of Peninsular Malaysia, Sumatra and Borneo in 2015 with changes since 1990. *Glob Ecol Conserv* 6:67–78. <https://doi.org/10.1016/j.gecco.2016.02.004>
- Miettinen J, Gaveau DLA, Liew SC (2018) Comparison of visual and automated oil palm mapping in Borneo. *Int J Remote Sens* 40(21):8174–8185. <https://doi.org/10.1080/01431161.2018.1479799>
- Mohd Najib NE, Kanniah KD, Cracknell AP, Yu L (2020) Synergy of active and passive remote sensing data for effective mapping of oil palm plantation in Malaysia. *Forests* 11(8):858. <https://doi.org/10.3390/F11080858>
- Mutanga O, Kumar L (2019) Google Earth engine applications. *Remote Sens* 11(5):591. <https://doi.org/10.3390/rs11050591>
- Olaniyi AO, Abdullah AM, Ramli MF, Sood AM (2013) Agricultural land use in Malaysia: an historical overview and implications for food security. *Bulg J Agric Sci* 19(1):60–69
- Omout H (2005) Roundtable on sustainable palm oil—RSPO. The second RSPO meeting in Jakarta in October 2004. In: OCL—oleagineux corps gras lipides (vol 12, no. 2). <https://doi.org/10.1051/occl.2005.0125>

- Oon A, Mohd Shafri HZ, Lechner AM, Azhar B (2019a) Discriminating between large-scale oil palm plantations and smallholdings on tropical peatlands using vegetation indices and supervised classification of LANDSAT-8. *Int J Remote Sens* 40(19):1–17. <https://doi.org/10.1080/01431161.2019.1579944>
- Oon A, Ngo KD, Azhar R, Ashton-Butt A, Lechner AM, Azhar B (2019b) Assessment of ALOS-2 PALSAR-2 L-band and Sentinel-1 C-band SAR backscatter for discriminating between large-scale oil palm plantations and smallholdings on tropical peatlands. *Remote Sens Appl Soc Environ* 13:183–190. <https://doi.org/10.1016/j.rsase.2018.11.002>
- Pekel JF, Cottam A, Gorelick N, Belward AS (2016) High-resolution mapping of global surface water and its long-term changes. *Nature* 540(7633):418–422. <https://doi.org/10.1038/nature20584>
- Pflugmacher D, Cohen WB, Kennedy RE (2012) Using Landsat-derived disturbance history (1972–2010) to predict current forest structure. *Remote Sens Environ* 122:146–165. <https://doi.org/10.1016/j.rse.2011.09.025>
- Pittman AM, Carlson KM, Curran LM, Ponette-Gonzalez A (2013) NASA satellite data used to study the impact of oil palm expansion across Indonesian Borneo. *The Earth observer (NASA)*, pp 12–16
- Rathnayake CWM, Jones S, Soto-Berelov M (2020) Mapping land cover change over a 25-year period (1993–2018) in Sri Lanka using Landsat time-series. *Land* 9(1):27. <https://doi.org/10.3390/land9010027>
- Razak JAA, Shariff ARM, Ahmad N, Ibrahim Sameen M (2018) Mapping rubber trees based on phenological analysis of Landsat time series data-sets. *Geocarto Int* 33(6):627–650. <https://doi.org/10.1080/10106049.2017.1289559>
- Razali SM, Marin A, Nuruddin AA, Shafri HZM, Hamid HA (2014) Capability of integrated MODIS imagery and ALOS for oil palm, rubber and forest areas mapping in tropical forest regions. *Sensors (Switzerland)* 14(5):8259–8282. <https://doi.org/10.3390/s140508259>
- RSPO (2015) RSPO remediation and compensation procedures related to land clearance without prior HCV assessment. http://www.rsपो.org/file/2_RSPOremediationandCompensationProcedures_May2014.pdf
- Samat N, Mahamud MA, Tan ML, Tilaki MJM, Tew YL (2020) Modelling land cover changes in peri-urban areas: a case study of George Town Conurbation, Malaysia. *Land* 9(10):373. <https://doi.org/10.3390/land9100373>
- Schneibel A, Stellmes M, Röder A, Frantz D, Kowalski B, Haß E, Hill J (2017) Assessment of spatio-temporal changes of smallholder cultivation patterns in the Angolan Miombo belt using segmentation of Landsat time series. *Remote Sens Environ* 195:118–129. <https://doi.org/10.1016/j.rse.2017.04.012>
- Senf C, Pflugmacher D, van der Linden S, Hostert P (2013) Mapping rubber plantations and natural forests in Xishuangbanna (Southwest China) using multi-spectral phenological metrics from Modis time series. *Remote Sens* 5(6):2795–2812. <https://doi.org/10.3390/rs5062795>
- Senf C, Pflugmacher D, Wulder MA, Hoster P (2015) Characterizing spectral-temporal patterns of defoliator and bark beetle disturbances using Landsat time series. *Remote Sens Environ* 170:166–177. <https://doi.org/10.1016/j.rse.2015.09.019>
- Shaharum NSN, Shafri HZM, Ghani WAWAK, Samsatli S, Al-Habshi MMA, Yusuf B (2020) Oil palm mapping over Peninsular Malaysia using Google Earth Engine and machine learning algorithms. *Remote Sens Appl Soc Environ* 17:100287. <https://doi.org/10.1016/j.rsase.2020.100287>
- Shen WJ, Li MS (2017) Mapping disturbance and recovery of plantation forests in southern China using yearly Landsat time series observations. *Shengtai Xuebao/Acta Ecologica Sinica* 37(5). <https://doi.org/10.5846/stxb201510142074>
- Shen W, Li M, Wei A (2017) Spatio-temporal variations in plantation forests' disturbance and recovery of northern Guangdong Province using yearly Landsat time series observations (1986–2015). *Chin Geogr Sci* 27(4):600–613. <https://doi.org/10.1007/s11769-017-0880-z>
- Stibig HJ, Achard F, Carboni S, Raši R, Miettinen J (2014) Change in tropical forest cover of Southeast Asia from 1990 to 2010. *Biogeosciences* 11(2):247–258. <https://doi.org/10.5194/bg-11-247-2014>

- Sun Z, Leinenkugel P, Guo H, Huang C, Kuenzer C (2017) Extracting distribution and expansion of rubber plantations from Landsat imagery using the C5.0 decision tree method. *J Appl Remote Sens* 11(2):026011. <https://doi.org/10.1117/1.jrs.11.026011>
- Swee-Hock S (2018) The population of Peninsular Malaysia. Institute of Southeast Asian Studies, Singapore. <https://doi.org/10.1355/9789812307309>
- Tang KHD, Al Qahtani HMS (2020) Sustainability of oil palm plantations in Malaysia. In: Environment, development and sustainability: a multidisciplinary approach to the theory and practice of sustainable development, vol 22, issue 6. Springer, Berlin. <https://doi.org/10.1007/s10668-019-00458-6>
- Tang D, Fan H, Yang K, Zhang Y (2019) Mapping forest disturbance across the China–Laos border using annual Landsat time series. *Int J Remote Sens* 40(8):2895–2915. <https://doi.org/10.1080/01431161.2018.1533662>
- Tangang FT, Juneng L, Salimun E, Sei KM, Le LJ, Muhamad H (2012) Climate change and variability over Malaysia: gaps in science and research information. *Sains Malaysiana* 41(11):1355–1366
- Trisasongko BH, Paull D (2020) A review of remote sensing applications in tropical forestry with a particular emphasis in the plantation sector. *Geocarto Int* 35(3):317–339. <https://doi.org/10.1080/10106049.2018.1516245>
- Trisasongko BH, Panuju DR, Paull DJ, Jia X, Griffin AL (2017) Comparing six pixel-wise classifiers for tropical rural land cover mapping using four forms of fully polarimetric SAR data. *Int J Remote Sens* 38(11):3274–3293. <https://doi.org/10.1080/01431161.2017.1292072>
- Wang X, Huang H, Gong P, Biging GS, Xin Q, Chen Y, Yang J, Liu C (2016) Quantifying multi-decadal change of planted forest cover using airborne LiDAR and Landsat imagery. *Remote Sens* 8(1):62. <https://doi.org/10.3390/rs8010062>
- Wang Z, Lechner AM, Yang Y, Baumgartl T, Wu J (2020) Mapping the cumulative impacts of long-term mining disturbance and progressive rehabilitation on ecosystem services. *Sci Total Environ* 717:137214. <https://doi.org/10.1016/j.scitotenv.2020.137214>
- Xu Y, Yu L, Li W, Ciais P, Cheng Y, Gong P (2020) Annual oil palm plantation maps in Malaysia and Indonesia from 2001 to 2016. *Earth Syst Sci Data* 12(2):847–867. <https://doi.org/10.5194/essd-12-847-2020>
- Yang Y, Erskine PD, Lechner AM, Mulligan D, Zhang S, Wang Z (2018) Detecting the dynamics of vegetation disturbance and recovery in surface mining area via Landsat imagery and LandTrendr algorithm. *J Cleaner Prod* 178:353–362. <https://doi.org/10.1016/j.jclepro.2018.01.050>
- Ye L, Liu M, Liu X, Zhu L (2021) Developing a new disturbance index for tracking gradual change of forest ecosystems in the hilly red soil region of southern China using dense Landsat time series. *Ecol Inform* 61:101221. <https://doi.org/10.1016/j.ecoinf.2021.101221>
- Yoshino K, Ishida T, Nagano T, Setiawan Y (2010) Landcover pattern analysis of tropical peat swamp lands in Southeast Asia. In: Networking the world with remote sensing, vol 38
- Zakaria R, Mohd Said MN, Ibrahim FH (2019) Association of tree communities with soil properties in a semi deciduous forest of Perlis, Peninsular Malaysia. *Biotropia-Southeast Asian J Trop Biol* 27(1):69–79. <https://doi.org/10.11598/btb.2020.27.1.1122>
- Zhu Z (2017) Change detection using Landsat time series: a review of frequencies, preprocessing, algorithms, and applications. *ISPRS J Photogrammetry Remote Sens* 130:370–384. <https://doi.org/10.1016/j.isprsjprs.2017.06.013>
- Zhu L, Liu X, Wu L, Tang Y, Meng Y (2019) Long-term monitoring of cropland change near Dongting Lake, China, using the landtrendr algorithm with landsat imagery. *Remote Sens* 11(10):1234. <https://doi.org/10.3390/rs11101234>

Part V

Remote Sensing of Mangrove Ecosystems



Geospatial Technology: Unlocking the Management and Monitoring in Malaysian Mangrove Forests

Norizah Kamarudin, Rhyma Purnamasayangasukasih Parman, Zulfa Abdul Wahab, Jamhuri Jamaluddin, and Mohd Hasmadi Ismail

Abstract

Mangroves are multifunctional ecosystems providing resource provisions and various ecosystem services critical to the local livelihood and national economy. The anthropogenic activities in the mangrove forest and the threat to these ecosystems remain a daunting and challenging task to the ecologist, especially in the management. This chapter attempted to present monitoring works conducted for mangrove forests as geospatial analytics helps in the decision-making and management. Geospatial technology offers a more accurate way of measuring the mangrove forest ecosystem and a more efficient tool in mangrove forest plan, management, and conservation. The application and discussion of this chapter focus on the Malaysian mangrove forest.

Keywords

Malaysian mangroves · Geospatial analysis · Tropical forest · Systematic literature review

N. Kamarudin (✉)

Department of Forestry Science and Biodiversity, Faculty of Forestry and Environment, Universiti Putra Malaysia, Serdang, Selangor, Malaysia

Institute of Tropical Forestry and Forest Products, Universiti Putra Malaysia, Serdang, Selangor, Malaysia

e-mail: norizah_k@upm.edu.my

R. P. Parman · Z. Abdul Wahab · J. Jamaluddin · M. H. Ismail

Department of Forestry Science and Biodiversity, Faculty of Forestry and Environment, Universiti Putra Malaysia, Serdang, Selangor, Malaysia

1 Introduction

Geospatial technology is essential technology of forestry research in this era. Exploring gaps in forestry research, especially in managing and monitoring spatial- and temporal-related problem-solving, can be evaluated by validating and qualifying with the knowledge advancement in geospatial technology. Fundamentally, the manager or the data analyser must be advancing the knowledge on geospatial data analyses before existing work.

Works in mangrove forests are challenging due to their unique ecosystems (Faridah-Hanum et al. 2019; Rhyma et al. 2015). The limitation of these challenges has intensified the geospatial technology used in management and monitoring work. Although Malaysia has limited satellite sensors and depends on other global companies providing satellite images, the management and monitoring work is not limiting for researchers and managers. The availability of sensors from low to high resolutions gives options to researchers and managers to choose the best satellite images applicable to their applications. Many freely available satellite images can be used in forestry-related work and finding solutions to problems, even though the cost is a barrier factor in geospatial technology-related work (Zulfa and Norizah 2018; Rhyma and Norizah 2016). With advanced image processing and existing skills, forestry-related issues and problems can be resolved quickly, without incurring high costs—the reliability, validity, and quality of the problem-solving produced matters.

This chapter discusses the use of geospatial technology in Malaysian mangrove forests. This chapter is organized as follows: The next section presents the characteristics and figures of Malaysian mangrove forests, followed by a section that discusses the application of geospatial technology. The discussion is designed by systematic literature review (SLR) consisting of the methodology and the summary of findings. Later, the last section concludes the chapter with suggestion on how to improve the quality and consistency of literature reviews.

2 Mangrove Forests in Malaysia

Mangrove forests are commonly found in the coastline and estuaries of tropical and subtropical regions. These forests are most abundant in tropical Asia, Africa, and the islands of the Southwest Pacific. Malaysia's coastlines stretch at an estimate of 4810 km attributed from the West Coast Peninsular Malaysia with 1110 km, East Coast of Peninsular Malaysia with 860 km, Sabah with 1800 km, and Sarawak with 1040 km.

Mangrove forests are characterized by unique ecosystems influence a diverse range of tree species. Mangrove areas are difficult to access because of the extension of dense root systems over a wide area, dense stands of mangrove species, and the regular occurrence of high and low tides with deep mudflats. Most mangrove species survive under high and low tides with special root system characteristics. Tomlinson (1986) describes, within a tide-dominated shore, mangroves were zoned to four parts, viz. (1) seaward zone, (2) mesozone, (3) landward zone, and (4) terrestrial

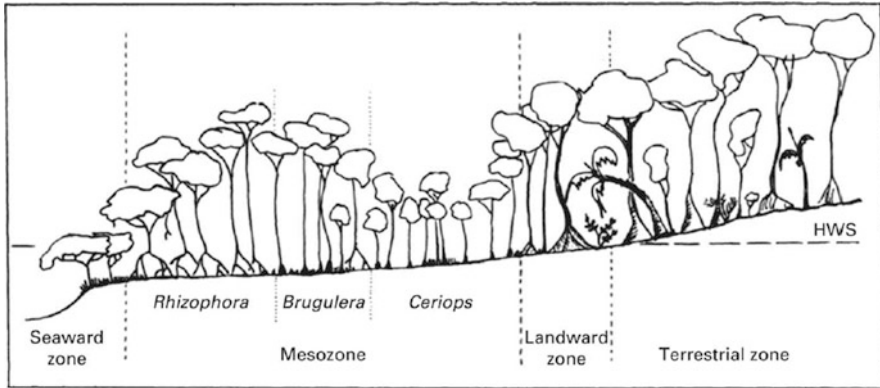


Fig. 1 Mangrove zonation profile as suggested by Tomlinson

zone. He added mangrove species zonation often appears as a clear sequence of species colonization with *Avicennia* on the seaward zone, followed by *Rhizophora*, *Bruguiera*, and *Ceriops* in the mesozones (Fig. 1). Different areas influence a mangrove; thus, zonation patterns may vary at both global and local scales. For example, mangrove zonation in the South America region contradicts the Asia region. *Rhizophora mangle* (red mangrove) is found at seaward zone, *Avicennia germinans* (black mangrove), and *Laguncularia racemosa* (white mangrove) are found in the landward zone in South America region. Meanwhile in Asia region, *Avicennian* communities are found in the seaward zone, *Rhizophora* community adaptable at soft, deep mud zone—middle zone, followed by the *Bruguiera* community that is more adaptable at landward zone (Fig. 2). According to Feller and Sitnik (1996), differences in species occurrence can be found across an estuary, which may be influenced by the fresh and saltwater source at local scales.

Malaysia is endowed with approximately 630,000 ha of mangrove forests lying on Malaysia’s East and West coasts. According to the annual report by the three Forestry Department in Malaysia, Sabah occupies the most extensive mangrove forest composition, about 234,700 ha, followed by Sarawak, 780,000 ha, and Peninsular Malaysia, about 90,000 ha. The mangrove area reported by Hamdan et al. (2020) was based on a 2017 satellite image, the most updated information of mangroves available. The other work reported that mangrove forests experienced deforestation 0.1% per year between 1990 and 2017 (Hamdan et al. 2018).

Since the threat to the mangrove forests is alarming, the management and monitoring work for understanding the conservation and protection measures has been widely conducted nationally. The following section discusses the spatial analysis application in Malaysian mangrove forests.

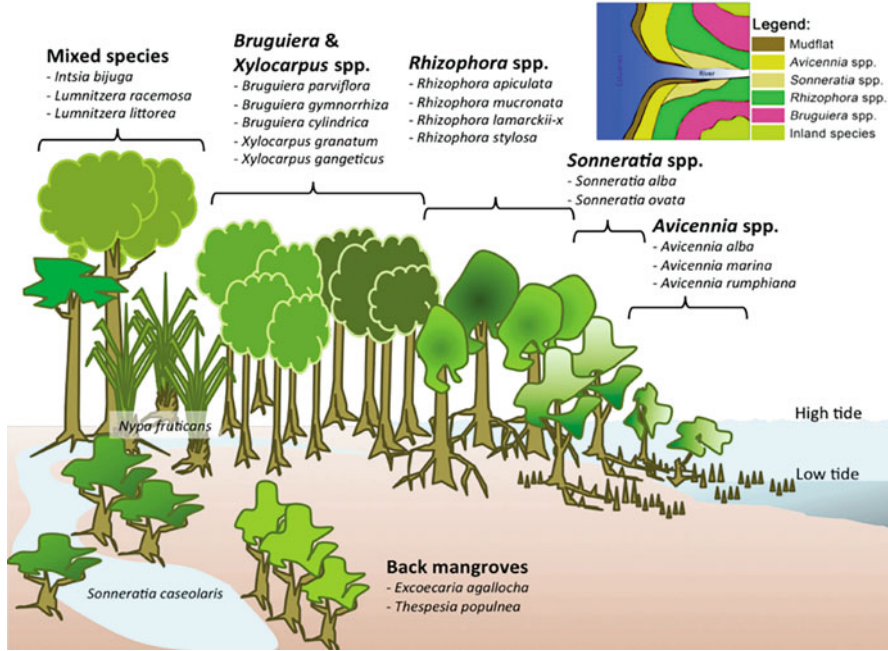


Fig. 2 Mangrove zonation profile in Malaysia

3 Mangrove and Geospatial Technology

3.1 Methodology

The discussion presented in this section was based on the SLR study (Mohamed Shaffril et al. 2021). The keyword search is the first step in SLR. The search was conducted on the selected database, Scopus, Science Direct, Google Scholars, and Google engine search. The content of the search focus on “Malaysian mangrove,” “geographic information system,” “remote sensing,” and “spatial analysis.” From the preliminary search of the title and the abstract, there is no limitation on literature and information type, as long as the content is related to mangrove forests in Malaysia. Since researchers and managers have extensively used geospatial technology as a precision forestry application in Malaysia since the 2000s; thus, the literature search includes all information published from 2000. In addition, all articles written in English and Malay are considered in the literature.

The comprehensive search obtained 9750 articles based on the title and the abstract. After the information extraction and evaluation, 42 articles were discussed in this chapter. Figure 3 shows the simplified methodological flowchart for this chapter.



Fig. 3 The flowchart for systematic literature review search

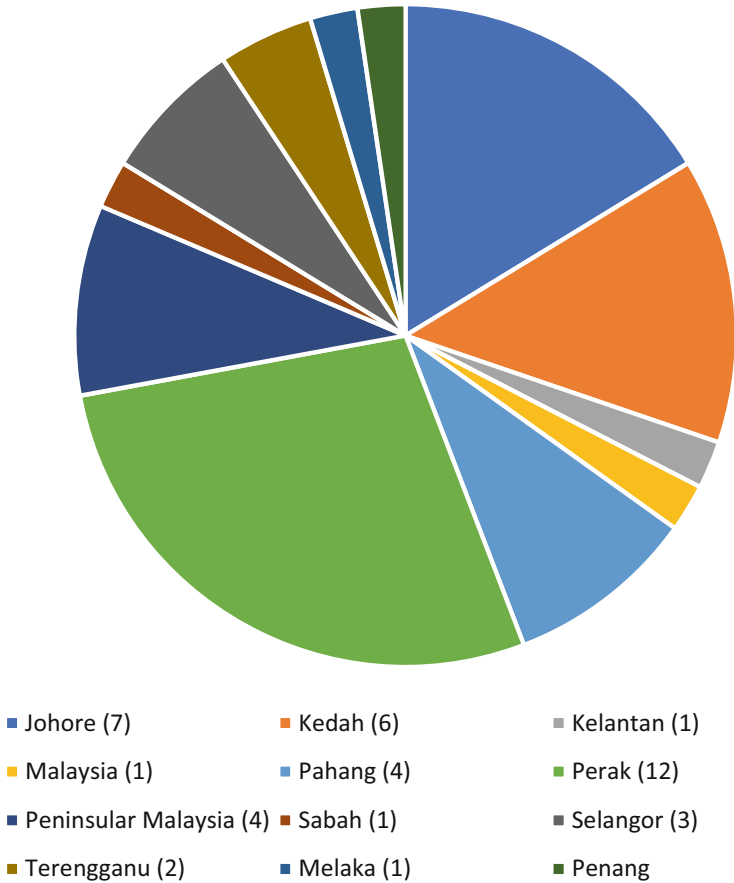


Fig. 4 The area of interest for geospatial technology application in mangrove forest application across Malaysia

3.2 Finding and Discussion

Figure 4 presents the distributions of mangrove forests and the geospatial technology study area conducted in Malaysia based on the 42 literature searches.

Known as the best-managed mangrove forest globally (Rhyma et al. 2020; Zulfa et al. 2021), Matang Mangrove Forest Reserve (MMFR), located at Perak, has

become the focus of researchers from within and outside countries. About 28% of the literature studies were conducted in this mangrove forest. The researchers' second most attractive mangrove forest is Johore by 16%. Most of the research was conducted at Southern Johore, covering Kukup and Sungai Pulai. Kilim and Sungai Merbok mangrove forest in Kedah is the third most attractive research area for geospatial application by 14%, followed by Pahang and Selangor by 10% and 7%, respectively. The other states in Peninsular are Terengganu by 5% and Kelantan, Malacca, and Penang by 2%. Although Sabah is attributed to the most extensive coastlines and mangrove forest cover, there is a lack of studies related to the geospatial application with only 2%. While Sarawak, the second largest mangrove forest cover, has no geospatial application studies reported from the literature search. There are four studies focused on Peninsular Malaysia, and one focused on Malaysia using geospatial technology. Most of these five studies monitor the changes in land use and land cover of mangrove forests using temporal-spatial data.

The extraction and evaluation of literature search compiled several geospatial applications. Mapping and monitoring are the most extensive application. This includes land use and land cover changes (LULC) (1, 4, 7, 8, 9, 10, 13, 15, 19, 24, 26, 30, 37, 39, 40), vegetation mapping (3, 12, 14, 16, 20, 23, 25, 27, 28, 31, 33, 38, 41), monitoring the anthropogenic activities along the coastal mangrove areas (6, 11), including riverbank erosion (2) and sea-level rise monitoring (5), and, last but not least is carbon monitoring (22, 32, 35, 37). Three literature searches applied geospatial technology in modelling the mangrove ecosystem in terms of environmentally sensitive areas (18), environmental vulnerability (36), and mangrove quality index (34). In addition, there are three literature searches found to use geospatial technology as a tool in finding the habitat suitability for *Aedes* (17), fish abundance (21), migratory birds (29), and firefly (42).

LULC changes are at an alarming rate. This is also not exempted from the mangrove forest. Most LULC studies found that the mangrove forest is decreasing, highlighted by Hamzah et al. (2009), Shahbudin et al. (2012), Khuzaimah et al. (2013), Kanniah et al. (2015), Nurul (2016), Hamdan et al. (2018), Ahmad et al. (2019), Hashim et al. (2019), Hamzah et al. (2020), and Kanniah et al. (2021). The study of LULC using the oldest temporal data is by Gopalakrishnan et al. (2021). They used the historical hardcopy map from 1853 in Peninsular Malaysia. They monitor the temporal changes of mangrove forests until 2018 and the available satellite images only from 1988. Since they have used temporal data for several years, the Google Earth Pro for Desktop software is an alternative to assess image processing accuracy and classification by activating the history tab in the software. The other LULC studies also used this method to measure the accuracy assessment since collecting on-site data was not feasible within the study period (Hamzah et al. 2020; Rhyma et al. 2020; Zulfa et al. 2021). While temporal images from the past years limit the confirmation of actual ground cover attributes, the available geospatial related software provides the solution to the users.

The occurrence of LULC can be explained by the opening of mangrove forest areas, particularly in the coastal areas. The development of coastal areas due to anthropogenic activities including agriculture, aquaculture and urbanization are the

significant causes of a mangrove forest opening. Due to these anthropogenic activities, the impact of forest canopy opening to the coastal areas leads to erosion, environmental problems, carbon offsets, and community services. Hamzah et al. (2009), Ahmad et al. (2019), Mohamad (2019), Hamzah et al. (2020), Kanniah et al. (2021) and Zakaria et al. (2021) used temporal-spatial data to detect the LULC, including erosion occurrence and carbon offsets. While monitoring the environmental problems, including mangrove ecosystem health and sensitive areas, Leman et al. (2016), Zulkifli et al. (2017), Yunus et al. (2018) and Faridah-Hanum et al. (2019) used biotic and abiotic data acquired from the measurements conducted on the field. These data were later combined with spatial data obtained from the satellite images with relevant image processing and spatial analyses algorithm. Although geospatial technology is an advanced application in helping decision-makers plan and solves the problem, integrating the ground survey data is essential to ensure the survival and sustainability of mangrove-associated biodiversity (Satyanarayana et al. 2011). Meanwhile, Khuzaimah et al. (2013) integrate the social aspects with geospatial technology application to understand socioeconomic impacts from the changes of mangrove forests. Hashim et al. (2020) studied mangrove carbon stocks by integrating the physical vegetation data with geospatial technology. Later, they developed an equation to estimate mangrove carbon stocks.

The vegetation distributions also come into effect from the mangrove forest opening and anthropogenic activities. A study by Zulfa et al. (2021) found that mangrove zonation by vegetation is likely disappeared. Identifying individual mangrove species is a challenging task to ensure the conservation of mangrove species and the management of mangrove forests as a whole. The use of high spatial resolution data conducted by Kanniah et al. (2007), Satyanarayana et al. (2011) and Roslani et al. (2013) confirms the accuracy of species identification. However, a recent study conducted by Zulfa et al. (2021) and Ibharim et al. (2015) show that moderate spatial resolution data is useful in identifying individual mangrove species. Acquisition of high spatial resolution data for mangrove forest mapping and monitoring is not compulsory at this day since there are lots of advanced processing algorithms available for geospatial data.

Geospatial technology's capability to examine the occurrence of biotic factors on the mangrove forests is a benefit that researchers and managers need to explore. For example, Jamizan and Chong (2017), Azimah and Tarmiji (2018), and Saffawati et al. (2019) used geospatial technology through Geographic Information System (GIS) software to identify the suitable areas for fish, migratory birds and *Aedes* in the mangrove forest, respectively. The selection of several attributes, mostly the abiotic factors that attract fish, migratory birds and *Aedes* to mangrove forests, is examined before the geospatial analyses. The selection of appropriate spatial analysis was later determined according to the objective. These geospatial modelling and decision-making help ease the management and the conservation of mangrove forest that benefits the mangrove ecosystem, including biotic and abiotic factors.

Kanniah et al. (2015) suggested promoting tourism-based activities in the mangrove forest for conservation purposes. Aminu et al. (2013) has developed the procedure to evaluate and plan to support tourism planning in mangrove forests by

integrating the expert's opinion with geospatial analyses. On the other hand, Mohd Razali et al. (2020) conducted mangrove density mapping to examine the essential conservation for mangrove forests. Ramsar site known as the unique wetlands and having important biological diversity requires conservation is the study area characteristics chosen by Aminu et al. (2013) and Mohd Razali et al. (2020). Such effortless work to sustain the mangrove forest areas with biological diversity can be a simple task by geospatial technology since the information provided by the satellite images and the advanced processing algorithm can monitor mangrove changes over a large spatial extent in a continuous manner. This includes mapping and monitoring mangrove forest cover, anthropogenic activities, carbon, and impact on the environments and community, which also changes following the changes of mangrove forest areas (Zuhairi et al. 2019; Ahmad et al. 2019; Amran et al. 2020; Mohd Razali et al. 2020; Rhyma et al. 2020; Otero et al. 2020; Kanniah et al. 2021).

Image processing is a significant step in monitoring temporal LULC changes, examining the distribution of vegetation and mapping, and monitoring and assessing the environments. Several procedures are available for image processing, such as pixel-based classification, object-based classification, and vegetation indices; several indices are available where the selection of indices algorithm is based on the study objective. Satellite images of SPOT and Landsat images are the common medium spatial resolution data source used in most geospatial technology applications in Malaysia. While the high spatial resolution data commonly used are RapidEye, Quickbird, and Pleiades images. The efficiency of using these images in mangrove forest conservation and management has been proven and reported in the literature search. On the other hand, Ruwaimana et al. (2018) describe the uses of unmanned aerial vehicle (UAV) remote sensing equipped with red, green, blue (RGB) and infra-red (IR) cameras is capable of doing the mapping and monitoring works in mangrove forests. The use of hyperspectral data is also reported by Zulfa et al. (2021) and Chung (2011) in identifying individual mangrove species by wavelength separation. Since there are many available satellite images and processing algorithms nowadays, geospatial technology is a must in managing mangrove forests at the strategic, tactical and operational level and for monitoring and conservation purposes.

4 Concluding Remarks

This chapter discusses geospatial technology applications for mangrove forests that have been conducted with an SLR. This chapter aimed at summarising the benefits of geospatial technology application to enable effortless plan, management and conservation of mangrove forests providing information on mangrove status and changes over a large spatial extent and in a continuous manner, study the impacts on the environment, vegetation distribution, biotic and abiotic factors, carbon, the health of the ecosystem and socials. Thus, this chapter draws the following conclusions and recommendations:

1. The inclusion and exclusion of titles and abstracts require a systematic evaluation to separate research articles, proceedings, dissertations, and other publications. From the SLR conducted in this chapter, different types of literature search give different understandings, and the explanation of the research is also different. For example, literature found from articles and dissertation is comprehensive in explaining the problem statements, objective, and methodology, while the others make a simpler explanation.
2. Limiting the selection of materials for SLR at specific periods or categorizing the periods of study helps the author and readers understand the evolution or trend of the geospatial technology applications in mangrove forests.

References

- Ahmad Z, Suharni MLM, Taib SNA, Shaheed M (2019) Impact of coastal development on mangrove distribution in Cherating Estuary, Pahang, Malaysia. *Malays J Fundam Appl Sci* 15(3):456–461
- Aminu M, Ludin ANBM, Matori AN, Wan Yusof K, Dano LU, Chandio IA (2013) A spatial decision support system (SDSS) for sustainable tourism planning in Johor Ramsar sites. *Malays Environ Earth Sci* 70(3):1113–1124
- Amran NFA, Isnan S, Nordin NH, Rahman A, Thanakodi S, Rosly A, Aziz A (2020) Identification of mangrove area using Landsat image in Kuala Selangor Nature Park. *Int J Bus Technol Manag* 2(4):1–9
- Azimah AR, Tarmiji M (2018) Habitat requirements of migratory birds in the Matang Mangrove Forest Reserve, Perak. *J Trop For Sci* 30(3):304–311
- Chung AYC (2011). Mangrove fauna of Sabah. Talk presented at the Sabah Tourist Guides Association MTGA Board and Affiliates Meeting, Kota Kinabalu, Sabah, 8 May, 2011
- Faridah-Hanum I, Yusoff FM, Fitrianto A, Ainuddin NA, Gandaseca S, Zaiton S, Norizah K, Nurhidayu S, Roslan MK, Hakeem KR, Shamsuddin I, Adnan I, Awang Noor AG, Balqis ARS, Rhyma PP, Siti Aminah I, Hilaluddin F, Fatin R, Harun NZN (2019) Development of a comprehensive mangrove quality index (MQI) in Matang Mangrove: assessing mangrove ecosystem health. *Ecol Indic* 102:103–117
- Feller IC, Sitnik M (1996) *Mangrove ecology: a manual for a field course*. Smithsonian Institution, Washington, DC, pp 1–135
- Gopalakrishnan L, Satyanarayana B, Chen D, Wolswijk G, Amir AA, Vandegehuchte MB et al (2021) Using historical archives and Landsat imagery to explore changes in the mangrove cover of Peninsular Malaysia between 1853 and 2018. *Remote Sens* 13(17):3403
- Hamdan O, Misman MA, Linggok V (2018) Characterizing and monitoring of mangroves in Malaysia using Landsat-based spatial-spectral variability. *IOP Conf Ser Earth Environm Sci* 169(1):012037. IOP Publishing
- Hamdan O, Husin TM, Ismail P (2020) Status of mangroves in Malaysia. Forest Research Institute Malaysia, Ministry of Energy and Natural Resources, Malaysia, p 288
- Hamzah KA, Omar H, Ibrahim S, Harun I (2009) Digital change detection of mangrove forest in Selangor using remote sensing and geographic information system (GIS). *Malays For* 72:61–69
- Hamzah ML, Amir AA, Maulud KNA, Sharma S, Mohd FA, Selamat SN et al (2020) Assessment of the mangrove forest changes along the Pahang coast using remote sensing and GIS technology. *J Sustain Sci Manag* 15(5):43–58
- Hashim NI, Zaharin NF, Hashim NH, Halim MA (2019) Temporal changes of mangrove distribution in Mukim Kuala Selangor using GIS approach. *IOP Conf Ser Earth Environ Sci* 385(1): 012027. IOP Publishing

- Hashim TMZT, Suratman MN, Singh HR, Jaafar J, Bakar AN (2020) Predictive model of mangroves carbon stocks in Kedah, Malaysia using remote sensing. *IOP Conf Ser Earth Environ Sci* 540:012033. <https://doi.org/10.1088/1755-1315/540/1/012033>
- Ibharim NA, Mustapha MA, Lihan T, Mazlan AG (2015) Mapping mangrove changes in the Matang Mangrove Forest using multi temporal satellite imageries. *Ocean Coast Manag* 114: 64–76. <https://doi.org/10.1016/j.ocecoaman.2015.06.005>
- Jamizan AR, Chong VC (2017) Demersal fish and shrimp abundance in relation to mangrove hydrogeomorphological metrics. *Sains Malays* 46(1):9–19
- Kanniah KD, Wai NS, Shin A, Rasib AW (2007) Per-pixel and sub-pixel classifications of high-resolution satellite data for mangrove species mapping. *Appl GIS* 3(8):1–22
- Kanniah KD, Sheikhi A, Cracknell AP, Goh HC, Tan KP, Ho CS, Rasli FN (2015) Satellite images for monitoring mangrove cover changes in a fast growing economic region in southern Peninsular Malaysia. *Remote Sens* 7(11):14360–14385
- Kanniah KD, Kang CS, Sharma S, Amir AA (2021) Remote sensing to study mangrove fragmentation and its impacts on Leaf Area Index and gross primary productivity in the South of Peninsular Malaysia. *Remote Sens* 13(8):1427
- Khuzaimah Z, Ismail MH, Mansor S (2013) Mangrove changes analysis by remote sensing and evaluation of ecosystem service value in Sungai Merbok's mangrove forest reserve, Peninsular Malaysia. In: International conference on computational science and its applications. Springer, Berlin, Heidelberg, pp 611–622
- Leman N, Ramli MF, Khirotudin RPK (2016) GIS-based integrated evaluation of environmentally sensitive areas (ESAs) for land use planning in Langkawi, Malaysia. *Ecol Indic* 61:293–308
- Mohamad N (2019) Evaluation of riverbank erosion based on mangrove boundary changes identification using multi-temporal satellite imagery. Doctoral dissertation, Master Thesis, Universiti Teknologi Malaysia, Faculty of Built Environment & Surveying Acknowledgments The authors feel grateful to the Universiti Teknologi Malaysia for funding this manuscript under UTM High Impact Research (UTM HR) Vote Q
- Mohamed Shaffril HA, Samsuddin SF, Abu Samah A (2021) The ABC of systematic literature review: the basic methodological guidance for beginners. *Qual Quant* 55(4):1319–1346
- Mohd Razali S, Nuruddin AA, Kamarudin N (2020) Mapping mangrove density for conservation of the Ramsar site in Peninsular Malaysia. *Int J Conserv Sci* 11(1)
- Nurul ABK (2016) Application of REMote sensing and geographic information system techniques to monitoring of protected mangrove forest change in Sabah, Malaysia
- Otero V, Lucas R, Van De Kerchove R, Satyanarayana B, Mohd-Lokman H, Dahdouh-Guebas F (2020) Spatial analysis of early mangrove regeneration in the Matang Mangrove Forest Reserve, Peninsular Malaysia, using geomatics. *For Ecol Manag* 472:118213
- Rhyma PP, Norizah K (2016) Kriging analysis-optimizing values in unknown areas using known data point. In: Sustainable forest development in view of climate change SFDC2016, p 96
- Rhyma PP, Norizah K, Ismail Adnan AM, Faridah-Hanum I, Ibrahim S (2015) Canopy density classification of Matang Mangrove Forest reserve using machine learning approach in remote sensing for transect establishment. *Malaysian Forester* 78(1–2):75–86
- Rhyma PP, Norizah K, Hamdan O, Faridah-Hanum I, Zulfa AW (2020) Integration of normalised different vegetation index and soil-adjusted vegetation index for mangrove vegetation delineation. *Remote Sens Appl Soc Environ* 17:100280. <https://doi.org/10.1016/j.rsase.2019.100280>
- Roslani MA, Mustapha MA, Lihan T, Juliana WW (2013) Classification of mangroves vegetation species using texture analysis on Rapideye satellite imagery. *AIP Conf Proc* 1571(1):480–486. American Institute of Physics
- Ruwaimana M, Satyanarayana B, Otero VM, Muslim A, Syafiq AM, Ibrahim S et al (2018) The advantages of using drones over space-borne imagery in the mapping of mangrove forests. *PLoS One* 13(7):e0200288
- Saffawati T, Ismail T, Kassim NF, Rahman AA, Hamid SA, Yahya K, Webb CE (2019) The application of geographic information system (GIS) to assess the population abundance of *Aedes albopictus* (Skuse) in mangrove forests of Penang, Malaysia. *Int J Mosq Res* 6:50–54

- Satyanarayana B, Mohamad KA, Idris IF, Husain ML, Dahdouh-Guebas F (2011) Assessment of mangrove vegetation based on remote sensing and ground-truth measurements at Tumpat, Kelantan Delta, East Coast of Peninsular Malaysia. *Int J Remote Sens* 32(6):1635–1650
- Shahbudin S, Zuhairi A, Kamaruzzaman BY (2012) Impact of coastal development on mangrove cover in Kilim River, Langkawi Island, Malaysia. *J For Res* 23(2):185–190
- Tomlinson PB (1986) *The botany of mangroves*. Cambridge University Press, Cambridge, p 413
- Yunus MZM, Ahmad FS, Ibrahim N (2018) Mangrove vulnerability index using GIS. *AIP Conf Proc* 1930(1):020007. AIP Publishing LLC
- Zakaria R, Chen G, Chew LL, Sofawi AB, Moh HH, Chen S et al (2021) Carbon stock of disturbed and undisturbed mangrove ecosystems in Klang Straits, Malaysia. *J Sea Res* 176:102113
- Zuhairi A, Zaleha K, Nur Suhaila MR, Muhammad Shaheed S (2019) Mapping mangrove degradation in Pahang River Estuary, Pekan Pahang by using remote sensing. *Sci Herit J* 3(2):01–05
- Zulfa AW, Norizah K (2018) Remotely sensed imagery data application in Mangrove Forest: a review. *Pertanika J Sci Technol* 26(3):899–922
- Zulfa AW, Norizah K, Hamdan O, Faridah-Hanum I, Rhyma PP, Fitrianto A (2021) Spectral signature analysis to determine mangrove species delineation structured by anthropogenic effects. *Ecol Indic* 130:108148
- Zulkifli M, Yunus M, Ahmad FS, Omar CM (2017) Spatial management on mangrove response to sea level rise (SLR) in Kukup Island. *IOP Conf Ser Mater Sci Eng* 226(1):012065. IOP Publishing



Effect of Tidal Regime, Relative Sea Level and Wind Intensity on Changes of Mangrove Area Using Remote Sensing Approach

Noorita Sahriman, Arnis Asmat, Fazlina Ahmat Ruslan, Ismail Maarof, and Abd Manan Samad

Abstract

Mangroves are very well known for their contribution to wildlife, human and ecosystem. Mangroves provide habitat, food, medicine and building material make them so valuable and important. However, despite all the benefits they offer, mangroves are being threatened all over the world. Mangrove loss and deforestation have become a worldwide issue. The destruction and replacement of mangrove forests spread widely for various reasons. This study focuses on determining the effect of environmental parameters towards mangrove areas. Three indicators were taken as a primary parameter in this study. Those parameters were tidal regime, wind intensity and relative sea level. The three information were obtained from Forest Research Institute Malaysia (FRIM), Forestry Department Peninsular Malaysia (FDIM) and Malaysian Meteorological Department (MMD) as well as from previous studies. The study area for this research covered the east and west coast of Malaysia. For the east coast was Chendering in Terengganu, whereas for the west coast was Kuala Perlis in Perlis. The detection of mangrove areas was performed using Landsat 5 TM and Landsat

N. Sahriman (✉) · I. Maarof · A. M. Samad

Centre of Studies Surveying Science and Geomatics, Faculty of Architecture, Planning and Surveying, Universiti Teknologi MARA, Shah Alam, Selangor Darul Ehsan, Malaysia

A. Asmat

Faculty of Applied Sciences, School of Chemistry and Environment, Universiti Teknologi MARA, Shah Alam, Selangor Darul Ehsan, Malaysia

F. Ahmat Ruslan

Centre of Studies Surveying Science and Geomatics, Faculty of Architecture, Planning and Surveying, Universiti Teknologi MARA, Shah Alam, Selangor Darul Ehsan, Malaysia

School of Electrical Engineering, College of Engineering Studies, Universiti Teknologi MARA, Shah Alam, Selangor Darul Ehsan, Malaysia

© The Author(s), under exclusive license to Springer Nature Singapore Pte Ltd. 2022

289

M. N. Suratman (ed.), *Concepts and Applications of Remote Sensing in Forestry*, https://doi.org/10.1007/978-981-19-4200-6_14

8 OLI satellite imageries in PCI Geomatica 2013 software. The process of determining the mangrove area was done using supervised classification with maximum likelihood classifier and supported with site verification. The area covered was 5 km × 5 km per image or 25 km² with the range period of 10 years from 2005 to 2015, and the satellite images selected were in the years of 2005, 2010 and 2015. The changes of mangrove areas were determined. Chendering mangrove areas increased 3243 m² during 2005–2015, while in Kuala Perlis mangrove increased 1892 m² during the same period. The relationships between tidal regime, relative sea level and wind intensity were analysed based on the results from mangrove area changes that was obtained through supervised classification and correlation analysis. The final result shows several responses that accomplished the objectives of this study. The classification processing for the mangrove area was successfully acquired with more than 85% accuracy. The mangrove areas have shown some changes during the years of 2005, 2010 and 2015.

Keywords

Mangrove · Remote sensing · Supervised classification · Maximum likelihood

1 Introduction

Mangrove is known as a small tree or forest vegetation of salt-tolerant tropical shrubs that can be found and grows in a particular area such as tidal marshes or river estuaries that are covered by the sea at high tide existing along estuary or coastline which are located between the land and the sea (Goh 2016). It connects the terrestrial with sea and usually can be found in tropical and subtropical regions. Usually they live within 0 and 5 m above mean sea level. Mangrove forests are mostly abundant in tropical Asia, Africa and the islands of the Southwest Pacific. Less than 0.1% of mangrove forest covers the Earth's surface. Mangrove forests are very complex however known for their multiple benefits to human, wildlife and ecosystem (Lewis 2005; Ghosh et al. 2017; Kong and Chung 2019). It provides building material, food, medicine, fuel, habitat and breeding location for variety of species such as fish, birds, monkey and reptiles. Mangrove helps to protect the ecosystem and stabilize the shorelines from any natural disasters such as hurricanes, coastal erosion, tsunamis, trapping silt and wastes. They also offer a renewable source of wood, carbon, nutrients, contaminants and accumulation sites for sediments. During the tsunami back in 2004, mangroves gave major contribution in reducing the impact along the Malaysia coastline area mostly in Perlis, Penang, Kedah, Perak and Selangor (Ahmadun et al. 2020).

Despite various benefits that have been offered by mangroves, however they cannot escape from deforestation and disappearance. Over the past century, mangrove forests are facing a replacement and deforestation all over the world. Among major factors include human interference, urbanization, development and natural

processes. As a result, the number of mangroves globally declined significantly (Goh, 2016; Ávila-Flores et al. 2020). In 2010, FAO in their report stated that the global area of mangroves has decreased from around 16.1 million hectares in 1990 to 15.6 million hectares in 2010. The decrease was about 0.5 million hectares at the annual rate of 25,000 ha per year. A parallel trend in Malaysian mangrove has been identified (Omar and Hamzah 2012). Since 1990, there has been about 1282 ha or about 1% mangrove loss in some major states in Peninsular Malaysia every year. Therefore, it is important for action to be taken in order to protect the mangrove loss from becoming worse. The first step is doing an early detection of mangrove forest changes, analyse factors or parameters that are affecting the changes and try to control the factors that threaten the mangroves (Ávila-Flores et al. 2020). The next stages are to plan on how to replant and rehabilitate of mangroves. Previously, several techniques and methods were applied to protect mangrove forest. This include the building of costal structure such as detach breakwater to become a protection measures for shore and coast area from by wave action, erosion and sediment deposition (Hashim et al. 2009). By using detach breakwater, it may contribute to mangrove restoration and protect them from the wave that might destroy the seed or new tree (Kamali and Hashim 2011). The concept of mangrove rehabilitation and conservation has already been implemented in Malaysia with the aid of remote sensing technique.

In this study, the dynamism and relationship of mangrove and parameter were studied as to see the changes of mangrove and which parameter affects the mangrove ecosystem the most. According to the previous study by Gelfenbaum et al. (2009), the dynamism of mangrove was associated with four factors. These include sediment supply, tidal regime, relative sea level and wind intensity. The ecosystem productivity for mangrove and its surrounding area was ensured based on the balance between these four factors. Factors that has been selected were tidal regime, relative sea level and wind intensity. Data used in this study were Landsat 5 TM and Landsat 8 OLI satellite imagery, relative sea level data from the Department of Survey and Mapping Malaysia (DSMM), wind intensity data from the Malaysian Meteorological Department (MMD) and mangrove information from Forestry Department Peninsular Malaysia (FDPM) and Forest Research Institute Malaysia (FRIM). Image processing was done in PCI Geomatica 2013 which involved supervised classification analysis. The results from this study were shown as line chart, analysis and mangrove vulnerable map.

The detection of mangrove changes has been frequently done by previous studies. Researches in this area help in determining whether area of mangroves are increasing or decreasing. Changes mangrove areas occurred due to monsoon, hurricanes, storms, climate changes or anthropogenic changes (Hamzah et al. 2020; Jupiter et al. 2007; Adams and Rajkaran, 2020; França et al. 2013). Another aspect that contribute to the mangrove changes is the deforestation as a result from activities such as firewood collection, clearing for agricultural purposes and extension of shrimp farming area (Thu and Populus, 2007). Mangrove forest concession, shrimp farming and tin mining are also lead to the degradation and ecological disturbances as well (Sremongkontip et al. 2000). When human natural uncertainties disturbance

occurs, it is a vital action to monitor the mangrove ecosystem closely (Nguyen et al. 2020; Uni et al. 2016; Upanoi et al. 2003; Nascimento et al. 2013; Sari and Rosalina 2016). The contributions and benefits of mangrove make it a compulsory to quantify and record the mangrove changes especially consistent on different date intervals (Upanoi and Tripathi 2012; Ibharm et al. 2015).

2 Study Area

The first study area was Chendering. It is located in east coastal side of Terengganu state, Malaysia. This area was selected as one of the study areas because it covers several criteria that were required in this study. Chendering coastal areas are covered with diurnal tide. Diurnal tide is a tide that has one-time high tide and one-time low tide in a day. The second reason was because Chendering is experiencing Northeast Monsoon. This monsoon happens at the Chendering's coastline from November until March every year. As for the three parameters, the relative sea level data represent the tide value, the diurnal tide represents the wave, and the Northeast Monsoon represents the wind intensity.

The second study area was Kuala Perlis. It is located in Perlis west coastal side of Perlis state, Malaysia. This area was selected as one of the study areas because it covers several criteria that were required in this study. Kuala Perlis coastal area is covered with semidiurnal tide. Semidiurnal tide is a tide that has two times high tide and two times low tide in a day. The monsoon occurs at the Kuala Perlis's coastline from May until September every year. As for the three parameters, while the tide represents the tide itself, the diurnal tide represents the wave and current, and the Southwest Monsoon represents the wind intensity. The study areas were identified based from the mangrove data which consists of location and distribution of mangrove forests in Malaysia coastal area (Fig. 1).

3 Environmental Parameters

In detection for mangrove changes, guidelines or keys need to be set first to see changes that happened before and after. In this study, there are three environmental parameters that have been selected to correlate with the results that have been gathered from mangrove area changes. In the previous study, Asbridge et al. (2016) have applied rainfall, runoff and sea level to detect the changes of mangrove area in Australia's Gulf of Carpentaria. The response of mangrove towards several parameters was also recorded by Soares (2009). The ecosystem of each mangrove is not same from one region to another; therefore, the selected of parameters must be suitable and available on the study area. In this study, three parameters which include tidal regime, wind intensity and relative sea level rise were selected. Particular information has been gathered from the Malaysia Meteorological Department (MMD), Department of Survey and Mapping Malaysia (DSMM) and the Forestry and Research Institute Malaysia (FRIM) in 3 years' interval of 2005, 2010 and 2015.



Fig. 1 Direction of Southwest Monsoon and Northeast Monsoon in Malaysia

4 Tidal Regime

Tidal regime occurs from the effect from the daily routine of tide movement amplitude. The tide is a periodic rise and fall of a body of water resulting from gravitational interactions between the Sun, Moon and Earth. It is also known as the vertical component of the particulate motion of a tidal wave. Although the accompanying horizontal movement of the water is part of the same phenomenon, it is preferable to designate this motion as tidal current (Spring 2000). The daily action of tide with the movement then produced a tidal wave. Tidal waves were produced from the act of shallow water waves that were caused by the gravitational interactions between the Sun, Moon and Earth. The high water is the crest of a tidal wave and low water is the trough. Meanwhile, tidal current is the horizontal component of the particulate motion, while tide is manifested by the vertical component. The observed tide and tidal current can be considered the result of the combination of several tidal waves, each of which may vary from nearly pure progressive to nearly pure standing and with differing periods, heights, phase relationships and direction.

The classification of tide is based on the characteristic forms of a tide curve. Semidiurnal tide happens when the two high waters and two low waters of each tidal day are approximately equal in height. It is also called two flood/maxima and two ebb/minima periods each tidal day. Semidiurnal tide is known as the predominant type of tide throughout the world. Mixed diurnal tide happens when there is a relatively large diurnal inequality in the high or low waters or both, while diurnal

tide happens when there is only one high water and one low water on each tidal day. It is also called a single flood/maxima and single ebb/minima periods of a reversing current in the tidal day. A rotary current is diurnal if it changes its direction through all points of the compass once each tidal day (Spring 2000).

This every routine of tide phenomenon is called a tidal regime. Tidal regimes consist of several important elements such as duration, timing, tidal amplitude and frequency especially if the tide is experienced in different parts of the intertidal zone. Each different tidal regime responds differently to various species of mangroves. A study in the Indian part of the Sundarban shows that a mangrove stands that experiences total diurnal inundation is dominated by *Avicennia alba* and *Avicennia marina* while *Acanthus ilicifolius*, *Ceriops dacandra* and *Excoecaria agallocha* dominate at sites that are not completely inundated (Hanum et al. 2016). For this study, tidal regimes were presented as diurnal and semi-diurnal only, and they were helped by the relative sea level data that carries the value of tide. The study area in Chendering consists of diurnal tide, while Kuala Perlis consists of semi-diurnal tide. Therefore, both study areas managed to cover both main tidal regimes in Malaysia.

5 Wind Intensity

One of the common features for marine environment is the existence of wind and currents or waves. Current is generally known as a horizontal movement of water. Currents were classified as tidal and also non-tidal (Spring 2000). Meanwhile, wind plays an important role for mangrove propagule dispersal (Van Der Stocken et al. 2013). Wind influence the mangrove ecosystem by its action of dispersing mangrove trees or seed. The current basically influences the integrated of wave parameters on long-term ocean wave climate. When the currents are strong, they produced a wave propagation. Once the waves are propagating towards an oncoming current, the current will tend to upsurge the steepness of the waves by increase in wave height and decrease in wavelength. The changing of wave energy might modify the surface waves when the current causes an exchange of energy between wave and current. Wave energy may gain or lost influenced by the movement of current (Sanil Kumar and Ashok Kumar 2010). It can be concluded that both wind and currents are very important for coastal and offshore engineering because both of them need these two factors as for the interaction between them in several coastal aspects. In this study, wind intensity covers the wind and current action. It was also represented by monsoon. Chendering consists of Northeast Monsoon, while Kuala Perlis consists of Southwest Monsoon.

6 Relative Sea Level

Relative sea level is the third environmental parameter that was selected in this study. Relative sea level is the mean sea level related to the local reference land level, mean sea level is the mean of everyday sea level in a month, while sea level rise

happened when there are changes in the relative sea level and that may be due to the global warming or the vertical motions of the land level (Gregory et al. 2019). Relative sea level might change due to the effect of eustatic sea level rise and local geomorphological changes in elevation. Tides are known as the regular and predictable change in the height of the ocean which is driven by gravitational and rotational forces between the Earth, Moon and Sun, combined with centrifugal and inertial forces. The experience of diurnal or semi-diurnal tides happens in every country's coastal areas which occur at different times in different locations around the Earth (Lewis et al. 2011). Relative sea level most of the time gets affected through different kinds of phenomena from marine ecosystem. These reasons could be from natural factors, global climate change, global warming and man-made issue such as development and sea reclamation. The changes on relative sea level might also give a huge impact to the coastal ecosystem. According to Hensel et al. (2014), every mangrove that have different criteria or types have different sensitivities, and this includes the influence of relative sea level.

7 Methods and Techniques

7.1 Supervised Classification (Maximum Likelihood)

Multiple techniques and methodologies have been practised for mangrove study since the 1970s. Several methods that usually have been applied in mangrove studies are Random Forest Classifier, NDVI, REDD, visual interpretation and supervised classification. In this study the supervised classification method with maximum likelihood classifier was applied in satellite image processing by using PCI Geomatica (2013) remote sensing software. The decision of using supervised classification is because the supervised classification methods are the most applied methods of classification. The supervised classification method is a dependent method that is controllable than the unsupervised classification method. This method requires creating a signature based on the region of interest or on training sites. Then, the classification process was run automatically in the software. Different sub-classification methods can be applied in the supervised classification. Those sub-classification methods are parallelepiped, minimum distance, mahalanobis distance, maximum likelihood and spectral angle mapper. However, the most commonly used technique is the maximum likelihood to natural nearby neighbour algorithm (Nguyen et al. 2013; Ghebregabher et al. 2016).

The maximum likelihood classifier method has been the most applied among high-resolution multi-spectral data sources by researchers and scholars to extract ground objects and convenience to be apply in the early stage of extraction data (Liao et al. 2020). This method offers simplicity and convenience in its application. The theoretical basis of the maximum likelihood method is mainly BAYES which means to describe the probability of an event, based on prior knowledge of conditions that might be related to the event, theory and fusion classification of prior knowledge of ground objects (Liao et al. 2020). This method also has been

used to see the different results between several methods (Purnamasayangasukasih et al. 2016). Maximum likelihood classifier has mostly been implemented alone or along with the different techniques as to classify and analysed the land use and land cover (Kamil et al. 2020; Ibhari et al. 2015; Sulong et al. 2002). Maximum likelihood algorithm also was selected for running classification using a threshold distance (Sremongkontip et al. 2000). The application of supervised maximum likelihood classifier has been proven as the most effective and robust method for classifying mangroves based on traditional satellite remote sensing data (Kuenzer et al. 2011). Since it is applicable and at the same time included in PCI Geomatica software, the supervised classification with maximum likelihood classifier method was chosen.

The selection of classes in this study was based on the main and basic details that have been found in the satellite imagery. Six main classes were selected which include agriculture, water bodies, urban area, empty space, cloud and mangrove. The quantification and investigation of the mangrove boundary changes in the year of 2005, 2010 and 2015 were proceed after the classification processes were completed. It began with distinguishing the total area from the satellite image classes that have been generated. In this stage, the analysis and mapping from the classification result were done together followed by accuracy assessment. The image classification for the mangrove area was successfully acquired with more than 85% accuracy. The results show that changes in mangroves occurred during the years of 2005, 2010 and 2015.

7.2 Correlation Analysis

Correlation analysis was applied to study whether relationships exist between two or more variables. This process is basically used to test relationships between quantitative variables or categorical variables. It measures how both variables are related. In this study, a correlation analysis was done between mangrove area and relative sea level and wind intensity to study the relationships between them.

7.3 Relationship of Mangrove Area Changes and Environmental Parameter

The result from supervised classification only is insufficient to prove the changes of mangrove area. The information needs to be supported by some other related information or variables to make it more solid and convincing. Therefore, three other parameters were selected, combined and overlaid together through the correlation analysis and the relationships between the parameters and mangrove changes can be analysed.

8 Results

8.1 Changes of Mangrove Boundary Area Quantification

The mangrove changes, whether it decreases or increases, will give some thoughts and ideas about the condition situation of mangroves. In this study, the mangrove area changes were obtained through the result of supervised classification. Mangrove classes were distinguished based on the specific spectral reflectance value for mangroves. This spectral signature was in the visible and near-infrared region into four-band spectra which were in the blue (400–500 nm), green (500–600 nm), red (600–700 nm) and near-infrared (700–800 nm) regions. Figure 2 shows the changes of mangrove area for Chendering. From the result, it shows that in the Northeast Monsoon which happens from November till March every year, the areas of mangrove changes were from 683 m² in 2005. The areas were increased to 4780 m² in 2010. However, the areas were then decreased to 3926 m² in 2015.

According to this result, there are a few possibilities and convincing factors that are believed to contribute to these changes. Back in 2005, during that time, most of the country's coastline areas were in the middle of recovering from the tsunami event that happened in December 2004 (Hashim et al. 2009). Tsunami that happened carried a high wave and a very strong wind causing a lot of damage.

The mangrove area in Kuala Perlis in Fig. 3 that has been obtained is 1590 m² in 2005. The value increased to 2574 m² in 2010, while in 2015 it increased even more to 3482 m². During the tsunami event back in 2004, Kuala Perlis was more affected than Chendering.

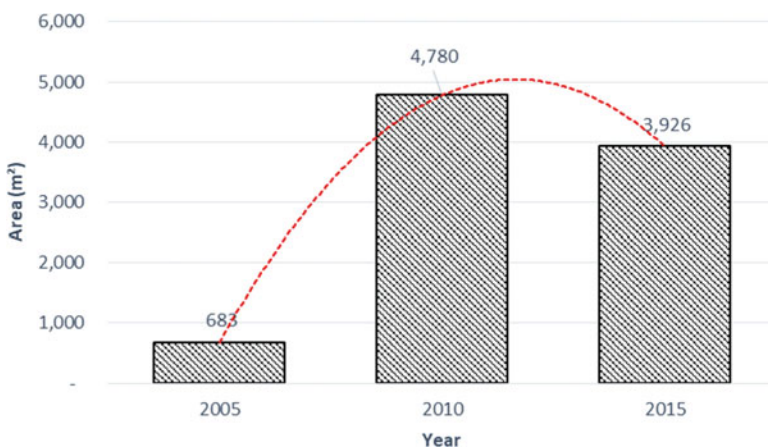


Fig. 2 Mangrove area changes for Chendering (10 years) in m²

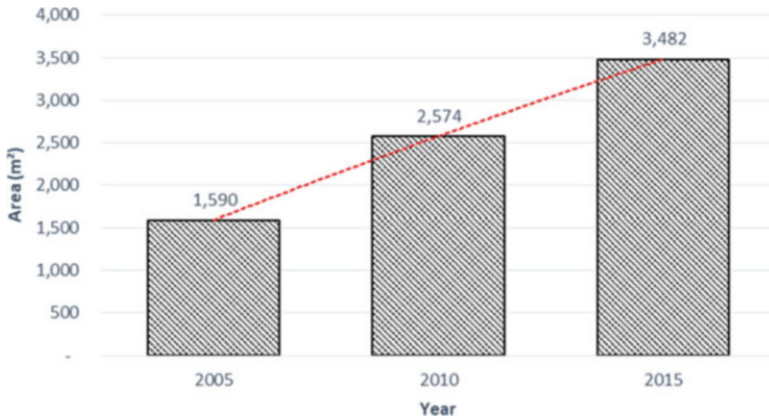


Fig. 3 Mangrove area changes for Kuala Perlis (10 years) in m²

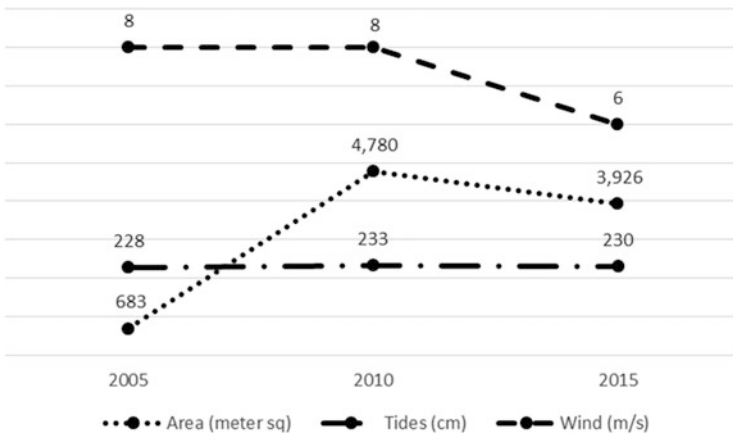


Fig. 4 Mangrove response on relative sea level and wind intensity for Northeast Monsoon in Chendering

8.2 Analyses of the Relationship Determination Between Mangrove Area with Tidal Regime, Wind Intensity and Relative Sea Level

The next stage was to see the response of mangrove on relative sea level and wind intensity for both study areas. Figure 4 shows the response of mangrove on relative sea level and wind for Chendering. Even though two monsoons highlighted in this study were Northeast Monsoon and Southwest Monsoon, the result that is important to be discussed is the monsoon that is related to the study area. Therefore, Chendering focuses on the Northeast Monsoon, while Kuala Perlis focuses on the Southwest Monsoon. From the result, the mangrove area was recorded at 683 m² in

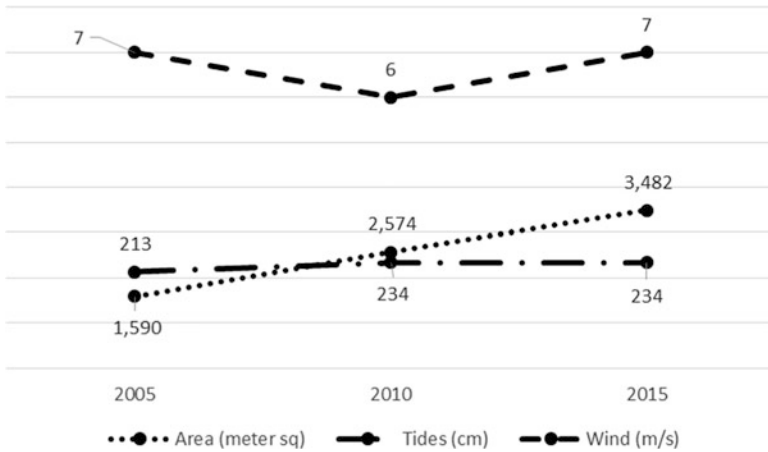


Fig. 5 Mangrove response on relative sea level and wind intensity for Southwest Monsoon in Kuala Perlis

2005 with the velocity of wind intensity at 8 m/s and the relative sea level value at 228 cm. In 2010, the mangrove area increased to 4780 m² with the same wind intensity at 8 m/s and the relative sea level value at 233 cm, while in 2015, mangrove area decreased to 3926 m² with wind intensity at 6 m/s and relative sea level value at 230 cm.

The response of mangrove on relative sea level and wind intensity for Southwest Monsoon in Kuala Perlis is shown in Fig. 5. The result indicates that the value of mangrove area at 1590 m² in 2005 with the velocity of wind intensity at 7 m/s and the relative sea level value at 213 cm. In 2010, the mangrove area increased to 2574 m² with velocity of wind intensity at 6 m/s and the relative sea level value at 234 cm, while in 2015, the value of mangrove area increased to 3482 m² with wind intensity at 7 m/s and relative sea level value at 234 cm.

The result in Figs. 4 and 5 explained the relationships between mangrove areas with all three environmental parameters. From this result, it shows that the mangrove area along with the parameters plays their own role very well. The gradual process and movement from the environmental parameters do give an impact to the mangrove area. Even though the value of wind intensity and relative sea level might be small and too obvious, the consistency activities that they bring on everyday routine prove that it did gave impact to the mangrove ecosystem.

8.3 Correlation Analysis

Correlation analysis is essentially used to test the relationships between quantitative or category variables. Pearson’s correlation coefficient (*r*) was used to indicate the occurrence of significant linear relationship between two variables to the other (Mohamad Hamzah et al. 2020). In this study, a correlation analysis was done for

Table 1 Correlations between mangrove area, relative sea level rise and wind intensity in Chendering

Environmental parameter	<i>r</i>
Relative sea level rise	0.95
Wind intensity	-0.32
Tidal regime	0

Table 2 Correlations between mangrove area, relative sea level rise and wind intensity in Kuala Perlis

Environmental parameter	<i>r</i>
Relative sea level rise	0.88
Wind intensity	-0.02
Tidal regime	0

mangrove area with relative sea level, mangrove area with wind intensity and mangrove area with tidal regime to see the relationship between these three variables towards mangrove area.

The results in Tables 1 and 2 show positive relationships exist between mangrove area and relative sea level. It explains the significance of relative sea level in determining the total mangrove area through time. For wind intensity, it shows that negative relationships exist with the mangrove area. It explains that the insignificant of wind intensity in determining the total mangrove area through time. However, there is no relationship between mangrove area and tidal regime ($r = 0$).

The correlation analysis for relative sea level shows a positive relationship, and it proves significant towards the mangrove areas in both study areas. It also has been stated by previous studies that relative sea level plays a huge role in influencing the mangrove area (Mcivor et al. 2013; Mallinson et al. 2014; Soares 2009; Gilman et al. 2007). The wind intensity parameter shows a negative relationship and it is uniform both study areas. Even though wind area is famously known for bringing an impact, however, for mangrove area in this study, it explained that wind intensity does not give impact towards the changes of mangrove area. It can happen due to the value of wind data that this study collected which is quite consistent. Meanwhile, the tidal regime or known as diurnal and semidiurnal has constant value for each of them. The correlation analyses are unable to produce a specific result. Therefore, it can be concluded that the relationship between the mangrove areas and the tidal regime is constant.

8.4 Vulnerable Map Establishment

A map is known as a diagrammatic representation of an area of land or sea showing physical features, cities, roads and other important details. There are several maps that can be created based on the purpose of the study. By using maps, details of things or information can be portrayed visually and seen. Map basically can make

any layman understand the information a little further. It indicates the changes of the mangrove area and at the same time shows the distribution of each class in the map. The mangrove vulnerable maps were used as guidelines to explore further possibilities that resulted in changes to the mangrove area.

8.4.1 Chendering

The vulnerable maps in Fig. 6 show the distribution of mangroves in Chendering in 2005, 2010 and 2015, respectively. The area for mangroves in Chendering has increased from 683 m² in 2005 to 4780 m² in 2010 and increased again to 3926 m² in 2015 with a total increment of 3243 m². The maps show that the distribution of mangrove along the coastline has increased in 2010 and 2015. The increased distribution can be found along the coastline.

8.4.2 Kuala Perlis

The vulnerable map in Fig. 7 shows the distribution of mangroves in Kuala Perlis in 2005, 2010 and 2015, respectively. The area for mangrove in Kuala Perlis has increased from 1590 m² at 2005 to 2574 in 2010 and increased more to 3482 m² in 2015 with the total increment of 1892 m² in 2005. Not only focused on the coastline, the increase in mangrove areas are scattered and concentrated in the coastline and landward area.

9 Perspectives and Conclusion

The application of remote sensing helps in determining the changes in mangrove areas in Chendering and Kuala Perlis. However, site verification is important to confirm the study area condition in order to gain more accurate findings. In addition,

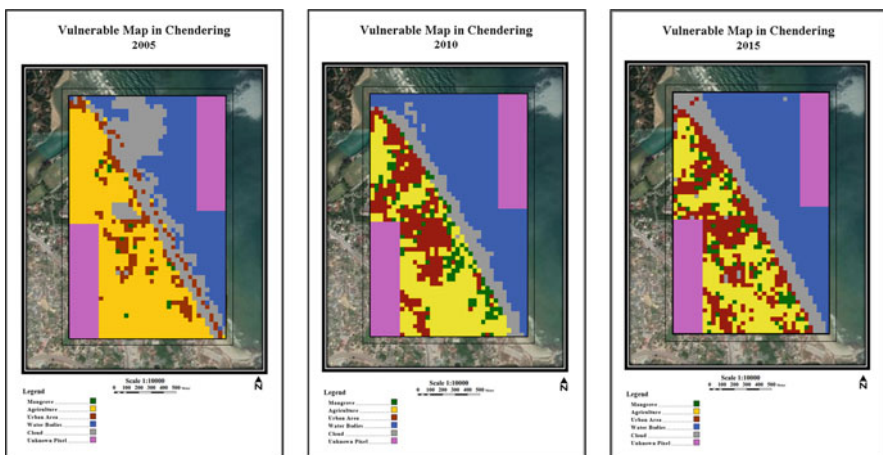


Fig. 6 Vulnerable map in Chendering for years 2005, 2010 and 2015

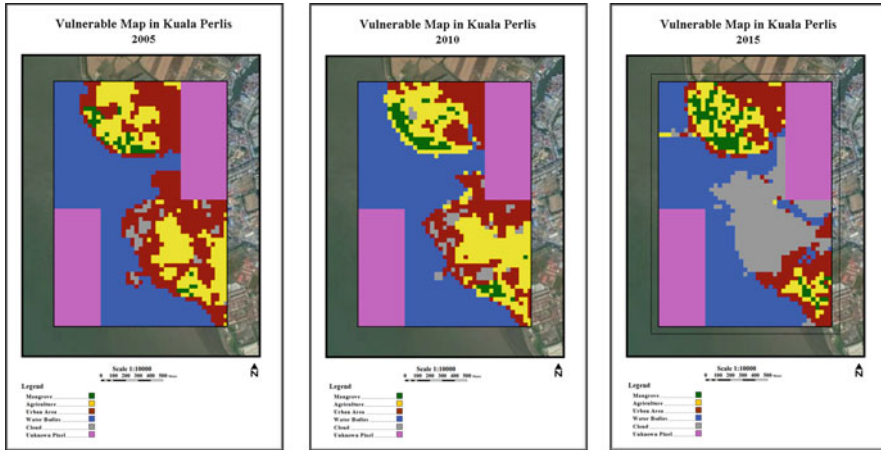


Fig. 7 Vulnerable map in Kuala Perlis for years 2005, 2010 and 2015

the ground truthing data on both study areas will help this study to become more reliable. The results show that the variables studied contributed a part in mangrove areas changes. This may suggest that other environmental parameters that exist surrounding mangrove areas may have impacts towards the changes in the mangrove area.

Acknowledgements Special thanks dedicated to Department of Survey and Mapping Malaysia (JUPEM), Malaysian Meteorological Department (MMD), Forestry Department Peninsular Malaysia (FDPM), and Forest Research Institute Malaysia (FRIM) for providing research data and guidance during the pre-consultation. Thank you to Research Management Centre (RMC-UiTM) for providing research grants and Ministry of High Education Centre (MOHE) for the scholarship. Last but not least to Automation and Robotics Research Group (AUROB), Universiti Teknologi MARA (UiTM) Perlis and Universiti Teknologi Malaysia (UTM) for the collaboration, guidance and support along this study.

References

- Adams JB, Rajkaran A (2020) Changes in mangroves at their southernmost African distribution limit. *Estuar Coast Shelf Sci* 247:106862
- Ahmadun FR, Wong MMR, Mat SA (2020) Consequences of the 2004 Indian Ocean Tsunami in Malaysia. *Saf Sci*
- Asbridge E, Lucas R, Ticehurst C, Bunting P (2016) Mangrove response to environmental change in Australia's Gulf of Carpentaria. *Ecol Evol* 6(11):3523–3539
- Ávila-Flores G, Juárez-Mancilla J, Hinojosa-Arango G, Cruz-Chávez P, López-Vivas JM, Arizpe-Covarrubias O (2020) A practical index to estimate mangrove conservation status: the forests from La Paz Bay, Mexico as a case study. *Sustainability* 12(3):858
- França MC, Cohen MCL, Pessenda LCR, Rossetti DF, Lorente FL, Álvaro A, Macario K (2013) Catena mangrove vegetation changes on Holocene terraces of the Doce River, Southeastern Brazil. *Catena* 110:59–69

- Gelfenbaum G, Stevens AA, Elias E, Warrick J (2009) Modeling sediment transport and delta morphology on the dammed Elwha River, Washington State, USA. *Coastal Dynamics*, (109), Paper 109
- Ghebregabher MG, Yang T, Yang X, Wang X (2016) Extracting and analyzing forest and woodland cover change in Eritrea based on landsat data using supervised classification. *Egypt J Remote Sens Space Sci* 19(1):37–47
- Ghosh MK, Kumar L, Roy C (2017) Climate variability and mangrove cover dynamics at species level in the Sundarbans, Bangladesh. *Sustainability* 9(5):805
- Gilman E, Ellison J, Coleman R (2007) Assessment of mangrove response to projected relative sea-level rise and recent historical reconstruction of shoreline position. *Environ Monit Assess* 124(1–3):105–130
- Goh HC (2016) Assessing Mangrove conservation efforts in Iskandar, Malaysia. *Malaysia Sustainable Cities Program, Working Paper Series*. pp 1–33
- Gregory JM, Griffies SM, Hughes CW, Lowe JA, Church JA, Fukimori I, Van de Wal RSW (2019) Concepts and terminology for sea level: mean, variability and change, both local and global. *Surv Geophys* 40
- Hamzah ML, Amir AA, Maulud KNA, Sharma S, Mohd FA, Selamat SN, Begum RA (2020) Assessment of the mangrove forest changes along the Pahang coast using remote sensing and GIS technology. *J Sustain Sci Manag* 15(5):43–58
- Hanum F, Latiff A, Hakeem KR, Ozturk M (2016) *Mangrove ecosystems of Asia*. Springer
- Hashim R, Kamali B, Tamin NM, Zakaria R (2009) An integrated approach to coastal rehabilitation: mangrove restoration in Sungai Haji Dorani, Malaysia. *Estuar Coast Shelf Sci* 86:118–124
- Hensel P, Proffitt EC, Delgado P, Shigenaka G, Yender R, Hoff R, Mearns AJ (2014) Oil spills in mangroves: Planning and response considerations, (September), 96
- Ibharim NA, Mustapha MA, Lihan T, Mazlan AG (2015) Ocean and coastal management mapping mangrove changes in the Matang Mangrove Forest using multi temporal satellite imageries. *Ocean Coast Manag* 114:64–76
- Jupiter SD, Potts DC, Phinn SR, Duke NC (2007) Natural and anthropogenic changes to mangrove distributions in the Pioneer River Estuary (QLD, Australia). *Wetl Ecol Manag* 15(1):51–62
- Kamali B, Hashim R (2011) Mangrove restoration without planting. *Ecol Eng* 37(2):387–391
- Kamil EA, Takaijudin H, Hashim AM (2020) Distribution of mangroves in Kedah, Malaysia: a remote sensing and ground-truth based assessment. *IOP Conf Ser Earth Environ Sci* 549(1)
- Kong H, Chung G (2019) Forum: use mangrove trees to fight rising waters. *The Straits Times*
- Kuenzer C, Bluemel A, Gebhardt S, Quoc TV, Dech S (2011) Remote sensing of mangrove ecosystems: a review. *Remote Sens* 3:878–928
- Lewis RR (2005) Ecological engineering for successful management and restoration of mangrove forests. *Ecol Eng* 24:403–418
- Lewis A, Estefen S, Huckerby J, Musial W, Pontes T, Torres-Martinez J (2011) IPCC ocean energy, pp 497–534
- Liao Y, Liao Y, Zhao W, Chen Q, Li T, Yang T (2020) Study on mangrove of maximum likelihood: reclassification method in Xiezhou Bay. *J Coast Res* 102(sp1):334–343
- Mallinson DJ, Culver SJ, Corbett DR, Parham PR, Shazili NAM, Yaacob R (2014) Holocene coastal response to monsoons and relative sea-level changes in northeast Peninsular Malaysia. *J Asian Earth Sci* 91:194–205
- Mcivor A, Spencer T, Möller I, Spalding MD (2013) The response of mangrove soil surface elevation to sea level rise natural coastal protection series: Report 3. *Natural Coastal Protection Series* ISSN, 2050–7941
- Nascimento WR, Souza-Filho PWM, Proisy C, Lucas RM, Rosenqvist A (2013) Mapping changes in the largest continuous Amazonian mangrove belt using object-based classification of multisensor satellite imagery. *Estuar Coast Shelf Sci* 117:83–93
- Nguyen HH, McAlpine C, Pullar D, Johansen K, Duke NC (2013) The relationship of spatial-temporal changes in fringe mangrove extent and adjacent land-use: case study of Kien Giang coast, Vietnam. *Ocean Coast Manag* 76:12–22

- Nguyen A, Le BVQ, Richter O (2020) The role of mangroves in the retention of heavy metal (Chromium): a simulation study in the Thi Vai river catchment, Vietnam. *Int J Environ Res Public Health* 17(16):1–22
- Omar H, Hamzah KA (2012) Aboveground biomass and carbon stock forest of Peninsular Malaysia using L-Band forest in Malaysia
- Purnamasayangasukasih P, Norizah K, Ismail AAM, Shamsudin I (2016) A review of uses of satellite imagery in monitoring mangrove forests. *IOP Conf Ser Earth Environ Sci* 37(1):012034
- Sanil Kumar V, Ashok Kumar K (2010) Waves and currents in tide dominated location off Dahej, gulf of Khambhat, India. *Marine Geodesy* 33(2):218–231
- Sari SP, Rosalina D (2016) Mapping and monitoring of mangrove density changes on tin mining area. *Procedia Environ Sci* 33:436–442
- Soares MLG (2009) A Conceptual model for the responses of mangrove forests to sea level rise. *J Coast Res* 2009(56):267–271
- Spring S (2000) Tide and current glossary national oceanic and atmospheric administration national ocean service center for operational oceanographic products and services, (January)
- Sremongkontip S, Hussin YA, Groenindijk L (2000) Detecting changes in the mangrove forests of southern Thailand using remotely sensed data and GIS. *Int Arch Photogramm Remote Sens* 33(1):567–574
- Sulong I, Mohd-Lokman H, Mohd-Tarmizi K, Ismail A (2002) Mangrove mapping using Landsat imagery and aerial photographs: Kemaman District, Terengganu, Malaysia. *Environ Dev Sustain* 4(2):135–152
- Thu PM, Populus J (2007) Status and changes of mangrove forest in Mekong Delta: case study in Tra Vinh, Vietnam. *Estuar Coast Shelf Sci* 71(1–2):98–109
- Uni K, Bürger R, Phua M (2016) Monitoring deforestation in Malaysia between 1985 and 2013: insight from South-Western Sabah and its protected peat swamp area. *Land Use Policy* 57:418–430
- Upanoi T, Tripathi NK (2012) A Satellite based monitoring of changes in mangroves in Krabi, Thailand (December), 2–6
- Upanoi T, Tripathi NK, Luang K, Marine P (2003) Map Asia 2003 natural resource management a satellite based monitoring of changes in mangroves in map Asia 2003 natural resource management
- Van Der Stocken T, De Ryck DJR, Balke T, Bouma TJ, Dahdouh-Guebas F, Koedam N (2013) The role of wind in hydrochorous mangrove propagule dispersal. *Biogeosciences* 10(6):3635–3647



Spatiotemporal Distribution of Mangrove at Kuala Sepetang Forest Reserve, Malaysia, Using Remotely Sensed Data

Zulkiflee Abd Latif, Nuraisah Anuar, Nurul Ain Mohd Zaki, Hamdan Omar, Mohd Nazip Suratman, and Biswajeet Pradhan

Abstract

Mangrove plays an important role in mitigating the impact of climate change by sequestering CO₂ as the main greenhouse gas emission. They maintain water quality and clarity, filtering pollutants and trapping sediments originating from

Z. Abd Latif (✉)

Institute for Biodiversity and Sustainable Development, Universiti Teknologi MARA, Shah Alam, Selangor Darul Ehsan, Malaysia

Centre of Studies for Surveying Science and Geomatics, Faculty of Architecture, Planning and Surveying, Universiti Teknologi MARA, Shah Alam, Selangor Darul Ehsan, Malaysia
e-mail: zulki721@uitm.edu.my

N. Anuar

Centre of Studies for Surveying Science and Geomatics, Faculty of Architecture, Planning and Surveying, Universiti Teknologi MARA, Shah Alam, Selangor Darul Ehsan, Malaysia

N. A. Mohd Zaki

Institute for Biodiversity and Sustainable Development, Universiti Teknologi MARA, Shah Alam, Selangor Darul Ehsan, Malaysia

Centre of Studies for Surveying Science and Geomatics, Faculty of Architecture, Planning and Surveying, Universiti Teknologi MARA, Perlis Branch, Arau, Perlis, Malaysia

H. Omar

Geoinformation Programme, Division of Forestry and Environment, Forest Research Institute Malaysia (FRIM), Kepong, Selangor, Malaysia

M. N. Suratman

Faculty of Applied Sciences and Institute for Biodiversity and Sustainable Development, Universiti Teknologi MARA (UiTM), Shah Alam, Malaysia
e-mail: nazip@uitm.edu.my

B. Pradhan

Centre for Advanced Modelling and Geospatial Information Systems (CAMGIS), School of Civil and Environmental Engineering, University of Technology Sydney, Ultimo, NSW, Australia

land. However, mangroves have been reported to be threatened by land conversion for other activities. The objectives of this chapter were: (1) to derive Normalized Difference Vegetation Index (NDVI) in the study area and (2) to map the status of the mangrove species distribution from year 2004 to 2019. Matang Mangrove Forest Reserves (MMFR) at Kuala Sepetang, Perak, Malaysia were determined using multi-temporal satellite imageries by Landsat TM and Sentinel-2 from year 2004 to 2019. The classification of land use land cover (LULC) was performed using the ISODATA Clustering method and Maximum Likelihood Classifier (MCL) method along with vegetation index differencing technique. The overall classification accuracy was 90% with Kappa statistic accuracy of 0.89. The results indicated changes in area of the mangrove forest to a cleared area occurred at 1340.01–1666.30 ha. (2004–2019). Combinations of these approaches were useful for change detection and an indication of the nature of these changes. The result also revealed that *Rhizophora apiculata* and *Avicennia sonneratia* are still being preserved and estimated to be 70% of the total species. Temporal changes of mangrove species for the 15–period showed that the mangrove species of *R. apiculata* was 58%, *A. sonneratia* was 6%, *Bruguiera parviflora* 8% and other mangrove species 28% in year 2019 as compared to 2004 in which *R. apiculata* was 71%, *A. Sonneratia* 6%, *B. parviflora* 10% and other mangrove species 14%. The findings indicated that the status and loss of mangroves due to direct impacts from surrounding land development activities.

Keywords

Spatiotemporal · Mangrove · LULC · Remote sensing

1 Introduction

Mangroves are trees that grow near the coast and protect the coastal land against the destruction of tsunamis and storms in the tropics, subtropics and temperate coast (Sheridan and Hays 2003). Mangroves are not only play important roles in ensuring stability and sustainability of coastal ecosystems, but also in fulfilling important socio-economic benefits to coastal communities (Suratman 2008). Mangroves are also important to coastal ecosystems for the shoreline stabilization, ecosystem biology coastal, water quality maintenance, habitat for various aquatic, bird immigrants, recreation, tourism, fishing activities, a supply of forest products and provides the carbon (C) storage in biomass and soil. According to the National Oceanic and Atmospheric Administration (NOAA), mangroves can sequester carbon at the rate of two to four times greater than mature tropical forests. In addition, the soil of mangrove forests stores a significant amount of carbon compared with other types of forest given its high sediment concentration (Zhu et al. 2015). Thus, there is a need to quantify the carbon (C) storage in different components of this ecosystem. According to Azahar et al. (2003), the total area of mangrove forests was

approximately 2% (645,852 ha) of the total land area in Malaysia in 1994. The distribution of mangroves area in Malaysia from year 1990 to 2017 are mainly at the west coast of Peninsular Malaysia (17%), east coast of Sabah (61%) and Sarawak coastlines (22%) (Hamdan et al. 2018). The factors that mainly contributed to the changes the biomass was direct conversion to other land uses in the form of aquaculture, developments of infrastructure, industry, and settlements. Besides, factors such as coastal erosion and pollution also affect the mangroves. To control mangrove, the proper and timely diagnosis will facilitate appropriate treatments to maintain a healthy forest of replanted mangrove trees (Ong et al. 2018). They are about over 30 species of mangroves in Malaysia, but the major species are *Rhizophora apiculata* (Bakau minyak), *R. mucronata* (Bakau kurap), and *Bruguiera parviflora* (Lenggadai) (Hamdan et al. 2013).

Several remote sensing methods have been developed for tree species identification such as using multispectral satellite images, hyperspectral images and airborne LiDAR (Abd Latif et al. 2012; Mohd Zaki and Abd Latif 2017). In this chapter, the Landsat TM and Sentinel-2 data were used in mapping the spatial patterns of mangroves with different wavelengths to distinguish biomass estimation and carbon stocks. Normalized Differential Vegetation Index (NDVI) is the most commonly used proxy for biomass estimation. According to (Aziz 2014), NDVI is a valuable tool to quantify vegetation biomass (Mohd Zaki et al. 2020). However, the use of NDVI sometimes underestimate the biomass of some woody mangroves because it represents only canopy properties (Hamdan et al. 2014). The use of remotely sensed images, such as a satellite image, can be cost and time-efficient. Remote sensing techniques and computer science made it possible to analyze mangrove biomass and productivity at present to compare them with global maps obtained with the classical technique (Ibrahim et al. 2015). The assessment of monitoring with satellite sensing based on the monthly, weekly, or daily recording the NDVI in several wavelengths which differ from day to day with the seasonal progress and development urban area. For example, the land use/cover of Pulau Indah, in Selangor, Malaysia was found to have changed dramatically over the year intervals of 1995, 1999, 2005 as detected by Landsat TM satellite driven by an expansion of urban areas and built-up land for West Port and cruise terminal development in the island (Suratman and Ahmad 2012).

2 Materials and Method

2.1 Study Area

The study area was located in the coast of Perak shoreline at Larut Matang, Kuala Sepetang which covers an area of 40,711 ha and along a 52 km stretch of the northern coast of Perak (Fig. 1). Kuala Sepetang consists of two zones namely Kuala Sepetang (North) and Kuala Sepetang (South). The study was carried out in North and South Kuala Sepetang. Kuala Sepetang consist of forest reserves namely Pulau Gula, Cabai Malai, Pulau Kelumpang, Sungai Baharu, Sungai Sepetang, Pulau



Fig. 1 Kuala Sepetang Mangrove Forest in study area (OpenStreetMap 2016)

Kecil, Pulau Selinsing, Jebong, Jebong (Tambahan), Pulau Sangga Besar, Pulau Sangga Kecil, and Telok Kertang a part of Sungai Limau.

Firstly, the validation of data from Google Earth and Forest Type in MMFR, then the second step from Sentinel-2 in 2019, Sentinel-2 in 2015, Landsat TM in 2009 and Landsat TM in 2004 satellite imagery data which was known as satellite measured data. There are several steps involved for processing the satellite imagery. First, the pre-processing was carried to the satellite image data. This is followed by an extraction of the image to obtain reflectance data. Then, images were classified using an Iterative Self-Organizing Data Analysis Techniques (ISODATA) algorithm. An ISODATA algorithm requires the user to choose the initial estimates of class means, and then each pixel was assigned to classes with a similar mean. The unsupervised and supervised classification methods were used to differentiate the land cover classes and reference map was used to determine the classification accuracy. Lastly, the maps of the mangroves area were developed. The summary of methodology work flow is shown in Fig. 2.

2.2 Data Processing

Satellite images of Sentinel-2 (2015 and 2019), Landsat TM (2004 and 2009) were downloaded from the USGS website. Forest type maps in MMFR at Kuala Sepetang, Perak were obtained for validation of the classification data. False color composite image of Kuala Sepetang Mangrove Forest was generated with the band combination of 1, 4, 7 and 2, 3, 8 for Landsat TM and Sentinel-2 images, respectively.

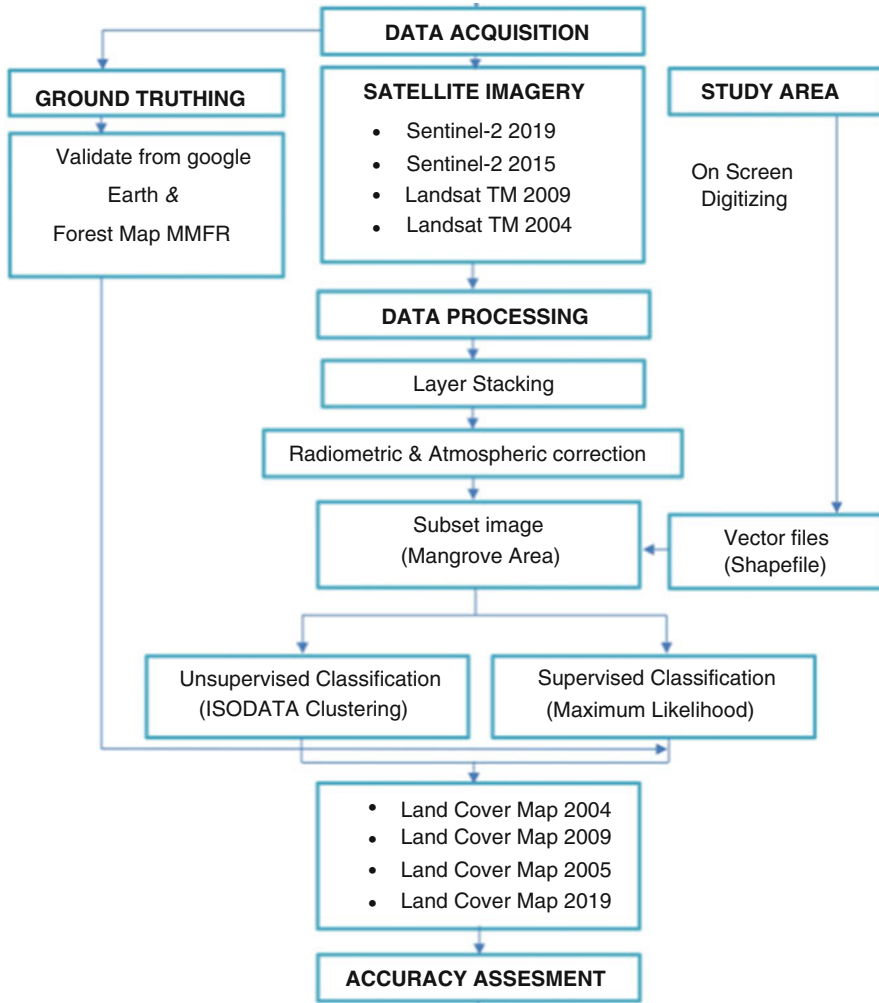


Fig. 2 Flowchart of the general methodology

2.3 Calibration and Validation Data

In order to analyze the spectral characteristics of typical land cover types in the study area and assess the accuracy for mangrove forest classification, calibration (or training) and validation (or reference) pixels for all land cover categories were collected from the Landsat TM and Sentinel-2 images by validating data with visual interpretation of Google Earth. Calibration pixels were selected using a visual interpretation, prior knowledge of the study area and from the MMFR map.

2.4 Land Use Land Cover Classification

ISODATA clustering and Maximum Likelihood were used to evaluate the performance of the decision-tree (DT) algorithm for mapping mangrove forests. Unsupervised (ISODATA) and supervised classifications (Maximum Likelihood) were made after radiometric corrections were performed. Unsupervised classification is the process which is computer determines the spectrally separable class and then defines their information value. For supervised classification, analysts identify the information classes of interest in the image. The result of this classification was five classes with different pixel values. Then, these five classes were grouped as *R. apiculata*, *Bruguiera* and *Avicennia*, Dryland and Unproductive area. The classification was made with the reference of the Google Earth and map of MMFR.

2.5 Normalized Difference Vegetation Index (NDVI)

The NDVI was derived from the pre-processed satellites data:

$$\text{NDVI} = \frac{\rho_{\text{NIR}} - \rho_{\text{R}}}{\rho_{\text{R}} + \rho_{\text{R}}}$$

where ρ_{R} and ρ_{NIR} are the reflectance values for the red and NIR channels, respectively. Mangrove is a part of vegetation that absorbs solar radiation in different bands.

3 Results and Discussion

Figure 3 shows the NDVI images of the Kuala Sepetang mangrove forest in 2004, 2009, 2015, and 2019. The mangrove high vegetation is indicated in dark green with a high value of NDVI meanwhile low vegetation is indicated in white with low value of NDVI.

Figure 4 shows a graph of the crown density of mangroves area based on the NDVI values in the year 2004 and 2019. The non-vegetation, lower dense, moderate dense, dense and higher dense are increased in 15 years. The area of moderate dense show an increasing area change of 72,341.15 ha compared to dense vegetation of 48,866.69 ha. Hence, this situation can conclude that the NDVI of mangrove areas is increasing at a very high rate in Kuala Sepetang.

The mangrove area in the year 2004–2019 tend to be reduced, however the cleared area tends to increase from 1340.01 to 1666.30 ha. These findings are in line with the findings of Giri et al. (2011). Changes also occurred along the intertidal zone due to erosion and occurred in between the mangrove forest due to changes in species and tree harvesting rotation system. The overall change of area during the 15-year period indicated the loss mangrove area at 344.07 ha, while the cleared area is increase at 326.29 ha. Therefore, mangrove forest has lost 34.41 per year ha during

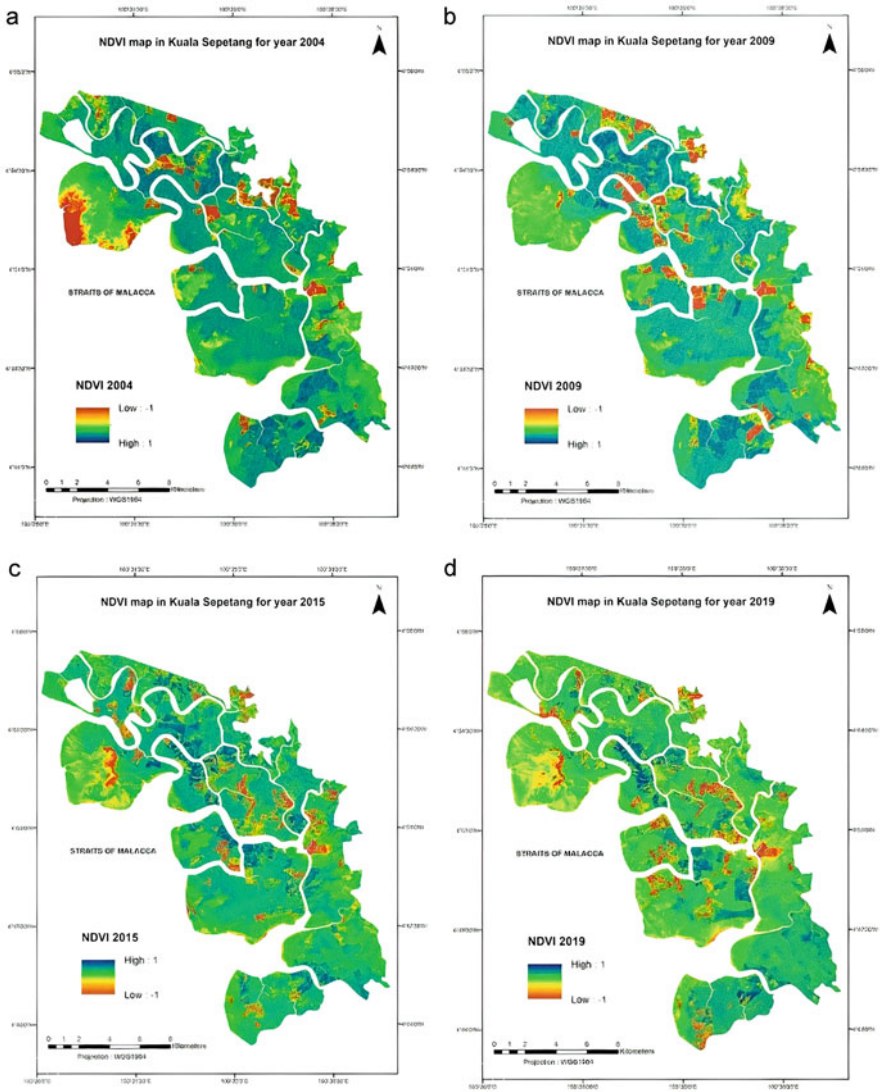


Fig. 3 NDVI map of Kuala Sepetang Mangrove Forest for years (a) 2004, (b) 2009, (c) 2015, and (d) 2019

2004–2019 interval. The cleared area increased 32.63 ha per year ha during 2004–2019.

Distribution of mangrove species from the supervised classification from 2004, 2009, 2015 to 2019 are shown in Fig. 5. Results indicated that five major classes are classified comprising of *R. apiculata*, *Bruguiera-Parviflora*, *Avicennia sonneratia*, Dryland Forest, and Unproductive area.

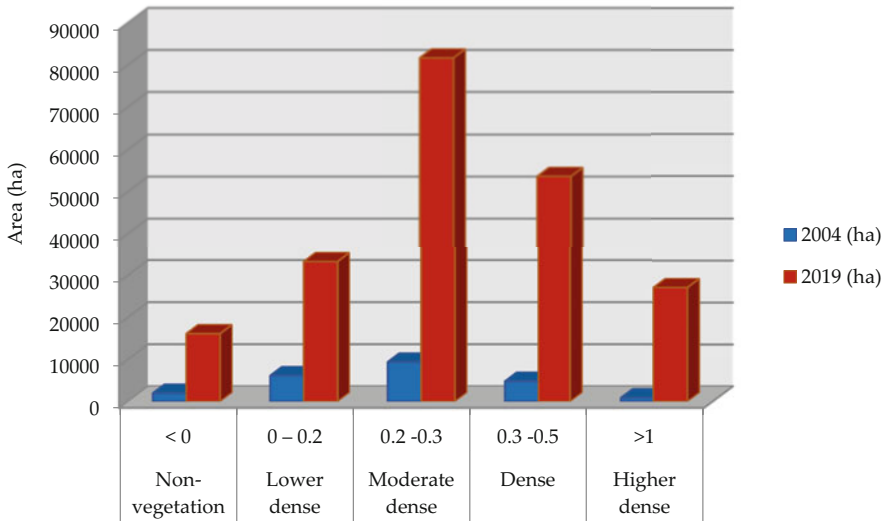


Fig. 4 Crown density based on NDVI value for years 2004 and 2019

Table 1 shows the area of mangroves species from 2004 to 2019. *R. apiculata* is the most dominant species for the years 2004, 2009, 2015 and 2019. *B. parviflora* is the second-highest species which consist of 10% in 2004, 11% in 2009, 7% in 2015, and 8% in 2019, respectively. Both *R. apiculata* and *B. parviflora* area decreased by 58% and 8% within 15 periods of year. It indicates that the total area of these the dominant species has decreased to 23,465.09 ha in 2019 from 23,482.87 ha in 2004. The Dryland forest had an increase of 21% in the year 2019 than 8% in the year 2004. Analysis of the 2004 Landsat TM image estimated the total mangrove area is 23,482.87 ha, in which the areas of *R. apiculata* and *B. parviflora* were 16,767.7 ha and 2252.79 ha respectively. Unproductive area covered area of 1340.01 ha, Dryland Forest 1771.74 ha, and *Avicennia-Sonneratia* 1350.63 ha. For the analysis of the 2009 Landsat TM image, it is estimated that the total mangrove area is 24,102.26 ha, in which the areas of *R. apiculata* was 15,727.4 ha, *B. parviflora* was 2568.06 ha, Unproductive area was 1215.72 ha, Dryland Forest was 2337.12 ha and *Avicennia-Sonneratia* was 2253.96 ha. Meanwhile, analysis of the 2015 Sentinel-2 image indicated the mangrove area at 23,465.25 ha, with the highest proportion recorded by *R. apiculata* at 15,730.5 ha, followed by *B. parviflora*, Unproductive area, Dryland Forest, and *Avicennia-Sonneratia* at 1582.85 ha, 2002.79 ha, 2327.55 ha and 1821.56 ha respectively. As for 2019s Sentinel-2, *R. apiculata* showed the value at 13,706.7 ha, followed by *B. parviflora*, Unproductive area, Dryland Forest, and *Avicennia-Sonneratia* at 1800.13 ha, 1666.3 ha, 4933.04 ha, and 1358.92 ha respectively. Changes in the mangrove species forest types from 2004 to 2019 are indicated in Table 1. Based on the table, 13% of loss in mangrove area is from *Rhizophora* species during the 2004–2019 study period. *Rhizophora* forest area decreased by 4% from 2004 to 2009, and was constantly decreasing in 2019. Generally, from 2004 to

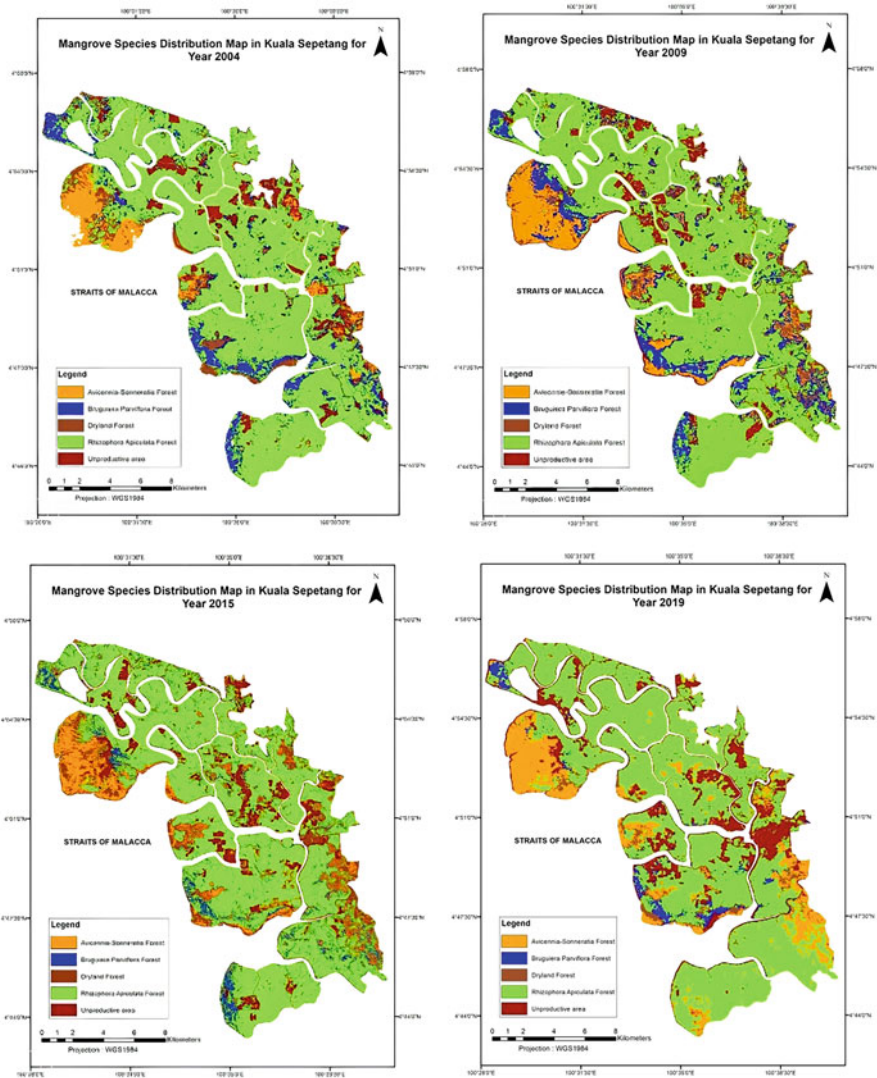


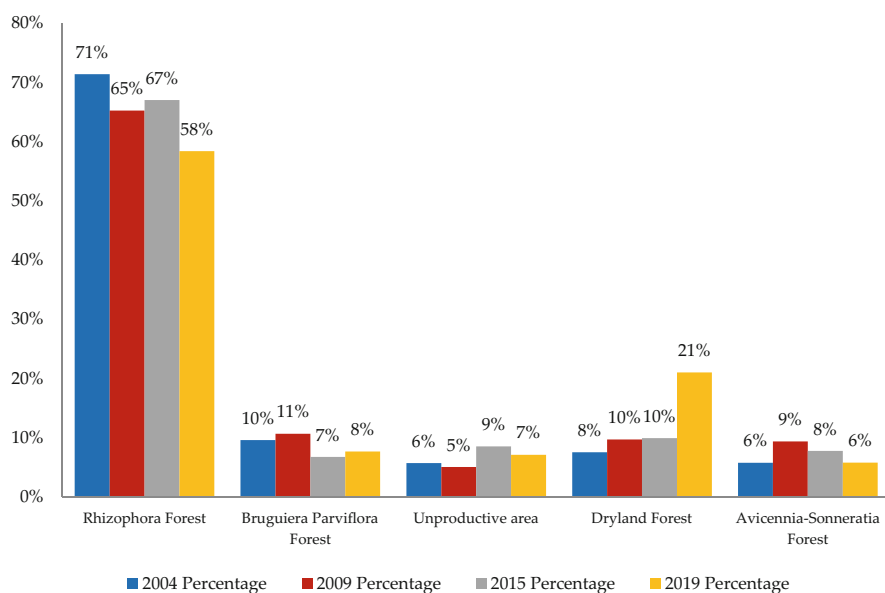
Fig. 5 Mangrove types distribution for years 2004, 2009, 2015, and 2019

2019, *Rhizophora, B. parviflora* had a loss of mangrove species at 3061 and 452.66 ha, while the Unproductive area, Dryland forest, and *Avicennia-Sonneratia* area increased at approximately 326.29, 316.13, and 8.29 ha.

Figure 6 shows the percentage area changes of different land use category. The spatial distribution of mangrove species classification at Kuala Sepetang indicated that *Rhizophora* species dominated the study area image. In Kuala Sepetang, *Rhizophora* forest is a major forest type that comprises about 71% of the total forested area in the year 2019. *Avicennia-Sonneratia* recorded the lowest value at

Table 1 Area of mangrove land use and percentage changes

Land use category	2004–2009		2009–2015		2015–2019		2004–2019	
	Area change		Area change		Area change		Area change	
	(ha)	%	(ha)	%	(ha)	%	(ha)	%
Rhizophora forest	— 1040.30	— 4	3.10	0	— 2023.80	— 9	— 3061.00	— 13
Bruguiera-Parviflora forest	315.27	1	— 985.21	— 4	217.28	1	— 452.66	— -2
Unproductive area	— 124.29	— 1	787.07	3	— 336.490	— 1	326.29	1
Dryland forest	565.38	2	-9.57	0	2605.49	11	316.13	1
Avicennia-Sonneratia forest	906.33	4	— 432.40	2	— 462.64	— 2	8.29	0

**Fig. 6** Percentage of species distribution

6% in the year 2004, 9% in the year 2009, 8% in the year 2015, and 6% in the year 2019.

Referring to Table 1, the area of mangrove changes that have occurred in Rhizophora forest loss at 13% over the study period from 2004 to 2019. Rhizophora forest area decreased by 4% from 2004 to 2009 and constantly decreasing to 2019. Generally, from 2004 to 2019, Rhizophora, Bruguiera-Parviflora had a loss of mangrove species at 3061 and 452.66 ha, while the Unproductive area, Dryland forest, and Avicennia-Sonneratia area increased approximately 326.29, 316.13, and 8.29 ha.

For the accuracy assessment in this study, simple random sampling was adopted. A total of 37, 45, 38, and 41 random pixels were extracted from the classified images of 2004, 2009, 2015, and 2019. The overall accuracies for 2004, 2009, 2015, and 2019 were 95%, 92%, 94%, and 94% respectively. Kappa statistics were 90%, 86%, 89%, and 90%. Kappa statistic was implemented to evaluate the accuracy of change detection and classification maps by measuring the agreement between the two images. User's and producer's accuracies of the individual class were relatively high, ranging from 34% to 100% which indicated a good agreement between the reference data and thematic maps generated from the images.

4 Conclusion

Understanding of spatial distribution of Kuala Sepetang Mangrove Forest helps to determine the location of deforestation, transitional forest, and erosion for the next future mangrove forest management. Hence, remote sensing application is a reliable method to monitor deforestation by comparing the temporal data by daily, monthly, yearly for large mangrove forest areas. In this study, mapping of mangrove area can contribute to the effectiveness of the area management as a whole since the conventional method of ground inventory for the mapping area is tremendously difficult, time-consuming and costly. Continuous monitoring of mangrove status using moderate resolution remote sensing imageries is essential for the large mangrove area for protection and restrictive productive forest. Hence, remote sensing is the best technique to estimate the changes of mangrove distribution. In conclusion, the present information on the status and changes of mangrove forest area will be useful for further studies and to monitor the mangrove ecosystem. It will help to formulate the strategic plans and afforestation of mangroves in the study area.

Acknowledgments The authors would like to thank Malaysia Space Agency (MySA) for providing the Landsat images and Sentinel-1 used in this study and Universiti Teknologi MARA (UiTM), Malaysia for the facilities in implementing this research. This research was funded by the UiTM Internal Grant (600-IRMI/PERDANA 5/3 BESTARI (079/2018)).

References

- Abd Latif Z, Zamri I, Omar H (2012) Determination of tree species using Worldview-2 data. In: Proceedings—2012 IEEE 8th international colloquium on signal processing and its applications, CSPA 2012, (March), pp 383–387
- Azahar M, Nik M, Shah NM (2003) A working plan for the Matang Mangrove Forest Reserve, Perak: the third 10-year period (2000–2009) of the second rotation. State Forestry Department of Perak, Ipoh
- Aziz AA (2014) Integrating a REDD+ project into the management of a production mangrove forest in Matang Forest Reserve, Malaysia. p 242
- Giri C, Ochieng E, Tiezan LL, Zhu Z, Singh A, Masek J, Duke N (2011) Status and Distribution of Mangrove forests of the world using earth observation satellite data. *Glob Ecol Biogeogr* 20: 154–159




- Hamdan O, Khairunnisa M, Ammar A et al (2013) Mangrove carbon stock assessment by optical satellite imagery. *J Trop For Sci* 25:554–565
- Hamdan O, Khali Aziz H, Mohd Hasmadi I (2014) L-band ALOS PALSAR for biomass estimation of Matang Mangroves, Malaysia. *Remote Sens Environ* 155:69–78
- Hamdan O, Mohamad A, Samsudin M et al (2018) Are we losing the mangroves? FRIM in focus. Forest Research Institute Malaysia, Kepong
- Ibrahim NA, Mustapha MA, Lihan T, Mazalan AG (2015) Mapping mangrove changes in the Matang mangrove forest using multi temporal satellite imageries. *Ocean Coast Manag* 114:64–76
- Mohd Zaki NA, Abd Latif Z (2017) Carbon sinks and tropical forest biomass estimation: a review on role of remote sensing in aboveground-biomass modelling. *Geocarto Int* 32(7):701–716
- Mohd Zaki NA, Rajuli MF, Abd Latif Z, Suratman MN, Omar H, Norashikin S, Zainal MZ, Talib N (2020) Analysis of canopy height model (CHM) extraction using quick terrain modeller (QTM) for tropical forest area. *IOP Conf Ser Earth Environ Sci* 540(1):012045
- Ong S et al (2018). Can we control mangrove and casuarina pests? FRIM in focus. MS ISO 9001: 2015 – ISSN 1394-5467
- Sheridan P, Hays C (2003) Are mangroves nursery habitat for transient fishes and decapods? *Wetlands* 23:449–458
- Suratman MN (2008) Carbon sequestration potential of mangroves in Southeast Asia. In: Bravo F, Jandl R, LeMay V, von Gadow K (eds) *Managing forest ecosystems: the challenge of climate change*. Springer, pp 297–315
- Suratman MN, Ahmad S (2012) Multi temporal Landsat TM for monitoring mangrove changes in Pulau Indah, Malaysia. In: *Proceedings IEEE symposium on business, engineering and industrial applications (ISBEIA2012)*. pp 163–168
- Zhu Y, Liu K, Liu L, Wang S, Liu H (2015) Retrieval of mangrove aboveground biomass at the individual species level with WorldView-2 images. *Remote Sens* 7:12192–12214

Part VI

Remote Sensing of Urban Forestry



Determination of the Effect of Urban Forests and Other Green Areas on Surface Temperature in Antalya

Mehmet Cetin , Fatih Adiguzel , and ilknur Zeren Cetin 

Abstract

Climate affects the entire life of humans such as physiological development and characteristics, housing and house structures, food and cloth selections, and distribution on land. It is projected that global climate change would cause important changes in climate parameters in the near future and affect the lives of all organisms on earth directly or indirectly. These changes would cause significant changes in forest area zones. Additionally, global population is rapidly increasing. Naturally, population density is also on the rise. Antalya, with its surface area, witnessed intense population movements to it due to its critical location between the West and East Mediterranean Sea. This situation has changed the city and its land uses drastically. Therefore, urban living conditions have become difficult in Antalya. In the cities, the temperatures are higher than the rural areas due to the rapid population growth and the increase in construction. The forest and other green areas in the city reduce the temperature relatively

M. Cetin (✉)

Faculty of Architecture, Department of City and Regional Planning, Ondokuz Mayıs University, Samsun, Turkey

e-mail: mehmet.cetin@omu.edu.tr

F. Adiguzel

Faculty of Arts and Sciences, Department of Geography, Nevsehir Haci Bektas Veli University, Nevsehir, Turkey

e-mail: fadiguzel@nevsehir.edu.tr

i. Zeren Cetin

Department of Park and Garden Plants, Program of Landscape and Ornamental Plants Cultivation, Samsun Vocational School, Ondokuz Mayıs University, Samsun, Turkey

Department of Forest Engineering, YOK 100/2000 Scholarship, Program of Sustainable Forestry, Institute of Graduate School, Bartın University, Bartın, Turkey

e-mail: ilknur.zerencetin@ogrenci.bartın.edu.tr; ilknur.cetin@omu.edu.tr

compared to the places where there is more construction. As a result of the rapid increase in urbanization in the city of Antalya, urban heat islands are formed at many points. The aim of our study is to determine the effect of urban forests and other green areas on the temperature in the city of Antalya. In this context, land use/cover, NDVI analysis, and surface temperature maps were produced with QGIS and ArcGIS software using Landsat-8 OLI and Sentinel-2 satellite images. Machine learning algorithms were used to detect land use/cover. As a result of the research, it has been determined that the surface temperature is high in places where buildings and asphalt surfaces are high, and an urban cold island is formed in the urban forest and other green areas and the temperature is low. The temperature differences were determined to be between 3 and -10 °C. The economical use of natural resources, the preference of genotypes with lower water needs in agriculture and forestry, the inclusion of foresights regarding the process in forestry studies in the management plans, the reduction of hard ground in urban areas, the increase of plant use, and the widespread use of roof and terrace gardens are used as measures. Climate change should be considered toward a healthy forest management plans and sustainability in forestry areas.

Keywords

Urban forest · Surface temperature · Urban heat island · Antalya · Green spaces

1 Introduction

Throughout the world, urbanization and the urban population show a rapid increase due to various reasons, especially industrialization. As a matter of fact, the rate of urban population in the world is now over 55% (Paul and Meyer 2001; Dye 2008; Gómez-Baggethun and Barton 2013; Dinç and Adıgüzel 2021). The fact that more than half of the world's population has begun to live in urban areas brings along a rapid construction in these areas and various problems can be encountered in these built environments. At the beginning of these problems, there are some negative effects of local or regional warming—which is specific to cities—on the population living in cities. Indeed, the results of the cumulative effects of climatic events on each other can adversely affect human health and the life of living things, especially in the mid-latitude zone and tropical regions (Şimşek and Şengezer 2012; Tzenkova et al. 2007; Cetin et al. 2010, 2018, 2019; Ataei and Hasheminasab 2012; Cetin 2015, 2016, 2020a, b; Monteiro et al. 2016; Deniz and Güngör 2020; Adıguzel et al. 2020, 2021; Kilicoglu et al. 2020, 2021; Gungor et al. 2021). While this is the case, it is noteworthy that in recent years, studies on urban climate have gained weight (Alkan et al. 2017).

Urban climate is defined by the World Meteorological Organization (WMO) and Marsh (1991) as the local climate that differs as a result of the interactions between the built areas and the regional climate (Adıgüzel 2018). Based on this definition, it is understood that urban climate is an important concept used in separating the

climate characteristics of cities from the climate characteristics of rural areas (Santamouris et al. 2015). Urban climate emphasizes the profound changes created by various climatic elements within the highly complex built environment of cities (Taha 1997; Arnfield 1998, 2003; Kanda 2006; Tzenkova et al. 2007; Cetin et al. 2010, 2018, 2019; Ataei and Hasheminasab 2012; Cetin 2015, 2016, 2020a, b; Monteiro et al. 2016; Deniz and Güngör 2020; Adiguzel et al. 2020, 2021; Kilicoglu et al. 2020, 2021; Gungor et al. 2021). Thus, each climate element, together with the components that make up the built environment of the cities, reveals some characteristic features of the urban climate. As a matter of fact, it is seen that “wind speed is lower, wind speed changes, temperature is higher, humidity is less, radiation is prevented, precipitation is less, and clouding is more” in cities compared to rural areas (Finke 1980).

As a result of the intense population growth in the cities, changes have also occurred in the land cover. Natural landscape elements are being pushed further and further away from the city center, leaving their place to hard floor coverings, and more industrial, commercial, and transportation services are being developed to serve the growing city (Tzenkova et al. 2007; Cetin et al. 2010, 2018, 2019; Ataei and Hasheminasab 2012; Cetin 2015, 2016, 2020a, b; Monteiro et al. 2016; Deniz and Güngör 2020; Adiguzel et al. 2020, 2021; Kilicoglu et al. 2020, 2021; Gungor et al. 2021). Today, global climate change and environment in the intense industrialization and urbanization phenomenon problems have arisen. In addition to climate change in the global sense, modern cities, which have developed in limited settlement areas as a result of urbanization, are also experiencing microclimatic changes (Tzenkova et al. 2007; Cetin et al. 2010, 2018, 2019; Ataei and Hasheminasab 2012; Cetin 2015, 2016, 2020a, b; Monteiro et al. 2016; Deniz and Güngör 2020; Adiguzel et al. 2020, 2021; Kilicoglu et al. 2020, 2021; Gungor et al. 2021; Zeren Cetin and Sevik 2020; Zeren Cetin et al. 2020).

In cities where the greatest change in climatic factors is experienced on temperatures, the increasing temperatures have become a worrying phenomenon for millions of people living in cities (Oke 1982; Adigüzel 2018). In urban areas, the built environment generates or absorbs more heat. In areas with high building density, the temperature level is higher than in open green areas, forest areas, and rural areas (Schwarz et al. 2012; Topay 2012; Feyisa et al. 2014; Dursun and Yavas 2016; Lehoczky et al. 2017; Cetin et al. 2019). This temperature phenomenon, which causes urban areas to be warmer than the surrounding rural areas and the natural environment, is defined as the urban heat island (Oke 1982). In this respect, heat island is the main product of the manifestation of urban climate and constitutes one of the important environmental problems of the twenty-first century (Rizwan et al. 2008).

Urban open green spaces shape the city by revealing the physical structure of the city. Urban open green spaces are among the most important formations that can minimize the effects of climate change in cities. Because of urban open green spaces, it creates the opportunity for shading and evaporation by reducing the urban heat island effect in cities. It creates a breeze and coolness effect on vegetated surfaces on hot days. It reduces carbon and pollutants that change their composition by filtering

them. Green areas, which create positive effects in cities, decrease horizontally and vertically. This negative situation affects people both psychologically and physiologically. It increases the longing for the natural environments in the city and people move toward rural areas. It creates orientation. The planning of green areas in urban is for decreasing for effecting of climate in urban areas, increasing impermeable surfaces, infrastructure systems and urban planning criteria have started to gain importance (Grassl 1976, 1979, 1981, 1989, 2006, 2011; Tzenkova et al. 2007; Cetin et al. 2010, 2018, 2019; Ataei and Hasheminasab 2012; Cetin 2015, 2016, 2020a, b; Monteiro et al. 2016; Deniz and Güngör 2020; Adiguzel et al. 2020, 2021; Kilicoglu et al. 2020, 2021; Gungor et al. 2021; Zeren Cetin and Sevik 2020; Zeren Cetin et al. 2020).

Humidity is another climatic element that is as effective as temperature in the formation of the urban heat island. In recent years, when the studies on the urban climate are examined, it is seen that the changes in the humidity values as well as the temperature have been drawn attention. As a matter of fact, the intense consumption of fossil fuels and the widespread use of water in cooling towers and pools involve the formation of moisture and therefore heat. In addition, other anthropogenic activities such as irrigation of urban vegetation also provide important moisture sources, especially in greener residential neighborhoods and urban parks (Richards 2005; Grassl 1976, 1979, 1981, 1989, 2006, 2011). The effects of moisture sources on the built environment of cities manifest themselves in the form of differences in evaporation levels. Evaporation is less in the city than in the environment, and this difference is more pronounced in relative humidity. During summer, both relative humidity and vapor pressure values are lower in cities. In winter, the differences due to steam pressure are largely eliminated. This shows that the relative humidity differences vary depending on the temperature (Kratzer 1968; Grassl 1976, 1979, 1981, 1989, 2006, 2011).

In addition to temperature and humidity, winds are one of the climate elements that are very effective on the urban climate. The rougher surface structure in cities and the changes in the radiation balance cause a change in wind speed and direction. Winds have a significant impact on urban heat islands due to their ability to disperse the clustered hot and dense air. In urban areas, human life can be adversely affected in cases where the wind directions and speeds go beyond the required values (Oke 1979). Some of these disadvantages can be avoided with adequate street width and building design. Occasional street guidance can reduce difficulties, especially when certain wind directions and speeds are expected to create adverse conditions (Wilmer 1975).

While climate elements such as temperature, precipitation, and wind are the factors that directly affect the urban climate, the characteristics of the elements that make up the built environment of the cities (such as the color of the surface coatings, roughness, reflection properties) are also determinative in the urban climate. In this case, it becomes clear how much climate elements are related to urban land use. The relations of climate elements and especially temperature with floor coverings in cities affect the quality of life and thermal comfort of people first of all. Therefore, surface temperatures are of great importance in urban climate studies (Voogt and Oke 2003). High temperatures created by floor coverings in urban areas cause

unhealthy comfort areas. This situation affects people negatively in terms of health, happiness, economy, and recreation; thermal stress cannot be controlled outdoors (Patz et al. 2005; Feyisa et al. 2014; Alkan et al. 2017).

In cities, the temperature is observed to be higher than in rural areas and natural landscape areas on the urban fringe. Building materials, roofing, asphalt, concrete, and pavement roads absorb more energy from the sun than other natural surfaces. On one hand, this energy spreads as warmth and the spread continues at night (Oke 1982). However, unlike the objects in question, urban open and green spaces minimize the anthropogenic effect in climate regulation; it contributes to the creation of healthier and more comfortable living spaces by reducing the heat island effect. Tree plantations in the city increase thermal comfort by reducing the negative effect of air temperature (Avissar 1996; Gómez et al. 2008; Topay 2012; Bozdogan and Sogut 2015; Estoque et al. 2017; Atwa et al. 2020; Bozdogan Sert et al. 2021). As a matter of fact, in many academic studies, it clearly reveals that urban forests and other green areas play an important role in reducing heat islands. It has been shown that as the area of green areas and tree communities is expanded, they are more effective in controlling the temperature in the city (Alkan et al. 2017).

Cities have begun to experience changes in microclimatic conditions. As a result of the intense population growth in the cities, changes have also occurred in the land cover. Natural landscape elements are being pushed further and further away from the city center, leaving their place to hard floor coverings in cities, and more industrial, commercial, and transportation services are developed to serve the growing city. When evaluated in this context, the changes that occur in cities due to climate change are stated in the study, and examples are given. Urban open green spaces is planning of the suggestions to be taken for this current problem in the design and planning stages are included.

In this study, the effect of urban forests and other green areas on the temperature in Antalya, which is located in the Antalya part of the Mediterranean Region and is the largest city of this part, was investigated. In the city of Antalya, which has been in a rapid urbanization process for almost half a century as a result of industry and tourism investments and has witnessed an intense construction, an urban heat island has been formed at many points, especially in recent years. This has undoubtedly increased the importance of open and green spaces in the city. The main motivation of this study is to draw attention to the importance in question and to make suggestions in terms of planning by identifying the heat islands in the city. In the study, the importance of urban building designs and green space arrangements in reducing urban warming is emphasized.

2 Materials and Methods

2.1 Study Area

Konyaaltı, Kepez, Muratpaşa, and Döşemealtı districts of Antalya province, located in the west of the Mediterranean Region, were chosen as the study areas. The most important reason for choosing it as a study area is that it is the place where

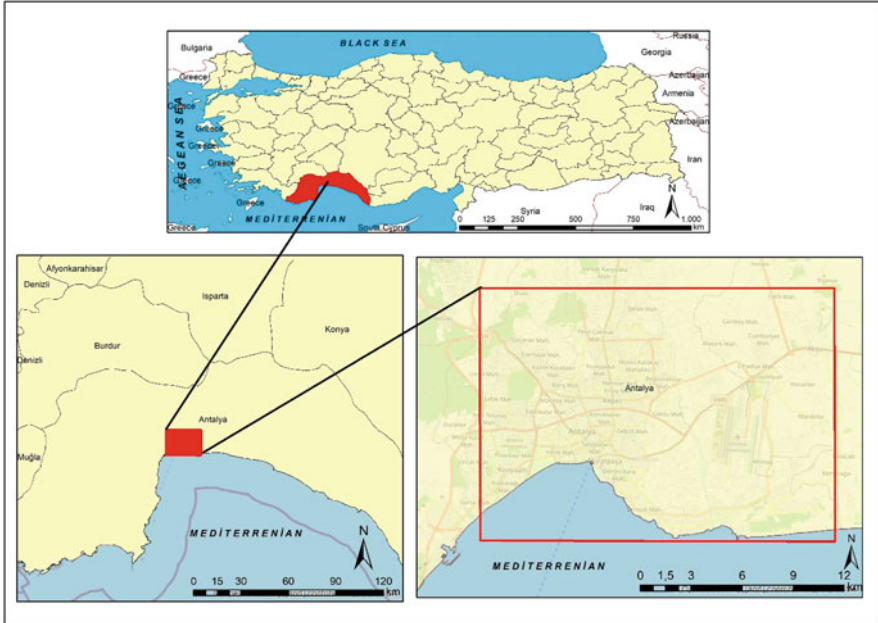


Fig. 1 Location map of the study area

urbanization and population are the highest. The study area is located between $36^{\circ} 15' - 36^{\circ} 45'$ north latitudes and $30^{\circ} 22' - 30^{\circ} 58'$ east longitudes (Fig. 1).

The scrub plants, which are the vegetation of the Mediterranean climate, also constitute the vegetation of Antalya. The climate of Antalya is Mediterranean climate. The summers are hot and dry, and the winters are warm and rainy. The average temperature in summer varies between $30 - 34$ and $9 - 15$ °C in winter. Meteorological events such as snowfall and frost are almost never experienced in the city. Average relative humidity per year is around 64%. It is cloudy and rainy only 40–50 days of the year (Antalya Metropolitan Municipality 2022).

2.2 Method

Within the scope of this study, two types of data were used to determine the land use of Antalya province Konyaaltı, Kepez, Muratpaşa, and Döşemealtı districts between 2021 and to determine the relationship between land use and surface temperature in 2021. First of these, Landsat 8 OLI satellite image data of August 2021 was used as research material. As the second data, NDVI analysis was performed with Sentinel-2 satellite images. Another type of data used in the study is the Landsat 8 OLI image obtained to be used in the calculation of the ground surface temperature (Land Surface Temperature-LST).

Landsat OLI satellite image dated 23.08.2021 was used to calculate the surface temperature of the study area. Sentinel-2 satellite image dated 29.08.2021 was used to calculate the NDVI analysis.

Using formula for calculating of Sentinel-2 NDVI:

$$\text{NDVI} = \text{float} ((b8 - b4) / (b8 + b4))$$

For Landsat OLI surface temperature:

1. TOA (Top of Atmospheric) = $0.0003342 * \text{"band10"} + 0.1$
2. BT (Brightness Temperature) = $(1321.08 / \text{Ln}((774.89 / \text{"TOA"} + 1)) - 273.15$
3. TM NDVI = $(\text{Band 5} - \text{Band 4}) / (\text{Band 5} + \text{Band 4})$
4. PV = Square $((\text{"NDVI"} - \text{NDVImin}) / (\text{NDVImax} - \text{NDVImin}))$
5. E = $0.004 * \text{"PV"} + 0.9866$ LST = $\text{"BT"} / (1 + (10.8 * \text{"BT"} / 14388) * \text{Ln}(\text{"e"}))$
(Avdan and Jovanovska 2016)

3 Results

The increase in the population living in cities and the rapid urbanization process lead to global climate change. Climate change causes an increase in temperatures, the formation of urban heat islands, and heat stress on people. The issue of climate change and adaptation strategies comes to the fore more frequently, with high rates of deaths as a result of both increasing temperatures and other climate change-related disasters.

In a city like Antalya, where the air temperature and humidity are very high, and urbanization is increasing day by day, especially as a result of touristic activities, it is of great importance to reveal the features that will minimize the effects of climate change. For this reason, in this study, urban forests and other green areas and their impact capacities in the city of Antalya were examined together with urbanization.

In this study, the transformation of dense urban areas into urban heat islands and the effect of urban forests and other green areas in reducing these urban heat islands were examined. Landsat OLI 8, Sentinel-2 satellite images and Urban Atlas land use data were used for this study. Thanks to these data, surface temperature relationships between land use, urban forests/other green areas, and urban areas were determined (Fig. 2). As a result of this relationship, the surface temperature of Antalya, one of the largest cities in Turkey, was determined and the effect of green areas on the surface temperature was determined (Fig. 3).

Since the summer months are the most prominent periods of the urban heat island, the month of August was chosen in this study. When the surface temperature of 23.08.2021 is examined, it is seen that it changed between 20.8 and 46.64 °C. When the map is examined, it is seen that the places where the surface temperature is the lowest in the city are in the urban forests, parks, and other green areas. Urban forests are located in the northwest of the city. The altitude of the north, northwest, and northeast of the city is relatively higher compared to other places, and the rate of

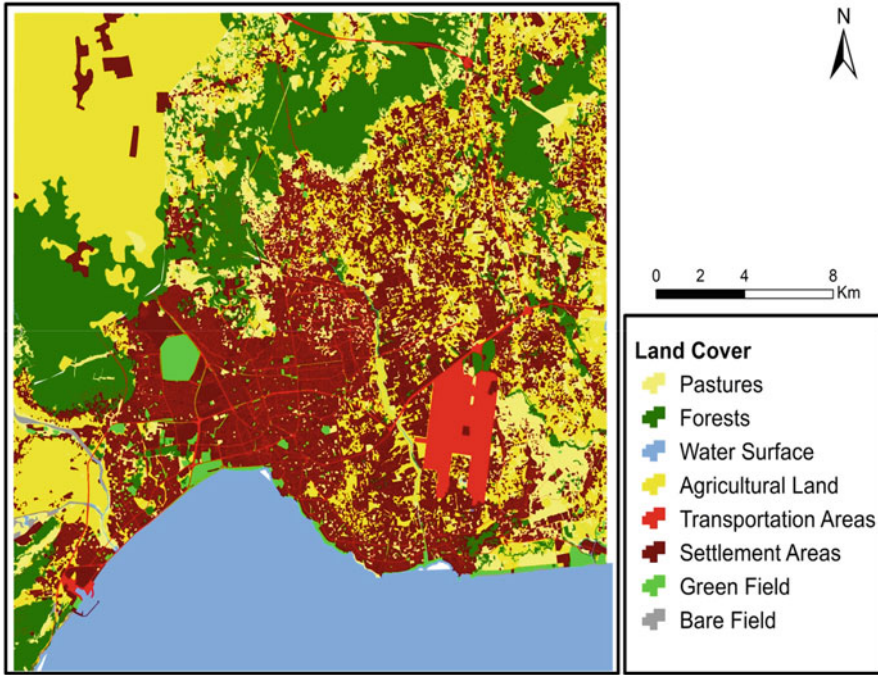


Fig. 2 Land use map of the study area

green space is higher. In addition, considering that the city has gained speed in spreading to the north and west, we can see that agricultural areas have turned into urban areas. Transportation networks have been the determining factor in urban development. The increase in tourism pressure in coastal areas has also increased the need for housing in these areas. Considering the distribution of the existing active and passive green area cover throughout the city, it is convenient to create a green infrastructure as it is connected with forest areas in the north, agricultural areas in the east, forest and agricultural areas in the west, and the Mediterranean coastline in the south. Surface temperatures in these regions are around 20.8–30 °C. In the districts of Teomanpaşa, Konuksever, Şirinyalı, Hurma, and Yenigün, where the urbanization is intense, the temperature values were found to be around 31–40 °C. The areas with the highest surface temperature were measured in the agricultural areas around the city. In these areas, the surface temperature values go up to 47 °C.

Areas devoid of green areas around cities heat up faster and more than urban areas. Since the Landsat satellite image capture of the study area coincides with the morning hours, agricultural lands and empty areas heat up faster than the city, and the surface temperature values are higher. However, in the evening and at night, the surface temperature of urban areas is higher than in agriculture and empty lands.

The normalized difference vegetation index (NDVI) is extremely important in explaining surface temperature and its relationship. NDVI values take values

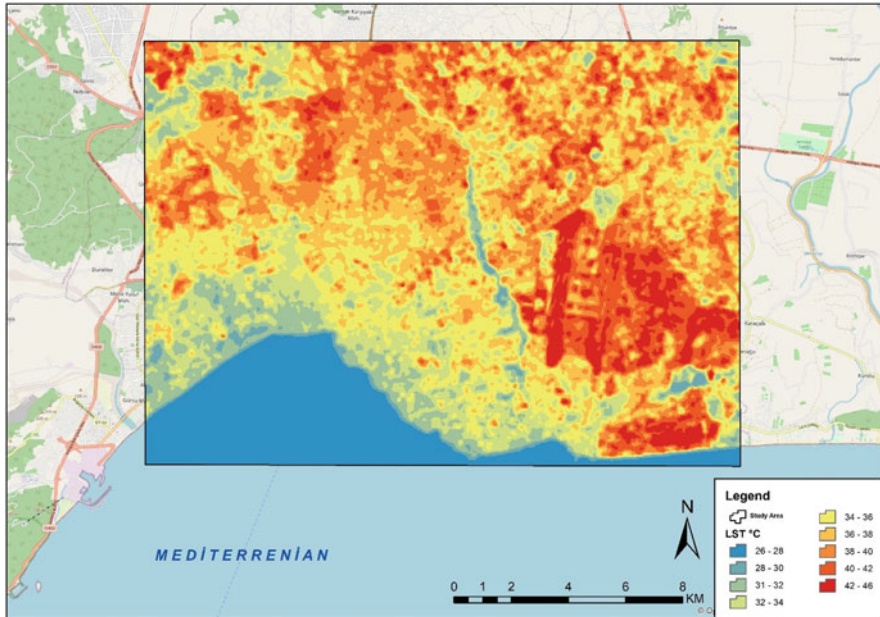


Fig. 3 Surface temperature map of the study area

between $(-1) - (+4)$. If it is covered with very healthy vegetation, it is greater than the NDVI value of $->0.66$. If it has a value between $0.33 - >0.66$, it has a healthy vegetation. If it is between $0 - >0.33$ values, it has a bad vegetation. A value of <0 and below refers to objects such as water, dead plants, buildings, and roads. The values obtained as a result of the NDVI analysis of the Sentinel-2 satellite image of the study area are -0.51 to $+0.78$ (Figs. 4 and 5).

When the NDVI map of the study area dated 29.08.2021 is examined, the forest cover in the north, northwest, and northeast and the NDVI values of the urban forests found in the city are 0.4 and 0.78. This shows the areas where the vegetation is dense and healthy. The NDVI values of the green areas in the dense construction are between 0.35 and 0.60. In addition, it is seen that the surface temperature of the settlements close to this vegetation is relatively lower than the other places (Figs. 4 and 5).

When the surface temperature and NDVI values are evaluated together, it is seen that in the city of Antalya, the surface temperature of urban forests and other green areas has a significant effect on the atmospheric temperature and bioclimatic comfort naturally. It is seen that green areas create an urban cold island in summer temperatures and create refreshing environments for urban residents.

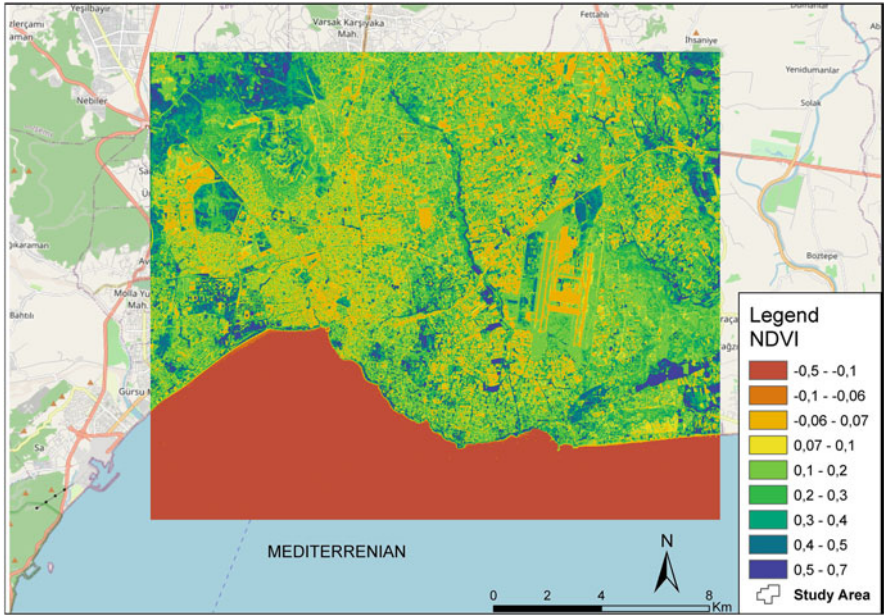


Fig. 4 NDVI map of the study area

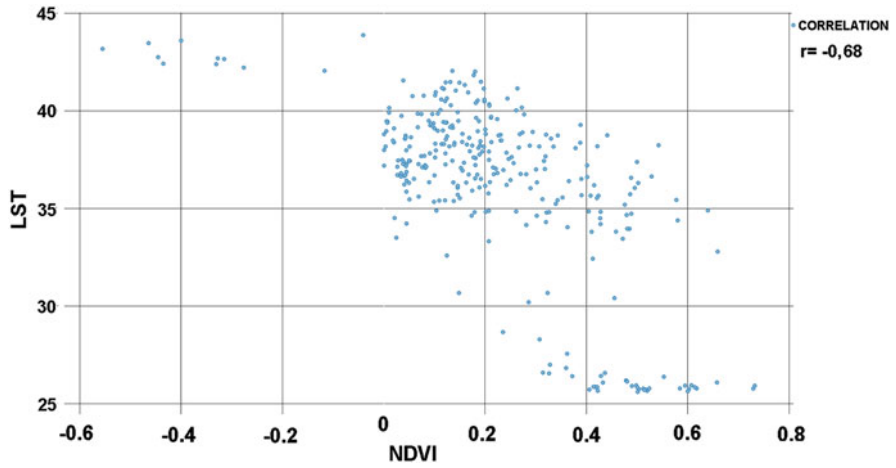


Fig. 5 Correlation between NDVI and LST

4 Discussions

In order to reduce the possible effects of climate change, ecological corridors and reserve areas with spatial distribution are needed (Upmanis et al. 1998; Heidt and Neef 2008; Yang et al. 2012; Vardoulakis et al. 2003). Green areas create an urban cold island in summer temperatures and create refreshing environments for urban residents (Alkan et al. 2017; Tzenkova et al. 2007; Cetin et al. 2010, 2018, 2019; Ataei and Hasheminasab 2012; Cetin 2015, 2016, 2020a, b; Monteiro et al. 2016; Deniz and Güngör 2020; Adiguzel et al. 2020, 2021; Kilicoglu et al. 2020, 2021; Gungor et al. 2021; Zeren Cetin and Sevik 2020; Zeren Cetin et al. 2020). The ecosystem, which exists spontaneously as a result of the interaction of different branches of science in the historical process, becomes a reference in the fight against climate change with its biological richness and climatic features. Recent disasters reveal the necessity of urban green space planning, especially in the city center and its surroundings, where urban fragility is high. The issue of climate change, which should be handled interdisciplinary in the morphological approach, is evaluated in an integrated manner in the context of ecological planning and urban morphology. Thus, it is aimed to improve the urban ecosystem and to create resistance to climate change.

Ecological urban green plans should be created by making use of urban green areas that give an idea about the development direction of the city and ecological heritage. Conservation development plans, landscaping, and urban design projects should be made for the protection and improvement of green areas. Urban green areas with residential and non-residential functions should play a role in the control of the urban pattern by strengthening public uses. Any intervention to the city should be handled in accordance with the characteristics of the place and the context in which it is located, without ignoring the environmental connections (Grassl 1976, 1979, 1981, 1989, 2006, 2011; Tzenkova et al. 2007; Cetin et al. 2010, 2018, 2019; Ataei and Hasheminasab 2012; Cetin 2015, 2016, 2020a, b; Monteiro et al. 2016; Deniz and Güngör 2020; Adiguzel et al. 2020, 2021; Kilicoglu et al. 2020, 2021; Gungor et al. 2021; Zeren Cetin and Sevik 2020; Zeren Cetin et al. 2020).

Ensuring harmony between geographical conditions and spatial structure minimizes the damage caused by climate change. When green areas are evaluated together with threshold lines sensitive to climate change (coastal areas, river beds, valleys, mountains, etc.), a mutualistic relationship emerges. Green areas define a protection zone around the threshold lines; threshold lines also prevent the areal shrinkage of green areas and protect the ecological heritage. Urban green areas constitute a habitat transition corridor with their rich biological diversity and ecological values. Ecological networks defined between inner, middle, and outer green areas increase the resistance against climate change and increase the comfort of climate-friendly transportation circulations such as public transportation, bicycle, and pedestrian (Oke 1984; Grassl 1976, 1979, 1981, 1989; 2006, 2011; Tzenkova et al. 2007; Cetin et al. 2010, 2018, 2019; Ataei and Hasheminasab 2012; Cetin 2015, 2016, 2020a, b; Monteiro et al. 2016; Deniz and Güngör 2020; Adiguzel et al.

2020, 2021; Kilicoglu et al. 2020, 2021; Gungor et al. 2021; Zeren Cetin and Sevik 2020; Zeren Cetin et al. 2020).

In this sense, in a study conducted in the city of Frankfurt in previous studies, it has been determined that small-scale vegetative areas around the city reduce the air temperature up to 3.5 °C (Georgii 1969). Similarly, it is seen that the temperature difference between parks and built-up areas varies between 3 and 6 °C depending on time for Mexico City (Oke et al. 1999; Spronken-Smith and Oke 1998). It has been determined that open green areas cause a temperature decrease of 4 °C in the urban climate and create a cooling effect between 2 and 8 °C for larger urban open green spaces.

The effect of urban open green spaces on climate change varies according to the structure of the area. It has been determined that factors such as the size of the area, its surrounding texture, traffic density, and the climatic structure of the area have an effect (Heidt and Neef 2008; Yang et al. 2012; Vardoulakis et al. 2003; Upmanis and Chen 1999). According to Upmanis et al. (1998), large parks have more cooling effects than smaller ones. In the same study conducted in Gothenburg, it was determined that the difference between the park area and the built-up area was 5.9 °C in the summer period, and the cooling effect of the 156 ha park area was observed up to 1100 m (Upmanis et al. 1998; Upmanis and Chen 1999). As a result of climate change and rapid increase in urbanization, water resources are decreasing and policies for life without water are being prepared. However, there is a strong relationship between the organization of the urban fabric and the development of urban water infrastructure systems. This existing relationship has become even more important with the decrease of urban green spaces.

Land surface temperatures are considered as the most basic indicator of the urban heat island phenomenon, as they are reflections of the surface temperatures. It is known that the density or health of the vegetation also affects the surface temperature and urban heat island formation depending on evapotranspiration. For this reason, it is of great importance to determine the relationship between land surface temperatures and NDVI, to determine the regions where the urban heat island effect is most intense and to take measures to reduce this effect.

It is widely accepted that reducing the urban heat island effect and increasing vegetation cover is a simple and effective way to mitigate the adverse effects of urban climate change. Therefore, significant research has been carried out recently to increase awareness of the functionality provided by urban vegetation. For example, a recent study found that a 10% increase in the amount of vegetation in urban areas in Manchester, with current climate change models, could potentially lower temperatures by as much as 4 °C (Gill et al. 2007, 2013; Skelhorn et al. 2016). Another important benefit of urban vegetation in relation to climate change is the reduction of the total energy consumption used for air conditioning, which will reduce greenhouse gas emissions and related air pollution (Solecki et al. 2005; Zhang et al. 2014; Santamouris et al. 2019; Santamouris 2020).

As a result, in Antalya province, when the land use and NDVI are evaluated together, “Building surfaces” and “Open Areas with Little or No Vegetation” trigger the formation of heat island in the summer months when the air temperature is the

highest, while the plant surface, water, and wetlands reduce this effect detected. When the land surface temperature values in the study area were examined spatially, it was concluded that the plant surfaces in the urban settlement areas reduced the heat island effect. Therefore, in order to reduce the heat island effect in urban areas, it is necessary to increase the amount of median planting, road afforestation, and open green space.

5 Conclusions

Climate change is the most important global threat today. Climate change negatively affects the structure, composition, productivity, geographical distribution, and morphology of many ecosystems. Changing climatic conditions also transform cities and increase the importance of climate plans in line with sustainability. However, ignoring the climatic areas that define morphological regions with unique characteristics in the plans made, the search for new parcels in the city due to the land values and increasing population leave the urban forest areas under the threat of alienation. This situation negatively affects green space plans in terms of ecological sustainability. Existing open green areas, which are scattered and in small pieces in the city and do not show a unity, should be of a quality to meet the needs of the urban people in terms of the aesthetic and functional properties of the structural plant elements and equipment.

Master and application development plans should be planned and designed rationally, aesthetically, and functionally according to the conditions of the day, taking into account the ecological, social, economic, and cultural characteristics of the city. For this purpose, not only city planners but also other related professional disciplines (architect, landscape planner, forest engineer, sociologist, geologist, ecologist) should be involved in the planning and implementation phase. The zoning legislation should not only have an understanding of controlling the structure within the parcel but also an understanding that controls the distribution and density of open and green areas.

While implementing zoning plans, scientific and technical criteria should always be prioritized, especially instead of political purposes and land renting tendencies. In addition, the local administration has to provide planning, implementation and supervision works in integrity.

Plant materials used in urban open green areas should be used aesthetically and functionally in accordance with their intended use. For this purpose, it is beneficial to increase the number of technical personnel such as landscape architect, forest engineer, and agricultural engineer in municipality.

It is possible to plan, implement, and ensure its continuity by taking into account the technical criteria. All open green spaces in the city should be integrated with the plans that include the urban management decisions and should be created in a way that provides continuity and flexibility for changes over time. In addition, Antalya city people and non-governmental organizations must be more active in terms of

influencing and directing the local government in creating conscious open green space.

As a result, ecological planning and urban green generation planning should support and complement each other. Urban green generation planning with the climatic approach method will form the basis for ecological planning. Thanks to the climatic green approach, which offers a different perspective against climate change in city planning, climate comfort and urban ecological sustainability will be ensured. Against climate change, it is necessary to define the jurisdictions in the city planning discipline, to ensure the planning hierarchy and to make legal arrangements for ecological values. In this context, it is recommended to include green generation planning in climate change strategies and action plans that include mitigation and adaptation strategies on a local, national, and global scale and to develop legal regulations that will regulate the harmony and superiority between other plans concerning the city and urban periphery plans. In this study, the effect of urban green areas on climate change has been emphasized in the context of the climatic green approach.

There is an inverse relationship between vegetation and ground surface temperature. The increase in the land surface temperature values indicates the regions where the area covered by any land use green area and vegetation decreases or the impermeable surfaces increase. Therefore, it is thought that it will guide planners, designers, and decision-making mechanisms in landscape planning and design studies on the development of proposals that can reduce the surface temperature and heat island effect formation in these determined regions.

In this study, the province of Antalya has been selected and examined in order to determine the factors with which the heat island effect, which has gained momentum in recent years, has started to increase. Migration from rural areas to urban areas, along with urbanization and industrialization, has led to rapid construction and climatic changes. As a result of the intense constructions experienced, the increase in vertical constructions in the city centers, uncontrolled energy consumption in the buildings, the opening of the green areas for development, the destruction of natural areas, and covering them with impermeable surface materials such as asphalt and concrete have caused temperature changes in urban areas, and these changes have caused climatic deterioration. As a result of the researches, the factors that cause the urban heat island effect, which can be defined as the urban heat island effect, which can be defined as the urban areas being warmer than the surrounding rural areas, have been observed and the relationship between the urban forests and green areas, which are effective in reducing the urban heat island effect of Antalya Province, with this effect. In the study, when the surface temperature map of Antalya Province was examined, it was determined that the temperature values were lower in areas with more green areas, and the temperature was higher in areas with dense construction. Green areas, which are one of the parameters of regulating and improving the climate, serve the ecosystem by balancing the heating and absorption needs of the buildings, acting as a source of moisture, making the ground surface less warm during the day, and preventing cooling by reducing energy loss at night. For this reason, it is very important to consider both the sustainable environment principle

and human comfort conditions in strategic plans for urbanization, taking into account the relationship between urban areas and people. In balancing the urban climate, winds as well as temperature and humidity play an important role in regulating the climate. Winds are an important factor that provides natural ventilation. Because it provides the exchange of bad air in the environment with fresh air for living life. Looking at the data of the International Energy Agency, it was seen that the dense construction that occurred with urbanization could not benefit enough from the natural wind effect, and the temperature and the amount of disturbing humidity increased due to the positioning of the buildings in the city in such a way that the winds could not interfere. For this reason, considering the wind factor, attention should be paid to the height and location of the buildings that will prevent the wind circulation in the city, and the wind inlets and outlets should be kept at an optimum level. The lands of Antalya province have a very important place in Turkey's agriculture. However, the natural opportunities of the city are decreasing over time due to urbanization and intense construction. While three quarters of the population made a living from agricultural activities in the 1970s, it was determined that this rate was 49% in the 2000s. In addition, Bogazici University Climate Change and Policy Research Manager Levent Kurnaz said "Antalya will be as hot as Cairo in 2100." In line with this information, it can be clearly stated that the temperature in the Mediterranean region has increased rapidly and will continue to increase. Considering all these results, preserving the vegetation in the cities, paying attention to the building forms that will provide air currents in the constructions, and choosing the ground surfaces that will balance the heat and temperature from materials with high albedo will affect the livability in urban areas.

Acknowledgments The authors thank the support by the Republic of Turkey Ministry of Agriculture and Forestry, General Directorate of Forest Engineering, and the General Directorate of Meteorology for their prompt responses to our requests.

References

- Adigüzel G (2018) Investigation of the micro-climatic effects of urban green areas in the example of İzmir-Bornova, PhD. Thesis, Ege University, Science Institute, Landscape Dept., 119pp, İzmir
- Adiguzel F, Cetin M, Kaya E, Simsek M, Gungor S, Sert EB (2020) Defining suitable areas for bioclimatic comfort for landscape planning and landscape management in Hatay, Turkey. *Theor Appl Climatol* 139(3):1493–1503
- Adiguzel F, Bozdogan Sert E, Dinc Y, Cetin M, Gungor S, Yuka P, Sertkaya Dogan O, Kaya E, Karakaya K, Vural E (2021) Determining the relationships between climatic elements and thermal comfort and tourism activities using the tourism climate index for urban planning: a case study of Izmir Province. *Theor Appl Climatol* 147(14):1–16. <https://doi.org/10.1007/s00704-021-03874-9>
- Alkan A, Adigüzel F, Kaya E (2017) Batman Kentinde Kentsel Isınmanın Azaltılmasında Yeşil Alanların Önemi. *Coğrafya Dergisi* 34:62–76
- Antalya Metropolitan Municipality (2022) Information about Antalya from Antalya Metropolitan Municipality. <https://www.antalya.bel.tr/BilgiEdin/Cografya>. Accessed 1 Feb 2022
- Arnfield AJ (1998) Micro-and mesoclimatology. *Progress in physical geography* 22(4):533–544

- Arnfield AJ (2003) Two decades of urban climate research: a review of turbulence, exchanges of energy and water, and the urban heat island. *Int J Climatol* 23(1):1–26
- Ataei H, Hasheminasab F (2012) Comparative assessment of human bioclimatic in Isfahan City using Terjunde, TCI, PET, PMV. *Urban Reg Stud Res* 4(14):17–19
- Atwa S, Ibrahim MG, Murata R (2020) Evaluation of plantation design methodology to improve the human thermal comfort in hot-arid climatic responsive open spaces. *Sustain Cities Soc* 59: 102198
- Avdan U, Jovanovska G (2016) Algorithm for automated mapping of land surface temperature using LANDSAT 8 satellite data. *J Sensors* 2016:1480307. <https://doi.org/10.1155/2016/1480307>
- Avissar R (1996) Potential effects of vegetation on the urban thermal environment. *Atmos Environ* 30(3):437–448. [https://doi.org/10.1016/1352-2310\(95\)00013-5](https://doi.org/10.1016/1352-2310(95)00013-5)
- Bozdogan Sert E, Kaya E, Adiguzel F, Cetin M, Gungor S, Zeren Cetin I, Dinc Y (2021) Effect of the surface temperature of surface materials on thermal comfort: a case study of Iskenderun (Hatay, Turkey). *Theor Appl Climatol* 144(1):103–113. <https://doi.org/10.1007/s00704-021-03524-0>
- Bozdogan E, Sogut Z (2015) Green solution suggestions within the concept of sustainability in Eastern Mediterranean cities. In: Avcikurt C, Dinu M, Hacioğlu N, Efe R, Soykan A (eds) *Tourism, environment and sustainability*. St. Kliment Ohridski Univ. Press, Sofia, pp 468–485
- Cetin M (2015) Determining the bioclimatic comfort in Kastamonu City. *Environ Monit Assess* 187:640–649. <https://link.springer.com/article/10.1007/s10661-015-4861-3>
- Cetin M (2016) Determination of bioclimatic comfort areas in landscape planning: a case study of Cide Coastline. *Turk J Agric Food Sci Technol* 4(9):800–804. <http://www.agrifoodscience.com/index.php/TURJAF/article/view/872>
- Cetin M (2020a) The changing of important factors in the landscape planning occur due to global climate change in temperature rain and climate types: a case study of Mersin city. *Turk J Food Agric Sci* 8(12):2695–2701
- Cetin M (2020b) Climate comfort depending on different altitudes and land use in the urban areas in Kahramanmaraş City. *Air Qual Atmos Health* 13(8):991–999
- Cetin M, Topay M, Kaya LG, Yılmaz B (2010) Efficiency of Bioclimatic Comfort in Landscape Planning Process: Case of Kutahya. *Fac For J Süleyman Demirel Univ Ser A* 1:83–95. <https://www.cabdirect.org/cabdirect/abstract/20123177909>
- Cetin M, Yildirim E, Canturk U, Sevik H (2018) Investigation of bioclimatic comfort area of Elazig city centre. In: *Recent researches in science and landscape management*. pp 324–333
- Cetin M, Adiguzel F, Gungor S, Kaya E, Sancar MC (2019) Evaluation of thermal climatic region areas in terms of building density in urban management and planning for Burdur, Turkey. *Air Qual Atmos Health* 12(9):1103–1112. <https://doi.org/10.1007/s11869-019-00727-3>
- Deniz A, Güngör Ş (2020) Mapping with unmanned aerial vehicles systems: a case study of Nevşehir Hacı Bektaş Veli University Campus. *Kastamonu Univ J Eng Sci* 6(1):27–32
- Diñç Y, Adigüzel F (2021) Şehir planlama içinde coğrafi planlama (Editörler: Mesut DOĞAN, Mustafa KÖSE ve Fatih AYHAN). Pegem Akademi Yayıncılık, Ankara
- Dursun D, Yavas M (2016) Urbanization and the use of climate knowledge in Erzurum, Turkey. *Procedia Eng* 169:324–331
- Dye C (2008) Health and urban living. *Science* 319(5864):766–769. <https://doi.org/10.1126/science.1150198>
- Estoque RC, Murayama Y, Myint SW (2017) Effects of landscape composition and pattern on land surface temperature: an urban heat island study in the megacities of Southeast Asia. *Sci Total Environ* 577:349–359
- Feyisa GL, Dons K, Meilby H (2014) Efficiency of parks in mitigating urban heat island effect: an example from Addis Ababa. *Landsc Urban Plan* 123:87–95
- Finke L (1980) Kent planlaması açısından yeşil alanların kent iklimini ve kent havasını iyileştirme yetenekleri. *İstanbul Üniversitesi Orman Fakültesi Dergisi* 30(2):224–256

- Georgii HW (1969) The effects of air pollution on urban climates. *Bull World Health Organ* 40(4): 624
- Gill SE, Handley JF, Ennos AR, Pauleit S (2007) Adapting cities for climate change: the role of the green infrastructure. *Built Environ* 33(1):115–133
- Gill SE, Rahman MA, Handley JF, Ennos AR (2013) Modelling water stress to urban amenity grass in Manchester UK under climate change and its potential impacts in reducing urban cooling. *Urban For Urban Green* 12(3):350–358
- Gómez F, Montero L, De Vicente V, Sequi A, Castilla N (2008) Vegetation influences on the human thermal comfort in outdoor spaces: criteria for urban planning. *WIT Trans Ecol Environ* 117:151–163
- Gómez-Baggethun E, Barton DN (2013) Classifying and valuing ecosystem services for urban planning. *Ecol Econ* 86:235–245. <https://doi.org/10.1016/j.ecolecon.2012.08.0>
- Grassl H (1976) The dependence of the measured cool skin of the ocean on wind stress and total heat flux. *Boundary-Layer Meteorol* 10(4):465–474
- Grassl H (1979) Possible changes of planetary albedo due to aerosol particles. *Dev Atmos Sci* 10: 229–241
- Grassl H (1981) The climate at maximum entropy production by meridional atmospheric and oceanic heat fluxes. *Q J R Meteorol Soc* 107(451):153–166
- Grassl H (1989) Extraction of surface temperature from satellite data. In: *Applications of remote sensing to agrometeorology*. Springer, Dordrecht, pp 199–220
- Grassl H (2006) Climate change, new weather extremes and climate policy. In: *Earth system science in the Anthropocene*. Springer, Berlin, Heidelberg, pp 41–50
- Grassl H (2011) Climate change challenges. *Surv n Geophys* 32(4–5):319
- Gungor S, Cetin M, Adiguzel F (2021) Calculation of comfortable thermal conditions for Mersin urban city planning in Turkey. *Air Qual Atmos Health* 14(4):515–522
- Heidt V, Neef M (2008) Benefits of urban green space for improving urban climate. In: *Ecology, planning, and management of urban forests*. Springer, New York, pp 84–96
- Kanda M (2006) Progress in the scale modeling of urban climate. *Theor Appl Climatol* 84(1): 23–33. <https://doi.org/10.1007/s00704-005-0141-4>
- Kilicoglu C, Cetin M, Aricak B, Sevik H (2020) Site selection by using the multi-criteria technique—a case study of Bafra, Turkey. *Environ Monit Assess* 192(9):1–12
- Kilicoglu C, Cetin M, Aricak B, Sevik H (2021) Integrating multicriteria decision-making analysis for a GIS-based settlement area in the district of Atakum, Samsun, Turkey. *Theor Appl Climatol* 143:379–388. <https://doi.org/10.1007/s00704-020-03439-2>
- Kratzer P (1968) Beitrage Zum Münchner Stadtklima. *Wetterund Leben* 20:110–116
- Lehoczky A, Sobrino JA, Skoković D, Aguilar E (2017) The urban heat island effect in the city of Valencia: a case study for hot summer days. *Urban Sci* 1(9):1–18
- Marsh MM (1991) *Landscape planning: environmental applications*. Wiley, Toronto, p 528
- Monteiro MV, Doick KJ, Handley P, Peace A (2016) The impact of greenspace size on the extent of local nocturnal air temperature cooling in London. *Urban For Urban Green* 16:160–169
- Oke TR (1979) Review of urban climatology 1973-1976 WMO Technical Notes, No. 134. Geneve (No. 04; QC875. 5, 04.)
- Oke TR (1982) The energetic basis of the urban heat island. *Q J R Meteorol Soc* 108(455):1–24
- Oke TR (1984) Methods in urban climatology. *Appl Climatol* 14(18):19–29
- Oke TR, Spronken-Smith RA, Jáuregui E, Grimmond CS (1999) The energy balance of central Mexico City during the dry season. *Atmos Environ* 33(24–25):3919–3930
- Patz JA, Campbell-Lendrum D, Holloway T, Foley JA (2005) Impact of regional climate change on human health. *Nature* 438(7066):310–317
- Paul MJ, Meyer JL (2001) Streams in the urban landscape. *Annu Rev Ecol Syst* 32(1):333–365
- Richards K (2005) Urban and rural dewfall, surface moisture, and associated canopy-level air temperature and humidity measurements for Vancouver, Canada. *Boundary-Layer Meteorol* 114(1):143–163

- Rizwan AM, Dennis LY, Chunho LIU (2008) A review on the generation, determination and mitigation of Urban Heat Island. *J Environ Sci* 20(1):120–128
- Santamouris M (2020) Recent progress on urban overheating and heat island research. Integrated assessment of the energy, environmental, vulnerability and health impact. Synergies with the global climate change. *Energy Build* 207:109482
- Santamouris M, Cartalis C, Synnefa A, Kolokotsa D (2015) On the impact of urban heat island and global warming on the power demand and electricity consumption of buildings—a review. *Energy Build* 98:119–124
- Santamouris M, Ding L, Osmond P (2019) Urban heat island mitigation. In: Decarbonising the built environment. Palgrave Macmillan, Singapore, pp 337–355
- Schwarz N, Schlink U, Franck U, Großmann K (2012) Relationship of land surface and air temperatures and its implications for quantifying urban heat island indicators—an application for the city of Leipzig (Germany). *Ecol Indic* 18:693–704
- Şimşek ÇK, Şengezer B (2012) İstanbul metropoliten alanında kentsel Isınmanın Azaltılmasında Yeşil Alanların Önemi. *Megaron* 7(2):116–128
- Skelhorn CP, Levermore G, Lindley SJ (2016) Impacts on cooling energy consumption due to the UHI and vegetation changes in Manchester, UK. *Energy Build* 122:150–159
- Solecki WD, Rosenzweig C, Parshall L, Pope G, Clark M, Cox J, Wiencke M (2005) Mitigation of the heat island effect in urban New Jersey. *Glob Environ Change B Environ Hazards* 6(1):39–49
- Spronken-Smith RA, Oke TR (1998) The thermal regime of urban parks in two cities with different summer climates. *Int J Remote Sens* 19(11):2085–2104
- Taha H (1997) Urban climates and heat islands: albedo, evapotranspiration, and anthropogenic heat. *Energy Build* 25(2):99–103
- Topay M (2012) Importance of thermal comfort in the sustainable landscape planning. *J Environ Protect Ecol* 13(3):1480–1487
- Tzenkova A, Ivancheva J, Koleva E, Videnov P (2007) The human comfort conditions at Bulgarian Black Sea side. In: Matzarakis A, de Freitas CR, Scott D (eds) *Developments in tourism climatology*, pp 150–157
- Upmanis H, Chen D (1999) Influence of geographical factors and meteorological variables on nocturnal urban-park temperature differences—a case study of summer 1995 in Göteborg, Sweden. *Climate Res* 13(2):125–139
- Upmanis H, Eliasson I, Lindqvist S (1998) The influence of green areas on nocturnal temperatures in a high latitude city (Göteborg, Sweden). *Int J Climatol* 18(6):681–700
- Vardoulakis S, Fisher BE, Pericleous K, Gonzalez-Flesca N (2003) Modelling air quality in street canyons: a review. *Atmos Environ* 37(2):155–182
- Voogt JA, Oke TR (2003) Thermal remote sensing of urban climates. *Remote sensing of environment* 86(3):370–384
- Wilmers F (1975) *Temperaturstudien in Gartenhofen*. Prof
- Yang X, Zhao L, Bruse M, Meng Q (2012) An integrated simulation method for building energy performance assessment in urban environments. *Energy Build* 54:243–251
- Zeren Cetin I, Sevik H (2020) Investigation of the relationship between bioclimatic comfort and land use by using GIS and RS techniques in Trabzon. *Environ Monit Assess* 192(2):71
- Zeren Cetin I, Ozel HB, Varol T (2020) Integrating of settlement area in urban and forest area of Bartın with climatic condition decision for managements. *Air Qual Atmos Health* 13(8): 1013–1022
- Zhang B, Gao JX, Yang Y (2014) The cooling effect of urban green spaces as a contribution to energy-saving and emission-reduction: a case study in Beijing, China. *Build Environ* 76:37–43



Conceptualising the Citizen-Driven Urban Forest Framework to Improve Local Climate Condition: Geospatial Data Fusion and Numerical Simulation

Siti Aekbal Salleh, Zulkiflee Abd. Latif, Faezah Pardi,
Emad Mushtaha, and Yarina Ahmad

Abstract

Rapid urbanisation has boosted demand for ecosystem goods and services, accelerating land-use development. This is concerning because urban forest acreage and biodiversity would be on the declining trend. With the heat island effect, radiant heat, and soil moisture evaporation all on the rise, this “urban infill” may place additional strain on existing trees and natural spaces while limiting space for new trees. Due to the scarcity of urban land and soil resources, careful planning is required to provide adequate greenery while balancing carbon emissions. Continued global warming will have a negative impact on Malaysia’s biodiversity. Our urban forest ecosystem is just one of many. In cities where air

S. A. Salleh (✉) · Z. Abd. Latif

Institute for Biodiversity and Sustainable Development, Universiti Teknologi MARA, Shah Alam, Malaysia

Faculty of Architecture Planning and Surveying, Universiti Teknologi MARA, Shah Alam, Malaysia

e-mail: aekbal@uitm.edu.my

F. Pardi

Institute for Biodiversity and Sustainable Development, Universiti Teknologi MARA, Shah Alam, Malaysia

Faculty of Applied Sciences, Universiti Teknologi MARA, Shah Alam, Malaysia

E. Mushtaha

Department of Architectural Engineering, University of Sharjah, Sharjah, United Arab Emirates

Y. Ahmad

Institute for Biodiversity and Sustainable Development, Universiti Teknologi MARA, Shah Alam, Malaysia

Faculty of Administrative Science and Policy Studies, Universiti Teknologi MARA, Shah Alam, Malaysia

© The Author(s), under exclusive license to Springer Nature Singapore Pte Ltd. 2022

337

M. N. Suratman (ed.), *Concepts and Applications of Remote Sensing in Forestry*,
https://doi.org/10.1007/978-981-19-4200-6_17

pollution and water management are issues, urban forests provide essential ecosystem services such as air and water filtering, which are critical to human health. Findings show that the collective efforts of individuals under a citizen-driven urban forestry (CDUF) framework might have a substantial influence on reducing high urban air temperatures, suggesting that the collective actions of individual citizens to increase urban forest cover can produce a significant effect on the mitigation of high air temperatures due to the urban heat island effect and climate change. Leveraging the richness of satellite data archive, geospatial technology, and several numerical simulation methods availability, the urban forest's vulnerability and adaptive capacity are sought to be quantified. Thus, conceptualising and reviewing the existing approach and framework of CDUF are critical, as they may aid in the conservation of urban forest biodiversity while mitigating the impacts of climate change.

Keywords

Urban forest · Geospatial · Citizen-driven · SDG13 · Urban climate

1 Introduction

1.1 Trees Outside Forest

Large-scale tree plantings that achieve goals such as commercial timber and fibre production, watershed protection, and habitat preservation are commonly referred to as planted forests. Agroforestry systems and community woodlots, on the other hand, plant trees at much smaller scales to provide a variety of products and services to resident households, local communities, and regional cultures.

Home gardens, alley cropping, improved fallows, intercropped trees for shade and fodder production, and trees planted in hedgerows and along fence lines are examples of these systems in tropical countries. A diverse range of indigenous practises and species mixtures can be found throughout the tropics, reflecting these systems' adaptations to meet localised needs and opportunities. While R&D programmes have aided in the expansion and refinement of many of these systems over the last two decades, land-tenure practises, population pressures that confine agroforestry practises to degraded lands, subsistence needs that preclude extended periods of tree growth, and an insufficient supply of technical information or technology remain significant constraints on tree planting. However, it is possible to conclude that incorporating green surfaces and parks into the urban environment is the most effective measure for mitigating urban heat islands.

Community forests typically involve planting a few species in small woodlots adjacent to farms, around villages, along roads, and as riparian buffers. While species diversity is important in all agroforestry systems, community forests typically involve planting a few species in small woodlots adjacent to farms, around villages, along roads, and as riparian buffers. The production of fuelwood for local

consumption and other marketable tree products, as well as soil stabilisation, reclamation, and improvement, and water quality protection are the primary objectives of these forests. As in many other planted forests, the number of species widely used in community forests has been limited, with the genera *Eucalyptus*, *Pinus*, and *Acacia* accounting for the majority of species. The major issues with these “planted forests” are product rights, responsibility for tree care once trees are established, protection of trees until they reach the appropriate size for their designated use, growing interest in using “native” species, and increased community involvement in planning and management.

In many urban and peri-urban landscapes, trees planted alongside streets and waterways, or as woodlots in parks and other public spaces, make up a significant portion of the planted forest. In addition to many of the same environmental benefits as agroforests and community forests, these urban plantings provide distinct aesthetic and recreational benefits. For a large portion of the world’s ever-growing urban population, these may be the only tangible points of reference for understanding planted forests.

2 Geospatial for Environmental Urban Solution

Open geospatial data and tools are becoming an increasingly important paradigm, with the potential to promote democratisation of geographical information, transparency of governments and institutions, and social, economic, and environmental opportunities. Over the last decade, there has been a significant improvement in the development of open geospatial data and open-source geospatial software. Many members of the scientific community genuinely think that integrating free and open software, open data, and open standards results in the creation of a sustainable ecosystem that accelerates new discoveries and aids in the resolution of global cross-disciplinary societal challenges ranging from climate change mitigation to sustainable cities. This thematic collection was inspired by the consistent pervasiveness of open-source geographic information systems (GIS) studies.

Geospatial technology has made it possible to use satellite and space techniques to solve a variety of environmental issues. This includes research on urban sprawl and slums, the threat of flooding and erosion, environmental degradation caused by oil spills, crop health, and early warning signals. Urban changes have been tracked using widely available remotely sensed imagery and aerial photographs with varying spatiotemporal resolutions, which can be analysed using the appropriate software, algorithms, and human capacity. The application of this technology improves data capture and distribution methods. This could be done in real time, reducing the time and energy required for data acquisition in order to solve environmental problems.

Urban forests are one-of-a-kind and highly valuable resources. However, due to soil compaction, limited growing spaces, high temperatures, and exposure to air and water pollution, trees in urban forests are frequently subjected to greater stress than those in rural or undeveloped areas. Furthermore, conditions in urban areas change faster than in rural and undeveloped areas. As a result, proactive management of

urban forests can be difficult and necessitates the availability of current and comprehensive information. Geospatial tools such as GIS, global positioning systems (GPS), and remote sensing work extremely well together for data collection, analysis, and reporting. Many urban forest management issues could be addressed quickly and effectively using geospatial methods and tools. Geospatial tools can provide timely and comprehensive spatial data from which urban forest attributes like land cover, forest structure, species composition and condition, heat island effects, and carbon storage can be derived. Data fusion, virtual reality, three-dimensional visualisation, Internet delivery, modelling, and emergency response are examples of emerging geospatial tools that could be adapted for urban forest applications.

Social media georeferenced data can be considered as volunteered geographic information (VGI), and social media can be considered VGI sources. Geotagged Tweets from Twitter, geotagged photographs from Flickr and Instagram, and so on are examples of these (See et al. 2017). Users have access to powerful tools for creating maps and adding elements such as text, images, and video with open-source GIS mapping software. Especially when combined with initiatives like OpenStreetMap, HERE Map, and Google Map. Furthermore, a good urban forest narration can be visualised using storymap GIS, as done by the NYC Parks Stewardship Program—Our Urban Forest (arcgis.com).

Big data and analytics are two other emerging advances in geospatial technology. It has been one of the most significant shifts in recent years for businesses. Organisations across industries are constantly looking for ways to turn an ever-increasing volume of data into a competitive advantage, and many have discovered that GIST adds value to these efforts. Geospatial analytics uses geographic information to enable better decision-making and problem-solving agility. Analytics specialists can use GIS data to create visualisations, identify meaningful trends, and make predictions, resulting in reports that provide valuable context for strategy.

3 Numerical Simulation for Urban Climate

In previous decades, increased urbanisation resulted in significant changes to local microclimate conditions. Numerical simulations are an effective tool for determining the relationship between urban climate and energy consumption. Climate change has emerged as one of humanity's most serious challenges as a result of the rapid urbanisation of the world and the globalisation of the economy. The built environment has become a primary focus for researchers investigating ways to mitigate the effects of urban climate change. On the other hand, researchers wishing to model the performance of a large number of buildings are limited to using complex simulation methods, which require a massive amount of computation when run in a standard computer environment. A significant contribution would be to develop a more straightforward, efficient modelling process.

In the early 2000s, Kikegawa et al. (2003) developed a simple building energy model (BEM) capable of dynamically calculating energy demand and anthropogenic heat due to air conditioning use. This model was combined with a multilayer UCM

(CM-BEM) developed by Kondo et al. (2005) for weather and climate simulation. This coupled model has been applied to a variety of studies examining urban climate and energy demand. Kikegawa et al. (2014) combined the CM-BEM and the WRF models (hereafter WRF-CM-BEM). It has been used to evaluate urban climate, energy demand, the effects of heat islands on mitigation, and health effects (Nakajima et al. 2021; Kikegawa et al. 2022). The number of scientific configurations and expendables used in these numerical simulation models has been steadily increasing in recent years. Numerous prior studies have validated the WRF-SLUCM, which has been used to quantify the impacts of surface materials used in cooling strategies, as well as historical climate simulations, future climate projections, and urban climate mitigation strategies (Li and Liu 2021; Khan et al. 2022).

The need for passive cooling strategies on the exterior to mitigate the heat surge generated by buildings and other man-made features is demonstrated by the demands for electrical usage for cooling, which was primarily concentrated for indoor purposes. To save energy, these urban dwellings should make use of cooling strategies whenever possible. Passive cooling refers to solar and heat control, heat modulation, and heat dissipation techniques that rely on naturally occurring phenomena such as natural ventilation, radiative cooling, evaporative cooling, and ground cooling, all of which are influenced by land use and land cover (Santamouris and Kolokotsa 2013; Su et al. 2021; Gu and You 2022). Techniques for passive cooling have been studied in a variety of climates. High nighttime ambient temperature, cloud cover, high humidity, and insufficient wind speeds are just a few of the climatic factors that contribute to the inefficiency of various cooling approaches; these conditions are common in hot-humid climates.

4 Benefits and Uses of Urban Forests and Trees

There are numerous economic, environmental, and health benefits associated with urban forests. Urban forests are becoming increasingly popular. In order to reduce the heat island effect and energy consumption, trees are planted to absorb and block sunlight from reaching buildings and the ground. Shopping in commercial areas with street trees has been shown to increase shoppers' willingness to spend more time and money, as well as their ability to assign a higher overall desirability to the merchandise being offered in studies. It has also been demonstrated that street trees increase the value of a property as well as the amount of rent that can be charged.

Trees in urban settings play an important role in improving urban life by reducing runoff, air pollution and energy use, and improving human health and emotional well-being. The increasing size and proportion of the human population living in towns and cities has also resulted in greater emphasis on the maintenance and improvement of trees within these settings. An understanding of urban floristic composition can help the municipal in managing their resources sustainably. Biological diversity within populations is important in order to minimise plant maintenance needs and disease tolerance of urban tree populations. Low species

diversity may leave the tree population more vulnerable to the new stress environments: both abiotic and biotic. Urban forestry literature generally recommends that not more than 10% of the trees be from any one species and the concern underlying this recommendation is with the possibility of a species-specific pest or disease sweeping through the area damaging or destroying a large segment of the trees.

Additionally, trees serve as a mediator for a variety of environmental pollutants, including the removal of ozone and sulphur dioxide from the air, the sequestration and storage of carbon, and the absorption and transformation of contaminants in soil. Furthermore, by providing habitat for wildlife, urban forests contribute to the conservation of biodiversity. When trees provide shade, they provide valuable protection from the sun's ultraviolet rays, and the benefits of improved air quality provided by urban forests may result in a reduction in respiratory illnesses such as asthma. Aside from that, trees absorb high-frequency noise and sound, which helps to reduce environmental stressors while also improving overall quality of life.

Urban environment is very stressful to the physiology of street trees, especially when the quality of air is very low due to high cases of pollution. Frequent pruning especially in places that have telephone or power wires will weaken trees, due to the fact less leaves after pruning resulted in lower rate of photosynthesis. Soil in urban areas is mostly reclaimed lands with low water-retention capacity and nutrient content (Webb et. al., 2000). Besides, soil compaction also interferes with the tree's access to water and nutrients.

5 Urban Biodiversity

Increasing urban greenness, vegetation, and urban tree canopy cover has become one of the most critical considerations for strategic planning within state and local government organisations. Urban trees and community green spaces have been identified as an important tool that can be used by policymakers to mitigate the many negative environmental effects of urbanisation.

Biodiversity had been considered as one of the key factors in the stability of the wayside tree population. The disease and insect hazards call up for the need of high species diversity to tolerate them, for example, the presence of colonies of aphids or other pests or wilting of leaves due to Dutch elm disease. The Dutch elm disease that wiped American native elms city was one good example of the catastrophic loss of using a high number of a single species. Therefore, low diversity results due to the practice of using a limited number of tree species that are more vulnerable to the challenges of the uncertain future even environmental species attack by a virulent pathogen. This practice would result in an increased maintenance cost in order to remove and replace these unhealthy trees that are unable to survive and thrive.

Whether the value of the urban forest is defined by its socioeconomic benefits or its monetary value, paramount to the understanding of the importance of trees within

urban environments is a quantitative understanding of how many trees there are and their spatial distribution throughout the community. City-wide assessments of urban tree canopy cover have become common foundations for national and local governments to measure, assess and increase the number of trees and green spaces within their government areas.

Accurate benchmarks and ongoing assessments of tree canopy cover and green spaces allow local government agencies to continuously review the performance of ongoing greening initiatives as well as ensuring that future policies are not only adequate but achievable. For a city-wide assessment of the urban forest to yield actionable results, it is critical that it accurately accounts for trees on private as well as public land, as private land can account for over 50% of both urban tree cover and open space, thus, making a large contribution to the urban forest and its positive benefits.

Trees require adequate space and light to develop, with different requirements depending on the species. Planting periods should be scheduled to avoid being stressed by harsh weather. Because trees and their roots might hinder infrastructure, trees and urban forests should be sited and selected with existing electricity lines and subterranean infrastructure utilities in mind. This issue can be avoided or lessened by choosing the right location and trees.

6 Local Climate Change Impacts

Numerous studies have shown that urban trees provide socioeconomic value to communities through a variety of positive effects on the urban environment, including economic benefits (Elmqvist et al. 2015; Donovan et al. 2019), positive effects on community health, well-being, and safety, improved air quality, and storm water attenuation. It can be difficult to translate the socioeconomic benefits of the urban forest into economic terms, which are frequently used in decision-making and policy development. Despite this, quantifying the monetary value of trees can be beneficial because it allows for a quantitative understanding of the balance of benefits and drawbacks associated with green assets, which can help state and local governments integrate economic assessments more effectively into decision-making processes.

Food and water shortages, heat stroke, air pollution, and increased energy demand, as well as environmental consequences, are all caused by the concentration of population in urban areas. If cities are not carefully planned in terms of spatial arrangement, climate change is likely to exacerbate these issues. Increased energy demand is one of the most serious social issues associated with urbanisation. Energy demand in developing countries will skyrocket as a result of population growth, urbanisation, and climate change.

In general, urban climate, which is influenced by the urban heat island effect (a local phenomenon) and climate change, is strongly related to energy demand, including the use of air conditioning (AC) systems (global phenomenon). Because of the increased use of air conditioning systems when urban temperatures rise due to the heat island effect and climate change, energy demand rises. This process causes an increase in anthropogenic heat transfer from indoor to outdoor locations during the summer. The released anthropogenic heat exacerbates the heat island effect.

Stormwater flow is reduced because rainwater is intercepted on the leaves, branches, and trunks of urban trees and forests. Some of the water that is intercepted evaporates into the atmosphere, while others soak into the ground. This reduces the amount of water that must be stored in containment facilities as well as the amount of runoff that must be managed in urban areas.

7 Urban Forest Policy and Planning

Policy and planning for urban forests are critical to realising the vision of a resilient and sustainable urban forest that supports a liveable city and natural environment while also contributing to community well-being (Act Government 2021). This aligns with the global 2030 Sustainable Development Goals (SDGs) agenda, which focuses on Sustainable Cities and Communities (SDG 11), make cities and human settlements inclusive, safe, resilient, and sustainable; Climate Action (SDG 13), take urgent action to combat climate change and its impacts; and Life on Land (SDG 15), protect, restore, and promote sustainable use of terrestrial ecosystems, sustainably manage forest, combat desertification, and halt climate change (United Nations 2021).

In general, forest management policy creation aids governments in implementing effective urban forest planning, decreasing climate change effects, providing green-liveable living infrastructure, and conserving living ecosystems (Act Government 2021). For example, urban forest policies and legislation in the United Kingdom are generated from statutes in a wide range of sectors, including planning, forestry, nature conservation, plant health, transportation, services/utilities, and security (Lawrence and Dandy 2012). While acknowledging the importance of integrating relevant sectors and stakeholders in the effective implementation of policies and plans, Van Der Jagt and Lawrence (2019) suggested that there should be more emphasis on the correlation between understanding, assessment, and co-creation of urban forest values. This will result in a systematic shift toward a new and generally shared sense of duty for urban forest stewardship.

The urban forest strategies created in Australia, on the other hand, aim to protect and sustain the current urban forest, increase canopy cover, improve urban forest variety, and increase community knowledge and engagement. These plans follow the principles of sustainable urban forest management, which include preserving biodiversity, productivity, regeneration capacity, and the ability to perform important ecological, economic, and societal functions (City of Sydney Urban Forest Strategy 2013). Further, other countries can benefit from the Australian local

government's creative forest governance, known as nature-based solutions (NbS), to maintain, manage, and enhance natural systems in order to address environmental, biodiversity, and social concerns. In this context, strategic initiatives, plans, or programmes aimed at preserving and improving urban forests are a visible and often dominant aspect of NbS in cities.

7.1 Key Elements of Urban Forest Policies and Planning

Indeed, urban forests have helped to support a bigger ecology and a more sustainable environment, as well as facilitating rapid urban development. There are numerous critical components that governments and policymakers must emphasise when formulating policies connected to urban forest in the context of policy and legislative framework. The roles and duties of stakeholders in managing or administering urban forest planning, including government agencies and policymakers, are the first crucial element that must be focused on. According to Schwab (2009), three tiers of duties and responsibilities should be considered when designing applicable policies: (1) forestry and parks professionals, (2) associated professionals, and (3) the general public, developers, and elected officials.

Aside from the roles and responsibilities of the stakeholders, funding is the next important factor to consider while drafting applicable policies (Urban Sustainability Exchange 2014; Vibrant Cities Lab 2021). Maximising financial allocation and collaborating with partners such as corporations and the private sector will result in a win-win situation for the government, society, community, and country. As a result, programmes and activities resulting from policies established have positive externalities for the ecosystem and structure of the environment. Finally, assets such as facilities and infrastructure, as well as active support from federal, state, regional, and local governmental jurisdictions, community, non-profits, the private sector, and others, will allow the country's capacity to be fully utilised to achieve success in urban forest policy and planning. Regardless, other supporting components including timeliness, transparency, compact and efficient planning, diversity, sustainability, and resilience, as well as liveable and accessible planning, would improve urban forest policy and planning (Urban Sustainability Exchange 2014; Vibrant Cities Lab 2021; Australian Capital Territory 2021).

7.2 Implementation and Measuring Success of Urban Forest Policy and Planning

The United Nations defines a forest as "somewhere that has at least 20% trees" in order to obtain such a status of resilient and healthy urban forestry. Many countries, including the United Kingdom (London) and Japan (Tokyo), have received global recognition for their efforts to create sustainable and resilient urban environments. For example, London has been named the world's greatest urban forestry, with 21% of the capital's trees and woodlands functioning as a vital part of green infrastructure

(Time Out England Limited 2022). The expression “not taken for granted” has come to represent London’s continual efforts to preserve, manage, and improve the city’s current urban forest. These are some of the indicators of successful urban forest strategy and planning.

In addition, the London Urban Forest Partnership’s Urban Forest Plan (2020) outlined six key indicators, including: (1) 21% canopy cover, (2) 700,000 trees planted in London streets, (3) proportion of trees planted by borough (administrative unit), (4) 25% of woods in good condition, (5) number of boroughs with local urban forest plans, and (6) area of ancient woodland. All of these indicators are critical for tracking actual progress toward completing the Urban Forest Plan’s actions. Furthermore, Barron et al. (2016) used the Delphi Technique to rank the important indicators based on the consensus of a group of forestry professionals in a previous study. The data found that two crucial measures, (1) urban tree diversity and (2) physical access to nature, had a high mean. Furthermore, the author noticed that the canopy cover that covers the city is a frequent indicator used in a few researches. Scholars and practitioners identified these metrics to track the progress of any state in the country toward resilient and healthy urban forestry (Barron et al. 2016).

7.3 Issues and Challenges

The lack of explicit legislation relating to urban forestry is among the popular issues debated among academics and researchers (Sharma and Ghimire 2019). The authors estimated that roughly 65% of Nepalese people are uninformed of urban forestry since they have not been exposed to the problem. As a result, various environmental effects, including pollution, have resulted as a result of this situation. Furthermore, a lack of public awareness of the benefits provided by urban forests is another concern that has to be addressed by the relevant authorities (Nowak and Dwyer 2007). Aside from that, urban trees are typically viewed as a financial burden or a risk, despite the fact that the benefits they provide are often overlooked by the general public and decision-makers. One of the concerns and challenges in efficiently implementing regulations and managing urban forests is a lack of resources for proper care (Driscoll et al. 2015). As a result, these problems and obstacles must be addressed in order to properly implement policies that maximise the benefits of urban forests while ensuring their long-term viability.

8 Urban Forestry: Innovative Solutions and Future Potential

Because of the numerous economic, social, and creative opportunities that cities provide, people continue to flock to them; large cities are more productive than rural areas. Environments in urban areas magnify global threats such as climate change, water and food security, as well as resource scarcity. The world’s fastest-growing cities have experienced difficulties adjusting to growth and industrialisation,

crushing under the weight of pollution, traffic congestion, and urban poverty, among other things. However, as the digital revolution gained momentum, the concept of the modern citizen emerged as a framework for addressing these issues. To be truly effective, innovation in urban forestry must evolve and change over time. This is especially true for optimising space and resources, developing minimal infrastructure with a large impact, and identifying the best way to do so, which may involve mobilising citizens and following universal design principles that are applicable to the people of all ages and abilities.

9 Remote Sensing and GIS Data Fusion for Urban Forest Management and Research

Various governments around the world are currently attempting to address the issue of climate change. However, there are some significant knowledge gaps that must be addressed. One of the most important factors is the role of urban forestry. It has been discovered that urban green spaces aid in mitigating the effects of climate change by absorbing various pollutants, including greenhouse emissions, and thus serve as an important carbon sink in the pursuit of a low-carbon society. Greenery and urban forests have been shown to have numerous tangible and intangible benefits. Its growth is one method of bridging the gap between people and nature. The carbon cycle is disrupted as a result of urbanisation, as large areas of land are covered by built-up areas.

The importance of urban forest ecosystem services and appropriate sustainable management of urban forests in maintaining environmental health, improving urban ecosystem resilience, and improving urban life quality is well understood. Successful urban forest management necessitates timely and accurate information on the status, trends, and information related to urban forests at various temporal and spatial scales in order to provide a full spectrum of ecosystem services. Traditionally, such data has been gathered through random field sampling and visual interpretation of aerial photos, both of which are labour-intensive, time-consuming, and costly and do not cover large areas of interest. Remote sensing, using the most advanced techniques and sensors (e.g. light detection and ranging (LiDAR) technology, hyperspectral imagery, and high spatial resolution satellite imagery), now provides useful observational and analytical tools for assessing and quantifying urban forest dynamics at various spatiotemporal scales. For example, remote sensing techniques can detect, measure, map, inventory, classify, monitor, model, and evaluate the 3D structural (tree height, volume and size of foliage and stems), compositional (species richness and diversity), and functional (ecological processes) characteristics of an individual tree, urban forest patch, or all urban forests in large areas. The use of remote sensing in urban forestry has increased, particularly in terms of spatial and spectral quantification of biophysical dimensions of urban forests and associated ecosystem services.

Though it is obvious that trees play an important role in such dry environments, urban planners and architects have largely ignored this fact. In an urban forest

ecosystem, trees are the most important component. The use of satellite imagery to monitor the health of city trees benefits urban ecosystems. It is possible to detect and classify features even faster and more accurately by combining traditional methods with other geospatial technologies, such as remote sensing, and artificial intelligence to achieve “geoAI”. Satellite data has been proven to be useful in quantifying aspects of vegetation productivity, health, and change, according to research. For a variety of functions, spectral vegetation index (SVI) algorithms have been developed, all based on specific mathematical expressions that combine visible light radiation, primarily from the green spectra region (from vegetation), and non-visible spectra to obtain proxy quantifications of vegetation health. A GIS in a city allows for spatial analysis and modelling, which can help with a variety of important urban tasks. GIS is now moving beyond image analysis and into image interpretation. We’re not only receiving more data on a daily basis, but we’re also gaining the ability to extract a lot more information from it. This level of real-time data collection and AI-based interpretation is critical to meeting the needs of tomorrow’s cities, and it is a cornerstone of the IoN.

10 Community-Based Approach of Urban Forest

Citizen science’s fundamental concept—Citizen science has grown in popularity in urban forestry over the last decade, with municipalities and non-profits enlisting volunteers to collect tree data. Participatory research and civic ecology are two examples of related forms of public engagement that have brought diverse stakeholders into the fold of knowledge production and stewardship of urban green spaces. While these various approaches have different methodological basis, they all connect as a way of interacting as well as engaging the public in the study and management of urban trees: what we call civic science in urban forestry. The citizen-led effort is also making an appearance on the climate action initiative, where their efforts are being projected to cool strategies, green materials, and even food waste disposal. Some programmes’ initiatives went beyond tree planting to halt the widespread and treatable destruction of our urban tree canopy.

The seven pillars of inclusion (access, attitude, choice, partnership, communication, policy, and opportunity) have brought together these committed citizens, along with a slew of city government officials, to hear the science, practicality, and well-reasoned sentiment behind the pressing need to stop tree loss, implement a programme to manage our urban forest, and build a green infrastructure to combat the local climate change effects. Several organisations have successfully instilled this culture in the community. The following are some examples of successful projects and community-based urban forests that are currently in operation:

Success story 1: The Citizen Forester programme provides an excellent opportunity for individuals to learn how to plant, prune, and maintain trees in an urban setting. It also gives interested individuals the opportunity to get involved with local authority and county government entities and help their community care for its

public trees. Since its inception in 2006, the programme has graduated over 300 volunteers who have dedicated their time to their communities. ([Citizen Forester | Cross Timbers Urban Forestry Council \(ctufc.org\)](#))

Success story 2: Become a Citizen Forester through Participate Melbourne (Citizen Forester Program). Since 2011, the City of Melbourne has collaborated with residents to develop the Urban Forest Strategy and Urban Forest Precinct Plans for each of the city's ten precincts. This collaboration has sparked a lot of interest and participation in making Melbourne greener. The Citizen Forester Program was created to foster an insightful and greater sense of community in order to grow and improve one of Melbourne's urban forest. ([Citizen Forester | Cross Timbers Urban Forestry Council \(ctufc.org\)\(melbourne.vic.gov.au\)](#)).

Success story 3: Community Greening is a collaborative initiative to promote the environment for people and nature. They worked with the community to create sustainable green spaces and a vibrant tree canopy in order to strengthen our environment, economy, society, and health in an equitable manner. Transforming Urban Green Spaces | Community Greening ([Transforming Urban Green Spaces | Community Greening](#)|[Transforming Urban Green Spaces | Community Greening](#)).

Success story 4: Communitree's mission is to empower people to green degraded spaces with locally indigenous vegetation, thereby contributing to socioecological restoration. Communitree primarily works in public spaces, training and guiding members of the local community to restore indigenous vegetation in their own backyard (<https://www.communitree-app.com>).

Success story 5: Econinja, in collaboration with the Johor State Forestry Department and the Malaysian Scout Federation, will implement the Malaysian Greening Program 2021–2025. ECONINJA is a community-based social entrepreneurship company that offers sustainable technology solutions through game-changing revolutionary approaches, while leading the way for socially conscious communities ([Tree Planting – Econinja.my](#)).

Another high-tech approach to community-based greening was the use of the crowdsourcing principle. This has recently piqued the interest of many urban foresters and urban planners as a solution for extracting data and information from communities (Cui et al. 2021). Despite the fact that the technology has been around for a while, the VGI is the use of tools to create, assemble, and disseminate geographic data provided voluntarily by individuals (Goodchild 2007) and has returned with more significant implications for the community. This exploratory study has also shown that it is necessary to assess the potential advantages and disadvantages of using VGI as a tool for cooperative urban planning, particularly the accuracy and dependability of the data collected. This is due to the fact that the users and volunteers may come from different backgrounds and may not have received formal training in data collection. However, if the data collected are within the reliability threshold, it will have a significant impact on the volume, scale and speed of the data gathering process. Therefore, it is highly possible that the technology can be expanded and used for the development of a comprehensive urban forests

inventory. These results raise concerns about a potential digital divide in the use of VGI tree mapping applications by indicating potential differences in digital citizenship and literacy by neighbourhood type, which is in line with a recent call for research on the implications of the democratisation of data gathering operations through crowdsourcing.

11 The “Coming of Age” of Urban Forestry: The Citizen-Driven of Urban Forest (CDUF)

VGI has been heralded as a potentially transformative new data source for urban planning and policymaking. However, despite the promotion of VGI as a means of increasing access to geographic knowledge production, there are concerns about uneven levels of participation and spatial coverage. By georeferencing VGI data, the spatial distribution and data richness of urban forest can be provided. Thus, with such spatial data, detailed analyses can be conducted to ascertain sociodemographic influences, environmental indicators, and other climatic dependencies of urban forests. GIS analyses such as ordinary least squares (OLS), general linear models (GLM), and spatial autoregressive models will aid urban foresters and policymakers in making sound judgements.

Inclusion of the community in urban greening initiatives serves as a transformational initiative for a smart community. This strategy has quickly gained traction in western countries as well as some Asian countries. As it turns out, community-based urban greening is probably the simplest and least expensive way to improve the liveability and sustainability of our cities. Over the last few decades, it has become clear that incorporating green space into the planning, construction, and operation of our cities is not only an extremely effective way to alleviate some of these challenges but also generates a slew of economic, social, and environmental benefits, both for individuals and the city as a whole.

While recent digital urban tree inventories offer significant opportunities for collaborative data collection, innovative research, intelligence gathering, and improved policymaking, data asymmetries in terms of quantity and quality may seriously compromise the applications' effectiveness. As a result, it is important to formulate and implement a strategy for resolving these issues.

One establishment that can be referred, founded on the principles of inclusion and collaboration, Mapping Green Dublin developed a just greening strategy for one Dublin neighbourhood through a collaborative process. In order to empower local communities to act on greening projects in their neighbourhoods, Mapping Green Dublin's mission is to inform more socially just urban greening policy and practise and to demonstrate how community-based strategy development can make a significant contribution to the achievement of climate action goals, liveability goals, and well-being goals. As a result of their efforts, a new approach to developing greening strategies has been developed that is grounded in community, collaborative efforts, and a more comprehensive understanding of social and environmental justice. It demonstrates how bottom-up greening strategies can be developed in response to

and informed by grassroots concerns and aspirations and how these strategies can be implemented in practise (Mapping Green Dublin 2021).

12 Conclusion/Summary

Heat, wildfires, and flooding are all climate-related disturbances that can be mitigated by identifying and developing suitable habitat within specific ecological communities. For urban foresters, fully recognising which characteristics are important and where they should be used will be a continuous land management component. In light of the uncertainties surrounding these effects, land managers will need to continue to observe and document the effects of climate change on tree species, as well as refine models and management strategies. Maintaining species diversity and selecting appropriate species for projected changes in habitat suitability will become more difficult tasks for everyone, from land managers to the nursery industry. Land managers and other decision-makers will have more opportunities to engage with their communities as a result of climate change challenges, develop new partnerships and programmes, expand their volunteer base, and invest in more resilient landscapes. The devaluation of science in modern civilisation, with the advent of geospatial technology, is completely incomprehensible, especially when one considers history and the role science played in developing humanity's understanding of its environment, health, and security, as well as how important science is in everything, we take for granted today. Scientific breakthroughs that have been nothing short of miraculous have shaped everything from procreation to the food we eat, our lifespan, and the way we communicate. Although technology aids decision-making, it also serves as a jumping-off point for considering the management implications of climate change in an urban setting, as shown above. Initiatives to address climate change and the urban tree canopy on a regional and state level, as well as the creation of our own Citizen-Driven Urban Forest, are areas of potential growth in order to address these challenges beyond municipal boundaries.

Acknowledgements The authors would like to gratefully acknowledge financial support from Universiti Teknologi MARA and the Ministry of Higher Education under the Fundamental Research Grant Scheme (FRGS), FRGS/1/2019/WAB03/UITM/02/1.

References

- Act Government (2021) Urban forest strategy. https://s3.ap-southeast-2.amazonaws.com/hdp.au.prod.app.actyoursay.files/1916/170/8000/ACTs_Urban_Forest_Strategy_2021-2045.pdf. Accessed 14 Mar 2022
- Australian Capital Territory (2021) Urban-forest strategy, 2021-2045. https://hdpauprodappactyoursayfiles.s3.ap-southeast2.amazonaws.com/5616/1710/4101/Urban_Forest_Strategy_2021-2045.pdf. Accessed 14 Mar 2022
- Barron S, Sheppard SRJ, Condon PM (2016) Urban forest indicators for planning and designing future forests. *Forests* 7(9)

- City of Sydney Urban Forest Strategy (2013) Urban forest strategy. https://www.cityofsydney.nsw.gov.au//media/corporate/files/202007migrated/files_u/urban-forest-strategy-adopted-feb-2013.pdf?download=true. Accessed 14 Mar 2022
- Cui N, Malleon N, Houlden V, Comber A (2021) Using VGI and social media data to understand urban green space: a narrative literature review. *ISPRS Int J Geoinf* 10(7):425
- Donovan GH, Landry S, Winter C (2019) Urban trees, house price, and redevelopment pressure in Tampa Florida. *Urban For Urban Green* 38:330–336
- Driscoll AN, Ries PD, Tilt JH, Ganio LM (2015) Needs and barriers to expanding urban forestry programs: an assessment of community officials and program managers in the Portland—Vancouver metropolitan region. *Urban For Urban Green* 14(1):48–55
- Elmqvist T, Setälä H, Handel SN, Van Der Ploeg S, Aronson J, Blignaut JN et al (2015) Benefits of restoring ecosystem services in urban areas. *Curr Opin Environ Sustain* 14:101–108
- Goodchild MF (2007) Citizens as sensors: the world of volunteered geography. *GeoJournal*. 69(4): 211–221. CiteSeerX 10.1.1.525.2435. <https://doi.org/10.1007/s10708-007-9111-y>. S2CID 2105836
- Gu Y, You XY (2022) A spatial quantile regression model for driving mechanism of urban heat island by considering the spatial dependence and spatial non-stationary: an example of Beijing China. *Sustain Cities Soc* 103:692
- Khan A, Carlouena L, Feng J, Khorat S, Khatun R, Doan QV, Santamouris M (2022) Optically modulated passive broadband daytime radiative cooling materials can cool cities in summer and heat cities in winter. *Sustainability* 14(3):1110
- Kikegawa Y, Genchi Y, Yoshikado H, Kondo H (2003) Development of a numerical simulation system toward comprehensive assessments of urban warming countermeasures including their impacts upon the urban buildings' energy-demands. *Appl Energy* 76(4):449–466
- Kikegawa Y, Tanaka A, Ohashi Y, Ihara T, Shigeta Y (2014) Observed and simulated sensitivities of summertime urban surface air temperatures to anthropogenic heat in downtown areas of two Japanese Major Cities, Tokyo and Osaka. *Theor Appl Climatol* 117(1):175–193
- Kikegawa Y, Nakajima K, Takane Y, Ohashi Y, Ihara T (2022) A quantification of classic but unquantified positive feedback effects in the urban-building-energy-climate system. *Appl Energy* 307:118–227
- Kondo H, Genchi Y, Kikegawa Y, Ohashi Y, Yoshikado H, Komiyama H (2005) Development of a multi-layer urban canopy model for the analysis of energy consumption in a big city: structure of the urban canopy model and its basic performance. *Boundary-Layer Meteorol* 116:395–421
- Lawrence A, Dandy N (2012) Governance and the urban forest. In: *Proceedings of the urban trees research conference*. pp 143–158
- Li XX, Liu X (2021) Effect of tree evapotranspiration and hydrological processes on urban microclimate in a tropical city: a WRF/SLUCM study. *Urban Climate* 40:101009
- London Urban Forest Plan (2020) Working together to protect, grow and enhance London's urban forest. file:///C:/Users/amaly/Downloads/londonurbanforestplan_final.pdf. Accessed 14 Mar 2022
- Mapping Green Dublin (2021) Strategic pathways to community-led greening: a collaborative research project across Dublin 8. University College Dublin, Dublin
- Nakajima K, Takane Y, Kikegawa Y, Furuta Y, Takamatsu H (2021) Human behaviour change and its impact on urban climate: Restrictions with the G20 Osaka Summit and COVID-19 outbreak. *Urban Climate* 35:100728
- Nowak DJ, Dwyer JF (2007) Understanding the benefits and costs of urban forest ecosystems. In: *Urban and community forestry in the northeast*. pp 25–46
- Santamouris M, Kolokotsa D (2013) Passive cooling dissipation techniques for buildings and other structures: the state of the art. *Energy Build* 57:74–94
- Schwab JC (2009) Planning the urban forest: ecology, economy, and community development. American Planning Association. https://planning-org-uploaded-media.s3.amazonaws.com/legacy_resources/research/forestry/pdf/555.pdf. Accessed 14 Mar 2022

- See L, Estima J, Póddór A, Arsanjani JJ, Bayas JCL, Vatseva R (2017) Sources of VGI for mapping. *Mapp Citiz Sens* 13:13–35. <https://www.ubiquitypress.com/site/chapters/e/10.5334/bbf.b/>. Accessed 3 Mar 2021
- Sharma P, Ghimire P (2019) Assessment of opportunities and challenges of urban forestry in Nawalparasi District, Nepal. *Grassroots J Nat Resour* 2(1):1–2
- Su MA, Ngarambe J, Santamouris M, Yun GY (2021) Empirical evidence on the impact of urban overheating on building cooling and heating energy consumption. *Iscience* 24(5):102495
- Time Out England Limited (2022) Did you know that London is the world’s largest urban forest? <https://www.timeout.com/london/things>. Accessed 14 Mar 2022
- United Nations (2021). Department of Economic and Social Affairs Sustainable Development. <https://sdgs.un.org/>. Accessed 14 Mar 2022
- Urban Sustainability Exchange (2014) Urban Forest Management Plan (UFMP). <https://use.metropolis.org/case-studies/urban-forest-management-plan-ufmp>. Accessed 14 Mar 2022
- Van Der Jagt AP, Lawrence A (2019) Local government and urban forest governance: insights from Scotland. *Scand J For Res* 34(1):53–66
- Vibrant Cities Lab (2021) Planning: best practices in urban forestry. <https://www.vibrantcitieslab.com/toolkit/plan-the-total-program/>. Accessed 14 Mar 2022
- Webb RW, Rosenzweig CE, Levine ER (2000) Global soil texture and derived water holding capacities. Oak ridge national laboratory distributed active archive center. <http://www.daac.ornl.gov>

Part VII

Remote Sensing of Forest Engineering and Restoration



State of the Art on Airborne LiDAR Applications in the Field of Forest Engineering

Burak Aricak, Michael G. Wing, and Abdullah E. Akay

This chapter is dedicated to the cherished memory of
Mehmet Şahin ARICAK,
beloved father of Burak ARICAK.

Abstract

Managing forest resources in large landscape can be a highly time- and resource-consuming task requiring significant amounts of data collection in the field. Airborne Light Detection and Ranging (LiDAR) is one of the most effective remote sensing technologies for data collection and is capable of providing quick and accurate 3D point clouds from which vegetative cover and the ground surfaces can be discerned. LiDAR-based 3D point clouds and derivative products are used in a number of forestry activities including forest inventory and management, forest operations, fire modeling and biomass and carbon storage estimations. In particular, high-resolution digital elevation models (DEMs) produced from point clouds can assist forest engineers in performing harvesting planning and forest road design. Also, LiDAR-produced tree lists can be mapped on a DEM and can be used for planning of landing areas, skid roads, and cable corridors. In this chapter, a comprehensive overview to the use of LiDAR technology in the field of forest engineering is discussed by reviewing previously conducted studies. Firstly, basic principles of operating LiDAR technology are provided, and then the progress and opportunities of using LiDAR technology in

B. Aricak (✉) · A. E. Akay

Faculty of Forestry, Forest Engineering Department, Bursa Technical University, Bursa, Turkey
e-mail: burak.aricak@btu.edu.tr

M. G. Wing

Forest Engineering, Resources and Management Department, College of Forestry, Oregon State University, Corvallis, OR, USA

various forest engineering applications are presented. These applications include 3D forest road design, road geomatics, road construction, earthwork allocation, forest transportation, forest operation, sediment prediction, and logging impact assessment. The results derived from these previous studies suggested that LiDAR technology has the potential to offer highly reliable and accurate 3D surface data when compared to the estimations of ground-based surveys. Thus, airborne LiDAR is a rapidly developing technology which provides a great potential for efficiently performing forest engineering activities quickly and accurately over large landscape areas.

Keywords

Airborne LiDAR · 3D road design · Earthwork allocation · Transportation network · Forest operation planning · Impact assessment

1 Introduction

In order to ensure multiple uses of forest resources while protecting the forest ecosystems, the forests should be planned and managed by using modern methods and cutting-edge technologies. In this context, using information technologies such as remote sensing, Geographic Information Systems (GIS), and digital image analysis has increased in variety of the forestry applications. Thus, the need for spatial data with high accuracy and resolution about forest resources has increased accordingly. Typically, spatial data used in the field of forestry were products derived from satellite images, aerial photographs, and topographic maps.

In recent decades, airborne laser scanning (LiDAR, Light Detection and Ranging) technology has been used quite effectively in forestry applications (Akay et al. 2014). Even though LiDAR technology is considered to be a cost-intensive method due to the high initial setup cost, generation of spatial data with LiDAR technology is a quick and less expensive method when compared to photogrammetric methods and terrestrial measurements. Using LiDAR technology, a digital elevation model (DEM) with high resolution and accuracy can be produced for open areas as well as for sparse or dense forested areas. In addition, high-quality spatial data on the structural properties of forest trees can be obtained with LiDAR technology (Li et al. 2013). Laser-based high-resolution DEMs and structural data are used in a number of forestry activities including taking forest inventory, developing forest fire models, planning forest harvesting, and estimating biomass and carbon storage (Akay et al. 2009). In this chapter, an overview of the state of the art studies related to airborne LiDAR applications in the field of forest engineering was given under three research lines including basic principles of LiDAR technology, 3D forest road design and road geomatics, forest transportation and forest operations, and logging impact assessment.

2 Basic Principles of LiDAR Technology

LiDAR laser scanning technology has been applied in forested settings for several decades with published studies beginning to appear with consistency in the early 2000s (Reutebuch et al. 2005). LiDAR sensors that are ground-based and mounted on a tripod or other platform are referred to as terrestrial LiDAR systems. LiDAR sensors mounted on moving ground-based vehicles are sometimes referred to as mobile LiDAR systems (MLS). LiDAR sensors can also be mounted on manned or unmanned aircraft systems (UAS). There are great differences in the cost and functionality of each of these primary LiDAR platforms, but the operating principles are the same regardless of platform.

LiDAR scanning involves directing discrete pulses of light toward landscapes and structures in order to return feature positions and dimensions. LiDAR scanning pulses are located in the near-infrared position of the electromagnetic spectrum. LiDAR sensor pulses are emitted from a sensor and travel until reaching an object. The structure and reflectivity of the object affect whether a light pulse, or some portion of it, is reflected back to the sensor or continues to travel until reaching a solid surface, such as the ground, and is reflected back. Up to five reflected values can be returned from a single pulse with each representing a difference distance, referred to as range, from the LiDAR sensor. By comparing the reflection return time to the speed of light, the range to a feature can be calculated. Repeat return combinations can be fused with other return pulses to create a LiDAR point cloud that supports a three-dimensional visualization of landscape features from which feature measurements can be taken.

Terrestrial LiDAR objectives are typically much more limited in scale in comparison to airborne applications as the sensor is generally mounted on a fixed tripod or on a moving vehicle that must follow a trail or road (Garms et al. 2020). Regardless of mounting configuration, airborne applications will usually cover larger areas and have the advantage of less constrained positioning.

With airborne LiDAR applications, the round-trip travel time of individual light pulses is measured and stored by an airborne sensor that is coordinated with an on-board global positioning system (GPS). The combination of pulse and GPS measurements results in the geo-referencing of return pulses that allows coordinates (longitude and latitude) and height (elevation) to be associated with each returned pulse. In addition, an inertial navigation system (INS) mounted on the aircraft tracks irregularities in flight path and attitude (yaw, pitch, and roll), and all measurement data are stored on an on-board data storage. Up to 2,000,000 pulses per second can be generated with modern aerial LiDAR systems (Leica 2022) with pulse rates for the typically smaller LiDAR UAS-mounted sensors averaging around 300,000 pulses per second. Pulse rates at high frequencies can lead to LiDAR databases that require hundreds of gigabytes for even modest sized areas (e.g., 2000 ha). A variety of commercial and freely available image processing software can be used to convert the millions or more of return pulses that are typical of LiDAR data projects into two- and three-dimensional representations of landscape characteristics including streams, roads, vegetation, and structures (Fig. 1).

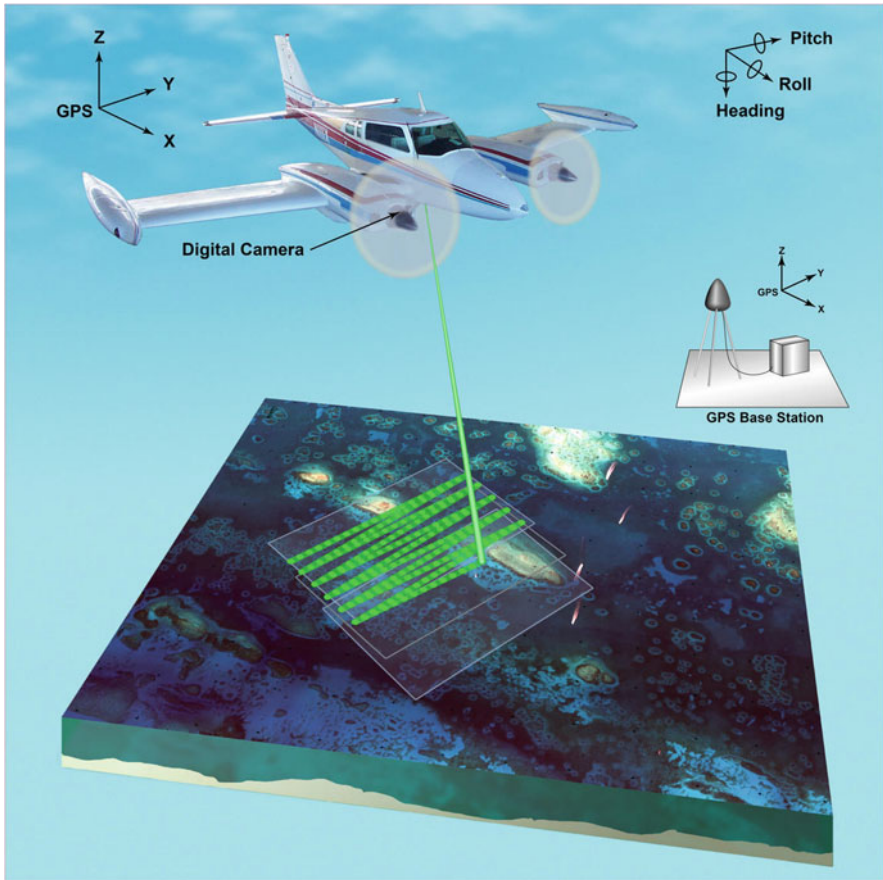


Fig. 1 LiDAR plane (URL-1 n.d.)

Costs vary substantially between manned and UAS LiDAR platforms with manned systems costing substantially more. For manned aircraft, a minimum crew of two is usually involved with a pilot and LiDAR operator. The aircraft itself will cost at least approximately \$300,000, and a very basic the LiDAR sensor will be at least approximately \$100,000. In addition, a survey-grade GPS and an INS will be needed with costs beginning in the tens of thousands of dollars for each of these devices. The strong benefit of manned LiDAR applications is that they will typically be able to cover a much larger area than UAS.

UAS platforms for LiDAR sensors will vary between approximately \$15,000 and \$60,000 depending in part at least on the quality of GPS and INS components. LiDAR sensors with multiple pulse return capability will vary between approximately \$12,000 and \$40,000 depending on size and functionality. Ranges to objects will be more constrained with UAS LiDAR sensors and will need to be within a



Fig. 2 Velodyne HDL-32 LiDAR sensor (silver cylinder on bottom of aircraft) mounted on a DJI s1000 quadcopter

range of approximately 100–200 m. Within the USA, only a single operator is required to pilot a UAS, but this rule varies in other countries (Fig. 2).

Potential LiDAR products that are relevant to forest engineering include point clouds, from which digital elevation models (DEMs) and digital surface models (DSMs) can be produced. A point cloud is the combination of all LiDAR pulse returns with each being stored as a point with latitude, longitude, and elevation coordinates (Fig. 3). A DEM is the ground surface with aboveground objects such as structures or trees not being considered. A DSM represents features above the ground surface and can be used to create a canopy surface model (CSM) to represent canopy heights. A variety of software packages and approaches are available to work

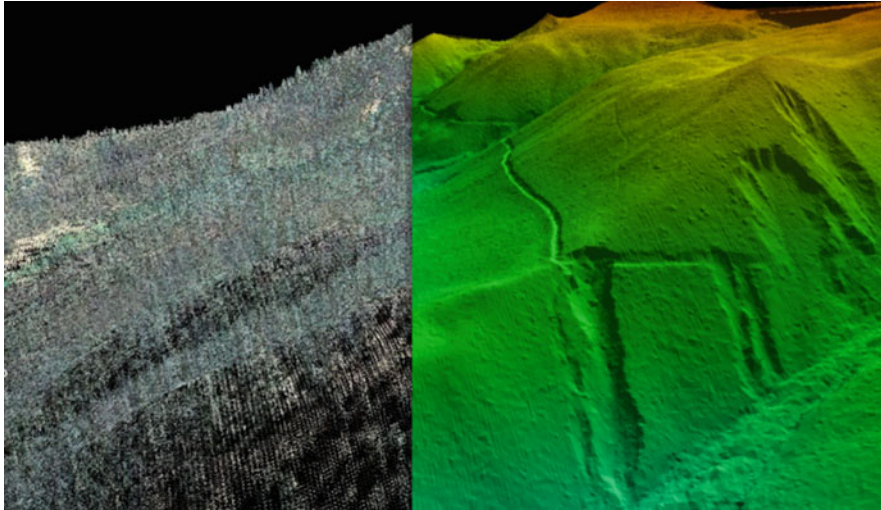


Fig. 3 LiDAR point cloud on left and digital elevation model on right (URL-2 [n.d.](#))

with point clouds and CSMs to create a tree list that represents the locations and heights of individual trees (Edson and Wing 2011; Maturbongs et al. 2019).

In addition to calculating position and height measurements, the reflectance intensity of each LiDAR pulse can be measured and geo-referenced. Researchers have found that the strength of reflectance intensity values can be analyzed to provide descriptive information about landscape features that goes beyond distances, areas, and volumes. Reflectance intensity is quantified by comparing the strength of the reflected pulse to that of the emitted pulse to create a ratio. Reflectance intensity provides a spectral signature that can be used to determine the health or nature of landscape objects and has been applied in previous studies related to forest engineering topics. Wing et al. (2010) used intensity values to discriminate live from mortally burned trees in a postfire landscape. Li et al. (2021) applied intensity values to assist in road detection. Li et al. (2021) found that intensity values helped improve tree species classification.

LiDAR has shown great potential in forest engineering applications in generating high-resolution point clouds from which DEMs, DSMs, and tree lists can be created. The cost of LiDAR per hectare is variable and depends on study area size with larger areas providing stronger economies of scale than smaller areas. Although the cost of acquiring LiDAR data may still be prohibitive for many organizations, larger areas (>5000 ha) can likely be flown at a cost of approximately \$2–5/ha with costs expected to decrease in the future.

3 Forest Road Design and Road Construction

Traditional forest road design methods employing topographic maps and aerial photos are not capable of locating optimum road alignment. However, computer-assisted forest road design models using high-resolution DEMs can provide optimum alignment by systematically searching a large number of alternative paths while considering economic, social, and environmental constraints. In recent years, LiDAR-derived DEMs have been effectively used in forest road design models (Akay et al. 2014).

The average-end area method and prismatic method are traditionally used for estimating earthwork, but the average-end area potentially overestimates the volume, while the prismatic method is more suitable for linear profiles. To overcome the drawbacks of conventional methods, Dodson et al. (2001) developed a new computer-based model to perform earthwork allocation by using a high-resolution DEM generated based on airborne LiDAR data. In this model, road engineers only need the series of center points along the road section to compute earthwork volume. The earthwork volume is the difference between actual ground surface elevation and the designed road surface elevation (Fig. 4). Dodson et al. (2001) reported that the model using LiDAR-derived DEM could accurately and quickly estimate the earthwork volume while spending less time for field measurements. In addition, the model allowed road engineers to evaluate a large number of alternatives and to select the optimum solution from among them.

Aruga et al. (2005) developed a road design model that simultaneously optimized the horizontal and vertical alignment of a forest road. In the solution process, the “Tabu Search” method was used to search for the optimum road alignment among computer-generated alternative solutions. In the model, a DEM was generated based on airborne LiDAR data taken from the Capitol State Forest in Western Washington (USA). In the model, the vertical alignment was first optimized, and then the horizontal and vertical alignments were optimized simultaneously. The results suggested that the model using LiDAR-derived DEM would be an effective tool

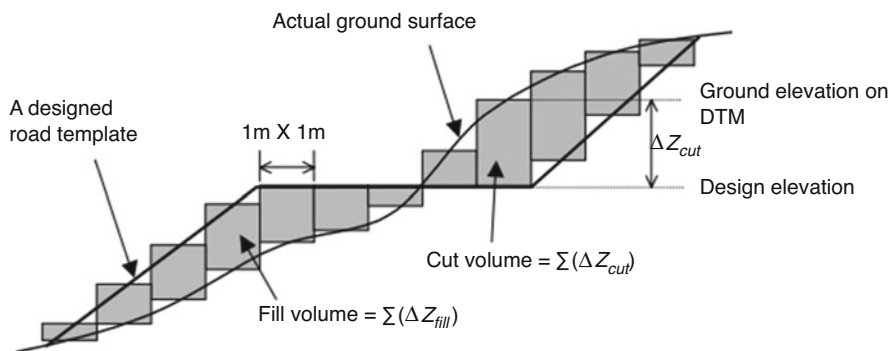


Fig. 4 Cross-section view of the road template (Dodson et al. 2001)

for designing optimum forest road alignment while eliminating the time-consuming process of road surveys.

Akay and Sessions (2005), using modern optimization methods and GIS techniques, developed a 3D interactive forest road alignment optimization model (TRACER) to help determine the forest road route with the minimum total road cost. In this model, “simulated annealing,” a “heuristic” method, was used to determine the vertical route with the least total road cost, while a linear program (DP) was used to balance the cut and fill volumes, which also minimized the earthwork cost. The starting route was developed by interactively locating intersection points on the on-screen 3D image of the terrain generated based on LiDAR-derived high-resolution DEM. At the same time, the model presents information such as soil type, distance to the nearest stream, road slope, length of road section, and deflection angle in horizontal and vertical alignment for determination of curves to the user in real time. Then, the model automatically places the horizontal and vertical path, taking into account the geometric, environmental, and driver safety conditions.

Saito et al. (2008) conducted a study where forest road constructions based on a topographic map-based DEM (with 10 m GSD) and LiDAR-based high-resolution DEM (with 1 m GSD) were compared. The LiDAR data was taken by a helicopter from the Funiyu Experimental Forest in Japan. The results indicated that the differences between actual road profiles of road constructed before the LiDAR measurements and LiDAR-derived DEM-based road profile were less than that of road profile generated based on the 10 m grid DEM. Saito et al. (2008) reported that the ground surfaces produced by LiDAR data accurately represented actual ground surfaces. Thus, using LiDAR-derived DEMs can assist road engineers to evaluate number of alternative road alignments to determine the optimum one with minimum construction costs.

Craven and Wing (2014) investigated the accuracy of airborne LiDAR data for examining the condition of forest roads to make sure that a stinger-steered log truck could be used for hauling. The field-based observation of forested road conditions was compared to measurements of forest roads estimated based on LiDAR technology which could detect the ground surface under tree canopies. The horizontal and vertical accuracy of LiDAR to locate centerlines along existing forest roads was considered within four stand structures including clear-cut, evenage, unevenage, and mature. The capability of estimating road grade and horizontal curve radius using the LiDAR-based approach was evaluated. The results indicated that airborne LiDAR would be sufficient to evaluate specified road geometries such as road grade and curve radius. In addition, the curves that are limiting can be defined by the LiDAR-based approach and further field inspection could verify limiting conditions.

4 Forest Transportation and Forest Operations

LiDAR data obtained from forest lands can provide high-quality 3D data on stand characteristics and terrain conditions. LiDAR-derived 3D data has been effectively used in forestry applications such as planning forest transportation and operations in

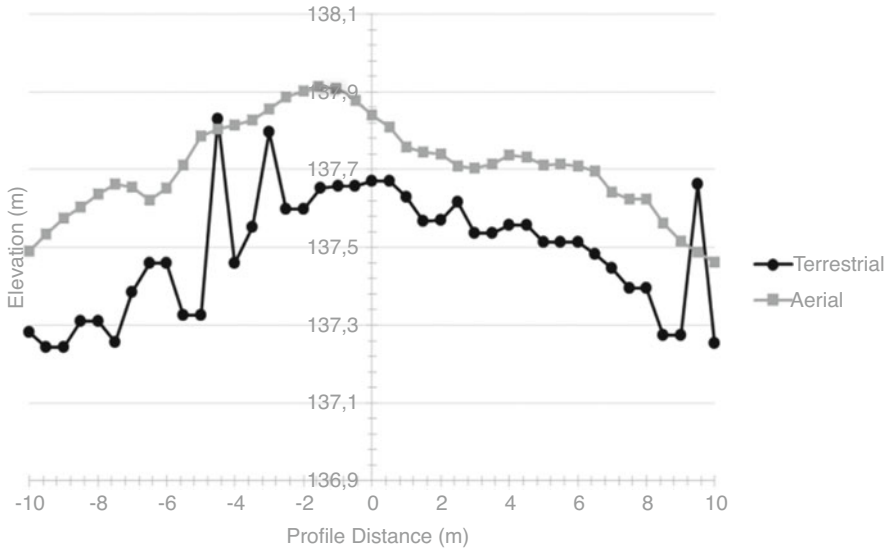


Fig. 5 The road profiles developed by using aerial LiDAR datasets compared to terrestrial dataset (Beck et al. 2015)

that manner. Utilization of GIS techniques can assist forest managers to search for the optimum timber extraction paths among a large number of alternatives and to determine hauling routes for truck transportation from landing to the mills. Chung et al. (2004) used a network-based heuristic algorithm to generate a solution for a cable logging and forest transportation planning problem based on a high-resolution DEM developed from airborne LiDAR. The results indicated that employing LiDAR-derived DEM with high-resolution improved the capabilities of the model.

González et al. (2008) stated that LiDAR-derived data allowed the recognition of ground morphology to assign with the accuracy of the forest harvesting machinery allowing the delineation of harvest units for spatial forest planning in their study in the eastern of the coast mountain of BioBio Region, Chile. González et al. (2008) presented the evaluation of the LiDAR DTM data over a planted forest field in order to use a forest harvest machinery assignment procedure in order to finally delineate harvest units for spatial forest planning.

Beck et al. (2015) conducted a study where a model was developed to generate a digital database for forest transportation planning using airborne LiDAR data. The road extraction process was implemented based on LiDAR data from McDonald-Dunn Research Forest located near the city of Corvallis, Oregon (USA). Two main attributes including LiDAR intensity data and ground return density were utilized. Figure 5 indicates the road profiles generated based on terrestrial and aerial LiDAR datasets in the study. The results proved that this methodology is useful in evaluating the accessibility of the hauling vehicles through extraction of the road geometry

considering the whole forest road network. Based on road geometry data, hauling vehicles with suitable sizes could be selected to transport large size forest products.

Waga et al. (2020) conducted a study to evaluate the forest road status by using airborne LiDAR data obtained from a coastal forest in northern Vancouver Island in Canada. Considering the vegetation existence, the road segments were classified in four groups including no vegetation, minor vegetation, dense understory vegetation, and dense overstory vegetation. The results obtained based on LiDAR data were compared to the field observation data. It was found that LiDAR-based classification was correct for about 75% of road segments when compared with the field observations. The accurate identification of road conditions provided valuable information for the road engineers to locate the road segments that might need repair or maintenance. In addition, Waga et al. (2020) suggested that LiDAR-derived DEM and canopy cover data could be effectively used for planning forest operations.

5 Logging Impact Assessment

Forest operations, particularly logging activities, may cause significant impact on forest resources when they are not planned or not implemented appropriately in the field. In order to detect logging impact on forest ecosystems, stand properties and forest ground conditions should be accurately measured. Capable of detecting both the forest floor and canopy elements, airborne LiDAR can estimate forest structure parameters with accuracy and precision. d'Oliveira et al. (2021) found the location and magnitude of the stand disturbance as a result of logging activities based on airborne LiDAR data and a RGB camera mounted on an unmanned aerial vehicles (UAV). In the solution process, the loss of above-ground biomass (AGB) due to logging was determined by using two methods including LiDAR-based method and RGB-photogrammetry integrated with LiDAR. The study area was located in the Antimary State forest within the border of Amazon Forests in Brazil. The results demonstrated that once the terrain is represented accurately, the location of the selective logging and its impact can be determined by using RGB-photogrammetry.

In a study conducted by Ellis et al. (2016), the impact of forestry operations including hauling, skidding, and felling was measured during a selective harvesting activity in a tropical forest. For this purpose, a model based on LiDAR-derived DEM was used to generate the digital layers for skidding paths and truck transportation road network in East Kalimantan in Indonesia, LiDAR-delineated skidding/felling impact zones (blue), and hauling impact zones (orange) in the cutting block which are shown in Fig. 6. According to the results, logging impacts can be effectively measured using airborne LiDAR data.

Akay et al. (2014) used a road design model, TRACER (Akay and Sessions 2005) developed based on an airborne LiDAR-derived high-resolution DEM, to estimate the sediment reduction cost for the forest roads. In the study, LiDAR data was obtained from the McDonald-Dunn Research Forest in Corvallis, Oregon (USA). In the solution process, optimum road alignments were generated for two scenarios. In the first scenario, TRACER searched for the optimum road alignment that

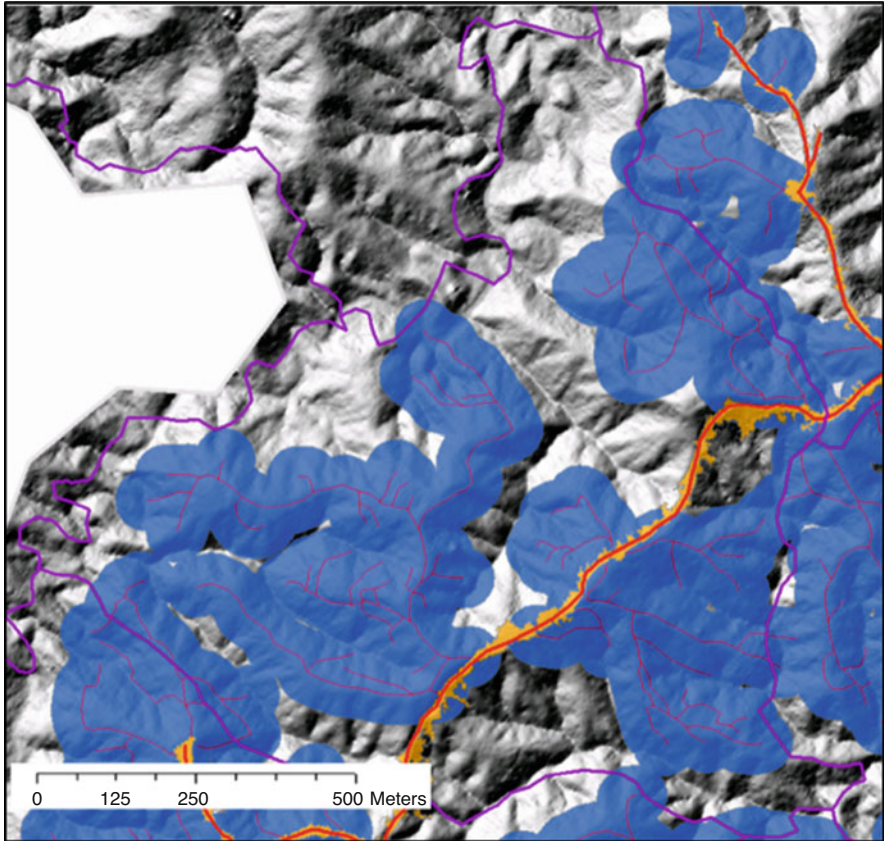


Fig. 6 LiDAR-delineated skidding/felling impact zones (blue) and hauling impact zones (orange) in the cutting block (Ellis et al. 2016)

minimized the minimum total cost, while the road alignment with minimum sediment yield delivered to stream was found in the second scenario. The average annual volume of sediment delivered to a stream from road networks was estimated based on a GIS-based sediment prediction model (SEDMODL). Then, additional cost of minimizing sediment yield in the second scenario was computed by computing the difference between the total road cost in both scenarios. The results indicated that the cost of reducing sediment delivery to the streams was about \$10,702/ton.

6 Conclusion

LiDAR capabilities continue to mature in terms of sensors and options for mounting sensors. This maturation also includes prices that tend to decrease over time for LiDAR data capture and processing. Forest engineering operations have benefited greatly from LiDAR data with the ability to discern, map, and measure individual features such as trees and roads. DEMs and DSMs can be derived from point clouds with both commercial and freely available software. The combination of these three databases can provide one of the most fundamental needs for forest engineers: a tree list containing the coordinates and height of all trees in a landscape. Tree lists will, at least currently, not be 100% accurate, but LiDAR has the ability to produce very reliable tree lists that are suitable for planning forest operations and for estimating forest inventory. It is likely that LiDAR will continue to improve with enhanced sensors and with greater flexibility in how sensors can be brought to the forest.

Authors' Contributions All authors performed the same effort in this study. All authors wrote, read, reviewed, and decided to submit chapters of the book.

Conflict of Interest No conflict of interest

References

- Akay AE, Sessions J (2005) Applying the decision support system, TRACER, to forest road design. *West J Appl For* 20(3):184–191
- Akay AE, Oguz H, Karas IR, Aruga K (2009) Using LiDAR technology in forestry activities. *Environ Monit Assess* 151(1):117–125
- Akay AE, Wing MG, Sessions J (2014) Estimating sediment reduction cost for low-volume forest roads using a LiDAR-derived high-resolution DEM. *Baltic J Road Bridge Eng* 9(1):52–57
- Aruga K, Sessions J, Akay AE (2005) Application of an airborne laser scanner to forest road design with accurate earthwork volumes. *J For Res* 10(2):113–123
- Beck SJ, Olsen MJ, Sessions J (2015) Automated extraction of forest road network geometry from aerial LiDAR. *Eur J For Eng* 1(1):21–33
- Chung W, Sessions J, Heinimann HR (2004) An application of a heuristic network algorithm to cable logging layout design. *Int J For Eng* 15(1):11–24
- Craven M, Wing MG (2014) Applying airborne LiDAR for forested road geomatics. *Scand J For Res* 29(2):174–182
- d'Oliveira MVN, Figueiredo EO, de Almeida DRA, Oliveira LC, Silva CA, Nelson BW et al (2021) Impacts of selective logging on Amazon forest canopy structure and biomass with a LiDAR and photogrammetric survey sequence. *For Ecol Manag* 500:119648
- Dodson E, Chung W, Akay AE, Sessions, J (2001). Optimization of forest road layout using a high resolution digital terrain model generated from LIDAR data, first international precision forestry symposium, 17–20 June. University of Washington, College of Forest Resources, Seattle, Washington, USA. pp 125–129
- Edson C, Wing MG (2011) Airborne light detection and ranging (LiDAR) for individual tree stem location, height, and biomass measurements. *Remote Sens* 3(11):2494–2528
- Ellis P, Griscom B, Walker W, Gonçalves F, Cormier T (2016) Mapping selective logging impacts in Borneo with GPS and airborne Lidar. *For Ecol Manag* 365:184–196

- Garms CG, Simpson CH, Parrish CE, Wing MG, Strimbu BM (2020) Assessing lean and positional error of individual mature Douglas-fir (*Pseudotsuga menziesii*) trees using active and passive sensors. *Can J For Res* 50(11):1228–1243
- González D, Becker J, Torres E, Albistur J, Escudero M, Fuentes R et al (2008) Using LiDAR technology in forestry harvest planning. In: 8th International conference on LiDAR applications in forest assessment and inventory, Edinburgh, UK
- Leica (2022) Leica TerrainMapper-2 flexible linear-mode LiDAR sensor. <https://leica-geosystems.com/en-us/products/airborne-systems/topographic-lidar-sensors/leica-terrainmapper-2>. Last Accessed 18 Feb 2022
- Li J, Hu B, Noland TL (2013) Classification of tree species based on structural features derived from high density LiDAR data. *Agric For Meteorol* 171–172:104–114
- Li H, Hu B, Li Q, Jing L (2021) CNN-based individual tree species classification using high-resolution satellite imagery and airborne LiDAR data. *Forests* 12(12):1697
- Maturbongs B, Wing MG, Strimbu B, Burnett J (2019) Forest inventory sensitivity to UAS-based image processing algorithms. *Ann For Res* 62(2):87–108
- Reutebuch SE, Andersen HE, McGaughey RJ (2005) Light detection and ranging (LIDAR): an emerging tool for multiple resource inventory. *J For* 103(6):286–292
- Saito M, Aruga K, Matsue K, Tasaka T (2008) Development of the forest road design technique using LiDAR data of the Funyu experimental forest. *J For Plan* 13(Special Issue):147–156
- URL-1 (n.d.). <https://www.usgs.gov/media/images/lidar-plane>. Last Accessed 15 Feb 2022
- URL-2 (n.d.). <https://www.usgs.gov/media/images/lidar-point-cloud-vs-bare-earth-dem>. Last Accessed 15 Feb 2022
- Waga K, Tompalski P, Coops NC, White JC, Wulder MA, Malinen J, Tokola T (2020) Forest road status assessment using airborne laser scanning. *For Sci* 66(4):501–508
- Wing MG, Eklund A, Sessions J (2010) Applying LiDAR technology for tree measurements in burned landscapes. *Int J Wildland Fire* 19(1):104–114



Restoration of Damaged Forest and Roles of Remote Sensing

Kyungil Lee, Jieun Ryu, and Seung Hee Kim

Abstract

Ecological damage refers to the reduction in the value of the environment due to human activities and natural disasters such as climate change and biological disease. The area where ecological damage mainly occurs is the forest, and restoration and management of damage are more important than other ecosystems. If a damaged forest is left unattended, secondary damage such as landslides is highly likely, so it should be restored prior to other ecosystems. The intensity of forest damage is worsening worldwide, and the importance of forest restoration projects at the national level is increasing. However, it is difficult to proceed forest restoration owing to lack of data on location and features of damaged forestry or vegetation species. In the absence of data on damaged forest, policy decision such as restoration prioritization and planning becomes difficult. In this chapter, we provide an overview of the current state of research to detect damaged forest using remote sensing and of the main findings and methodological challenges therein. In addition, the use and role of remote sensing to establish legally appropriate ecological restoration including forest at the national level will be introduced. The results will suggest the importance of remote sensing for the identification and appropriate restoration approaches for damaged forests.

K. Lee (✉)

AI Semiconductor Research Center, Seoul National University of Science and Technology,
Nowon-gu, Seoul, Republic of Korea
e-mail: leedake@seoultech.ac.kr

J. Ryu

Inchoen Climate and Environment Research Center, Yeonsu-gu, Incheon, Republic of Korea
e-mail: jjieun@ii.re.kr

S. H. Kim

Schmid College of Science and Technology, Chapman University, Orange, CA, USA
e-mail: sekim@chapman.edu

Keywords

Optical remote sensing · Change detection · Forest restoration · Earth observation · Deep learning

1 Introduction

Forest ecosystems are an integral part of many terrestrial ecosystems, providing a wide range of ecological, economic, social, and cultural services (Chen et al. 2015). In addition, many more depend on forests for other critical ecosystem services, such as climate regulation, carbon storage, human health, and the genetic resources underpin wood products (Wingfield et al. 2015). However, both natural and managed forests are more profoundly threatened than before. Forest degradation is generally recognized as disturbance caused by human actions in a forested landscape and is usually defined by FAO as a reduction of the capacity of the forest to provide goods and services (FAO 2010). Various environmental change caused by anthropogenic activities or natural phenomena has increased forest vulnerability to a range of natural disturbances including diseases and insects (Boyd et al. 2013; Reed et al. 2007). Natural disasters such as forest fires and landslides are mainly human-caused damage, so it is difficult to restore them. In particular, forest fires threaten not only forest vegetation and habitats but also the underlying environment for restoration through changes in physical and chemical properties of soil due to oxidation and incineration of soil seeds. Large-scale damage to forest ecosystems causes not only ecological damage to forest resources and wildlife but also natural disasters such as landslides and global carbon emissions.

The social demand for restoration of damaged forest is increasing, as is the importance of the role of policy for restoration projects. However, in the absence of information of the damaged forests such as location, area, and damaged type, difficulties in policy decisions for restoration inevitably arise. Monitoring deforestation for restoration requires an estimate of the area clearly, and characteristics for restoration such as average carbon content for each hectare of a given forest type should also be measured (Goetz et al. 2015). In this regard, the role of remote sensing in restoration planning and monitoring has increased, especially in the last decade, owing to improved sensor technology and data availability (Nagendra et al. 2013). Remote sensing tools and technologies have been used to track land-cover change around various areas including forest (Reif and Theel 2017; Scharsich et al. 2017). Its main advantages involve its capacities to provide extensive information on land cover and areas of damaged forest as well as analyze natural biophysical characteristics for restoration (Lu et al. 2004).

In this chapter, we present an overview of remote sensing research, focusing on meta-studies, case study research that detect damaged or changed forests using various methods including artificial intelligence technology and implications for restoration. This chapter is organized into four sections: Sect. 2 an introduction to the research on remote sensing applications in forestry, Sect. 3 a review of the

findings of these studies on the trends of remote sensing in forest monitoring, and Sects. 4 and 5 classifications of approaches for ecological restoration and the role of remote sensing techniques in forest restoration.

2 Remote Sensing Application in Forestry

Historically, the most important change in land use which is done by people has been destroying forests and converting forests into agricultural lands and habitats (Lausch and Herzog 2002). So, assessment of forest degradation is one of the main targets of monitoring land-cover changes over the past decade (Miettinen et al. 2014). Foresters and researchers have relied on aerial photography, aerial sketch mapping, and ground sampling techniques to check this forest degradation and renew forest inventory records (Heller et al. 1959; Nelson 1983). However, inventory techniques like ground surveys are useful and possible to detect accurately but burdensome, and catastrophic disasters such as forest fire can quickly change the quantity and quality of the forest (Nelson 1983). For example, leaf area index (LAI) is one of the most significant indicators in forestry studies. It is an indicator of forest ecological processes such as rate of photosynthesis, transpiration, and net primary production, and it can predict and analyze the state of the forest (Pierce and Running 1988; Meyers 1987). Around 1980, before the use of remote sensing was activated in forestry, most research on LAI estimation used ground-based data and methods, which were exceedingly time-consuming and difficult to acquire the large-scale spatial and temporal variability (Lagomasino et al. 2014; Wang et al. 2019; Weaver et al. 1986).

Remote sensing methods are suited for early-stage detection and evaluations when accessibility for ground surveys is difficult or still not possible, as the area needs to be cleared to provide access and security (Mokroš et al. 2017). Since the late 1970s after Landsat 1 was launched in 1972, remote sensing instruments such as multispectral scanner (MSS) and thematic mapper (TM) on Landsat satellite have been recognized for offering a synoptic view data acquiring from an altitude of 705 km (Rock et al. 1986). A single Landsat scene produced an image of a ground area measuring 185 km on a side which make researchers design damage assessment surveys, but traditional aerial photography was not able to provide this information (Heller 1978). In addition, TM's spectral coverage extends out into the reflected infrared that was being used for vegetation biomass and physiological status monitoring (Tucker 1979). Due to these reasons, researchers have suggested that satellite images might best be utilized as the first stage in a multistage sampling design, for various areas including forest and researchers have begun to perform analysis using satellite images (Heller 1978; Robinove et al. 1981). Unlike traditional aerial photography for monitoring, satellite images such as Landsat are provided as bands separated by spectral values over a wide area. Temporal Landsat data have been useful for monitoring noteworthy levels of forest canopy alteration, as only change versus unaltered areas need to be described, and once change areas are identified, ground observations would be proceed more easily to provide the

details necessary for making management decisions. Therefore, the researchers tried to study various approaches to detect, identify, and quantify forest decline symptoms through using of this multispectral and multitemporal data sets (Heller 1978; Maxwell 1976; Rock et al. 1986; Rouse Jr et al. 1973; Tucker 1979).

Forest change detection approaches using digital satellite data could be distinguished by (1) the data transformation procedure and (2) the analysis techniques used to delineate areas of significant modifications (Nelson 1983). Representative methods of the data transform procedure approach include simple visual differencing, rationing, and vegetation index differencing. The ratio transformation is a mathematical operand on the same data sets. Todd (1977) made temporal overlays combining Landsat band 5 data from October 1972 and 1974 using General Electric Image 100 system for rationing. The 1972 data were divided by the 1974 data, and low ratios indicate areas where land cover had changed. The vegetative index difference means to monitor vegetation biomass and physiological status by using the difference and combination of spectral reflectance for each band (Maxwell 1976). Many researchers tried to derive the vegetation indices by calculating the bands of Landsat images in various ways such as perpendicular vegetation index (PVI), soil brightness index (SBI), and green vegetation index (GVI) (Kauth and Thomas 1976; Richardson and Wiegand 1977). Banner and Lynham (1981) suggest that the sensitivity of the near infrared (NIR) wavelengths to the vegetation within the clear-cut boundaries resulted in their research. The normalized difference vegetation index (NDVI) calculated by using of NIR and red linear combination is one of the most used indices by researchers for vegetation monitoring (Borowik et al. 2013; Tucker 1979). NDVI also has been having correlation to different vegetation attributes such as net primary production (NPP), percentage of photosynthetically active radiation (PAR), LAI, and quantitative biomass such as crop productivity (Broge et al. 1997; Persson et al. 1993; Sellers et al. 1992). In addition, recent studies have suggested more various NDVI applications in animal ecology, confirming the suitability of NDVI as a proxy for linking vegetation status with animal diversity, distribution, and dynamics (Ryan et al. 2012; Wiegand et al. 2008; Wu et al. 2021).

If the data transformation procedure simply uses multispectral bands, the analysis techniques are methods to improve the accuracy and applicability of forest change detection. A wide variety of forest change detection algorithms have been analyzed over the last two decades. The algorithms can be roughly divided into (1) spectral change detection and (2) post-classification change detection methods (Singh 1989). In post-classification change detection, two images from different dates are separately classified and labelled. And then the changed area is extracted through the direct comparison of the classification results (Howarth and Wickware 1981). The benefit of post-classification change detection is that it bypasses the problems in forest change detection associated with the analysis of images acquired at different sensors or by different times of year, but this method has the high sensitivity to the individual classification accuracies (Deng et al. 2008). Spectral change detection techniques depend on the principle that surface changes result in permanent changes in the spectral signature of the affected forest. These techniques include the transformation of two original images to a new single-band or multiband image in which the

changed forest is highlighted (Coppin and Bauer 1996). The benefit of the spectral change detection technique is that they are based on the detection of physical changes between image dates so most of the forest change detection techniques are in the spectral change detection category (Lunetta and Elvidge 1998). One of the most important algorithms for spectral change detection that have been used since the 1980s is the principal component analysis (PCA). PCA is a method of analyzing correlated multidimensional data which can be used to facilitate the visual interpretation of a mass of data having uniform a priori significance, by reducing redundancy, correlation between channels (Byrne et al. 1980). Richards (1984) applied a PCA algorithm to two-date MSS imagery to monitor brush-fire damage and vegetation regrowth over extensive areas in Australia confirming that areas of localized change were enhanced in the lower components. Multivariate alteration detection (MAD) is also an important method of spectral change detection. MAD is an extension of the traditional canonical correlations analysis and is invariant to linear scaling of the input data, but it has been less implemented (Nielsen et al. 1998). Change vector analysis (CVA) is a multivariate change detection technique that processes the full dimensionality (spectral + temporal) of the image data and produces two outputs: change magnitude and direction (Coppin et al. 2002). Johnson and Kasischke (1998) showed the capability of CVA to be an effective technique to capture all changes and not just a priori defined change events. In addition to these algorithms, a mathematical regression model which describes the fit between two multi-date images of the same area or various machine learning algorithms also exists.

The study of forestry change detection has become principally comprehensive, not only because forestry are the most extensive land-cover types in the world but also because they have significant impacts on the provision of a wide range of services and on the environment. At the same time, remote sensing data analyses become more difficult and more expensive with smaller spatial units. More detailed spatial units increase mapping efforts and decrease forest change detection accuracy. Recently, for the quantification of the greenhouse gas (GHG) and reducing emissions from deforestation and forest degradation (REDD+) project, the role of remote sensing in the forestry field is being emphasized more (Achard et al. 2014). Whatever change detection algorithm and classification routine is applied, it is evident that a broad range of alternatives exist and that all have varying degrees of flexibility and availability. In this sense, although Landsat imagery has become the standard relied upon by many forest ecologists and other researchers who use remotely sensed data, remote sensing data sets depends on the objectives and requirements of projects and research (Cohen and Goward 2004; Deng et al. 2008).

Considering the different objectives and questions addressed, Goetz et al. (2015) identified some functions of remote sensing for forestry management in the context of REDD+ needs:

- *Monitoring deforestation:* Deforestation is defined as the conversion of forest to a non-forest land use and remotely sensed data such as Landsat images enable

mapping and monitoring of forest cover and change over large areas at regular intervals, providing information on where and how changes are taking place.

- *Monitoring forest degradation*: Forest degradation is defined as the loss of aboveground biomass within forested land but without a change in the designated type of land use. Imagery with high resolution can be used to map local losses of tree cover that result from various types of degradation.
- *Monitoring the 'plus' from regrowth*: Monitoring of tree cover gain requires the tracking of regrowth over time before a determination of recovery to a forested state can be established. Regrowth in forest areas can be measured with a combination of field and LiDAR data.
- *Distinguishing forest trait diversity with remote sensing*: Characterizing the tree species diversity of forests, understood here as the number and distribution of individual species or assemblages of species, was considered beyond the capability of remote sensing technologies until recently. Technologies to measure and monitor forest biodiversity in forest ecosystems have developed rapidly because of the advancement of new sensor classes including LiDAR and hyperspectral remote sensing.

Based on these functions of remote sensing, we present an overview of the findings of 15 studies on recent remote sensing for forest monitoring trends with various algorithms and data sets and points for forest restoration in the next section (see Table 1).

3 Trends in Remote Sensing Techniques for Forest Monitoring

A recent large-scale analysis of detecting ecologically damaged areas including forest undertaken by Lee et al. (2020) serves as a proper starting point to introduce this section and the direction of the chapter. In this study, as a post-classification change detection method study, ecologically damaged areas for restoration in South Korea were detected using remote sensing and field surveys. For post-classification change detection, land-cover maps constructed nationally for South Korea at different times were used as a main analysis tool. In addition, by using land use zoning map, environmental impact assessment (EIA) data, and Google Earth data, illegally damaged ecological areas were derived along with specific areas in m². Results of this study showed ecologically damaged areas distributed in South Korea and 62% of the ecological damage occurred in forest ecosystems (Figs. 1 and 2; Lee et al. 2020). The damaged areas were mostly smaller than 50,000 m², and through field surveys, the cause and type of damaged areas were investigated, and the direction of restoration was suggested (Lee et al. 2020).

Goetz et al. (2015) emphasize the synergistic role of integrating field inventories with remote sensing for best practices in monitoring, reporting, and verification. However, it is not easy for researchers to directly perform field measurements because it is time-consuming and comparatively expensive. So, some studies

Table 1 Studies synthesized in this chapter

Study	Data/main approach	Major contribution to remote sensing research for forest restoration
Chen et al. (2015)	Airborne images and pre-established field measurement data/spectral change detection (object-based image analysis)	Assessed postfire burn severity in forests affected by three different stages of pre-fire mortality. Indicated that PCA and MNF are promising for balancing computation efficiency and the performance of burn severity models
Šimić Milas et al. (2015)	Landsat images (OLI)/change detection using vegetation indices	Suggested the total damaged area covers 45,265.32 ha of forests in five Croatian counties. Indicate that proposed index NDVI approach performs sufficiently well in detecting the forest damages for restoration
Fassnacht et al. (2016)	Review	Provided an overview of current research practices in focusing on tree species classification and local scale approaches have been presented for several sensor suggesting a concrete hypothesis or a targeted application
Einzmann et al. (2017)	RapidEye scenes/spectral change detection (random forest classifier)	Identified windthrow areas and the large-scale mean shift algorithm were chosen for image segmentation and identified over 90% of the windthrow areas. Helps monitor forest disturbances due to storms and select restoration sites
Mokroš et al. (2017)	UAS and ALS imagery/spectral change detection (semiautomatic approach)	Estimated the forest areas affected after windthrow and the volume of salvage logging using combination of UAS/ALS imagery. The windthrow areas were successfully identified within the forest land of the study site showing potential for application to early-stage surveys of damaged forest
Jahanifar et al. (2018)	Landsat images (TM and ETM+)/spectral change detection (linear multiple regression)	Detection satellite images showed that during the studied period, there was found a reduction of forest areas up to approximately 257,331 ha for agricultural purposes. The results can be used as an efficient tool to manage and improve forests regarding physiographical and human characteristics
Puletti et al. 2018	Sentinel-2 images/spectral difference detection (random forest classification)	Suggested multitemporal Sentinel-2 images collected at different phenological periods are required for to discriminate forest categories and

(continued)

Table 1 (continued)

Study	Data/main approach	Major contribution to remote sensing research for forest restoration
		types. The best configuration yielded an accuracy >83% in all considered forest types
Wessel et al. (2018)	Sentinel-2 images/spectral difference detection (support vector machines and random forest)	Indicated a high potential of Sentinel-2 data for forest classification using a hierarchical semiautomatic algorithms achieving overall classification accuracies of 88%
Hamdi et al. (2019)	Aerial orthophotos/spectral change detection (convolutional neural networks)	The algorithm achieved an accuracy of 92%, and the sum of the non-detected damaged areas amounted to 0.1 km ² , which represented 13% of the manually delineated damaged area. Provided the potential of deep learning on high-resolution imagery and for fast and efficient post-disaster damage assessment as a first step of disaster management on forest
Hościło and Lewandowska (2019)	Sentinel-2 images/spectral difference detection (random forest classification)	The overall accuracy for the forest/non-forest cover reached 98.3% and 94.8% for the classification of the forest type. The accuracy of eight tree species classification improved from 75.6% to 81.7% with the multitemporal Sentinel-2 data at the regional scale
Lee et al. (2020)	Land use land-cover maps and Google Earth image/post-classification change detection and field survey	Legally damaged areas were derived through remote sensing using national standardized vector data sets and satellite images and verified through field surveys. It is necessary to establish an effective restoration plan by related ministries and regional local governments
Axelsson et al. (2021)	Sentinel-2 images/spectral difference detection (maximum likelihood with Bayesian inference)	An overall accuracy of 87% was obtained for four tree species classes: <i>Betula spp.</i> , <i>Picea abies</i> , <i>Pinus sylvestris</i> , and <i>Quercus robur</i> suggesting that Bayesian inference is a practical way to provide a high classification accuracy
Onishi and Ise (2021)	UAV images/spectral difference detection (convolutional neural networks)	The algorithm succeeded in classifying seven tree classes, including several tree species with more than 90% accuracy showing that the CNN classified trees

(continued)

Table 1 (continued)

Study	Data/main approach	Major contribution to remote sensing research for forest restoration
		according to their shapes and leaf contrasts
Tarazona et al. (2021)	Landsat images (TM and OLI) and SAR images/spectral change detection (machine learning algorithms)	Showed the benefits of combining optical and SAR data for detecting deforestation compared to using only optical data. The calibration of the machine learning algorithms revealed that all classifiers had overall accuracy of more than 90%
Yu et al. (2021)	UAV images/spectral difference detection (Faster R-CNN and YOLOv4)	The accuracy of Faster R-CNN (60.98–66.7%) was higher than that of YOLOv4 (57.07–63.55%) for detecting pine wilt disease (PWD). The accuracy of early detection of PWD infection showed an increase of 3.72–4.29%, from 42.36–44.59% to 46.08–48.88%, when broad-leaved trees were considered

apply pre-established field data rather than directly performing field measurement. As an example, Chen et al. (2015) examined the three stages of impacts of fire and exotic disease on forests by applying Geographic Object-Based Image Analysis (GEOBIA) to MASTER (MODIS/ASTER) airborne images that were acquired immediately following the forest fire for assessment and contained both high spatial (4 m) and high spectral (50 bands) resolutions. Chen et al. (2015) also assessed two widely used band reduction algorithms, PCA (principal component analysis), and MNF (minimum noise fraction) to increase computation efficiency (Fig. 3; Chen et al. 2015). They suggested that the spectral variation removed by PCA and MNF was essential for distinguishing between the spectral reflectance from disease-induced dried crowns (still retaining high structural complexity) and fire ash.

Since forest damage mostly occurs over a large area, most research tried to study algorithms to improve the accuracy of change detection by using various imagery acquired from satellite system or a digital aerial survey camera system. Jahanifar et al. (2018) used Landsat TM (Thematic Mapper) data of 1995 and Landsat ETM+ (Enhanced Thematic Mapper Plus) data of 2015 for classification and investigated the changes in the forest area using linear multiple regression. The results of regression analysis indicated that the linear combination of income per capita, rain, and temperature with determined coefficient 0.4 as independent variables could estimate the reduction of forest area. Hamdi et al. (2019) implemented an algorithm based on convolutional neural network (CNN) for automatic detection and mapping of damaged areas using aerial orthophotos of 109 km² forest acquired with for spectral bands (blue, green, red, near infrared). Šimić Milas et al. (2015) evaluated the capability of Landsat-8 optical data and vegetation indices such as NDVI, LAI, and fraction of photosynthetically active radiation (fPAR) for mapping forest

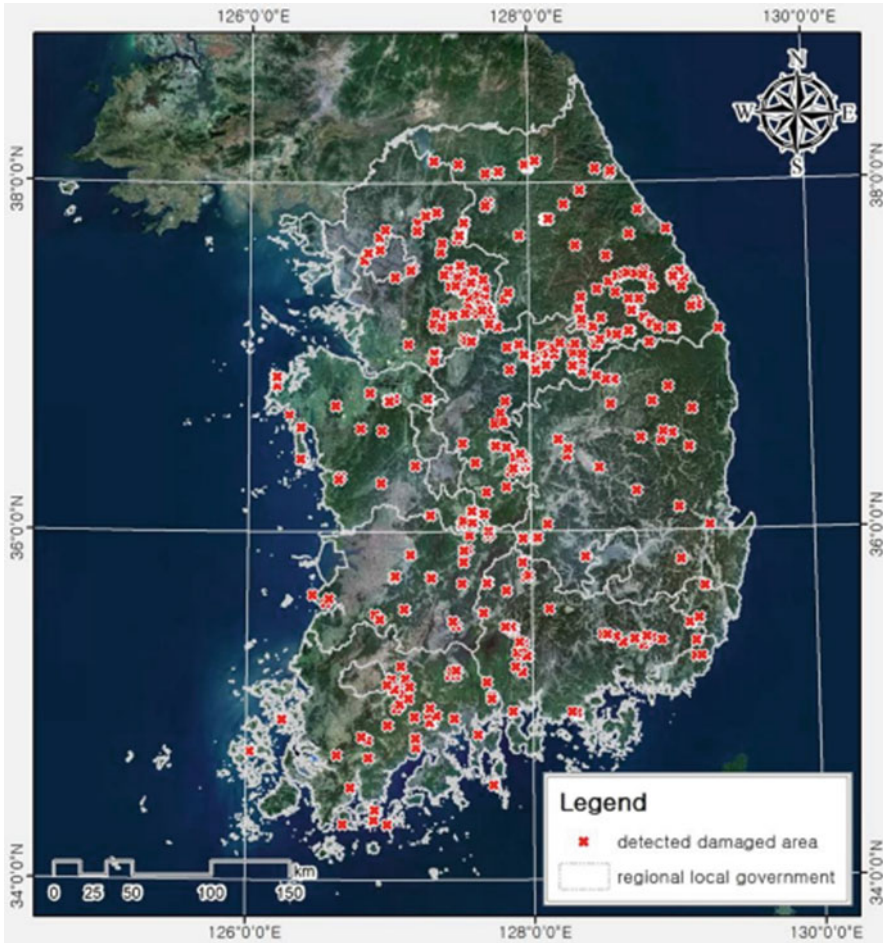


Fig. 1 Distribution status of damaged areas in South Korea derived through remote sensing. (Source: Lee et al. (2020))

damage in Croatia. Tarazona et al. (2021) fused Landsat images (TM & Operational Land Imager (OLI)) and synthetic aperture radar (SAR) images using PCA algorithm and used machine learning classification such as support vector machine (SVM) to detect deforestation in tropical forest of Peru. Einzmann et al. (2017) suggested forest change detection approach using RapidEye scenes before and after the storm damage on the forest areas in Bavaria, Germany. Einzmann et al. (2017) used a supervised random forest (RF) algorithm for an object-based bitemporal change analysis to identify windthrow areas, and the large-scale mean shift algorithm was chosen for image segmentation and identified over 90% of the windthrow areas as a result (Fig. 4; Einzmann et al. 2017).

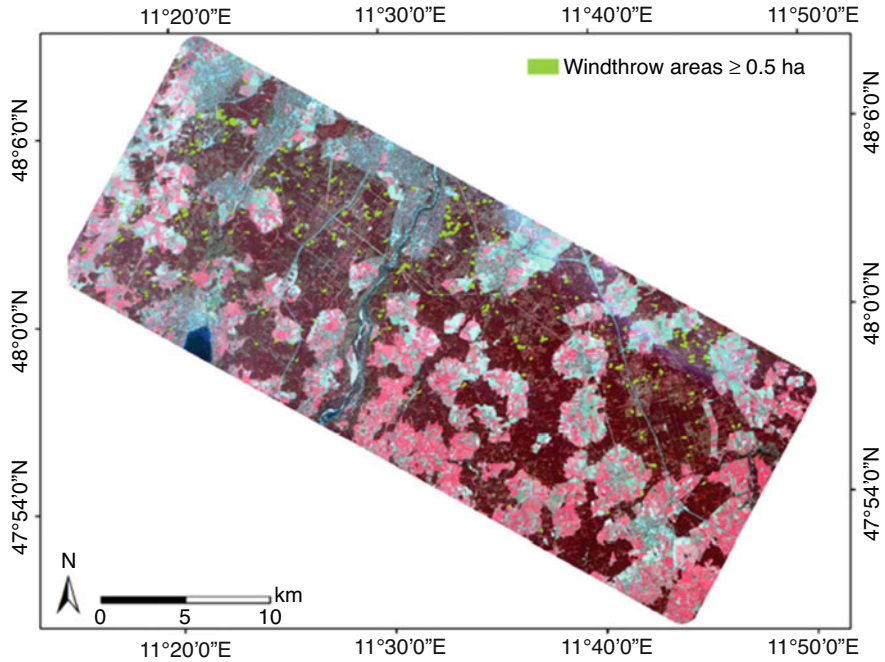


Fig. 4 Occurrence of windthrow areas ≥ 0.5 ha (green areas) in the *Munich South* study area. As background is the false color composite (band combination: near infrared-red-green) post-storm RapidEye scene depicted. (Source: Einzmann et al. (2017))

Sweden. Axelsson et al. (2021) acquired an overall accuracy of 87% for four tree species classes: *Betula* spp., *Picea abies*, *Pinus sylvestris*, and *Quercus robur* as a result. Puletti et al. (2018) used three Sentinel-2 images from spring, summer, and autumn in a random forest classification to classify between coniferous, broad-leaved, and mixed forest and achieved a maximum overall accuracy of 86.2% using a separate validation data set. Wessel et al. (2018) also used available S2 data and forest inventory data to evaluate machine learning approaches (SVM and RF) to classify tree species in two forest regions in Bavaria, Germany. Hościło and Lewandowska (2019) used S2 data in combination with topographic information to classify types of land, forest, and eight tree species (beech, oak, alder, birch, spruce, pine, fir, and larch) using RF algorithm. The overall accuracy for the forest/non-forest cover reached 98.3% and declined slightly to 94.8% for the classification of the forest type, and the classification of eight tree species improved from 75.6% to 81.7%.

Recently, unmanned aerial vehicle (UAV) has been supposed to be an easy-to-use, cost-effective tool and high-resolution images for monitoring forests. Yu et al. (2021) collected multispectral imagery by UAV with a real-time kinematic (RTK) module and used two target detection algorithms including faster region-based CNN and two machine learning algorithms based on feature extraction (random forest and

support vector machine) to detect early infected pine trees. Onishi and Ise (2021) used a commercially available UAV and deep learning algorithm to construct a machine vision system for the automatic classification of trees. They segmented a UAV photography image of forest into individual tree crowns and carried out object-based deep learning, and the system was able to classify seven tree types at overall 89.0% accuracy (Fig. 5; Onishi and Ise 2021). Mokroš et al. (2017) also used a fixed-wing type of unmanned aircraft system (UAS) with a compact digital camera to identify damaged forest. They used semiautomatic approach based on the UAS imagery and on the combination of UAS imagery with airborne laser scanning (ALS). The results from the UAS and the combined UAS/ALS methods were statistically significant with the reference data measured by global navigation satellite system (GNSS) devices.

Summing up, for forest change detection using remote sensing, selection of appropriate data according to spatial scale is becoming more important. UAV-based remote sensing is efficient and flexible in efficient and flexible in small and middle scale, and the device can be equipped with various remote sensors that generate high-resolution images (Tang and Shao 2015). However, when the spatial scale to check change detection is large, the time and cost for image acquisition could increase exponentially. In addition, it seems important to use an appropriate analysis method according to the data. Even if the same data and similar algorithm are used, it can be confirmed that the accuracy can vary greatly depending on the phenomenon to be detected and the difference in the algorithm process (Tarazona et al. 2021).

4 Approaches for Ecological Restoration

Ecological restoration projects or programs include one or more targets that identify the native ecosystem to be restored (as informed by the reference model) and project goals that establish the level of recovery sought (Gann et al. 2019). The restoring forest is especially dynamic ecosystem, with changing species composition and forest structure, but interventions and management steer the forest toward a desired climax or pre-disturbance community structure (Aerts and Honnay 2011). Therefore, for successful forest restoration, it is important to appropriately select the restoration approaches according to the restoration method, volume, and other goals considering different ecosystem. Ministry of Environment (MOE) in South Korea proposed some major approaches to restoration of damaged ecosystem including forest environment: conceptual approach (e.g., restoration, rehabilitation, replacement, enhancement), policy approach (e.g., department in charge, restoration space), and technical approach (e.g., physical and chemical restoration, biological restoration, management) (MOE 2011). It is important to notice that for the restoration of a specific ecological environment, all approaches must be combined to determine one restoration model. Here, we describe definitions and examples for each approach.

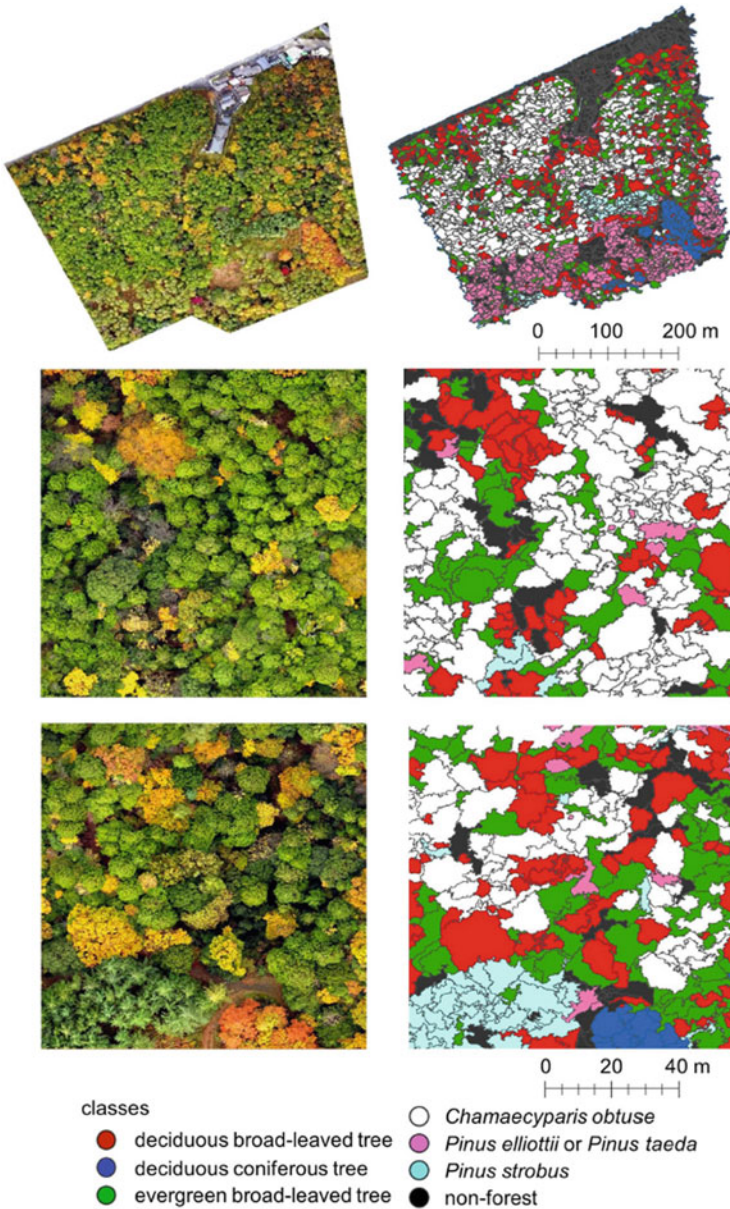


Fig. 5 Orthomosaic photos and classification maps obtained with the CNN classifier. The topmost images each gives an overall view of one area, and the lower images in each column show the respective enlarged area. The tree classes found in the images are identified in the legend at the bottom of the figure. (This figure was created using ArcGIS Desktop v10.6 software (<https://www.esri.com>, Environmental Systems Research Institute, Inc., Redlands, United States). *Source*: Onishi and Ise (2021))

5 Conceptual Approach

Over the many years, ecologists working on the arboretum restoration projects learned much about the structure and function of ecological systems through trial and error (Covington et al. 1999). The United Nations documented ecosystem restoration as a central concern in the Rio Declaration on Environment and Development in Principle 7 which declares, “States shall cooperate in a spirit of global partnership to conserve, protect and restore the health and integrity of the Earth’s ecosystems.” The concept of natural environment restoration has undergone changes and development along with this history of restoration. In this chapter, the conceptual approaches of restoration were divided into four categories (restoration, rehabilitation, reclamation, enhancement).

The dictionary definition of “restoration” is the act of bringing back to an original or unimpaired condition. Thus, ecological restoration has had as its goal the restoration of degraded ecosystems to emulate more closely, although not necessarily duplicate, conditions which prevailed before disruption of natural structures and processes (Covington et al. 1999). However, returning the damaged area to the original ecosystem consumes a lot of time and costly and is very difficult to put into practice. On the other hand, rehabilitation of an ecosystem means to repair and replace the essential or primary ecosystem structures and functions which have been altered or eliminated by disturbance (Cooke 2005). Rehabilitation of ecosystems could be an alternative view of the problem that could be more appropriate and attainable than restoration. In the study of Martin et al. (2002), they used different types of species: industrially produced, native, and wild cultivated species for rehabilitation. Comparing to restoration, this method integrates the benefits of using available low-costing seeds that are already used on large-scale projects with better adapted species, issued from the cultivation of native species and seed production for their use on smaller scale and more costly but more effective results (Martin et al. 2002). In the case of the restoration definition proposed in the recent convention on biological diversity (CBD), it seems to be mixing rehabilitation rather than the relatively strict definition of restoration in the past. The definition is as follows: the process of managing or assisting the recovery of an ecosystem that has been degraded, damaged, or destroyed as a means of sustaining ecosystem resilience and conserving biodiversity (CBD 2016).

Ecological reclamation means the creation of an original ecosystem elsewhere to improve the current condition, and although structurally simple, it is often highly effective in terms of productivity, and replacement usually applies to severely degraded land generally devoid of vegetation (Stanturf et al. 2014). Ecological enhancement focuses on improving the functional aspects of an ecosystem and aims to develop the ecosystem in terms of quality, importance, and attractiveness beyond the current ecosystem.

6 Policy Approach

Ecological restoration policy and practice are value-laden, involving multiple interests and actors, each prioritizing different project objectives and types of action (Baker and Eckerberg 2016). Ecological restoration projects for damaged ecosystems are being carried out sporadically by department, space, and medium. For more effective restoration of the natural environment, policy directions for each department, space, and media should be approached to induce an integrated restoration.

- *Department:* Most countries have several departments responsible for various restoration activities (Douglas 2002). Therefore, restoration projects often overlap because the restoration target, purpose, and approach are different for each department. For this reason, if the restoration space overlaps or it is difficult to clearly distinguish between the restoration projects by department, conflicts between departments such as project promotion entities and responsible workshops are concerned. To solve this problem, there is a way to first form an organization in charge of restoration projects for the entire country beyond ministries or a council organization. In addition, even within one department, the fields are divided according to the spatial scope, so a general organization is needed to systematically lead the restoration projects promoted by each department.
- *Space:* The restoration project aims at the circulation of ecosystems in areas and regions damaged by development, restoration of original ecological services, and restoration of appearance. Therefore, restoration at the watershed level should be considered in consideration of the linkage of the ecosystem. In general, restoration at the watershed level has been regarded as important in the river ecosystem, but it is desirable to apply it to the entire ecosystem due to the nature of the ecosystem that affects each other. The need for an approach at the watershed level has been raised by experts, and recent studies and guidelines related to domestic and foreign restoration have also applied the watershed level approach as important. Steiner et al. (2000) described that the watershed level approach emphasizes interrelationships to clarify the relationship between biophysical and sociocultural processes, and watershed-based planning is the most appropriate method for ecological planning for limitedly sensitive areas.
- *Components:* Ecological components such as vegetation, soil, water, and atmosphere composing an ecosystem influence each other and cycle. The concept of the cycle of this ecosystem should be applied equally to the restoration project, so that the integrated restoration between the components should be done. Most of the budget for restoration projects is supported by the collection fee imposed on development activities or the national treasury, and these budgets are often used redundantly for similar restoration projects by departments. Therefore, for an efficient restoration project, it is necessary to present a standard for restoration priority by type of ecosystem. In addition, for efficient budget execution, an integrated restoration system is needed, such as sequential restoration projects

or simultaneous implementation of restoration projects for the same space through a cooperative system between related ministries.

7 Technical Approach

Based on the damaged state and the properties of the ecosystem, the technical approaches for restoration could be largely divided into the state requiring restoration of the ecological infrastructure, restoration of the ecological environment, and management.

- *Physical and chemical restoration:* The field that requires physical and chemical restoration is the ecological-based environment field, which includes nonliving fields such as topography, hydrology, hydrology and water quality, and soil and geology. This kind of restoration could prevent ongoing deterioration, remediate substrates, some level of native biota present (Gann et al. 2019). As a representative example, when the contaminants are removed through soil construction suitable for the original topography by restoring the physical structure of the topography and an environment in which microorganisms in the soil can inhabit is secured, nutrients are accumulated through decomposers and other soil organisms are actively activated (MOE 2011). As this ultimately contributes to the restoration of the ecological environment such as forests, the restoration of the ecological base environment becomes the basis for the restoration of the ecological environment.
- *Biological restoration:* Ecological environment is a field for biological and ecological restoration and restoration (including introduction) of species and ecosystem components such as flora and vegetation restoration including habitat and biotope restoration and fauna. Biological restoration is the restoration of lost ecosystem components, such as species and habitats where species can inhabit. This includes the combination and dispersal of species, predation relationship, interaction, disturbance, and succession model, and it can be said to be the stage of attracting wild animals through restoration of plant species. Reforestation is kind of biological restoration.
- *Management:* Ecosystem management is principally focused on large, relatively natural, and autonomous landscapes (Aplet 1998). The ecological level of the restored space is determined depending on which management technique is applied in the process of returning to the original ecosystem through physical and chemical restoration and biological restoration. A restored space maintained under high management intensity can represent an externally excellent natural environment, but in terms of energy and material circulation, the space is operated by human activities such as continuous monitoring, irrigation, use of fertilizer, and spraying of pesticides. This can be judged as an ecosystem with low autogenesis, and such restored ecosystem can be easily culled when management is neglected or stopped, and the effect or result of restoration can be lost. Therefore, the improved management technique should induce the restored

ecosystem to maintain its own ecosystem and develop without excessive external help, based on the principle of adaptive management (MOE 2011).

8 Roles of Remote Sensing for Forest Restoration

The first thing to be done in the forest restoration is to identify the exact cause and area of the damaged forest. Through this, the purpose of restoration, approach direction, and restoration technique that can remove or reduce the cause of damage is determined according to the degree and condition of forest damage. Using field methods to monitor the success of reforestation is also a complicated task involving considerable temporal and financial resources. In this regard, remote sensing methods are especially suited for early-stage detection, and it can help cope with the widespread lack of timely, long-term, homogeneous, and reliable ground information for restoration and monitoring management (Meroni et al. 2017). Here, we use our review to summarize the major contributions and derive key opportunities to make advancements in remote sensing application for forest restoration:

- **Analysis of damaged forest:** Examples of causes of damage are anthropogenic pollution, climate change, and silvicultural activities. Other damaging agents are biotic, e.g., insects and fungi; their effects on trees and forest ecosystems depend on interactions between them, the trees and ecosystem processes, which may be synergistic or antagonistic (Lovett et al. 2006). Physical damage like deforestation can be detected by monitoring through remote sensing data such as Landsat since the late 1970s. Nowadays, airborne laser scanning (ALS) and radar images are widely used in forestry because they provide accurate information about canopy height and structure and the underlying terrain (Hyypä et al. 2012). Many studies related to forestry also use quantitative statistical method and indices such as the leaf area index to assess change in the forest phenology and structure (Fang et al. 2019). In addition, it is possible to acquire high-resolution remote sensing data by using UAV and detect forest change caused by biological damage such as PWD using deep learning algorithms (Yu et al. 2021).
- **Selection of damaged forest for restoration:** To establish an effective restoration plan by related ministries and methods, the data base for the damaged forest that was built in advance is needed. Most of the previous studies related to remote sensing for forest restoration have been carried out to detect changes targeting the area where the damage may have occurred. However, change detection alone is not sufficient data for restoration projects. Based on the results of Lee et al. (2020), by applying national standardized vector data sets institutionally used for change detection worldwide, such as LULC maps and EIA maps, it can be confirmed that it is possible to judge whether the detected forest damage is illegal or not. In addition, if a data base for damaged forest is primarily established through remote sensing analysis, the information necessary for the restoration project was collected through field surveys with relatively less time and cost.

- **Management after forest restoration:** The concept of forest management refers to the process of planning and executing practices for the administration and use of forests with the objective of meeting specific environmental, economic, social, and cultural objectives (Abad-Segura et al. 2020). Remote sensing has been used in a diverse range of forest management applications from mapping invasive species to monitoring land-cover changes after restoration (Lechner et al. 2020). For sustainable forest management, systematic monitoring and maintenance are necessary. In addition, monitoring data can be helpful in planning new forest restoration projects in the future by enabling the establishment of a direction adjustment, improvement, and supplementation plan through detection when unexpected problems occur after forest restoration.

9 Conclusion

Huge areas of the world's forests are being degraded, and these changes are affecting substantial losses of biodiversity. Destruction of forest ecosystems makes it impossible for large mammals or highly mobile wild animals that require a wide habitat to live, which may eventually become extinct or cause friction with humans by invading into residential spaces. Therefore, forest restoration is an important practice that would increase levels of biodiversity and human well-being. The economic circumstances may determine the level of resources available and approaches for restoration. Especially, monitoring is recognized as a costly and time-consuming operation, and it is often not performed before and after a restoration project. However, if monitoring is not performed, the evaluation of damage and restoration recovery trajectories becomes impossible.

We have presented an overview of the current state and capabilities of remote sensing in forestry. Remotely sensed data enable large area mapping and monitoring of forest cover and change at regular intervals, providing various information. In addition, remote sensing techniques to restore and monitor forest have advanced remarkably in recent years. In parallel with the advance in sensor technology and platforms, the processing and classification of remote sensing imagery are advancing significantly. Techniques from computer vision, along with the use of artificial intelligence algorithms including deep learning, are being applied to remote sensing, and we are likely to see a transformation in the algorithms being applied, especially for specific types of applications, such change detection, and species classification. In addition, a mix of remote sensing and field measurements is necessary for restoration projects and purposes. The technique of forest monitoring using both remote sensing and field survey would increase the data quality compared to a simple remote sensing monitoring, while reducing the cost compared to a simple filed survey for forest restoration.

Lastly, it should be noted that various research on remote sensing applied in the forestry to optimize forest restoration and management shows an upward trend. However, in most laws or guidelines, there are no regulations for monitoring and follow-up management using remote sensing, so it is difficult to link to actual

restoration projects. It is necessary to prepare a plan for the use of remote sensing in terms of institutional and policy aspects.

References

- Abad-Segura E, González-Zamar MD, Vázquez-Cano E, López-Meneses E (2020) Remote sensing applied in forest management to optimize ecosystem services: advances in research. *Forests* 11(9):969
- Achard F, Boschetti L, Brown S, Brady M, DeFries R, Grassi G et al (2014) A sourcebook of methods and procedures for monitoring and reporting anthropogenic greenhouse gas emissions and removals associated with deforestation, gains and losses of carbon stocks in forests remaining forests, and forestation (No. COP20-1). GOF-C-GOLD
- Aerts R, Honnay O (2011) Forest restoration, biodiversity and ecosystem functioning. *BMC Ecol* 11(1):1–10
- Aplet GH (1998) On the nature of wildness: exploring what wilderness really protects. *Denv UL Rev* 76:347
- Axelsson A, Lindberg E, Reese H, Olsson H (2021) Tree species classification using Sentinel-2 imagery and Bayesian inference. *Int J Appl Earth Obs Geoinf* 100:102318
- Baker S, Eckerberg K (2016) Ecological restoration success: a policy analysis understanding. *Restor Ecol* 24(3):284–290
- Banner A, Lynham TJ (1981) Multitemporal analysis of LANDSAT data for forest cutover mapping: a trial of two procedures
- Borowik T, Pettorelli N, Sönnichsen L, Jędrzejewska B (2013) Normalized difference vegetation index (NDVI) as a predictor of forage availability for ungulates in forest and field habitats. *Eur J Wildl Res* 59(5):675–682
- Boyd IL, Freer-Smith PH, Gilligan CA, Godfray HCJ (2013) The consequence of tree pests and diseases for ecosystem services. *Science* 342(6160):1235773
- Broge, NH, Hvidberg M, Hansen BU, Andersen HS, Nielsen AA (1997) Analyses of spectral-biophysical relationships for a wheat canopy. In: *Proceedings of the 3rd international airborne remote sensing conference and exhibition*, vol 2. pp 373–379
- Byrne GF, Crapper PF, Mayo KK (1980) Monitoring land-cover change by principal component analysis of multitemporal Landsat data. *Remote Sens Environ* 10(3):175–184
- Chen G, Metz MR, Rizzo DM, Dillon WW, Meentemeyer RK (2015) Object-based assessment of burn severity in diseased forests using high-spatial and high-spectral resolution MASTER airborne imagery. *ISPRS J Photogramm Remote Sens* 102:38–47
- Cohen WB, Goward SN (2004) Landsat's role in ecological applications of remote sensing. *Bioscience* 54(6):535–545
- Convention on Biological Diversity (2016) Decision adopted by the conference of the parties to the convention on biological diversity
- Cooke GD (2005) Ecosystem rehabilitation. *Lake Reserv Manag* 21(2):218–221
- Coppin PR, Bauer ME (1996) Digital change detection in forest ecosystems with remote sensing imagery. *Remote Sens Rev* 13(3–4):207–234
- Coppin P, Lambin E, Jonckheere I, Muys B (2002) Digital change detection methods in natural ecosystem monitoring: a review. In: *Analysis of multi-temporal remote sensing images*. pp 3–36
- Covington WW, Niering WA, Starkey E, Walker J (1999) Ecosystem restoration and management: scientific principles and concepts. In: Szaro RC, Johnson NC, Sexton WT, Malk AJ (eds) *Ecological stewardship: a common reference for ecosystem management*, vol II, pp 599–617
- Deng JS, Wang K, Deng YH, Qi GJ (2008) PCA-based land-use change detection and analysis using multitemporal and multisensor satellite data. *Int J Remote Sens* 29(16):4823–4838
- Díaz S, Cabido M (2001) Vive la différence: plant functional diversity matters to ecosystem processes. *Trends Ecol Evol* 16(11):646–655

- Douglas T (2002) Ecological restoration guidelines for British Columbia. Ministry of Water, Land and Air Protection [Ministry of Environment and Climate Change Strategy]
- Einzmann K, Immitzer M, Böck S, Bauer O, Schmitt A, Atzberger C (2017) Windthrow detection in European forests with very high-resolution optical data. *Forests* 8(1):21
- Fang H, Frédéric B, Plummer S, Schaepman-Strub G (2019) An overview of global leaf area index (LAI): methods products validation and applications. *Rev Geophys* 57(3):739–799
- Fassnacht FE, Hooman L, Krzysztof S, Modzelewska A, Lefsky M, Waser LT, Straub C, Ghosh A (2016) Review of studies on tree species classification from remotely sensed data. *Remote Sens Environ* 186:64–87
- Food and Agriculture Organization of the United Nations. Forestry Department (Rome) (2010) Global forest resources assessment 2010: main report. Food and Agriculture Organization of the United Nations
- Gann GD, McDonald T, Walder B, Aronson J, Nelson CR, Jonson J et al (2019) International principles and standards for the practice of ecological restoration. *Restor Ecol* 27(S1):S1–S46
- Goetz SJ, Hansen M, Houghton RA, Walker W, Laporte N, Busch J (2015) Measurement and monitoring needs, capabilities and potential for addressing reduced emissions from deforestation and forest degradation under REDD+. *Environ Res Lett* 10(12):123001. <https://doi.org/10.1088/1748-9326/10/12/123001>
- Hamdi ZM, Brandmeier M, Straub C (2019) Forest damage assessment using deep learning on high resolution remote sensing data. *Remote Sens* 11(17):1976
- Heller RC (1978) Case applications of remote sensing for vegetation damage assessment. *PERS* 44: 1159–1166
- Heller RC, Aldrich RC, Bailey WF (1959) An evaluation of aerial photography for detecting southern pine beetle damage
- Hościło A, Lewandowska A (2019) Mapping forest type and tree species on a regional scale using multi-temporal Sentinel-2 data. *Remote Sensing* 11(8):929
- Howarth PJ, Wickware GM (1981) Procedures for change detection using Landsat digital data. *Int J Remote Sens* 2(3):277–291
- Hyypä J, Holopainen M, Olsson H (2012) Laser scanning in forests. *Remote Sensing* 4(10): 2919–2922
- Jahanifar K, Amirnejad H, Mojaverian M, Azadi H (2018) Land change detection and effective factors on forest land use changes: application of land change modeler and multiple linear regression. *J Appl Sci Environ Manag* 22(8):1269–1275
- Johnson RD, Kasischke ES (1998) Change vector analysis: a technique for the multispectral monitoring of land cover and condition. *Int J Remote Sens* 19(3):411–426
- Kauth RJ, Thomas GS (1976) The tasseled cap—a graphic description of the spectral-temporal development of agricultural crops as seen by Landsat. In: LARS symposia. p 159
- Lagomasino D, Price RM, Whitman D, Campbell PK, Melesse A (2014) Estimating major ion and nutrient concentrations in mangrove estuaries in Everglades National Park using leaf and satellite reflectance. *Remote Sens Environ* 154:202–218
- Lausch A, Herzog F (2002) Applicability of landscape metrics for the monitoring of landscape change: issues of scale, resolution and interpretability. *Ecol Indic* 2(1-2):3–15
- Lechner AM, Foody GM, Boyd DS (2020) Applications in remote sensing to forest ecology and management. *One Earth* 2(5):405–412
- Lee K, Sung HC, Seo JY, Yoo Y, Kim Y, Kook JH, Jeon SW (2020) The integration of remote sensing and field surveys to detect ecologically damaged areas for restoration in South Korea. *Remote Sens* 12(22):3687
- Lovett GM, Canham CD, Arthur MA, Weathers KC, Fitzhugh RD (2006) Forest ecosystem responses to exotic pests and pathogens in eastern North America. *Bioscience* 56(5):395–405
- Lu D, Mausel P, Brondizio E, Moran E (2004) Change detection techniques. *Int J Remote Sens* 25(12):2365–2401
- Lunetta RS, Elvidge CD (1998) Remote sensing change detection: environment monitoring methods and applications. Ann Arbor Press, Chelsea, MI

- Martin A, Khater C, Mineau H, Puech S (2002) Rehabilitation ecology by revegetation. Approach and results from two Mediterranean countries. *Korean J Ecol* 25(1):9–17
- Maxwell E (1976) Sensor design for monitoring vegetation canopies. *Photogramm Eng Remote Sens* 42:1399–1410
- Meroni M, Schucknecht A, Fasbender D, Rembold F, Fava F, Mauclair M et al (2017) Remote sensing monitoring of land restoration interventions in semi-arid environments with a before–after control–impact statistical design. *Int J Appl Earth Obs Geoinf* 59:42–52
- Meyers TP (1987) Modelling the plant canopy micrometeorology with higher-order closure principles. *Agric For Meteorol* 41(1–2):143–163
- Miettinen J, Stibig HJ, Achard F (2014) Remote sensing of forest degradation in Southeast Asia—aiming for a regional view through 5–30 m satellite data. *Glob Ecol Conserv* 2:24–36
- Ministry of Environment (2011) Research for the systematic restoration of the damaged natural environment; Republic of Korea. Ministry of Environment, Sejong City. (In Korean)
- Mokroš M, Výboštok J, Merganič J, Hollaus M, Barton I, Koreň M et al (2017) Early stage forest windthrow estimation based on unmanned aircraft system imagery. *Forests* 8(9):306
- Nagendra H, Lucas R, Honrado JP, Jongman RH, Tarantino C, Adamo M, Mairota P (2013) Remote sensing for conservation monitoring: assessing protected areas, habitat extent, habitat condition, species diversity, and threats. *Ecol Indic* 33:45–59
- Nelson RF (1983) Detecting forest canopy change due to insect activity using Landsat MSS. *Photogramm Eng Remote Sens* 49(9):1303–1314
- Nielsen AA, Conradsen K, Simpson JJ (1998) Multivariate alteration detection (MAD) and MAF postprocessing in multispectral, bitemporal image data: new approaches to change detection studies. *Remote Sens Environ* 64(1):1–19
- Onishi M, Ise T (2021) Explainable identification and mapping of trees using UAV RGB image and deep learning. *Sci Rep* 11(1):1–15
- Persson P, Hall-Könyves K, Sjöström G, Pinzke S (1993) NOAA/A VHRR data for crop productivity estimation in Sweden. *Adv Space Res* 13(11):111–116
- Pierce LL, Running SW (1988) Rapid estimation of coniferous forest leaf area index using a portable integrating radiometer. *Ecology* 69(6):1762–1767
- Puletti N, Chianucci F, Castaldi C (2018) Use of Sentinel-2 for forest classification in Mediterranean environments. *Ann Silvicult* 42(1):32–38. <https://doi.org/10.12899/ASR-1463>
- Reed MS, Dougill AJ, Taylor MJ (2007) Integrating local and scientific knowledge for adaptation to land degradation: Kalahari rangeland management options. *Land Degrad Dev* 18(3):249–268
- Reif MK, Theel HJ (2017) Remote sensing for restoration ecology: application for restoring degraded, damaged, transformed, or destroyed ecosystems. *Integr Environ Assess Manag* 13(4):614–630
- Richards JA (1984) Thematic mapping from multitemporal image data using the principal components transformation. *Remote Sens Environ* 16(1):35–46
- Richardson AJ, Wiegand CL (1977) Distinguishing vegetation from soil background information. *Photogramm Eng Remote Sens* 43(12):1541–1552
- Robinove CJ, Chavez PS Jr, Gehring D, Holmgren R (1981) Arid land monitoring using Landsat albedo difference images. *Remote Sens Environ* 11:133–156
- Rock BN, Vogelmann JE, Williams DL, Vogelmann AF, Hoshizaki T (1986) Remote detection of forest damage: plant responses to stress may have spectral “signatures” that could be used to map, monitor, and measure forest damage. *Bioscience* 36(7):439–445
- Rouse Jr JW, Haas RH, Schell JA, Deering DW (1973) Monitoring the vernal advancement and retrogradation (green wave effect) of natural vegetation (No. NASA-CR-132982)
- Ryan SJ, Cross PC, Winnie J, Hay C, Bowers J, Getz WM (2012) The utility of normalized difference vegetation index for predicting African buffalo forage quality. *J Wildl Manag* 76(7):1499–1508
- Scharsich V, Mtata K, Hauhs M, Lange H, Bogner C (2017) Analysing land cover and land use change in the Matobo National Park and surroundings in Zimbabwe. *Remote Sens Environ* 194:278–286

- Sellers PJ, Heiser MD, Hall FG (1992) Relations between surface conductance and spectral vegetation indices at intermediate (100 m² to 15 km²) length scales. *J Geophys Res Atmos* 97 (D17):19033–19059
- Šimić Milas A, Rupasinghe P, Balenović I, Grosevski P (2015) Assessment of forest damage in Croatia using Landsat-8 OLI Images. *South-east Eur For SEEFOR* 6(2):159–169
- Singh A (1989) Review article digital change detection techniques using remotely-sensed data. *Int J Remote Sens* 10(6):989–1003
- Stanturf JA, Palik BJ, Dumroese RK (2014) Contemporary forest restoration: a review emphasizing function. *For Ecol Manag* 331:292–323
- Steiner F, Blair J, McSherry L, Guhathakurta S, Marruffo J, Holm M (2000) A watershed at a watershed: the potential for environmentally sensitive area protection in the upper San Pedro Drainage Basin (Mexico and USA). *Landsc Urban Plan* 49(3–4):129–148
- Tang L, Shao G (2015) Drone remote sensing for forestry research and practices. *J For Res* 26(4): 791–797
- Tarazona Y, Zabala A, Pons X, Broquetas A, Nowosad J, Zurqani HA (2021) Fusing Landsat and SAR data for mapping tropical deforestation through machine learning classification and the PVts-β non-seasonal detection approach. *Can J Remote Sens* 47(5):677–696
- Todd WJ (1977) Urban and regional land use change detected by using Landsat data. *J Res US Geol Surv* 5(5):529–534. <https://pubs.er.usgs.gov/publication/70112341>
- Tucker CJ (1979) Red and photographic infrared linear combinations for monitoring vegetation. *Remote Sens Environ* 8(2):127–150
- Wang L, Jia M, Yin D, Tian J (2019) A review of remote sensing for mangrove forests: 1956–2018. *Remote Sens Environ* 231:111223
- Weaver PL, Medina E, Pool D, Dugger K, Gonzales-Liboy J, Cuevas E (1986) Ecological observations in the dwarf cloud forest of the Luquillo Mountains in Puerto Rico. *Biotropica* 18:79–85
- Wessel M, Brandmeier M, Tiede D (2018) Evaluation of different machine learning algorithms for scalable classification of tree types and tree species based on Sentinel-2 data. *Remote Sens* 10(9):1419
- Wiegand T, Naves J, Garbulsky MF, Fernández N (2008) Animal habitat quality and ecosystem functioning: exploring seasonal patterns using NDVI. *Ecol Monogr* 78(1):87–103
- Wingfield MJ, Brockerhoff EG, Wingfield BD, Slippers B (2015) Planted forest health: the need for a global strategy. *Science* 349(6250):832–836
- Wu J, Li H, Wan H, Wang Y, Sun C, Zhou H (2021) Analyzing the relationship between animal diversity and the remote sensing vegetation parameters: the case of Xinjiang, China. *Sustainability* 13(17):9897
- Yu R, Luo Y, Zhou Q, Zhang X, Wu D, Ren L (2021) Early detection of pine wilt disease using deep learning algorithms and UAV-based multispectral imagery. *For Ecol Manag* 497:119493



Recent Advances in UAV-Based Structure-from-Motion Photogrammetry for Aboveground Biomass and Carbon Storage Estimations in Forestry

Sercan Gülci, Abdullah Emin Akay, Burak Arıcak, and Temel Sariyildiz

Abstract

Due to economical, ecological, and social changes over the last decade, managers and researchers in nature-based disciplines intend to use both traditional and innovative remote sensing (RS) technologies for best management practices. RS, which has grown interest in forestry, offers rapid and reliable assessment tool to monitoring and observing. Several successful studies in literature have indicated that the RS use in forestry is light the way of the most effective evaluating various forest ecosystems. Recent developing unmanned aerial platforms play as a low-cost and inexperienced user-based multi-image processing by using computer vision techniques for forestry studies. Forests, where are essential natural resources for the future, are the pool of biomass and carbon storage, and they need periodical monitoring to sustain. A sustainable management of carbon balance and biomass in mountainous forests includes exhausting effort in field-based studies. However, the RS as a tool for study on biomass and carbon storage can be received as the most effective prediction and nondestructive method in combination with structure-from-motion techniques. Considering recent opportunities in data science and unmanned aerial vehicles (UAVs), RS and photogrammetry in forestry have still played an indispensable role in the evolution of forests. This chapter aims to review the recent advanced knowledge on the progress of the use of UAV technologies in accordance with advanced photogrammetry-related applications in the quantification of forest aboveground biomass and carbon

S. Gülci (✉)

Faculty of Forestry, Forest Engineering Department, Kahramanmaraş Sütçü İmam University, Kahramanmaraş, Turkey
e-mail: sgulci@ksu.edu.tr

A. E. Akay · B. Arıcak · T. Sariyildiz

Faculty of Forestry, Forest Engineering Department, Bursa Technical University, Bursa, Turkey

© The Author(s), under exclusive license to Springer Nature Singapore Pte Ltd. 2022

M. N. Suratman (ed.), *Concepts and Applications of Remote Sensing in Forestry*, https://doi.org/10.1007/978-981-19-4200-6_20

storage. A comprehensive literature search has been performed on the use of UAV-based SfM photogrammetry for UAV-based forest biomass and carbon storage studies.

Keywords

UAV-SfM · Digital aerial photogrammetry · Remote sensing · Stand parameters · Timber volume · Carbon stock

1 Introduction

Studies on forest biomass estimation can provide important results for determining the distribution and flow of materials in ecosystems and are necessary to understand the dynamics of the forest ecosystem (Andersson 1971). Estimation of forest woody biomass plays an important role in forestry for several reasons. Firstly, the planning of forest woody assortments production, for main commercial roundwood assortment and for assortments like “waste wood” or “recovered wood” as a potential for energy purposes (firewood, wood bricks, wood pellets, etc.). Secondly, the estimation of different parts of forest woody biomass as bole, branches, and foliage can be used to better manage forest resources. Thirdly, forest woody biomass estimations are useful to evaluate and understand (a) the stocks and fluxes of several biogeochemical elements and (b) the amount of net primary energy production from forests as a cleaner alternative to fossil fuels. In addition, forest biomass is an essential variable mostly used in several ecological and ecophysiological models (Brown 1997; Chave et al. 2005; Návar 2009a, b; Richardson et al. 2002). Finally, in last two decades, forest biomass estimation studies have received much attention due to its importance in the evaluation of carbon sequestration and the carbon balance capacity of forest ecosystems. It is well-known that forest ecosystems, being the most important carbon sink, are a good tool to reduce the carbon content of the atmosphere. Estimating the amount of carbon stored by forests is essential to support climate change mitigation and promote the transition to a low-carbon emission economy.

It is well-known by researchers, authorities, and publics that forests are major terrestrial C sinks and sequester large amounts of atmospheric carbon dioxide (CO₂). Forest ecosystems contain large amounts of C in above- and below-ground biomass, dead organic matter, and soil and contribute to significant annual C exchanges with the atmosphere. All these components may play an important role in the carbon storage and cycling of forest ecosystems. Article 2.1 of The Kyoto Protocol addresses issues related to global warming and holds signatories accountable to protect sinks and reservoirs of greenhouse gases, increase afforestation and reforestation, and promote sustainable forest management (Yavaşlı 2012). Thus, in the last few decades, many local, regional, and national studies have been carried out to quantify the biomass of forest ecosystems and its potential carbon fixation. Those

studies have reported that both forest plants and soils can sequester 60–80% of the global terrestrial carbon (Perruchoud and Fischlin 1995).

Most studies have focused on precise assessment of CO₂ emissions due to land-use changes, forest fire, degradation, and other anthropogenic activities in order to understand global carbon cycle and hence to make policies. So, biomass estimation studies of forest ecosystems all over the world have received much attention to reduce the uncertainties related to carbon cycle and emissions and find out the sources and sinks of carbon (C) as a result of forest to degraded land and vice versa as well as their temporal variations (Yavaşlı 2012).

In many studies, the standard methodology for the estimation of tree, plot, and regional aboveground biomass has been mostly allometric equations (Brown 1997; Lingner et al. 2018). Dry weight measurements conducted on harvested trees, fresh and dry weights of biomass components, and recording independent tree variables are required to construct allometric equations at the species, stands, or tree community levels. However, measuring forest biomass through field survey at a large spatial scale is time-consuming and cost-expensive and thus is difficult to popularize (Hermosilla et al. 2014; Van Leeuwen and Nieuwenhuis 2010; Dittmann et al. 2017). In addition to the large forest areas with the structural and geographical complexity and heterogeneity of forests and the conflicts in methods for forest measurements, precise mensuration of tree attributes with sufficient spatial and temporal resolution is also time-consuming and cost-intensive, especially in natural forest lands. Consequentially, the quantity, the frequency, and the parameter richness of in situ forest measurements reveal the constraints in accordance with the budget and the accessibility in forests.

The use of unmanned aerial vehicles (UAVs) both for small- and large-scale forest management inventories has become quite widespread and also produce accurate results (Wallace et al. 2012; Tuominen et al. 2015; Puliti et al. 2017, 2018b). The UAVs have high capacity to capture high- and ultrafine resolution information on the forest canopy and also their versatility and availability increase their uses for estimating forest management inventories. UAV systems represent a low-cost, agile, and autonomous opportunity and thus make them an alternative platform to satellites and aircrafts for forest inventory (Dandois et al. 2015; Sankey et al. 2017; Puliti et al. 2019). Considering recent applications of UAVs, demands on the usage of UAV-assisted surveys have increased suddenly in the last decade due to the technological advancements on various fronts such as structure-from-motion (SfM), machine learning, and robotics. The SfM photogrammetry provides surveys with little cost and low technical expertise. Therefore, the potential of using UAVs and consumer-grade cameras for terrestrial SfM-based surveys in forestry should be considered in measuring for large-scale forest inventories.

Within the scope of this study, researchers conducted on aboveground biomass and carbon storage in forest areas (coniferous or deciduous trees) were evaluated. Particularly studies in which UAV-SfM techniques are used in biomass and carbon measurements, which are the most important indicators for the reduction of pressures in forest areas, especially climate change, and the management of forests and the continuation of ecosystem services in a sustainable way have been reviewed.

Advanced research option under web of science search engines was used to identify the most up-to-date applications and researches. In the web of science core collection, the research area was chosen as “forestry.” A total of 15 recent publications related to aboveground biomass (AGB) and carbon storage estimations with UAV-SfM techniques were identified in the literature search made in the web of science database. In the review process, AGB and carbon estimation publications produced by manned flight, other than tree species, were excluded from the evaluation.

2 A Very Brief Historical UAV Technology

Considering the history of remotely controlled unmanned aerial vehicles, hot-air balloons can be seen on the development of the first attempts for UAV before 1800s. The main technological development concepts of different type of UAV and mounted equipment or payloads (human, sensors, or weapons) have been used in the military and civilian purposes since early 1900s. In emerged unmanned flight platforms from past to today, inventors, manufacturers, and beneficiaries have used different terms, namely, “remote controlled aerial vehicles,” “remote controlled aircraft,” “remotely piloted aerial systems,” “unmanned air platform,” “unmanned aircraft,” “unmanned aerial systems,” “unmanned aerial vehicle” “drone,” “hexacopter,” “octocopter,” “quadcopter,” “delta-wing,” as well as other specific names such as “special purpose aircraft” and “unmanned combat aerial vehicle.” All mentioned terms have still been use in the history of continued UAV development in accordance with the technical usage function and the features of vehicles (Newcome 2004; Gupta et al. 2013; Keane and Carr 2013).

With the development of technology, there are many types of UAVs used for civilian purposes today. This type of vehicle uses inertial measurement unit (IMU), Global Navigation Satellite System (GNSS) receivers, sensors (different type of camera, radar, and laser detection systems), digital memory cards for recording, and telemetry system that transmits a data back to ground control station (González-Jorge et al. 2017). Remotely controlled aerial platforms with many different features, produced for fully automatic or semiautomatic hobby purposes, have become widespread.

UAVs (capable of short-term flight with vertical or horizontal take-off feature), which are used for nonmilitary purposes, are widely used today in different studies in the field of science or social sciences, with the use of commercial or open source software or self-programming. There are multipurpose vehicles that are almost the size of a mobile phone and can be loaded with photogrammetric flight plans thanks to the microprocessors inside. In addition, even amateur users have appeared as “robots” with artificial intelligence that can safely return and land after the flight, without experiencing an accident, by overcoming obstacles.

3 UAV Photogrammetry in Forestry

UAV usage techniques and terms have increased rapidly in forestry, which has become very popular in recent years. UAV-based SfM photogrammetry studies, which are considered new in terms of forestry, have been used in various countries in America, Europe, and Asia. With the widespread use of deep learning methods in photogrammetry (metric photography), its usage area has increased rapidly. The terms “close-range photogrammetry,” “digital aerial photogrammetry,” and “drone/UAV photogrammetry” are used for UAV photogrammetry, which does not comply with the definition of classical aerial photogrammetry classes. The term remote sensing has started to be used with the use of satellites and the development of technology. Similar methods can be applied for image processing and evaluation stages in digital photogrammetry, which is currently used.

The use of UAV platforms and their sensors is increasing rapidly due to the safety/security, cost, and time savings they provide in forested areas with difficult terrain conditions (Banu et al. 2016). Within the scope of forestry studies, preferred sensor combination expresses the use of both active and passive sensors. According to the intensity of use, visible range (RGB), multispectral, and LiDAR sensors are used in forestry (Dainelli et al. 2021). UAV-based forestry studies are carried out not only to collect data from hard-to-reach forest areas but also to use remote sensing techniques in all terrain conditions (Fig. 1).

As a result of recent advances and developments in UAV technology, the use of UAVs, especially for photogrammetry, is becoming even more common in forestry. In fact, the use of UAV photogrammetry has paved the way for the development of numerous methods, applications, research, and strategies by enabling to look at the problems that need to be solved in forestry from different perspectives. The diversity of data obtained from the scientific studies using UAV photogrammetry (observation, cartography, and 3D modeling) has carried the forestry research to whole new dimensions.

With various sensors mounted on UAV platforms, they have been used as spatial data production tools in many scientific researches and variety of applications in the field of forestry (Nex and Remondino 2014; Pajares 2015; Guimarães et al. 2020). In forestry, cameras in the RGB (R = Red, G = Green, and B = Blue) and NIR (Near infrared) spectral ranges are mostly preferred within the scope of UAV-assisted photogrammetry studies. Then, hyperspectral cameras and LiDAR sensors are preferred in the second place due to the cost constraints in applications. Currently, LiDAR sensor or hyperspectral camera and data processing costs are still higher than RGB and NIR band cameras (Torresan et al. 2017; Stone et al. 2016).

Aerial photography and satellite imagery, which have been used traditionally in forestry for many years, use of deep learning techniques (i.e., random forest, support vector machine, and convolutional neural networks) and UAV-imagery based photogrammetry, which can be evaluated within the scope of digital aerial photogrammetry, is structure-from-motion (SfM), paired with multi-view stereo algorithms provide significant advantages for forest practitioners and researchers (Iglhaut et al. 2019). The SfM technique, which includes traditional photogrammetric foundations,

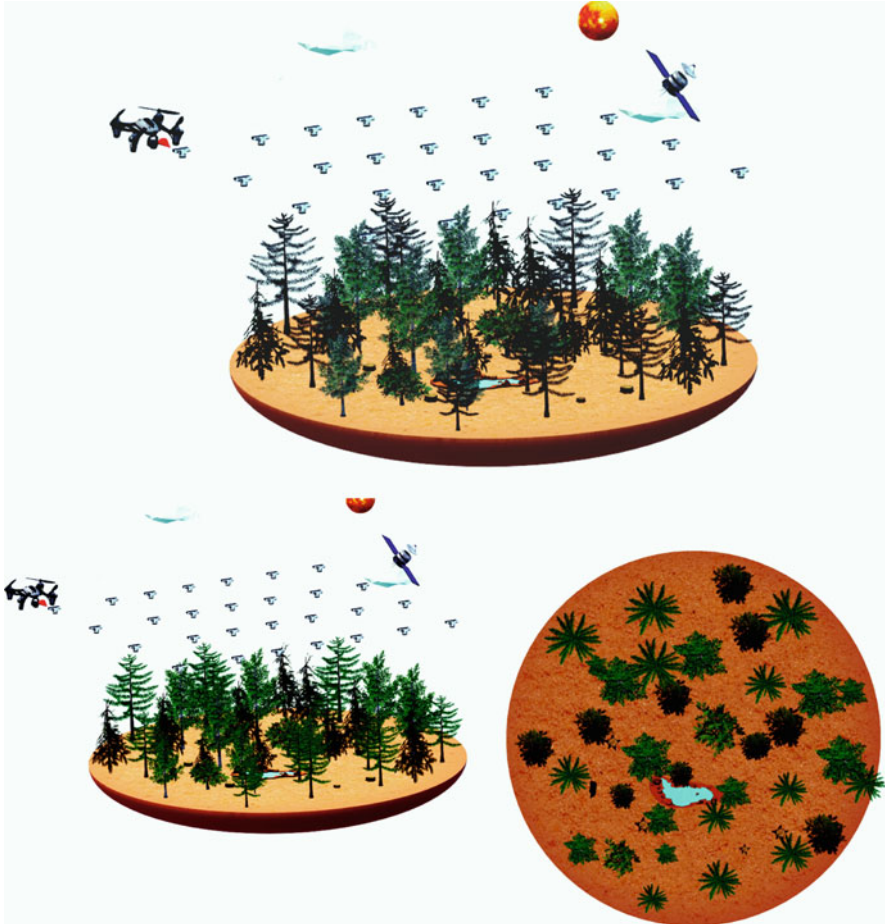


Fig. 1 Photogrammetric flight mission with drone

has led to an increase in measurement studies within the scope of close-range photogrammetry.

Through technological developments such as the development of more user-friendly photo processing algorithms and the production of various cost-effective sensors that can obtain various forestry-related data attract the attention of researchers in utilizing advanced remote sensing technologies in the field of forestry (Tang and Shao 2015). In the coming years, UAV photogrammetry use in forestry will increase its popularity especially in estimating individual tree parameters (used in tree recognition or disease detection in forests) with the decrease in the cost of camera and image processing programs in hyperspectral bands (Dainelli et al. 2021). For this reason, with UAV-SfM photogrammetry use in forestry, the next section focuses on studies using consumer-grade cameras in the visible range RGB and NIR.

4 UAV-SfM Photogrammetry Use in Forestry

Structure from motion (SfM) paired with multi-view stereo (MVS), namely, SfM, is a technique that converts stereopairs taken with a UAV from a 2D plane to a 3D point cloud. UAV-mounted consumer-grade RGB cameras or NIR cameras have been used in the generation of image-based 2D or 3D models using various software (i.e., Photoscan, Pix4D, MicMac, ReCap, VisualSfM, etc.), which effectively run SfM-based algorithms (Lisein et al. 2013). To generate self-calibrated image-derived products, UAV-SfM pipeline involves four basic steps: (1) image acquisition, (2) sparse dense cloud producing, (3) georeferencing, and (4) 3D dense cloud producing. Then, the generation of high-resolution models (orthophoto, mesh, texture, and digital elevation models) can be derived by using 3D dense point clouds (Fig. 2) (Remondino et al. 2014; Smith et al. 2015).

There is no standard for the values of the image processing quality that must be entered by the user in the image processing steps with SfM. UAV-SfM imagery-based derivation of 3D point clouds, which are LiDAR-like point clouds, can be prepared for further processing in forest stand parameters (i.e., individual tree detection, canopy cover, or canopy height model). To obtain stand-specific estimations, image-derived point clouds can be processed by using local maxima, marker-controlled watershed algorithm, template matching, valley following, scale-space theory, and Markov random fields (Wallace et al. 2016; Mohan et al. 2021).

Cost-effectiveness, temporal resolution, and flexibility in working within the scope of forestry increase the use of UAV-SfM method. Estimation of individual tree parameters (i.e., tree height and crown widths) with UAV-SfM photogrammetry has promising accuracy. Many variables are being investigated to increase the quality of 3D point cloud. For example, closure, species, species compositions, topographic structure, and other factors affecting locality can be taken into consideration. The carrier platform and system features used in photogrammetric flights, photogrammetric flight plan (such as flight altitude, flight speed, overlapping rates, camera calibration), environmental conditions during flight (such as stand feature and meteorological birds), image processing methods, and parameters are still being

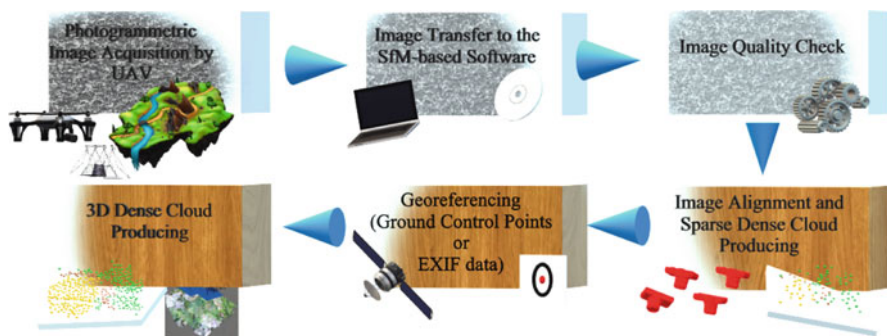


Fig. 2 Simplified workflow of UAV-SfM

investigated (Gülci 2019; Yurtseven et al. 2019; Kameyama and Sugiura 2020; Eker et al. 2020; Nasiri et al. 2021; Swayze et al. 2021). Studies on the variables and conditions that affect the prediction success of the UAV-SfM technique continue to increase. Therefore, the success of estimation of stand parameters has been increasing gradually.

The SfM techniques are effectively used in following subjects in forestry: (1) individual tree detection and inventory parameters; (2) aboveground volume estimations; (3) pest and disease detection; (4) species recognition and invasive plant detection; (5) conservation, restoration, and fire monitoring; and (6) setting and accuracy of imagery products (Dainelli et al. 2021). Among these subjects, the most popular research topics are individual tree detection and inventory parameters such as basal area, number of trees, diameter, and volume, which are crucial in decision making process, and followed by the pest and disease detection.

There are recent examples of UAV-SfM-based forestry-related researches, which mostly involve visible and NIR bands photogrammetry derived 3D point clouds. These researches were conducted on forest uniformity (Michez et al. 2016; Hentz et al. 2018); the characterization of vertical and horizontal variations of the forest canopy (Jayathunga et al. 2020); an assessment of the estimation success in tree height; tree crown cover and tree count for young stone pine stand and comparison of SfM processing quality (Gülci 2019); tree crown parameter estimations by using object-based image classification (Yurtseven et al. 2019); the mapping and classification of forest tree species comparing field- and UAV-SfM-based timber volume estimations by using allometric formulas (Gülci et al. 2021); mapping forests at the species level (Grybas and Congalton 2021); monitoring health status in priority riparian forests and detection of infects (Woellner and Wagner 2019; Guerra-Hernández et al. 2021; Miraki et al. 2021); tree-stump detection, segmentation, classification, and measurement (Puliti et al. 2018a); and forest road construction and earthwork (Bugday 2018; Akgul et al. 2018).

Based on the results derived from the previous studies, the success in estimated tree parameters of UAV imagery has great potential to use in forestry. For example, biomass estimations of tree parameters determined by UAV-SfM have been carried out with the help of allometric formulas for more than a decade (Dandois and Ellis 2010). On the other hand, UAV-SfM-derived orthophotos with high resolution provide as a basis of image classification techniques (i.e., unsupervised or supervised) for land cover analysis.

5 UAV-SfM Studies in Aboveground Biomass and Carbon Estimation

Precise measurement of a tree biomass includes felling, weighing, and costly and difficult stages. This cost will increase exponentially in forested areas depending on the rough conditions of the land structure. In addition, ecological bases may not be appropriate in many studies, depending on the amount of sample tree use. For this

reason, more cost-effective biomass and carbon measurement techniques, which can be alternatives in tree mass measurement, are used (Dittmann et al. 2017).

The techniques generally used in biomass estimations include (1) allometric equations (field- and laboratory-based equations), (2) optical images (aircraft- and satellite-based passive sensors), (3) radar (aircraft- and satellite-based active sensors), (4) LiDAR (aircraft- and satellite-active sensor), and (5) SfM (UAV-based passive sensors) techniques.

Alonzo et al. (2018) carried out inventory studies in coniferous and broad-leaved forest areas. Tree density, basal area, and AGB estimates were made for white spruce, black spruce, birch, and aspen species in the study, which was carried out for a total of five different lands. In the study carried out with UAV-SfM photogrammetry, oblique and vertical photogrammetric image acquisitions were performed with a DJI Phantom 4 Pro quadcopter with a 20 megapixel camera. In oblique acquisitions, the nadir angle is set to 90° at a 90% overlapping rate at 100 m flight altitude. In their vertical flights, they flew with the camera at a narrow angle (20° off nadir) from a height of 70 m. The total duration of single grid flights for 100 m and double grid flights for 70 m was 12 min. They have established a total of five ground control points (GCPs). In the study, firstly, with the RGB point cloud from UAV-SfM, it was investigated how accurately boreal forest tree species could be classified at the crown scale. Five basic steps have been followed to achieve this goal: (1) identifying the crown areas from the point cloud; (2) estimating structural and spectral variables for each segment; (3) classifying each segment as birch, aspen, white spruce, black spruce, or shrub; (4) calculating crowns at USDA FIA subplot level to estimate tree density (TD), basal area (BA), and AGB; and (5) comparing the TD, BA, and AGB model without segmentation at the subplot level. In the study application, Pix4D software was used for digital photogrammetric processes. They preferred watershed segmentation and then mean-shift segmentation methods in generating canopy height model (CHM) from point clouds. Except for one of the trial areas, the height errors were calculated to be below 1 m. With the help of allometric formulas, estimations were made for conifers by using tree height values ($R^2 = 0.75$, RMSE = 2.5 cm). On the other hand, the diameter at breast height (DBH) estimates based on crown width was lower ($r^2 = 0.35$, RMSE = 5 cm). Segment volumes substantially improved modeled AGB compared to subplot-level height metrics ($R^2 = 0.92$, RMSE = 13.5 Mg ha^{-1} , %RMSE = 27.1) in their study, where they stated that the TD values calculated on a single tree basis and on a trial area basis varied.

Otero et al. (2018) obtained CHM from the point cloud produced by the UAV-SfM technique. Biomass estimations of *Rhizophora apiculata* Blume and *R. mucronata* Lamk species were performed. They produced orthomosaic and digital surface model (DSM) with Photoscan software. Tree height information was estimated with CHM, in which Gaussian filter was applied. The package program "rLidar" (Silva et al. 2015) in R was used to process the CHM. CHMs have been introduced with the local maximum function with a fixed window size application. According to forest inventory, different values for Gaussian filter and a window size were compared for the best thresholds. A quadratic formula ($R^2 = 0.75$) that explains

the relationship between height and AGB by making use of allometric formulas was used in the calculations of AGB (Mg ha^{-1}) (Eq. 1):

$$\text{AGB} = 23.5 - 6.5 \times \text{Height} + 0.8 \times \text{Height}^2 \quad (1)$$

Fernandes et al. (2020) used a combined field and multispectral imagery approach to assess C stock of three dominant species (i.e., *Acacia dealbata* Link, *Alnus glutinosa* (L.) Gaertner, and *Salix salviifolia* Brot.), understory, and soil biomass in the Mediterranean riparian. Object-based image analysis (OBIA) was performed for species classification and segmentation from unmanned aerial vehicle (UAV)-based images. UAV SenseFly eBee platform is used as an aerial platform with RGB camera and Sequoia Parrot (multispectral camera). The photogrammetric flight height was 120 m with 80% of forwarding and side overlaps for RGB and 100 m for multispectral images. In the data acquisition, a total of 12 GCPs were used. Working with SfM logic, Pix4DMapper was used to process block images. Then, the aboveground biomass was calculated based on the allometric formula. A simple nonlinear model ($R^2 = 0.94$, $\text{MSE} = 4.5$) was developed for *Salix salviifolia*, an endemic species (Eq. 2). A coefficient of 0.5 (tC ha^{-1}) was used as the carbon conversion factor:

$$\text{AGB} = 0.1758 \times \text{DBH}^{2.1314} \quad (2)$$

In their study, based on image classification, it was concluded that multiband UAV image data directly supports the conservative ability to classify in-forest waterfront species and indirectly predict tree AGB. No metrics are specified for the estimated carbon content and AGB prediction accuracy.

Wang and Lin (2020) performed photogrammetric flight with a RGB sensor platform mounted on a fixed-wing type UAV and performed biomass estimations. DSM, DEM, and CHM were obtained by processing the 3D point clouds produced with SfM in an area with sparse coniferous species. Tree crown widths were determined using the OBIA technique on the orthorectified map. Tree heights were estimated using CHM. Photogrammetric flight plans used SONY ILCE-5100 brand camera from 400 m height with 60% side and 80% front overlap. In the processing of photo blocks, point cloud and orthorectified map were obtained with Acute3d context capture. They have established 24 GCPs in the field. TerraScan software with the gradual encryption algorithm was used to generate CHM from point cloud. They used new height estimates using a linear regression model between tree height measurements and estimates. In tree height estimations, $R^2 = 92$ and RMSE value was calculated as 1.08 m.

Castellanos-Galindo et al. (2021) studied comparison of ground-based, UAV-based, and radar-based measurements in estimation of stand characteristics. They performed a photogrammetric flight from 100 m using the DJI Phantom Mavic Pro and the Drone Deploy app. GCPs could not be established in the mangrove forest, which is very densely closed. Point cloud and orthomosaic were produced from block images taken at nadir angles with Agisoft Metashape. Tree diameter

(Gülci et al. 2021) and thus the carbon amount will increase. In addition, since even the same species may show different morphological characteristics in different forest ecosystems, it is necessary to develop site-specific formulas by classifying them (Tiwari and Singh 1984).

There are difficulties in performing biomass estimations with UAV-SfM due to the presence of trees of different closures, ages, and types in protected areas:

- Detection of errors caused by point cloud estimations due to tree crown forms.
- Preferring UAV platforms with sensitive GNSS modules (such as D-RTK or RTK) in difficult conditions where GCPs cannot be obtained.
- Reducing the losses incurred when processing images.
- SfM-based programs should be designed in an easier and more understandable way, as it can be complex for people who are not experienced in processing point cloud.

6 Conclusion

AGB and carbon storage in forestlands cannot be directly measured by using UAV-SfM; however, some of biophysical attributes can be obtain by using UAV-mounted optical sensors considering SfM technique. Our findings show UAV-SfM photogrammetry can provide individual tree attributes such as tree height and canopy cover area via processing 3D point clouds. On the other hand, SfM-based generated orthomosaics can be classified by using supervised or unsupervised classification techniques. To improve image classification accuracies, different vegetation indexes, which can be derived from multispectral camera, can improve AGB estimations in forests with high canopy cover or riparian zones. Furthermore, research on carbon storage will be increased in forestry when the cost of hyperspectral camera and LiDAR sensor reduce by time. UAV-SfM-based AGB estimation, which is a nondestructive method, will be increased with the help of developed computer vision technology as well as experts.

Authors' Contributions All authors performed the same effort in this study. All authors wrote, read, reviewed, and decided to submit as chapters of a book.

Conflict of Interest No conflict of interest

References

- Akgul M, Yurtseven H, Gulci S, Akay AE (2018) Evaluation of UAV-and GNSS-based DEMs for earthwork volume. *Arab J Sci Eng* 43(4):1893–1909
- Alonzo M, Andersen H-E, Morton DC, Cook BD (2018) Quantifying boreal forest structure and composition using UAV Structure from Motion. *Forests* 9(3):119

- Andersson F (1971) Methods and preliminary results of estimation of biomass and primary production in south Swedish mixed deciduous woodland. In: Du-Vigneaud P (ed) Productivity of forest ecosystems. UNESCO, Paris, pp 281–288
- Banu TP, Borlea GF, Banu C (2016) The use of drones in forestry. *J Environ Sci Eng B* 5:557–562
- Brown S (1997) Estimating biomass and biomass change of tropical forests. Forest Resources Assessment Publication. FAO Forestry Papers 134:55 pp. Rome
- Bugday E (2018) Capabilities of using UAVs in forest road construction activities. *Eur J Forest Eng* 4(2):56–62
- Castellanos-Galindo GA, Casella E, Tavera H, Zapata Padilla LA, Simard M (2021) Structural characteristics of the tallest mangrove forests of the American continent: a comparison of ground-based, drone and radar measurements. *Front For Glob Change* 4:732468
- Chave J, Andalo C, Brown S, Cairns MA, Chambers JQ, Eamus D, Fölster H, Fromard F, Higuchi N, Kira T, Lescure J-P, Nelson BW, Ogawa H, Puig H, Riera B, Yamakura T (2005) Tree allometry and improved estimation of carbon stocks and balance in tropical forests. *Oecologia* 145(1):87–99
- Chave J, Réjou-Méchain M, Burquez A, Chidumayo E (2014) Improved allometric models to estimate the aboveground biomass of tropical trees. *Glob Chang Biol* 20:3177–3190
- Dainelli R, Toscano P, Di Gennaro SF, Matese A (2021) Recent advances in unmanned aerial vehicle forest remote sensing—a systematic review. Part I: a general framework. *Forests* 12:327
- Dandois JP, Ellis EC (2010) Remote sensing of vegetation structure using computer vision. *Remote Sens* 2:1157–1176
- Dandois J, Olano M, Ellis E (2015) Optimal altitude, overlap, and weather conditions for computer vision UAV estimates of forest structure. *Remote Sens* 7:13895–13920
- Dittmann S, Thiessen E, Hartung E (2017) Applicability of different non-invasive methods for tree mass estimation: a review. *For Ecol Manag* 398:208–215
- Eker R, Alkan E, Aydın A (2020) A comparative analysis of UAV-RTK and UAV-PPK methods in mapping different surface types. *Eur J Forest Eng* 7(1):12–25
- Fernandes MR, Aguiar FC, Martins MJ, Rico N, Ferreira MT, Correia AC (2020) Carbon stock estimations in a Mediterranean riparian forest: a case study combining field data and UAV imagery. *Forests* 11(4):376
- González-Jorge H, Martínez-Sánchez J, Bueno M, Arias AP (2017) Unmanned aerial systems for civil applications: a review. *Drones* 1(1):2
- Grybas H, Congalton RG (2021) A Comparison of multi-temporal RGB and multispectral UAS imagery for tree species classification in heterogeneous New Hampshire Forests. *Remote Sens* 13(13):2631
- Guerra-Hernández J, Díaz-Varela RA, Álvarez-González JG, Rodríguez-González PM (2021) Assessing a novel modelling approach with high resolution UAV imagery for monitoring health status in priority riparian forests. *For Ecosyst* 8(1):1–21
- Guimarães N, Pádua L, Marques P, Silva N, Peres E, Sousa JJ (2020) Forestry remote sensing from unmanned aerial vehicles: a review focusing on the data, processing and potentialities. *Remote Sens* 12(6):1046
- Gülci S (2019) The determination of some stand parameters using SfM-based spatial 3D point cloud in forestry studies: an analysis of data production in pure coniferous young forest stands. *Environ Monit Assess* 191(8):495. <https://doi.org/10.1007/s10661-019-7628-4>
- Gülci S, Akay AE, Gülci N, Taş İ (2021) An assessment of conventional and drone-based measurements for tree attributes in timber volume estimation: a case study on stone pine plantation. *Ecol Inform* 63:101303
- Gupta SG, Ghonge MM, Jawandhiya PM (2013) Review of unmanned aircraft system (UAS). *Int J Adv Res Comput Sci Eng Inf Technol* 2(4):1646–1658
- Hentz ÂMK, Silva CA, Dalla Corte AP, Netto SP, Strager MP, Klauberg C (2018) Estimating forest uniformity in *Eucalyptus* spp. and *Pinus taeda* L. stands using field measurements and structure from motion point clouds generated from unmanned aerial vehicle (UAV) data collection. *For Syst* 27(2):17

- Hermosilla T, Ruiz LA, Kazakova AN, Coops NC, Moskal LM (2014) Estimation of forest structure and canopy fuel parameters from small-footprint full-waveform LiDAR data. *Int J Wildl Fire* 23:224–233
- Ighhaut J, Cabo C, Puliti S, Piermattei L, O'Connor J, Rosette J (2019) Structure from motion photogrammetry in forestry: a review. *Curr Forest Rep* 5(3):155–168
- Jayathunga S, Owari T, Tsuyuki S, Hirata Y (2020) Potential of UAV photogrammetry for characterization of forest canopy structure in uneven-aged mixed conifer–broadleaf forests. *Int J Remote Sens* 41:53–73
- Kameyama S, Sugiura K (2020) Estimating tree height and volume using unmanned aerial vehicle photography and SfM technology, with verification of result accuracy. *Drones* 4(2):19
- Keane JF, Carr SS (2013) A brief history of early unmanned aircraft. *Johns Hopkins APL Technical Digest* 32(3):558–571
- Lingner S, Thiessen E, Müller K, Hartung E (2018) Dry biomass estimation of hedge banks: allometric equation vs. structure from motion via unmanned aerial vehicle. *J For Sci* 64:149–156
- Lisein J, Pierrot-Deseilligny M, Bonnet S, Lejeune P (2013) A photogrammetric workflow for the creation of a forest canopy height model from small unmanned aerial; system imagery. *Forests* 4:922–944
- Michez A, Piégay H, Lisein J, Claessens H, Lejeune P (2016) Classification of riparian forest species and health condition using multi-temporal and hyperspatial imagery from unmanned aerial system. *Environ Monit Assess* 188:146
- Miraki M, Sohrabi H, Fatehi P, Kneubuehler M (2021) Detection of mistletoe infected trees using UAV high spatial resolution images. *J Plant Dis Prot* 128:1679–1689
- Mohan M, Leite RV, Broadbent EN, Jaafar WSWM, Srinivasan S, Bajaj S et al (2021) Individual tree detection using UAV-lidar and UAV-SfM data: a tutorial for beginners. *Open Geosci* 13(1): 1028–1039
- Nasiri V, Darvishsefat AA, Arefi H, Pierrot-Deseilligny M, Namiranian M, Le Bris A (2021) Unmanned aerial vehicles (UAV)-based canopy height modeling under leaf-on and leaf-off conditions for determining tree height and crown diameter (case study: Hyrcanian mixed forest). *Can J For Res* 51(7):962–971
- Návar J (2009a) Allometric equations for tree species and carbon stocks for forests of northwestern Mexico. *For Ecol Manag* 257:427–434
- Návar J (2009b) Biomass component equations for Latin American species and groups of species. *Ann For Sci* 66:208–216
- Newcome LR (2004) Unmanned aviation: a brief history of unmanned aerial vehicles. Reston, VA, American Institute of Aeronautics and Astronautics, Inc., pp 45–50
- Nex F, Remondino F (2014) UAV for 3D mapping applications: a review. *Appl Geomatics* 6:1–15
- Otero V, Van De Kerchove R, Satyanarayana B, Martinez-Espinosa C, Bin Fisol MA, Bin Ibrahim MR, Sulong I, Mohd-Lokman H, Lucas R, Dahdouh-Guebas F (2018) Managing mangrove forests from the sky: forest inventory using field data and Unmanned Aerial Vehicle (UAV) imagery in the Matang Mangrove Forest Reserve, peninsular Malaysia. *For Ecol Manag* 411: 35–45
- Pajares G (2015) Overview and current status of remote sensing applications based on unmanned aerial vehicles (UAVs). *Photogramm Eng Remote Sens* 81(4):281–329
- Perruchoud DO, Fischlin A (1995) The response of the carbon cycle in undisturbed forest ecosystems to climate change: a review of plant-soil models. *J Biogeograph* 22:759–274
- Puliti S, Ene LT, Gobakken T, Næsset E (2017) Use of partial-coverage uav data in sampling for large scale forest inventories. *Remote Sens Environ* 194:115–126
- Puliti S, Talbot B, Astrup R (2018a) Tree-stump detection, segmentation, classification, and measurement using Unmanned aerial vehicle (UAV) imagery. *Forests* 9:102
- Puliti S, Saarela S, Gobakken T, Ståhl G, Næsset E (2018b) Combining UAV and Sentinel-2 auxiliary data for forest growing stock volume estimation through hierarchical model-based inference. *Remote Sens Environ* 204:485–497

- Puliti S, Solberg S, Granhus A (2019) Use of UAV photogrammetric data for estimation of biophysical properties in forest stands under regeneration. *Remote Sens* 11(3):233
- Remondino F, Spera MG, Nocerino E, Menna F, Nex F (2014) State of the art in high density image matching. *Photogramm Rec* 29:144–166
- Richardson J, Bjorheden R, Hakkila P, Lowe AT, Smith CT (2002) *Bioenergy from sustainable forestry: guiding principles and practice*. Kluwer Academic Publishers, Dordrecht, p 344
- Sankey T, Donager J, McVay J, Sankey JB (2017) UAV Lidar and hyperspectral fusion for forest monitoring in the southwestern USA. *Remote Sens Environ* 195:30–43
- Silva CA, Crookston NL, Hudak AT, Vierling LA (2015) Package ‘rLiDAR’: LiDAR data processing and visualization. Available in CRAN repository. <https://cran.r-project.org/web/packages/rLiDAR/rLiDAR.pdf>. Accessed 15 Dec 2021
- Smith MW, Carrivick JL, Quincey DJ (2015) Structure from motion photogrammetry in physical geography. *Prog Phys Geogr* 40:247–275
- Stone C, Webster M, Osborn J, Iqbal I (2016) Alternatives to LiDAR-derived canopy height models for softwood plantations: a review and example using photogrammetry. *Aust For* 79:271–282
- Swayze NC, Tinkham WT, Vogeler JC, Hudak AT (2021) Influence of flight parameters on UAS-based monitoring of tree height, diameter, and density. *Remote Sens Environ* 263:112540
- Tang L, Shao G (2015) Drone remote sensing for forestry research and practices. *J For Res* 26:791–797
- Tiwari AK, Singh JS (1984) Mapping forest biomass in India through aerial photographs and nondestructive field sampling. *Appl Geogr* 4:151–165
- Torresan C, Berton A, Carotenuto F, Di Gennaro SF, Gioli B, Matese A, Miglietta F, Vagnoli C, Zaldei A, Wallace L (2017) Forestry applications of UAVs in Europe: a review. *Int J Remote Sens* 38(8–10):2427–2447
- Tuominen S, Balazs A, Saari H, Pölonen I, Sarkeala J, Viitala R (2015) Unmanned aerial system imagery and photogrammetric canopy height data in area-based estimation of forest variables. *Silva Fenn* 49(5):1348
- Van Leeuwen M, Nieuwenhuis M (2010) Retrieval of forest structural parameters using LiDAR remote sensing. *Eur J For Res* 129:749–770
- Wallace L, Lucieer A, Watson C, Turner D (2012) Development of a UAV-LiDAR system with application to forest inventory. *Remote Sens* 4:1519
- Wallace L, Lucieer A, Malenovský Z, Turner D, Vopěnka P (2016) Assessment of forest structure using two UAV techniques: a comparison of airborne laser scanning and structure from motion (SfM) point clouds. *Forests* 7:62
- Wang M, Lin J (2020) Retrieving individual tree heights from a point cloud generated with optical imagery from an unmanned aerial vehicle (UAV). *Can J For Res* 50(10):1012–1024
- Woellner R, Wagner TC (2019) Saving species, time and money: application of unmanned aerial vehicles (UAVs) for monitoring of an endangered alpine river specialist in a small nature reserve. *Biol Conserv* 233:162–175
- Yavaşlı DD (2012) Recent approaches in aboveground biomass estimation methods. *Aegean Geogra J* 21(1):39–49
- Yurtseven H, Akgul M, Coban S, Gulci S (2019) Determination and accuracy analysis of individual tree crown parameters using UAV based imagery and OBIA techniques. *Measurement* 145: 651–664

Part VIII

**Hyperspectral and Multi Source Remote
Sensing**



Hyperspectral Identification of Selected Dipterocarp Montane at the Species Level

Nisfariza Mohd Noor

Abstract

The ecosystems of rainforests in Peninsular Malaysia are complex. The assessment and monitoring using the traditional land-based survey methods for these ecosystems are costly and time-consuming. It is an advantage for remote surveillance, especially when dealing with inaccessible areas. Remote sensing for forests mapping, species distribution, aboveground biomass, and carbon stocks allocation is emerging at this very moment. The technology enables regular monitoring of difficult forest areas and data captured from remote sensors analysed for the deduction and information gathering of the local and world forest cover. Each object reflects unique electromagnetic radiation, which is the foundation behind spectral identification. Vegetation covers such as agricultural plots, urban forestry, or urban landscape are simple due to the accessibility of the and limited numbers of species. However, remote sensing of tropical forests is a big challenge due to the hilly surface and the abundant species. Remote sensors are developed using different utility types of sensing approaches for observing the earth surfaces, namely, the optical sensors (multispectral and hyperspectral), RADAR, and LiDAR. Hyperspectral can harvest the minute disparity or changes of the reflectance of a vegetation cover. The use of hyperspectral for vegetation spans from vegetation species identification, pest and disease detection, and many more. This chapter presents the use of spectroscopy sensors and analytics to discriminate the several species of dipterocarp in forest areas of Semangkok, Selangor, and their spectral library and general distribution of the forest species with their biophysical properties in the montane strata.

N. Mohd Noor (✉)

Department of Geography, Faculty of Arts and Social Sciences, University Malaya, Kuala Lumpur, Malaysia

e-mail: nish@um.edu.my

© The Author(s), under exclusive license to Springer Nature Singapore Pte Ltd. 2022

M. N. Suratman (ed.), *Concepts and Applications of Remote Sensing in Forestry*, https://doi.org/10.1007/978-981-19-4200-6_21

413

Keywords

Dipterocarp · Hyperspectral · Species identification · Spectral reflectance

1 Introduction

Research on remote sensing vegetation is one of the main interests of many researchers; vegetation covers such as agricultural plots, urban forestry, or urban landscape are easier to study due to the accessibility to the study area and minute numbers of species. However, remote sensing of forests especially in the tropics is quite a challenge due to the enormous numbers of species and hilly surfaces. This chapter presents the species identification of selected dipterocarp trees in montane structures of Semangkok Forest Reserve. Remote sensing technology is not a replacement for field surveys, but a complementary tool for supporting the research and analytics and should be conducted simultaneously until a significant correlation or model between ground assessment and remote sensing is developed. During the data collection campaign, we manage to obtain spectral datasets of 16 dipterocarp species in the montane forest of Semangkok. However, only four dipterocarp species were presented. The spectral analysis of selected dipterocarp species is focusing on identifying the spectral curve of floral biodiversity using the hyperspectral remote sensing technique in the Semangkok forest.

2 General Introduction of Tropical Rainforests

The tropical rainforest (in Malaysia is called Hutan Hujan Tropika) is one of the utmost miscellaneous ecosystems on this planet (Denslow 1987; Myers et al. 2000; Kettle 2010). Salinas et al. (2021) generally referred to as the tropical montane forest (TMF) and are found on most of Earth's continents along variable elevation ranges, the area covered by tropical and subtropical montane forests is around 305 million hectares, and about 13% of the area covered by tropical and subtropical forests. Tropical rainforests cover less than 7% of the planet's land mass, which is about half of the forest in this planet (Wilson 1988; Bierregaard et al. 1992). Amazingly, these ecosystems are habitat to half to two thirds of the species of flora and fauna on the earth (Newman 2002). The eco-region of the Malaysian rainforest is categorised into the Tropical and Subtropical Moist Broadleaf Forests in the Indo-Malaya biogeographic realms (Olson et al. 2001). Approximately about 40–75% of all living creatures on this planet originated from this type of forest (Denslow 1987), and for this reason, the tropical rainforest is also called a jewel of the earth and the “world's largest pharmacy” due to over one-quarter of natural antidote (mostly derived from vegetation) that has been discovered within this forest (Maiti and Maiti 2011).

Tropical rainforests can be found in three major geographical zones between the latitudes of 22.5° north and 22.55° south of the equator which is in the regions of Central America (in the Amazon River basin), Africa (Zaire basin, with all small

zone in West Africa and eastern Madagascar), and Indo-Malaya (west coast of India, Assam, Southeast Asia, New Guinea, and Queensland, Australia) (Denslow 1987; Olson et al. 2001). Unfortunately, it was approximated that at least 70 million ha of forest are depleted and extensively logged in Southeast Asia (SEA) (Adjers et al. 1996; Myers et al. 2000). The biodiversity of tropical montane in Southeast Asian forests are solemnly in danger (Sodhi et al. 2010; Chechina 2015) due to the high deforestation rate and threat to loss the biodiversity in 2100 (Sodhi et al. 2010).

Characterisation of spatial distribution of global forest in terms of extent, loss, and gain are reported by Hansen et al. (2013). Globally 2.3 million km² were lost, and 0.8 million km² were gained from replanting program in 12 years. The topics exhibit greatest losses and gains.

Recently, Feng et al. (2021) reveals increasing mountain forest loss across Southeast Asia using high-resolution satellite and indication and quantification of carbon loss from forest clearance. Encroachment of forest at higher altitudes influenced the roles tropical forests play in the context of global climate mitigation, biodiversity conservation, and global carbon cycling. The acceleration in forest loss also affects biodiversity conservation in the region because a substantial number of endemic species are found in the mountains of SEA (Sodhi et al. 2010).

Peninsular Malaysia encompasses an area of 13.2 million ha. This region is situated between latitudes 1°20' and 6°45' N and 100° and 104°30' E. A mountain range runs along peninsula region with peaks more than 2000 m, more than 60% of the region is undulating lowland surface, less than 300 m above sea level about 35% is hilly with elevations of 300–1300 m, and the remainder peninsula surface is extremely mountainous (FAO 1981; Brown et al. 1994).

The lowland dipterocarp forests of Peninsular Malaysia were cut for agriculture purposes before 1966. Thus, Peninsular Malaysian forests have been placed on Conservation International's list "hot spot" due to its megadiversity which plays especially key role in maintaining present and future diversity of the world. The tropical rainforests can be responsible to numerous ecosystem services including freshwater management, carbon storage, and soil protection (Myers et al. 2000).

3 Introduction on Dipterocarp Species

Dipterocarps are tropical evergreen rain forest trees, biologically suitable for warm and uniform moist conditions. Climatic variations contribute to the distribution of the dipterocarp forest at altitude lower than 1200 meters. The dipterocarp forest is divided into low dipterocarp forest and hill dipterocarp forest. It is the predominant family of timber trees in the tropical evergreen rainforest of Malay Peninsula (now Peninsular of Malaysia) and are closely related ecologically and floristically to Borneo and Sundae Shelf. Several Malayan genera can be found in India, Ceylon, the Philippines, and New Guinea (Symington 1974). Dipterocarpaceae (or "two-winged fruit") is a tree family of 17 genera (Maury-Lechon and Curtet 1998), and 13 genera are restricted to Asia (Bawa and Seidler 2008; Myers et al. 2000). In addition, around 695 dipterocarp species managed to be identified all over the world

(Bawa 1998). Studies have shown that up to 90% of the dipterocarp species are restricted to Asia (Myers et al. 2000) and, surprisingly, 10 genera and 99 species are exclusively only can be found in South Asia (FAO 1985). Numerous numbers of dipterocarp trees can be found in the Philippines (65 spp.), Sumatra (106 spp.), the Malay Peninsula (155 spp.), and Borneo (267 spp.) (Chechina 2015; Corlett and Primack 2005; Myers et al. 2000). According to Symington (2004), *Shorea* (196 species), *Hopea* (104 species), *Dipterocarpus* (70 species), and *Vatica* (65 species) are top four of the biggest genera in Dipterocarpaceae family. Corlett and Primack (2005) stated that it is a common thing to find 25 or more species of *Shorea* and 6 or more species of the other tree (*Hopea*, *Dipterocarpus* and *Vatica*) genera in any one forest in Sumatra, Borneo, or Malay Peninsula.

Symington (2004) stated that the greatest diversity of Dipterocarpaceae occurs in Borneo. Most of the Malaysian pristine tropical rainforest is commonly featured by the dominance existence of trees from Dipterocarpaceae family (Symington 2004), and this tree family typically forms high portion (nearly 30%) of the floristic composition in the emergent and canopy strata (Schulte and Schöne 1996; Whitmore and Burnham 1975). In addition, Appanah and Turnbull (1998) and Chechina (2015) stated that dipterocarp trees generally inhabit mature stages of primary forest, and sometimes they also seem able to colonise secondary forest.

4 Hyperspectral Remote Sensing of Forest

Remote sensing has been shown to play an important role in providing more continuous and detail monitoring data in many fields such as forestry (Berry and Ripple 1996; Dalponte et al. 2011) even at the most isolated and unreachable areas (Kalacska and Sánchez-Azofeifa 2008). The study of vegetation spectra is one of the most important remote sensing applications since vegetation covers a large area of the earth and plays important role in assuring its sustainability. Hyperspectral remote sensing refers to a lot of wavelengths measured by the hyperspectral sensor. This means that hyperspectral remote sensing provides ample spectral information to identify and distinguish spectrally unique materials, thus providing the potential for more accurate and detailed information extraction than other types of remotely sensed data. The spectral library is a key to exploring the hyperspectral imaging detection and mapping of dipterocarp species on airborne or UAVs (Jusoff 2007). Hyperspectral remote sensing is divided into imaging and non-imaging systems. The non-imaging usually refers to as spectroscopy or spectroradiometry. Hyperspectral data have details and accuracy that allow phenomena and concepts to be extended beyond traditional remote sensing. Thus, provide opportunities to precisely identify earth surface phenomena than is normally possible with broadband sensors (Campbell and Wynne 2011).

Energy interactions between objects are often specific. Specificity is the key to distinguishing objects for ascertaining certain characteristics. Spectral reflectance is a function of wavelength and of the properties of the object. This means that the spectral reflectance of different objects almost equal at certain wavelengths but

different at other wavelengths. The image of vegetation from an aerial viewpoint integrates the effects of leaves, stems and branches, flowers, and other elements of the plants with the background soil; it is called the spectral signature.

The spectral signatures of vegetation are modified by leaf type and morphology (Sims and Gamon 2002), leaf physiology, and chlorophyll content (Blackburn 1998). Spectral analysis or spectrum analysis is analysis in terms of a spectrum of electromagnetic frequencies or related quantities such as energies. In specific areas it may refer to spectroscopy in chemistry and physics, a method of analysing the properties of matter from their electromagnetic interactions.

According to Roberts et al., most narrowband or hyperspectral systems are able to accumulate a big capacity of data in wavelengths that are extremely correlated from one another. One of the advantages of the hyperspectral data is the sample data can be utilised for statistical analysis during the discrimination of tree species utilising reflectance spectra. Different tree species have different spectral signatures due to different plant materials, nitrogen content, amount of pigment, carbon content, water content and other plant properties (Asner 1998). Hyperspectral remote sensing is believed to be more practicable compare to other remote sensing systems due to its special features like possessing high spatial resolution with contiguous and narrow bandwidths that permit this spectral technology to be examined earth surface topographies more clearly and precisely. Compared to multispectral imagery; hyperspectral imagery can be utilized to map tree species within forested areas (Mohd Azahari et al. 2011). Biodiversity mapping have been attempted by several researchers using airborne hyperspectral systems in Afizzul et al. (2021), Kishore et al. (2020), Vaglio Laurin et al. (2014), Mohd Azahari et al. (2011), Mohamad Hasmadi et al. (2010), Jusoff (2006), Jusoff (2009), Jusoff (2013).

5 Study Area

The Semangkok Forest Reserve is located in Ulu Selangor, Selangor, Malaysia (3° 37' N, 101° 44' E) . The estimated terrain elevation of Semangkok forest is approximately 950 MSL. The Semangkok Forest Reserve is a 28-ha virgin jungle reserve surrounded by secondary forests that were selectively logged in the 1980s (Niiyama et al. 2016, Nakaya and Tani 2016) the dipterocarps trees are undergoing fast disappearing mostly due to the influence of human interference such as logging. This has bad impacts on economic growth and eventually on the Mother Nature as a whole. These consequences have then drawn considerable attention to forest management in order to conserve and preserve this unique dipterocarps forest ecosystem. During the random sampling of the Semangkok Forest Reserve, we observed several plots with plot markings, and the dipterocarp trees were also tagged. The Semangkok Forest Reserve has been studied comprehensively under the joint research between the Forest Research Institute of Malaysia and the Japanese International Research Center for Agricultural Sciences (JIRCAS) for research development and monitoring of forest regeneration (Tani et al. 2015). It is a challenging task to track down, categorize, and map dipterocarps trees, especially in highly mixed

heterogeneous and hilly tropical rainforests like in the Semangkok Forest Reserve. The average annual rainfalls are 2,414 mm, and the average annual minimum and maximum temperatures are 21.9 °C and 33.0 °C, respectively (Saifuddin et al. 1991). The periphery of Fraser's Hill and Semangkok is marked on the state border in between Selangor and Pahang in the road entrancing Fraser's Hill near the gap. Thus, this chapter eventually acquaints Frasers' Hill as a geographical or common reference on the location of the study area.

6 Biodiversity Profile and Biophysical of Selected Dipterocarp Species in Semangkok Forest

Studies of floristic composition of hill and montane forest in Semangkok Forest are not well diverse as compared to Fraser's Hill. Most of the studies were correlated with the montane forest structure, floristic variation, and physiognomic criteria consistently with altitudinal vegetation zones, forest regeneration, and sustainable forest management. (3° 37' N, 101° 44' E) The Semangkok Forest shown a well dynamic of floristic composition and vegetation changes along altitudinal gradient will be well explained according to variation of microhabitats and microclimate. The average annual rainfalls are 2,414 mm, and the average annual minimum and maximum temperatures are 21.9 °C and 33.0 °C, respectively (Saifuddin et al. 1991). Fraser's Hill and Semangkok Mountain (including Semangkok Forest Reserve) are in the undulating environment and on transboundary forest system, that is a sensitive with and fragile ecosystem and that holds a key area for highland biodiversity.

The condition of Semangkok Forest is good and stands as a reserved forest. The presence of various types of vegetation like *liana*, rattan, and palm species and various types of fauna makes a good indicator a virgin forest. Figure 1 exhibits Semangkok Forest with a variety of floristic and physiognomic criteria.

This chapter only focusses on Dipterocarpaceae due to its economical and ecological importance within Semangkok Reserve Forest region. The tree family Dipterocarpaceae plays a major role in both the economic and environmental values (Appanah and Turnbull 1998) such as providing many ecological services and goods to a rising population (Kettle 2010). According to Ghazoul (2016), there are about 157 dipterocarp species which can be found in Peninsular Malaysia and 30 dipterocarp species are endemic to Peninsular Malaysia. Besides playing a vital role as a supplier for excellent quality timber species, the member of this family also provides us with valuable secondary products (products that come out of a production process in addition to the main product) or non-timber products such as essential oils, balsam, and resin (Appanah and Turnbull 1998; Ghazoul 2016).



Fig. 1 Various of floristic and physiognomic criteria in Semangkok forest

7 Methodology

The methodology adopted in this chapter is presented in Fig. 2.

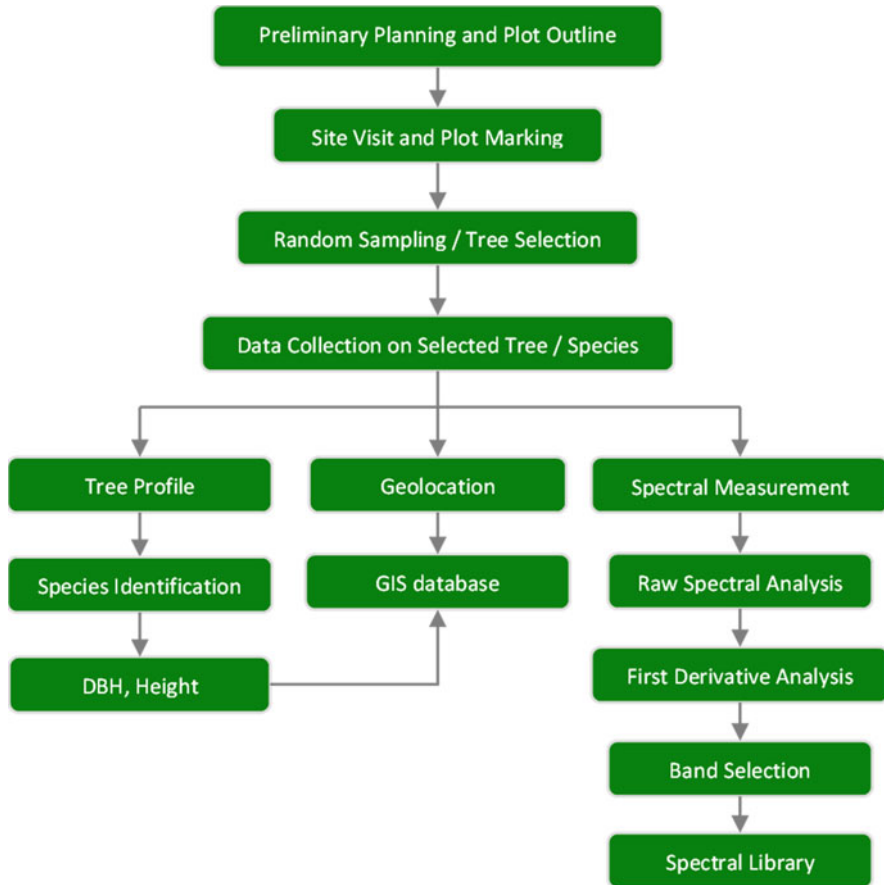


Fig. 2 Flowchart of the methodology adopted in the study

7.1 Random Sampling and Selection of Dipterocarp Species

The data collection was done in a primary hill dipterocarp forest in the Semangkok Forest Reserve. The field campaign was carried out from 2017 to 2018. Fresh leaves from randomly selected dipterocarp trees were collected within 6 ha of Semangkok Forest Reserve plot areas. The sampled tree stand was tagged using a metal tag, and the coordinate was recorded for mapping purposes using Trimble Juno 3D. In occasions trees were randomly sampled with tags from previous researcher's campaign. Random sampling was established for selection of the dipterocarp trees due to the random distribution of the species, challenging topography, and no previous census data.

The dipterocarp tree selection and leaf samples were collected with the help of indigenous people (Orang Asli Temuan) from nearby indigenous settlement in



Fig. 3 Field data collection

Kampung Pertak and experienced forester. Leaf samples were collected from crown of individual study trees manually using slingshot. Efforts and extra care were also taken to only collect healthy green, mature, and homogenous in colour (without anthocyanin pigmentation) as well as perfect (without visible symptoms of rot or disease). The tree species were identified later reconfirmed with herbarium records. The forest stand data acquisition was collected during the sampling; DBH Diameter at breast height (DBH) (diameter at breast height Diameter at breast height (DBH)), height, and altitude of each tree stand sampled were recorded accordingly using 20m DBH Diameter at breast height (DBH) tape and height using a rangefinder. Six to eight leaves were plucked using the sling shot slingshot for each tree samples. The leaves were kept in a transparent ziplock bag recorded, numbered, and kept in a cool box to maintain their freshness for spectral data collection. Figure 3 exhibits the data collection campaign.

A total of 320 leaves from 40 tree crowns were sampled. Ten individual trees for each dipterocarp species. In this campaign, we obtained pure spectral reflectance of twenty dipterocarp species. However, due to random sampling, challenging topography and rare occasion of the existence of certain species, spectral information on several species has yet to be completed for significant band selection. Only species with complete number of sample (ten trees per species) were analysed statistically.

7.2 Biophysical Information

Four species have been selected for this research which are *Dipterocarpus grandiflorus* (Keruing belimbing), *Shorea acuminata* (Meranti rambai daun), *Hopea dryobalanoides* (Merawan mata kucing hitam), and *Shorea macroptera* (Meranti melantai). Table 1 shows the details about data collection of four selected dipterocarp species.

7.3 Mapping of the Study Area

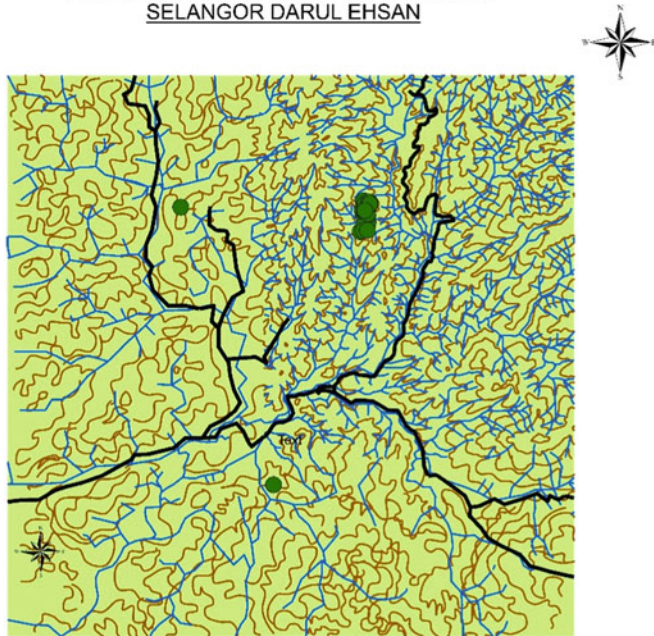
The restricted topography map with the scale of 1:50,000, Series L7030, Sheet No. 3759 and 3859 (Tanjong Malim and Raub) published by the Department of Survey and Mapping Malaysia (JUPEM) in 1993 was scanned, georectified to WGS1984, UTM Zone N47 and EPSG:32647 and digitised as the base map for reference on the spatial distribution of the dipterocarp species sampled. The geotagged coordinate of each tree stand were added into the base map of the study area. Figure 4 shows the study area with the distribution of dipterocarp sample in Semangkok Forest, Ulu Selangor.

During the campaign, samples were recorded on the following dipterocarp species: *Shorea maxwelliana* (Balau kumus hitam), *Shorea hopeifolia* (Damar hitam siput jantan), *Shorea ovalis* (Meranti kepong), *Anisoptera curtisii* (Mersawa kuning), *Shorea leprosula* (Meranti tembaga), *Anisoptera laevis* (Mersawa durian), *Shorea pauciflora* (Meranti nemesu), *Shorea parvifolia* (Meranti sarang punai), and *Shorea bracteolata* (Meranti pa'ang). All measurements of biophysical and spectral were observed, but the total number of samples is not up for the statistical analysis. Figure 5 shows the species of dipterocarp and their locations in the Semangkok Forest Reserve.

Table 1 Biophysical information on the selected dipterocarp species

Types of dipterocarp species	Status (IUCN/ Malaysia Plant Red List)	Size, DBH (cm)	Height (m)	Altitude (m)
<i>Dipterocarpus grandiflorus</i> (Keruing belimbing)	Endangered/least concern	7.4–35.4	13.0–30.0	545–559
<i>Shorea macroptera</i> (Meranti melantai)	Least concern	13.0–88.0	15.0–37.0	500–550
<i>Shorea acuminata</i> (Meranti rambai daun)	Least concern	9.0–72.0	7.0–32.0	494–541
<i>Hopea dryobalanoides</i> (Merawan mata kucing hitam)	Least concern	6.7–63.0	10.0–27.5	308–540

STUDY SITE OF DISTRIBUTION DIPTEROCARPS SAMPLE,
SEMANGKOK FOREST, ULU SELANGOR,
SELANGOR DARUL EHSAN



Legend

- Dipterocarp Sample
- Road
- River
- Contour 100 meter

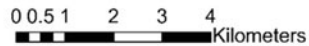


Fig. 4 GIS map exhibiting the sampling area and the highland topography and river streams of the sampling area

7.4 Spectral Reflectance of Selected Dipterocarp Species

Spectral information and plant canopy functional traits and biodiversity have been developed in the Spectranomics approach, to provide time-varying and scalable methods for remote sensing of forest biodiversity (Martin 2020). Spectral measurements of the leaves were taken using the GER 1500 field handheld spectroradiometer manufactured by Spectra Vista Corporation, New York, USA. The spectroradiometer covers the wavelength range from 350 to 1050 nm with 514 spectral bands separated at 1.5nm. The GER 1500 was attached to a leaf probe with light source to record the spectral signature of each dipterocarp species. Dipterocarps leaves were sampled from the upper portion of tree crowns to avoid

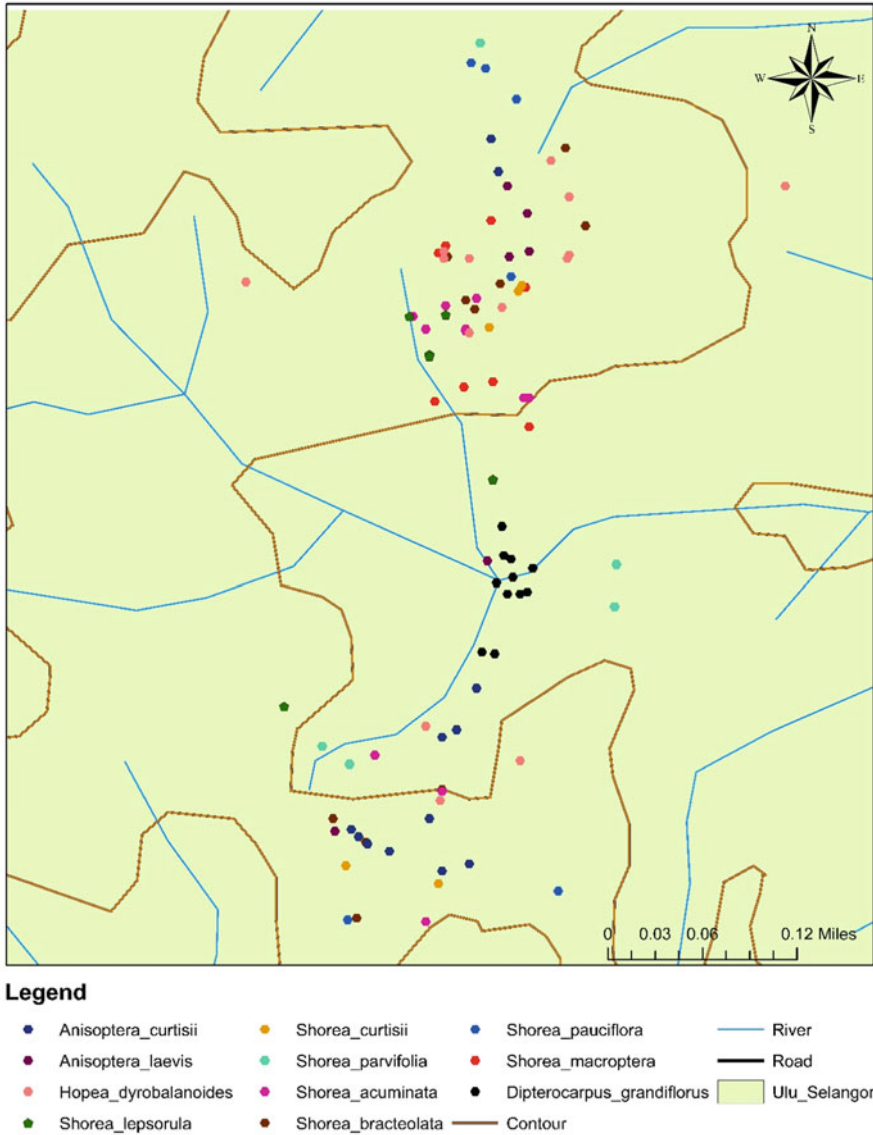


Fig. 5 The distribution of Dipterocarp samples in Semangkok Forest Reserve

sample variability caused by the light environment. Leaf samples that are exposed to sunlight are more applicable for the remote sensing context of this study owing to at the top of a tree canopy they powerfully affect remote spectral measurements (Rivard et al. 2008). Six best leaves from each individual dipterocarp tree were chosen and wiped with a paper towel to remove any water and other substance. The spectroradiometer was set to reference mode by obtaining the reflectance of a

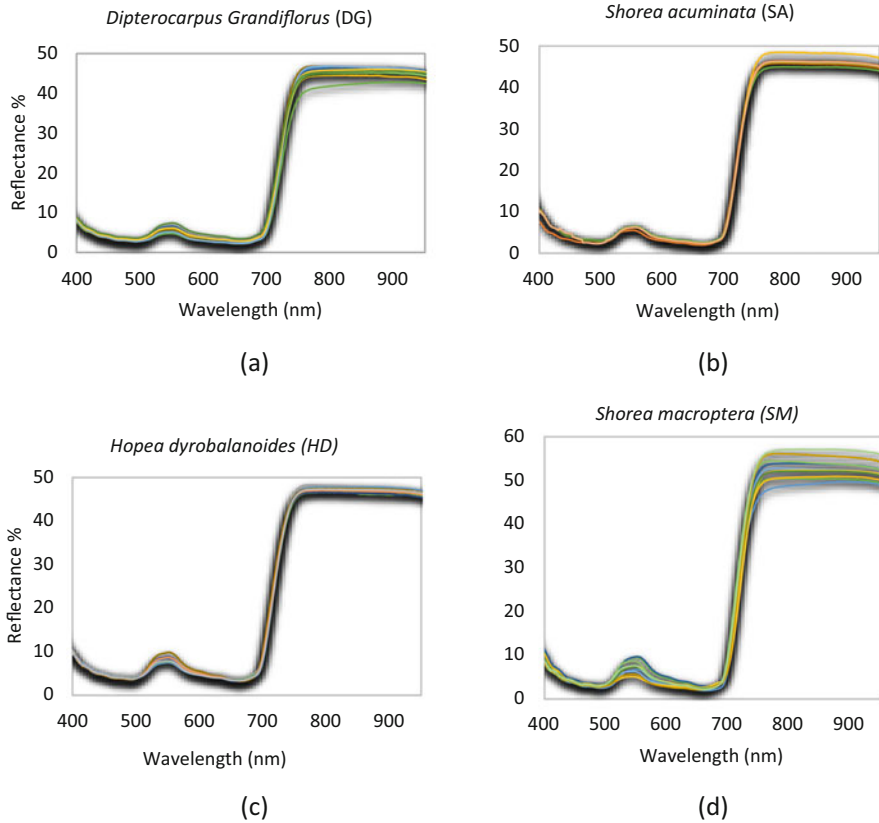


Fig. 6 The first derivative spectra of the (a) *Dipterocarpus grandiflorus*, (b) *Shorea acuminata*, (c) *Hopea dryobalanoides*, and (d) *Shorea macroptera*

white reference. A black cloth with high absorbing material was used in the GER1500 equipment set-up to remove any background signal and increase spectral purity during the spectral measurement. The spectroscopy measurement for spectral reflectance is also known as non-imaging hyperspectral technique. Hyperspectral can pick up the minute difference or changes of the reflectance of the vegetation cover. A massive ground samples are required to develop dipterocarp spectral signatures with ancillary data (tree height, DBH, biomass, biophysical information) at the same time of spectral data sampling.

A number of 320 leaf samples were plucked/slingshot from 40 trees that represent the dipterocarp species; Fig. 6 portrays reflectance curve or spectral signature of four dipterocarp species, namely, (a) *Dipterocarpus grandiflorus* (Keruing belimbing) (b) *Shorea acuminata* (Meranti rambai daun), (c) *Hopea dryobalanoides* (Merawan mata kucing hitam), and (d) *Shorea macroptera* (Meranti melantai).

Figure 7 shows the spectral reflectance for (a) *Dipterocarpus grandiflorus* (Keruing belimbing), (b) *Shorea acuminata* (Meranti rambai daun), (c) *Hopea*

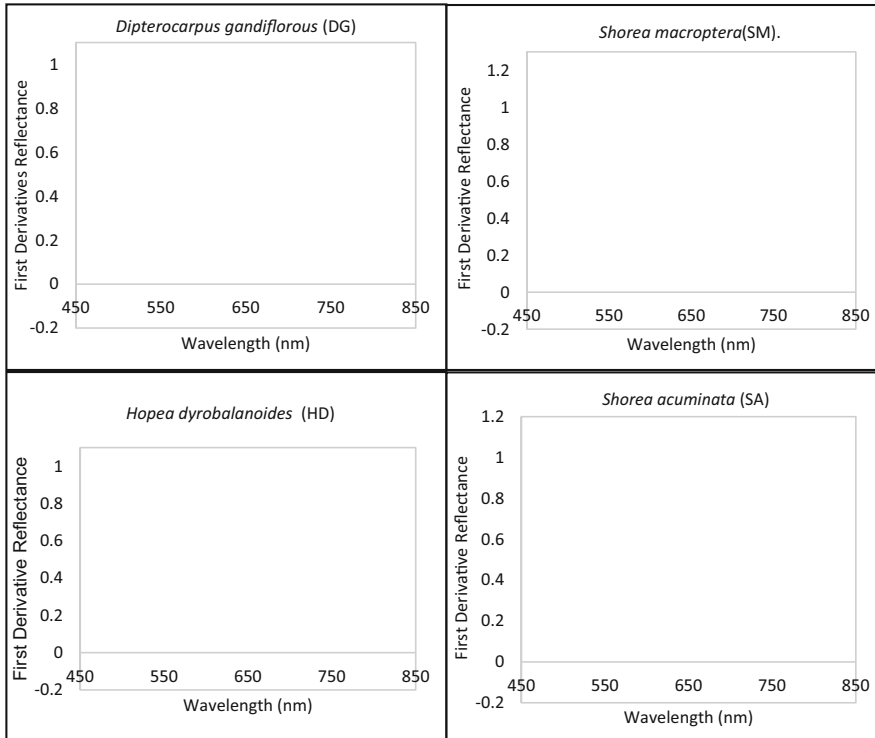


Fig. 7 First derivative analysis (without smoothing) of *Dipterocarpus gandiflorous*, *Shorea acuminata*, *Hopea dryobalanoides*, and *Shorea macroptera*

dryobalanoides (Merawan mata kucing hitam), and (d) *Shorea macroptera* (Meranti melantai).

8 Spectral Analysis of Dipterocarp Species

8.1 Derivative Analysis

First derivative analysis of spectra is the most common and simple analysis in spectroscopy to analyse contiguous spectra through reflectance measurements (Demetriades-Shah et al. 1990; Dawson and Curran 1998; Zarco-Tejada et al. 2003; Nisfariza 2012). It involves the calculation of the slope or rate of change of reflectance with wavelength. Derivatives are useful to reduce the effect of multiple scattering of radiation due to sample geometry and surface roughness and for locating the positions of absorption features and inflection points in the spectra.

The derivative analysis of spectra reflectance was used primarily to locate the position and height of the inflection point of the red edge. The first difference transformation of the reflectance spectrum was obtained from the polynomial fit

by calculating the first derivative. In this case, the red-edge peak in the derivative spectra was composed of the peak maximum usually between 680 and 750 nm and calculated by the XLSTAT. The first derivative was calculated using a first difference transformation of the reflectance spectrum (Dawson and Curran 1998).

Data and manipulation for the raw data were carried out in XLSTAT; the spectral reflectance features of each dipterocarp trees species and the average reflectance were calculated for each distinct species of tree leaves. Each of the individual spectra is plotted as a spectral curve graph and examined to make sure no incorrect values to be amalgamated into the subsequent analysis as well as to determine tree species curves for dipterocarp trees.

The first derivative reflectance (FDR) of all four species are shown in Fig. 7 from average of all leaf samples of each dipterocarp species, while Fig. 6 shows a set of reflectance spectra of based on every sample taken on *Dipterocarpus grandiflorus*, *Shorea acuminata*, *Hopea dryobalanoides*, and *Shorea macroptera*. From the set of spectral reflectance of each sample, the derivative analysis has been made through all the reflectance of leaf samples. The result of derivative analysis of reflectance for each species is shown in Fig. 7a–d.

8.2 Ratio of Derivative Peak

The reflectance spectra for each group of four selected dipterocarp species were all plotted together. Figure 8 illustrates that the most intense difference in terms of shapes and amplitude observed from derivative spectra lies in between wavelength 711.16 and 714.29 nm; the highest peak is at 718.99 nm, and the amplitude change can be also observed at wavelength 723.68 nm. These peaks can be further analysed

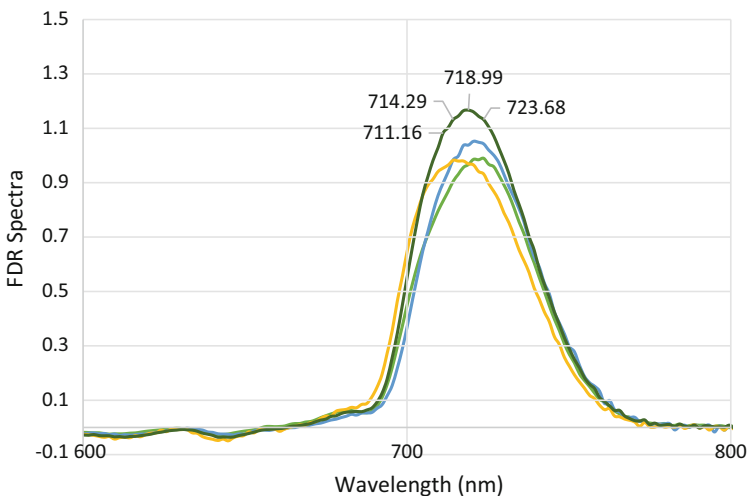


Fig. 8 The reflectance spectra for each group of four selected dipterocarp species plotted together

for the ratio of derivative peaks to evaluate for the performance in explaining the variation of greenness and vigorousness of the dipterocarp trees.

9 Results and Discussion

9.1 Statistical Analysis and Significance Tests

The results of spectral reflectance were analysed using derivative analysis as variables of ANOVA test to determine the separability of four dipterocarp species. The statistical analyses were based on averaged values of leaf samples on 40 trees of *Dipterocarpus grandiflorus*, *Shorea acuminata*, *Hopea dryobalanoides*, and *Shorea macroptera*. The analysis of variance (ANOVA) test was used to determine whether the measured variable differed among the classification groups based on the species. The null hypothesis was stated as follows: there is no difference between the variance of the compared group of derivative spectral reflectance. The test was run on six pairs of DP, *Dipterocarpus grandiflorus*; SA, *Shorea acuminata*; HD, *Hopea dryobalanoides*; and SM, *Shorea macroptera* – HD versus SA, HD versus SM, HD versus DG, DG versus SA, DG versus SM, and SM versus SA. The idea of stating the null hypothesis is to analyse or demonstrate whether the null hypothesis can be rejected, and we can accept the alternative hypothesis. The statement of hypothesis can be written as:

H_o : The difference of variance between the derivatives of spectral reflectance four dipterocarp species is equal to 0.

H_a : The difference of variance between the derivatives of spectral reflectance four dipterocarp species is different from 0.

The comparison of the significance was analysed using the ANOVA test, the null hypothesis had no effect or significance difference between the derivatives of spectral reflectance based on same wavelength in the paired classification. If the computed p -value is the lower than significance level (α) = 0.05 or 95% confidence level, we should reject the null hypothesis H_o . In other words, the decision is to reject the null hypothesis of equality of the variance, and the difference between the variance is significant. In the following tables, the p -values are of significance levels.

9.2 ANOVA on First Derivative Spectra of Four Dipterocarp Species

The first derivative spectra for each group of dipterocarp species were all plotted and compared. Changes in slope and location of inflection points were characterised. The significance of differences of the variance of the first derivative spectra was analysed per wavelength to evaluate the chain of significant wavelengths in separating groups of spectral reflectance of dipterocarp species. The visual appearance examination of

Table 2 Significant wavelengths of the first derivative spectra for all interaction of four dipterocarp species

Sensor	Species ANOVA test					
	HD vs SA	HD vs SM	HD vs DG	DG vs SA	DG vs SM	SM vs SA
Key wavelengths (nm)	412–413	412	501	525–542	521–540	512–522
	427	423	509–529	550	566–601	558–571
	440–442	493	561–579	558	604	676
	493–495	501–506	585	574–580	609–628	693–726
	501–521	509–516	595	655–684	649	898
	555–571	558	601	711–722	700–729	
	633–644	633–641	609	757		
	673–709	678–698	682–715			
	717–765	709–761	723–753			
	793	764	756			
		770				

the first derivative spectra often gives a straightforward perspective on the chlorophyll contents of the dipterocarp tree leaves.

Independent ANOVA test results of the first derivative spectra of four selected species with six interactions between four species tabulated in Table 2. As ANOVA test showed, it is observed that there are several significant wavelengths were found when comparing the four dipterocarp species.

This is a series of significant wavelengths when comparing DG, *Dipterocarpus grandiflorus* (Keruing belimbing); SA, *Shorea acuminata* (Meranti rambai daun); HD, *Hopea dryobalanoides* (Merawan mata kucing hitam); and SM, *Shorea macroptera* (Meranti melantai): HD versus SA, HD versus SM, HD versus DG, DG versus SA, DG versus SM and SM versus SA.

There are six interactions of each type of dipterocarp species which have been made to look the significant different between species for identifying the classification of the four species on specific wavelength.

This study has shown that hyperspectral remote sensing through spectral reflectance of the dipterocarp species is feasible by testing first derivative spectra by using ANOVA. Hence, the detection of dipterocarp species was all plotted and compared to classify them. The significance of differences of the variance of the first derivative spectra was analysed per wavelength to evaluate the chain of significant wavelengths in separating groups of spectral reflectance of dipterocarp species.

It shows a positive result on several runs of significant wavelengths found when comparing the species. However, there are few recommendations to strengthen this study:

- The number of leaf sample of each tree's species must be standardised for an equal average of spectral reflectance of each species.
- The location of sample taken should be more specifically instead of randomly to make sure the relationship between the samples is stronger.

- The species identification should be clearer by using vegetation indices for display the classification of the study area.
- To get more reliable result, variance analysis is suggested as a comparison to ANOVA.

10 Discussion and Conclusion

In this chapter it was found that it is possible to detect and characterise the dipterocarp species using hyperspectral remote sensing using several hyperspectral techniques. At this stage it is not possible to identify a generic technique identifying dipterocarp species, due to differences of leaf structure, thickness, and leaf chlorophyll content as well as spatial and spectral resolution of the sensors. These findings suggest that reflectance spectra of dipterocarp species are able to be identified using spectral analysis. However, the spectral matching or classification of species is highly dependent on the spectral reflectance of each species. With the advancement of current remote sensing technology, the aerial detection of forest is possible.

In-depth analysis of vegetation indices as well as continuum removal will be done to comprehensively denote the series of key wavelengths for each species. It will be a continuous effort by stakeholders and researchers to develop and add to this spectral library for Malaysian dipterocarp species. This spectral signature will be useful in the future whereby the utilisation and readiness of UAV hyperspectral systems with availability of durable batteries increase BVLOS (beyond line of sight) capabilities. The upscaling from leaf to canopy/airborne will be established using the spectral match analysis to produce a classification map accordingly. The classification map is then used as the base information in the GIS system. Finally, linkage between the datasets with the spatial information is accomplished.

Acknowledgement This project is funded by University of Malaya Research Grant RP017A-15SUS: Hyperspectral Species Identification and Mapping of Bukit Fraser Forest. The author thanks Jabatan Perhutanan Semenanjung Malaysia for the research permits, Forest Research Institute of Malaysia (FRIM), and Japan International Research Center for Agricultural Sciences (JIRCAS) for supplementary information in this research.

References

- Adjers G, Kuusipalo J, Hadengganan S, Nuiyanto K, Vesa L (1996) Performance of ten dipterocarp species in restocking logged-over forest areas subjected to shifting cultivation. *J Trop For Sci* 9(2)
- Afizzul MM, Omar H, Yasmin YS, Ayop N, Amira AA, Hajar ZSN (2021) UAV-based hyperspectral imaging system for tree species identification in tropical forest of Malaysia. *J Adv Geospatial Sci Technol* 1(1) <https://jagst.utm.my>
- Appanah S (1998) Introduction. In: Appanah S, Turnbull JM (eds) *Review of the dipterocarps: taxonomy, ecology, silviculture*. CIFOR, Bogor, pp 1–4
- Asner GP (1998) Biophysical and biochemical resources of variability on canopy reflectance. *Remote Sens Environ* 63:155–165

- Bawa KS (1998) Conservation of genetic resources in the Dipterocarpaceae. In: Appanah S, Turnbull JM (eds) A review of dipterocarps, taxonomy, ecology and silviculture. CIFOR, Bogor, pp 45–56
- Bawa KS, Seidler R (2008) Natural forest management and conservation of biodiversity in tropical forests. *Conserv Biol* 12(1):46–55. <https://doi.org/10.1111/j.1523-1739.1998.96480>
- Berry JK, Ripple WJ (1996) Emergence of geographic information systems in forestry. In: McDonald P, Lassoie J (eds) The literature of forestry and agroforestry. Cornell University Press, Ithaca, NY, pp 107–128
- Bierregaard RO, Lovejoy TE, Kapos V, Hutchings RW (1992) The biological dynamics of tropical rainforest fragments. *Bioscience* 42(11):859–866. <https://doi.org/10.2307/1312085>
- Blackburn GA (1998) Quantifying chlorophylls and carotenoids at leaf and canopy scales: an evaluation of some hyperspectral approaches. *Remote Sens Environ* 66:273–285
- Brown S, Iverson LR, Lugo AE (1994) Land-Use and biomass changes of forests in peninsular malaysia from 1972 to 1982: a GIS approach. In: Dale, V.H. (eds) Effects of land-use change on atmospheric CO₂ concentrations. Ecological studies, vol 101. Springer, New York. https://doi.org/10.1007/978-1-4613-8363-5_4
- Campbell JB, Wynne RH (2011) Introduction to remote sensing, Fifth edn. The Guilford Press, New York
- Chechina M (2015) Sustainable management of dipterocarp forests in the Philippines. PhD Thesis. University of Alberta, Canada. https://sites.ualberta.ca/~ahamann/people/pdfs/Chechina_2015_PhD.pdf
- Corlett RT, Primack RB (2005) Tropical rain forests: an ecological and biogeographical comparison, 2nd edn. Wiley-Blackwell
- Dalponte M, Bruzzone L, Gianelle D (2011) Tree species classification in the Southern Alps with very high geometrical resolution multispectral and hyperspectral data. 3rd workshop on hyperspectral image and signal processing: evolution in remote sensing (WHISPERS)
- Dawson TP, Curran PJ (1998) A new technique for interpolating red edge position. *Int J Remote Sens* 19(11):2133–2139
- Demetriades-Shah TH, Steven MD, Clark JA (1990) High resolution derivative spectra in remote sensing. *Remote Sens Environ* 33:55–64
- Denslow JS (1987) Tropical rain forest gaps and tree species diversity. *Annu Rev Ecol Syst* 18:431–451. <https://doi.org/10.1146/annurev.es.18.110187.002243>
- FAO (Food and Agriculture Organization) (1981) Tropical forest resources assessment project (in the Framework of GEMS). Forest Resources of Tropical Asia, UN3216.1301-78-04, Technical Report 3. FAO, Rome
- FAO (Food and Agriculture Organization) (1985) Tropical forestry action plan. Food and Agriculture Organization of the United Nations, Committee on Forest Development in the Tropics, Rome. 159 pp
- Feng Y, Ziegler AD, Elsen PR et al (2021) Upward expansion and acceleration of forest clearance in the mountains of Southeast Asia. *Nat Sustain* 4:892–899. <https://doi.org/10.1038/s41893-021-00738-y>
- Ghazoul J (2016) Dipterocarp biology, ecology, and conservation. Oxford Scholarship Online
- Hansen MC et al (2013) High-resolution global maps of 21st-century forest cover change. *Science* 342:850–853
- Jusoff K (2006) Individual mangrove species identification and mapping in Port Klang using airborne hyperspectral imaging. *J Sustain Sci Manag* 1:27–36
- Jusoff K (2007) Advanced processing of UPMAPSB's AIS airborne hyperspectral images for individual timber species identification and mapping. *Int J Syst Applied Eng Dev* 2:21–26
- Jusoff K (2009) Airborne hyperspectral sensor for individual species counting and mapping of Karas (*Aquilaria malaccensis*) in Bukit Nanas F. R, Malaysia. *World Appl Sci J* 7(10): 1246–1251
- Kalaska M, Sánchez-Azofeifa G (2008) Hyperspectral remote sensing of tropical and sub-tropical forests. CRC Press, Boca Raton

- Kettle CJ (2010) Ecological considerations for using dipterocarps for restoration of lowland rainforest in Southeast Asia. *Biodivers Conserv* 19(4):1137–1151. <https://doi.org/10.1007/s10531-009-9772-6>
- Kishore BSPC, Kumar A, Saikia P, Lele N, Pandey AC, Srivastava P, Bhattachary BK, Khan ML (2020) Major forests and plant species discrimination in Mudumalai forest region using airborne hyperspectral sensing. *J Asia Pac Biodivers* 13(4):637–651. <https://doi.org/10.1016/j.japb.2020.07.001>
- Maiti PK, Maiti P (2011) Biodiversity: perception, peril and preservation. PHI Learning Pvt. Ltd
- Martin RE (2020) Lessons learned from spectranomics: wet tropical forests. In: Cavender-Bares J, Gamon JA, Townsend PA (eds) Remote sensing of plant biodiversity. Springer, Cham. https://doi.org/10.1007/978-3-030-33157-3_5
- Maury-Lechon G, Curtet L (1998) Biogeography and evolutionary systematics of Dipterocarpaceae. In: Appanah S, Turnbull JM (eds) A review of dipterocarps: taxonomy, ecology and silviculture. CIFOR, Bogor, pp 5–44
- Mohamad Hasmadi I, Kamaruzaman J, Nurul Hidayah MA (2010) Analysis of crown spectral characteristic and tree species mapping of tropical forest using hyperspectral imaging. *J Trop For Sci* 22(1):67–73. Forest Research Institute of Malaysia (FRIM)
- Mohd Azahari F, Khali Aziz H, Hamdan O (2011) High-resolution airborne hyperspectral data for mapping of ramin distribution in peat swamp forest. FRIM, Kuala Lumpur
- Myers N, Mittermeier RA, Mittermeier CG, da Fonseca GAB, Kent J (2000) Biodiversity hotspots for conservation priorities. *Nature* 403(6772):853–858. <https://doi.org/10.1038/35002501>
- Nakaya T, Tani N (2016) Suitable habitats for the establishment of *Shorea curtisii* seedlings in a primary hill forest in Malaysia. *J Trop For Sci*. <https://www.researchgate.net/publication/306479441>
- Newman A (2002) Tropical rainforest: our most valuable and endangered habitat with a blueprint for its survival into the third millennium, 2nd edn. Checkmark. ISBN: 0816039739
- Niiyama K, Iida S, Kimura K, Sato T, Azizi R, Abdul Rahman K (2016) Survivorship of *Shorea curtisii* seedlings in a hill Dipterocarp forest, Peninsular Malaysia. *J Trop For Sci* 28:334–341
- Nisfariza MN (2012) Early detection of *Ganoderma* basal stem rot disease of oil palm by hyperspectral remote sensing. PhD thesis, University of Nottingham, United Kingdom
- Olson DM, Dinerstein E, Wikramanayake ED, Burgess ND, Powell GVN, Underwood EC, D'Amico JA, Itoua I, Strand HE, Morrison JC, Loucks CJ, Allnutt TF, Ricketts TH, Kura Y, Lamoreux JF, Wettengel WW, Hedao P, Kasse KR (2001) Terrestrial ecoregions of the world: a new map of life on Earth. *Bioscience* 51(11):933–938
- Rivard B, Sanchez-Azofeifa GA, Foley S, Calvo-Alvarado JC (2008) Species classification of tropical tree leaf reflectance and dependence on selection of spectral bands. In: Kalacska M, Sanchez-Azofeifa GA (eds) Hyperspectral remote sensing of tropical and subtropical forests, 1st edn. CRC Press
- Saifuddin S, Abdul Rahim N, Muhammad Farid AR (1991) Watershed research in forest plantation: I. Establishment and physical characteristics of Bukit Tarek watershed. Research Pamphlet No. 110. Forest Research Institute Malaysia, Kepong
- Salinas N, Cosio EG, Silman M, Meir P, Nottingham AT, Roman-Cuesta RM, Malhi Y (2021) Editorial: tropical montane forests in a changing environment. *Front Plant Sci* 12. <https://doi.org/10.3389/fpls.2021.712748>
- Schulte A, Schöne DH-F (1996) Dipterocarp forest ecosystems: towards sustainable management. World Scientific
- Sims DA, Gamon JA (2002) Relationships between leaf pigment content and spectral reflectance across a wide range of species, leaf structures and developmental stages. *Remote Sens Environ* 81(2002):337–354
- Sodhi NS, Posa MRC, Lee TM, Bickford D, Koh LP, Brook BW (2010) The state and conservation of Southeast Asian biodiversity. *Biodivers Conserv* 19(2):317–328. <https://doi.org/10.1007/s10531-009-9607-5>

- Suzuki R, Numata S, Okuda T, Supardi MN, Kachi N (2009) Growth strategies differentiate the spatial patterns of 11 dipterocarp species coexisting in a Malaysian tropical rain forest. *J Plant Res* 122:81–93
- Symington CF (1974) Forester's manual of Dipterocarps. Malaysian forest records No. 16 (First Published in 1943, Reprinted in 1974). Kuala Lumpur, Malaysia
- Symington CF (2004) 1905-1943. Foresters' manual of dipterocarps by Symington CF; revised by Ashton PS and Appanah S; Barlow HS (ed). Forest Research Institute Malaysia: Malaysian Nature Society, Kuala Lumpur
- Tani N, Tsumura Y, Fukasawa K, Kado T, Taguchi Y, Lee SL, Lee CT, Muhammad N, Niiyama K, Otani T, Yagihashi T, Tanouchi H, Ripin A, Kassim AR (2015) Mixed mating system are regulated by fecundity in *Shorea curtisii* (Dipterocarpaceae) as revealed by comparison under different pollen limited conditions. *PLoS One* 10(5). <https://doi.org/10.1371/journal.pone.0123445>
- Whitmore TC, Burnham CP (1975) Tropical rain forests of the far east. Clarendon Press
- Wilson EO (1988) The current state of bio-logical diversity. In: Wilson EO (ed) Biodiversity. National Academy Press, Washington, DC, pp 3–18
- Zarco-Tejada PJ, Pushnik JC, Dobrowski S, Ustin SL (2003) Steady-state chlorophyll-a fluorescence detection from canopy derivative reflectance and double-peak red-edge effects. *Remote Sens Environ* 84:283–294



Tree Biophysical Parameter Retrieval from Multi-source Remote Sensing Data Fusion

Nafisah Khalid, Noraain Mohamed Saraf, Juazer Rizal Abdul Hamid, and Zulkiflee Abd. Latif

Abstract

Malaysian tropical forest consists of marketed tree species such as *Hopea*, *Neobalanocarpus* and *Shorea*. According to the International Union for Conservation of Nature and Natural Resources (IUCN) Red list 2021, 160 tree species from the genus of *Shorea* are threatened. From this list, *Shorea resinosa*, *Shorea exelliptica* and *Shorea macrantha* are categorized as critically endangered species. Due to the current list, mapping and monitoring the tropical trees are deemed necessary. The recent remote sensing technology that allows for accurate operational and managerial inventories in a cost-effective and timely manner is constantly in demand. Multispectral remote sensing imagery such as WorldView-2, WorldView-3, GeoEye-1, Pleiades and SPOT 7 is extensively used in extracting the tree crown and classifying the tree species. Besides, airborne LiDAR is utilized mainly for accurate estimation of individual tree height. The fusion of multispectral imagery with airborne LiDAR data is believed to improve the estimation of tree biophysical parameters with the additional information. Therefore, this chapter provides an overview and analysis focused on *Shorea* spp. biophysical parameter retrieval from the fusion of multispectral and airborne LiDAR data using object-based image analysis (OBIA). The information

N. Khalid (✉) · N. Mohamed Saraf · J. R. Abdul Hamid
Centre of Studies for Surveying Science and Geomatics, Faculty of Architecture, Planning and Surveying, Universiti Teknologi MARA, Selangor, Malaysia
e-mail: nafisahkhalid@uitm.edu.my

Z. Abd. Latif
Centre of Studies for Surveying Science and Geomatics, Faculty of Architecture, Planning and Surveying, Universiti Teknologi MARA, Selangor, Malaysia

Institute for Biodiversity and Sustainable Development (IBSD), Universiti Teknologi MARA, Selangor, Malaysia

provided should help readers to understand the characteristics, scale parameters, accuracy and limitations in retrieving the *Shorea* spp. in the tropical forest area.

Keywords

Airborne LiDAR · Remote sensing · Tropical forest · Object-based classification · *Shorea*

1 Introduction

Forests play an important role in the global carbon cycle, economic development and climate moderation. The diversity of forest ecosystems is generally classified according to its altitude, climate, location and soil suitability (FAO 2018). Tropical forests located in Southeast Asia are recognized to be the oldest forests and richer in biodiversity and have been known as the most productive forests and more effective in carbon sequestration. Major types of tropical forests recognized in Malaysia are lowland dipterocarp forest, hill dipterocarp forest, upper hill dipterocarp forest, peat-swamp forest, coastal forest and mangrove forest. Each forest type has different tree species such as lowland dipterocarp forest consists of commercial tree species from a family of Dipterocarpaceae including from the genera of *Hopea*, *Neobalanocarpus* and *Shorea*.

Based on FAO (2016), the net loss of seven million hectares per year of tropical forest in 2000–2010 was similar to the increase in agricultural area (six million hectares per year). Most of this deforestation is due to the conversion of tropical forest to agriculture occurred in South America, sub-Saharan Africa and South and Southeast Asia. Thus, the loss of forest area affected the extinction of some of the tree species.

Managing and conserving tropical forests are challenging due to the rareness and little knowledge of tree species. The tree parameters and species information are deemed necessary for aboveground biomass estimation and forest management daily activities. However, uncertainty in tropical forest inventory remains high due to the fact that measuring the tree biophysical parameters is too costly and laborious. Thus, recent and powerful approaches for improving the efficiency and accuracy of forest inventories, especially in remote locations, are in constant demand.

Advancement in remote sensing technology allows for accurate operational and managerial inventories in a cost-effective and timely manner till the compartment level over larger forest areas. Dating back to 1972, the first earth resource satellite Landsat was developed to provide optical remotely sensed data with coarse spatial resolution followed by a series of Landsat and SPOT satellites that gradually improved the spatial resolution of each product. From there, remote sensing has become an ever-increasing popular geospatial data acquisition method, and since 1999, commercial satellites such as IKONOS, QuickBird and most recently the Digital Globe's family of sensors, WorldView-2 to WorldView-4, provide high spatial resolution imagery of 1 m or less as well as increased radiometric resolutions.

Despite that, there are also active remotely sensed data in the likes of airborne laser scanning or Light Detection and Ranging (LiDAR), which could provide vertical information and complement the sub-metre spatial resolution data (Zhen et al. 2016). It has been proven that LiDAR remote sensing is capable of retrieving the tree information by focusing on utilizing tree height. Therefore, detailed and accurate information of individual tree parameters could be extracted from the synergism of the finer spatial resolution imagery with LiDAR data, through curtains of image processing techniques.

2 Genus of *Shorea*

Dipterocarp forest also known as an inland forest is an evergreen forest with mean annual rainfall exceeding 1000 mm (Appanah 1998). The preservation of lowland dipterocarp forests (LDF) is made through the implementation of forest reserve. There are beautiful and relatively undisturbed LDF in Malaysia which are Taman Negara in Peninsular Malaysia, Lambir Hills National Park in Sarawak, and Sepilok Forest Reserve and Danum Valley in Sabah. Unfortunately, lowland forests reserved near urban centres such as the Sungei Buloh Reserve, Kanching Forest Reserve and Ampang Forest Reserve are under intense pressure from development.

The dipterocarp forests in Malaysia are mostly dominated by trees from the Dipterocarpaceae family. Generally, Dipterocarpaceae are a family of 17 genera and approximately 500 species such as from genera of *Shorea*, *Hopea*, *Dipterocarpus*, *Neobalanocarpus*, and *Vatica*. Specifically, in Peninsular Malaysia, the family Dipterocarpaceae comprises 157 species (Guan and Yen 1999). Trees from this family often emerge from forest canopy and typically reach heights of 40–70 m tall, some even over 80 m.

Shorea spp. (Meranti, Balau, Damar Hitam) is commonly known as dominant and emergent trees. A study carried out by Fangliang and James (1997) in Pasoh Reserve Forest found that the emergent tree species are *Dipterocarpus cornutus* (Keruing gombang), *Shorea maxwelliana* (Balau kumus) and *Neobalanocarpus heimii* (Chengal) and the upper canopy is dominated by red meranti. Based on Khalid et al. (2013), there is a good correlation between tree height and crown diameter for *Shorea* spp. with an r^2 for linear model which is 0.738. The good correlation could reveal significant contributions in various studies. Thus, it is important to extract tree biophysical parameters, and remote sensing technology could be utilized especially for large forest areas.

3 Extracting Tree Biophysical Parameters Using Remote Sensing Data Sets

Remote sensing technology can be divided into two categories which are passive and active sensors. Passive or optical sensors record the reflected or emitted natural energy from the earth surface. Optical sensors are characterized into low spatial

resolution (MODIS, AVHRR), medium spatial resolution (Landsat, SPOT) and high spatial resolution imagery (WorldView-3, IKONOS) which are used globally in forest studies and land-cover mapping. Very high resolution of optical remote sensing data is providing new opportunities for exploring and enumerating the forest structure at both the stand and individual tree level.

In contrast, active sensors such as RADAR and LiDAR use their own energy source for illumination to map the earth surface. This technology promises to increase the accuracy of tree structural measurements and provide the accurate three-dimensional distribution of tree crowns. The RADAR data is capable of detecting and delineating the tree crown over forest area, and LiDAR data has been extensively used in the forest study. LiDAR is one of the active sensors that provide data that is possible to detect and isolate individual trees. It has been proven that LiDAR remote sensing is capable of retrieving the tree information by focusing on utilizing tree height.

4 High-Resolution Remote Sensing Images

Remote sensing sensors evolve from coarse to fine spatial resolution with new additional spectral bands. This evolution offers foresters an additional source of data for forest inventory purposes. The ability to directly estimate the individual trees from high spatial resolution data may improve other parameters estimation such as crown areas and volume and subsequently improve estimation of aboveground biomass. High spatial resolution remote sensing provides a potential for trees to be visible in the imagery unlike medium resolution satellite images. Characterization of remote sensing imagery is based on the spatial, spectral, radiometric and temporal resolutions. Spatial resolution refers to the ability of a sensor to detect the smallest possible size of the features. The earth features appear clearly in the high spatial resolution imagery, while features appear blurry in low spatial resolution imagery which gives difficulty to interpret the imagery.

The spectral resolution refers to the ability of a sensor to identify fine wavelength intervals. Different remote sensing systems have different capability in recording the wavelength intervals. The sensors that only define one band refer to the panchromatic sensors. Commonly the sensors have the ability to define three to eight bands which are known as multispectral sensors, while the sensors that have ability to detect hundreds of narrow spectral bands are known as hyperspectral sensors.

Numerous studies incorporate high spatial resolution with multispectral imagery to improve the classification accuracy. Gebreslasie et al. (2011) used IKONOS imagery which has four bands to detect the individual tree with 85% overall accuracy. In addition, Whiteside and Ahmad (2008) found that the tree detection and delineation accuracy is acceptable with 79.5%, and Song et al. (2010) found that IKONOS and QuickBird produce an identical result in estimating the tree crown size.

Several researchers have been applied WorldView-2 and Worldview-3 imageries for individual tree crown detection and delineation (Heumann 2011; Ozdemir and

Karnieli 2011; Immitzer et al. 2012; Latif et al. 2012; Mora et al. 2013; Jakubowski et al. 2013; Varin et al. 2020; Tong et al. 2021). Based on Immitzer et al. (2012), WorldView-2 imagery has good capability in discriminating tree species with the overall classification accuracy more than 82%.

Heumann (2011) has compared the result of tree species classification in mangrove forest between QuickBird and WorldView-2 imagery using object-based image analysis (OBIA) and concluded that WorldView-2 sensor produces high classification accuracy with more than 94%. Heumann (2011) also mentioned that the WorldView-2 imagery has better spectral separability between vegetation classes than the QuickBird imagery which leads to the better classification result.

According to Latif et al. (2012), the infrared band in WorldView-2 imagery is very useful for vegetation studies due to its sensitivity towards the chemical composition of vegetation thus making them useful to be differentiated and identified. However, the classification on the tropical forest trees can be a bit low in accuracy. Trees in the tropical forest are randomly distributed and are located too close to each other making it hard to be differentiated.

5 Extracting Tree Parameters from Airborne LiDAR

LiDAR is an active remote sensing system that uses laser pulses to capture the earth surface. LiDAR provides an excellent amount of vertical and textural information about the forest structure complement to passive remote sensing images. LiDAR records the time interval of laser pulses traveling from the laser scanner to hit the objects and return laser pulses which are backscattered from an object with a known constant velocity. The return of LiDAR pulses generates a 3D representation of the earth surface in which each point is characterized by X , Y and Z coordinates.

Full waveform sensor or discrete return sensor could be used to record the return pulses. Full waveform sensor records the amount of energy returned to the sensor in the continuous signal form (Hancock et al. 2015). Conversely, a discrete return sensor allows for one (single-return systems) or more returns (multiple-return systems) to be recorded for each pulse during flight. Both sensors are typically used in combination with Global Positioning System (GPS) receivers and inertial navigation systems (INS). A GPS receiver is used to obtain the position of the platform, while the INS is used to measure the roll, pitch and yaw of the LiDAR sensor. In addition, the GPS on the ground base station is also necessary for differential GPS (DGPS) to improve the positional accuracy given from LiDAR sensor.

Discrete return sensor has the advantage of providing data over a large area but is restricted by the laser pulse return density as points/m² ratio. In contrast, the problem in discrete return sensor particularly in biomass studies can be solved with full waveform sensor where this technology records the amplitude of the return signal at fixed time intervals by digitizing the waveform.

In forestry application, the first returned laser pulses are the most significant return as it will be associated with the highest feature in the forest landscape like a

treetop. The conversion of the emitted point cloud from first return to a raster model is called Digital Surface Model (DSM). The last return usually hits the ground surface. Conversely, in the dense forest area, the last return may always hit the understory vegetation. The conversion of these pulses to raster models is called digital terrain model (DTM). Then the Digital Canopy Height Model (DCHM) was created by subtracting the DTM from the Digital Surface Model (DSM).

The accuracy obtained for detection of individual trees using airborne LiDAR depends on the structure of the forest, quality of images and density of laser point clouds and applied processing technique. Trees usually can be recognized only in the dominant tree layer, and LiDAR data has a tendency to underestimate tree height in dense forests. Previous studies advocate that LiDAR tends to underestimate the tree height. The underestimation increased with the decrease of the sampling density due to a large probability of missing treetops. Zahidi et al. (2015) stated that the recommended pulses per square metre (ppsm) for vegetation analysis is at least 4, and yet they mentioned that 1.4 ppsm is sufficient for DEM creation in delineating the tropical trees.

6 Synergism of Satellite Images and LiDAR Data in Forestry

The synergism of high spatial resolution imagery with LiDAR data has been widely used and believed to improve the derivation accuracy of tree structural parameters. Based on Machala (2014), the synergism of both data sets provides extra valuable information complementing the sub-metre spatial resolution imagery for estimating other structural elements of the tree canopy.

Several studies have synergized high spatial resolution imagery and LiDAR data set. The integration of both data sets can significantly improve classification accuracy at individual tree level. The fusion of both data sets could generate highest classification accuracy and give an accurate positional value for each feature, and apart from that, various tree attributes could be acquired from this operation such as species classification, tree height, crown area and finally estimating accurate above-ground biomass from the acquired parameters.

However, few studies have been found that fused the high spatial resolution imagery with LiDAR data particularly in evaluating the tropical forest. This might be due to the complexity of the tropical forest. As stated by Jakubowski et al. (2013), the accuracy of individual tree detection decreased in the dense forest areas, and they suggested that better accuracy would be yielded if the LiDAR and high spatial resolution data were collected simultaneously.

7 Object-Based Image Analysis (OBIA) for *Shorea* Classification

Robust object-based image analysis (OBIA) is an intrinsically multi-scalar and hierarchical approach developed to overcome high variation in high-resolution satellite imagery. The OBIA primarily consists of two steps which are image segmentation and classification. The attributes gathered from image segmentation make a knowledge-based for the sample objects, which can be called upon in the classification process. This method involves segmenting an image into objects through the use of spectral and spatial context. Tree biophysical parameters that could be extracted from OBIA are crown area and tree species. The knowledge about tree species should be supported with the spectral signature from in situ measurement.

8 Multi-resolution Image Segmentation

Image segmentation is a basic operation in computer vision and pattern recognition. The goal of segmentation is to subdivide the image to find the semantic regions. One of the image segmentation methods is multi-resolution. Multi-resolution image segmentation algorithm is used to produce an image object for a further classification process. Two main components of multi-resolution segmentation are decision heuristics to determine the image objects that will merge at each step and the homogeneity of image objects to pair with the merge of image objects (Dekavalla and Argialas 2018).

This segmentation process defines the size and shape of desired objects by defining the object homogeneity and calculating the heterogeneity between adjacent pixels. The other parameters used to define homogeneity of image objects are the shape factor and compactness.

The image is divided into homogeneous regions based on several user-defined parameters which affect the size, spectral and spatial homogeneity of the resulting image objects. The proper selection of setting parameters is critical to evade the under-segmentation or over-segmentation of features.

The scale parameter is one of the segmentation criteria that are used to control the average image object size. The evaluation of the scale parameter for the entire area is difficult and requires further analysis. Table 1 shows the close-up view for individual tree crowns delineation. Crown A represents a tree crown with less distinct brightness value with adjacent features, and crown B represents a tree crown with distinct brightness with adjacent features.

The crown delineation accuracy can be evaluated by using the goodness measures of segmentation (Phua et al. 2014). Based on the illustration in Table 1, the 10-scale parameter for both crowns is over-segmented, and the 20-scale parameter generates slightly under-segmentation of the crown. In addition, 30 and 40 scales generate relatively poor segmentation for crown A while producing good segmentation for crown B. The segmentation result produced using 30 and 40 scale parameters

Table 1 Selected crown segmentation using different scale parameter

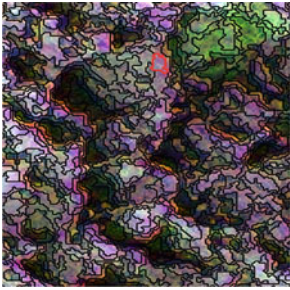
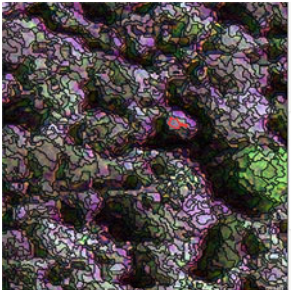
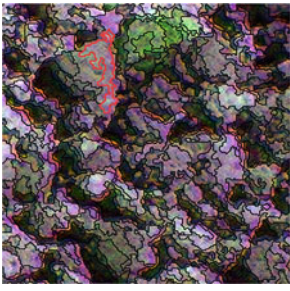
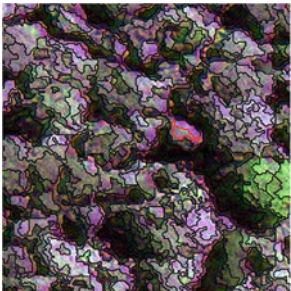
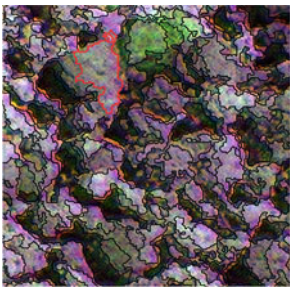
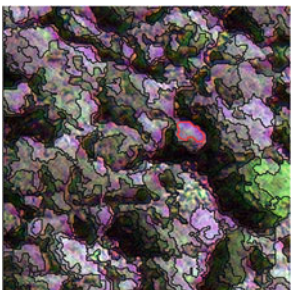
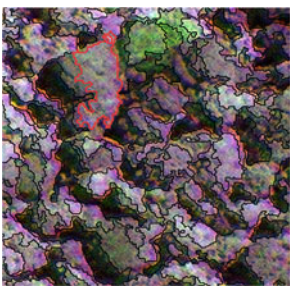
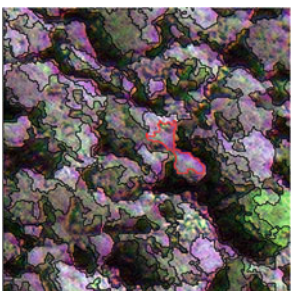
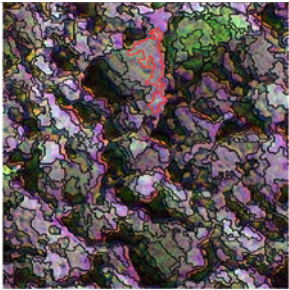
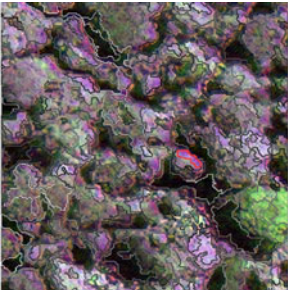
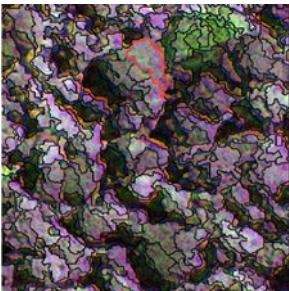
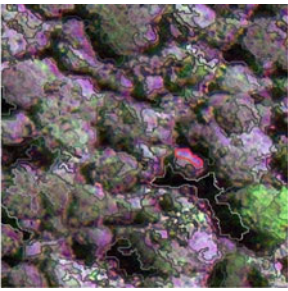
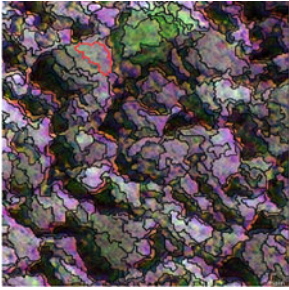
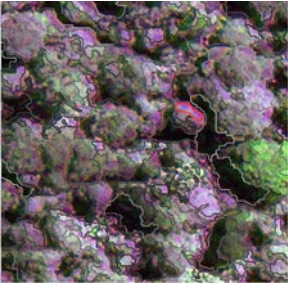
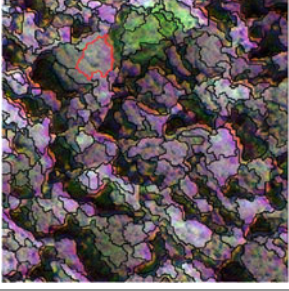
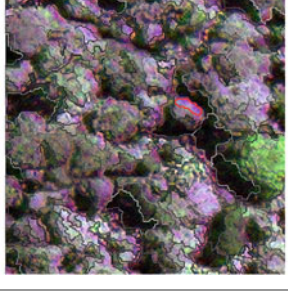
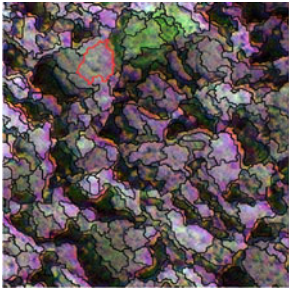
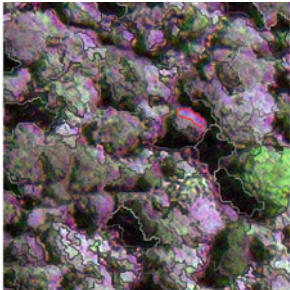
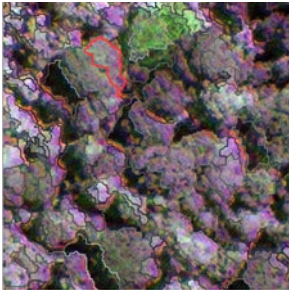
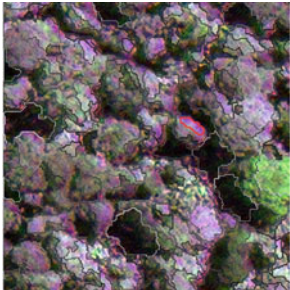
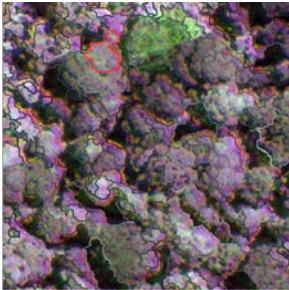
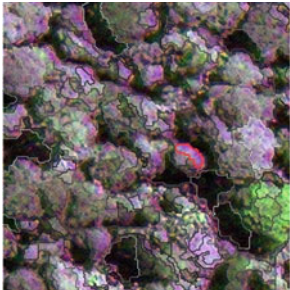
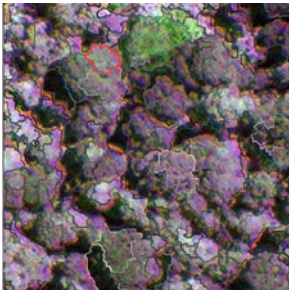
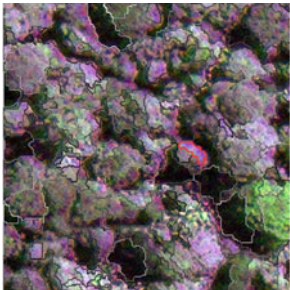
Scale parameter	Crown A	Crown B
10		
20		
30		
40		

Table 2 Selected crown segmentation using different shape parameter

Shape	Crown A	Crown B
0.1		
0.2		
0.3		
0.4		

merges with the adjacent features that have less distinct brightness value with the selected crowns and produce one object rather than several objects.

Table 3 Selected crown segmentation using different compactness value

Compactness	Crown A	Crown B
0.5		
0.6		
0.7		
0.8		

Tables 2 and 3 show the segmentation results for different shape and compactness parameters, respectively. The segmentation results for 0.2 and 0.3 of shape parameters show the improvement in the shape of the object. However, the highlighted object in the image object A cannot be separated from the adjacent object. The final selection of shape parameters is 0.4. This parameter generates a well-defined shape of selected crowns with the best closeness index. The higher selection of the shape criterion value (more than 0.9) could affect the spectral information of the image because the users are indirectly defining the colour criteria by modifying the shape criterion.

Compactness defines the weight of compactness of the image objects. The setting of compactness starts from 0.5 value because no significant finding is identified using compactness below this value. The closeness index for both selected crowns using different settings is good, but the best index generates from 0.8 of compactness value. Different features require different selection of parameters. Thus, it is important to identify the optimum parameters before proceeding with other processing stages.

9 Classification of Forest Structure

Image classification is the process of assigning groups of identical pixels into classes. Image classification is an adopted method used in order to obtain land-cover information from satellite images. In forest application, classification and mapping of forests over large spatial scales are generally used to substitute tedious traditional classification methods. Several image classification algorithms have been proven to produce good classification accuracy in the forest application.

A rule-based and support vector machine (SVM) are well-known image classifiers that are commonly being used to classify the tree species. Rule-based is a sequence of processes executed in the defined order. It is representing the code of rule ware assembling a set of functions based on the Definiens Cognition Network Language (DCNL). Each single process executes in the rule-based selected algorithm providing a solution to a specific image analysis problem.

SVM is a machine learning algorithm that separates classes by defining an optimal hyperplane between classes based on support vectors. The support vectors are defined by training data. This feature is very valuable specifically for object-based image analysis, where only small training sample size is used than in pixel-based approaches. The studies that compared the object-based and pixel-based classification techniques found that the overall accuracy of the object-based was better than pixel-based classification (Jakubowski et al. 2013; Machala 2014).

In addition, Zahidi et al. (2015) compared the performance of supervised SVM and rule-based techniques in classifying the tropical trees in floodplain areas, and they found that the overall accuracy for rule-based classification is 8% higher than SVM technique. Finally, a supervised nearest neighbour (NN) classification also is widely applied in detailed classification of the forest areas where the overall

accuracy using NN classification is comparable with other approaches with 90% (Machala 2014).

10 Spectral Range for *Shorea* Tree

The classification can be improved by analysing the spectral range according to the mean layer value for each feature as shown in Figs. 1, 2, and 3. Figures 1 and 2 compare the spectral range between gaps from *Shorea* and mixed tree species. There is clear range for gaps, mixed tree species and *Shorea* trees. However, the classification among tree species is a challenging process as there are no distinct characteristics between species. As shown in Fig. 3, the range for *Shorea* and mixed species is overlapping in each layer value except in the mean layer value 3 or

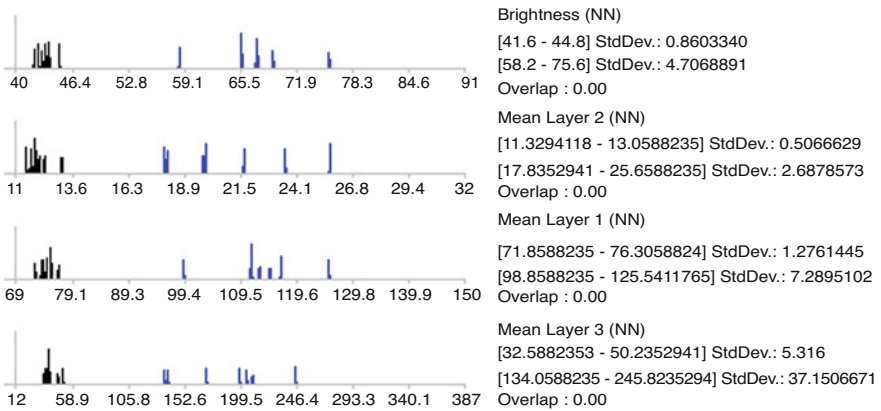


Fig. 1 Spectral range comparison between gaps and mixed species

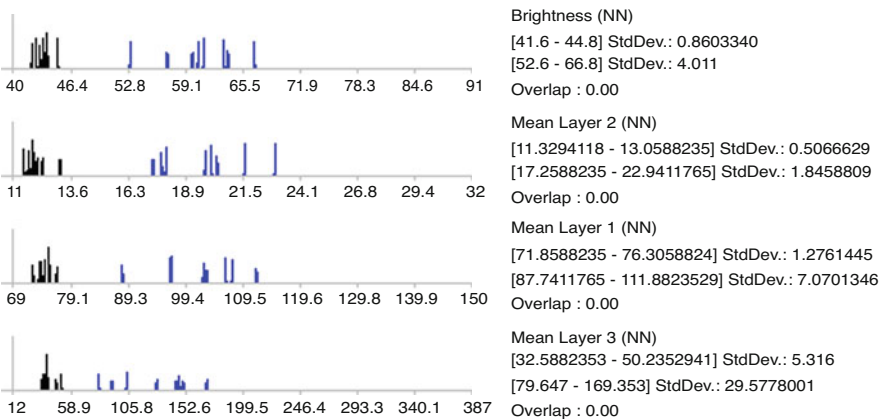


Fig. 2 Spectral range comparison between gaps and *Shorea* spp.

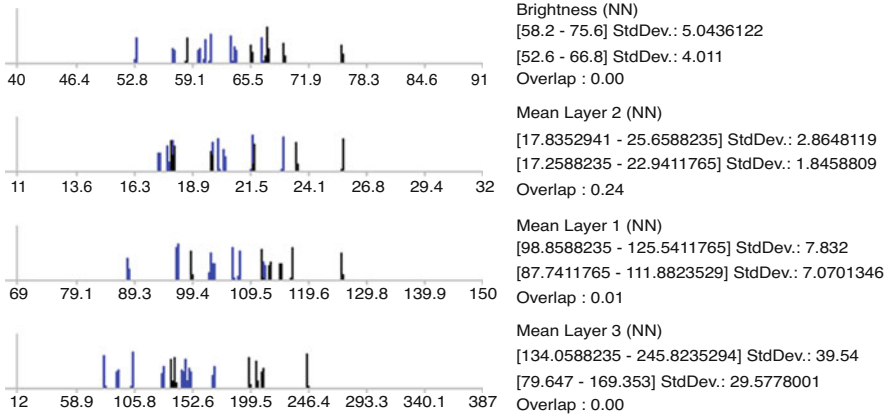


Fig. 3 Spectral range comparison between mixed species and *Shorea* spp.

near-infrared-2 (NIR2) band. Based on the spectral range, band NIR2 is suitable for species classification as there is no overlapping range for each feature and can be used to differentiate the features accurately.

11 Spectral Signature for Selected Tree Species

Spectral signature is the reflectance or emittance of a target over a variety of wavelengths that can be represented in a spectral plot. An understanding of spectral signatures is essential in the understanding and interpretation of a remote sensing image. The spectral reflectance of radiation is distinctive for different features. Similar features also have different spectral signatures because the reflectance pattern is very sensitive to the chemical contents in specific features. The classification between tree species can be analysed using a spectral reflectance curve. The site investigation using a field spectrometer is essential for accurate image generation and verification of image endmembers. A field spectrometer measuring the trees or other features over the range of 400–1050 nm would detect more detail of spectral information as compared to information given by WorldView-2 multispectral imagery. The selected species are *Shorea* spp. (Meranti and Balau), *Syzygium* spp. (Kelat), *Neobalanocarpus heimii* (Chengal) and *Palaquium* spp. (Nyatuh). For genus of *Shorea*, the spectral signature was obtained from four different species which are *Shorea maxwelliana* (Balau), *Shorea parvifolia* (Meranti sarang punai), *Shorea leprosula* (Meranti tembaga), and *Shorea ovalis* (Meranti kepong). Figure 4 shows the mean of spectral signatures of each species. The spectral range for each species is suitable to be analysed further in the near-infrared region.

In WorldView-2 imagery, Band 7 is known as near-infrared 1 (NIR1) covers a region from 770 to 895 nm. This band is very valuable for moisture content and plant biomass estimation. This band is also effective to separate the water bodies from

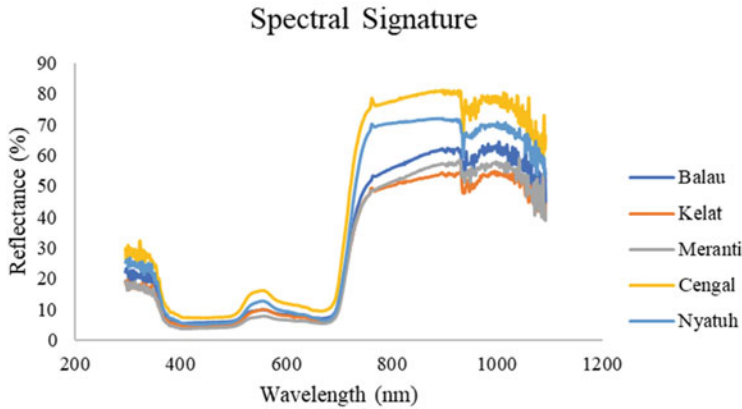


Fig. 4 Spectral signature of selected species

vegetation and useful to identify the tree species. Based on Lillesand et al. (2015), in the NIR portion of the spectrum at about 700–1050 nm, a plant leaf reflects about 50% of the energy incident upon it. Most of the remaining energy is transmitted, since absorption in this spectral region is minimal. Range from 700 to 1050 nm also can be used to detect the vegetation stress.

Near-infrared 2 (NIR2) covers a wavelength interval from 860 to 1045 nm. This band is effective for the broad analysis of tree species and valuable for biomass studies. Common vegetation reflectance peaks around 900–940 nm, and the absorption occurs at the 940 nm where 940–1010 nm is the moisture-sensitive region. The wavelength interval from 925 to 955 nm illustrates the distinct curves between tree species.

Each tree species has unique curves at this interval which provide researchers a broad region for tree species identification and analysis. At this interval, the *Neobalanocarpus heimii* (Cengal) and *Palaquium* spp. (Nyatuh) have very steep V-shaped valley while, *Shorea* spp. (Meranti and Balau) and *Syzygium* spp. (Kelat) have W-shaped valley. Based on Fig. 4, Meranti tree species has another valley similar signature with Balau at wavelength 950 nm. The unique signature of each species could improve the classification between tree species.

12 Distribution Map of *Shorea* Trees

The distribution of *Shorea* trees derived from rule-set and SVM classifiers are shown in Figs. 5 and 6, respectively. The overall classification accuracy generated from rule-set and SVM is above 80% (Khalid et al. 2018). However, the producer's and user's accuracy for *Shorea* tree species and mixed species is less than 80%. The good classification accuracy indicates that the object-based image classification based on selected threshold conditions and parameters has the high capability of achieving a good result. The generated accuracy assessment proved that rule-set and SVM

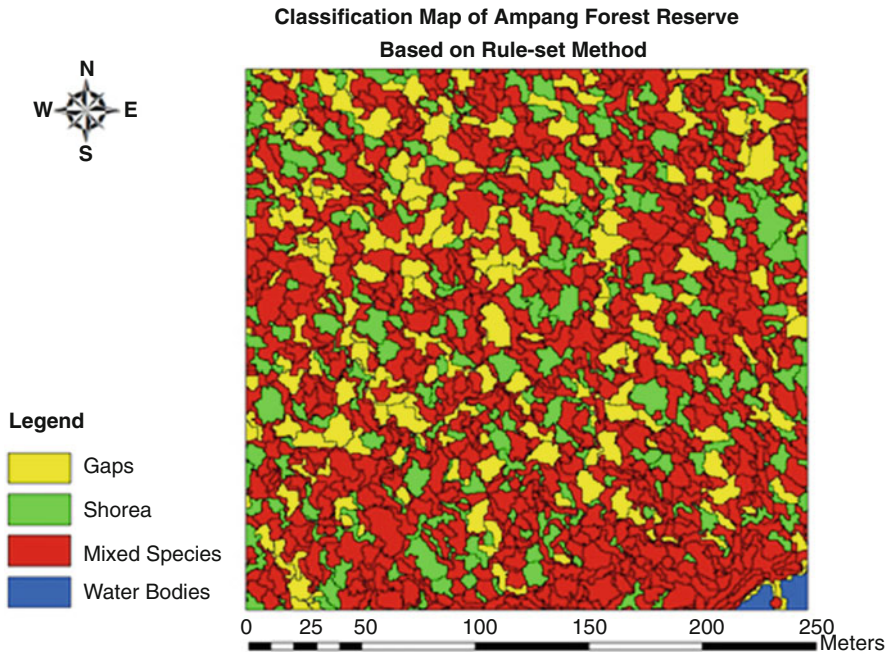


Fig. 5 Classification map based on rule-set method

classifiers have a high capability in mapping the *Shorea* tree species in the dense forest area.

13 Vertical Accuracy for LiDAR Data

ASPRS (2014) defined the horizontal and vertical accuracy in terms of the root mean square error (RMSE). The RMSE for horizontal accuracy for LiDAR data should not be less than 30 cm, and the vertical accuracy should be less than 15 cm. The vertical accuracy for LiDAR data with less than 1.4 ppsm could be higher than tolerance. Khalid et al. (2018) stated that the RMSE for the non-vegetated area with the undulating area is ± 0.479 m and the RMSEz for the vegetated area with the hilly area is ± 1.635 m. The results are classified in class VIII.

Tropical forest is occupied with the understory trees, bushes and trees with DBH less than 15 cm. It is demonstrated that the LiDAR observation has limitations in the dense forest area. The results indicate that the DTM given by LiDAR data does not really represent the ground in the dense forest area. This is consistent with the statement from ASPRS (2013) where most of the LiDAR pulses are reflected before reaching the forest floor. Therefore, a higher density data is needed to improve the vertical accuracy in the vegetated area.

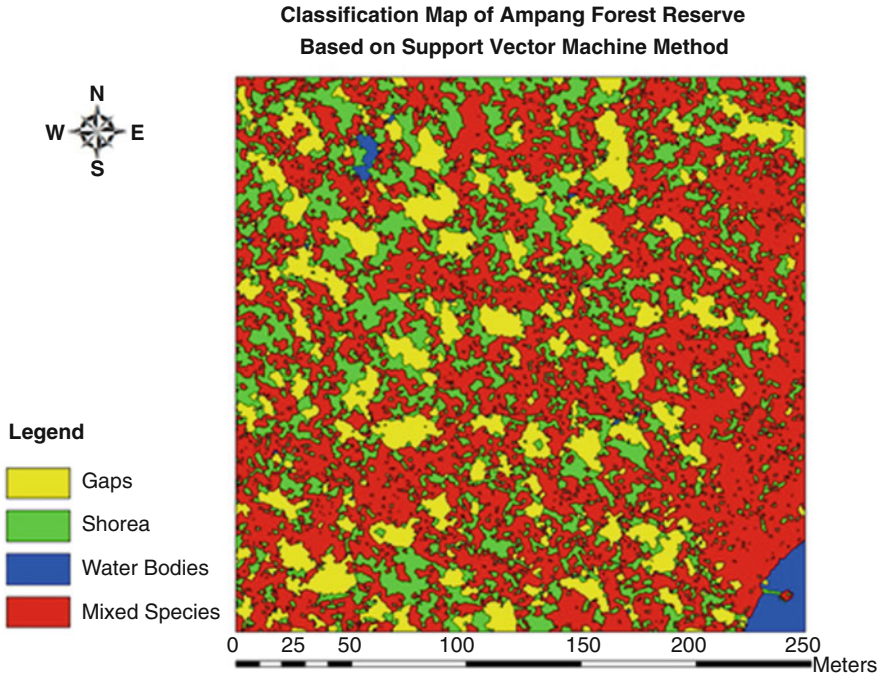


Fig. 6 Classification map based on SVM method

14 Conclusion

This chapter covers the theoretical review about forest heterogeneity and characteristics of *Shorea* spp. Tree biophysical parameters extracted from multi-source remote sensing data are presented and analysed in this chapter with the synergism of WorldView-2 imagery and LiDAR. The extraction results depend on the selection of the segmentation parameters, threshold conditions, training samples for classification and also the availability of the data set. This chapter also revealed the potential of LiDAR data in retrieving tree height and crown areas in the heterogeneous forest environment.

References

- Appanah S (1998) A review of dipterocarps taxonomy, ecology and silviculture
 ASPRS (2013) ASPRS accuracy standards for digital geospatial data
 ASPRS (2014) ASPRS positional accuracy standards for digital geospatial data draft for second public review draft revision 5, version 1

- Dekavalla M, Argialas D (2018) A region merging segmentation with local scale parameters: applications to spectral and elevation data. *Remote Sens* 10:2024. <https://doi.org/10.3390/rs10122024>
- Fangliang H, James V (1997) Distribution patterns of tree species in a Malaysian tropical rain forest. *J Veg Sci* 8(1):105–114
- FAO (2016) State of the world's forests 2016. Forests and agriculture: land-use challenges and opportunities. Rome. ISBN 978-92-5-109208-8
- FAO (2018) The state of the world's forests
- Gebreslasie MT, Ahmed FB, Van Aardt JAN, Blakeway F (2011) Individual tree detection based on variable and fixed window size local maxima filtering applied to IKONOS imagery for even-aged Eucalyptus plantation forests. *Int J Remote Sens* 15:4141–4154. <https://doi.org/10.1080/01431161003777205>
- Guan SL, Yen SY (1999) Conservation of dipterocarpaceae in Peninsular Malaysia. *J Trop For Sci* 12(3):593–615
- Hancock S, Armston J, Li Z, Gaulton R, Lewis P, Disney M, Danson FM, Strahler S, Schaaf C, Anderson K, Gaston KJ (2015) Waveform LiDAR over vegetation: an evaluation of inversion methods for estimating return energy. *Remote Sens Environ* 164:208–224
- Heumann BW (2011) An object-based classification of mangroves using a hybrid decision tree-support vector machine approach. *Remote Sens* 12:2440–2460. <https://doi.org/10.3390/rs3112440>
- Immitzer M, Atzberger C, Koukal T (2012) Tree species classification with random forest using very high spatial resolution 8-band WorldView-2 satellite data. *Remote Sens* 12:2661–2693. <https://doi.org/10.3390/rs4092661>
- Jakubowski MK, Li W, Guo Q, Kelly M (2013) Delineating individual trees from lidar data: a comparison of vector and raster-based segmentation approaches. *Remote Sens* 5:4163–4186. <https://doi.org/10.3390/rs5094163>
- Khalid N, Hamid JRA, Latif ZA (2013) Tree biophysical relationship in the Ampang Forest Reserve. In: 2013 IEEE international conference on control system, computing and engineering. pp 365–369. <https://doi.org/10.1109/ICCSCCE.2013.6719991>
- Khalid N, Hamid JRA, Latif ZA, Rasam AR, Saraf NM (2018) Mapping the 3D distribution of Shorea tree species based upon information extracted from Worldview-2 and LiDAR data. In: 2018 IEEE 8th international conference on system engineering and technology (ICSET). pp 128–132. <https://doi.org/10.1109/ICSEngT.2018.8606359>
- Latif ZA, Zamri I, Omar H (2012) Determination of tree species using Worldview-2 data. In: 2012 IEEE 8th international colloquium on signal processing and its applications. pp 383–387. <https://doi.org/10.1109/CSPA.2012.6194754>
- Lillesand T, Kiefer RW, Chipman J (2015) Remote sensing and image interpretation, 7th edn. Wiley, Toronto
- Machala M (2014) Forest mapping through object-based image analysis of multispectral and LiDAR aerial data. *Eur J Remote Sens* 47:117–131. <https://doi.org/10.5721/EuJRS20144708>
- Mora B, Wulder MA, White JC, Hobart G (2013) Modeling stand height, volume, and biomass from very high spatial resolution satellite imagery and samples of airborne LiDAR. *Remote Sens* 5:2308–2326. <https://doi.org/10.3390/rs5052308>
- Ozdemir I, Karnieli A (2011) Predicting forest structural parameters using the image texture derived from WorldView-2 multispectral imagery in a dryland forest, Israel. *Int J Appl Earth Obs Geoinf* 13:701–710. <https://doi.org/10.1016/j.jag.2011.05.006>
- Phua MH, Zing ZY, Wong W, Korom A, Ahmad B, Besar N, Tsuyuki S, Ioki K, Hoshimoto K, Hirata Y, Saito H, Takao G (2014) Estimation of above-ground biomass of a tropical forest in Northern Borneo using high-resolution satellite image. *J For Environ Sci* 30(2):233–242. <https://doi.org/10.7747/JFS.2014.30.2.233>
- Song C, Dickinson MB, Su L, Zhang S, Yaussey D (2010) Estimating average tree crown size using spatial information from IKONOS and Quickbird images: across-sensor and across-site comparisons. *Remote Sens Environ* 114:1099–1107. <https://doi.org/10.1016/j.rse.2009.12.02>

- Tong F, Tong H, Mishra R, Zhang Y (2021) Delineation of individual tree crowns using high spatial resolution multispectral WorldView-3 satellite imagery. *IEEE J Sel Top Appl Earth Obs Remote Sens*
- Varin M, Chalghaf B, Joannis G (2020) Object-based approach using very high spatial resolution 16-band WorldView-3 and LiDAR data for tree species classification in a broadleaf forest in Quebec, Canada. *Remote Sens* 12:3092. <https://doi.org/10.3390/rs12183092>
- Whiteside T, Ahmad W (2008) Estimating canopy cover from eucalypt dominant tropical savanna using the extraction of tree crowns from very high resolution imagery. In: *Proceedings of geobia 2008*
- Zahidi I, Yusuf B, Hamedianfar A, Shafri HZM, Mohamed TA (2015) Object-based classification of Quickbird image and low point density LiDAR for tropical trees and shrubs mapping. *Eur J Remote Sens* 423. <https://doi.org/10.5721/EuJRS20154824>
- Zhen Z, Quackenbush L, Zhang L (2016) Trends in automatic individual tree crown detection and delineation-evolution of LiDAR data. *Remote Sens* 2016(8). <https://doi.org/10.3390/rs8040333>

Index

A

- Above ground biomass (AGB), 15, 34, 36–43, 51, 63, 64, 76–80, 82–93, 117, 122, 123, 130, 187, 190, 193, 199, 203–205, 366, 398, 403–406
- Accuracy assessments, 81, 90, 119, 122, 126–128, 130, 131, 143, 162, 163, 233, 246–248, 255–261, 282, 296, 315, 448
- Active sensors, 11, 79, 196, 403, 437, 438
- Advanced Vegetation Index (AVI), 34
- Advanced Very High-Resolution Radiometer (AVHRR), 195, 200, 438
- Aerial photographs, v, 4, 8–10, 15, 16, 67, 193, 194, 200, 339, 358
- Afforestation, 179, 189, 315, 331, 396
- Agroforestry, 7, 8, 51, 186, 244, 338
- Airborne, v, 7, 29, 39, 40, 43, 52, 62, 67, 68, 81–84, 90, 93, 120, 197, 200, 307, 358–368, 377, 379, 417, 430, 440
- Airborne laser scanning (ALS), 40, 43, 52, 65, 68, 77, 78, 81–84, 89, 90, 93, 358, 377, 383, 388, 437
- Algorithm, 17, 30, 31, 35, 41, 44, 65, 85, 87, 92, 117–121, 123, 128, 130, 131, 162, 165, 196, 221, 222, 228, 240, 241, 243, 245, 246, 249, 267, 283, 284, 295, 296, 308, 310, 339, 348, 365, 374–380, 382, 383, 388, 389, 399, 401, 404, 441, 445
- Allometric equations, 35, 36, 64, 80, 81, 85–92, 117, 122, 199, 201–203, 205, 397, 403
- A priori knowledge, 221
- Artificial neural network (ANN), 39, 44, 117–119, 122–124, 126, 128, 130, 131, 157, 200, 201, 203

B

- Bioclimatic, 35, 137, 142, 147, 149, 150, 327
- Biodiversity, xi, 45, 51–54, 56, 58, 60–62, 67, 131, 137, 148, 168, 174, 283, 342, 344, 345, 376, 385, 389, 415, 417, 418, 436
- Biogeochemical, 190, 396
- Biomass, 7, 8, 15, 17, 29, 34–39, 42, 51, 52, 55, 63, 64, 76, 77, 80, 81, 83, 85–87, 89–91, 116–131, 157, 186–205, 306, 307, 358, 366, 373, 374, 376, 396–406, 425, 436, 438–440, 447, 448
- Biophysical parameters, 44, 80, 191, 436, 437, 441, 450
- Block plantation, 9
- Boreal forests, 18, 59, 403

C

- Canopy height model (CHM), 39, 43, 77, 80, 81, 90–92, 120, 125, 131, 200, 401, 403, 404
- Carbon dioxide (CO₂) emissions, 50
- Carbon sequestration, 61, 68, 87, 88, 90, 91, 93, 165, 186, 190, 201, 396, 436
- Carbon stocks, v, 7, 15, 34, 40, 51, 64, 76–93, 122, 123, 125, 126, 128, 130, 131, 186, 188, 191, 201, 202, 205, 239, 283, 307
- Carbon storage, 52, 165, 340, 358, 372, 396–406, 415
- Change vector analysis (CVA), 375
- Circular fixed plots, 7
- Citizen-driven urban forestry (CDUF), 350–351

- Classification, v, 9, 17, 29, 34, 40–42, 44, 64, 65, 67, 68, 81, 84, 117, 120, 121, 131, 157, 160–162, 165, 172, 191, 193–196, 201, 219, 221, 222, 225, 228–231, 233, 239, 241, 245–246, 253, 255, 266, 267, 282, 284, 293, 295, 296, 308, 310, 313, 315, 362, 366, 373–375, 377–383, 389, 402, 404, 428–430, 439–441, 445–448, 450
- Classification accuracy, 16, 17, 31, 34, 41, 63, 222, 223, 225–227, 229–231, 233, 239, 308, 374, 378, 406, 438–440, 445, 448
- Classification errors, 233
- Climate change, 50, 54, 57, 60, 61, 64, 76, 88, 116, 131, 137, 154, 165, 186, 189, 190, 192, 291, 295, 321, 323, 325, 329–333, 339, 340, 343–344, 346–348, 351, 388, 396, 397
- Cluster sampling, 5
- Coarse woody debris (CWD), 64, 65
- Commission error, 222, 225, 257, 258, 263, 265, 269
- Confusion matrix, 16, 225, 226, 231, 232, 243, 253, 255, 256, 258–260
- Convention on biological diversity (CBD), 385
- Convolutional neural network (CNN), 67, 68, 378, 379, 382, 399
- Correlation analysis, 83, 296, 299, 300
- Criteria and indicator (C & I), 169
- Crop productivity, 374
- Crown projection area (CPA), 77–82, 84, 90–93, 122–125, 127–131
- D**
- Damaged forests, 372, 376, 377, 379, 380, 383, 385, 386, 388
- Data fusion, 67, 340, 347, 436–450
- Data transformation, 374
- Decision support system (DSS), 100, 101, 105, 112
- Decision tree, 157, 240, 245, 310
- Diameter at breast height (DBH), 40, 42, 43, 77, 78, 80–92, 119, 122–125, 127–131, 155, 197, 202, 205, 403, 405, 422, 425, 449
- Digital canopy height model (DCHM), 440
- Digital elevation model (DEM), 12, 63, 67, 109, 137, 142, 144, 162, 358, 361–366, 368, 401, 404, 440
- Digital surface model (DSM), 77, 79–81, 91, 92, 361, 403–405, 440
- Digital terrain model (DTM), 13, 77, 79–81, 90–92, 365, 440, 449
- Dipterocarpaceae, 168, 170, 416, 418, 436, 437
- Dipterocarpus*, 416, 422, 425, 427–429, 437
- Disturbance, 14, 43, 44, 57, 58, 60, 160, 187, 196, 238–270, 291, 351, 366, 372, 377, 385, 387
- Double sampling, 7, 16
- E**
- Ecognition, 125, 128, 220
- Ecological niche models (ENMs), 136, 137, 150
- Ecophysiological models, 396
- Ecoregion, 54, 138, 142, 143, 145, 150
- Electromagnetic spectrum, 9, 11, 168, 359
- Electromagnetic wave, 157, 191
- Elevation coordinates, 361
- Enhanced Thematic Mapper (ETM+), 10, 31, 155, 379
- Enhanced vegetation index (EVI), 34, 139, 144, 147, 191
- Environmental impact assessments (EIA), 376, 388
- European Remote Sensing (ERS), 197
- F**
- Farm forestry, 9
- Fire modelling, 358
- Forest biomass, v, 12, 34, 35, 39, 76–93, 116, 187–189, 193–195, 197–200, 202, 396, 397, 405
- Forest cover, 13–16, 28–31, 33, 50, 58, 60, 147, 154–165, 168, 169, 174, 175, 177–179, 241, 282, 284, 290, 327, 376, 389
- Forest ecosystems, v, 28, 38, 45, 55, 60, 100–112, 116, 171, 175, 186, 347, 358, 366, 372, 376, 388, 389, 396, 397, 406, 436
- Forest engineering, 358–368
- Forest fires, 60, 67, 100–112, 189, 358, 372, 373, 379, 397
- Forest inventory, v, 4–19, 29, 40, 44, 52, 81, 84, 85, 119, 154, 160, 358, 368, 373, 382, 397, 403, 436, 438
- Forest landscape restoration (FLR), 50–68
- Forest management, v, 8, 14, 17, 28, 29, 44, 45, 64, 104, 105, 107, 112, 168, 169, 174, 179, 201, 315, 340, 344, 347, 389, 397, 436
- Forest operations, 358, 364–366, 368
- Forest restoration, 51, 53, 56, 61–63, 373, 376, 379, 383, 388–389
- Freshwater swamp forests, 28
- Fuelwood, 189, 216, 338

G

- Gaussian processes (GP), 118
- Generic algorithm for Rule-set Production (GARP), 136
- Geographic information system (GIS), 14, 15, 36, 100, 102–105, 107–109, 111, 112, 137, 160–162, 190, 193, 219, 220, 242, 280, 283, 339, 340, 347, 348, 350, 358, 364, 365, 430
- Geographic Object-Based Image Analysis (GEOBIA), 379
- Geomorphology, 43
- Georeferencing, 119, 120, 350, 401
- Geospatial technology, 278, 280–285, 339, 340, 348, 351
- Global carbon cycle, 64, 154, 189, 397, 436
- Global positioning system (GPS), 62, 120, 162, 340, 359, 360, 439
- Green areas, 320–333
- Green normalized difference vegetation index (GNDVI), 159, 161, 162
- Green vegetation index (GVI), 374
- Greenhouse gasses (GHG), 60, 186, 189
- Ground survey, 283, 373

H

- Heath forests, 28, 169
- High resolution vertical (HRV), 17, 18
- Homegarden, 219
- Hopea*, 41, 416, 422, 425, 427–429, 436, 437
- Hyperion, 10, 12

I

- IKONOS, 10–12, 40, 42, 194, 200, 436, 438
- Industrialization, 320, 321, 332
- International Tropical Timber Organization (ITTO), 169, 171, 176
- International Union for Conservation of Nature (IUCN), 53, 54, 422
- Iterative Self-Organizing Data Analysis Technique (ISODATA), 200, 308, 310

J

- Jackknife test, 144, 146, 147
- Japanese Earth Resources Satellite (JERS), 12, 43, 197
- Jeffries-Matusita (J-M) Distance, 221

K

- Kappa coefficient, 222, 225, 226, 229, 231
- K-nearest neighbour (kNN), 19
- Kyoto Protocol, 396

L

- Land surface temperature (LST), 325, 331, 332
- Land Surface Water Index (LSWI), 34
- Land use and land cover (LULC), 137, 172, 175, 261, 266, 270, 282–284, 296, 341, 388
- Land use change analysis (LUCA), 238–242, 270
- Landsat MSS, 14, 16
- Landsat TM, 10–12, 14, 17, 18, 37, 39, 195, 216–233, 243, 307–309, 312, 379
- LandTrendr, 238–270
- Latitude, 7, 57, 138, 145, 170, 217, 324, 359, 361, 414, 415
- Leaf area index (LAI), 34, 42, 52, 161, 163, 191, 203, 373, 374, 379, 388
- Linear regression, 81, 83, 88, 89, 91, 117, 118, 123, 161, 203, 404
- Longitude, 138, 170, 217, 324, 359, 361

M

- Machine learning (ML), 65, 116–131, 165, 375, 379, 380, 382, 397, 445
- Malayan rectified skew orthomorphic (MRSO), 120
- Mangrove forests, 16, 28, 29, 38, 41–43, 88–90, 278–285, 290–292, 306, 308–310, 315, 404, 436, 439
- Mangroves, 15, 16, 28, 31–33, 41–43, 90, 169, 171, 173, 201, 244, 278–285, 290–302, 306–315
- Maximum entropy modelling (MaxEnt), 136, 137, 139, 142–145, 147, 148, 150
- Maximum likelihood, 17, 157, 221, 222, 227, 233, 240, 295, 296, 310, 378
- Mean decrease in Gini index (MDG), 67
- Mid-infrared band, 11, 17, 36
- Minimum noise fraction (MNF), 41, 377, 379
- Mixed dipterocarp forests, 169
- Model application, 217, 222–225, 233
- Model building, 224
- Model validation, 88, 89, 91, 92, 103, 123, 129, 142

- Moderate Resolution Imaging Spectro-
Radiometer (MODIS), 42, 102, 103,
105, 107, 191, 195, 200, 204, 239–241,
379, 438
- Montane, 28, 169, 172, 173, 414–430
- Multicollinearity, 142, 144, 150
- Multi-layer perceptron neural networks (MPL
neural nets), 118
- Multilevel sampling, 5–7
- Multiphase sampling, 6, 7
- Multiple coefficients of determination (R^2), 130
- Multi-source remote sensing, 436
- Multispectral Scanner System (MSS), 10, 12,
14, 16, 93, 373, 375
- Multistage sampling, 6, 373
- N**
- National Oceanic Atmospheric Administration
(NOAA), 306
- Near-Infrared band, 11, 17
- Neobalanocarpus*, 41, 436, 437, 447, 448
- Net primary production (NPP), 188, 373, 374
- Network analyst, 100, 101, 111
- Normalised difference vegetation index
(NDVI), 34, 36, 37, 42, 68, 120, 121,
139, 144, 147, 158–163, 191, 195, 200,
203, 204, 240, 241, 270, 295, 307, 310,
324–327, 330, 374, 377, 379
- Normalized Burn Ratio (NBR), 243, 246, 252,
253, 270
- Numerical simulation, 340–341
- O**
- Object based image analysis (OBIA), 41, 77,
81, 118, 125, 126, 131, 404, 439, 441
- Oil palm, 7, 15, 31, 168, 194, 201, 216, 219,
221, 226–228, 230–232, 238–270
- Operational Land Imager (OLI), 15, 31, 34, 36,
43, 118, 138, 155, 160, 161, 163, 171,
243, 291, 324, 325, 377, 379, 380
- Optimised Soil Adjusted Vegetation Index
(OSAVI), 34
- Orthorectification, 119, 120
- Overall accuracy, 31, 41, 63, 81, 84, 126, 143,
145, 162, 222, 225, 229, 233, 248, 252–
256, 261, 266, 267, 269, 270, 315, 378,
379, 382, 438, 445
- P**
- Panchromatic, 11–14, 120, 438
- Parashorea*, 170
- Passive sensors, 157, 198, 240, 399, 403
- PCI Geomatica, 291, 295, 296
- Peat swamp forests, 28, 436
- Permanent sample plots, 7
- Perpendicular vegetation index (PVI), 374
- Phased Array type L-Band Aperture Radar
(PALSAR), 10, 12, 31, 38, 43, 89, 118,
197, 204, 241
- Photogrammetry, 44, 80, 90, 396–406
- Photosynthetically active radiation (PAR), 161,
374, 379
- Pixels, 10, 17, 19, 107, 117, 131, 143, 157, 160,
163, 196, 220–223, 225, 226, 229, 231,
232, 240, 245–247, 249, 253, 267, 268,
270, 308–310, 315, 441, 445
- Polygons, 84, 122, 125, 126, 220, 221, 224, 248
- Post classification change detection, 374, 376,
378
- Predictive models, v, 13, 34, 38, 216–233
- Primary forests, 28, 58–61, 174, 197, 202, 416
- Principal component analysis (PCA), 37, 67,
200, 375, 377, 379, 380
- Producer's accuracy, 222, 225–227, 230, 252,
254, 255, 257, 258, 266, 269
- Putrajaya, 219
- Q**
- Quickbird, 12, 13, 40, 42, 284, 436, 438, 439
- R**
- Radio Detection and Ranging (RADAR), 43,
438
- Rainforests, 13, 28, 43, 59, 65, 83, 87, 89,
167–179, 244, 414–416
- Random forest (RF), 41, 65, 67, 117–119,
122–124, 128–131, 157, 162, 201, 239,
243, 253, 270, 295, 377, 378, 380, 382,
399
- Reclamation, 61, 295, 339, 385
- Reconstruction, 61, 86, 87
- Red band, 158, 160, 162
- Reducing emissions from deforestation and
forest degradation (REDD+), 375
- Reflectance, v, 4, 17, 36, 37, 41, 68, 77,
155–160, 163, 172, 186, 187, 190, 191,
194, 195, 198, 204, 217, 227, 243, 297,
308, 362, 374, 379, 416, 417, 423–430,
447, 448
- Reforestation, 387, 388, 396
- Rehabilitation, 61, 291, 383, 385
- Remote sensing, v, xi, 4, 7, 9–19, 28–30,
34–36, 40, 42, 44, 45, 50–68, 76–93,

- 104, 117, 118, 124, 125, 128, 138, 142, 154–165, 167–179, 186–205, 217, 219, 233, 238–242, 245, 280, 284, 290–302, 307, 315, 340, 347, 348, 358, 372–383, 388–389, 399, 414, 416, 429, 430, 436–439, 447
- Replacement, 5, 61, 290, 383, 385, 414
- Replanting, 216, 242, 246, 247, 254, 255, 267, 415
- Resolution, 7, 9–14, 28–30, 36, 40, 42–44, 64, 68, 77, 79, 81, 93, 102, 104, 117, 121, 142, 147, 149, 155, 157, 160–162, 165, 194–196, 200, 203, 204, 253, 261, 266, 278, 283, 284, 315, 339, 347, 358, 376, 379, 381, 397, 401, 402, 430, 436–438, 440
- Riparian zones, 406
- Root mean squared error (RMSE), 38–40, 81–88, 90–92, 120, 126, 128, 130, 131, 220, 403, 404, 449
- Roundtable on Sustainable Oil Palm (RSPO), 238–240, 242, 244, 245
- Rubber industry, 216
- Rubber plantations, 7, 15, 186–188, 191, 192, 201, 204, 206, 216–233, 239, 242, 266, 269
- Rubber stand, 14, 15, 203, 220–222, 227, 229, 233
- Rubber trees, 186–205, 216–233, 240
- S**
- Sampling design, 5–7, 9, 373
- Satellite imagery, v, 9, 12–16, 19, 37, 39, 82, 160, 162, 163, 203, 240, 246, 261, 269, 291, 296, 308, 347, 348, 441
- Satellite Pour l'Observation de la Terre (SPOT), 10–13, 17, 37, 118, 195, 196, 200, 284, 436, 438
- Sea level, 170, 217, 282, 290–302, 415
- Secondary forests, 52, 58–61, 174, 190, 193–195, 201, 202, 204, 227, 244, 247, 416
- Segmentation, 42, 43, 77, 81, 84, 120, 122, 125, 126, 131, 160, 220, 222–224, 377, 380, 402–404, 441–445, 450
- Sensors, v, 9–13, 19, 28–45, 52, 65, 67, 76–93, 118, 155, 157, 158, 160–163, 186, 191, 193, 194, 196–198, 204, 219, 233, 278, 347, 359, 360, 368, 372, 374, 376, 377, 381, 383, 389, 398, 399, 403, 404, 406, 416, 429, 430, 436–439
- Sentinel, 239
- Shape file, 220
- Shorea*, 41, 81, 82, 170, 416, 422, 425–429, 436, 437, 441, 446–450
- Signature separability, 221, 228, 229
- Signature separation, 228, 229
- Simple random sampling, 5, 315
- Soil brightness index (SBI), 374
- Spaceborne Imaging Radar (SIR), 12, 200
- Spatial modelling, 99–112, 283
- Spatio-temporal, 160, 190, 305–315, 339, 347
- Species distribution, 142–144, 147
- Species distribution models (SDMs), 136, 147
- Spectral angle mapper (SAM), 40, 41, 295
- Spectral post-classification, 374
- Spectral signatures, 40, 41, 172, 203, 204, 231, 240, 297, 362, 374, 417, 423, 425, 430, 441, 447
- Spectral variability, 195, 223, 240
- Stand age, v, 17, 192, 201, 203
- Stand volume, v, 7, 13, 15, 77, 201, 216–233
- Stratified random sampling (STRS), 5
- Structure from Motion (SfM), 65, 79, 91, 401
- Superview-1, 127–129
- Supervised classification, 161, 220–222, 229, 233, 243–245, 253, 254, 261, 266, 291, 295–297
- Supervised classification, 171, 308, 310, 311
- Support vector machine (SVM), 31, 41, 44, 117, 157, 201, 240, 380, 382, 383, 399, 445, 448
- Support vector regression (SVR), 118
- Surface temperature, 320–333
- Sustainable Development Goals (SDGs), 344
- Sustainable forest management (SFM), xi, 8, 28, 45, 63, 169, 171, 175, 179, 389, 396, 418
- Synthetic aperture radar (SAR), 10, 12, 28, 29, 36, 38, 39, 43, 44, 78, 79, 87–89, 193, 196, 197, 204, 240, 379, 380
- Systematic sampling, 5, 7
- T**
- Temporal variations, 397
- Temporary sample plots, 7
- Terrain roughness index (TRI), 142, 144
- Terrestrial laser scanner (TLS), 39, 40, 43, 64, 65, 78, 82–87, 90
- Testing areas, 221, 228
- Thematic Mapper (TM), 14, 15, 17, 18, 31, 37, 118, 155, 160, 162, 171, 193, 200, 203, 219, 220, 228, 291, 325, 373, 377, 379, 380

- Threshold, 31, 57, 62, 143, 241, 242, 246,
248–250, 252, 254, 256, 267, 296, 329,
403, 448, 450
- Tidal regime, 290–302
- Time series, 43, 87, 164, 204, 239–241, 249
- Training areas, 221, 225, 233
- Transport accessibility, 104
- Tree crops, 8, 9, 216
- Trees outside forests, 338–339
- U**
- Unmanned aerial vehicle (UAV), 28, 29,
42–44, 64, 67, 79, 89–93, 284, 366, 378,
379, 382, 383, 388, 397–402, 404–406,
430
- Unmanned aircraft systems (UAS), 359–361,
377, 383
- Unsupervised classification, 34, 295, 310, 406
- Urban biodiversity, 342–343
- Urban climate, 320–322, 330, 333, 340–341,
344
- Urban forest policy, 344–346
- Urban forests, 320–333, 339–351
- Urbanization, 169, 177–179, 282, 290, 320,
321, 323, 325, 326, 330, 332, 333
- User's accuracy, 222, 225, 227–230, 252, 254,
255, 257, 258, 266, 448
- V**
- Vatica*, 170, 416, 437
- Village woodlots, 9
- Visible, 9, 11, 34, 41, 58, 155–157, 160, 191,
193, 195, 227, 253, 267, 297, 345, 348,
399, 400, 402, 421, 438
- Volume class, 221, 224, 228–233
- Vulnerable map, 291, 300, 301
- W**
- Wind intensity, 290–302
- WorldView, 13, 200